Mechanisms controlling microglial colonization of the forebrain

Cécile Bridlance

Sorbonne Université

Ecole Doctorale 515 – Complexité du Vivant

Institut de Biologie de l'Ecole Normale Supérieure

Centre Interdisciplinaire de Recherche en Biologie

Mechanisms controlling microglial colonization of the forebrain

Par Cécile Bridlance

Thèse de doctorat de Neurosciences

Dirigée par Morgane Thion et Sonia Garel

Présentée et soutenue publiquement le 22 juin 2023 devant un jury composé de :

Rosa Paolicelli Assistant Professor, University of Lausanne, Suisse	*Rapporteur*
Sophie Layé Directeur de recherche, Bordeaux Neurocampus, France	*Rapporteur, Président du jury*
Mélanie Greter Associate Professor, University of Zurich, Suisse	*Examinatrice*
Anne Desmazières Chargé de recherche, Institut du Cerveau, France	*Examinatrice*
Jean-Christophe Delpech Chargé de recherche, Bordeaux Neurocampus, France	*Invité*
Morgane Thion Chargé de recherche, IBENS, CIRB, France	*Co-Directrice de Thèse*
Sonia Garel Professeur, IBENS, CIRB, France	*Co-Directrice de Thèse*

Croyez ceux qui cherchent la vérité,
doutez de ceux qui la trouvent.

André Gide
Ainsi soit-il ou Les jeux sont faits, 1952

Acknowledgements

I first would like to thank members of my PhD jury: Rosa Paolicelli and Jean-Christophe Delpech for accepting to review my work, as well as Sophie Layé, Mélanie Greter and Anne Desmazières. I am grateful to have you in my jury. I would also like to thank members of my thesis committee: Laurence Goutebroze, Michel Mallat and again Anne Desmazières, thank you for your guidance and advise along my PhD.

I would like to express my deepest gratitude to both my co-directors, Morgane and Sonia: you bring different and complementary energies which was a great cocktail to work with. Sonia, I first met you as a professor, teaching neurodevelopmental biology with Nicolas David. You gave me the desire to pursue further in biology and specifically opened my mind to the beauty of this field. Thank you for later welcoming me in your lab so nicely. Most of all, thank you for your constant enthusiasm, energy and kind support through the years. Thank you very much Morgane for your guidance and patience through this journey. Your scientific efficiency and combativeness taught me a lot. Thank you for always being available to help and correct my work, and for giving me such trust and freedom during this last phase of the PhD.

Thank you to all members of the Garel lab, past and present. Thank you Lud for bringing a different vibe in the lab, always genuily passionate and ready to share your knowledge. Thank you Alex for greeting me in the lab. It was great to have your English vibes around. Thank you Akindé, my PhD buddy, for all the moments we shared – and for showing me the way! It was great having you around, always some good accent imitation to laugh in the good and in the tough moments. Thank you Ioana, both for your always lucid scientific insights and for your good-heartedness – without forgetting music recommendations! Thank you Hugues for everything, from the pranks to your always surprising stories. I somehow cherish the time spent with only us four in the lab after lockdown. Thank you Nicolas for your support in every moments. It has been a great adventure for me to supervise you during you M2 internship and I am happy that you stayed for a PhD and to have you around. Thank you Alice and Clarissa for bringing Italian vibes to the lab. Thank you for your help and support in so many ways during my PhD. Thank you so much Sarah, for all the help during the end of my PhD – I don't know how I would have done this without you! Thank you for always smiling and laughing, even drawn under billions of PCR. Thank you Edmond for your help with the RNAscope experiments and for settling in College. Most of all, thank you for your kindness and for being always ready to help. Thank you Nina for your help in this last crucial moment. Thank you so

much, Thandi, for always being a ray of sunshine in this lab, and especially for all the "chouquettes" you brought! Thank you Maryama, Jonathan, Feriel and Seiki for your help with the experiments and making the lab work smoothly.

Thank you all in the Garel lab and 5th floor for this great atmosphere we had and for all the nice drinks together.

Thank you very much to the people of the animal and imaging facilities at the IBENS doing such a good work. Thank you for handling so many mouse lines with patience and great care Eléonore, I could not have managed any of it without you! Thank you also to Gwendoline and Deborah, whose boxes I also colonized recently. And thank you Benjamin for the two-photon experiments: seeing microglia actually move was like a child's dream!

Thank you Julienne, Jean, Dimitri and Gustave amongst others, my friends and PhD partners, it's been great to discuss our PhD lives together along the way!

Thinking of how it all started, I am grateful to Claude Desplan for having me in his lab when I had absolutely no experience, and Vil for teaching me everything! I had a great time, full of intellectual and scientific stimulation as well as good atmosphere - and this is what made my think about doing a PhD. Vil, it was such a pleasure spending some time again with you in Ventura!

I am also grateful for the Ecole Polytechnique and the ARC foundation for my PhD fellowship and extension.

Last, I would like to thank my friends and family for all the support they showed me over the years and during this PhD journey, no matter how mysterious it could sound to them. Thank you Mum and Dad for never missing an occasion of asking how the little mice were doing: they're doing great, no worries! Thank you Louis for being by my side and supporting me in so many ways.

Table of contents

Table of figures

List of abbreviations

AD	Alzheimer's Disease
AGM	Aorto-Gonad-Mesonephros
ASD	Autism Spectrum Disorders
ATAC-seq	Assay for Transposase-Accessible Chromatin sequencing
ATM	Axonal Tract associated Microglia
ATP	Adenosine Triphosphate
BAMs	Border Associated Macrophages
BBB	Blood Brain Barrier
BDNF	Brain-Derived Neurotrophic Factor
BM	Bone Marrow
CA	Cornu Ammonis
CC	Corpus Callosum
CGE	Caudal Ganglionic Eminence
ChIP-seq	Chromatin-Immunoprecipitation followed by Sequencing
CNS	Central Nervous System
CSF	Cerebrospinal Fluid
CSF-1	Colony-Stimulating Factor 1
CSF-1R	Colony-Stimulating Factor 1 Receptor
DAM	Disease-Associated Microglia
DG	Dentate Gyrus
DIM	Disease Inflammatory Macrophages
E	Embryonic Day
ECM	Extra-Cellular Matrix
EMPs	Erythromyeloid Progenitors
FDA	Food and Drug Administration
GF	Germ-Free
GW	Gestational Week
HAM	Human Alzheimer's Microglia
HDLS	Hereditary Diffuse Leukoencephalopathy with Spheroids
HSC	Hematopoietic Stem Cells
IL	Interleukin

ION	InfraOrbital Nerve
L	Layer
LGE	Lateral Ganglionic Eminence
LPS	Lipopolysaccharide
MGE	Medial Ganglionic Eminence
NGF	Nerve Growth Factor
OPC	Oligodendrocyte Progenitor Cell
P	Postnatal day
PAM	Proliferative region Associated Microglia
PAMPs	Pathogen-Associated Molecular Patterns
PC	Principal Cell
PV	Parvalbumin
ROS	Reactive Oxygen Species
scRNA-seq	Single-Cell RNA-sequencing
TCA	Thalamo-Cortical Axon
TLR	Toll-Like Receptor
TNF-α	Tumor Necrosis Factor Alpha
VP	Ventral Posterior nucleus
VZ	Ventricular Zone
YAM	Youth-Associated Microglia
YS	Yolk Sac

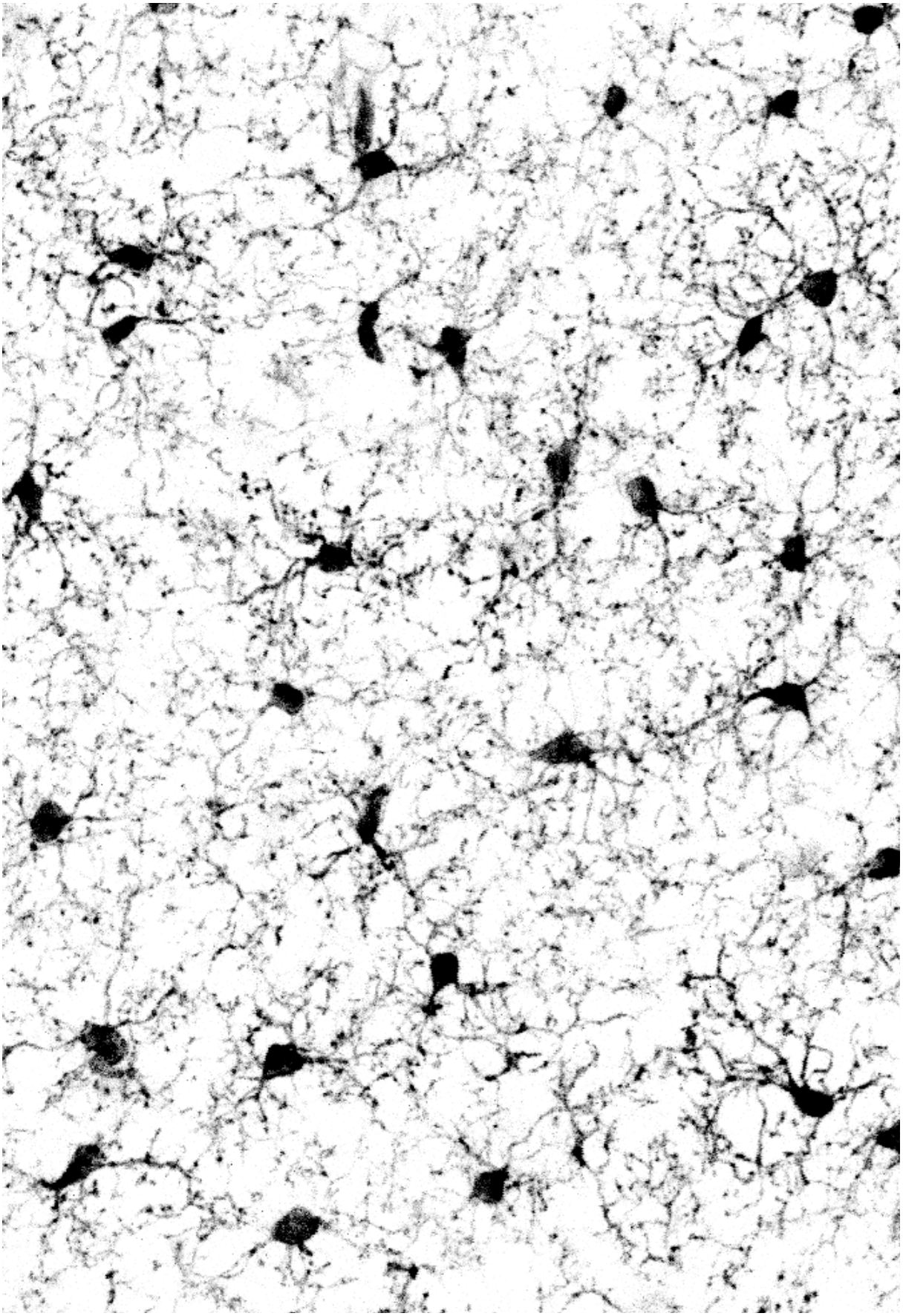

Microglia tiling the cortex with their ramified process at P20.

INTRODUCTION

1. The brain and its development

1.1. The brain: a complex and organized structure

The brain is the most rostral part of the Central Nervous System (CNS), protected by the skull. It is composed, from most rostral to caudal, of the forebrain, midbrain and hindbrain, and is connected to the spinal cord. The primitive function of the brain is to maintain homeostatic conditions for the body: ensuring appropriate heart rate, breathing or digestive functions, amongst others. While this still holds true, it has evolved through evolution to become a complex center integrating and processing external stimuli, generating abstract thinking, emotions or decisions – all of which mainly occurs in the forebrain. On the other hand, the cerebellum, which occupies part of the hindbrain and orchestrates balance maintenance and coordinated movements (Sciences, 1992), is increasingly recognized for its contribution to cognitive functions (Koziol *et al.*, 2014).

Overall, appropriate brain functioning results from the arrangement of billions of neurons and glial cells in spatially-organized and connected structures. These structures have their own functions and internal organization, and some are further detailed below. Importantly, the global organization of the brain is well-conserved amongst mammals. In particular, mouse, our animal model of study, is thus an appropriate tool to study the mammalian brain, including the human brain, and a schematic representation of the brain of both species is provided in **Figure 1.1**. The main differences across mice and human are further discussed along the text.

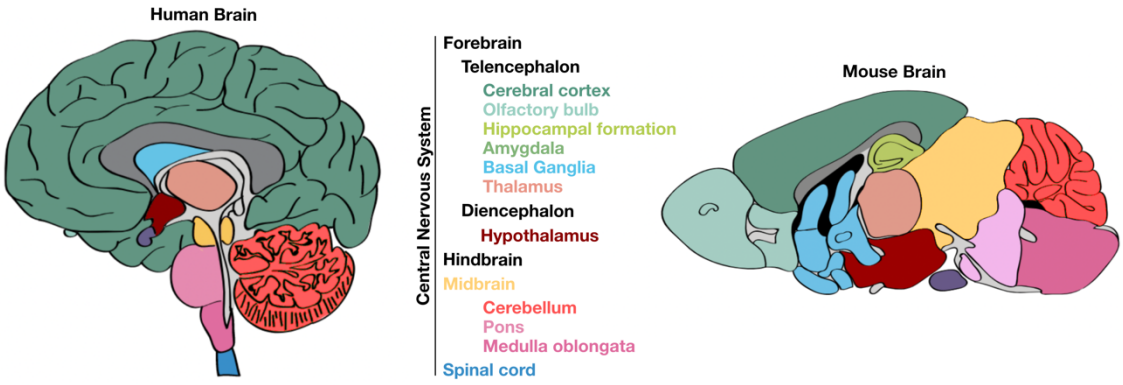

Figure 1.1 Schematic representations of the human and mouse brain

While the global organization of the brain is well-conserved between humans and mice, with color-coded correspondence between the different functional structures, there are some divergences. For example, human cortex is overdeveloped while the olfactory bulb is greatly reduced, coherently with our limited use of smell.
Adapted from www.proteinatlas.org/brain

1.1.1. Neuronal connectivity and diversity

Brain function is regulated by the coordinated activity of neuronal networks and neuronal activity relies on the communication between neurons: each of them receives inputs on its dendrites, while its cell body, the soma, integrates them and can further transmit information (**Figure 1.2**). If so, an electrical stimulus is sent through the axon and passed on to downstream neurons. The information thus propagates in specific neuronal networks: some are very local, while long-range connections allow to target distant regions of the brain. Neuron to neuron communication happens at synapses via the release of specific neurotransmitters and one single neuron can establish thousands of synapses with its neighbors. The constant and fascinating rearrangement of synapses allows the brain to learn, memorize and be reshaped by experience (Purves, 2001).

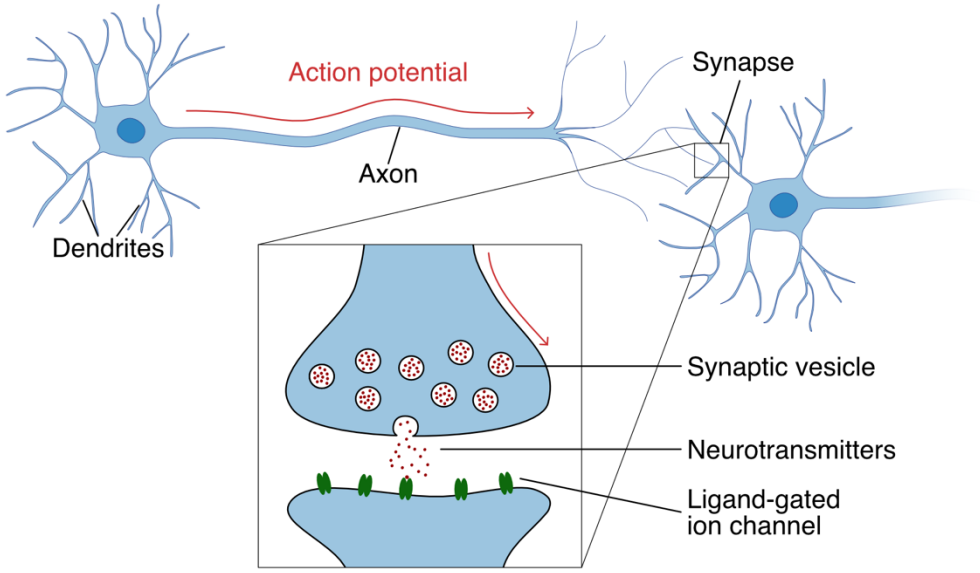

Figure 1.2 Schematic representation of neuronal transmission

The pre-synaptic neuron receives inputs on its dendrites, integrates this information and triggers - or not - an action potential that propagates as an electrical signal along its axon. Transmission from the pre-synaptic to the post-synaptic neuron occurs at the synapse (close-up) where neurotransmitters are released upon arrival of the action potential. They are recognized by specific ligand-gated ion channels on the surface of the post-synaptic neuron.

Neurons come in many different flavors: different types have specific locations, morphologies and functions. Importantly, they can be divided in two broad functional categories: neurons are excitatory or inhibitory. Through the use of different kind of neurotransmitters, they can respectively promote or prevent neuronal activity in their downstream neurons. In the cerebral cortex, inhibitory neurons only represent ~10 to 20% of

all neurons. A majority of them do not have long-range connections and they rather locally tune neuronal activity, thus ensuring an essential role. Indeed, appropriate Excitatory/Inhibitory balance is key to the normal functioning of the brain - and is impaired in diverse pathologies such as epilepsy or Austism Spectrum Disorder (ASD)(Uzunova, Pallanti and Hollander, 2016).

1.1.2. Architecture of the forebrain

While anatomists have extensively divided the brain and named its parts, each of them ensures specific functions. In this thesis, we will focus on the forebrain, which comprises the telencephalon and diencephalon. The telencephalon includes dorsally the cerebral cortex and hippocampus (originating from the pallium), and other ventral structures including the striatum and preoptic area (originating from the subpallium).

In particular, the cerebral cortex is the largest site of neural integration (Purves, 2001). It is divided into areas: some receive unimodal sensory information but others, called associative areas, are involved in complex tasks such as memory, abstraction or language. It has a laminar structure with six distinct layers, each composed of different types of neurons precisely organized within circuits. Information is processed through columnar functional units spanning all layers. Cortical neurons are mainly excitatory pyramidal neurons (80%) and the remaining are inhibitory interneurons. Pyramidal neurons are projection neurons: their axons project from one layer to the other, or to other brain regions, to establish connections. Interestingly, the cortex of mice is not “folded” like in humans, primates and most mammals, but its laminar and circuit organization remains very comparable.

The striatum is part of the basal ganglia, a group of subcortical nuclei principally important in the control of motor functions, habits and addiction. The striatum itself is known to initiate voluntary motor movements, but is also involved in other functions such as cognition and emotions (Albin, Young and Penney, 1989; Mink, 2003). It is mainly composed of medium spiny neurons that constitute 95% of striatal cells. Those neurons are GABAergic: they produce and release the neurotransmitter Gamma-Aminobutyric Acid (GABA), the main inhibitory neurotransmitter in the central nervous system, and are thus inhibitory neurons. The striatum receives inputs from the cortex, and projects to the rest of the basal ganglia. It in turn projects back to the cortex via the thalamus, a structure that relays sensory information to the cortex.

The hippocampus is adjacent to the neocortex and is mainly responsible for making new memories. It is divided in regions called Cornu Ammonis (CA) 1, CA2 and CA3, each of them composed of an outer molecular layer, a granular cell layer, and a hilus. The pyramidal neurons that compose the hippocampus have their cell bodies densely packed in the granular cell layer, while their dendrites and axons occupy much of the two other layers. This peculiar organization and identified function in memory made the hippocampus a popular object of study. Following this same organization, the Dentate Gyrus (DG) lies at the tip of the hippocampus and participate in memory formation mechanisms. It is also known to be one of the few regions where neurogenesis is maintained throughout adult life (Altman and Das, 1965; Cameron and Mckay, 2001).

The preoptic area (POA) is part of the hypothalamus, in the diencephalon. It is a functionally heterogeneous region further divided into multiple nuclei. It is involved in sleep, thermoregulation as well as sexual and parental behaviors and has been shown to be sexually dimorphic in rodents (Tsukahara and Morishita, 2020; Rothhaas and Chung, 2021).

1.1.3. The example of the somatosensory system

The somatosensory system of mice (see **Figure 1.3**) provides a nice example of how information is processed through different brain structures (for review: Petersen, 2007). Mice extensively use their whiskers to analyze and monitor their environment. Being awake at night, they thus compensate for their limited sight with their whiskers, that serve as sensors capable of discriminating texture or providing spatial maps of the surroundings. Whiskers are aligned in rows and columns on the mouse snout, and information is then collected by neurons of the infraorbital nerve (ION). They make synapses in the trigeminal nuclei of the brain stem with neurons that target the ventral posterior nucleus (VP) of the thalamus. From there, Thalamo-Cortical Axons (TCA) relay information to the primary somatosensory cortex. In particular, their dendrites contact neurons called principal cells (PCs) in cortical layer (L)IV. Strikingly, information arising from each whisker is segregated, forming topographic maps of whiskers all along the pathway: the barrelettes in the brain stem, the barreloids in the thalamus and the barrels in cortical LIV, as illustrated by the fact that a single barrel will be strongly activated by its corresponding whisker. In addition, multidimensional integration occurs in the somatosensory cortex so that the strength of barrel activation can be modulated by the context (motor behavior or stress, for example).

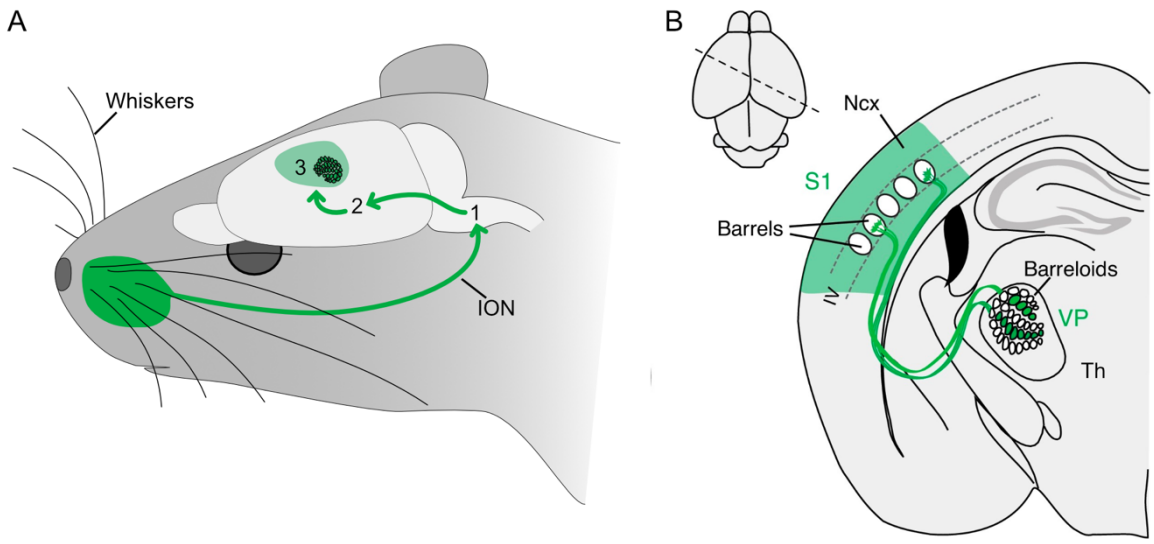

Figure 1.3 The rodent somatosensory system: from the whiskers to the cortex

(A) Information from each whisker is transferred via sensory neurons of the infraorbital nerve to the brain stem (1). It is relayed in the VP of the thalamus (2) before reaching Layer IV of the somatosensory cortex (3, green area). (B) Coronal brain hemisection representing the topographic map transfer from the thalamic barreloids to the barrels. ION: infraorbital nerve, S1: primary sensory area, Ncx: Neocortex, Th: Thalamus, VP: Ventroposterior nucleus. Adapted from Lokmane & Garel, 2014.

In addition to being spatially confined thanks to physical TCA aggregation in LIV, the barrel response is also temporally restricted via the specific structure of the neural circuit. Indeed, TCAs contact both PCs and Parvalbumin-expressing (PV) inhibitory interneurons. PV interneurons are fast-spiking and rapidly inhibit PCs after TCA activation, creating a feed-forward inhibition. This provides an important temporal resolution in information processing and illustrates the crucial role of inhibitory interneurons.

1.1.1. Glial diversity and varied roles

While neurons and their complex integration into circuits are fascinating, they are not the only cells in the brain: they cohabit and interact with glial cells. Long overlooked, the latter were primarily described by Rudolph Virchow in the 19th century as non-functional “glue” that structurally supports neurons (Ndubaku and de Bellard, 2008). Instead, glial cells play many

important roles in brain functioning (Freeman and Rowitch, 2013). Among them are mainly astrocytes, oligodendrocytes and microglia (**Figure 1.4**). Astrocytes provide nutrients to neurons, maintain homeostasis at the synapse and regulate blood flow (Sofroniew and Vinters, 2010). In addition, they react in case of injury and isolate the injured part from the rest of the brain. Most importantly, they now arise as key regulators of neuronal activity: astrocytes are involved in the promotion of synapses as well as their elimination through engulfment, and mediate synaptic plasticity (Freeman and Rowitch, 2013). Oligodendrocytes are responsible for the production of myelin, unsheathing axons to speed up signal propagation, and also provide trophic support to neurons (Bradl and Lassmann, 2010). Last, microglia are the immune cells of the brain and will be further described (see 2).

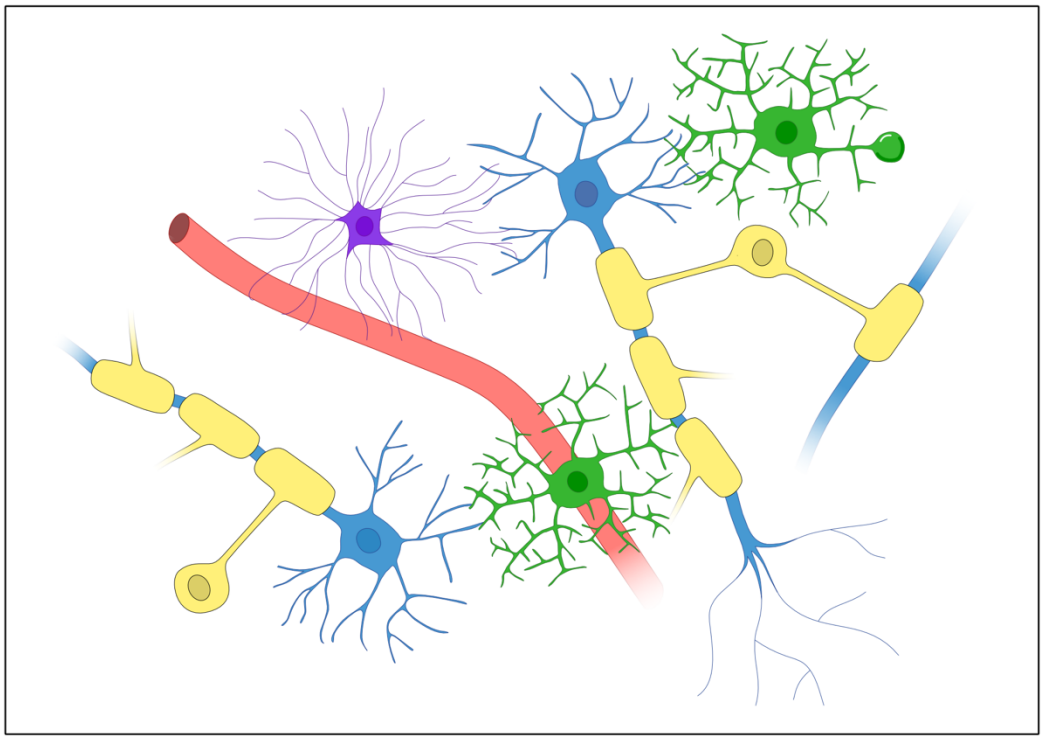

Figure 1.4 Neurons and principal glial cells

Schematic representation of neurons (in blue) with the principal populations of glial cells in the CNS: astrocytes (in purple) are in close contact with blood vessels (in red) and synapses; oligodendrocytes (in yellow) are responsible for the myelination of axons, and microglia (in green) with their highly ramified morphology. On the top right, one microglia displays a phagocytic cup.

1.2. Brain development

To achieve such complexity, brain development is a protracted and multistep process starting at early embryonic stages and lasting through adolescence. Both genetically regulated and influenced by the environment, it follows a stepwise program of dynamic and adaptive mechanisms. Here is a broad overview of its major events.

1.2.1. The early stages of embryogenesis and formation of the neural tube

In the early stages of embryonic development, while cells are actively proliferating, two cavities form: the amniotic cavity, which will later surround the embryo, and the primary yolk-sac. The amniotic sac is filled with liquid. It allows the embryo to move freely inside the uterus and protects it from trauma, but also acts as a reservoir of nutrients for the growing embryo. On the other hand, the primary yolk-sac, which will give rise to the yolk-sac, consists of a membranous sac ventrally attached to the embryo where primitive hematopoiesis occurs and which participates in the formation of the umbilical cord (Yamane, 2018). While in mice the yolk-sac persists throughout gestation and eventually surrounds the embryo (**Figure 1.5**), as does the amniotic sac, it is largely incorporated in the primary gut during Gestational Week (GW) 4 in humans (Freyer and Renfree, 2009; Yamane, 2018). During gastrulation, very early on in embryonic development (around GW3 in humans), the cells start differentiating and reorganize themselves to form three layers (Muhr and Ackerman, 2020): the ectoderm, which will give rise to skin cells and to the nervous system; the endoderm, giving rise to epithelial cells lining the internal surface of organs associated to the digestive and respiratory systems; and the mesoderm, giving rise to a large variety of organs and cell types, including heart, kidneys, gonads, bones, blood and muscle cells. Ectodermal cells of the dorsal portion of the embryo form the neural plate. It then invaginates and eventually forms the neural tube. The neuroepithelial cells that constitute its walls will proliferate and give rise caudally to the spinal cord and rostrally to brain rudiments, which drastically expand, undergoing morphogenesis and folding to create brain architecture. As the brain develops, ventricles form which are then filled with Cerebrospinal Fluid (CSF), providing protection, waste removal and nourishment to the brain (Spector, Robert Snodgrass and Johanson, 2015).

1.2.2. Generation of neurons and glial cells

Along the ventricles, the ventricular zone of the neural tube contains neural stem cells, mainly radial glia, that proliferate to give rise first to neurons, later to glial cells. In particular, the ventricular zone of dorsal telencephalon (or pallium) produces most cortical excitatory neurons. This process called corticogenesis occurs from Embryonic Day (E)10.5 and E18.5 in mice, and from GW7 to GW27 in humans (Götz and Huttner, 2005). The generated neurons migrate radially towards the pia along radial glia processes to form the 6 cortical layers in an "inside-out" fashion (newborn neurons cross early-born neuron layers)(**Figure 1.6**). The ventricular zone of the ventral telencephalon (or subpallium) transiently divides in three structures: the Lateral Ganglionic Eminence (LGE), Medial Ganglionic Eminence (MGE) and Caudal Ganglionic Eminence (CGE), defined by specific combination of gene expression (Nery, Fishell and Corbin, 2002). It abuts the POA which remains in place through adulthood. Newly-generated neurons form the different nuclei of the basal ganglia. Interestingly, additional neurons are generated in the ganglionic eminences (mainly MGE and CGE) as well as POA and migrate through the brain to reach the cerebral cortex. These future cortical interneurons follow different migratory streams, depending on their date of birth (Marín, 2013). When arriving in the cerebral cortex, they all undergo a phase of tangential migration followed by radial migration to reach their final position through the cortical layers (Guo and Anton, 2014).

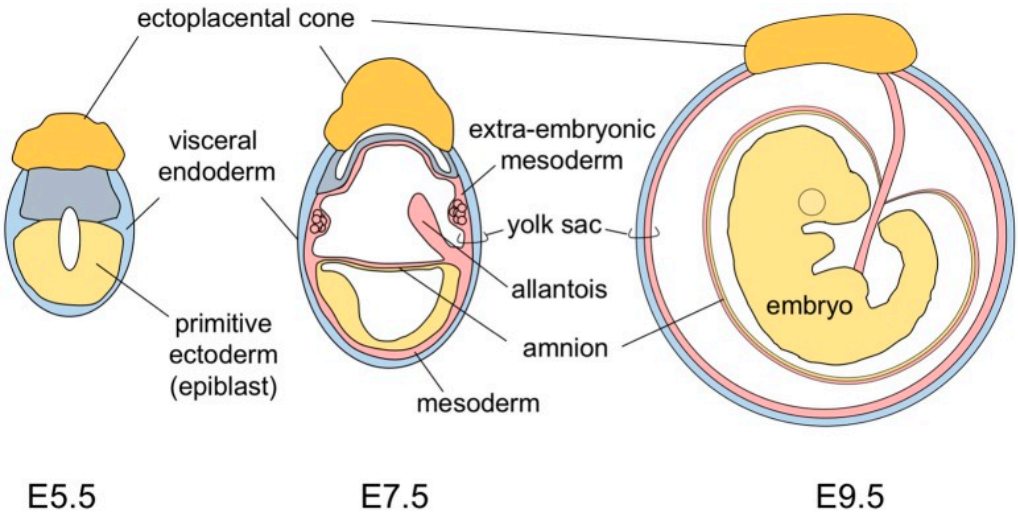

Figure 1.5 Schematic representation of early embryonic development in mice

Early in development, the cells will organize themselves in three layers: the endoderm, the ectoderm and the endoderm (not represented). Originating from cells of the extra-embryonic mesoderm, the yolk sac is ventrally attached to the embryo and later surrounds the embryo in mice. E: Embryonic day. From Yamane, 2018.

Importantly, in the meantime, other neurons need to grow their axons to reach their target region, thus allowing communication between different brain structures. While extending, axons are guided by gradients of guidance cues in their environment, that attract or repel them, but the complete understanding of how they achieve to find their target so accurately is still ongoing research (Zang, Chaudhari and Bashaw, 2021). Groups of axons often bundle, forming zones of white matter, as it is the case in the Corpus Callosum (CC), the main connection between the two cortical hemispheres. Regions enriched in neuron soma and dendrites are instead referred to as grey matter.

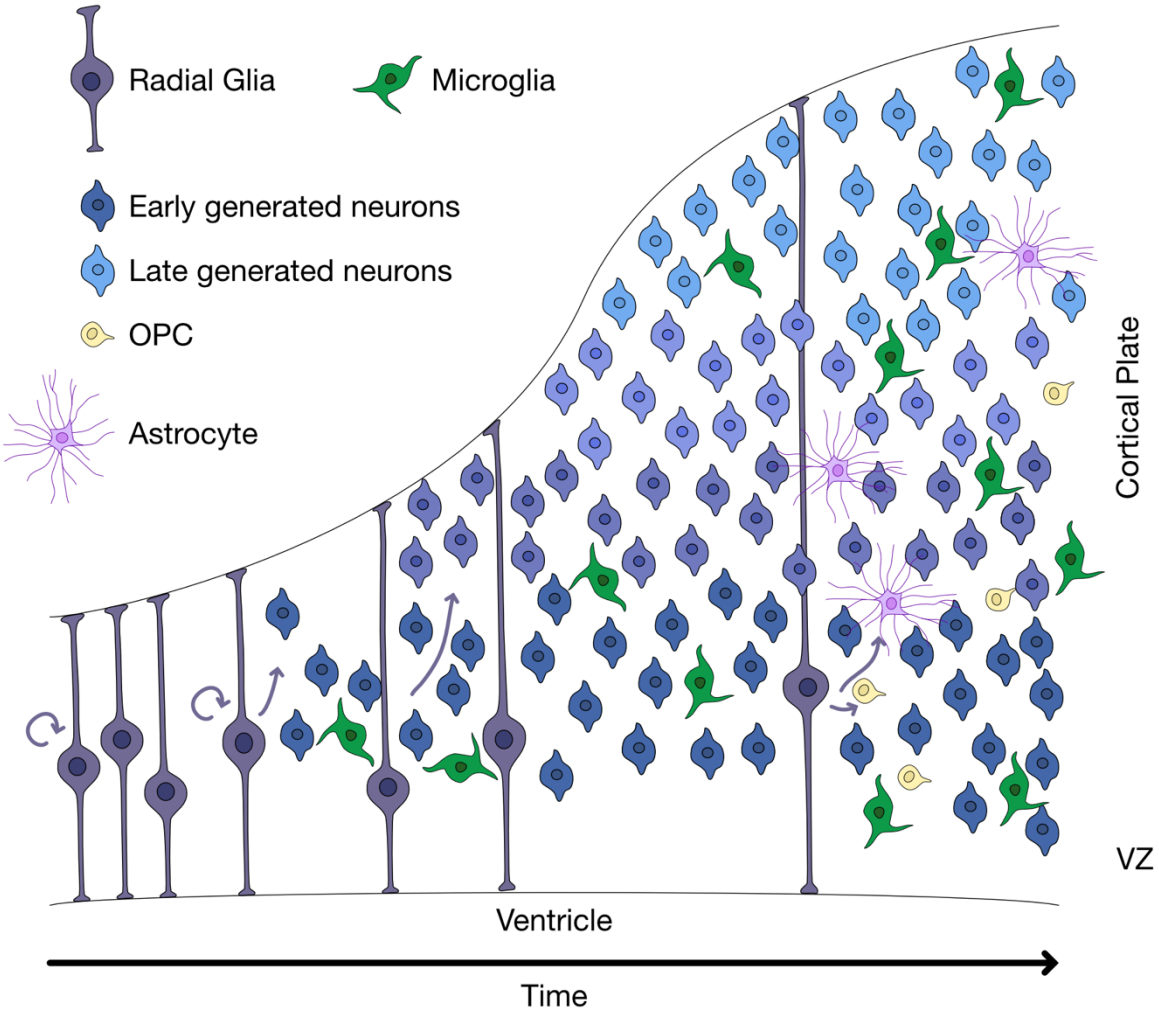

Figure 1.6 Schematic representation of cortical development in mice

Radial glia first proliferate, and later give rise to cortical excitatory neurons. Early-born neurons remain in the deep cortical layers while newly-generated neurons migrate to the upper layers. Then astrocytes and OPCs are generated, which themselves proliferate *in situ*. Microglia are present throughout this process. Cortical interneurons (not represented here) are not generated in the cerebral cortex, but migrate from the Ganglionic Eminences. VZ: ventricular zone, OPC: oligodendrocyte progenitor cell.

Around the end of embryogenesis, neurogenesis overlaps and is followed by gliogenesis: the cortical stem cells of the ventricular zones that were producing neurons then switch to produce astrocytes and Oligodendrocyte Progenitors Cells (OPCs). Timing of this switch is of course important to generate all cell types in appropriate numbers, and is orchestrated by a complex interplay between a variety of extracellular factors and intrinsic epigenetic cell state (Barber, Ali and Kucenas, 2022; Clavreul, Dumas and Loulier, 2022). Of note, OPCs are in fact generated in different waves, the first one starting early in the embryo (around E12.5 in mice), but these OPCs are mainly replaced postnatally by newly generated ones (Van Tilborg *et al.*, 2018). Both astrocytes and OPCs migrate and clonally expand, finally achieving a uniform tiling of the parenchyma where each cell occupies its own, non- or little-overlapping territory. OPCs continuously give rise to oligodendrocytes which once mature start to enwrap axons and produce myelin. Myelination is a slow process starting around birth in mice and actively lasting during the first post-natal years in humans. Constant remodeling of myelin is required along life and shaped by experience (Hughes *et al.*, 2018).

1.2.3. From spontaneous synchronous activity to functioning circuits

After the generation of a broad diversity of neurons and glial cells and their appropriate migration, there remains one crucial step: creating functional circuits. In fact, neuronal circuits are electrically active very early on (Cossart and Garel, 2022). After migration, neurons display some spontaneous activity. First uncorrelated, they further make connections through gap-junctions and their activity becomes locally synchronous with small groups of neighboring neurons. The synchronous spontaneous activity later propagates to whole brain areas, while neurons make chemical synapses. Around birth, neuronal activity shifts from spontaneous to evoked: it results from the integration of sensory stimuli or is task-oriented (motor behavior for example)(Molnár, Luhmann and Kanold, 2020). Activity gradually becomes sparser and more desynchronized (**Figure 1.7**). These transitions in neuronal activity are timed by neuronal maturation as well as environmental stimulations, and allow for appropriate building of functional networks. In particular, waves of neuronal death eliminate supernumerary neurons that are less integrated in circuits (Wong and Marín, 2019). Following a similar dynamic,

synapses are produced in excess and are later sorted: active synapses are strengthened while weaker synapses are eliminated.

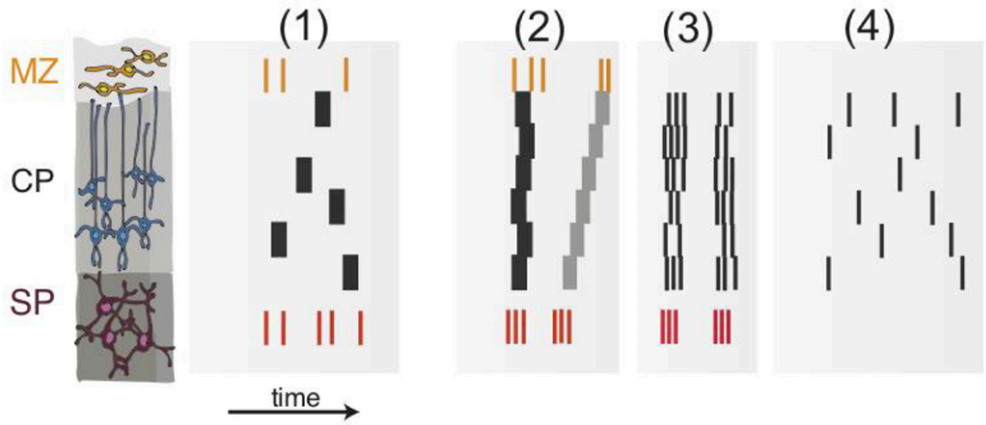

Figure 1.7 Changes in patterns of neuronal activity in the developing neocortex

(1) Cajal-Retzius and subplate neurons (yellow and purple bars, respectively), which are transient neuronal populations, already discharge faster action potentials and at higher frequency than cortical plate neurons (black bars). (2) Neurons electrically coupled by gap junctions generate either local synchronized activity or propagating activity waves. (3) Discharges become faster and local networks discharge in synchronized bursts. Transient early-born neurons start to disappear during this phase. (4) Appearance of adult-like sparse desynchronized activity independent of transient neurons and circuits. Adapted from Molnár *et al*., 2020.

Overall, brain morphogenesis is a complex step-wide program, that involves self-organization and activity-dependent adaptation of brain circuits, including transient circuits and neuronal activity patterns. The different steps of brain construction are important for its functioning, since developmental deficits have been involved in the etiology of a broad range of brain disorders, including mental retardation, epilepsy, autism spectrum disorders or schizophrenia.

2. Microglia: the brain resident macrophages – and more

After Virchow's termed all brain elements that were not neurons as "neuroglia", the field had to wait until new techniques were developed by Santiago Ramón y Cajal (1852-1934) to put forward the theory that neuroglia was actually constituted of cells. In 1913, Ramón y Cajal extensively described astrocytes and mentioned some poorly labelled cells he called the "third element". Nicolás Achúcarro (1880-1918) who was Cajal's student and later collaborator, further adapted the technique to better visualize glia. But it's his student, Pío del Río-Hortega (1882-1945), who described for the first time the morphological and functional features of both oligodendrocytes and microglia (**Figure 2.1**)(Sierra *et al.*, 2016). Using techniques that look archaic and extremely limited compared to what can be done now, nearly a century later, he was able to make assumptions about microglia that were proven right decades afterwards (Sierra, Paolicelli and Kettenmann, 2019). In particular, he suggested the mesodermal origin of these cells, their migrating and phagocytic capacities, and their ability to change from ramified to ameboid morphology in pathologic conditions.

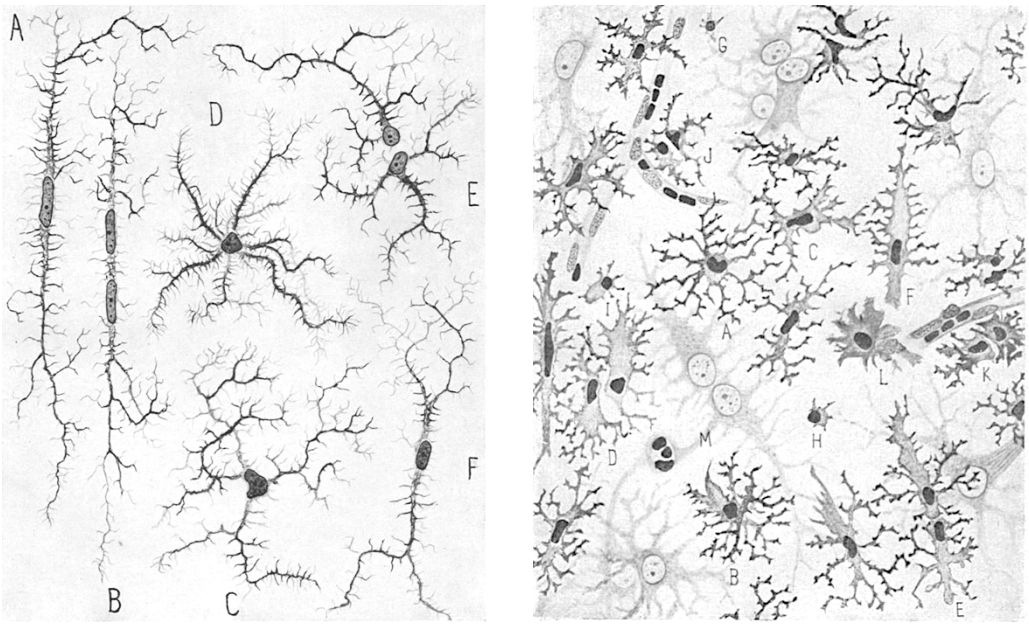

Figure 2.1 Pío del Río-Hortega's drawings from his 1919 papers

Left panel - Main types of normal human microglia: A, bipolar, rod-shaped cell; B, elongated cell with two nuclei; C, multipolar cell with branched expansions; D, multipolar cell with spiny appendages; E, isogenic couple ["dividing microglia"]; F bipolar corpuscle with forked appendages. Right panel - Microglial features in the rabbit stratum radiatum, close to the site of an injury produced two days before. (Note the morphological change that precedes the formation of the granuloadipose bodies). A, cell with the body slightly thickened. B, C, D, cells at different stages of thickening. E, F, elongated shapes. G, H, I, lymphocyte-like corpuscles with poorly developed processes. J, two small elements with thorny processes. K, L, cells with tuberous excrescences. M, protoplasmic neuroglia ["astrocytes"] showing hypertrophy and hyperplasia. Translation from Sierra *et al*., 2016.

2.1. The immune cells of the brain

Microglia are now known as the resident macrophages of the brain. As immune cells, their primary functions are thus to surveil the surrounding tissue, participate in the innate immune response and maintain brain homeostasis.

2.1.1. Microglial tiling and active surveillance of the brain parenchyma

Microglia are the brain immune sentinels: to efficiently surveil the parenchyma, they distribute homogeneously and monitor their own non-overlapping territories. While microglial densities and consequent territory size can vary from a region to the other, their distribution is carefully maintained (Askew *et al.*, 2017; Biase *et al.*, 2018). To maintain a stable density, one dying microglia will induce proliferation in some of its neighboring cells. Most of newly-generated cells rapidly undergo apoptosis, while one remains (Askew *et al.*, 2017). Thus, microglia self-renew following a stochastic process under steady-state conditions: every microglia is capable to proliferate, rather than having dedicated "progenitor-like" microglia (Lawson, Perry and Gordon, 1992; Ajami *et al.*, 2007; Askew *et al.*, 2017; Tay *et al.*, 2017). Turnover of microglia has been estimated through various techniques (Askew *et al.*, 2017; Füger *et al.*, 2017; Réu *et al.*, 2017; Tay *et al.*, 2017). It was proposed to be of several months, but appeared different across regions, with cortical microglia suggested to be long-lived (Tay *et al.*, 2017). In humans, taking advantage of changes in the atmospheric ^{14}C, microglia were estimated to be 4.2 years old on average, 28% of them renewing per year (Réu *et al.*, 2017). By long-term live-imaging through a cranial window, microglial average lifetime was estimated to be of 29 months in young mice (Füger *et al.*, 2017). On the other hand, microglia were shone to clonally expand in disease (Tay *et al.*, 2017), accompanied by global changes in density and morphology (Tan, Yuan and Tian, 2020).

As sketched by Pío del Río-Hortega, adult microglia have a ramified morphology, with a small cell body and several branched processes covering the neighboring parenchyma. Interestingly, this characteristic morphology is found across evolutionary distant species, from leech to human microglia, with varying degree of complexity (Geirsdottir *et al.*, 2019). It was long thought that these microglia were "resting" and waiting for signals in their microenvironment to adopt the ameboid morphology seen in various disease states. Instead, the use of *in vivo* two-photon live imaging on thinned skull, combined with the then new

Cx3cr1$^{GFP/+}$ mouse line allowing to fluorescently label microglia (Jung *et al.*, 2000), revolutionized our vision of microglia: microglial processes were observed rapidly extending and retracting (**Figure 2.2**)(Davalos *et al.*, 2005; Nimmerjahn, Kirchhoff and Helmchen, 2005). In this light, microglia are now understood as "surveilling" their environment, with their processes scanning the cell's territory. Microglial toolkit to perform this function is called the "sensome": it is a set of receptors allowing them to sense any changes in their environment, from chemokines, cytokines, purinergic signaling to inorganic substances, changes in pH or amino acid concentrations (Hickman *et al.*, 2013).

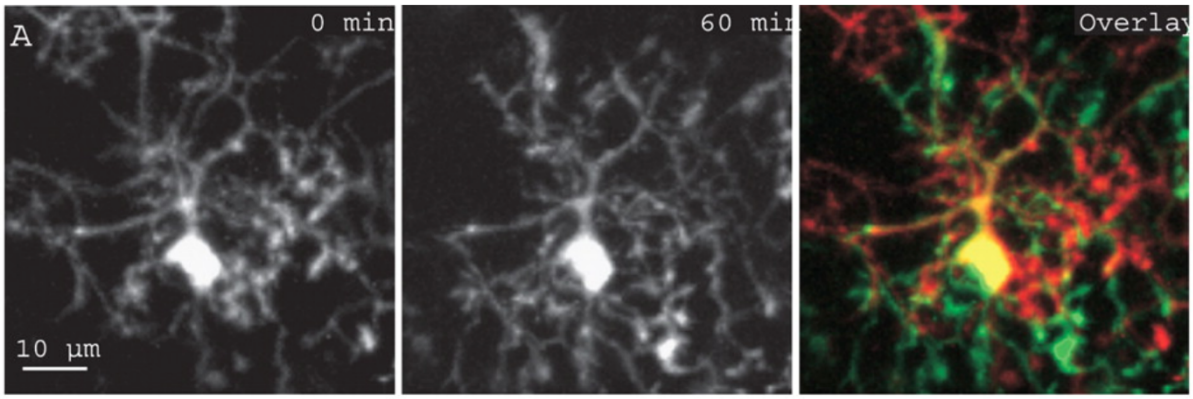

Figure 2.2 Microglial cells are highly dynamic in the resting state *in vivo*

Maximum-intensity projections of an individual microglial cell (45 to 75 µm below the pia) at the beginning (left) and 1 hour after (center) the start of a transcranial time-lapse recording. (Right) Overlay showing extensive formation (green) and deletion (red) of microglial processes. From Nimmerjahn *et al*., 2005.

2.1.2. Inflammation & phagocytosis

Not only do microglia sense their environment, but they also respond to it. In particular, like all macrophages, they constitute the first line of defense in the brain parenchyma and are mediators of inflammation. They detect pathogens through Toll-Like Receptors (TLR) that recognize Pathogen-Associated Molecular Patterns (PAMPs) present on the surface of some bacteria, viruses and fungi. They also identify apoptotic cells via the presentation of phosphatidylserine on the cell surface, and respond to molecules of the complement system.

In response to threats including injury, cell damage, ischemia, inflammation or infection, microglia can release pro-inflammatory cytokines and Reactive Oxygen Species (ROS), thus amplifying the inflammatory response, recruiting other immune cells on the site of

injury or promoting neuronal cell death (Smith *et al.*, 2012). Microglia can also migrate to the site of injury and rapidly send their processes to form a physical barrier, isolating the parenchyma from the detrimental compounds induced. This is mediated by the purinergic receptor P2RY12 that senses intracellular Adenosine Triphosphate (ATP) released upon injury and acts as a powerful "find me" signal (Davalos *et al.*, 2005; Haynes *et al.*, 2006). In addition, microglia can phagocytose pathogens like bacteria or viruses found in the brain parenchyma, as well as cell debris and dying cells. Indeed, phagocytosis is also a key component of brain homeostasis: rapid engulfment and digestion of dying or damaged cells prevents the release of toxic components and self-antigens that would be harmful to the tissue. This is mediated by

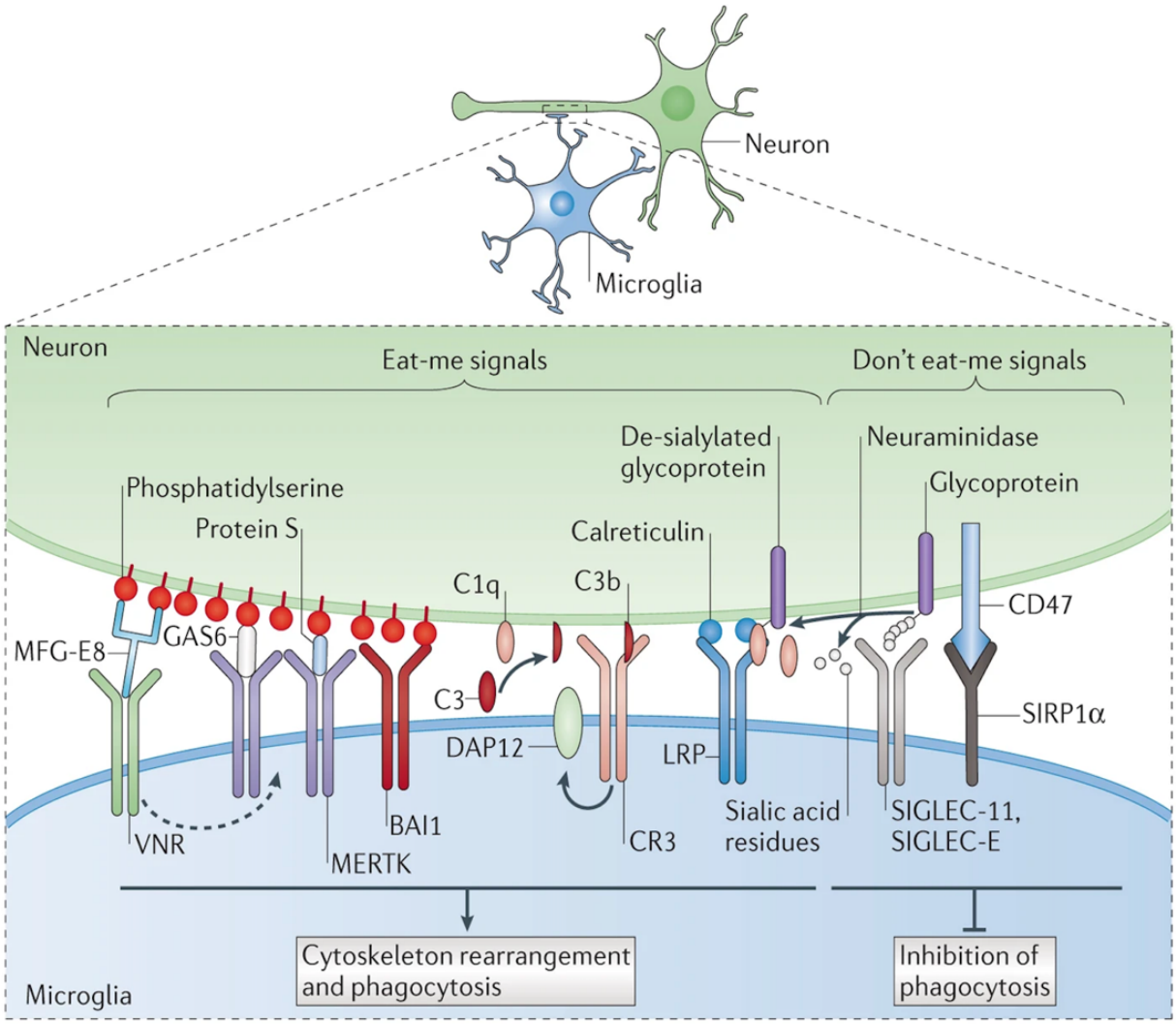

Figure 2.3 Different "eat me" and "don't eat me" signals in neurons recognized by microglia

"Eat-me" signals, like phosphatidylserine exposed on the membrane of dying neurons, are recognized by microglia and induce phagocytosis. Others, the "don't eat me" signals, prevent from excess phagocytosis, like CD47. From Brown & Neher, 2014.

microglial recognition of specific “eat me” and “don’t eat me” signals on brain cells (**Figure 2.3**)(Brown and Neher, 2014).

2.1.3. Other macrophages of the CNS

Though microglia are the only immune cells to be found in the brain parenchyma in physiological conditions, other macrophages inhabit the CNS. Called Border Associated Macrophages (BAMs) or CNS-associated macrophages, they can be found at the interface between the brain and the periphery: in the perivascular space, meninges and choroid plexus (**Figure 2.4**)(Goldmann *et al.*, 2016; Mildenberger, Stifter and Greter, 2022). Their position is highly strategic as the brain parenchyma is a protected environment known as “immune-privileged” (Shechter, London and Schwartz, 2013; Engelhardt, Vajkoczy and Weller, 2017): the Blood Brain Barrier (BBB), blood-CSF barrier and meningeal barrier preferentially isolate the brain from the circulation, cautiously filtering what can enter the brain. In particular, in the healthy brain, circulating immune cells are prevented from reaching the parenchyma (Ajami *et al.*, 2007; Mildner *et al.*, 2007; Bruttger *et al.*, 2015; Askew *et al.*, 2017).

Though still understudied, recent studies are shedding new light on their great heterogeneity (Kierdorf *et al.*, 2019; Van Hove *et al.*, 2019) and new specific tools should help investigate their respective roles. In particular, many tools to target microglia also target BAMs, to an extent that what has been described as microglial functions could also be attributed in part to BAMs (see Review).

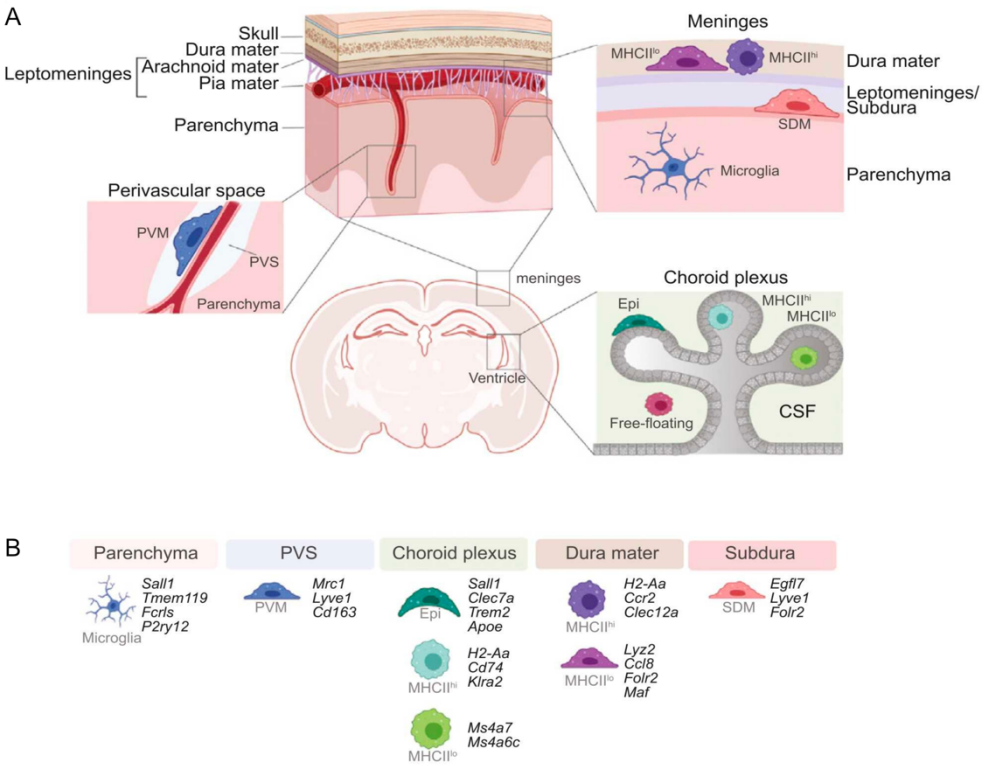

Figure 2.4 Microglia and BAMs localization at the CNS interfaces

(A) Non-parenchymal macrophages reside in different compartments of the brain, including perivascular spaces, the choroid plexus in the ventricles, and the meninges. The latter is composed of the dura mater and leptomeninges/subdural meninges, which consist of the arachnoid mater and pia mater. Several subsets of non-parenchymal macrophages exist, including PVMs in perivascular spaces, MHCII^{hi} and MHCII^{lo} macrophages in the dura mater and the choroid plexus epiplexus macrophages located on the choroid plexus epithelium, and subdural macrophages. (B) Signature genes identified for the different CNS macrophage populations. PVM: perivascular macrophage, SDM: subdural macrophage, Epi: epiplexus macrophage, PVS: perivascular space. Adapted from Mildenberger *et al*., 2022.

2.2. Both immune and glial cells

Microglia lie at the crossroad between immune and glial cells: as resident macrophages, microglia perform a panel of canonical immune functions, but the past few decades have also revealed their importance as glial cells, participating in key processes of brain development and functioning. We here focus on their non-immune functions in the healthy adult brain.

2.2.1. Neuronal roles of microglia

Microglia play important roles in monitoring and tuning neuronal activity which they finely sense. They express a wide array of receptors for neurotransmitters and purines, allowing them to directly sense synaptic communication (Hickman *et al.*, 2013; Butovsky *et al.*, 2014; Zhang *et al.*, 2014; York, Bernier and MacVicar, 2018). More interestingly, they are in turn capable of tuning neuronal activity via the secretion of factors such as Brain-Derived Neurotrophic Factor (BDNF)(Coull *et al.*, 2005; Parkhurst *et al.*, 2013), Interleukin (IL)-10 (Lim *et al.*, 2013; Pereira *et al.*, 2015), IL-1ß (Huang *et al.*, 2011; Hewett, Jackman and Claycomb, 2012) or Tumor Necrosis Factor Alpha (TNF-α)(Beattie *et al.*, 2002; Olmos and Lladó, 2014). They have also been shown recently to down-tone locally neuronal excitability (Badimon *et al.*, 2020): their processes are attracted in an activity-dependent manner at the synapse, by neuronal and astrocytic ATP released when the synapse is active (Akiyoshi *et al.*, 2018; Umpierre *et al.*, 2020). It is recognized through the microglial P2Y12 receptor and converted in adenosine monophosphate and then adenosine, which acts back on neuronal adenosine receptors leading to a decrease in excitability. This elegant negative feedback mechanism protects the brain from excessive activation, and in particular reduces seizure risk.

Microglial processes additionally engage in physical contacts with neurons (**Figure 2.5**). They contact synapses (Miyamoto *et al.*, 2016; Weinhard *et al.*, 2018), preferentially interacting with active ones (Wake *et al.*, 2009; Tremblay, Lowery and Majewska, 2010), both glutamatergic and GABA-ergic (Cserép *et al.*, 2020). In particular, microglial contacts with spines are regulated by spontaneous and evoked activity, and is impacted by the sleep-wake cycles (Hristovska *et al.*, 2022). While it could be useful to provide negative feedback at the synapse (Badimon *et al.*, 2020), the functions of these contacts are not fully understood in the healthy adult brain. On the other hand, they participate in microglial synapse elimination in development and disease (see 3.4.2 and 2.4)(Stephan, Barres and Stevens, 2012; Schafer and

Stevens, 2015). In addition, microglia had been shown to contact neuronal soma (Tremblay, Lowery and Majewska, 2010; Szalay *et al.*, 2016). In 2020, an elegant study by Cserép *et al.* detailed the molecular structure of the somatic purinergic junctions between microglial processes and neurons (Cserép *et al.*, 2020). They highlighted how microglial clusters of P2Y12 receptors align at the zone of contact, while diverse cellular nanostructures are recruited on the neuronal side, including increased density of mitochondria, vesicle-like structures and endoplasmic reticulum-plasma membrane contacts. This suggests dynamic intercellular communication and possible mitochondrial signaling. While it appears to be neuroprotective in case of acute brain injury by limiting neuronal hyperexcitability, the function of this novel microglia-neuron communication is not fully understood so far.

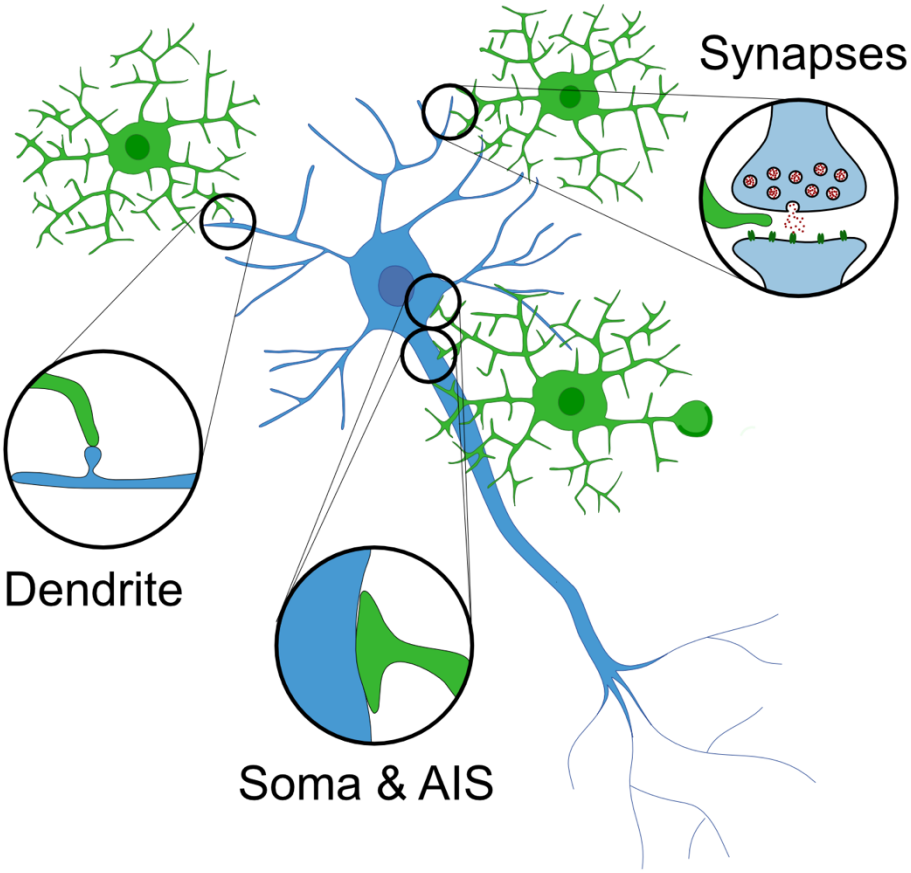

Figure 2.5 Types of Direct Microglia-Neuron Contacts Based on Neuronal Compartments

Microglia (in green) contact neurons (blue) along different compartment: their process can reach the synaptic cleft, and further modulate neuronal activity; interact with dendrites and participate in synapse formation or elimination as well as arborization; engage in physical contact on the neuron soma or AIS. AIS, Axon Intital Segment.

Last, microglia have been shown to contact myelinated neurons at the nodes of Ranvier in an activity dependent manner (Ronzano *et al.*, 2021). While this promotes remyelination in injury, whether microglia could modulate the structure and electrophysiological properties of these strategic zones in homeostasis remains to be investigated.

2.2.2. Microglia engage in brain homeostasis

Microglia don't only interact with neurons in the regulation of neuronal activity, but instead engage with most brain cells. As they interact with blood vessels, microglia have been associated to the neurovascular unit, along with endothelial cells, pericytes, smooth muscle cells and astrocytes. Though their roles were not fully understood in the healthy adult brain, microglia were shown to regulate diverse mechanisms in inflammation and disease, including the disruption of the BBB through release of pro-inflammatory cytokines that allows leukocyte extravasation (Dudvarski Stankovic *et al.*, 2016). Interestingly, microglia have very recently been shown to participate in the fine tuning of the cerebral blood flow, directly and simultaneously contacting neurons, pericytes and blood vessels (Császár *et al.*, 2022). In particular, they participate in neurovascular coupling through a P2Y12 receptor-mediated action (Császár *et al.*, 2022).

Microglia have additionally been shown to participate in adult neurogenesis in the hippocampus by promoting survival of newborn neuroblasts (Kreisel *et al.*, 2019). On the other end, they phagocyte apoptotic newborn cells (Sierra *et al.*, 2010). More precisely, microglia increase the number of newborn neurons in the DG in an experience-dependent manner (Nguyen *et al.*, 2020). The latter also illustrates how microglia remodel the Extra-Cellular Matrix (ECM) following neuronal production of IL-33. Engulfment of the ECM by microglia promotes synaptic plasticity and is needed for precise consolidation of long-term memory (Nguyen *et al.*, 2020).

2.2.3. Microglia: at the interface between brain and body

As professional sensors of their surroundings, microglia also constitute an interface between the brain and its hosting body. Microglia are shaped by their microenvironment as well as circulating signals, originating from different parts of the body and modulated by the external environment.

2.2.3.1. Microglia and environmental factors

Far from being isolated, the brain is connected to the body in many ways. As a consequence, microglia, its sensors, are impacted by a large panel of environmental factors, particularly during embryonic and early post-natal development (Hanamsagar and Bilbo, 2018; Catale *et al.*, 2020): pollution (Bolton *et al.*, 2017), maternal and early-life stress (Calcia *et al.*, 2016; Delpech *et al.*, 2016), nutrition (Leyrolle, Layé and Nadjar, 2019), sleep deprivation (Zhao *et al.*, 2014), alcohol exposure (Ruggiero *et al.*, 2018) or chemotherapy agents (Gibson *et al.*, 2018). Indeed, as will be developed in 3.4, microglia are emerging as key players of brain development, taking part in many different processes occurring during this critical period. Resultant effects of environmental perturbations are thus very dependent on their timing of occurrence and of the models used. For Maternal Immune Activation (MIA) for example, several models exist in mice, with injections of Lipopolysaccharide (LPS) or Poly(I:C) to mimic respectively bacterial or viral infections, and their effects have been shown to be modulated by various elements including timing and doses of injection, as well as the housing system or the genetic background (Mueller *et al.*, 2018). Nevertheless, they can durably alter brain function, mimicking some traits of neurodevelopmental disorders found in humans including deficits in cognitive performance, memory or processing of social stimuli (Catale *et al.*, 2020), for which environmental challenges are known risk factors (see 3.4.2).

2.2.3.2. Mediators of the gut-brain axis

The brain also responds to body signals. In particular, recent works characterized the extensive communication between the gut and the CNS (Haq *et al.*, 2018). Indeed, the gut microbiota, consisting of billions of microorganisms, and in particular of a great variety of bacteria, has been shown to regulate many aspects of brain functioning, from neurotransmitter signaling and myelination to neurogenesis (Haq *et al.*, 2018). Communication can occur through direct neuronal signaling through the vagus nerve, or via metabolites derived from gut bacteria, that join the circulation. Microglia is pointed out as one of the mediators of gut-brain communication (**Figure 2.6**). Indeed, they are shaped by the microbiota, which presence and

diversity are essential for their maturation (Matcovitch-Natan *et al.*, 2016). Microglia in embryos from Germ Free mice exhibit different densities and morphology through the brain, both at E18.5 (Thion *et al.*, 2018) and at birth (Castillo-Ruiz *et al.*, 2018), and were also impaired in the adult (Erny *et al.*, 2015; Thion *et al.*, 2018). Interestingly, these effects were sex-dependent (Thion *et al.*, 2018).

Importantly, evidence for a link between diet and brain function has been described for some years, in particular highlighting the negative consequences of a diet rich in unsaturated fats and refined carbohydrates, as seen more and more in the Western world (Francis and Stevenson, 2013). Microglia were shown *in vitro* to be sensitive to palmitic acid, a free fatty acid enriched in the serum in case of obesity, impairing microglial phagocytosis, motility and inducing an inflammatory profile (Yanguas-Casás *et al.*, 2018). Microglia were recently found *in vivo* to be directly affected by a maternal high-fat diet during pregnancy (Bordeleau *et al.*, 2022), and to be mediators of some of its effects in the mouse developing brain (Madore *et al.*, 2020). This field is now extensively growing and should bring new information on diet-induced alterations of microglia.

2.2.3.3. Microglia and sexualization of the brain

Microglia are important actors of brain sexualization (Lenz and McCarthy, 2017; Guneykaya *et al.*, 2018). Influenced both by their imprinting and by circulating hormones, microglia have been shown to colonize differently the developing male and female brains in rats, across different regions (hippocampus, parietal cortex, amygdala (Schwarz et al., 2012); preoptic area (Lenz *et al.*, 2013)). Microglia in male POA have larger cell bodies and shorter processes (Lenz *et al.*, 2013). In the neonate, microglial phagocytosis in the hippocampus is more active in the female brain (Nelson, Warden and Lenz, 2017), while it is the contrary in the amygdala (VanRyzin *et al.*, 2019). Sex differences in microglia were further investigated, from transcriptome to function (Guneykaya *et al.*, 2018), and found also in humans (Hanamsagar *et al.*, 2017). More importantly, while some microglial sexual dimorphism is possibly linked to sex chromosomes, it was shown to be in part mediated by sex hormones as injections of estradiol, the aromatized form of testosterone, at P0 and P1 in female pups led to masculinization of the POA with more ameboid microglia (Lenz *et al.*, 2013; Nelson, Warden and Lenz, 2017). Microglial dopamine receptors were also shown to impact sexualization of the brain and consequent differential behavior in adolescent rats (Kopec *et al.*, 2018). In the developing amygdala, testosterone impacts microglial phagocytic activity, shaping juvenile social play in rats (VanRyzin *et al.*, 2019). Interestingly, in the adult, microglia were shown to

be more inflammatory in male. When transplanted in depleted male brains, microglia isolated from females retained their “feminized” profile and still displayed a neuroprotective effect (Villa *et al.*, 2018).

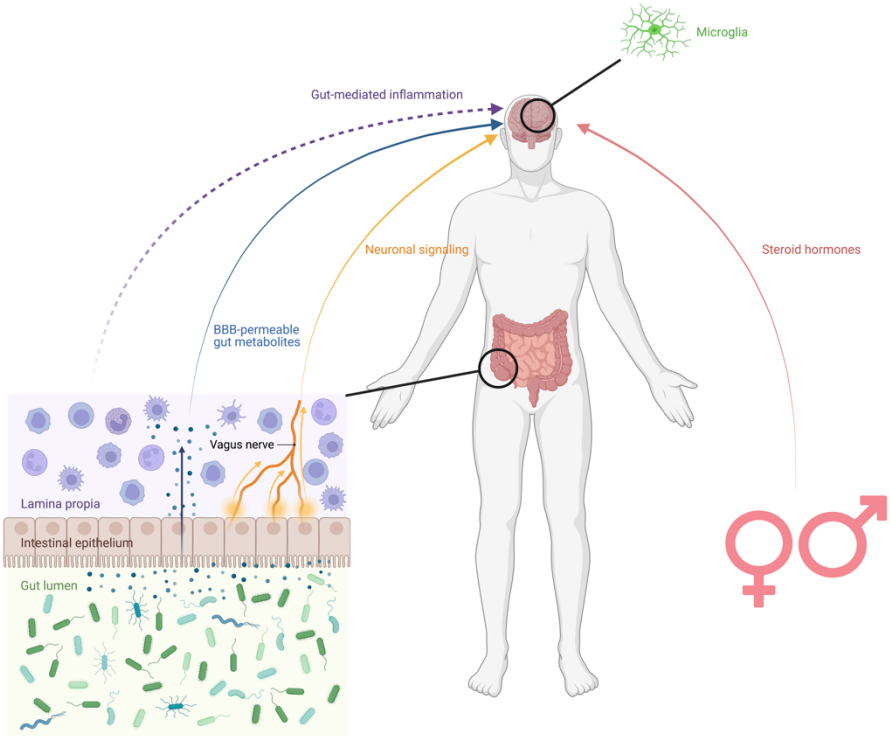

Figure 2.6 Microglia, mediators of brain sexualization and of the gut-brain axis

Steroid hormones can cross the BBB and directly impact on microglial maturation and functions. On the other hand, the gut-brain axis establishes a complex communication through which gut microbiota influences brain physiology and behavior, as well as microglial maturation and functions, either through direct neuronal signaling to the brain via the vagus nerve, through BBB-permeable gut-derived metabolites, or through peripheral gut-mediated inflammation. Created in biorender.com

2.3. Microglia in disease and neurodegeneration

Very early on, microglia drew attention in the context of pathology, in which they can dramatically change morphology and numbers. Whether they are a causal factor or only react to changes in their environment, microglia participate in almost all neurological pathologies.

2.3.1. Inflammation and 'reactive' microglia

Indeed, microglia respond to inflammation, which is part of most neurological diseases. Microglia adopt a different morphology in pathology, with less ramified processes and a larger cell body, and increase their density (microgliosis). Because they were found to express either pro-inflammatory or anti-inflammatory cytokines, they were classified, similarly to macrophages, as in M1 or M2 states respectively, the latter being recognized as neuroprotective and promoting tissue repair. This overly simplified nomenclature is nevertheless not reflecting the more subtle and numerous hues of microglia in disease (Paolicelli *et al.*, 2022). Indeed, more integrated studies and the use of new techniques including scRNA-seq and ATAC-seq showed the large diversity of profiles (or states) and functions of microglia in disease.

In this context, microglia appear protective or detrimental in different pathological contexts. For example, they have been studied a lot in Alzheimer's Disease (AD), as variants in *TREM2*, predominantly expressed in microglia in the brain, have been identified as risk factors for this disease. The different conclusions about the roles of microglia likely depend on the stage of the disease or of differences between models (Chen and Holtzman, 2022). More precisely, AD starts with amyloid-ß depositions in specific regions of the brain. These accumulate to form plaques and lead to a Tau pathology and neurodegeneration. In this context, depletion of microglia, which is later followed by microglial repopulation, has been shown to be detrimental, suggesting a protective role: microglia maintain plaque compacity, reduce neurotoxicity and progression of neurodegeneration (Condello *et al.*, 2015; Keren-Shaul *et al.*, 2017; Casali *et al.*, 2020). On the other hand, microglial depletion can also reduce amyloid deposition and rescue some cognitive functions, in particular with improved memory (Olmos-Alonso *et al.*, 2016; Sosna *et al.*, 2018; Son *et al.*, 2020), suggesting a detrimental role of microglia, collectively putting the manipulation of microglia as a therapeutic hope for the treatment of AD.

2.3.2. Disease-Associated Microglia

In particular, one substate of microglia has been described in the context of AD, called Disease-Associated Microglia (DAM) (Keren-Shaul *et al.*, 2017; Krasemann *et al.*, 2017). Using the 5XFAD mouse model that bears 5 mutations associated to familial forms of the disease in humans, they performed massively parallel scRNA-seq (MARS-seq) on all myeloid cells in control or 5XFAD brains and identified two small microglial clusters present only in AD. Microglia from these clusters were enriched in genes associated to metabolism and phagocytosis such as *Apoe* (Apolipoprotein E), *Lpl* (Lipoprotein lipase) and *Cst7* (Cystatin 7), as well as other markers including *Itgax* (CD11c), *Clec7a* and *CD63*; while they downregulate homeostatic microglial genes such as *P2ry12*, *Cx3cr1* and *Tmem119*. Importantly, one cluster (named DAM 1) appears as a transitory state towards the second one (DAM 2), and transition from DAM 1 to DAM 2 is TREM2-dependent (**Figure 2.7**). More precisely, TREM2 is an immunomodulatory receptor, which interacts with DAP12, its co-receptor, and broadly regulates microglial activation (Kober and Brett, 2017). DAM are phagocytic and found in proximity to Aß plaques. They display the same phenotype and specific markers (*APOE*, *AXL*, *TREM2*) in AD post-mortem human tissues (Keren-Shaul *et al.*, 2017; Krasemann *et al.*, 2017). Importantly, microglia with DAM characteristics were also identified in other models of AD (Holtman *et al.*, 2015; Kamphuis *et al.*, 2016; Krasemann *et al.*, 2017; Ajami *et al.*, 2018; Mrdjen *et al.*, 2018), other neurodegenerative diseases (Deczkowska *et al.*, 2018), like Amyotrophic Lateral Sclerosis (ALS) (Keren-Shaul *et al.*, 2017), Multiple Sclerosis (MS) (Krasemann *et al.*, 2017), and in aging (Holtman *et al.*, 2015; Keren-Shaul *et al.*, 2017; Mrdjen *et al.*, 2018).

Recently, Silvin and colleagues showed that two profiles commonly attributed to DAM actually coexist, with one resembling a subtype of developing microglia (see 3.3) and a second one, which they call Disease Inflammatory Macrophages (DIM), marked by a higher inflammatory profile, that are TREM2-independent and monocyte-derived, and accumulate in the brain in aging and neurodegeneration (Silvin *et al.*, 2022). Such dichotomy was also suggested by previous work, which performed scRNA-seq in AD murine models along disease progression, and highlighted the presence of activated response microglia (ARM) resembling canonical DAM, and interferon response microglia (IRM) enriched in genes involved in the innate immune response and interferon pathways (Frigerio *et al.*, 2019).

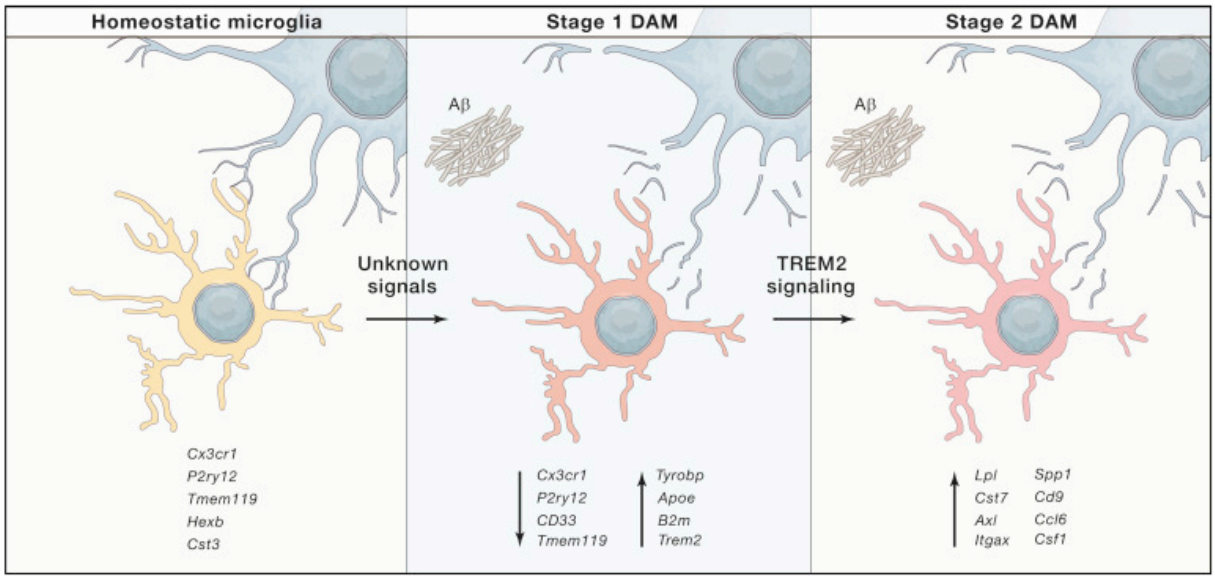

Figure 2.7 A two-step model of DAM induction

Unknown signals promote transition from homeostatic to stage 1 DAM, while TREM2 signaling is required for stage 2 induction. Each stage is characterized by a unique transcriptional signature. From Deczkowska *et al*., 2018.

2.3.3. Microglia in human pathology and its experimental models

Thanks to advances in technologies, Genome Wide Association Studies (GWAS) became more common, aiming at associating genetic variants to specific traits or disease in humans. Surprisingly, while investigating neurodegenerative disease, several mutations were pointing towards genes specific to microglia in the CNS such as *APOE* and *TREM2* which mutations are risk factors for AD (Nott *et al.*, 2019; Sierksma *et al.*, 2020). Microglia thus went under the spotlight in the context of neurodegeneration and several mouse models were developed like 5XFAD and APP/PS1 for AD; Tau 301L and Tau P301S for tauopathies; and others for ALS, MS or simply aged mice. In both humans and mice models of neurodegeneration, DAM are found in the same location, with a similar phagocytic morphology and displaying specific DAM markers. Nevertheless, mice models to study neurodegeneration are genetically induced. For AD for example, the 5XFAD mice develop an exacerbated version of the disease that does not parallel the sequential onset of the disease in humans (Edler, Mhatre-Winters and Richardson, 2021). In addition, sequencing studies were still limited on human tissue, but their use is now opening exponential research in the field. AD-related subtypes of microglia were highlighted in humans, but revealed to be more heterogeneous and quite diverse compared to their mouse counterparts (Del-Aguila *et al.*, 2019; Mathys *et al.*, 2019; Olah *et al.*, 2020; Srinivasan *et al.*, 2020; Chen and Colonna, 2021). Importantly, the scarcity of human

tissue and inherent choice of donors, as well as their quality, could explain to some extent exacerbated diversity of human microglial clusters. Though investigating with different experimental methods, Alsema and colleagues were not able to extract AD specific features of microglia when comparing control to AD patients in both bulk RNA sequencing and scRNA-seq (Alsema *et al.*, 2020). On the other hand, Srinivasan and colleagues identified a Human Alzheimer's Microglia (HAM) signature. HAM upregulate *APOE* and *SPP1* but their transcriptional signature is overall different from mouse DAM, and is enriched in human aging-associated genes (Srinivasan *et al.*, 2020). Nevertheless, microglial response to AD pathology also appears dependent on *TREM2* in humans (Krasemann *et al.*, 2017; Nguyen *et al.*, 2020). On the same note, differentially expressed genes in aging show little overlap between mice and humans, even though their homeostatic signatures are comparable (Dubbelaar *et al.*, 2018), raising the question of the difference of microglial response in neurodegeneration and aging between mice and humans, and the limitations inherent to our mice models.

3. Development of microglia: an atypical and heterogeneous population

3.1. Origin and maturation

Pío del Río-Hortega had already hypothesized the mesodermal origin of microglia in his 1919 papers (Sierra *et al.*, 2016). At the time, his assumption was principally based on the difference in staining of microglia compared to astrocytes and oligodendrocytes; and to their similarity in morphology and function with resident macrophages: they are morphologically shaped by their surrounding environment and are capable of migrating and phagocyting in case of pathology. Nevertheless, the debate of microglial origin remained highly controversial for decades, something that can be explained by the peculiar origin of these cells, and the complexity of fetal hematopoiesis.

3.1.1. Hematopoietic waves

The establishment of the Hematopoietic Stem Cells (HSCs) in the Bone Marrow (BM) where they will give rise to all myeloid cells, including monocytes, macrophages and lymphocytes, only occurs during late gestation (Ginhoux and Prinz, 2015). In rodents, this is preceded by three waves of hematopoiesis. The first wave, called “primitive hematopoiesis”, starts in the extra-embryonic yolk sac (YS) and gives rise to primitive c-kit+ erythromyeloid progenitors (EMPs) around E7.5. They differentiate into YS-derived resident macrophages that colonize the whole embryo (Gomez Perdiguero *et al.*, 2015; Hoeffel and Ginhoux, 2015). These macrophages depend on Colony Stimulating Factor 1 (CSF-1) receptor signaling (Ginhoux *et al.*, 2010; Erblich *et al.*, 2011), and on the transcription factors Pu.1 (or Sfpi) and Irf8, but not on c-Myb (Kierdorf *et al.*, 2013). Importantly, the first wave is also responsible for the production of the first red blood cells that bring oxygen to the growing embryo. The second wave of hematopoiesis generates late EMPs starting at E8.25, that express c-Myb. They migrate to the fetal liver (FL) and proliferate, and depending on the region, can contribute to macrophage resident populations in the adult (Gomez Perdiguero *et al.*, 2015). Around E9.5, the third wave generates fetal HSCs from the Aorto-Gonad-Mesonephros (AGM) which migrate to the fetal liver where they proliferate. They give rise to FL monocytes which colonize the embryo, replacing to some extent the YS-derived macrophages (Hoeffel and Ginhoux,

2015), and further participate in definitive hematopoiesis (Kumaravelu *et al.*, 2002; Kieusseian *et al.*, 2012) (**Figure 3.2**). HSCs later colonize other hematopoietic organs, including the bone marrow around E15, which will be the main site of hematopoiesis starting at E17 (Perdiguero and Geissmann, 2016).

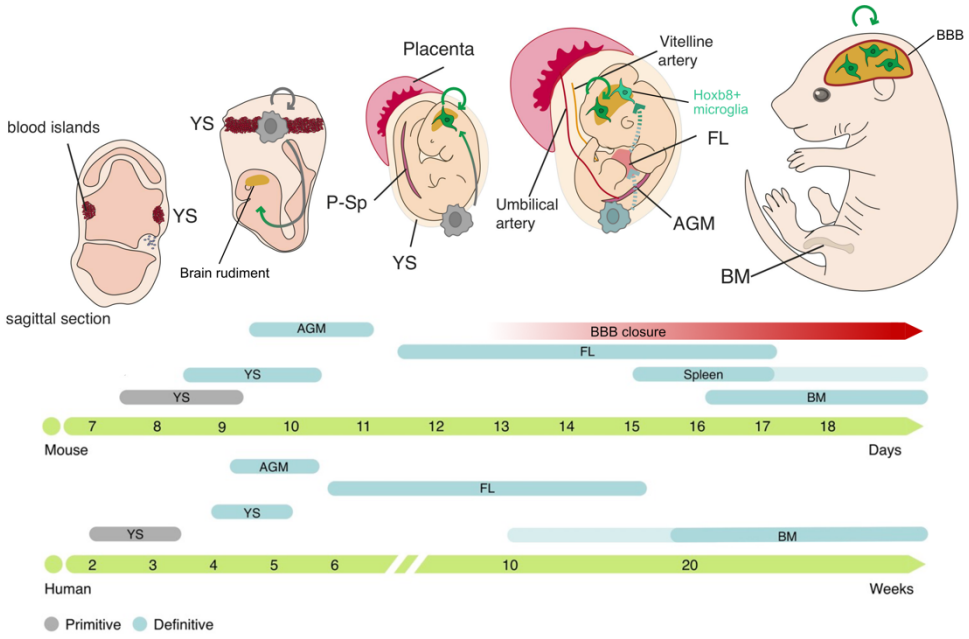

Figure 3.1 Ontogeny of microglia and timeline of hematopoiesis in mice and humans

Embryonic hematopoiesis is established in three distinct waves. In the first wave, primitive EMPs are generated in the blood islands of the YS, migrate through the embryo and enter in the brain, giving rise to microglia. During the second wave, definitive EMPs migrate to the fetal liver (FL) where they proliferate and give rise to most tissue macrophages. It is proposed that some migrate from the FL to the brain and give rise to a Hoxb8+ microglial population. After the closure of the BBB, microglia proliferate *in situ* and self-renew throughout life. Around E9.5,-E11 (GW4), HSCs emerge in the AGM region and migrate to the FL where they expand and differentiate into all mature blood cells lineage. They later migrate to the BM which becomes the major hematopoietic organ. YS, yolk sac; P-Sp para-aortic splanchnopleura; FL, fetal liver; AGM, aorta-gonads-mesonephros; BM, bone marrow; BBB, blood-brain-barrier. Adapted fom Soares-Da-Silva et al., 2020.

Because microglia can be observed in the brain parenchyma as early as E8 (Alliot, Godin and Pessac, 1999), it was hypothesized that microglia derive from primitive EMPs of the first hematopoietic wave. This was further confirmed through different fate-mapping studies (Ginhoux *et al.*, 2010; Kierdorf *et al.*, 2013). In particular, Ginhoux *et al.* used a *Runx1*^{CreER} mouse line combined with a fluorescent reporter. While Runx1 is expressed in both progenitors in the YS and FL, precise temporal tagging through injection of 4-hydroxytamoxifen allowed to label mainly YS progenitors (injection at E7.5) or FL progenitors (injection at E8.5).

Microglia were greatly labelled with E7.5 injections, while almost not at E8.0, highligting their YS origin. Their profound difference from HSC-derived macrophages was again shown by their c-Myb independence, microglia being present in *Myb*$^{-/-}$ mice which totally lack HSCs (Schulz *et al.*, 2012). It has been hypothesized that HSC-derived monocytes from the FL are prevented from replacing microglia by the closure of the BBB, occuring around E13.5 and isolating the brain from circulating cells. From the timing of fematopoietic events (**Figure 3.2**) as well as new single-cell analysis, this trajectory could be quite similar in humans (Bian *et al.*, 2020).

Though disputed, mystery remains about a possible second wave of microglia, that would derive from Hoxb8+ progenitors of the second wave of hematopoiesis: with a YS origin but that transiently settle and expand in the FL and AGM (**Figure 3.2**)(De *et al.*, 2018). This peculiar journey could provide them with specific features, and Hoxb8+ microglia were fisrt identified as involved in the control of compulsive behavior in mice (Chen *et al.*, 2010) – while they are molecularly similar to Hoxb8- microglia and participate in the same way to synaptic pruning or in response to brain injury.

Last, two fate-mapping studies found a monocyte contribution to the early post-natal microglial population (Askew *et al.*, 2017; Chen *et al.*, 2020). Askew *et al.* used E14 *in utero* injections, in the fetal liver, of lentiviral vectors carrying a fluorescent reporter. Some monocyte-derived microglia-like cells were found in the brain parenchyma at P0 and P3, but their number decreased by P6, probably through apoptosis. Instead, Chen *et al*. used a fate-mapping system suggesting CCR2+ monocytes infiltrate the brain during early post-natal development and adopt a microgia-like phenotype, displaying a ramified morphology and expressing canonical microglial markers such as TMEM119 and P2RY12 (Chen *et al.*, 2020). These don't undergo cell death and can still be seen in the brain at P24, while it is unknown if they remain later on. This raises the interesting questions of the contribution of monocyte-derived microglia to the general microglial population; of how different they could be and could thus differentially contribute to inflammation through life.

3.1.2. Entry in the brain

Microglial precursors migrate from the YS to the embryonic brain coincidently with the remodeling of the embryonic vasculature, from a simple circulatory loop to a complex and three-dimensional organization (Walls *et al.*, 2008). Interestingly, in the *Ncx-1*$^{-/-}$ mouse model where heart beat is impaired and thus lacking a functional blood circulation, microglia were

absent from the brain of E9.5-E10 embryos while the numbers of YS macrophages were comparable (Ginhoux *et al.*, 2010). In addition, thanks to intravital microscopy, embryonic YS macrophages were observed migrating away from the YS via the blood circulation, in a restricted developmental window peaking at E10.5 (Stremmel *et al.*, 2018). Thus, evidence suggest microglial progenitors use the bloodstream to migrate through the embryo and reach the developing brain.

How they properly enter in the brain parenchyma is nonetheless still unclear. From static analysis on human and rodent embryonic tissues, microglia were thought to enter the cortex from the pia, the ventricular walls and the choroid plexus, where they mainly accumulate early on (Monier *et al.*, 2006, 2007; Verney *et al.*, 2010; Menassa and Gomez-Nicola, 2018). Historically, some hotspots of microglial accumulation in white matter, where they have an ameboid morphology, were described as "fountains of microglia" by Kershman in 1939, and were thought to fuel the parenchyma with microglia, though no evidence clearly support this observation. It was also hypothesized that microglia could excavate from blood vessels to colonize the parenchyma (Navascués *et al.*, 2000). New techniques, such as two-photon *ex utero* live-imaging should provide new insights into these mechanisms. For instance, a recent study suggests that BAMs can enter from the ventricles to the brain parenchyma, where they become microglia (**Figure 3.2**)(Hattori, Kato, *et al.*, 2022).

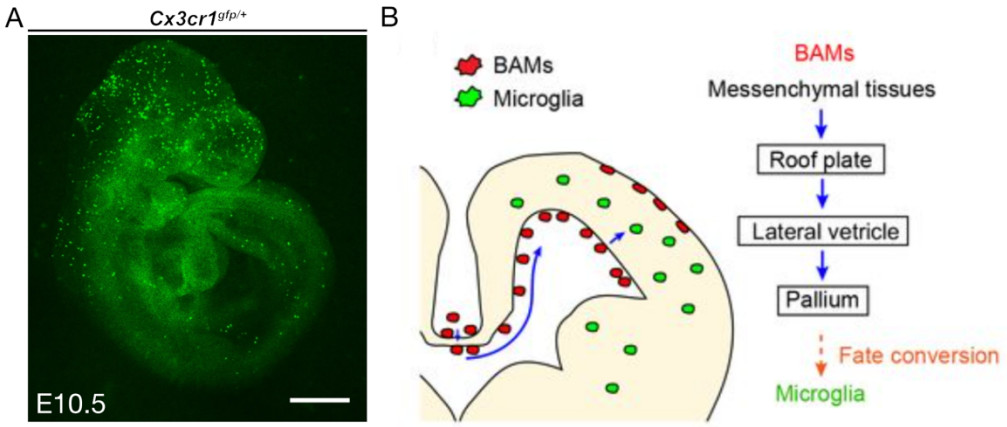

Figure 3.2 Exploring microglial progenitor journey using the *Cx3cr1*$^{gfp/+}$ mouse line
(A) Isolated E10.5 *Cx3cr1*$^{gfp/+}$ embryo. From Stremmel et al., 2018 (B) Model of BAMs infiltration. From Hattori, Kato *et al*., 2022.

Interestingly, while microglial entry in the brain seems comparable between mice and humans, it appears quite different in zebrafish. In this specie, microglial migration towards the brain was shown to be independent from blood circulation, and to be orchestrated by apoptotic cells (Xu *et al.*, 2016).

3.1.3. Microglia and BAMs, an intricate birth story

Our understanding of BAMs origin, diversity and functions has recently progressed, but still leaves open questions. In particular, their great heterogeneity has only recently been highlighted (Van Hove *et al.*, 2019). BAMs diverge in terms of location, ontogeny and transcriptional identities. They were long thought to derive from blood-monocytes, with a high turn-over. Instead, by combining parabiosis and fate-mapping analysis, recent work provided new insights into BAMs origin (Goldmann *et al.*, 2016; Van Hove *et al.*, 2019; Utz *et al.*, 2020; Cugurra *et al.*, 2021; Masuda *et al.*, 2022). BAMs of the subdural meninges have an embryonic origin and establish stable populations, while BAMs of the choroid plexus have a dual ontogeny, are short-lived and further replaced by BM-derived monocytes as well as BAMs of the dura mater (see a schematic representation in **Figure 3.3**) (Goldmann *et al.*, 2016; Van Hove *et al.*, 2019). More precisely, BAMs of the dura mater have recently been shown in mice to be replaced locally by monocytes of the skull bone marrow, with no contribution from circulating monocytes in the healthy brain (Cugurra *et al.*, 2021). On the other hand, BAMs of the perivascular space have been recently proposed to derive from meningeal BAMs postnatally (Masuda *et al.*, 2022).

Interestingly, BAMs of embryonic origin have been shown to originate from YS primitive EMPs as do microglia, though they already represent distinct populations as early as E10.5 in the YS (**Figure 3.3)**(Utz *et al.*, 2020). Both BAMs and microglia depend on IRF-8 (Van Hove *et al.*, 2019) and CSF-1 receptor signaling (Buttgereit *et al.*, 2016; Mrdjen *et al.*, 2018; Van Hove *et al.*, 2019). Nevertheless, in a new model presenting a mutated form of a conserved *Csf-1r* enhancer (Rojo *et al.*, 2019), some BAMs - mainly the epiplexus macrophages - were affected along microglia, while other BAMs were still present (Munro *et al.*, 2020). Emphasizing their early divergence, only microglial precursors depend on TGF-ß signaling (**Figure 3.3)**(Butovsky *et al.*, 2014; Buttgereit *et al.*, 2016; Utz *et al.*, 2020).

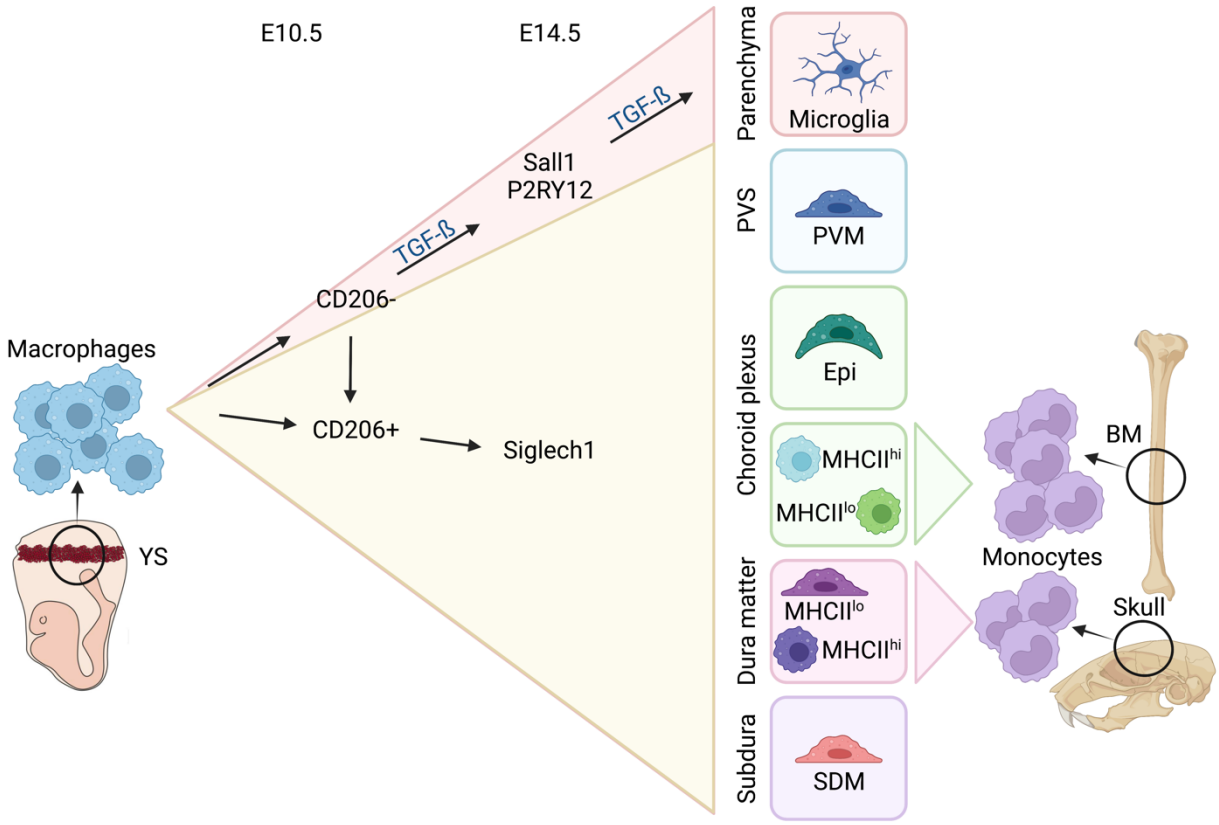

Figure 3.3 Origins of microglia and BAMs

BAMs and microglia share a close ontogeny. They all derive from primitive EMPs of the YS but segregate early in two distinct populations. Microglial maturation depends on TGF-ß signaling, while BAMs are TGF-ß independent. Some BAMs of the choroid plexus will progressively be replaced by BM-derived monocytes, while BAMs of the Dura matter are locally replaced by monocytes from the skull BM, without contribution from the circulation. YS: yolk-sac, PVS: perivascular space, PVM: perivascular macrophage, Epi: epiplexus macrophage, BM: bone marrow. Adapted from Mildenberger *et al.*, 2022. Created in Biorender.com

3.2. Microglial colonization of the forebrain

3.2.1. Proliferation and migration of microglia

3.2.1.1 Proliferation

Upon entry in the brain parenchyma, microglia were shown to be highly proliferative, which was observed by immunostaining (Alliot, Godin and Pessac, 1999; Dalmau *et al.*, 2003; Monier *et al.*, 2006, 2007; Swinnen *et al.*, 2013; Nikodemova *et al.*, 2015; Menassa *et al.*, 2021; Barry-Carroll *et al.*, 2023) and confirmed by scRNA-seq (Matcovitch-Natan *et al.*, 2016; Li *et al.*, 2019, 2022; La Manno *et al.*, 2021; Menassa *et al.*, 2021), in both rodents and humans. This was coherent with the increased numbers of microglia observed along development. These studies, made across different species, used different tools and focused on different regions so much so that they are difficult to compare. Nevertheless, they show convergent trends. More specifically, looking along mice brain development, Alliot *et al.* could identify microglia as early as E8 in the brain and quantify their exponentially increasing numbers. They also quantified microglial proliferation via PCNA staining: more than a third of microglia were PCNA positive at E16, postnatal day (P)0, P3 and P7, while this proportion drastically decreased in the following days. Dalmau *et al.* studied microglial dynamics in the rat brain from E16 to P18 and could show the same trend: high proliferation peaking at P9 where more than 90% of microglia were PCNA positive, and reduced at P18. Interestingly, they looked in different regions of the brain, in both grey and white matter (cortex, hippocampus, DG, fimbria and subcortical white matter), highlighting subtle differences across regions. In particular, the density appears heterogeneous amongst regions, and relatively stable across development, the increase in numbers compensating for brain expansion. In addition, Dalmau *et al*. mentioned microglial apoptosis as a rare event, that could marginally contribute to the decreased density. Both studies thus suggest that proliferation alone accounts for the increase in microglial numbers. A broader analysis was recently performed in mice, spanning the whole parenchyma thanks to automated image quantification, and reached the same conclusions: expansion of microglia is clonal and follows an allometric scaling (Barry-Carroll *et al.*, 2023). Focusing on the cortex and the ganglionic eminences during embryonic development, Swinnen *et al.* detailed microglial densities and proliferation from E11.5 to E17.5. They showed that the percentage of proliferative microglia were decreasing along time, starting around 40% at E11.5 and close to 0% by E16.5, thus bringing a more detailed view about the temporal modulation of microglial proliferation in the embryonic brain (Swinnen *et al.*, 2013). Last, Nikodemova *et*

al. investigated the post-natal global microglial numbers through whole-brain flow cytometry analysis. They showed that microglial numbers peak around P14 thanks to proliferation, and decrease by P21 through apoptosis, reaching their adult level (Nikodemova *et al.*, 2015). These embryonic and post-natal periods of microglial proliferation with a late decrease accompanied by microglial apoptosis, can to some extent parallel what has been shown recently during human brain development (Menassa *et al.*, 2022).

Importantly, the exceptional proliferative capacities of developmental microglia are needed to generate the adult population from the restricted pool of YS-derived progenitors that reach the brain before E12. Indeed, microglia not only generate a broad population, but they are also believed to self-maintain throughout life in non-pathological conditions, without contributions from circulating monocytes (Ginhoux *et al.*, 2010; Kierdorf *et al.*, 2013; Hoeffel and Ginhoux, 2015). Their expansion from a restricted pool of progenitors has been recently highlighted through an elegant technique of *in vivo* barcoding allowing lineage tracing studies (Ratz *et al.*, 2022).

3.2.1.2 Migration

In addition to proliferation, microglia need to seed the entire parenchyma during development. Though long-range dispersion has been evidenced by lineage tracing (Ratz *et al.*, 2022), processes of migration are not fully understood and were most studied in the case of retinal colonization in different species (for review see Navascués *et al.*, 2000). Here are a few specific examples where mechanisms of local microglial migration have been identified. Thanks to two-photon live-imaging on brain slices, cortical microglia were observed adopting a saltatory migration as illustrated in **Figure 3.4** (Swinnen *et al.*, 2013). Though heterogeneous, some microglia are highly mobile during embryonic development, particularly at E14.5. Their migration towards the Ventricular Zone (VZ) has been shown to depend on the Cxcl12/Cxcr4 signaling: basal progenitors secrete Cxcl12 that is recognized by the microglial receptor Cxcr4 and contribute to their accumulation in the VZ (Arnò *et al.*, 2014; Thion *et al.*, 2018). In addition, it was suggested that the same attracting pathway mediates microglial migration towards to marginal zone of the neocortex, thanks to meningeal Cxcl12 (Hattori *et al.*, 2020). This bidirectional attraction could explain the transient microglial absence from the cortical plate. In the developing spinal cord, microglia are thought to migrate along and through blood vessels: microglial numbers increase concomitantly with angiogenesis, and some cells can be seen inside capillaries, or halfway exiting its walls (Rigato *et al.*, 2011). In addition, they are in close interaction with radial glia processes, but dynamic analysis is needed to confirm if it

serves as a guide for microglia or not. On the other hand, microglia have been observed to migrate slowly along blood vessels in the somatosensory cortex at P7, but not in the adult (Mondo *et al.*, 2020).

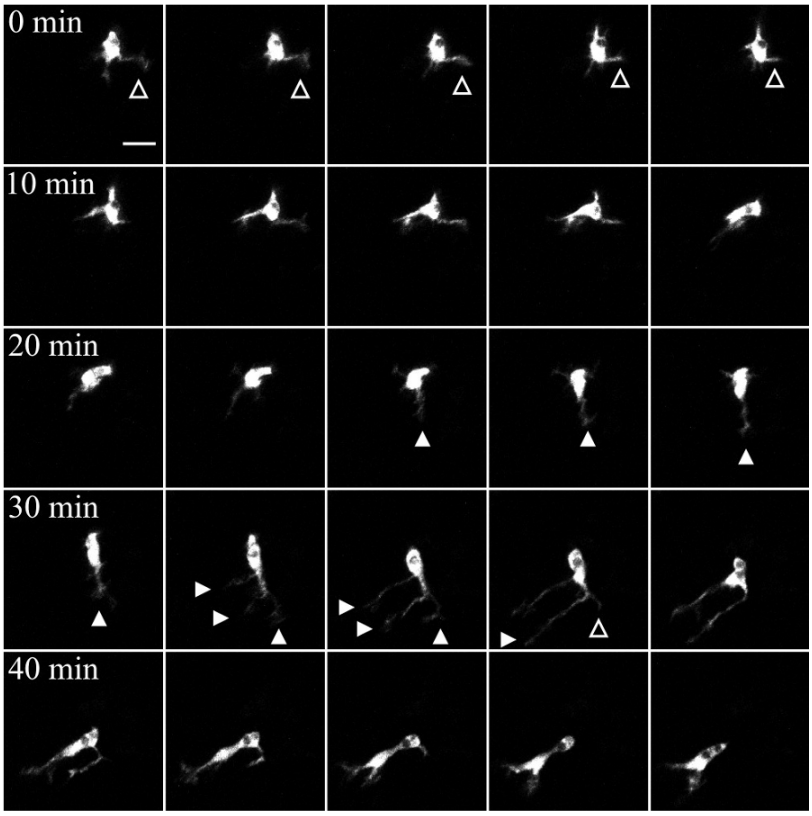

Figure 3.4 Saltatory migration of embryonic microglia

A microglial cell showing highly dynamic behavior. It seems to be scanning the environment by constantly sending out (closed arrowheads) and retracting (open arrowheads) protrusions. At 30 min the cell starts sending out more protrusions in the same direction after which it drags the cell soma in the same path, resulting in a displacement of the cell. Images are cropped z-projections (five optical slices with a z-step of 8 µm and time interval of 2 min). Scale bar=20 µm. From Swinnen *et al*., 2013.

3.2.2. Stepwise maturation

3.2.2.1 Cellular maturation: from ameboid to ramified

The first microglia that can be seen in the brain rudiment are ameboid, with almost no ramification, both in rodents and humans (see **Figure 3.5**)(Alliot, Godin and Pessac, 1999; Dalmau *et al.*, 2003; Orłowski, Sołtys and Janeczko, 2003; Monier *et al.*, 2006, 2007; Verney *et al.*, 2010; Menassa *et al.*, 2022). Through time, the size of their cell bodies decreases, and they get more ramified, with additional processes getting more branched. But it's not before the third post-natal week that they acquire their highly ramified morphology.

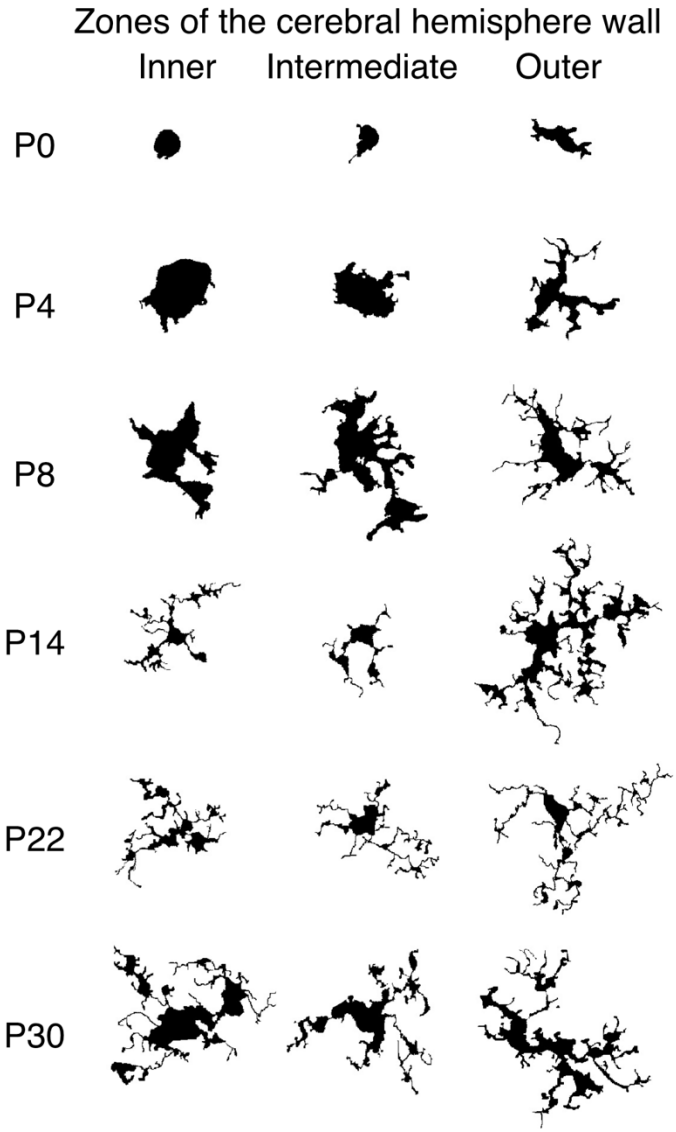

Figure 3.5 Microglial morphology along their maturation in the rat

Examples of microglial cells typical of consecutive developmental stages (P0–P30 presented in rows) from the inner, intermediate and outer zones within the cerebral hemisphere wall (presented in respective columns). Adapted from Orłowski *et al.*, 2003.

3.2.2.2 Molecular maturation

During their journey from the YS to their more mature phenotype, microglia mature. Indeed, in a pioneer study performed by Matcovitch-Natan and colleagues, progenitors of the YS and microglia were isolated at different time points of embryonic and early postnatal development, as well as from the adult (Matcovitch-Natan *et al.*, 2016). By performing a combination of scRNA-seq, ATAC-seq and Chromatin-Immunoprecipitation followed by

Sequencing (ChIP-seq), they could show that microglia follow a stepwise program of maturation: individual cells shift their regulatory networks in a coordinated manner during development. Three transcriptional stages, linked to changes in the chromatin landscape, were identified and temporally succeed one another: early microglia until E14.5, pre-microglia until a few weeks after birth, and adult microglia. This was later confirmed by a second study using bulk-RNAseq and showing that even at the level of the whole population, microglia follow a step-wise developmental program (Thion *et al.*, 2018). One key step of the maturation process depends on the transcription factor *SALL1*, which deletion leads to an immature phenotype of microglia, retaining their CD206 expression (Buttgereit *et al.*, 2016; Scott *et al.*, 2022). Furthermore, microglial developmental program is susceptible to changes in the environment, highlighted by sexual dimorphism arising in the adult (Thion *et al.*, 2018), and the use of models of Germ-Free (GF) mice deprived of microbiota (Matcovitch-Natan *et al.*, 2016; Thion *et al.*, 2018) and of MIA (Matcovitch-Natan *et al.*, 2016). Focusing on hippocampal microglia, another study compared developmental microglia (E18.5, P4 and P14) to adult microglia (P60) and could deduce a "microglial developmental index" which was perturbed both by sexual dimorphism and MIA (Hanamsagar *et al.*, 2017). Similarly in humans, scRNA-seq and bulk chromatin profiling from GW9 to GW18 showed that microglia progressively mature in the human fetal brain and acquire their immune sensing capacities (Kracht *et al.*, 2020).

Interestingly, it was shown that the proper maturation of microglia relies both on the ontogeny of these cells and on the local microenvironment (Lavin *et al.*, 2014; Gosselin *et al.*, 2017; Takata *et al.*, 2017; Bennett *et al.*, 2018). By transplanting different macrophage populations in a microglia-depleted brain, they could observe that YS-derived macrophages are able to turn on a mature microglial profile, even after a phase of *in vitro* culture during which they undergo dramatic transcriptional changes (Bennett *et al.*, 2018). Macrophages from other locations, though adopting a ramified morphology and canonical markers of microglia like TMEM119, never fully recapitulated a homeostatic microglial profile. Engraftment and progressive maturation towards the homeostatic microglial profile was also obtained with induced-pluripotent-stem-cell-derived primitive macrophages injected at birth in ventricles of depleted mouse brains (Takata *et al.*, 2017).

Last and intriguingly, microglial maturation was suggested to depend on their interaction with other immune cells: some CD4 T cells are resident in the brain parenchyma, both in mice and humans, and are necessary for microglial transition from their fetal to their adult phenotype (Pasciuto *et al.*, 2020).

3.2.3. Heterogeneity of microglial colonization

While global trends of microglial maturation can be observed, microglia actually colonize the brain in a very heterogeneous manner (**Figure 3.6**), following a conserved spatiotemporal pattern. First, starting between E12.5 and E14.5 in mice, microglia get heterogeneously distributed: microglia are transiently excluded from the cortical plate, as can be seen in **Figure 3.6A-C**. They progressively enter the cortical plate from E16.5 (Arnoux *et al.*, 2013; Swinnen *et al.*, 2013; Hattori *et al.*, 2020) in mice and GW10-13 in humans (Monier *et al.*, 2006, 2007; Verney *et al.*, 2010). In addition, microglia accumulate at hotspots, close to developing axonal tracts, mainly of the external capsule and corpus callosum, termed the "fountains of microglia" (Verney *et al.*, 2010). These accumulations were also described in rodents (Imamoto and Leblond, 1978; Ling, 1979; Ashwell, 1991), and an additional embryonic hotspot was associated to Tyrosine-Hydroxylase (TH)-positive midbrain dopamine axons crossing the subpallium (Squarzoni *et al.*, 2014). Importantly, microglia display heterogeneous morphologies across development, but also across the brain at any given timepoint, as shown in **Figure 3.6B**. In particular, in the hotspots of microglial accumulation, they appear particularly ameboid (Imamoto and Leblond, 1978; Ling, 1979; Ashwell, 1991; Verney *et al.*, 2010; Squarzoni *et al.*, 2014). This developmental heterogeneity strikingly contrasts with their homogeneous tiling of the mature parenchyma, with their highly ramified morphology, as can be seen as early as P20 in mice (**Figure 3.6**).

In addition, microglial maturation is shaped by their local environment. This was already pointed out in the rat that microglial proliferation and densities varied across development between forebrain regions (Dalmau *et al.*, 2003), as well as in mice between forebrain, hindbrain and midbrain (Barry-Carroll *et al.*, 2023), but were more precisely detailed during post-natal development across different basal ganglia nuclei, additionally analyzing microglial coverage and cell death (Hope *et al.*, 2020). This last study, though investigating the possible impact of surrounding cell death and proliferation on microglial phagocytic activity, could not highlight a process driving microglial proliferation and thus density in the nuclei. Interestingly, a complementary anterior study had already established the region-specific phenotypes of microglia in the basal ganglia nuclei, and had shown that after depletion, microglia repopulate the brain and re-establish the same region-specific patterns (Biase *et al.*, 2018). Insights into mechanisms of specific microglial maturation was recently provided by an elegant study combining single-cell and spatial transcriptomic profiling during postnatal

development of the neocortex, which showed that microglial states are finely regulated by the neighboring neuronal diversity (Stogsdill *et al.*, 2022).

Microglial regional specificities were further studied comparing cortical and spinal cord microglia, and their respective reaction in disease (Zheng *et al.*, 2021); comparing microglia from the cortex, striatum and cerebellum, which showed an epigenetic regulation of microglial phagocytic capacity (Ayata *et al.*, 2019); and was also highlighted in the human brain (Li *et al.*, 2022).

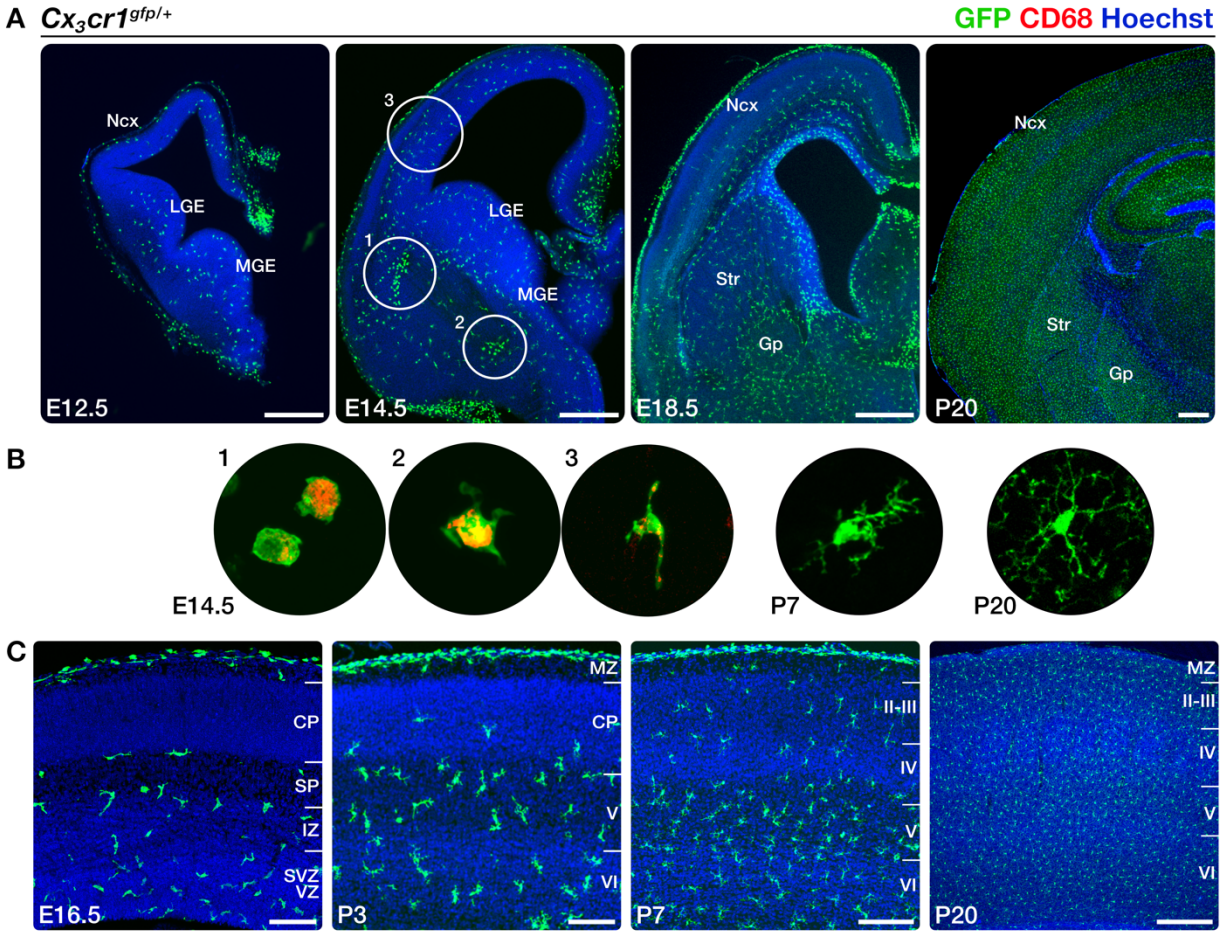

Figure 3.6 Heterogeneous colonization of the mouse developing brain

(A) Coronal sections of cx3cr1gfp/+ brains from E12.5 to P20 showing the transient uneven microglia distribution during development in contrast to homogeneous distribution in the adult. Note the presence of microglial hotspots at E14.5 (1) at the CSA, (2) at the extremity of dopaminergic axons (DA axons) and (3) in the neocortex. (B) Zooms of microglial morphology across the parenchyma at E14.5 and at P7 and P20. (C) Somatosensory cortex coronal sections of cx3cr1gfp/+ brains from E16.5 to P20 show progressive colonization of the cortical plate by microglia (CP). Note that at E16.5 microglia remain largely excluded from the CP. Ncx: Neocortex, MZ: marginal zone, CP: cortical plate, SP: subpallium, IZ: intermediate zone, SVZ: subventricular zone, VZ: ventricular zone. Scale bars represent 500 mm in (A), and 100 mm in (C) for E16.5, 250 mm for P3 and 300 mm for P7 and P20. Adapted from Thion and Garel, 2017.

3.3. Developmental heterogeneity

3.3.1. High developmental cellular heterogeneity

Studies have long been limited to the morphology, density, and expression of a few markers like CD68, a lysosomal marker suggesting phagocytic activity; or levels of F4/80, expressed by various macrophages including microglia. This suggested some degree of microglial heterogeneity, but it was only with technical advances that it became possible to get insights into spatial and temporal multiplicity of microglia at the single-cell level. Recent scRNA-seq studies strikingly revealed a high molecular diversity of developmental microglia,

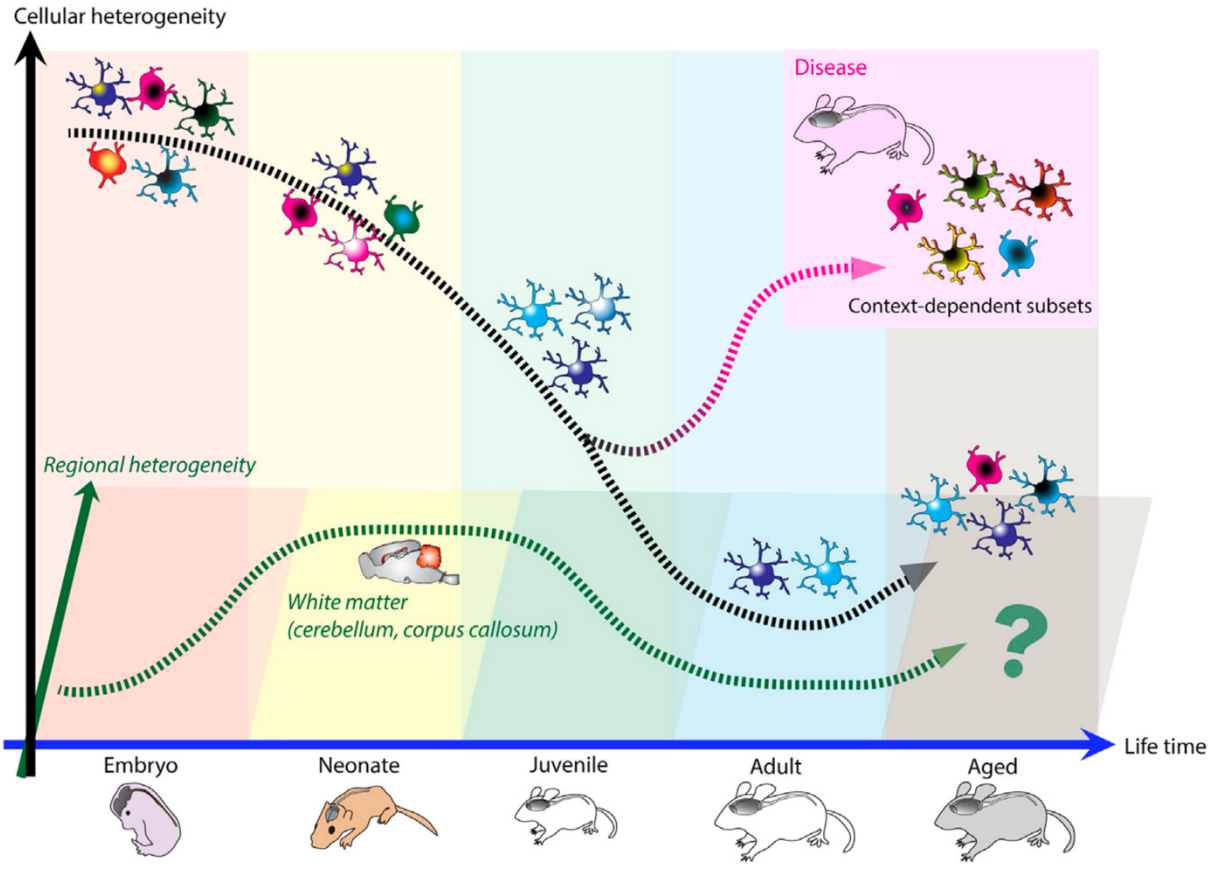

Figure 3.7 Dynamic changes in microglial heterogeneity during development, aging and disease

Highly transcriptionally diverse microglia clusters exist at embryonic time points in mice, the extent of which gradually decreases over the course of development, resulting in limited heterogeneity of microglia during adulthood. In contrast, the diversity of microglia increases again during aging, whereas less is known about region-specific diversity in the aged brain. On the other hand, higher regional heterogeneity is observed at early post- natal time points, especially in white-matter regions such as the cerebellum or the corpus callosum. During disease conditions, microglia are able to once again change their transcriptional phenotypes and give rise to more heterogeneous substates in a context-dependent manner. Differentially colored cells indicate diverse microglia transcriptional states. From Masuda, Sankowski, et al., 2020.

contrasting with a more homogeneous adult population (Hammond *et al.*, 2019; Li *et al.*, 2019; Masuda *et al.*, 2019). Diversity arises again in aging, disease and neurodegeneration (**Figure 3.7**)(Hammond *et al.*, 2019; Masuda, Sankowski, *et al.*, 2020).

More precisely, using the 10x technology, Hammond *et al.* analyzed the transcriptome of more than 76 000 microglia, extracted from whole brains of E14.5, P4/5, P30, P100, P540 and in condition of injury. On the other hand, Li *et al.* used a semi-automated Smart-seq2 platform to perform scRNA-seq on fewer microglia (close to 2 000) but with an enhanced depth (> 1 million raw reads per cell), from E14.5, P7 and P60 brains. Thus, both studies bring different information but importantly converge on several aspects: microglia form a highly heterogeneous population during development; an important proportion of microglia are proliferating in the developing brain; one cluster found in white matter present a specific set of genes, with similarities to DAMs. Another study focused on embryonic development and analyzed the whole brain (La Manno *et al.*, 2021). Even though the amount of microglia analyzed is limited, they could again identify proliferating microglia, as well as the microglial profile associated to white matter tracts that is further developed in the next paragraph.

Overall, our understanding of microglial diversity has greatly increased in the past years. The myriad of states that microglia can adopt appear to be both locally shaped, and dependent on the cell state (Paolicelli *et al.*, 2022). In this line, several methods of spatial transcriptomics have recently been developed, allowing to link cellular mRNA expression with the cell's location. Combined to their expanding use and increasing resolution, it will be crucial to refine our understanding of microglial subsets. Importantly, whether microglia are committed to specific fates or those are induced and by what, and whether they are transient and reversible, still needs further investigation.

3.3.2. Axonal Tract associated Microglia, or PAM-YAM-CD11c+…

One developmental cluster, corresponding to microglia accumulating along axonal tracts, specifically the corpus callosum and white matter of the cerebellum, and presenting an ameboid morphology, was thus identified. More specifically, they were called Axonal-Tract-associated Microglia (ATM)(Hammond *et al.*, 2019; La Manno *et al.*, 2021) because of their location - and which name we will keep hereafter; Proliferative-region-Associated Microglia (PAM)(Li *et al.*, 2019) as they were also found in neurogenic regions; or Youth-Associated Microglia (YAM)(Silvin *et al.*, 2022) as they transiently appear during development. They all

express, but at lower levels, the main signature genes of homeostatic microglia including *P2ry12*, *Tmem119* or *Siglech*, and are characterized by a set of specific genes such as *Spp1*, *Igf-1*, *Clec7a*, *Lgals3* or *Itgax* (coding for CD11c). Importantly, their location, morphology, transient appearance in the developing brain and their transcriptomic profile were highly reminiscent of a "subtype" of microglia that had been shown two years earlier to be of importance respectively for proper myelination through the release of IGF-1 (Wlodarczyk *et al.*, 2017), and for development and homeostasis of oligodendrocytes and their progenitors (Hagemeyer *et al.*, 2017); and which had been referred to as neonatal CD11c+ microglia or the aforementioned fountains of microglia. Additional observation by Li *et al.* suggest that ATM additionnally phagocyte newly formed oligodendrocytes and possibly astrocytes (Li *et al.*, 2019). While their presence in the embryonic brain had been suggested by whole brain scRNA-seq analysis, recent work from the laboratory showed their accumulation at hotspots of white matter under morphogenetic stress, namely the Cortico-Subpallial Boundary (CSB) and the Cortico-Striato-Amygdalar boundary (CSA), where they likely participate in the maintenance of tissue integrity (Lawrence *et al.*, under revision). Of note, presence of accumulated ameboid microglia displaying several core ATM markers was also identified in the embryonic human brain (Lawrence *et al.*, under revision). A similar ATM-like profile was also identified in the post-natal retina, which was partly induced by neuronal death (Anderson *et al.*, 2019).

Interestingly, ATM share several features with DAM (see 2.3.2), which also express *Spp1*, *Igf-1*, *Clec7a* or *Itgax* (Kamphuis *et al.*, 2016; Keren-Shaul *et al.*, 2017; Krasemann *et al.*, 2017). Their ameboid morphology and high phagocytic capacities (Keren-Shaul *et al.*, 2017; Krasemann *et al.*, 2017; Li *et al.*, 2019) raise the questions of possible shared functions in brain development and disease, and of the relationship between ATM and DAM. In particular, how both profiles are induced is still under investigation. Interestingly, loss of SIRP-α expression in microglia, or of its ligand CD47, has been shown to increase the numbers of CD11c+ microglia in white matter, mimicking the increase in DAM seen in aging and neurodegeneration (Sato-Hashimoto *et al.*, 2019). This led to reduced demyelination (Sato-Hashimoto *et al.*, 2019), as well as excess synaptic pruning in development during which SIRP-α is preferentially expressed by microglia (Lehrman *et al.*, 2018); and accelerated cognitive impairment in AD (Ding *et al.*, 2021). This highlights the double-edge effect, dependent on the specific environment, of the increased phagocytic activity associated to both ATM and DAM profiles. One main difference nevertheless is that DAM depend on TREM2 to turn on their full profile, while ATM have been observed in *Trem2*$^{-/-}$ and *Apoe*$^{-/-}$ (Hammond *et al.*, 2019). In

addition, though some microglia can be termed DAM in various disease conditions and aging, by displaying some core shared features, they appear nevertheless slightly different, possibly reflecting specific microglial functions and local environment they have to deal with.

3.3.3. Heterogeneity in human microglia

Microglial developmental heterogeneity has also been observed in humans (Kracht *et al.*, 2020; Li *et al.*, 2022). More strikingly, one subtype present in early and mid-gestation shares transcriptional features of mice ATM/DAM (Kracht *et al.*, 2020), as histological observations of Lawrence *et al.* tend to confirm (Lawrence *et al.*, under revision). By mid-gestation, microglia tend to adopt a more mature phenotype. The obvious scarcity of healthy adult brain tissue available still complicates our study of mature human microglia and their diversity. Human homeostatic microglia nevertheless appear more diverse than in mice: one subset shared most genes with mice homeostatic signatures, but others only partially overlapped, which functions are still unknown (Masuda *et al.*, 2019; Sankowski *et al.*, 2019). Region and age-related heterogeneity of human microglia were also illustrated (Böttcher *et al.*, 2019; Masuda *et al.*, 2019; Sankowski *et al.*, 2019; Li *et al.*, 2022).

3.4. Developmental roles of microglia

The appropriate building of the brain demands precise orchestration of several genetic and developmental programs in coordination with the environment. Because of their atypic ontogeny, microglia arrive in the brain at the beginning of neurogenesis: until the generation of astrocytes and OPCs, microglia are the main glial cell population present in the brain. This, along with their immune-glial identity, puts microglia in a privileged position to engage in brain development. And indeed, microglia now appear as key actors of this critical period, participating in a wide array of developmental processes (**Figure 3.8)**.

3.4.1. Microglia: Swiss army knife of brain development

Though some studies unquestionably unravel microglial functions, directly looking at their immediate action, many of the developmental roles of microglia were shown using depletion strategies broadly targeting microglia and other macrophages, including BAMs. Because microglia are the only one present in the brain parenchyma, they were considered the main effectors, but a contribution by BAMs or peripheral macrophages cannot be excluded.

3.4.1.1 Angiogenesis

Microglia have long been observed along blood vessels (Monier *et al.*, 2007; Verney *et al.*, 2010; Mondo *et al.*, 2020; Hattori, 2022). In addition, impaired angiogenesis in a model of microglial and macrophage loss (Kubota *et al.*, 2009) suggested that microglia could be involved in this process in the brain. It was later suggested that microglia in the embryonic zebrafish retina and hindbrain are responsible for vascular anastomosis by promoting tip cell fusion, and were thus responsible for proper vascular network complexity (Fantin *et al.*, 2010). How they participate in the formation of blood vessels in the mouse and human brain has not yet been clearly established.

3.4.1.2 Regulation of neuronal numbers, positioning and maturation

Microglia participate in the regulation of neuronal numbers in different manner. They interact with basal progenitors of the ventricular zones, and when microglia are absent using *Csf-1r*$^{-/-}$ or liposomal clodronate, basal progenitors numbers have respectively been reported to decrease (Arnò *et al.*, 2014) or increase (Cunningham, Martínez-Cerdeño and Noctor, 2013). More specifically, microglia were shown in the rat and monkey brain to phagocyte neural

progenitors throughout development, which is increased at the end of neurogenesis (Cunningham, Martínez-Cerdeño and Noctor, 2013). On the other hand, microglia have been shown to promote neurogenesis in the early postnatal brain of rats via the secretion of pro-inflammatory cytokines (Shigemoto-Mogami *et al.*, 2014). More recently, in a model of pericyte depletion which induced a decrease in microglial numbers, embryonic microglia were suggested to be responsible for the differentiation of neural stem cells into intermediate progenitors (Hattori, Itoh, *et al.*, 2022), while their transient absence from the cortical plate was needed for proper differentiation of promigratory cortical neurons (Hattori *et al.*, 2020). A recent study also suggests that microglia induce proliferation of neuronal progenitors (Cserép *et al.*, 2022).

Later in development, microglia have been shown to participate both in neuronal death and survival (Audinat and Arnoux, 2014; Schafer and Stevens, 2015; Thion, Ginhoux and Garel, 2018). In particular, they promote death of developing Purkinje cells of the cerebellum through oxidative stress, before phagocyting them (Marín-Teva *et al.*, 2004); of retinal neurons through the release of the neurotrophin Nerve Growth Factor (NGF) (Frade and Barde, 1998); of motoneurons of the spinal cord via TNF-α (Sedel *et al.*, 2004); and of developing neurons of the hippocampus via their release of ROS in a DAP12- and CD11b-dependent manner (Wakselman *et al.*, 2008). On the other hand, through the release of IGF-1 they promote LV neuron survival during the first postnatal week (Ueno *et al.*, 2013).

In addition to mediating neurogenesis and later survival of neurons or their elimination by apoptosis, microglia also participate in two critical step of brain circuitry: neuronal migration and positioning, and axonal growth and fasciculation. Indeed, embryonic microglia modulate the outgrowth of dopaminergic axons crossing the subpallium (Squarzoni *et al.*, 2014), and are also important for the fasciculation of the corpus callosum (Pont-Lezica *et al.*, 2014). They orchestrate the laminar positioning of *Lhx6*-positive interneurons (Squarzoni *et al.*, 2014), and regulate migration of postmitotic immature neurons through somatic dynamic contacts (Cserép *et al.*, 2022). Occurrence of these contacts was increased during the first postnatal week, and they form in a P2RY12-dependent manner. Indeed, knock-out of P2RY12 leads to an aberrant cortical distribution of neurons during development and in the adult (Cserép *et al.*, 2022).

3.4.1.3 From early circuit wiring to synaptic orchestration

Microglia also closely interact with synapses to sculpt the developing neuronal networks. They regulate activity-dependent synaptic pruning in different contexts (Paolicelli *et*

al., 2011; Schafer *et al.*, 2012; Filipello *et al.*, 2018; Weinhard *et al.*, 2018; Favuzzi *et al.*, 2021). Along with neuronal activity, several signaling pathways have been shown to be implicated in this process, such as the complement receptor pathway (Schafer *et al.*, 2012), TREM2 signaling (Filipello *et al.*, 2018) or Cx3cr1 signaling (Paolicelli *et al.*, 2011). Interestingly, Favuzzi and colleagues highlighted a GABA-receptive microglia subtype which specifically interacts with inhibitory synapses (Favuzzi *et al.*, 2021). Microglia have also been proposed to promote synapse formation, as two-photon live-imaging showed that microglial contacts with dendrites of pyramidal cells of the developing somatosensory cortex were followed by filopodia formation (Miyamoto *et al.*, 2016). Microglia also participate in the appropriate maturation of synapses through Cx3cr1/Cx3cl1 signaling, which disruption leads to a delayed maturation of thalamocortical synapses in the barrel cortex (Hoshiko *et al.*, 2012), and to global impaired functional connectivity and social behavior (Zhan *et al.*, 2014). In addition, they shape axonal extension of SST+ cortical interneurons (Gesuita *et al.*, 2022).

Coherent with the fact that microglia impact virtually all aspects of neuronal development, it has been shown that embryonic microglial depletion as well as activation in MIA both lead to impaired early positioning and wiring of PV inhibitory neurons of the somatosensory cortex (Squarzoni *et al.*, 2014; Thion *et al.*, 2019). While they induce a hyper-inhibition in the juvenile animals, it is converted to a hypo-inhibition in the adult. Even though mechanisms at stake are still unknown, it remarkably highlights not only the need of microglial presence, but also how their alterations through inflammation in this crucial period can alter brain wiring in the long-term.

3.4.1.4 Gliogenesis and myelination

Microglia have been suggested to participate in astrogenesis, with *in vitro* studies showing that neural progenitors displayed less proliferation and differentiation into astrocytes in the absence of microglia (Reemst *et al.*, 2016). On the other hand, in *Csf1r*$^{-/-}$ mice which lack microglia and macrophages, astrocyte density in the neocortex was increased (Erblich *et al.*, 2011), while postnatal depletion of microglia via BLZ945, a CSF-1R inhibitor, did not modify it (Hagemeyer *et al.*, 2017). More recently, sexual dimorphism in microglial phagocytic activity of newborn cells in the developing amygdala has been shown to impact astrocyte density in rats (VanRyzin *et al.*, 2019), a phenomenon also suggested in mice by the observation of substantial interactions between microglia and astrocytes (Li *et al.*, 2019).

Microglia, and more particularly ATM, have been instead associated to oligodendrogenesis and proper myelination. It has been shown that microglial inflammatory

state (Shigemoto-Mogami *et al.*, 2014) and presence (Erblich *et al.*, 2011; Hagemeyer *et al.*, 2017) is important for the generation and expansion of oligodendrocytes and further myelination. This is mediated by ATM IGF-1 (Wlodarczyk *et al.*, 2017) and Neuropilin-1 (Sherafat *et al.*, 2021) expression. Importantly, ATM were observed phagocyting both viable OPCs (Nemes-Baran, White and DeSilva, 2020) and newly formed oligodendrocytes (Li *et al.*, 2019). Interestingly, recent works in mice and zebrafish suggest that microglia further interact

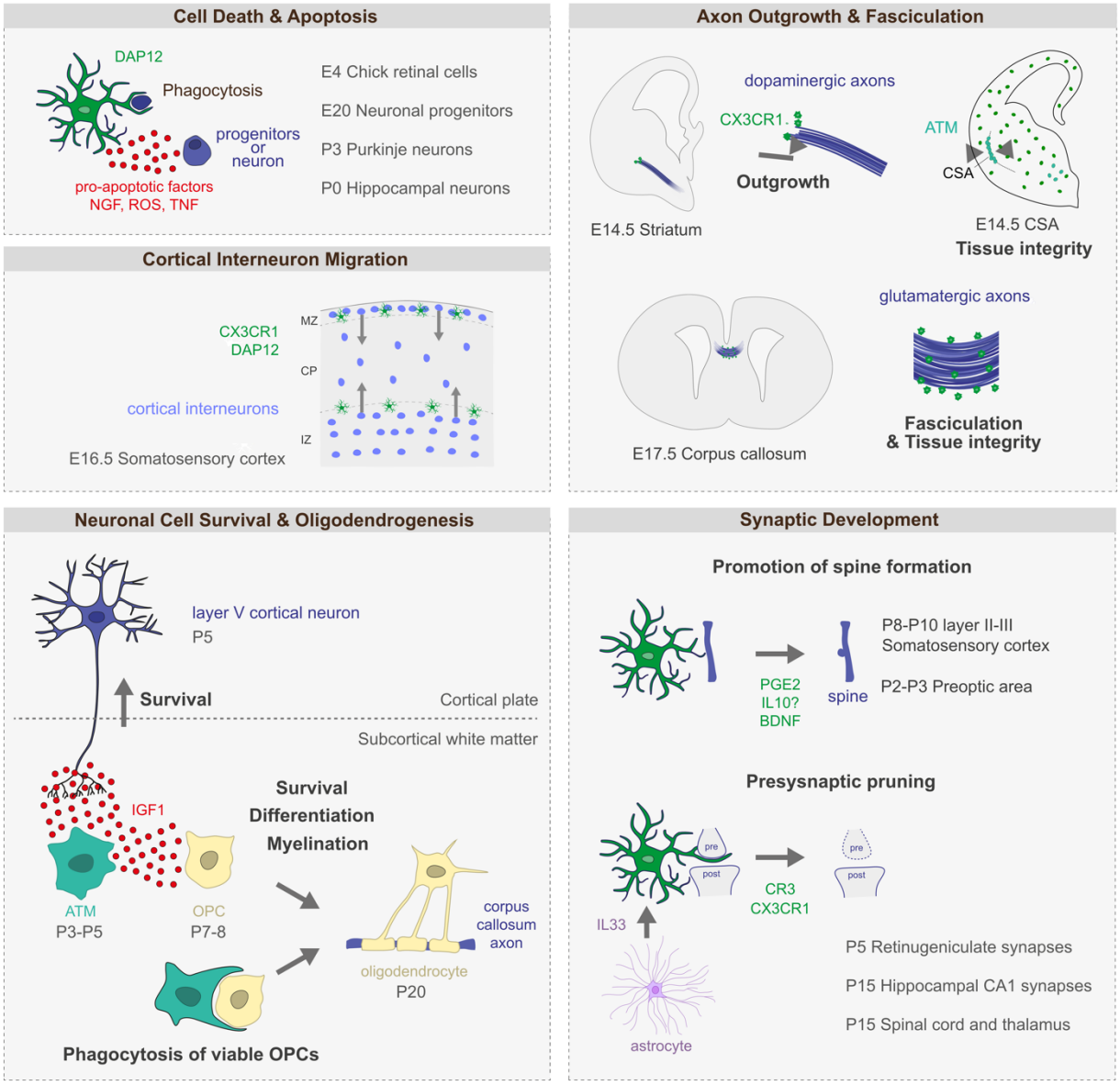

Figure 3.8 Main cellular functions of embryonic and postnatal microglia

Schematic representation of microglial functions during pre- and postnatal development. Microglia participate in diverse developmental processes: regulation of neuronal numbers through phagocytosis of progenitors and induction of apoptosis; interneuron positioning; maintenance of tissue integrity; axonal outgrowth and fasciculation; neuronal cell survival; oligodendrogenesis and myelination; synaptic development and maturation. Adapted from Thion, Ginhoux, *et al.*, 2018.

with developmental myelin, by phagocytosis of misfolding or excessive myelin (Hughes and Appel, 2020; Djannatian *et al.*, 2021). Yet, the specific roles of microglia versus BAMs have been recently questioned since myelin development seems to be occurring in *Csf1r*$^{\Delta FIRE/\Delta FIRE}$ mice, that lack microglia but somehow preserves BAMs (Rojo *et al.*, 2019; McNamara *et al.*, 2023). Deciphering the roles of cell types, states and potential compensatory mechanisms will thus be important in further studies.

3.4.2. Microglia and neurodevelopmental disorders

Thus, during this crucial phase of brain construction, microglia participate in the fine-tuning of many developmental processes. Environmental perturbations in this period, to which microglia are particularly sensitive, participate in the etiology of neurodevelopmental disorders (Scattolin, Resegue and Rosário, 2022). Increasing evidence points towards a role of microglial dysfunction in this process, including ASD, Epilepsy or Schizophrenia (Parikshak *et al.*, 2016; Gandal *et al.*, 2018; Velmeshev *et al.*, 2019; Lukens and Eyo, 2022). Few mutations identified as risk factor for neurodevelopmental disorders directly target microglia. In most cases, neuronal properties are affected, especially synaptic development or properties (Velmeshev *et al.*, 2019), for example resulting in altered excitation/inhibition balance or impaired brain oscillations, to which microglia can in turn respond, thereby potentially participating to some extent to disorders. Non-exclusively, early defects in microglia could alter early brain wiring and have long-term impact on the properties of these cells, thereby contributing to abnormal functioning of the circuits at later stages (Ikezu *et al.*, 2021; Hayes *et al.*, 2022).

In addition, neurodevelopmental disorders are not only genetically regulated: both genetic and environmental factors act in synergy, following a model of multiple hits. In this view, it is believed that both the fact that microglia do not perform their usual developmental functions in environmentally-challenged contexts, and their response to inflammation *per se*, could explain their contribution to neurodevelopmental disorders (Rahimian *et al.*, 2021). Interestingly, many of these environmental threats have sex-dependent consequences on microglia, reflecting the sex-biased prevalence of most neurodevelopmental disorders, and reinforcing the idea of microglial involvement in their onset (Rahimian *et al.*, 2021).

4. The CSF-1 Receptor pathway and microglia

The CSF-1 receptor (CSF-1R) pathway is essential for the development and life-long maintenance of tissue resident macrophages, including microglia. Importantly, microglia and other macrophages are dependent on CSF-1R signaling pathway for their survival at all the stages of prenatal and adult life (Stanley and Chitu, 2014). The CSF-1R is highly conserved across human and mice and its mutations are associated to Hereditary Diffuse Leukoencephalopathy with Spheroids (HDLS)(Pridans *et al.*, 2013), an adult-onset neurodegenerative disorder, as well as other neurologic disorders (Guo and Ikegawa, 2021) and even early death in the case of homozygous mutation (Oosterhof *et al.*, 2019).

4.1. General overview of the pathway

4.1.1. One receptor, two ligands

The CSF-1R is a tyrosine kinase receptor mainly expressed in HSCs, monocytes, osteoclasts, Paneth cells, myeloid dendritic cells and tissue resident macrophages (for review see Stanley & Chitu, 2014), so that in the brain it is mainly expressed by microglia and BAMs. It is expressed in neurons during injury (Wang, Berezovska and Fedoroff, 1999; Luo *et al.*, 2013) and its expression has been reported in cortical basal progenitors during development (Nandi *et al.*, 2012).

It has two known ligands: the cytokines CSF-1 and IL-34 (**Figure 4.1**). CSF-1 exists under three distinct biologically active isoforms: a secreted glycoprotein, a secreted proteoglycan and a membrane-spanning cell-surface glycoprotein - which have overlapping yet distinct effects. This was shown in the *Csf1*$^{op/op}$ mouse model bearing an inactivating mutation of *Csf-1* in which expression or injections of different isoforms only partially rescued the *Csf1*$^{op/op}$ phenotypes (Dai *et al.*, 2004; Nandi *et al.*, 2006). While the proteoglycan and membrane isoforms act locally, the glycoprotein isoform can be found in blood circulation. On the other hand, IL-34 actions are probably limited to its local environment. CSF-1R is thought to be the only receptor for CSF-1, while IL-34 also binds additional receptors: receptor-type protein tyrosine phosphatase-ζ (PTP-ζ)(Nandi *et al.*, 2013), not expressed on microglia nor macrophages but on neural and hematopoietic stem cells; and syndecan-1, a cell surface

chondroitin sulfate-containing proteoglycan, through which it can mediate migration of myeloid cells (Segaliny *et al.*, 2015).

CSF-1R activates a multitude of signaling pathways, resulting in pleiotropic cellular responses. This pathway is essential for microglial and macrophage survival and proliferation, and is involved in chemotaxis (Stanley and Chitu, 2014). It was suggested to be also important for macrophage differentiation, a view now revised at least in zebrafish (Endele *et al.*, 2017; Oosterhof *et al.*, 2018). Interestingly, CSF-1R induced proliferation can be mediated by DAP12/TYROBP, a transmembrane adaptor protein for TREM2 (Stanley and Chitu, 2014). This pathway is well conserved across species. In zebrafish, two homologs of the human receptor can be found, *csf1ra* and *csf1rb*, which are likely partially redundant. In humans, the CSF-1R has several oncogenic derivatives and was extensively studied in the context of tumor-associated macrophages.

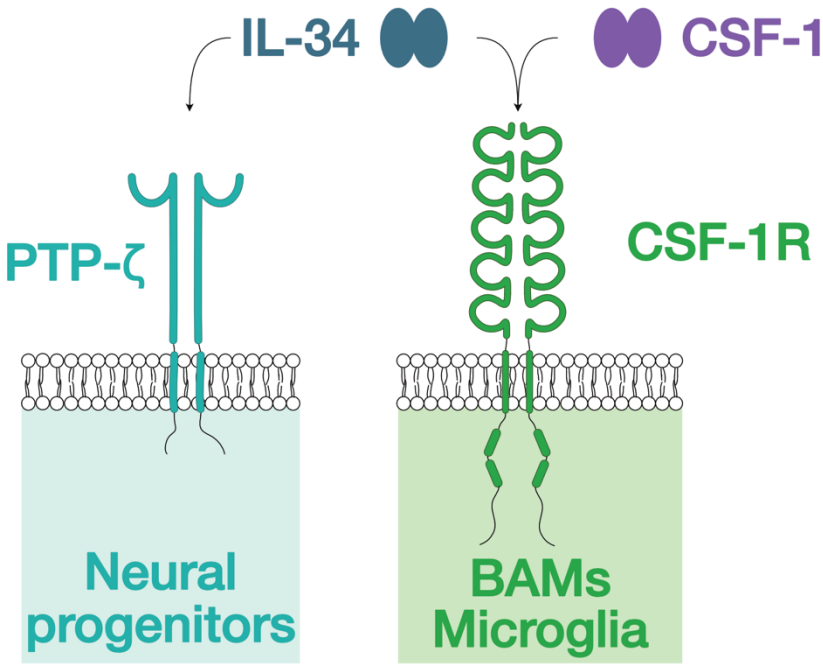

Figure 4.1 The CSF-1 receptor ligands and their respective receptors

The cytokines IL-34 and CSF-1 are the two known ligands of the CSF-1R. CSF-1 is thought to bind exclusively to CSF-1R, mostly expressed by microglia and BAMs in the CNS. IL-34 also binds to PTP-ζ and syndecan-1 (not shown here). IL-34: Interleukin-34, CSF-1: colony-stimulating factor 1, CSF-1R: colony-stimulating factor 1 receptor, PTP-ζ: protein tyrosine phosphatase-ζ, BAMs: border-associated macrophages.

4.1.2. CSF-1R signaling in the developing brain

Thanks to *Csf1r*$^{-/-}$ full mutants, it was established that the development of microglia, as well as of their YS progenitors, depends on CSF-1R signaling (Ginhoux *et al.*, 2010; Erblich *et al.*, 2011). On the other hand, while the dependency of microglia on each CSF-1R ligand and their respective distribution in the adult brain are now well-characterized (**Figure 4.2**), what happens during development is less understood. Both ligands can be detected in the brain at embryonic stages, with *Il-34* at higher levels than *Csf-1*, but it is not known by which cells they are respectively secreted (Wei *et al.*, 2010; Greter *et al.*, 2012). Using fluorescent RNA *in situ* hybridization, it was shown that at P1, *Il-34* was only detected in the meninges, but *Csf-1* was observed in low abundance in all regions observed (cerebral cortex, fimbria, dentate gyrus and meninges)(Easley-Neal *et al.*, 2019). Discrepancies in these results probably correspond to differential sensitivity of the techniques. By P8, the mature patterns of the ligands expression are already established, with *Il-34* expressed by neurons in zones of grey matter, and *Csf-1* by glia in white matter (Kana *et al.*, 2019).

Surprisingly, *Il-34*, even though present early on in the brain, has been suggested to be dispensable for microglial development, as flow cytometry analysis revealed normal numbers of microglia in the brain of *Il-34*$^{-/-}$ mice at E10.5, E14.5, E17.5 and in newborns (Greter *et al.*, 2012). Using the same technique, a parallel study instead found microglial numbers to be radically decreased at P2 (Wang *et al.*, 2012), thus interrogating on the possible early role of *IL-34*. On the other hand, *Csf-1* appears essential: microglial numbers are reduced at E17.5 in both forebrain and cerebellum of *Nestin*^{cre}*;Csf-1*$^{fl/fl}$ (Kana *et al.*, 2019), and at P0 and P4 with injections of anti-CSF-1 at E6.5 and E7.5 (Easley-Neal *et al.*, 2019).

4.1.3. Differential spatiotemporal regulation of CSF-1R signaling in the brain

In the adult brain, non-overlapping distribution of both ligands shapes their differential regulation of microglia. Indeed, *Csf-1* is expressed by glial cells, mainly astrocytes and oligodendrocytes, while *Il-34* is expressed by neurons (Cahoy *et al.*, 2008; Mizuno *et al.*, 2011; Greter *et al.*, 2012; Wang *et al.*, 2012; Zeisel *et al.*, 2015; Kana *et al.*, 2019). Thus, their expressions are restricted respectively to the white and grey matter. Microglia in each region specifically depend on the ligand expressed there. This was shown by systemic injections of anti-CSF-1 and anti-IL-34 antibodies, leading to decreased microglial numbers in regions of white and grey matter respectively (Easley-Neal *et al.*, 2019). Compensation from the other ligand was nevertheless observed, as injections of both antibodies most often led to a greater

decrease in microglial numbers. Similar results were obtained in models of genetic ablation of the ligands in all astrocytes, oligodendrocytes and neurons thanks to the *Nestin*^{cre}*;Csf-1*$^{fl/fl}$ and *Nestin*^{cre}*;Il-34*$^{fl/fl}$ mice (Kana *et al.*, 2019; Badimon *et al.*, 2020).

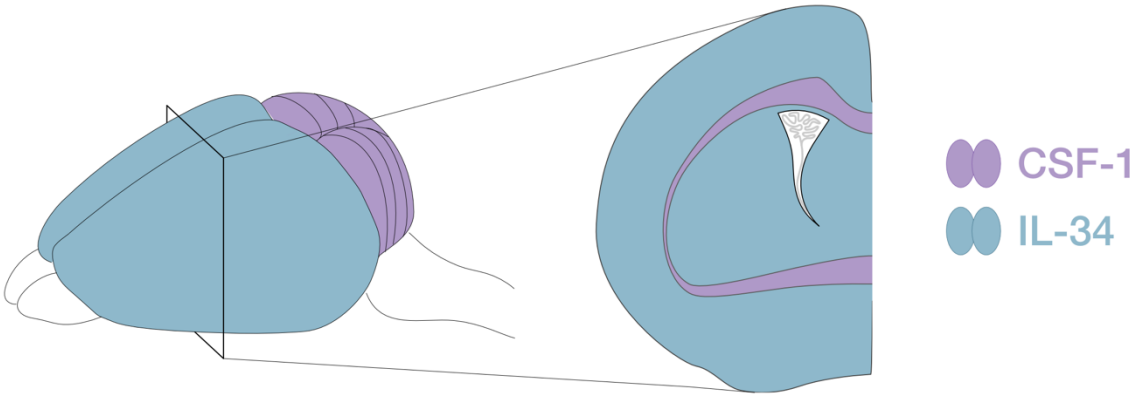

Figure 4.2 CSF-1 and IL-34 expression patterns in the adult forebrain

Schematic representation of patterns of expression of both CSF-1R ligands: IL-34, expressed by neurons, is abundantly found in grey matter; CSF-1, expressed mainly by oligodendrocytes as well as astrocytes, is mainly found in white matter regions of the forebrain and in the cerebellum. Microglia locally depend on the ligand accessible in its environment.

Importantly, CSF-1 and IL-34 respective signaling have been shown to differ, even though they both promote survival and proliferation (Chihara *et al.*, 2010). In microglia in particular, they possibly participate in the induction of an ATM/DAM profile: remaining microglia in *Csf-1* depleted cerebellum, a region mainly composed of white matter tracts and in which microglia principally depend on *Csf-1*, down-regulated genes associated to this profile (Kana *et al.*, 2019). Consistently with the protective role of ATM/DAM in response to demyelination and in remyelination, these processes were severely impaired in the *Csf1*$^{op/op}$ mice (Wylot *et al.*, 2019). On the contrary, microglia in the forebrain of IL-34 deficient mice showed up-regulation of ATM/DAM signature genes (Kana *et al.*, 2019). Thus, consistently with the white matter-specific location of ATM, differential signaling from CSF-1R ligands could modulate to some extent the local emergence or regulation of microglial states.

4.2. The CSF-1 receptor pathway: a key tool to deplete microglia

Depleting microglia has been challenging, but nevertheless allowed to unravel many functions of microglia and broaden our understanding of their contribution to normal brain development, homeostasis, as well as their role in neurodevelopmental disorders and neurological diseases. Plethora of depletion models exist (see Green, Crapser and Hohsfield, 2020; Bridlance and Thion, 2023), and their diversity illustrates the difficulty to obtain a specific, efficient and long-lasting depletion of microglia while limiting its off-target effects. Here, we will only focus on depletion models that target the CSF-1R pathway.

4.2.1. Genetic models

Genetic models with constitutive gene knock-out have been used to study microglial depletion, such as *Csfr1*$^{-/-}$, *Csf1*$^{op/op}$ or *Il34*$^{-/-}$ (Michaelson *et al.*, 1996; Erblich *et al.*, 2011; Greter *et al.*, 2012; Wang *et al.*, 2012). But because of the broad expression of the receptor and its ligands, and their essential functions, these models have important side effects. In *Csfr1*$^{-/-}$ mice, the absence of microglia is accompanied by the absence of most tissue macrophages, skeletal deformities, shortened lifespan, and neurodevelopmental abnormalities (Dai *et al.*, 2004; Erblich *et al.*, 2011). The overall microglial density in *Csf1*$^{op/op}$ mice has been reported to be similar to control or reduced by a third. Numbers of microglia in white matter tracts appear significantly decreased. Although less drastic than in *Csfr1*$^{-/-}$ mice, *Csf1*$^{op/op}$ mice also display brain abnormalities and morphologic defects (Michaelson *et al.*, 1996; Erblich *et al.*, 2011; Nandi *et al.*, 2012). In *Il34*$^{-/-}$ mice, microglial numbers are only partially reduced and other cells are affected, such as the resident skin macrophages or Langerhans cells (Greter *et al.*, 2012).

More subtle approaches were thus needed, and mice bearing flox alleles were generated for the receptor and its two ligands (Takasato *et al.*, 2004; Li *et al.*, 2006; Greter *et al.*, 2012; Wang *et al.*, 2012). Thus, the *Csf1r*$^{fl/fl}$ can be crossed to microglial cre lines to induce its specific deletion. This strategy has been used with *Sall1*^{CreER}*;Csf1r*$^{fl/fl}$ (Buttgereit *et al.*, 2016) and *Hexb*^{CreERT2}*;Csf1r*$^{fl/fl}$ mice (Masuda, Amann, *et al.*, 2020), with a respective efficiency varying across brain regions from 70% to 90% and of 60%. On the other hand, microglial regional dependence on each ligand allows both grey or white matter specific deletion of microglia using the *Nestin*^{cre};*Csf1*$^{fl/fl}$ and *Nestin*^{cre};*Il34*$^{fl/fl}$ (Kana *et al.*, 2019; Badimon *et al.*, 2020), with the *Nestin*^{cre} targeting all neurons, astrocytes and oligodendrocytes. Of note, the depletion is even

more drastic in all brain regions in *Nestin*^{cre};*Csf1*$^{fl/fl}$;*Il34*$^{fl/fl}$ (Kana *et al.*, 2019). Using more specific neuronal lines, Badimon *et al*. were even able to achieve a more restricted depletion: targeting D1 or D2 medium spiny neurons of the striatum led to a 50% decrease of microglial numbers in this region without impacting cortical microglia (Badimon *et al.*, 2020). Importantly, in these models, generation and life of other non-CNS macrophages are unaffected, while to our knowledge the presence and state of BAMs still need to be investigated.

An additional important model is the *Csf1r*$^{\Delta FIRE/\Delta FIRE}$ mice, in which a *Csf1r* enhancer is deleted (Rojo *et al.*, 2019). This leads to the absence of microglia from the brain parenchyma, of resident macrophages of the skin, kidney, heart and peritoneum, and differentially affects BAM populations (Munro *et al.*, 2020), while other macrophages and monocytes are unaffected. Importantly, these mice are healthy and fertile in a mixed B6CBAF1/C57BL\6J background, and do not display the strong developmental defects described in *Csf1r*$^{-/-}$ mice, indicating that they constitute a more specific and long-lasting model to explore microglial functions (McNamara *et al.*, 2023).

4.2.2. Pharmacological CSF-1R inhibitors

Pharmacological inhibitors of the CSF-1R injected or delivered non-invasively via food pellets have been broadly developed to deplete adult microglia, such as PLX3397 and PLX5622, the latter having a higher specificity and improved brain penetrance (Elmore *et al.*, 2014; Green, Crapser and Hohsfield, 2020). They allow for a rapid and very efficient depletion of microglia and can be administered during a controlled time-window. Of note, they also affect BAMs and bone-marrow derived monocytes (Spiteri *et al.*, 2022). Upon retrieval of the inhibitors, microglia rapidly repopulate the brain (see 4.3.1).

These CSF-1R inhibitors can also be given to pregnant dams, and efficiently deplete embryonic microglia (Lawrence *et al.*, under revision; Rosin, Vora and Kurrasch, 2018; Li *et al.*, 2020; Marsters *et al.*, 2020). Nevertheless, this treatment can affect lactation by depleting maternal macrophages essential for mammary gland development (O'Brien *et al.*, 2012), and it can impact pup survival following birth. For early postnatal depletion, direct subcutaneous injections of PLX3397 or PLX5622 during the first post-natal week allows for a lasting depletion of microglia (Li *et al.*, 2020; Favuzzi *et al.*, 2021; Gesuita *et al.*, 2022), while intraperitoneal injections of BLZ495 (200mg/kg) every two days from birth to P7 decreased microglial numbers predominantly in regions of white matter (Hagemeyer *et al.*, 2017).

4.2.3. Antibodies against CSF-1R, CSF-1 and IL-34

Injections of blocking antibodies has also been proposed to deplete microglia. Because they are circulating, possible side-effects occurring in periphery organs are yet to be investigated. Nevertheless, injections of an anti-CSF-1R antibodies in pregnant dams performed at E6.5 and E7.5 lead to a drastic depletion of microglia (Squarzoni *et al.*, 2014; Hoeffel and Ginhoux, 2015; Thion *et al.*, 2019). It also directly impacts myeloid progenitors and most macrophages. Repopulation then spans the first postnatal week (Squarzoni *et al.*, 2014; Hoeffel and Ginhoux, 2015; Thion *et al.*, 2019). On the other hand, as previously mentioned, injections of anti-CSF-1 and anti-IL-34 antibodies lead to depletion of white matter or forebrain microglia respectively, though to a lesser extent than with PLX3397 (Easley-Neal *et al.*, 2019).

4.3. Microglial depletion and repopulation

4.3.1. Repopulating microglia

In all models of acute microglial depletion and independently of their efficiency, microglia rapidly repopulate the brain (Green, Crapser and Hohsfield, 2020). For example, while microglial depletion can be drastically efficient (>99%) in a few days (7 days), microglia are back at their homeostatic densities within a week (or even show a transient phase of increased density)(**Figure 4.3**), both using a CSF-1R inhibitor (Elmore *et al.*, 2014) or targeting microglia with a diphtheria toxin-based system (Bruttger *et al.*, 2015). Several studies showed that microglia replenish the brain thanks to an intense proliferation of residual microglial cells, that were initially thought to transiently express *Nestin* (Elmore *et al.*, 2014), and without contribution from circulating monocytes (Elmore *et al.*, 2014; Bruttger *et al.*, 2015; Huang *et al.*, 2018; Zhan *et al.*, 2019; Hohsfield *et al.*, 2021). In particular, long-lasting depletion of microglia is followed by repopulation from the few remaining cells located in the ventricular zone and white matter regions. By local proliferation and suggested short-range migration, they replenish the brain following a wave-like pattern (**Figure 4.3**)(Hohsfield *et al.*, 2021).

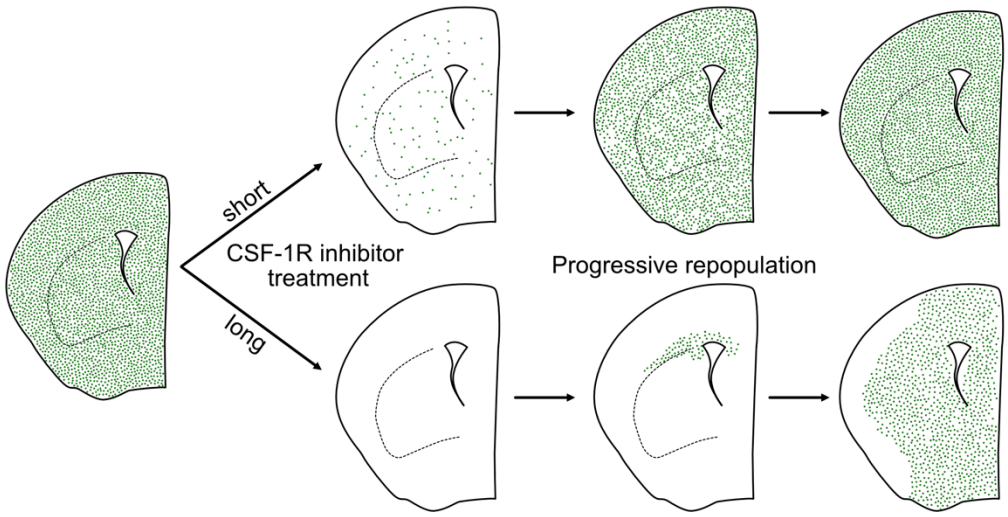

Figure 4.3 Microglial depletion & repopulation process

Schematic representation of different paradigms of microglial depletion and consequent repopulation: after treatment with CSF-1R inhibitors, like PLX3397, most microglia (green) are gone from the parenchyma. After shorter treatment (classical a week), few microglia remain dispersed, and progressively repopulate through active proliferation. After longer/stronger treatment, microglia are almost absent from the parenchyma but later repopulate in a wave-like pattern from white matter and ventricular regions. Summarizes the findings from (Elmore *et al.*, 2014; Zhan *et al.*, 2020; Hohsfield *et al.*, 2021)

Importantly, they re-establish their homeostatic region-specific densities, illustrating a fine regulation by the neural niche (Biase *et al.*, 2018). Microglial remarkable capacity to restore the whole population from a very restricted pool of remaining cells parallels their proliferative capacity seen in development and throughout life, when they self-maintain from few YS progenitors. This capacity nevertheless has limits, and successive depletion/repopulation phases show slower microglial repopulation (Najafi *et al.*, 2018).

4.3.2. Immature features of repopulating microglia

Repopulating microglia first display an immature morphology and profile: they are ameboid or poorly ramified, and lose the expression of canonical microglial markers like P2RY12, TMEM119 and SIGLEC-H. This is accompanied by a unique immature transcriptome signature that partially overlaps with that of neonatal P4 microglia (Zhan *et al.*, 2019). By 14 days of repopulation, microglia have recovered their highly ramified homeostatic morphology and the expression of homeostatic microglia signature genes (Elmore *et al.*, 2014; Zhan *et al.*, 2019, 2020).

More precisely, their transient immature transcriptome during early-repopulation was accompanied by the expression of *Axl* and *Clec7a* (Hohsfield *et al.*, 2021), core genes of the ATM profile, as well as Mac2 (*Lgals3*)(Zhan *et al.*, 2020), often associated to the ATM profile. This immature "progenitor-like" profile, sharing some similarities but not overlapping with the ATM profile, was further suggested to be present at very low-levels in the homeostatic brain and to be particularly resistant to CSF-1R inhibition (Zhan *et al.*, 2020). In line with this idea, retinal microglia have been shown to express ATM/DAM markers during development. This shift is dependent on Axl-regulated engulfment of apoptotic neurons (Anderson *et al.*, 2019, 2022), and is linked to a CSF-1R independency. Indeed, while depletion of microglia through CSF-1R inhibition was efficient in the brain, it was limited in the retina where the percentage of ATM was increased. Consistently, in the retina of the *Bax* knock-out model that limits neuronal apoptosis, less ATM were observed and depletion was much more efficient.

Interestingly, ATM as well as "progenitor-like" microglia from Zhan *et al*., have been shown to express *Csf-1* (**Figure 4.4**)(Li *et al.*, 2019; Zhan *et al.*, 2020; Anderson *et al.*, 2022), raising the possibility that intracrine signaling could allow them to become independent to environmental CSF-1R signaling.

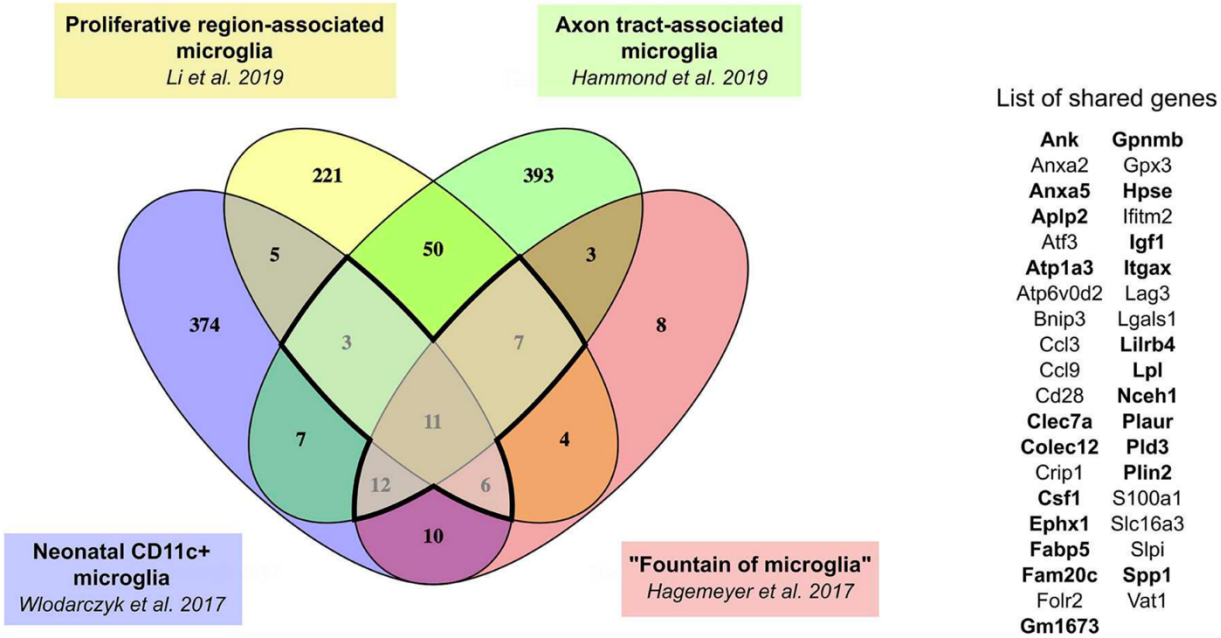

Figure 4.4 *Csf-1* expression is upregulated in ATM and DAM
Comparison of genes upregulated in four studies (Hagemeyer *et al.*, 2017; Wlodarczyk *et al.*, 2017; Hammond *et al.*, 2019; Li *et al.*, 2019) reveals a common signature for ATM of 39 genes upregulated in at least three of the studies (bold dark outline) which includes *Csf-1*. Genes also shared with the DAM signature are in bold. From Benmamar-Badel, Owens and Wlodarczyk, 2020.

4.3.3. Microglial depletion as a therapeutic approach?

Interestingly, microglial depletion/repopulation process is increasingly studied in the context of aging and disease (Priller and Prinz, 2019; Mahmood and Miron, 2022). Fast repopulation allows for the transient depletion of microglia, thus limiting their absence to a time-window where they could have detrimental effects, for example during acute injury (Rice *et al.*, 2015). Importantly, repopulating microglia can "reset" microglial population: in aging or after MIA in which microglia display altered transcriptomes, repopulating microglia came back to a more homeostatic profile and some synaptic and cognitive deficits were rescued in both cases (Elmore *et al.*, 2018; Ikezu *et al.*, 2021). Some CSF-1R inhibitors being already approved by the Food and Drug Administration (FDA) in context of glioblastoma, they are bringing hope for therapeutic development in other neurologic conditions. Yet, as mentioned in 1.1, microglial contribution to different pathologies can be both detrimental or protective and is highly dependent on the timing and context, so that the therapeutic use of CSF-1R inhibitors is still a complex path.

Aims of the study

Microglia, as immune cells of the brain, fascinatingly assume both immune and glial functions. In the course of discoveries of their diverse roles, microglia emerge as key actors of brain function and development. Importantly, their atypic origin and early entry in the brain allow them to mature within the developing parenchyma, in close interaction with neurons and before the generation of other glial cells. They are known to extraordinarily expand through proliferation and distribute themselves heterogeneously, before uniformly tiling the parenchyma later on. Along with a heterogeneous distribution, they were lately shown to display a great cellular heterogeneity lost in the adult microglial population. What drives their heterogeneous colonization and how it can be linked to their functions, is nevertheless poorly understood.

In this work, I first performed a longitudinal characterization of microglial distribution and proliferation in the developing brain, and investigated the role of the CSF-1R pathway in this process (Article 1). Next, I participated in a study characterizing a novel embryonic function of microglia in transient hotspots where they accumulate (Article 2). Last, through a review of the tools available to study microglia and BAMs during development (Review), we interrogate on their respective roles and future approaches available.

Overall, this work sheds new light on microglial colonization of the brain, its dependance on each CSF-1R ligands, and highlights how microglial heterogeneity can be linked to a novel microglial function in the embryonic brain. Importantly, it provides a new model for specific and local microglial depletion which we believe will be valuable for further study.

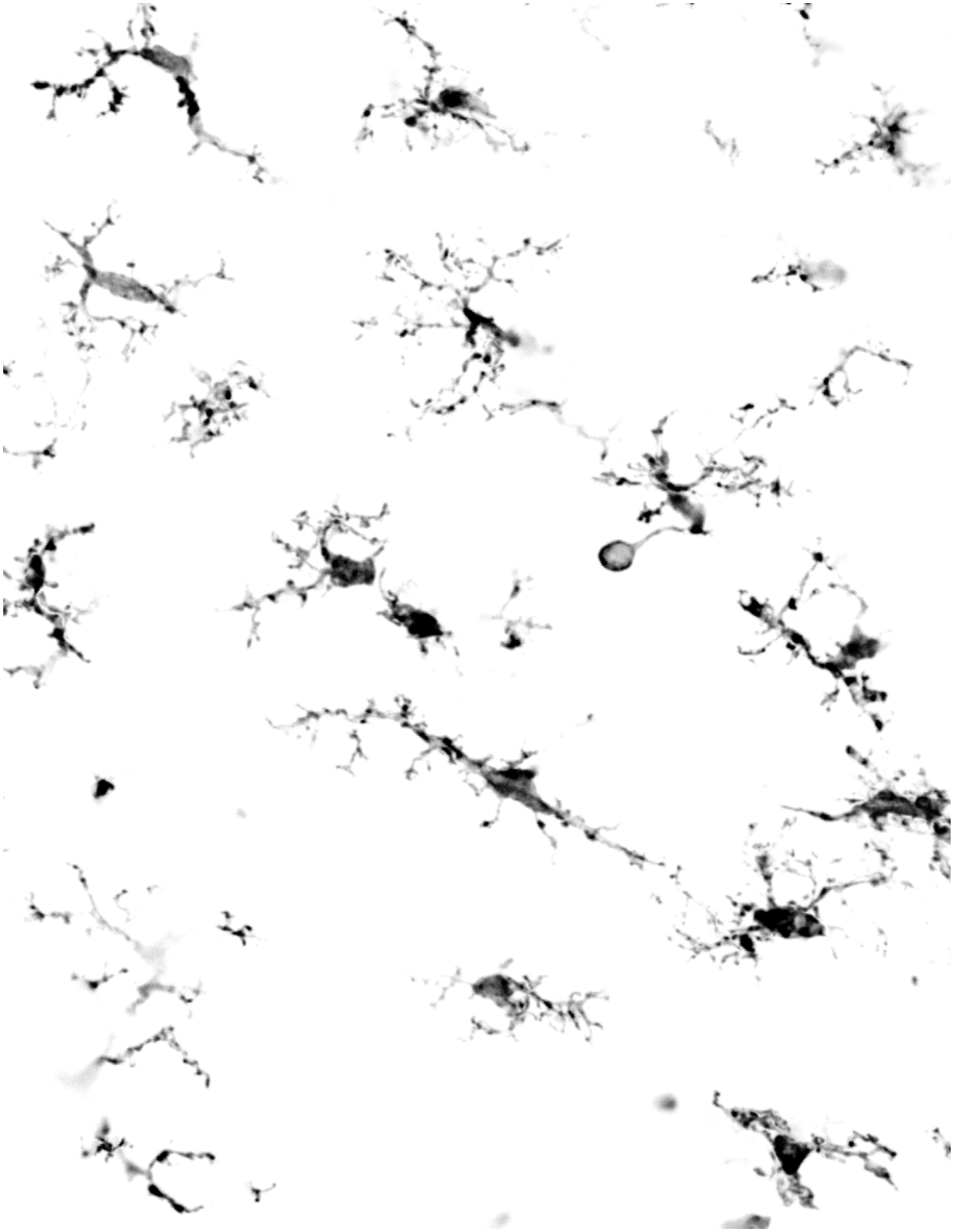

Microglia in the somatosensory cortex at P7.

RESULTS

Article 1

Microglial colonization is shaped by intrinsic and extrinsic CSF-1 during early forebrain development

Summary

Microglial colonization of the brain, known to result from intense proliferation of a restricted pool of progenitors, is still little understood. In particular, our knowledge of where, when and which microglia actually proliferate is fragmented. In addition, the CSF-1 receptor (CSF-1R) pathway regulates microglial survival and proliferation from embryogenesis up to adulthood, with its two ligands, the cytokines CSF-1 and IL-34, produced by the neural environment. Yet, how each ligand is involved in regulating microglial proliferation and numbers during development is only partially known.

Herein, we performed a detailed analysis of microglial proliferation and distribution during mouse forebrain development, and examining how the neural environment may regulate this pattern, either through neuronal activity or CSF-1 expression. We first highlighted the existence of two waves of microglial proliferation: a first global and intense phase during mid-embryogenesis, and a second postnatal phase which intensity and timing vary across forebrain regions. In addition, we found that some transient developmental hotspots of microglia were particularly proliferative. Using two-photon live-imaging on acute brain slices, we confirmed local proliferation and redistribution, but found no evidence of long-range migration. Collectively, our findings indicate that proliferation is an important driver of microglial colonization and contributes to its heterogeneous pattern.

Focusing on the cerebral cortex, we first tested during this second wave of proliferation the role of neuronal activity, which emerges at these developmental stages and is known to be monitored by microglia. We found that perturbations of neuronal activity, using genetic tools or modulations of sensory inputs, had no broad effect on microglial numbers and distribution. Next, we examined the roles of CSF-1, using conditional mutants in specific neural populations. Through distinct cre drivers, we showed that CSF-1 from both cortical progenitors and neurons is required for microglial embryonic colonization. More specifically, CSF-1 acts in a dose-dependent manner and has a remarkably local effect, without severely affecting other

populations of macrophages in the meninges. Consistently, CSF-1 cortical inactivation leads to a drastic absence of microglia, sparing other macrophages, only during embryogenesis, supporting a later role of IL-34, as previously reported. In parallel, we examined proliferative hotspots and observed that microglia displayed a distinct state in part characterized by high expression of *Csf-1*. Using conditional mutants, we revealed that autocrine CSF-1 production by microglia contributes to the intense proliferation in hotspots. Our findings thus highlight a dual contribution of local neural CSF-1 and microglial CSF-1 in regulating their early developmental distribution.

Altogether, our study sheds light on how microglia proliferate and distribute to colonize the brain as well as on their focal and cell-type dependency on CSF1. In addition, our conditional cortical mutants provide a groundbreaking tool to study the local and specific roles of microglia during prenatal cortical development and opens the path to further dissect the relative contributions of CSF-1R ligands.

Please note that this is a draft of the article, which needs further experiments and modifications before submission.

Microglial colonization is shaped by intrinsic and extrinsic CSF-1 during early forebrain development

Bridlance Cécile[1,2,3], Edmond Dupont[2], Sarah Viguier[1,2], Nicolas Olivié[1,2], Benjamin Mathieu[1], Sonia Garel[1,2,*,#] and Morgane Sonia Thion[1,2,*,#]

[1]Institut de Biologie de l'École Normale Supérieure (IBENS), École Normale Supérieure, CNRS, INSERM, Université PSL, 75005 Paris, France.

[2]Centre Interdisciplinaire de Recherche en Biologie (CIRB), Collège de France, CNRS, INSERM, Université PSL, Paris, France.

[3]Sorbonne Université, Collège Doctoral, F-75005 Paris, France.

*These authors contributed equally to this work.

[#]Corresponding authors: morgane.thion@college-de-france.fr (MST); sonia.garel@bio.ens.psl.eu (SG).

Keywords: microglia, development, colonization, neocortex, proliferation, cytokine, CSF-1R, CSF-1, IL-34.

Abstract

Microglia, the brain resident macrophages, are instrumental for cerebral development, function and homeostasis. Derived from yolk sac myeloid progenitors, these immigrants distribute in the brain following a stereotypical spatiotemporal pattern and expand through proliferation. They display a remarkable cellular and transcriptional heterogeneity during development. Some features of their heterogeneous distribution are highly conserved among mammalian species and have been associated to specific microglial developmental functions. However, the regulation of early microglial distribution and heterogeneity remains largely to be investigated. Herein, we showed that microglia display two dynamic broad waves of proliferation in the mouse developing forebrain, as well as transient hotspots of highly proliferative microglia, where they exhibit a specific state resembling Axon-Tract associated Microglia (ATM). Furthermore, we found that microglial broad colonization is not altered by early postnatal neuronal activity. Using conditional inactivation of *Colony Stimulating Factor 1 (Csf-1)*, we showed that embryonic cortical microglia critically rely on neural CSF-1, coming both from progenitors or post-mitotic neurons, and that the action of CSF-1 is transient, local and dose-dependent. In contrast, intrinsic microglial *Csf-1* specifically expressed by ATM contributes to sustained proliferation at developmental hotspots. Altogether, our work highlights that microglia rely on distinct, local and cell-type specific sources of CSF-1 to adopt their developmental distribution. In addition, our conditional cortical mutants provide a groundbreaking tool to study the local and specific roles of microglia during prenatal development and opens the path to further dissect the relative contributions of CSF-1R ligands.

INTRODUCTION

Microglia, the brain resident macrophages, play key roles in maintaining brain homeostasis. Through dynamic scanning of their environment (Nimmerjahn, Kirchhoff and Helmchen, 2005) and expression of an extensive set of receptors, called the "sensome" (Hickman *et al.*, 2013), microglia surveil the parenchyma and constitute the first line of defense of the brain. Beyond their immune functions, microglia constantly interact with the neural tissue, closely monitoring and modulating neuronal activity (Tremblay, Lowery and Majewska, 2010; Schafer *et al.*, 2012; Parkhurst *et al.*, 2013; York, Bernier and MacVicar, 2018; Badimon *et al.*, 2020; Umpierre and Wu, 2021). Importantly, microglia are also key actors of brain development (Thion, Ginhoux and Garel, 2018). In particular, they participate in synaptogenesis and synaptic pruning (Paolicelli *et al.*, 2011; Schafer *et al.*, 2012; Miyamoto *et al.*, 2016; Weinhard *et al.*, 2018), regulate cell death and survival of neurons, oligodendrocytes and their progenitors (Cunningham, Martínez-Cerdeño and Noctor, 2013; Shigemoto-Mogami *et al.*, 2014; Hagemeyer *et al.*, 2017; Nemes-Baran, White and DeSilva, 2020), participate in axon tract formation (Pont-Lezica *et al.*, 2014; Squarzoni *et al.*, 2014) and to the development and functionality of inhibitory circuits (Squarzoni *et al.*, 2014; Thion *et al.*, 2019; Favuzzi *et al.*, 2021; Gesuita *et al.*, 2022). In agreement with such a wide array of functions, microglial dysfunctions have been associated to almost all brain pathologies, from neurodevelopmental to neurodegenerative diseases (Mosser *et al.*, 2017; Li and Barres, 2018; Prinz, Jung and Priller, 2019; Thion and Garel, 2020).

In contrast to most brain cells that are locally generated, microglia arise from myeloid progenitors of the yolk sac and enter in the brain as early as Embryonic day (E)9 in mice, or Gestational Week (GW) 5 in humans (Monier *et al.*, 2007; Ginhoux *et al.*, 2010; Verney *et al.*, 2010; Menassa and Gomez-Nicola, 2018). Along development, microglial population progressively extend through proliferation (Alliot, Godin and Pessac, 1999; Dalmau *et al.*, 2003; Nikodemova *et al.*, 2015; Matcovitch-Natan *et al.*, 2016; Adaikkan *et al.*, 2019; Li *et al.*, 2019; Menassa *et al.*, 2022; Barry-carroll *et al.*, 2023), but where and when do microglia proliferate remains poorly characterized. After the closure of the blood-brain barrier occurring around E14.5 in mice, microglia self-renew throughout life in steady-state conditions, without contribution from circulating cells (Ginhoux *et al.*, 2010; Kierdorf *et al.*, 2013). Microglia progressively mature in the brain, in close interaction with their neural environment (Matcovitch-Natan *et al.*, 2016; Bennett *et al.*, 2018; Thion *et al.*, 2018; Stogsdill *et al.*, 2022). While they homogeneously tile the brain parenchyma in the adult and maintain appropriate

densities across regions (Askew *et al.*, 2017; Tay *et al.*, 2017; Biase *et al.*, 2018), their colonization follows a highly stereotypical spatiotemporal pattern with conserved features amongst mammalian species (Swinnen *et al.*, 2013; Squarzoni *et al.*, 2014; Menassa *et al.*, 2022). Notably, microglia are excluded from the developing cortical plate and accumulate in several hotspots (Swinnen *et al.*, 2013; Squarzoni *et al.*, 2014; Hattori *et al.*, 2020; Nemes-Baran, White and DeSilva, 2020). This developmental heterogeneity in location comes along an important morphological and cellular diversity of developing microglia (Hammond *et al.*, 2019; Li *et al.*, 2019, 2022; Masuda *et al.*, 2019; Hope *et al.*, 2020). In particular, in the postnatal white matter, ameboid microglia have been transiently found to be in a peculiar state expressing a specific set of genes including *Spp1*, *Lgals3*, *Gpnmb*, *Clec7a*, *Itgax* or *Igf1* (Hagemeyer *et al.*, 2017; Wlodarczyk *et al.*, 2017; Hammond *et al.*, 2019; Li *et al.*, 2019; Silvin *et al.*, 2022). Described in several studies, these microglia will thereafter be referred to as Axon-Tract associated Microglia, or ATM. Importantly, microglial heterogeneity in distribution and transcriptional states have been linked to specific developmental functions. In particular, their exclusion from the cortical plate have been implicated in proper differentiation of cortical neurons (Hattori *et al.*, 2020) while ATM have been shown to participate in the regulation of oligodendrogenesis and appropriate myelination (Hagemeyer *et al.*, 2017; Wlodarczyk *et al.*, 2017; Nemes-Baran, White and DeSilva, 2020). Thus, their exceptional capacity to proliferate and generate a long-lived, self-renewing population from a restricted pool of progenitors as well as their finely regulated pattern of distribution in the parenchyma appear crucial for proper microglial shaping of the developing brain. Yet, how early microglial distribution and heterogeneity are regulated and the potential contributions of the neural tissue to these complex processes, remain largely to be investigated.

One key signaling pathway for microglial development and maintenance is the Colony Stimulating Factor-1 Receptor (CSF-1R) pathway. Importantly, it is also shared with all resident macrophages, and in particular with the other Central Nervous System (CNS) macrophages. These Border Associated Macrophages (BAMs) can be found at the interfaces of the brain, such as the meninges, choroid plexus and perivascular space (Lee *et al.*, 2021) and some share a close ontogeny with microglia (Goldmann *et al.*, 2016; Mrdjen *et al.*, 2018; Kierdorf *et al.*, 2019; Utz *et al.*, 2020; Mildenberger, Stifter and Greter, 2022). Microglia and BAMs are the main populations expressing the CSF-1R in the CNS, and their survival, proliferation and recruitment rely on its signaling. A promising model, the *Csf1r*$^{\triangle FIRE\triangle/FIRE}$ mouse line, has recently been published and shown to lack microglia while sparing most BAMs and other tissue resident macrophages (Rojo *et al.*, 2019; Munro *et al.*, 2020; McNamara *et al.*,

2023). Instead, commonly used depletion strategies involve CSF-1R inhibitors and thus target all macrophages (Eme-Scolan and Dando, 2020; Green, Crapser and Hohsfield, 2020; Bridlance and Thion, 2023), making it difficult to untangle the relative contributions of BAMs and microglia to brain development and homeostasis (Goldmann *et al.*, 2016; Kierdorf *et al.*, 2019; Van Hove *et al.*, 2019; Mildenberger, Stifter and Greter, 2022). The CSF-1R ligands known so far are two cytokines, CSF-1 and interleukin 34 (IL-34), with overlapping yet slightly different functions (Stanley and Chitu, 2014). In the adult brain, CSF-1 is mainly secreted by astrocytes and oligodendrocytes, and required for white matter and cerebellar microglia, while IL-34 produced by neurons is important for grey matter microglia (Wei *et al.*, 2010; Nandi *et al.*, 2012; Easley-Neal *et al.*, 2019; Kana *et al.*, 2019; Badimon *et al.*, 2020). In addition, ATM have been suggested to express *Csf-1* (Hristova *et al.*, 2010; Hagemeyer *et al.*, 2017; Wlodarczyk *et al.*, 2017; Hammond *et al.*, 2019; Li *et al.*, 2019; Benmamar-Badel, Owens and Wlodarczyk, 2020), though the role of this potential intrinsic CSF-1 signaling has not been investigated so far. Both ligands can be detected in the embryonic brain (Wei *et al.*, 2010; Greter *et al.*, 2012; Nandi *et al.*, 2012), but their location and sources during early development remain to be fully characterized. Last, microglia have been shown to rely on CSF-1 during embryonic development (Easley-Neal *et al.*, 2019), but the early postnatal contribution of IL-34 remains controversial (Greter *et al.*, 2012; Wang *et al.*, 2012).

Here, we performed a broad characterization of microglial distribution and proliferation in several regions of the murine forebrain, thereby completing the information provided by previous studies (Dalmau *et al.*, 2003; Swinnen *et al.*, 2013; Nikodemova *et al.*, 2015; Barry-carroll *et al.*, 2023). Combining analysis of proliferation on fixed tissue and live-imaging through development, we showed that microglial colonization mostly relies on local proliferation, which follows two waves: one global occurring during mid-embryogenesis, while a second burst around the end of the first postnatal week displays more regional heterogeneity. In the cortex, local proliferation allows for a redistribution of microglia throughout the cortical layers, while microglial broad numbers are unaffected by early postnatal neuronal activity. In parallel, highly proliferative microglia transiently accumulate in developmental hotspots. Using genetic models of conditional inactivation of *Csf-1* or *Il-34* in different neural populations, we interrogated the CSF-1R ligands sources and their contribution to early microglial colonization. We showed that embryonic microglial survival and proliferation transiently and locally rely on CSF-1 from both progenitors and neurons, independently of IL-34. In parallel, intrinsic microglial *Csf-1*, associated to an ATM-like state found in developmental hotspots, is involved in their sustained proliferation. Our study thus sheds new light on how microglia colonize the

developing forebrain, and deepens our understanding of the CSF-1R pathway. Most importantly, it also provides a new model for local, transient and specific depletion of cortical microglia, not affecting BAMs, which should be instrumental to investigate and disentangle microglial versus BAMs embryonic functions.

RESULTS

Microglial colonization of the brain relies on two broad dynamic waves of proliferation

To investigate how microglia distribute and proliferate during forebrain development, we characterized microglial density and proliferation along embryogenesis (embryonic day (E)12.5, E14.5, E16.5 and E18.5), in pups (postnatal day (P)0, P3, P5, P7, P9 and P14), juveniles (P20) and adults (P60). Using *Cx3cr1*$^{gfp/+}$ heterozygous mice (Jung *et al.*, 2000), we focused on the somatosensory cortex (SSC) or presumptive SSC, the hippocampus, the striatum and the PreOptic Area (POA) (**Figure 1A**) and excluded BAMs from this analysis (**Figure S1A and S1B**). Proliferation was assessed using Ki-67 immunofluorescence which labels cells in the different cell cycle phases except the resting G0 phase (**Figure 1B**). At stages where a large proportion of microglia were positive for Ki-67 (namely E14.5, P7 and P9), we also performed a single injection of 5-ethynyl-2'-deoxyuridine (EdU) to tag cells in replication and further collected the tissue two hours following injection. EdU revelation combined with Ki-67 labeling allowed us to confirm that Ki-67-positive cells were indeed dividing, with roughly half of Ki-67-positive cells also labelled by EdU (**Figure 1C, S1C and S1D**).

At E12.5, while microglial densities across our regions of interest was low, the majority of microglia were actively proliferating (around 60%) (**Figure 1D and 1F**) and a large portion of microglia (around 35%) still displayed a sustained proliferation at E14.5 (**Figure 1D and 1F**). Their proliferation drastically decreased to reach an average of 5% by E16.5 (**Figure 1D and 1F**). In agreement with brain expansion, microglial numbers increased over this period while their density remained stable (**Figure S2A-C**). Following this early embryonic proliferative wave, we observed a second proliferative wave around P9, which timing and intensity vary across regions (**Figure 1D and 1F**). Microglial density peaked at P14 (**Figure 1E and 1G**) and further decreased after the 3rd postnatal week to reach adult levels (**Figure 1E and 1G**). Interestingly, in the POA, microglia followed a different trajectory: postnatal proliferation remained at low levels, solely compensating for the area extension, and thus maintaining a stable density over time with little refinement at adult stage. Consistently with what has been described in humans (Menassa *et al.*, 2022), we observed no differences in microglial numbers nor proliferation in females and males (data not shown). Thus, microglial expansion follows two waves of proliferation: a first global and intense phase during mid-neurogenesis, and a second postnatal phase which intensity and timing vary across forebrain regions.

Cortical microglia locally proliferate and redistribute but their numbers are unaffected by early postnatal modulations of neuronal activity

We then focused on the somatosensory cortex in which microglial pattern of colonization is highly stereotypical and heterogeneous (Arnoux *et al.*, 2013; Squarzoni *et al.*, 2014; Hattori *et al.*, 2020). During early embryogenesis, microglial proliferation is homogenous while they remain excluded from the cortical plate until E16.5. They do accumulate in the intermediate zone before progressively colonizing the deep layers (**Figures 2A, 2B and 2C**). At postnatal stages, microglial proliferation dropped at P14 concomitantly to a homogenization of their distribution across cortical layers (**Figures 2A, 2B and 2C**). While increases in microglial densities thus appear to be associated to local proliferation (**Figure 2B and 2C**), we wondered if long-range migration could redistribute microglia across different forebrain regions. We thus performed two-photon live imaging on brain slices at different timepoints. Consistently with previous work (Swinnen *et al.*, 2013), we found that microglia are highly mobile at E14.5 in the neocortex contrary to meningeal BAMs (**Figure 2D and 2E**) or striatal microglia at the same age (data not shown). Interestingly, we witnessed a few microglial cells crossing the cortical plate at E14.5, highlighting redistribution of microglia within the cortex through local migration in absence of coordinated migratory patterns (**Figure 2D**). Their sustained cortical mobility was further decreased by E16.5 (data not shown). Furthermore, we found that microglial cell bodies show little displacement by P7, while their processes actively scan their surrounding environment, similarly to what has been observed in adulthood (Nimmerjahn, Kirchhoff and Helmchen, 2005; Haynes *et al.*, 2006)(data not shown).

Interestingly, microglial proliferation is intense during the end of the first postnatal week (**Figure 2B**), when activity switches from spontaneous to sensory-evoked (Molnár, Luhmann and Kanold, 2020). As microglia finely sense neuronal activity (Nimmerjahn, Kirchhoff and Helmchen, 2005; Schafer *et al.*, 2012), we thus wondered if this remodeling in neuronal activity could shape microglial colonization pattern, *i.e.* their numbers and distribution. We first modulated sensory inputs coming from the whisker pad by performing either unilateral infraorbital nerve section (ION) at P1, which impairs the formation of the barrels (White *et al.*, 1990) (**Figure S2D and S2G**), as well as daily bilateral plucking of the whiskers. These did not induced major changes in microglial numbers (**Figure 2F and 2G**), nor distribution (**Figure S2E**) within the SSC at P7 or at P14 following ION (**Figure S2F, S2H and S2I**). We then used genetic models and overexpressed excitatory Designer Receptor Exclusively Activated by a Designer Drugs (DREADDs)(Roth, 2016) in all excitatory cortical neurons using the *Emx1*$^{cre/+}$

mouse line. We injected clozapine-N-oxide (CNO) twice a day in our mutants and their control littermates to control for possible off-target effects of CNO injections. After stimulation between P5 and P7, the numbers and distribution of microglia in the SSC appeared unchanged in this context of cortical hyperexcitability (**Figure 2H**). Altogether, this suggests that early microglial colonization is mainly shaped by local waves of proliferation rather than the surrounding neuronal activity.

Highly proliferative microglia accumulate in developmental hotspots

In parallel to these canonical regions of interest, we studied microglial dynamics in hotspots where they form transient and specific accumulations, a feature conserved across mammalian species (Rio-Hortega, 1932; Kershman, 1939; Hristova *et al.*, 2010; Verney *et al.*, 2010; Lawrence *et al.*, under revision). We focused on two specific microglial hotspots: the cortico-striatal-amygdalar boundary (CSA)(**Figure 3A**), and the early dorsal white matter (EDWM), located in the cingulum bundle, a part of the corpus callosum located below the anterior cingular cortex (**Figure 3I**). While microglia appear mostly heterogeneously scattered through the parenchyma at E12.5, ameboid microglia accumulate at the CSA at E14.5, spanning the whole dorso-ventral axis (**Figure 3A**). Although most microglia are ramified in the region by E16.5, few ameboid microglia accumulate at the lateroventral tip of the striatum during the first postnatal week. Their numbers are variable during this period and this hotspot is no further present by P14 (**Figure 3D**). In parallel, ameboid microglia start to accumulate at birth in the EDWM accumulation, peak in numbers by the end of the first postnatal week, and are further undetectable by P14 (**Figure 3I and 3L**). In both regions, accumulating microglia displayed a important proliferative capacity relative to neighboring regions, and the amount of proliferation at a given timepoint was correlated to the number of ameboid microglia (**Figure 3B, 3D, 3J and 3L**).

Importantly, it was shown that microglia accumulating at the CSA at E14.5 display features resembling postnatal ATM (Lawrence *et al.*, under revision). ATM have also been described in the developing corpus callosum, and are thus found in the EDWM accumulation (Hagemeyer *et al.*, 2017; Wlodarczyk *et al.*, 2017; Hammond *et al.*, 2019; Li *et al.*, 2019). We confirmed in both regions that a high proportion of accumulating microglia were Spp1-positive, an established core marker of ATM (**Figure 3E and 3M**). Focusing on the CSA at E14.5 and EDWM at P7, when microglia were highly proliferative in both regions, we wondered if microglial proliferation at the hotspots was specific to their ATM profile. By performing EdU

injections, we found that Spp1-positive microglia were more proliferative than Spp1-negative microglia in both hotspots (**Figure 3C, 3F, 3K and 3N**).

Last, coherent with microglial accumulation and active proliferation at these hotspots, we wanted to verify that they could be "fountains of microglia", *i.e.* reservoirs where microglia would proliferate before fueling the parenchyma. While two-photon live imaging on brain slices at E14.5 at the CSA confirmed microglial proliferation at these hotspots, we observed little or no migration towards the neighboring regions (**Figure 3G and 3H**). Similarly, focusing on P7, our preliminary experiments suggest that EDWM microglia do not redistribute across adjacent regions. Thus, our data show that these hotspots of accumulating ameboid microglia in the developing brain display a sustained proliferation, in part associated to their ATM profile. Contrary to what could be expected, microglia nevertheless do not appear to migrate away from the CSA, and this needs to be further investigated for the EDWM.

Local cortical CSF-1 is essential for embryonic microglia but not for meningeal BAMs

Apart from neuronal activity sensed by microglia, there are numerous pathways involved in neuron-microglia communication. We investigated how CSF-1R signaling from the neural environment could regulate microglial brain colonization. It has been shown that both ligands are expressed in the embryonic brain as early as E12.5, with a higher abundance of *Il-34* mRNA, and that their expression is maintained in the adult (Greter *et al.*, 2012; Nandi *et al.*, 2012). Nevertheless, little is known about which cell types are expressing either *Il*-34 or *Csf-1* during this developmental time window.

We took advantage of a publicly available dataset of single-cell RNA sequencing of the neocortex throughout corticogenesis, spanning embryogenesis up to early postnatal stages (Di Bella *et al.*, 2021). Through reanalysis of this dataset, we found that *Csf-1* is expressed at low levels in progenitors across development, as well as in migrating and immature neurons from E14 onwards (**Figure 4A**). At early postnatal stages, it is expressed by oligodendrocytes and more strongly by astrocytes. *Il-34* instead is mainly found after E18.5 in mature neurons of deep cortical layers (**Figure 4B**). Of note, apart from microglia, we found no expression of *Csf-1r* throughout cortical development except for very low levels in P1 intermediate precursor cells (**Figure S3A**).

Using genetic tools, we thus conditionally inactivated *Csf-1* in all progenitors and excitatory neurons of the neocortex using the $Emx1^{cre}$; $Csf1^{fl/fl}$ mice (**Figure 4C**). This led to a drastic depletion of microglia at E14.5 specifically in the neocortex while microglia in adjacent

regions such as the CSA or the neighboring striatum remained unaffected (**Figure 4D, 4E, S3C and S3D**). Interestingly, *Emx1^{cre}; Csf1$^{fl/+}$* heterozygous mice displayed an intermediate phenotype, highlighting a dose-dependent effect of neural CSF-1 (**Figure 4E**). This depletion was highly specific to microglia, with no effect on the number of meningeal BAMs (**Figure 4F**). The local absence of microglia from the neocortex was already present at E12.5 (**Figure 4G and 4I**), although a very scarce number of cortical microglia expressed cleaved-caspase 3, suggesting that cell death could be involved in their later disappearance (**Figure S3E**). Moreover, it suggested that some microglial progenitors could invade the brain parenchyma even in absence of neural CSF-1. Lack of microglia at E14.5 was later followed by a progressive repopulation, completed by P7 (**Figure 4G and 4I**). Early repopulating microglia displayed a less ramified morphology and little or no expression of P2RY12, the latter being associated to canonical markers of mature homeostatic microglia, suggesting that neural CSF-1 could modulate microglial differentiation and maturation once they reach the brain parenchyma (**Figure 4H**). In addition, inactivation of *Csf-1* only in cortical neurons using *Nex1^{cre}; Csf1$^{fl/fl}$* mice tended to decrease the number of microglia specifically in the intermediate zone and subplate, but not in the ventricular zone where apical progenitors are located (**Figure S3F-H**). Last, preliminary results suggest that inactivation of *Il-34* from the neocortex in *Emx1^{cre}; Il34$^{fl/fl}$* mice has no effect on embryonic microglia (**Figure S3J-L**). Importantly, the number of BAMs in the meninges were not affected in both conditions (**Figure S3I and S3M**).

Altogether, our data show that embryonic microglia drastically depend on extrinsic CSF-1 from both progenitors and neurons, but not on IL-34, and that CSF-1 action is extremely local and dose-dependent. On the contrary, meningeal BAMs were unaffected, suggesting that their survival and recruitment are most probably locally regulated independently of signaling from the underlying brain parenchyma.

Neural and microglial *Csf-1* both contribute to the regulation of microglial proliferation

We further wondered if neural *Csf-1*, found to be essential for embryonic microglia, could also impact their proliferation *in vivo*. We thus took advantage of our *Emx1^{cre}; Csf1$^{fl/+}$* heterozygous animals, in which CSF-1 levels are mildly impacted and reduced microglial density are found in the neocortex. We monitored microglial proliferation through EdU injections and found that the number of EdU positive microglia tended to be decreased in these animals as compared to controls (**Figure 5A and 5B**). While reduced microglial proliferation probably accounts in part for their altered density in heterozygotes, we also found an increase in the proportion of cleaved-

caspase 3 positive microglia, coherent with an effect of CSF-1 on survival (**Figure S4A and S4B**).

In addition to extrinsic neural CSF-1, we aimed at investigating the role of intrinsic microglial CSF-1. Indeed, as previously mentioned, *Csf-1* belongs to ATM core genes (Hagemeyer *et al.*, 2017; Wlodarczyk *et al.*, 2017; Hammond *et al.*, 2019; Li *et al.*, 2019; Benmamar-Badel, Owens and Wlodarczyk, 2020)(**Figure 5A, 5C, S4C and S4D**). Using RNAscope experiments, we confirmed that ameboid microglia at the CSA at E14.5 and in the EDWM (as well as subcortical white matter) at postnatal stages express *Csf-1*, in contrast to adjacent ramified microglia that lacked *Csf-1* transcripts (**Figure 5D and 5E**). To investigate the role of intrinsic *Csf-1*, we used $Cx3cr1^{creER};Csf1^{fl/fl}$ mice to inactivate *Csf-1* in all microglia and macrophages upon tamoxifen injections, as confirmed by RNAscope (**Figure S4E and S4F**). Proliferation was then assessed through EdU labelling and administration of tamoxifen at E12.5 led to a partial decrease in microglial *Csf-1*, and a specific reduction of the proportion of EdU-positive microglia at the CSA (**Figure 5F and 5G**). When microglial *Csf-1* inactivation was performed at P3, it triggered a significant decrease of microglial *Csf-1* and of EdU-positive microglia at the EDWM (**Figure 5H and 5I**). Importantly, in this context, microglial proliferation in the SSC was unchanged, coherently with microglial expression of *Csf-1* being restricted to ameboid microglia in the accumulations and other white matter regions, matching Spp1 pattern of expression (**Figure S4G and S4H**). Intrinsic *Csf-1* expression was not necessary for microglial expression of Spp1 (**Figure 5F and 5I**), suggesting *Csf-1* is neither required for the induction of the ATM profile nor for their accumulation at the hotspots. Finally, *Spp1* and *Gpnmb*, two ATM signature genes known to promote proliferation in other contexts, were not implicated in microglial proliferation at the CSA at E14.5, as assessed by analyses of full mutants for these genes (data not shown).

Overall, our data suggest that in addition to extrinsic neural CSF-1, which is locally needed for microglial survival and proliferation, intrinsic CSF-1 signaling is specific to ameboid microglia accumulating at the hotspots and can regulate in part their proliferation. Taken together, our study sheds new light on how microglia colonize the brain and on the modes of action of CSF-1, but also provide a new model of local, transient and specific microglial depletion.

DISCUSSION

Microglia are observed in both the murine and human brain parenchyma very early on during development, coincident with the beginning of neurogenesis. During development, they have been shown to be highly proliferative through immunostaining (Alliot, Godin and Pessac, 1999; Dalmau *et al.*, 2003; Verney *et al.*, 2010; Swinnen *et al.*, 2013; Menassa and Gomez-Nicola, 2018; Barry-carroll *et al.*, 2023) or single-cell RNA sequencing studies (Hammond *et al.*, 2019; Li *et al.*, 2019; La Manno *et al.*, 2021), which is coherent with microglial population being generated from a restricted pool of progenitor cells that settle in the parenchyma early on. By performing a longitudinal study of murine microglial proliferation along development and in different regions of the forebrain, we here highlighted that early microglial proliferation is not linear. Similarly to what has been observed in developing human fetuses (Menassa *et al.*, 2022), microglia undergo dynamic phases of expansion. We identified an early phase of intense and global proliferation, followed by an arrest in proliferation before birth. Between E16.5 and birth, when microglial proliferation is reduced, we showed that it is correlated to decreased microglial densities across regions. This suggests that, during this phase of brain expansion that induces microglial dilution in the absence of proliferation, entry of microglia in the brain parenchyma is scarce or absent. We observed a second postnatal phase of proliferation which timing and intensity depend on the region observed. After the second postnatal week, proliferation is greatly reduced and microglial densities progressively decrease to reach adult levels, as previously described and thought to be mediated by microglial death (Nikodemova *et al.*, 2015; Hope *et al.*, 2020; Menassa *et al.*, 2022). In parallel, we showed that the transient hotspots of white matter where ameboid microglia accumulate during development (Kershman, 1939; Hristova *et al.*, 2010; Verney *et al.*, 2010) actually display a sustained proliferation.

What drives microglial proliferation still remains to a large extent unknown: shown to be independent from surrounding cell death or cell proliferation (Hope *et al.*, 2020), little is known about what induces the different proliferative waves as well as the regional disparities that we and others have highlighted (Dalmau *et al.*, 2003; Hope *et al.*, 2020). In this context, it is interesting to stress out that perturbations of neuronal activity, which changes in a region specific manner during crucial phases of microglial development, had no broad effect on microglial numbers nor distribution even though microglia have been shown to respond to patterns of activity in other contexts (Iaccarino *et al.*, 2016). Instead, both through *in vitro* (Stanley and Chitu, 2014) and *in vivo* overexpression studies (De *et al.*, 2014), CSF-1 has been known to promote microglial proliferation. Our study suggests that CSF-1 indeed regulates

microglial proliferation in physiological conditions, in a dose-dependent manner. In addition, we showed that the sources of neocortical CSF-1 are mainly progenitors, as well as immature neurons, coherent with our reanalysis of available single-cell datasets (Di Bella *et al.*, 2021). We found that CSF-1 action is extremely local, suggesting that circulating CSF-1, found in the blood early on and throughout life (Stanley and Chitu, 2014), is not sufficient for microglial maintenance at embryonic stages.

In our *Emx1^{cre}; Csf1$^{fl/fl}$* model, microglia are absent from the neocortex at E14.5, which could either result from their incapacity to reach the parenchyma, because of lack of a CSF-1 chemoattractant effect, or because they do not survive without CSF-1. Nevertheless, few progenitors are able to reach the brain parenchyma as we found some microglial cells in the neocortex at E12.5. Interestingly and consistently with previous findings (Nandi *et al.*, 2012; Easley-Neal *et al.*, 2019; Kana *et al.*, 2019), CSF-1 is only transiently essential to microglia, and their drastic depletion in the *Emx1^{cre}; Csf1$^{fl/fl}$* mice is followed by microglial progressive repopulation of the neocortex at postnatal stages, possibly migrating from neighboring regions. The ameboid morphology and lack of P2RY12 expression of microglia in the early phase of repopulation is reminiscent of repopulating microglia following depletion through CSF-1R inhibitors (Elmore *et al.*, 2014; Zhan *et al.*, 2020). This signature is commonly associated to "immature" states of microglia, raising the question of the role of CSF-1 signaling in microglial maturation and acquisition of homeostatic signature. How these microglia are altered and if they recover or not at later stages is currently under investigation in part through scRNA-seq analysis. In parallel, coherent with the little expression of *Il-34* found in cells of the parenchyma during brain development, our *Emx1^{cre};Il-34$^{fl/fl}$* model suggests that IL-34 is not required for embryonic microglia proliferation and survival, in good agreement with the absence of effect observed at birth in full *Il-34* knockout (Greter *et al.*, 2012). Other non-neural sources of both *Csf-1* and *Il-34*, such as pericytes or endothelial cells, could nevertheless marginally contribute to microglial maintenance and remain to be investigated.

In parallel, the field lacks specific and efficient tools to study and deplete microglia (Bridlance and Thion, 2023), most of them displaying important side effects or targeting both microglia and BAMs. Here, our study provides a new model for specific microglial depletion that is local and transient. This is promising to investigate local roles of microglia, but also to decipher if BAMs contribute to some functions previously attributed to microglia. In our model, while no striking defect could be observed in corpus callosum fasciculation or myelination in the cortex at P14 (data not shown), we are currently investigating, using scRNA-seq, how the

different cell populations could be affected by the transient absence of microglia in the neocortex.

Last, further than neural *Csf-1*, we showed that intrinsic microglial *Csf-1*, associated to the ATM profile found in developmental hotspots, is also important for their sustained proliferation. This surprising finding suggests ATM-like state could allow microglia to be independent from surrounding sources of neural CSF-1, to increase their proliferation and density. While microglial recruitment and induction of their ATM profile is still little understood, it is thought to be locally regulated by their microenvironment and linked to specific functions played by these cells in the hotspots, such as maintenance of tissue integrity at the CSA (Lawrence *et al.*, under revision) or engulfment of OPCs in the EDWM (Nemes-Baran, White and DeSilva, 2020). These functions could require their increased density at these specific developmental hotspots. Similarly, Disease-Associated Microglia (DAM), which share many characteristic with ATM, including *Csf-1* expression (Keren-Shaul *et al.*, 2017), could potentially use the same mechanisms to expand in neurodegenerative conditions. Microglial intrinsic expression of *Csf-1* also raises the intriguing question of the disappearance of these hotspots. Though our study suggests that microglia do not massively migrate away from the CSA at E14.5 or EDWM at P7, this might be happening later on, a feature that we are further investigating. If so, this would mean that ATM could then turn on a homeostatic profile, and loss their core genes expression, or undergo cell death, since very few ATM can be detected later on. Indeed, microglia in both hotspots studied are highly phagocytic (Lawrence *et al.*, under revision; Hagemeyer *et al.*, 2017; Li *et al.*, 2019; Nemes-Baran, White and DeSilva, 2020), which might contribute to their elimination, as observed in the case of remyelinating microglia (Lloyd *et al.*, 2019) or as suggested during zebrafish development in a recent study (Gordon, Schafer and Smith, 2023).

Overall, our study highlights the broad waves and hotspots of proliferation enabling microglia to acquire their stereotypical pattern of distribution, essential for their developmental functions in the forebrain. We furthermore reveal that such pattern is regulated by distinct sources of CSF-1, of both neural and microglial origin, that jointly act at short range, providing key insights on how important immune cells colonize the brain during a critical developmental time window.

Limitations of the study

Our study provides a characterization of microglial proliferation and densities in different regions of the brain through development as well as the implication of local expression of CSF-1, a ligand of the CSF-1 receptor, which signaling is required for microglial survival and proliferation. Nevertheless, microglia being highly sensitive to the environment, such as the maternal environment during prenatal life, environmental stress factors or the gut microbiota, we believe that the global pattern of microglial colonization could be variable amongst conditions, genetic background or animal facilities. In addition, while we do not observe overt changes in heterozygous *Cx3cr1*$^{gfp/+}$ mice compared to control animals, this mutation might alter their pattern of brain colonization. Nonetheless, our findings shed light on how microglia proliferate and distribute to colonize the brain as well as on their focal and cell-type dependency on CSF-1.

MATERIAL AND METHODS

EXPERIMENTAL MODELS

Mouse Lines

All animals were housed in a 12 h light-dark cycle at constant temperature and humidity with ad libitum access to food and water. Both males and females were used in this study. Wild-type littermates were used as controls for mutant mice. Animals were genotyped by tail biopsy and PCR using primers specific for the different alleles as defined by the provider or initial publications. The day of the vaginal plug was considered E0.5 and the birth date was considered as postnatal day 0 (P0). Animals were handled in accordance with European regulations and the local ethics committee. *Cx3cr1*$^{gfp/+}$ (JAX:005582)(Jung *et al.*, 2000), *Cx3cr1*^{creER} (JAX:020940)(Yona *et al.*, 2013), *Emx1*$^{cre/+}$ (JAX:005628)(Gorski *et al.*, 2002), *Nex1*$^{cre/+}$ (Goebbels *et al.*, 2006), *R26*$^{hM3Dq\text{-}DREADD}$ (JAX :026220)(Zhu *et al.*, 2016), *Il34*$^{fl/fl}$ (Greter *et al.*, 2012), *Csf1*$^{fl/fl}$ (Harris *et al.*, 2012), *Gpnmb*$^{-/-}$ (Nickl, Qadri and Bader, 2021) and *Spp1*$^{-/-}$ (JAX:004936)(Liaw *et al.*, 1998) mice were kept in a C57BL/6J background.

To achieve DREADD-mediated modulations of neuronal excitability, *R26*$^{hM3Dq\text{-}DREADD}$ mice were crossed to the *Emx1*$^{cre/+line}$. Excitatory DREADD receptors were activated through injections of its exogenous ligand Clozapine N-oxide (CNO) (Zhu *et al.*, 2016). CNO (Tocris 4936) was diluted in 0.9% saline to 0.1 mg/mL. Both control (cre negative) and mutant pups were injected with CNO (1 mg/kg animal) subcutaneously, twice a day, from P5 to P7.

To conditionally inactivate *Csf-1* in the monocyte and macrophage lineage, *Csf1*$^{fl/fl}$ mice were backcrossed to *Cx3cr1*^{creER} to obtain *Csf1*$^{fl/fl}$;*Cx3cr1*$^{creER/+}$ animals. Tamoxifen induction of Cre-ERT2 driven recombination was performed at E12.5 by gavage administration to pregnant dams of 300µl tamoxifen (Sigma) dissolved in corn oil to achieve a final concentration of 2mg/10g animal; or at P3 by subcutaneous injections of 10µl/g animal of tamoxifen dissolved in corn oil to achieve a final concentration of 2mg/10g animal.

To conditionally inactivate *Csf-1* in cortical progenitors and neurons, or in cortical neurons only, *Csf1*$^{fl/fl}$ mice were backcrossed to *Emx1*$^{cre/+}$ or *Nex1*$^{cre/+}$ animals respectively. Last, to conditionally inactivate *Il-34* in cortical progenitors and neurons, *Il34*$^{fl/fl}$ mice were backcrossed to *Emx1*$^{cre/+}$ animals.

Sensory deprivation

Whisker plucking of pups was performed bilaterally from P1 to P7 as previously described (Genescu *et al.*, 2022). Pups were removed from the mother, anesthetized by hypothermia for 3 min and whiskers were plucked with sterile forceps. The Infraorbital Nerve (ION) lesion was performed unilaterally at P1, as previously described (White *et al.*, 1990; Frangeul *et al.*, 2014). In brief, pups were removed from the mother and anesthetized by hypothermia for 3 min. Using a sterile scalpel, an incision was made between the eye and the right whisker pad, enabling the section of the ION. Pups were put on a heating pad to recover from the lesion and anesthesia. The efficiency of the manipulation was systematically checked by anti-vGlut2 immunostaining to assess for the absence of barrels in the contralateral somatosensory cortex.

METHODS DETAILS

Tissue preparation and immunohistochemistry

For experiments at embryonic stages, pregnant females were sacrificed by cervical dislocation, embryos were collected from the womb and their brains were immediately dissected, except for E12.5 embryos for which the whole head was kept intact. For experiments at postnatal stages, pups were anesthetized in ice (until P5) or with isoflurane, and were transcardially perfused with 4% paraformaldehyde (PFA) in PBS preceding brain dissection. Brains were then fixed in 4% PFA at 4°C overnight (2 hours at room temperature for E12.5 embryos). Brains were cut into coronal floating sections of 80µm (embryonic and P0 brains) or 60µm (postnatal brains) thickness. Slices were first incubated for 1 h at room temperature (RT) in 0.2% Triton X-100, 0.2% Gelatin in PBS (blocking solution), and then incubated in the same blocking solution with the following primary antibodies overnight at 4°C: chicken anti-GFP (1/1000; Aves Labs Cat# GFP-1020, RRID:AB_10000240), rabbit anti-IBA1 (1/500; FUJIFILM Wako Shibayagi Cat# 019-19741, RRID:AB_839504), chicken anti-IBA1 (1/400; Synaptic Systems Cat# 234 009, RRID:AB_2891282), rabbit anti-P2Y12 (1/500; AnaSpec; EGT Group Cat# 55043A, RRID:AB_2298886), goat anti-SPP1 (1/400; R and D Systems Cat# AF808, RRID:AB_2194992), rabbit anti-KI67 (1/200; Abcam Cat# ab15580, RRID:AB_443209), rat anti-CD206 (1/200; Bio-Rad Cat# MCA2235, RRID:AB_324622), anti-VGlut2 (1/2000; Millipore Cat# AB2251-I, RRID:AB_2665454), rabbit anti active Caspase-3 (R and D Systems Cat# AF835, RRID:AB_2243952). Sections were rinsed in PBS-0.1% TritonX-100 and

incubated from 2 h to overnight at 4°C with secondary antibodies (1/400 in PBS, Jackson ImmunoResearch Labs): Alexa 10 Fluor® 488-conjugated donkey anti-chicken (Cat# 703-545-155, RRID:AB_2340375), Alexa 10 Fluor® 488-conjugated donkey anti-goat (Cat# 705-545-147, RRID:AB_2336933); Alexa 10 Fluor® 488-conjugated donkey anti-rat (Cat# 712-545-150, RRID:AB_2340683); Alexa 10 Fluor® 488-conjugated donkey rabbit (Cat# 711-545-152, RRID:AB_2313584); Cy3-conjugated donkey anti-goat (Cat# 705-165-147, RRID:AB_2307351), Cy3-conjugated donkey anti-rabbit (Cat# 711-165-152, RRID:AB_2307443), Cy3-conjugated donkey anti-rat (Cat# 712-165-150, RRID:AB_2340666), Alexa 10 Fluor® 647-conjugated donkey anti-goat (Cat# 705-605-147, RRID:AB_2340437), Cy5-conjugated donkey anti-goat (Cat# 705-175-147, RRID:AB_2340415), Cy5-conjugated donkey anti-goat (Cat# 705-175-147, RRID:AB_2340415), Cy5-conjugated donkey anti-rat (Cat# 712-175-150, RRID:AB_2340671). Hoechst (1/1000; Sigma-Aldrich 33342) was used for fluorescent nuclear counterstaining and Vectashield for mounting (Vector Labs).

EdU administration and detection

To monitor microglial proliferation, 50 mg/kg body weight (8 mg/ml stock, dissolved in filtered PBS) of EdU (Thermo Fisher Scientific) was administered to pregnant mice by intra- peritoneal injection or to pups by subcutaneous injections. Sacrificed of animals were performed 2 hours after injections, to insure good EdU incorporation in dividing cells but limit the numbers of cells that divided in the meantime. EdU incorporation was detected using the Click-iT EdU Alexa Fluor imaging kit (Thermo Fisher Scientific for Alexa Fluor 647 staining), and the protocol was adapted from (Podgorny *et al.*, 2018). Briefly, brains were processed as described above, and floating slices were first blocked and incubated overnight at 4°C with primary antibodies as for an immunostaining. After three washes in PBS, slices were permeabilized in 4% Triton X-100 in PBS for one hour. Slices were again washed in PBS three times and incubated for 1 hour with the Click-iT reaction cocktail, protected from light. After three washes in PBS, sections were incubated with secondary antibodies and Hoechst for 2 hours, washed three times in PBS and mounted as described above.

RNAscope *in situ* hybribization

Brains were processed as described above, and floating slices were first blocked and incubated overnight at 4°C with primary antibodies as for an immunohistochemistry staining. After

washes in PBS, slices were blocked with H_2O_2 for 10 minutes at room temperature before being rinsed in TBS-T (50mM Tris-HCl pH 7.6, 150mM NaCl, 0,1% Tween 20). Slices were then mounted on Superfrost+ slices and left to dry one hour at room temperature, one hour at 60°C in a dry oven, and overnight at room temperature. Slices were then treated with Protease + for 30 minutes at room temperature, and then incubated with the probes for 2 hours at 40°C. The following steps were done according to the manufacturer's protocol. Briefly the probes were amplified sequentially and ultimately labeled with OPAL 570nm or 690nm dyes with the Thyramide signal amplification (TSA) system while being kept away from light here on. After completion of the RNAscope, slides were immerged overnight at 4°C in PBS minus Ca^{2+}/Mg^{2}. Then slices were incubated with secondaries and Hoechst for 2 hours at room temperature, then mounted as previously described. The probes used come from ACD: CSF-1 targeting exon 6 (that is excised in the *Csf-1*$^{fl/fl}$): 122261-C3; regular CSF-1: 315621-C3; IL-34: 428201 and CSF-1R: 428191-C2.

Two-photon live imaging

Cx3cr1$^{gfp/+}$ pups were sacrificed by decapitation, and their brain were dissected and kept in an ice-cold solution consisting of L-15 Medium without phenol red (SIGMA-Aldrich) supplemented with 3% Glucose. For embryos, pregnant dams were sacrificed by cervical dislocation and their brains dissected as before. Brains were included in 3,5% low-melting agarose (Promega) in L-15 Glucose^{+} solution and 300-µm-thick coronal slices were cut on a vibratome. Slices were allowed to equilibrate for one hour at 37°C, in the L-15 Glucose^{+} solution at 37 °C and bubbled with O_2/CO_2 (95% / 5%). They were then imaged using a Custom-designed AOD-based multi-photon microscope (AODscope, IBENS Imaging Platform) over a period of up to 6 hours, while being constantly perfused (L-15 Glucose^{+} at 37 °C, bubbled with 5% CO_2). Laser was tuned to 900 nm. Fluorescence was detected after 510-84 nm band-pass filter to acquire GFP signals. Starting and finishing more than 100 µm away from the surface of the slice, 100-µm-thick z-stacks were imaged every 30 seconds with a z-step of 1µm. Individual slices could be imaged for over 6 hours without loss of GFP signals from microglia nor signs of microglial death. For time-lapse movie analysis, eventual drift in the three dimensions was first corrected using IMARIS software (Bitplane, Oxford). To track microglial movements and analyze their migratory speed and directions, the functionality 'Spots' was used and further manually corrected. Potential BAMs were also manually removed from the analysis.

Image acquisition and quantification

Immunofluorescence images were acquired using a confocal microscope (Leica TCS SP5 and SP8) with a 10X objective or a fluorescence microscope (Leica DMi8). RNAscope images were obtained with a microscope ECHO Revolve. Microglial quantifications were performed at each stage and region on whole stack projections (Standard Deviation function) using the ImageJ software, with Cell Counter plug-in. Microglial proliferation was assessed by performing an automated segmentation of the Ki-67 channel (or alternatively EdU channel), followed by the 'Analyze particle' function. Results of the latter analysis was exported as ROIs and visualized in the microglial channel to perform counting. For the cortex, quantification was done for each individual cortical layer defined using the Hoechst staining across a width of 500µm, and BAMs of the meninges and perivascular space were excluded based on their location and morphology (Fig. S1). While most slices we acquired entirely at 10X using a 2 µm step, EDWM images were acquired on a 20µm-thick region at the center of the slice, with a 0.5µm z-step, because of microglial density in the EDWM.

Statistical analysis

All data were expressed as mean ± SD or ± SEM dependent on the types of data plotted, as specified in legends. A P-value inferior to 0.05 was considered significant. According to the data structure, we systematically performed non-parametric tests namely Mann-Whitney U Test, Kruskal-Wallis Tests with Dunn's correction, and 2 ways ANOVA test with Dunnett's or Sidak's correction, depending on whether we performed single or multiple group comparisons with individual or common controls. Statistics and plotting were performed using GraphPad Prism 7.00 (GraphPad Software Inc., USA). $^{*}p < 0.05$, $^{**}p < 0.01$, $^{***}p < 0.001$.

FIGURES

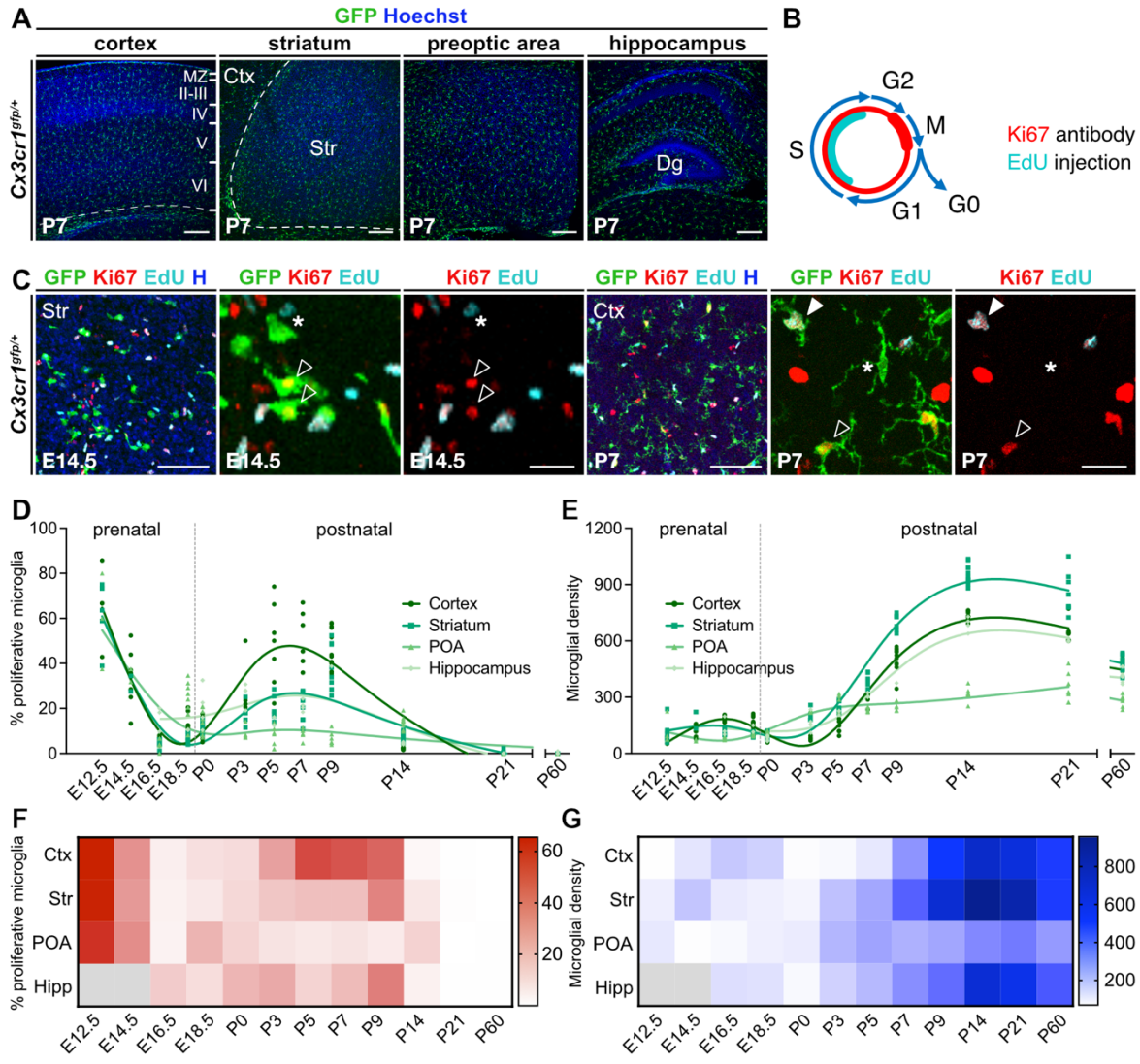

Figure 1. Microglial brain colonization relies on two dynamic waves of proliferation

(A) Representative pictures at P7 of the four regions analyzed in *Cx3cr1*$^{gfp/+}$ animals. Scale bar, 250µm. **(B)** Schematic representation of labeling of the different phases of the cell cycle by either Ki-67 or EdU injections. **(C)** Illustration of double labelling with Ki-67 and EdU at E14.5 and P7 respectively in the striatum and cortex. Stars point at non proliferating (Ki-67 and EdU negative) microglia, open arrowheads point at proliferating (Ki-67 positive) microglia and the solid arrowhead points at a proliferating (Ki-67 and EdU positive) microglia. Scale bars are 100µm at E14.5, and 25µm at P7. **(D)** and **(E)** Proportion of proliferative (Ki-67 positive) microglia and microglial densities (GFP+ cells/mm^2) in each region from E12.5 to P60 (E12.5: n=5, E14.5: n=9, E16.5: n=8, E18.5: n=10, P0: n=8, P3: n=4, P5: n=6, P7: n=6, P9: n=6, P14: n=8, P20: n=7, P60: n= 8). The curves plotted for each region are non-parametric regressions,

as centered polynomial models were not fitting the data and were thus unsuitable here. **(F)** and **(G)** Heatmaps of the proportion of proliferative (Ki-67 positive) microglia and of microglial densities (GFP+ cells/mm^2) in each region from E12.5 to P60 (E12.5: n=5, E14.5: n=9, E16.5: n=8, E18.5: n=10, P0: n=8, P3: n=4, P5: n=6, P7: n=6, P9: n=6, P14: n=8, P20: n=7, P60: n=8).

Ctx, cortex; Dg, dentate gyrus; Hipp, hippocampus; POA, preoptic area; Str, striatum.

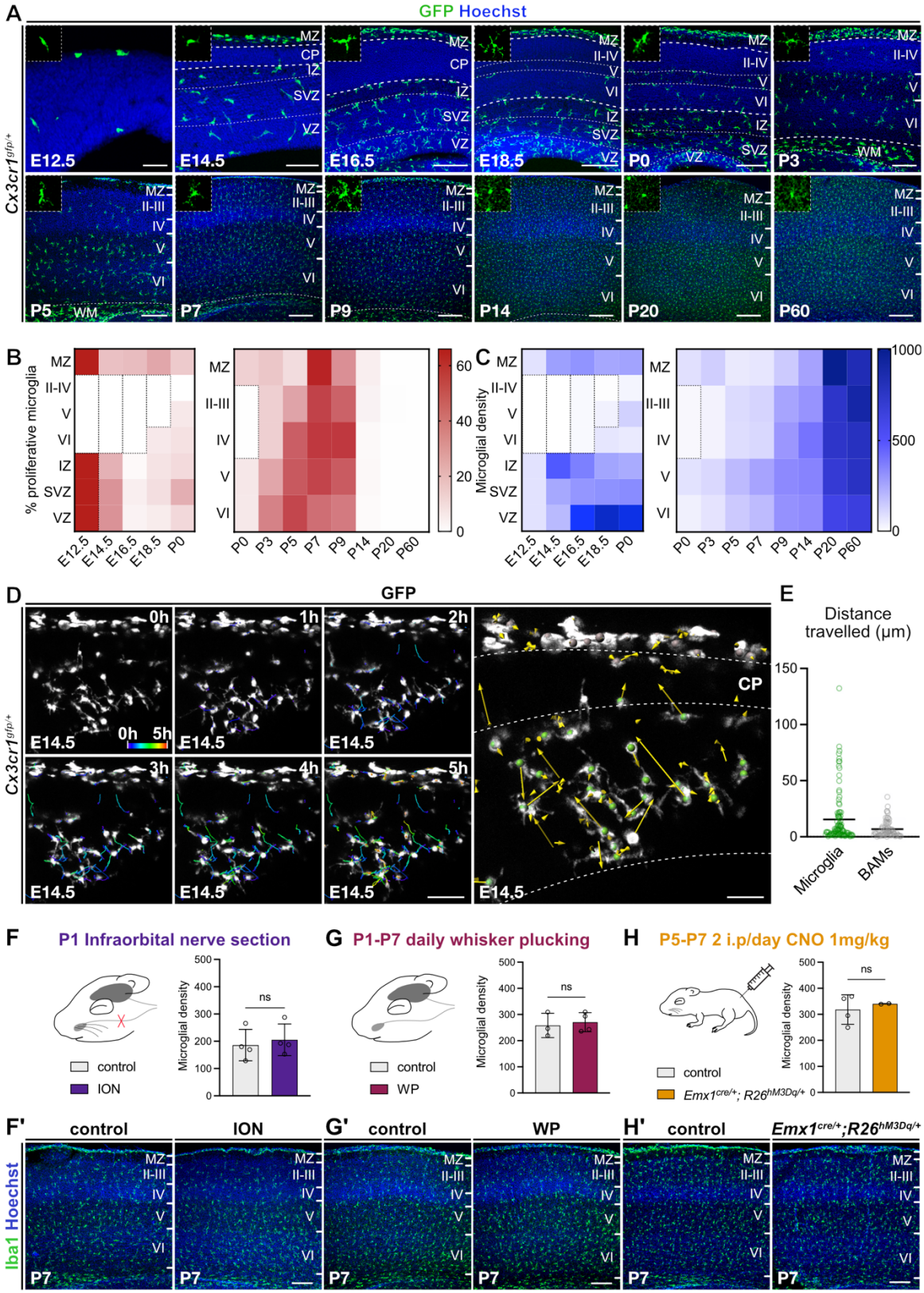

Figure 2. Cortical microglia locally proliferate and redistribute through migration independently of early postnatal neuronal activity

(A) Timeline of microglial colonization of the cortex in *Cx3cr1*$^{gfp/+}$ animals, from E12.5 to P60. Until P3, the cortical plate is underlined by bold dotted lines. Microglial close-ups, delineated by dotted lines, show only GFP and are 75µm wide. Scale bars: E12.5, 50µm; E14.5, 100µm; E16.5, E18.5, P0 and P3, 200µm; P5 to P60, 250µm. **(B)** and **(C)** Heatmaps of the proportion of proliferative (Ki-67 positive) microglia and of microglial densities (cells/mm^2) in each cortical layer from E12.5 to P60 (E12.5: n=5, E14.5: n=9, E16.5: n=8, E18.5: n=10, P0: n=8, P3: n=4, P5: n=6, P7: n=6, P9: n=6, P14: n=8, P20: n=7, P60: n= 8). In each case, the first graph represents all layers of the neocortex, and the second one is restricted to the postnatal cortical plate. Dotted rectangles correspond to layers not distinguished for quantification. **(D)** Representation of microglial migration at E14.5 in the neocortex with two-photon live-imaging on slices (length recording, 5h). Left panels show the progressive displacement of each cell analyzed with Imaris software. Color scale corresponds to time of displacement. The right panel displays their initial positions (green dots for microglia, grey dots for BAMs) and total displacement (yellow arrows). Scale bar left panel, 100µm; right panel, 50µm. **(E)** Total distance travelled by individual microglia (green) and BAMs (grey) tracked during imaging using Imaris software analyses. **(F-H)** Schematic paradigm, microglial densities (Iba1+ cells/mm^2) in the cortical plate at P7 and **(F'-H')** representative images of Iba1 immunolabeling of microglia for (F-F') unilateral infraorbital nerve section performed at P1 (n=4, controls are the cortex of the ipsilateral hemisphere and ION of the contralateral hemisphere); (G-G') bilateral daily whisker plucking from P1 to P7 (control, n=3; WP, n=4. All are littermates); (H-H') two injections a day of CNO from P5 to P7 (control, n=4; mutant, n=2. All are littermates and received CNO). Scale bars, 200µm. Data are presented as mean ± SEM. Two-sided unpaired Mann-Whitney tests were performed to assess differences. n.s., non significant.

BAMs, border associated macrophages; CP, cortical plate; CNO, clozapine-N-oxyde; ION, infraorbital nerve section; IZ, intermediate zone; MZ, marginal zone; SVZ, subventricular zone; VZ, ventricular zone; WM, white matter; WP, whisker pluck; II, III, IV, V and VI are respectively cortical layers II, III, IV, V and VI.

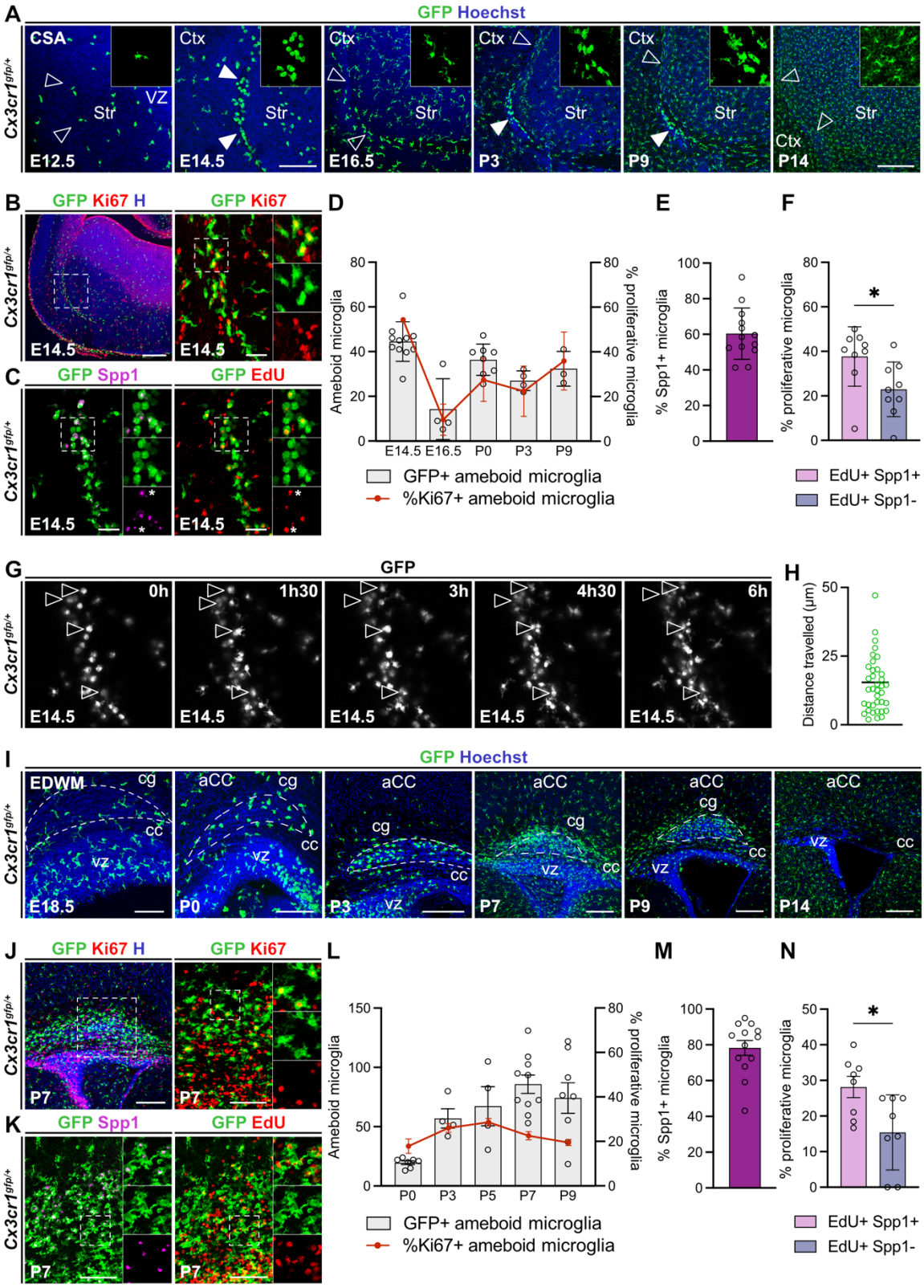

Figure 3. Developmental hotspots comprise highly proliferative microglia

(A) Representative images of accumulating ameboid microglia at the CSA along development in *Cx3cr1*$^{gfp/+}$ animals. Open arrowheads show the absence of accumulated microglia and closed

arrowheads their accumulations. Microglial close-ups show only GFP and are 150µm wide. Scale bars: 150µm for E12.5-E14.5; 250µm for E16.5-P14. **(B)** Proliferative microglia at the CSA at E14.5, evaluated with Ki-67 staining. Scale bars left image, 250µm; right image, 50µm. Close-ups are 75µm wide. **(C)** Accumulating ameboid microglia at the CSA display the ATM marker Spp1 at E14.5 and are proliferative, evaluated with EdU. Scale bars, 50µm. Close-ups are 75µm wide. Stars highlight double positive microglia (Spp1 and EdU positive cells). **(D)** Number of accumulating ameboid microglia and proportion of proliferative (Ki67 positive cells) ameboid microglia at the CSA along development (E14.5, n=11; E16.5, n=4; P0, n=8; P3, n=4; P9, n=3). Data are presented as mean ± SD. **(E)** Percentage of Spp1-positive ameboid microglia at the CSA at E14.5 (n=13). Data are presented as mean ± SD. **(F)** Percentage of EdU-positive ameboid microglia at the CSA at E14.5 amongst Spp1-positive or Spp1-negative ameboid microglia (n=13). Data are presented as mean ± SD. Two-sided unpaired Mann-Whitney test was performed to assess differences. * $p<0.05$. **(G)** Representation of microglial proliferation at the CSA at E14.5, with two-photon live-imaging on slices (length recording, 6h). Open arrowheads allow to track single microglia dividing over the course of imaging. Scale bar, 100µm. **(H)** Total distance travelled by individual microglia tracked during imaging using Imaris. **(I)** Representative images of accumulating ameboid microglia at the EDWM along development in *Cx3cr1*$^{gfp/+}$ animals. Dotted lines delineate the zone of cellular accumulation (intense Hoechst staining) between the cingulum bundle and ventral part of the corpus callosum, where quantifications were made. Scale bars: E18.5, 100µm; P0, 150µm; P3 to P14, 200µm. **(J)** Proliferative microglia at the EDWM at P7, evaluated with Ki-67 staining. Scale bars: left image, 250µm; right image, 50µm. Close-ups are 75µm wide. **(K)** Accumulating ameboid microglia at the CSA display the ATM marker Spp1 at E14.5 and are proliferative, evaluated here with EdU. Scale bars, 50µm. Close-ups are 75µm wide. Stars highlight double positive microglia (Spp1 and EdU positive). **(L)** Number of accumulating ameboid microglia and proportion of proliferative (Ki67 positive) ameboid microglia at the EDWM from E18.5 to P14 (quantifications have been done on two images per brain: P0, n=7; P3, n=4; P5, n=4; P7, n=10; P9, n=8). Data are presented as mean ± SEM. **(M)** Percentage of Spp1-positive ameboid microglia at the EDWM at P7 (n=13). Data are presented as mean ± SEM. **(N)** Percentage of EdU-positive ameboid microglia at the CSA at E14.5 amongst Spp1-positive or Spp1-negative ameboid microglia (n=9). Data are presented as mean ± SEM. Two-sided unpaired Mann-Whitney test was performed to assess differences. * $p<0.05$.

aCC, anterior cingulate cortex; cc, corpus callosum; cg, cingulum bundle; Ctx, cortex; Str, striatum; vz, ventricular zone.

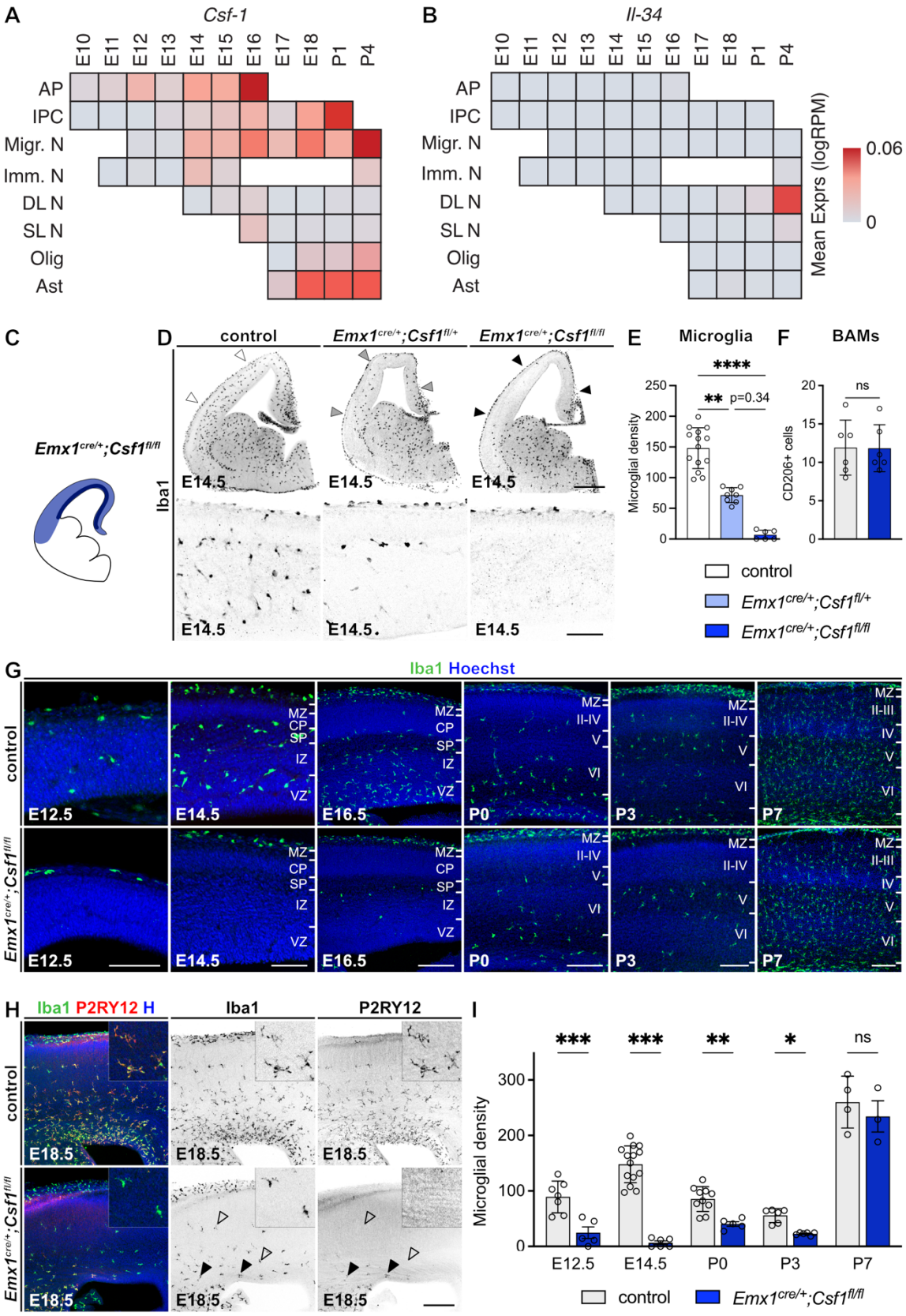

Figure 4. Local cortical CSF-1 is required for microglial colonization in a transient and dose-dependent manner

(A-B) Heatmaps of single-cell gene expression of *Csf-1* (A) and *Il-34* (B) in neural cells of the neocortex along development in mean reads per millions. Data extracted from the available dataset produced by (Di Bella *et al.*, 2021). Squares were left empty when data was not available. **(C)** Schematic representation of the pattern of expression of the $Emx1^{cre}$ line in the embryonic brain, including all progenitors and excitatory neurons of the neocortex. **(D)** Representative images showing Iba1 expressing microglia at E14.5 in control, $Emx1^{cre/+};Csf1^{fl/+}$ and $Emx1^{cre/+};Csf1^{fl/+}$ animals, and highlighting the local depletion of microglia in heterozygotes (grey arrowheads) and homozygotes (black arrowheads). Iba1 also stains BAMs present in the meninges. Scale bars top, 500µm; bottom, 100µm. **(E)** Quantification of microglial densities (Iba1+ cells/mm^2) in the neocortex at E14.5 (control, n=17; heterozygote, n=8; homozygote, n=6). Data are presented as mean ± SD. Kruskal Wallis with Dunn's multiple comparisons post hoc test was performed to assess differences. n.s., non significant, ** $p<0.01$, *** $p<0.001$. **(F)** Quantification of BAMs numbers in the meninges (over a 500µm length) of the neocortex at E14.5 (control, n=6; homozygote, n=6). Data are presented as mean ± SD. Two-sided unpaired Mann-Whitney test was performed to assess differences. n.s., non significant. **(G)** Representative images showing Iba1 expressing microglia in the neocortex along development in control and $Emx1^{cre/+};Csf1^{fl/+}$ animals, illustrating the progressive repopulation by microglia. Scale bar E12.5 and E14.5, 100µm; E16.5 to P7, 200µm. **(H)** Representative images showing Iba1 expressing microglia in the neocortex at E18.5 in control and $Emx1^{cre/+};Csf1^{fl/+}$ animals. Repopulating microglia are less ramified and are not expressing P2RY12 (closed arrowheads). Microglial close-ups are 150µm wide. Scale bar, 250µm. **(I)** Quantifications of microglial densities (Iba1+ cells/mm^2) in the neocortex across development in control and $Emx1^{cre/+};Csf1^{fl/+}$ animals (E12.5: $n_{control}=7$, $n_{homo}=5$; E14.5: $n_{control}=6$, $n_{homo}=6$; P0: $n_{control}=10$, $n_{homo}=5$; P3: $n_{control}=6$, $n_{homo}=6$; P7: $n_{control}=4$, $n_{homo}=3$). Data are presented as mean ± SD. A Two-way ANOVA with Fisher's post hoc test was performed to assess differences. n.s., non significant, * $p<0.05$, ** $p<0.001$, *** $p<0.0001$.

AP, apical progenitors; Ast, astrocytes; BAMs, border associated macrophages; CP, cortical plate; DL N, deep layer neurons; Imm. N, immature neuron; IPC, intermediate progenitor cell; IZ, intermediate zone; Migr. N, migrating neuron; MZ, marginal zone; Olig, oligodendrocytes; RPM, reads per millions; SL N, superficial layer neurons; SVZ, subventricular zone; VZ, ventricular zone; II, III, IV, V and VI are respectively cortical layers II, III, IV, V and VI.

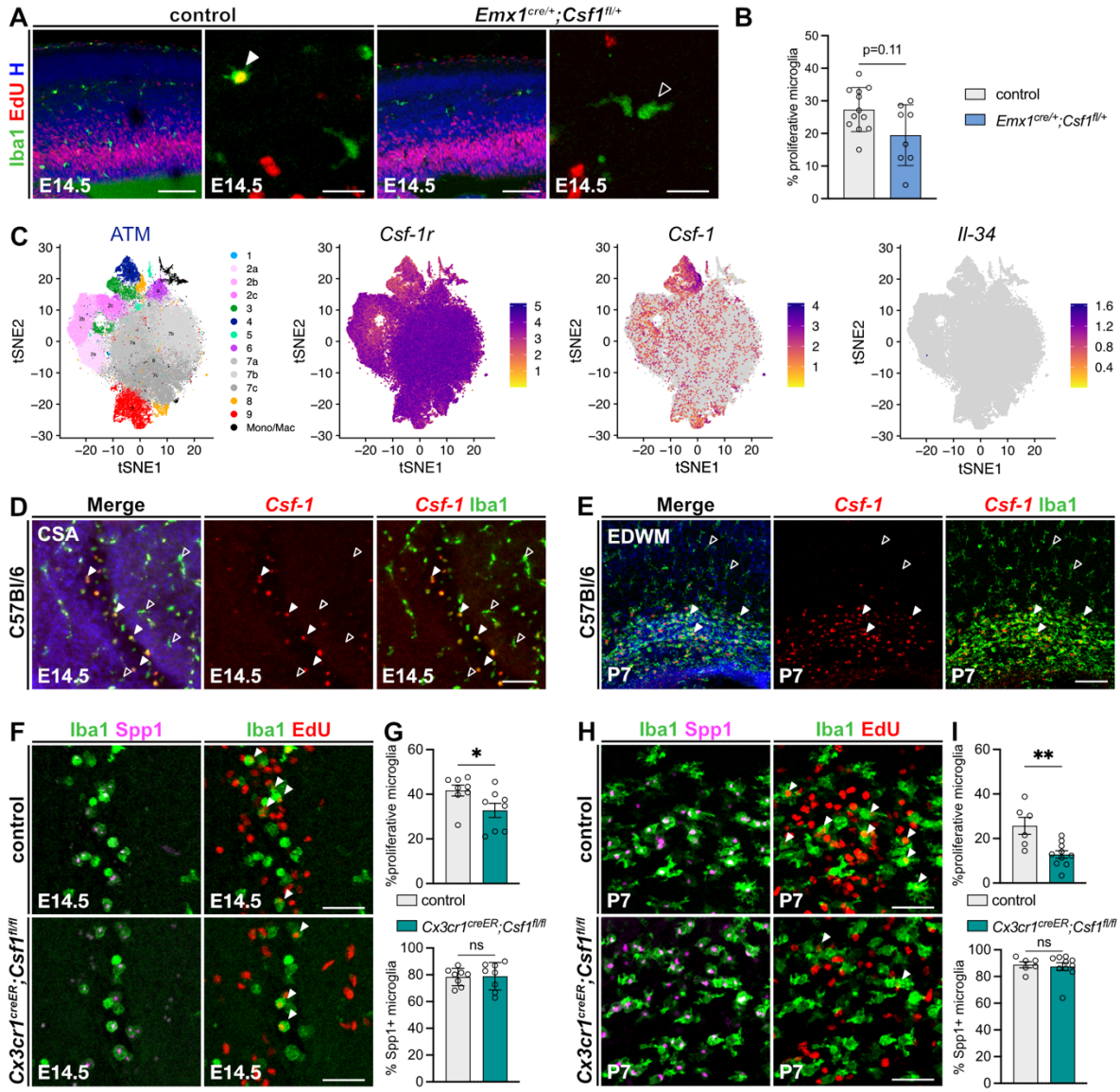

Figure 5. Cortical and microglial *Csf-1* regulate proliferation of developing microglia

(A) Representative images of the cortex at E14.5 in controls and *Emx1*$^{cre/+}$;*Csf1*$^{fl/+}$ animals, in which proliferation is assessed with EdU. Scale bar neocortex, 100µm; close-up, 25µm. **(B)** Proportion of proliferative (EdU positive) microglia in all the neocortex except the ventricular zone at E14.5 (control, n=12; mutant, n=9). Data are presented as mean ± SD. Two-sided unpaired Mann-Whitney test was performed to assess differences. **(C)** Reproduced tSNE plot of the 76,149 cells characterized by scRNA-seq in the dataset from (Hammond *et al.*, 2019) where ATM are present in cluster 4, and projections of the respective expression of *Csf-1r*, *Csf-1* and *Il-34*. *Csf-1* expression in particular overlaps with cluster 4, while microglia don't express *Il-34*. **(D-E)** Representative images of the CSA at E14.5 and EDWM at P7 in control animals. RNAscope experiments show *Csf-1* expression in ameboid microglia of the accumulation

(closed arrowheads), but not in ramified microglia in neighboring regions (open arrowheads). Scale bar, 100µm (D) and 150µm (E). **(F)** Representative images of microglia at the CSA at E14.5 in control and *Cx3cr1*$^{creER/+}$;*Csf1*$^{fl/fl}$ animals, which received tamoxifen at E12.5. Closed arrowheads point at proliferating (EdU positive) microglia. Scale bar, 50µm. **(G)** Proportion of proliferating (EdU positive) microglia and of Spp1-positive microglia at the CSA at E14.5 (control, n=8; mutant, n=8). Data are presented as mean ± SEM. Two-sided unpaired Mann-Whitney test was performed to assess differences. n.s., non significant, * $p<0.05$. **(H)** Representative images of microglia at the EDWM at P7 in control and *Cx3cr1*$^{creER/+}$;*Csf1*$^{fl/fl}$ animals, which received tamoxifen at P3. Closed arrowheads point at proliferating (EdU positive) microglia. Scale bar, 50µm. **(I)** Proportion of proliferating (EdU positive) microglia and of Spp1-positive microglia at the EDWM at P7 (control, n=6; mutant, n=10). Data are presented as mean ± SEM. Two-sided unpaired Mann-Whitney test was performed to assess differences. n.s., non significant, * $p<0.05$, ** $p<0.01$.

ATM, axon-tract associated microglia; CSA, cortico-striato-amygdalar boundary; EDWM, early-dorsal white matter.

SUPPLEMENTARY DATA

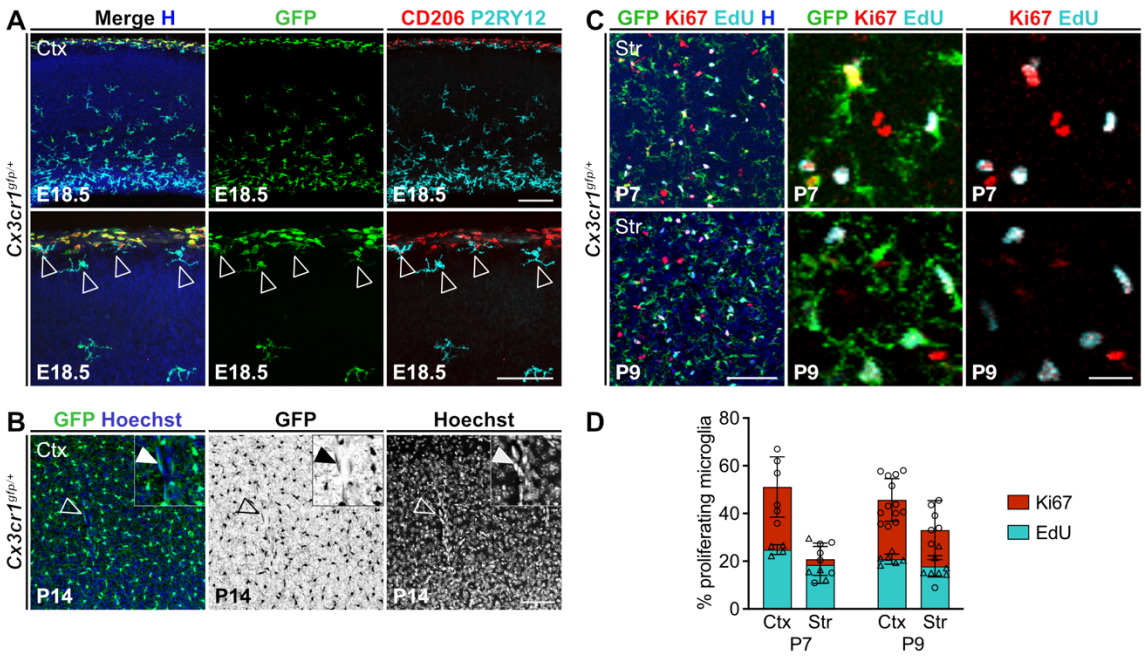

Figure S1, related to Figure 1. Identification of microglia and BAMs and double Ki-67/EdU staining

(A) Representative images of the cortex at E18.5 in *Cx3cr1*$^{gfp/+}$ animals. The *Cx3cr1*$^{gfp/+}$ labels all microglia and BAMs with GFP. At the border between the marginal zone and meninges, where BAMs and microglia are close, microglia (open arrowheads) can be distinguished by their ramified morphology and location in the marginal zone, whereas BAMs are round and restricted to the meninges. Scale bars top, 150µm; bottom, 100µm. **(B)** Representative images of a blood vessel in the cortex at P14 in *Cx3cr1*$^{gfp/+}$ animals. Amongst BAMs, the *Cx3cr1*$^{gfp/+}$ labels perivascular macrophages (open arrowhead), found in the perivascular space. Their morphology and low GFP intensity allow them to be distinguished from microglia, alongside with their location along blood vessels which is visible as a Hoechst intense line. Scale bar, 100µm. Close-ups are 100µm wide. **(C)** Representative images of double proliferative labeling with Ki-67 and EdU, in the striatum at P7 and cortex at P9 in *Cx3cr1*$^{gfp/+}$ animals. Virtually all EdU positive cells are also Ki-67 positive. Scale bars: left, 100µm; right, 25µm. **(D)** Quantification of the proportion of proliferative microglia (Ki-67 positive or EdU positive) in the striatum at P7 and cortex at P9 in *Cx3cr1*$^{gfp/+}$ animals. Roughly half of Ki-67 positive microglia are also EdU positive, coherent with the fact that Ki-67 labels all phases of the cell cycle whereas EdU only targets cells in S-phase. Ki-67 positive microglia are thus not arrested in G0.

BAMs, border associated macrophages; Ctx, cortex; Str, striatum.

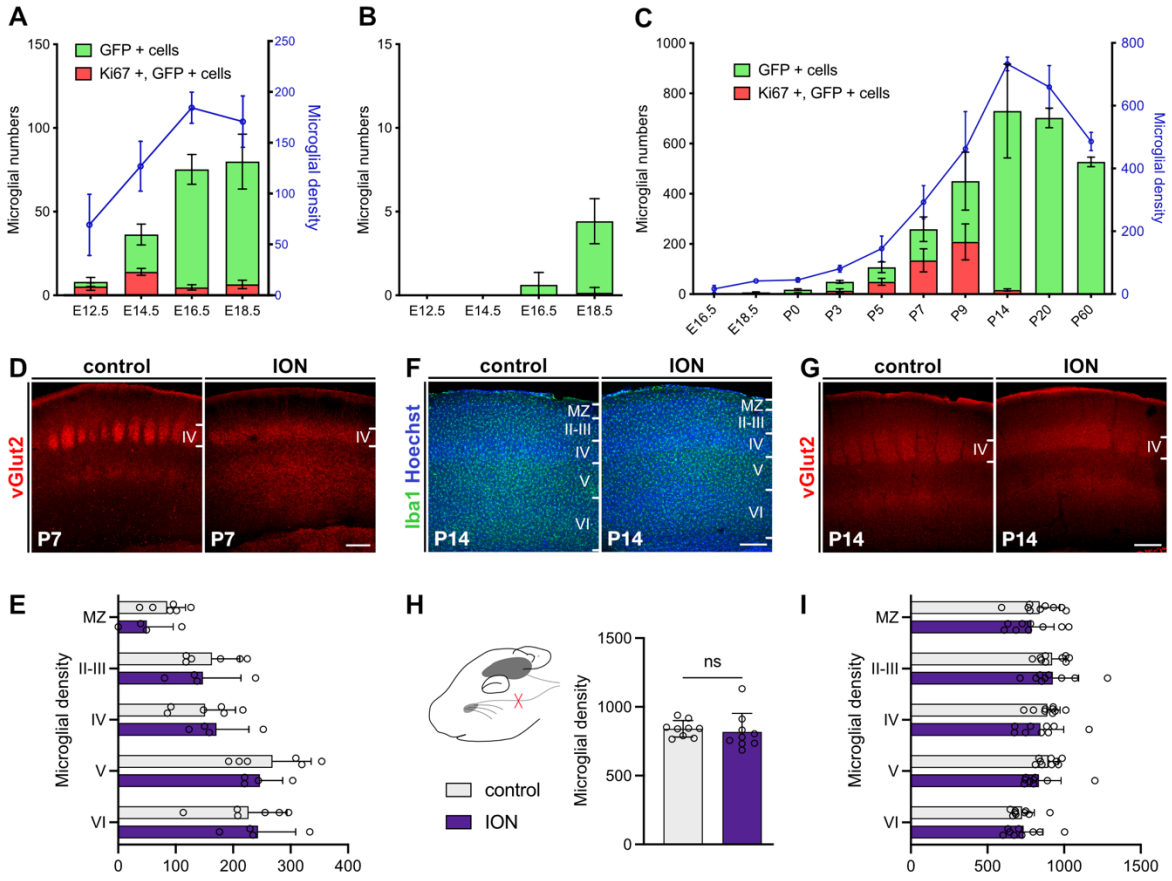

Figure S2, related to Figure 2. Kinetics of cortical microglial numbers and densities and absence of effect of ION on microglial densities

(A) Number of Ki-67 positive, Ki-67 negative microglia and microglial density (blue line, cells/mm^2) in all layers of the neocortex of *Cx3cr1*$^{gfp/+}$ animals. **(B-C)** Detail of the numbers of Ki-67 positive, Ki-67 negative microglia and of microglial density (blue line, cells/mm^2) in the cortical plate of *Cx3cr1*$^{gfp/+}$ animals. **(D,G)** Representative images of cortical layer IV afferences labelled by vGlut2 at P7 (D) and P14 (F). Scale bars, 250µm. **(E,I)** Microglial density (Iba1+ cells/mm^2) across cortical layers at P7 (E) or P14 (I) for unilateral infraorbital nerve section performed at P1 (P7, n=4; P14, n=9; controls are the cortex of the ipsilateral hemisphere and ION of the contralateral hemisphere). **(F,H)** Schematic paradigm, microglial densities (Iba1+ cells/mm^2) in the cortical plate at P14 and representative images of Iba1 immunolabeling of microglia for unilateral infraorbital nerve section performed at P1 (n=9, controls are the cortex of the ipsilateral hemisphere and ION of the contralateral hemisphere). Scale bar, 250µm. Data are presented as mean ± SD. Two-sided unpaired Mann-Whitney tests were performed to assess differences. n.s., non significant.

ION, infraorbital nerve section; MZ, marginal zone; II, III, IV, V and VI are respectively cortical layers II, III, IV, V and VI.

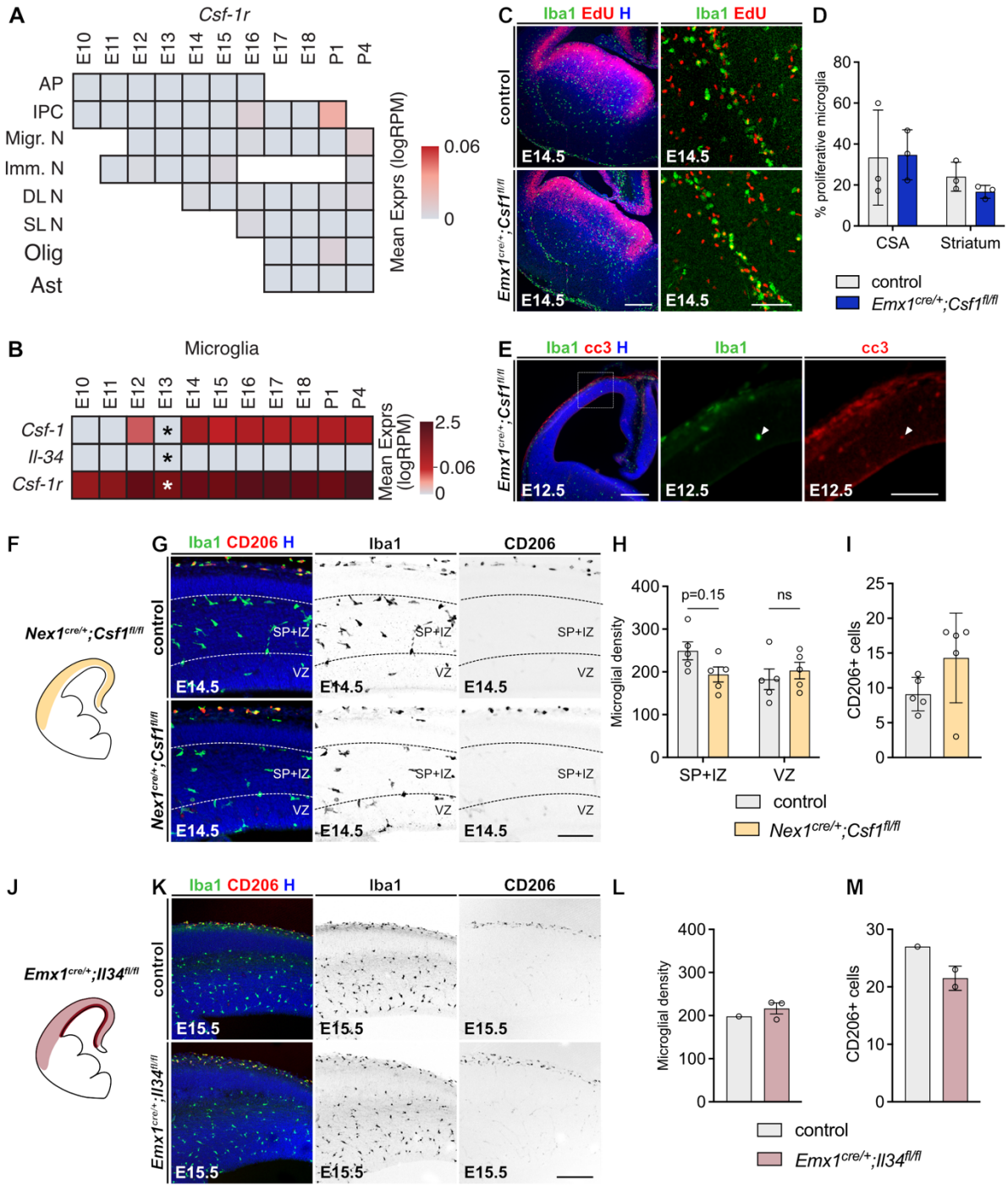

Figure S3, related to Figure 4. Effects of local inactivation of CSF-1R ligands during embryogenesis

(A,B) Heatmaps of single-cell gene expression of *Csf-1r* in neural cells of the neocortex (A), and of *Csf-1, Il-34* and *Csf-1r* in microglia (B) along development in mean reads per millions. Data extracted from the available dataset produced by (Di Bella *et al.*, 2021). Squares were left empty when data was not available. At E13 and marked by stars, only 5 microglial cells were identified. **(C)** Immunolabeling of Iba1 combined with EdU showing microglial proliferation

at the CSA and striatum of E14.5 control and *Emx1$^{cre/+}$;Csf1$^{fl/fl}$* animals. **(D)** Quantification of microglial proliferation (EdU positive) in the CSA and striatum of E14.5 control and *Emx1$^{cre/+}$;Csf1$^{fl/fl}$* animals (control, n=3; mutant, n=3). **(E)** Immunolabeling of a cc3 positive microglia found in an E12.5 *Emx1$^{cre/+}$;Csf1$^{fl/fl}$* animal. **(F)** Schematic representation of the pattern of expression of the *Nex1^{cre}* line in the embryonic brain, including excitatory neurons of the neocortex but not progenitors. **(G)** Representative images showing Iba1 expressing microglia at E14.5, and CD206 BAMS, in control and *Nex1$^{cre/+}$;Csf1$^{fl/fl}$* animals. Scale bar, 100µm. **(H)** Quantification of microglial densities in the neocortex at E14.5 (control, n=5; mutant, n=5). Data are presented as mean ± SD. Two-sided unpaired Mann-Whitney test was performed to assess differences. n.s., non significant. **(I)** Quantification of BAMs numbers in the meninges (over a 500µm length) of the neocortex at E14.5 (control, n=6; homozygote, n=6). Data are presented as mean ± SD. **(J)** Schematic representation of the pattern of expression of the *Emx1^{cre}* line in the embryonic brain, including progenitors and excitatory neurons of the neocortex. **(K)** Representative images showing Iba1 expressing microglia at E15.5, and CD206 BAMS, in control and *Emx1$^{cre/+}$;Il34$^{fl/fl}$* animals. Scale bar, 100µm. **(L)** Quantification of microglial densities (Iba1+ cells/mm^2) in the neocortex at E15.5 in control and *Emx1$^{cre/+}$;Il34$^{fl/fl}$* animals (control, n=1; mutant, n=3). Data are presented as mean ± SD. **(M)** Quantification of BAMs numbers in the meninges (over a 500µm length) of the neocortex at E15.5 in control and *Emx1$^{cre/+}$;Il34$^{fl/fl}$* animals (control, n=1; homozygote, n=3). Data are presented as mean ± SD.
AP, apical progenitors; Ast, astrocytes ; BAMs, border associated macrophages; cc3, cleaved-caspase 3; CSA, cortico-striato-amygdalar boundary; DL N, deep layer neurons; Imm. N, immature neuron; IZ, intermediate zone; IPC, intermediate progenitor cell; Migr. N, migrating neuron; Olig, oligodendrocytes; RPM, reads per millions; SL N, superficial layer neurons; SP, subplate; VZ, ventricular zone.

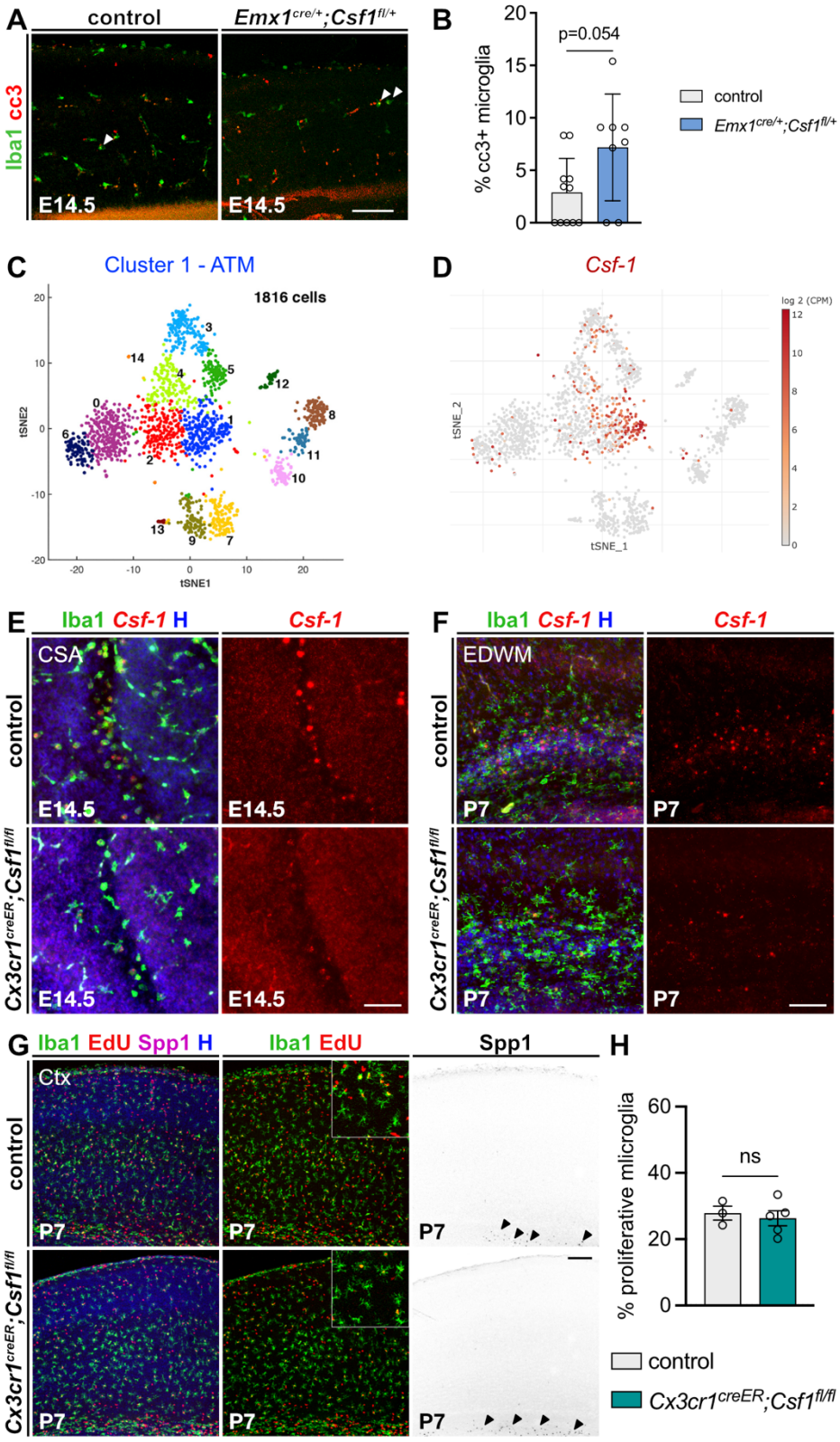

Figure S4, related to Figure 5. Role of neural and microglial *Csf-1* in the regulation of microglial proliferation

(A) Representative images of cc3 positive microglia in the cortex of control and *Emx1*$^{cre/+}$*;Il34*$^{fl/+}$ animals at E14.5. **(B)** Quantification of the proportion of cc3 positive microglia in the cortex of control and *Emx1*$^{cre/+}$*;Il34*$^{fl/+}$ animals at E14.5 (control, n=12; mutant, n=9). Data are presented as mean ± SD. Two-sided unpaired Mann-Whitney test was performed to assess differences. **(C-D)** Reproduced tSNE plot of the 1,816 cells characterized by scRNA-seq in the dataset from (Li *et al.*, 2019) (C) where ATM are present in cluster 1, and (D) projections of the expression of *Csf-1*. *Csf-1* expression again overlaps with the ATM cluster. **(E-F)** Representative images of RNAscope experiments showing *Csf-1* expression in microglia in control and *Cx3cr1*$^{creER/+}$*;Csf1*$^{fl/fl}$ animals at E14.5, which all received tamoxifen at E12.5 (E); and at P7, which all received tamoxifen at P3 (F). Scale bars, 100µm. **(G)** Representative images of microglial proliferation (EdU positive) in the cortex of control and *Cx3cr1*$^{creER/+}$*;Csf1*$^{fl/fl}$ animals which all received tamoxifen at P3. Microglia in the cortex do not express *Csf-1* (not shown) nor Spp1, found only in microglia of the white matter (closed arrowheads). Scale bar, 200µm. Close-ups are 200µm wide. **(H)** Quantification of the proportion of proliferating (EdU positive) microglia at P7 in control and *Cx3cr1*$^{creER/+}$*;Csf1*$^{fl/fl}$ animals, which all received tamoxifen at P3 (control, n=3; mutant, n=5). Data are presented as mean ± SD. Two-sided unpaired Mann-Whitney test was performed to assess differences. n.s., non significant.

ATM, axon-tract associated microglia; cc3, cleaved-caspase 3; CPM, counts per million; CSA, cortico-striatal-amygdalar boundary; EDWM, early dorsal white matter.

REFERENCES

Adaikkan, C. *et al.* (2019) 'Gamma Entrainment Binds Higher-Order Brain Regions and Offers Neuroprotection', *Neuron*. Elsevier Inc., 102(5), pp. 929-943.e8. doi: 10.1016/j.neuron.2019.04.011.

Alliot, F., Godin, I. and Pessac, B. (1999) 'Microglia derive from progenitors, originating from the yolk sac, and which proliferate in the brain', *Developmental Brain Research*, 117(2), pp. 145–152. doi: 10.1016/S0165-3806(99)00113-3.

Arnoux, I. *et al.* (2013) 'Adaptive phenotype of microglial cells during the normal postnatal development of the somatosensory "Barrel" cortex', *GLIA*. John Wiley & Sons, Ltd, 61(10), pp. 1582–1594. doi: 10.1002/glia.22503.

Askew, K. *et al.* (2017) 'Coupled Proliferation and Apoptosis Maintain the Rapid Turnover of Microglia in the Adult Brain', *Cell Reports*, 18(2), pp. 391–405. doi: 10.1016/j.celrep.2016.12.041.

Badimon, A. *et al.* (2020) 'Negative feedback control of neuronal activity by microglia', *Nature*. Springer US, 586(7829), pp. 417–423. doi: 10.1038/s41586-020-2777-8.

Barry-carroll, L. *et al.* (2023) 'Microglia colonize the developing brain by clonal expansion of highly proliferative progenitors, following allometric scaling', *CellReports*. The Author(s), 42(5), p. 112425. doi: 10.1016/j.celrep.2023.112425.

Di Bella, D. J. *et al.* (2021) 'Molecular logic of cellular diversification in the mouse cerebral cortex', *Nature*. Springer US, 595(7868), pp. 554–559. doi: 10.1038/s41586-021-03670-5.

Benmamar-Badel, A., Owens, T. and Wlodarczyk, A. (2020) 'Protective Microglial Subset in Development, Aging, and Disease: Lessons From Transcriptomic Studies', *Frontiers in Immunology*, 11(April). doi: 10.3389/fimmu.2020.00430.

Bennett, F. C. *et al.* (2018) 'A Combination of Ontogeny and CNS Environment Establishes Microglial Identity', *Neuron*, 98(6), pp. 1170-1183.e8. doi: 10.1016/j.neuron.2018.05.014.

Biase, L. M. De *et al.* (2018) 'Local cues establish and maintain region-specific phenotypes of basal ganglia microglia', *Neuron*, 95(2), pp. 341–356. doi: 10.1016/j.neuron.2017.06.020.Local.

Bridlance, C. and Thion, M. S. (2023) 'Multifaceted microglia during brain development: Models and tools', *Frontiers in Neuroscience*, 17(March). doi: 10.3389/fnins.2023.1125729.

Cunningham, C. L., Martínez-Cerdeño, V. and Noctor, S. C. (2013) 'Microglia regulate the number of neural precursor cells in the developing cerebral cortex', *Journal of Neuroscience*, 33(10), pp. 4216–4233. doi: 10.1523/JNEUROSCI.3441-12.2013.

Dalmau, I. *et al.* (2003) 'Dynamics of microglia in the developing rat brain', *Journal of Comparative Neurology*, 458(2), pp. 144–157. doi: 10.1002/cne.10572.

De, I. *et al.* (2014) 'CSF1 overexpression has pleiotropic effects on microglia in vivo', *Glia*, 62(12), pp. 1955–1967. doi: 10.1002/glia.22717.

Easley-Neal, C. *et al.* (2019) 'CSF1R Ligands IL-34 and CSF1 Are Differentially Required for Microglia Development and Maintenance in White and Gray Matter Brain Regions', *Frontiers in Immunology*, 10(September). doi: 10.3389/fimmu.2019.02199.

Elmore, M. R. P. *et al.* (2014) 'Colony-stimulating factor 1 receptor signaling is necessary for microglia viability, unmasking a microglia progenitor cell in the adult brain', *Neuron*. Elsevier Inc., 82(2), pp. 380–397. doi: 10.1016/j.neuron.2014.02.040.

Eme-Scolan, E. and Dando, S. J. (2020) 'Tools and Approaches for Studying Microglia In vivo', *Frontiers in Immunology*, 11(October), pp. 1–10. doi: 10.3389/fimmu.2020.583647.

Favuzzi, E. *et al.* (2021) 'GABA-receptive microglia selectively sculpt developing inhibitory circuits', *Cell*, 184(15), pp. 4048-4063.e32. doi: 10.1016/j.cell.2021.06.018.

Frangeul, L. *et al.* (2014) 'Specific activation of the paralemniscal pathway during nociception', 39(January), pp. 1455–1464. doi: 10.1111/ejn.12524.

Genescu, I. *et al.* (2022) 'Dynamic interplay between thalamic activity and Cajal-Retzius cells regulates the wiring of cortical layer 1', *Cell Reports*, 39(2). doi: 10.1016/j.celrep.2022.110667.

Gesuita, L. *et al.* (2022) 'Microglia contribute to the postnatal development of cortical somatostatin-positive inhibitory cells and to whisker-evoked cortical activity', *Cell Reports*, 40(7). doi: 10.1016/j.celrep.2022.111209.

Ginhoux, F. *et al.* (2010) 'Fate mapping analysis reveals that adult microglia derive from primitive macrophages', *Science*, 330(6005), pp. 841–845. doi: 10.1126/science.1194637.

Goebbels, S. *et al.* (2006) 'Genetic targeting of principal neurons in neocortex and hippocampus of NEX-Cre mice', *Genesis (United States)*, 44(12), pp. 611–621. doi: 10.1002/dvg.20256.

Goldmann, T. *et al.* (2016) 'Origin, fate and dynamics of macrophages at central nervous system interfaces', *Nature Immunology*, 17(7), pp. 797–805. doi: 10.1038/ni.3423.

Gordon, H., Schafer, Z. T. and Smith, C. J. (2023) 'A paradox promoted by microglia cannibalism shortens the lifespan of developmental microglia', *bioRxiv*, p. 2023.03.15.532426. Available at: https://www.biorxiv.org/content/10.1101/2023.03.15.532426v1%0Ahttps://www.biorxiv.org/content/10.1101/2023.03.15.532426v1.abstract.

Gorski, J. A. *et al.* (2002) 'Cortical excitatory neurons and glia, but not GABAergic neurons, are produced in the Emx1-expressing lineage', *Journal of Neuroscience*, 22(15), pp. 6309–6314. doi: 10.1523/jneurosci.22-15-06309.2002.

Green, K. N., Crapser, J. D. and Hohsfield, L. A. (2020) 'To Kill a Microglia: A Case for CSF1R Inhibitors', *Trends in Immunology*, 0(0), pp. 771–784. doi: 10.1016/j.it.2020.07.001.

Greter, M. *et al.* (2012) 'Stroma-Derived Interleukin-34 Controls the Development and Maintenance of Langerhans Cells and the Maintenance of Microglia', *Immunity*. NIH Public Access, 37(6), pp. 1050–1060. doi: 10.1016/j.immuni.2012.11.001.

Hagemeyer, N. *et al.* (2017) 'Microglia contribute to normal myelinogenesis and to oligodendrocyte progenitor maintenance during adulthood', *Acta Neuropathologica*, 134(3), pp. 441–458. doi: 10.1007/s00401-017-1747-1.

Hammond, T. R. *et al.* (2019) 'Single-Cell RNA Sequencing of Microglia throughout the Mouse Lifespan and in the Injured Brain Reveals Complex Cell-State Changes', *Immunity*. Cell Press, 50(1), pp. 253-271.e6. doi: 10.1016/j.immuni.2018.11.004.

Harris, S. E. *et al.* (2012) 'Meox2Cre-mediated disruption of CSF-1 leads to osteopetrosis and osteocyte defects', *Bone*. Elsevier Inc., 50(1), pp. 42–53. doi: https://doi.org/10.1016/j.bone.2011.09.038.

Hattori, Y. *et al.* (2020) 'Transient microglial absence assists postmigratory cortical neurons in proper differentiation', *Nature Communications*. Springer US, 11(1). doi: 10.1038/s41467-020-15409-3.

Haynes, S. E. *et al.* (2006) 'The P2Y12 receptor regulates microglial activation by extracellular

nucleotides', *Nature Neuroscience*, 9(12), pp. 1512–1519. doi: 10.1038/nn1805.

Hickman, S. E. *et al.* (2013) 'The microglial sensome revealed by direct RNA sequencing', *Nature Neuroscience*. Nature Publishing Group, 16(12), pp. 1896–1905. doi: 10.1038/nn.3554.

Hope, K. T. *et al.* (2020) 'Maturation of the microglial population varies across mesolimbic nuclei', *European Journal of Neuroscience*, 52(7), pp. 3689–3709. doi: 10.1111/ejn.14740.

Van Hove, H. *et al.* (2019) 'A single-cell atlas of mouse brain macrophages reveals unique transcriptional identities shaped by ontogeny and tissue environment', *Nature Neuroscience*, 22(6), pp. 1021–1035. doi: 10.1038/s41593-019-0393-4.

Hristova, M. *et al.* (2010) 'Activation and deactivation of periventricular white matter phagocytes during postnatal mouse development', *Glia*, 58(1), pp. 11–28. doi: 10.1002/glia.20896.

Iaccarino, H. F. *et al.* (2016) 'Gamma frequency entrainment attenuates amyloid load and modifies microglia', *Nature*. Nature Publishing Group, 540(7632), pp. 230–235. doi: 10.1038/nature20587.

Jung, S. *et al.* (2000) ' Analysis of Fractalkine Receptor CX 3 CR1 Function by Targeted Deletion and Green Fluorescent Protein Reporter Gene Insertion ', *Molecular and Cellular Biology*, 20(11), pp. 4106–4114. doi: 10.1128/mcb.20.11.4106-4114.2000.

Kana, V. *et al.* (2019) 'CSF-1 controls cerebellar microglia and is required for motor function and social interaction', *Journal of Experimental Medicine*, 216(10), pp. 2265–2281. doi: 10.1084/jem.20182037.

Keren-Shaul, H. *et al.* (2017) 'A Unique Microglia Type Associated with Restricting Development of Alzheimer's Disease', *Cell*. Elsevier, 169(7), pp. 1276-1290.e17. doi: 10.1016/j.cell.2017.05.018.

Kershman, J. (1939) 'Genesis of microglia in the human brain', *Archives of Neurology & Psychiatry*. American Medical Association, 41(1), pp. 24–50.

Kierdorf, K. *et al.* (2013) 'Microglia emerge from erythromyeloid precursors via Pu.1-and Irf8-dependent pathways', *Nature Neuroscience*, 16(3), pp. 273–280. doi: 10.1038/nn.3318.

Kierdorf, K. *et al.* (2019) 'Macrophages at CNS interfaces: ontogeny and function in health and disease', *Nature Reviews Neuroscience*. Springer US, 20(9), pp. 547–562. doi: 10.1038/s41583-019-0201-x.

Lawrence, A. *et al.* (no date) 'Microglia maintain structural integrity during fetal brain morphogenesis', *in preparation*.

Lee, E. *et al.* (2021) 'Distinct features of brain-resident macrophages: Microglia and non-parenchymal brain macrophages', *Molecules and Cells*, 44(5), pp. 281–291. doi: 10.14348/molcells.2021.0060.

Li, Q. *et al.* (2019) 'Developmental Heterogeneity of Microglia and Brain Myeloid Cells Revealed by Deep Single-Cell RNA Sequencing', *Neuron*. Elsevier Inc., 101(2), pp. 207-223.e10. doi: 10.1016/j.neuron.2018.12.006.

Li, Q. and Barres, B. A. (2018) 'Microglia and macrophages in brain homeostasis and disease', *Nature Reviews Immunology*. Nature Publishing Group, 18(4), pp. 225–242. doi: 10.1038/nri.2017.125.

Li, Y. *et al.* (2022) 'Decoding the temporal and regional specification of microglia in the developing human brain', *Cell Stem Cell*. Elsevier Inc., pp. 1–15. doi:

10.1016/j.stem.2022.02.004.

Liaw, L. *et al.* (1998) 'Altered wound healing in mice lacking a functional osteopontin gene (spp1).', *Journal of Clinical Investigation*, 101(7), pp. 1468–1478. doi: 10.1172/jci2131.

Lloyd, A. F. *et al.* (2019) 'Central nervous system regeneration is driven by microglia necroptosis and repopulation', *Nature Neuroscience*. Springer US, 22(7), pp. 1046–1052. doi: 10.1038/s41593-019-0418-z.

La Manno, G. *et al.* (2021) 'Molecular architecture of the developing mouse brain', *Nature*. Springer US, 596(7870), pp. 92–96. doi: 10.1038/s41586-021-03775-x.

Masuda, T. *et al.* (2019) 'Spatial and temporal heterogeneity of mouse and human microglia at single-cell resolution', *Nature*. Springer US, 566, pp. 388–392. doi: 10.1038/s41586-019-0924-x.

Matcovitch-Natan, O. *et al.* (2016) 'Microglia development follows a stepwise program to regulate brain homeostasis', *Science*, 353(6301). doi: 10.1126/science.aad8670.

McNamara, N. B. *et al.* (2023) 'Microglia regulate central nervous system myelin growth and integrity', *Nature*. Springer US, 613(7942), pp. 120–129. doi: 10.1038/s41586-022-05534-y.

Menassa, D. A. *et al.* (2022) 'The spatiotemporal dynamics of microglia across the human lifespan', *Developmental Cell*, pp. 1–13. doi: 10.1016/j.devcel.2022.07.015.

Menassa, D. A. and Gomez-Nicola, D. (2018) 'Microglial dynamics during human brain development', *Frontiers in Immunology*, p. 1014. doi: 10.3389/fimmu.2018.01014.

Mildenberger, W., Stifter, S. A. and Greter, M. (2022) 'Diversity and function of brain-associated macrophages', *Current Opinion in Immunology*. Elsevier, 76, p. 102181. doi: 10.1016/j.coi.2022.102181.

Miyamoto, A. *et al.* (2016) 'Microglia contact induces synapse formation in developing somatosensory cortex', *Nature Communications*. Nature Publishing Group, 7(1), p. 12540. doi: 10.1038/ncomms12540.

Molnár, Z., Luhmann, H. J. and Kanold, P. O. (2020) 'Transient cortical circuits match spontaneous and sensory-driven activity during development', *Science*. doi: 10.1126/science.abb2153.

Monier, A. *et al.* (2007) 'Entry and distribution of microglial cells in human embryonic and fetal cerebral cortex', *Journal of Neuropathology and Experimental Neurology*, 66(5), pp. 372–382. doi: 10.1097/nen.0b013e3180517b46.

Mosser, C. A. *et al.* (2017) 'Microglia in CNS development: Shaping the brain for the future', *Progress in Neurobiology*, 149–150, pp. 1–20. doi: 10.1016/j.pneurobio.2017.01.002.

Mrdjen, D. *et al.* (2018) 'High-dimensional single-cell mapping of central nervous system immune cells reveals distinct myeloid subsets in health, aging, and disease', *Immunity*. Elsevier, 48(2), pp. 380–395. doi: 10.1016/j.immuni.2018.01.011.

Munro, D. A. D. *et al.* (2020) 'CNS macrophages differentially rely on an intronic Csf1r enhancer for their development', *Development (Cambridge, England)*, 147(23). doi: 10.1242/dev.194449.

Nandi, S. *et al.* (2012) 'The CSF-1 receptor ligands IL-34 and CSF-1 exhibit distinct developmental brain expression patterns and regulate neural progenitor cell maintenance and maturation', *Developmental Biology*. Elsevier, 367(2), pp. 100–113. doi: 10.1016/j.ydbio.2012.03.026.

Nemes-Baran, A. D., White, D. R. and DeSilva, T. M. (2020) 'Fractalkine-Dependent Microglial Pruning of Viable Oligodendrocyte Progenitor Cells Regulates Myelination', *Cell Reports*. ElsevierCompany., 32(7), p. 108047. doi: 10.1016/j.celrep.2020.108047.

Nickl, B., Qadri, F. and Bader, M. (2021) 'Anti-inflammatory role of Gpnmb in adipose tissue of mice', *Scientific Reports*. Nature Publishing Group UK, 11(1), pp. 1–10. doi: 10.1038/s41598-021-99090-6.

Nikodemova, M. *et al.* (2015) 'Microglial numbers attain adult levels after undergoing a rapid decrease in cell number in the third postnatal week', *Journal of Neuroimmunology*. Elsevier, 278, pp. 280–288. doi: 10.1016/j.jneuroim.2014.11.018.

Nimmerjahn, A., Kirchhoff, F. and Helmchen, F. (2005) 'Resting microglial cells are highly dynamic surveillants of brain parenchyma in vivo', *Neuroforum*, 11(3), pp. 95–96. doi: 10.1515/nf-2005-0304.

Paolicelli, R. C. *et al.* (2011) 'Synaptic pruning by microglia is necessary for normal brain development', *Science*, 333(6048), pp. 1456–1458. doi: 10.1126/science.1202529.

Parkhurst, C. N. *et al.* (2013) 'Microglia Promote Learning-Dependent Synapse Formation through Brain-Derived Neurotrophic Factor', *Cell*, 155(7), pp. 1596–1609. doi: https://doi.org/10.1016/j.cell.2013.11.030.

Podgorny, O. *et al.* (2018) 'Triple S-Phase Labeling of Dividing Stem Cells', *Stem Cell Reports*. ElsevierCompany., 10(2), pp. 615–626. doi: 10.1016/j.stemcr.2017.12.020.

Pont-Lezica, L. *et al.* (2014) 'Microglia shape corpus callosum axon tract fasciculation: Functional impact of prenatal inflammation', *European Journal of Neuroscience*, 39(10), pp. 1551–1557. doi: 10.1111/ejn.12508.

Prinz, M., Jung, S. and Priller, J. (2019) 'Microglia Biology: One Century of Evolving Concepts', *Cell*. Elsevier Inc., 179(2), pp. 292–311. doi: 10.1016/j.cell.2019.08.053.

Rio-Hortega, del P. (1932) 'Microglia', *Cytology and cellular pathology of the nervous system*. Hoeber, pp. 482–534.

Rojo, R. *et al.* (2019) 'Deletion of a Csf1r enhancer selectively impacts CSF1R expression and development of tissue macrophage populations', *Nature Communications*. Nature Publishing Group, 10(1), p. 3215. doi: 10.1038/s41467-019-11053-8.

Roth, B. L. (2016) 'DREADDs for Neuroscientists', *Neuron*. Elsevier Ltd, 89(4), pp. 683–694. doi: 10.1016/j.neuron.2016.01.040.

Schafer, D. P. *et al.* (2012) 'Microglia Sculpt Postnatal Neural Circuits in an Activity and Complement-Dependent Manner', *Neuron*, 74(4), pp. 691–705. doi: 10.1016/j.neuron.2012.03.026.

Shigemoto-Mogami, Y. *et al.* (2014) 'Microglia enhance neurogenesis and oligodendrogenesis in the early postnatal subventricular zone', *Journal of Neuroscience*, 34(6), pp. 2231–2243. doi: 10.1523/JNEUROSCI.1619-13.2014.

Silvin, A. *et al.* (2022) 'Dual ontogeny of disease-associated microglia and disease inflammatory macrophages in aging and neurodegeneration', *Immunity*. Elsevier Inc., 55(8), pp. 1448-1465.e6. doi: 10.1016/j.immuni.2022.07.004.

Squarzoni, P. *et al.* (2014) 'Microglia Modulate Wiring of the Embryonic Forebrain', *Cell Reports*. The Authors, 8(5), pp. 1271–1279. doi: 10.1016/j.celrep.2014.07.042.

Stanley, E. R. and Chitu, V. (2014) 'CSF-1 receptor signaling in myeloid cells', *Cold Spring*

Harbor Perspectives in Biology, 6(6), pp. 1–22. doi: 10.1101/cshperspect.a021857.

Stogsdill, J. A. *et al.* (2022) 'Pyramidal neuron subtype diversity governs microglia states in the neocortex', *Nature*, 608(7924), pp. 750–756. doi: 10.1038/s41586-022-05056-7.

Swinnen, N. *et al.* (2013) 'Complex invasion pattern of the cerebral cortex bymicroglial cells during development of the mouse embryo', *GLIA*, 61(2), pp. 150–163. doi: 10.1002/glia.22421.

Tay, T. L. *et al.* (2017) 'A new fate mapping system reveals context-dependent random or clonal expansion of microglia', *Nature Neuroscience*, 20(6), pp. 793–803. doi: 10.1038/nn.4547.

Thion, M. S. *et al.* (2018) 'Microbiome Influences Prenatal and Adult Microglia in a Sex-Specific Manner', *Cell*. Elsevier Inc., 172(3), pp. 500-507.e16. doi: 10.1016/j.cell.2017.11.042.

Thion, M. S. *et al.* (2019) 'Biphasic Impact of Prenatal Inflammation and Macrophage Depletion on the Wiring of Neocortical Inhibitory Circuits', *Cell Reports*, 28(5), pp. 1119-1126.e4. doi: 10.1016/j.celrep.2019.06.086.

Thion, M. S. and Garel, S. (2020) 'Microglial ontogeny, diversity and neurodevelopmental functions', *Current Opinion in Genetics and Development*. Elsevier Ltd, pp. 186–194. doi: 10.1016/j.gde.2020.06.013.

Thion, M. S., Ginhoux, F. and Garel, S. (2018) 'Microglia and early brain development: An intimate journey', *Science*. American Association for the Advancement of Science, 362(6411), pp. 185 LP – 189. doi: 10.1126/science.aat0474.

Tremblay, M. Ě. M.-E. `, Lowery, R. L. and Majewska, A. K. (2010) 'Microglial interactions with synapses are modulated by visual experience', *PLoS Biology*. Edited by M. Dalva. Public Library of Science, 8(11), p. e1000527. doi: 10.1371/journal.pbio.1000527.

Umpierre, A. D. and Wu, L.-J. J. (2021) 'How microglia sense and regulate neuronal activity.', *Glia*. United States, 69(7), pp. 1637–1653. doi: 10.1002/glia.23961.

Utz, S. G. *et al.* (2020) 'Early Fate Defines Microglia and Non-parenchymal Brain Macrophage Development', *Cell*. Elsevier, 181(3), pp. 557-573.e18. doi: 10.1016/j.cell.2020.03.021.

Verney, C. *et al.* (2010) 'Early microglial colonization of the human forebrain and possible involvement in periventricular white-matter injury of preterm infants', *Journal of Anatomy*, 217(4), pp. 436–448. doi: 10.1111/j.1469-7580.2010.01245.x.

Wang, Y. *et al.* (2012) 'IL-34 is a tissue-restricted ligand of CSF1R required for the development of Langerhans cells and microglia', *Nature Immunology*, 13(8), pp. 753–760. doi: 10.1038/ni.2360.

Wei, S. *et al.* (2010) 'Functional overlap but differential expression of CSF-1 and IL-34 in their CSF-1 receptor-mediated regulation of myeloid cells', *Journal of Leukocyte Biology*, 88(3), pp. 495–505. doi: 10.1189/jlb.1209822.

Weinhard, L. *et al.* (2018) 'Microglia remodel synapses by presynaptic trogocytosis and spine head filopodia induction', *Nature Communications*. Springer US, 9(1). doi: 10.1038/s41467-018-03566-5.

White, F. A. *et al.* (1990) 'Neonatal infraorbital nerve transection in the rat: Comparison of effects on substance P immunoreactive primary afferents and those recognized by the lectinBandierea simplicifolia-I', *The Journal of Comparative Neurology*. John Wiley & Sons, Ltd, 300(2), pp. 249–262. doi: 10.1002/cne.903000208.

Wlodarczyk, A. *et al.* (2017) 'A novel microglial subset plays a key role in myelinogenesis in

developing brain', *The EMBO Journal*, 36(22), pp. 3292–3308. doi: 10.15252/embj.201696056.

Yona, S. *et al.* (2013) 'Fate Mapping Reveals Origins and Dynamics of Monocytes and Tissue Macrophages under Homeostasis', *Immunity*. Elsevier, 38(1), pp. 79–91. doi: 10.1016/j.immuni.2012.12.001.

York, E. M., Bernier, L. P. and MacVicar, B. A. (2018) 'Microglial modulation of neuronal activity in the healthy brain', *Developmental Neurobiology*, 78(6), pp. 593–603. doi: 10.1002/dneu.22571.

Zhan, L. *et al.* (2020) 'A MAC2-positive progenitor-like microglial population is resistant to CSF1R inhibition in adult mouse brain', *eLife*, 9, pp. 1–22. doi: 10.7554/elife.51796.

Zhu, H. *et al.* (2016) 'Cre-dependent DREADD (Designer Receptors Exclusively Activated by Designer Drugs) mice', *genesis*. John Wiley & Sons, Ltd, 54(8), pp. 439–446. doi: https://doi.org/10.1002/dvg.22949.

Article 2

Microglia maintain structural integrity during fetal brain morphogenesis

Summary

During development, microglia transiently accumulate in a specific developmental hotspot, the early dorsal white matter (EDWM) during the first postnatal week. These accumulating microglia have an atypic profile, called axon-tract associated microglia (ATM), and have been associated to appropriate oligodendrogenesis and myelination. Here, taking advantage of available scRNA-seq datasets, we showed that a similar ATM signature could be found amongst embryonic microglia. We identified microglial hotspots in the embryonic brain of both mice and humans, the cortico-striatal-amygdalar boundary (CSA) and cortical-septal boundary (CSB), where microglia indeed share great similarities with postnatal ATM. These two hotspots of embryonic ATM (eATM) accumulations are at the interface between structures growing at different pace and particularly prone to morphogenetic tensions. Indeed, while this was described for the CSB, we highlighted normally occurring and transient microlesions at the CSA. Using several genetic models, we modulated morphogenetic stress at the CSA and found that it correlates with eATM accumulation. Through diverse models of microglial embryonic depletion, we found that absence of microglia leads to the formation of cavitary lesions at both the CSA and CSB. They are later resorbed postnatally, concomitant with microglial repopulation. While inactivation of different signaling pathways key in microglial functions did not alter the CSA nor CSB, we found that the ATM-derived extracellular-matrix interacting protein Spp1/Osteopontin was involved in both lesion prevention and repair.

These findings reveal a novel contribution of immune cells to fundamental aspects of brain construction and architecture, acting as bona fide “glia/glue” cells, and provide new evidence for microglia stage and state-specific functions. This work is currently uder review in Cell.

Author's contribution

I participated in this study by setting up the paradigm of embryonic microglial depletion through the use of PLX3397 and its characterization, specifically during repopulation. I also conducted experiments of laser injury on two-photon live-imaging of embryonic brain slices, which are not shown here. Finally, I tried to set up other models of microglial depletion: I first aimed for a local depletion of microglia located at the CSA through a conditional *Csf-1* knock-out, which was unfortunately not specific enough to the region of the CSA; I also tried to develop a microglial specific depletion model using the $p2ry12^{creER};R26^{dta}$, but we found that tamoxifen doses needed to induce microglial death were detrimental to the tissue.

Microglia maintain structural integrity during fetal brain morphogenesis

Akindé Lawrence[1], Alice Canzi[1,˚], Cécile Bridlance[1,˚], Nicolas Olivié[1], Claire Lansonneur[2], David A. D. Munro[3], Aurélien Fortoul[4], Davide Boido[5], Guillaume Oller[1], Paola Squarzoni[1], Feriel Zehani[1], Adrien Candat[6], Julie Helft[7], Cécile Allet[8], Francoise Watrin[4], Jean-Bernard Manent[4], Denis Thieffry[2], Laura Cantini[2], Clare Pridans[9,10], Josef Priller[3,11,12], Antoinette Gélot[13], Paolo Giacobini[14], Luisa Ciobanu[5], Florent Ginhoux[15,16], Morgane Sonia Thion[1,#], Ludmilla Lokmane[1,#] and Sonia Garel[1,17,*,#]

[1]Team Brain Development and Plasticity, Institut de Biologie de l'École Normale Supérieure (IBENS), École Normale Supérieure, CNRS, INSERM, Université PSL, 75005 Paris, France.

[2]Team Computational Systems Biology, Institut de Biologie de l'École Normale Supérieure (IBENS), École Normale Supérieure, CNRS, INSERM, Université PSL, 75005 Paris, France.

[3]UK Dementia Research Institute at the University of Edinburgh, Centre for Clinical Brain Sciences, University of Edinburgh.

[4]INMED, Inserm, Aix-Marseille University, Turing Centre for Living Systems, Marseille, France.

[5]NeuroSpin, CEA, Gif-sur-Yvette, Paris-Saclay University, Saclay, France.

[6]Electron Microscopy Facility, Institut de Biologie de l'École Normale Supérieure (IBENS), École Normale Supérieure, CNRS, INSERM, Université PSL, 75005 Paris, France.

[7]Université Paris Cité, INSERM U1016, CNRS UMR8104, Institut Cochin, 75014 Paris, France.

[8]UMR-S 1172 - JPArc - Centre de Recherche Neurosciences et Cancer, University of Lille, Lille, France.

[9]University of Edinburgh Centre for Inflammation Research, Edinburgh EH16 4TJ, UK.

[10]Simons Initiative for the Developing Brain, University of Edinburgh, Edinburgh, UK.

[11]Department of Psychiatry and Psychotherapy, School of Medicine, Technical University Munich, 81675 Munich, Germany.

[12]Neuropsychiatry and Laboratory of Molecular Psychiatry, Charité – Universitätsmedizin and DZNE Berlin, 10117 Berlin, Germany.

[13]Service D'anatomie Pathologique, Hôpital Trousseau APHP, 75571 Paris Cedex 12, France.

[14]University of Lille, CHU Lille, Inserm, Laboratory of Development and Plasticity of the Neuroendocrine Brain, Lille Neuroscience and Cognition, UMR-S 1172, F-59000 Lille, France.

[15]Singapore Immunology Network (SIgN), Agency for Science, Technology and Research, Singapore 138648, Singapore.

[16]INSERM U1015, Gustave Roussy Cancer Campus, Villejuif 94800, France.

[17]Collège de France, Université PSL, 75005 Paris, France.

[˚,#] These authors contributed equally to this work

[*]Corresponding author and lead contact. Email: sonia.garel@bio.ens.psl.eu

Keywords: microglia; microglial state; development; cerebral cortex; repair; cavity; lesion; Spp1; osteopontin; morphogenesis; amygdala; corpus callosum.

SUMMARY

Microglia, the brain-resident macrophages, play key roles in health and disease via a diversity of cellular states. While embryonic microglia display a large heterogeneity of cellular distribution and transcriptomic states, their functions remain poorly characterized. Here, we uncovered a novel role for microglia in the maintenance of structural integrity at two fetal cortical boundaries. At these boundaries between structures that grow in distinct directions, embryonic microglia accumulate, display a state resembling postnatal Axon-Tract associated Microglia (ATM) and prevent the progression of microcavities into large cavitary lesions, in part via a mechanism involving the ATM-factor Spp1. Microglia and Spp1 furthermore contribute to the rapid repair of lesions, collectively highlighting protective functions that preserve the fetal brain from physiological morphogenetic stress and injury. Our study thus highlights novel functions for embryonic microglia and Spp1 in maintaining structural integrity during morphogenesis, with major implications for our understanding of microglia functions and brain development.

INTRODUCTION

Microglia, the brain-resident macrophages, play key roles in the development and maintenance of brain circuits throughout life [1-8]. These immune sentinels are involved in key steps of neural network assembly, for instance by regulating neuronal numbers, synaptic development and refinement, maturation of myelin, synaptic transmission or neuronal excitability[1-15]. In agreement with the diverse roles of microglia, their dysfunction has been linked to almost all brain pathologies, ranging from developmental disorders to neurodegenerative diseases[1-7]. Anatomical and recent single-cell transcriptomic studies have shown that microglia exist in distinct cellular and transcriptomic states, particularly during development, ageing and neurodegeneration[16-33]. This transcriptomic diversity, as shown in the white matter and cerebral cortex[29,32], can be driven by the local environment, revealing a symbiotic relationship between microglia and their local cerebral niches[33]. Yet, how such heterogeneity relates to specific locations and functions of these multifaceted cells, especially during the dynamic period of prenatal development, remains poorly understood.

Microglia originate from yolk sac-derived macrophages that migrate and seed the brain primordium during early embryogenesis[34]. This process starts from embryonic day (E) 9 in mice, and gestational week (GW) 4 in humans [2,35,36]. Microglia subsequently colonize the parenchyma during the dynamic phases of cerebral development, characterized by a prolonged phase of neuronal generation, migration and wiring, as the brain grows, folds and changes of shape[37]. In both human and mice, microglia colonize the brain in a progressive, highly stereotyped manner[2,4,36,38] characterized by an uneven distribution: microglia accumulate at hotspots, avoid selective regions such as the developing cortical plate[39], and exhibit a diverse range of morphologies, cellular behaviors and transcriptomic states[5,7,21,22,27,31,32]. Although this heterogeneity and diversity are progressively lost as development proceeds, they can reemerge in the context of ageing and disease[17-20,22-24,29-31,33]. In physiological conditions, microglial heterogeneity spans both the prenatal and postnatal periods [2,4,21,22,38,40,41]. In particular, specific populations of amoeboid microglia present in the

postnatal cortical white matter, including the corpus callosum [21,22,40,41], display a specific transcriptomic state and have been variously termed Axon-Tract-associated Microglia (ATM) [22], proliferative associated microglia (PAM) [2], youth-associated microglia (YAM)[31] or Cd11c-positive (+) microglia[40,41]. Postnatal ATM/PAM/YAM/Cd11c^{+} microglia, or ATM, are characterized by the expression of *Spp1* (encoding osteopontin or OPN), *Lgals3*, *Gpnmb, Clec7a, Itgax* (encoding Cd11c) and *Igf1*, sharing transcriptomic features with Disease-Associated Microglia (DAM), initially identified in mouse models of Alzheimer's disease and observed in various neurodegenerative contexts [17-19,24,29,31]. Functionally, postnatal ATM are involved in the engulfment of nascent glial cells, regulation of myelination, and promotion of neuronal survival, in part through *Igf1* expression [21,22,40-43]. While these studies highlight a link between postnatal microglial hotspots, specific transcriptomic states and functions, the roles of prenatal microglia and their potential cellular heterogeneity remain largely to be deciphered.

Here, by combining transcriptomic analyses, imaging and genetically-modified mouse models, we reveal that microglia maintain the structural integrity at the fetal cortico-striato-amygdalar and cortico-septal boundaries, where embryonic microglia accumulate and display a specific state resembling postnatal ATM [21,22,40,41]. These boundaries, which are vulnerable to developmental tensions linked to brain growth and morphogenesis, rely on microglia to prevent the formation of large cavitary lesions, in part via a mechanism involving the pleiotropic ATM-factor Spp1/Osteopontin (OPN). Microglia and Spp1 furthermore contribute to the rapid repair of large lesions, which highlights their protective functions in preserving the fetal brain from physiological morphogenetic tensions and injuries. Our study thus reveals that embryonic microglia and ATM-factor Spp1 play a critical role in maintaining the structural integrity of the developing brain during normal morphogenesis, with major implications for our understanding of microglia functions and cerebral development.

RESULTS

Embryonic ATM accumulate at the cortico-striato-amygdalar boundary

While the developmental heterogeneity of microglia has been established by anatomical [2,4,36,38] and single cell transcriptomic studies[21,22,27,32], whether transient accumulations or hotspots of microglia in the embryonic brain composed of cells in specific states is yet to be determined.

As a first step toward selectively exploring the heterogeneity of microglia during embryogenesis, we took advantage of a longitudinal brain single-cell (sc) transcriptomic dataset generated by La Manno et al. for each day between embryonic day (E)9 and E18 [30]. By extracting and analyzing the microglia from this dataset, we identified 3 distinct clusters: cycling microglia (MG), non-cycling MG, and embryonic microglia that resemble postnatal ATM/PAM/YAM/Cd11c^{+} microglia [30] (Fig. 1A). Embryonic ATM (eATM) are notably present from E14 to E18.5 (Fig. 1A, S1A and Table S1) and share a core genetic signature with previously described postnatal white matter ATM (Fig. 1B,C) [22] and PAM (Fig. S1B,C) [21]: they notably express *Spp1*, which codes for Osteopontin (OPN), *Igf1*, *Lgals3*, which codes for Galectin3/Mac2 and *Gpnmb* (Table S1) [21,22]. Consistently, eATM [30] and PAM [21] gene signatures are present mainly in cells of the ATM cluster (Fig. S1D-F) as described by Hammond and colleagues [22], highlighting the similarities between these transcriptomic signatures.

To assess whether eATM may locate in specific regions, we first focused on mid-neurogenesis (E14.5), when the eATM transcriptomic signature is first detected and microglial distribution starts to be noticeably uneven across the developing forebrain [38,39]. Using the *Cx3cr1^{gfp}* mouse line, which labels all macrophages, we observed a significant accumulation of GFP^{+} microglia at the boundary between the cerebral cortex, striatum and amygdala [38,39], which we called the cortico-striato-amygdalar boundary (CSA)(Fig 1D). These cells exhibited an amoeboid morphology, expressed high levels of the lysosomal marker CD68 and were

notably phagocytic as assessed in *ex vivo* slices (Fig. S1H-I). Their bona fide microglial identity was confirmed by their location in the parenchyma (Fig. 1D) and expression of the microglial marker P2Y12 receptor but not the perivascular macrophage marker LYVE1 (Fig. 1D) [2,23]. These cells were most abundant at E15 and co-expressed ATM-specific markers at this time point (Fig.1E and S1G). Using *Cd11c-eYFP* mice and immunostainings we found that approximately 60% of CSA microglia labeled by IBA1 immunostaining or *Cx3cr1^{gfp}* labelling, co-expressed proteins encoded by ATM "core" signature genes: Cd11c, Mac2, Clec7A, Spp1 and GPNMB (Fig. 1E and S1G). This contrasted with adjacent regions, where only few sparse cells expressed these markers (Fig. 1E), highlighting a very local and dense accumulation of eATM at the CSA between E14.5 and E16.5, with only few cells restricted to the ventro-caudal CSA after E16.5 (data not shown). To investigate whether a similar accumulation occurs in humans, we labelled fetal brains from GW 9 to 14, and detected a conserved pattern of microglia expressing ATM core factors at the CSA throughout these stages (Fig. 1F and S1J). These data show that, in both mice and humans, microglia expressing an ATM-like signature accumulate at the early embryonic CSA.

Microglia maintain structural integrity at the cortico-striato-amygdalar boundary

Accumulation of eATM at the CSA occurs much earlier than the extensive generation of other glial cells or the development of myelin, both of which have been associated with postnatal ATM functions. To investigate the potential role of microglia in the development of the CSA, we examined various established and novel models of macrophage and microglia depletions by mainly targeting the Colony stimulating factor 1 receptor (CSF1R) signaling pathway, which is required for microglial survival [44,45]. We first administered a CSF1R-blocking antibody (AFS98) to dams at E6.5 and E7.5, causing a transient depletion of microglial progenitors and a severe depletion of microglia until E18.5[11,38,46] (Fig. S2A), followed by a progressive microglial repopulation during the first postnatal week[11,38,46]. We also achieved similar depletion/repopulation by feeding pregnant dams with PLX3397[47,48], a pharmacological

inhibitor of CSF1R, between E6.5 and E15 (Fig. S2B) and compared with *Pu.1* mutant embryos that lack all myeloid cells [49]. As these models target both microglia and other macrophage populations over a broad embryonic period, we also performed more transient depletions by treating pregnant dams with PLX3397 for only 3 days, between E12.5 and E15, covering the timing of microglial accumulation at the CSA (Fig. S2C). Finally, and importantly, we examined *Csf1r*$^{\triangle FIRE\triangle/FIRE}$ that lack microglia yet retain most other brain macrophages [50,51], and enable to interrogate microglia-specific roles in brain circuits [10,52]. In all the models we examined, including the three-days short PLX3397 treatment and *Csf1r*$^{\triangle FIRE\triangle/FIRE}$ embryos, we found that the lack of microglia induced a large "cavitary lesion" at the CSA boundary starting at E14.5 (Fig. 2A) and persisting until E18.5 (Fig. 2B). These cavities, which formed where eATM normally accumulate (Fig. 1D), lacked cell bodies and showed no contact with the ventricle, prompting us to examine them using electron-microscopy (Fig. S2D). As observed in PLX3397-treated embryos, the cavitary lesions did not contain cells or displayed a basal lamina (Fig. S2D), but rather displayed sparse irregular membrane debris, resembling cysts or pseudocysts that are reported in several human pathologies, including cystic leukoencephalopathies [53]. In contrast, we did not observe such cavitary lesions in models perturbing already known developmental functions of microglia, such as *Cx3cr1*, *Dap12/TyroBP* and *Complement receptor 3* (*CR3*) mutants, or in embryos exposed to a mild prenatal inflammation (MIA) (Fig. S1E).

To rule out the possibility that the cavities were caused by tissue damage during sectioning, we analyzed whole brains using iDISCO clearing and magnetic resonance imaging (MRI) [54,55]. iDISCO clearing and 3D hemibrain reconstruction performed in both CSF1R depletion models revealed CSA lesions located in the caudal third of the telencephalic vesicles, at the border between the caudal insular cortex, claustrum, striatum and amygdala (Fig. 2C and Supplementary movies S1-2). Similarly, whole-head MRI scans of fixed *Csf1r*$^{\triangle FIRE\triangle/FIRE}$ and PLX3397-treated embryos and newborns pups showed bright bilateral hyperintensities after contrast enhancement, unequivocally confirming the presence of CSA cavitary cystic

lesions in the absence of microglia (Fig. 2D,E). Our results thus demonstrate that microglia maintain the structural integrity of the fetal CSA, a site where eATM normally accumulate, revealing a novel physiological function of these cells during early development.

Microglia maintain integrity at another ATM-dense cortical boundary

Since the eATM transcriptomic signature is detected throughout prenatal life, we investigated whether accumulations of eATM were present at later embryonic stages, at sites where microglia could exert conserved roles in the maintenance of structural integrity. To this aim, we conducted a longitudinal study of the embryonic forebrain after E14.5. In addition to the CSA, found only one large and dense accumulation of eATM cells in the midline between E16.5 and E18.5, at the cortico-septal boundary (CSB) (Fig. 3A). This hotspot was located below the corpus callosum, consistent with where postnatal ATM reside later in life [21,22,40,41,56] and indicating a continuum of ATM-like cell accumulations that spans the prenatal and postnatal periods. A few scattered eATM cells were also observed in the subpallium and hippocampus (data not shown). Using a conserved combination of core ATM markers (Spp1, Clec7A, GPNMB, Mac2), we found that approximately 70% of microglia accumulating at the CSB co-expressed ATM markers (Fig. 3A). To further assess the impact of microglial depletion on this cortical boundary where eATM accumulate during late embryogenesis, we examined all the aforementioned models of microglia depletion (Fig. 2 and S2). We found that, similarly to what we observed at the CSA, the absence or depletion of microglia induced the formation of midline cavities at the spot where microglia normally accumulate (Fig. 3B). This cavitary lesion was observed with iDISCO transparization (Supplementary movies S3,4), and in MRI scans when the contrast at the midline enabled visualization (data not shown). Thus, overall, the absence of microglial during prenatal development leads to a sequential loss of structural integrity at the CSA and CSB, two sites where eATM normally accumulate.

ATM-factor Spp1 contributes to structural integrity at cortical boundaries

The involvement of microglia in maintaining tissue integrity at the hotspots of accumulating eATM raises the question of the underlying molecular mechanisms. As mentioned, we did not observe cavitary lesions in genetic models perturbing known developmental functions of microglia, such as *Cx3cr1*, *Dap12/TyroBP* and *Complement receptor 3* (*CR3*) mutants (Fig. S2E), suggesting the involvement of alternative pathways. We focused on ATM-specific molecules known to modulate immune functions and contribute to adhesion and tissue remodeling, such as Spp1 and GPNMB [57,58]. In particular, Spp1, which encodes OPN, has been linked to a various tissue remodeling and repair processes, and has recently been shown to promote microglial phagocytosis in the context of neuronal damage and early stages of Alzheimer's Disease [59,60]. We took advantage of available global knock-outs, as these factors are highly and specifically expressed by microglia in the prenatal brain at these developmental timepoints (Fig. S3A). While mice lacking *Gpnmb* displayed normal brain structure (Fig. S3B-C), approximately 50% of those lacking *Spp1* showed cavitary lesions at the CSA at E14.5 (Fig. 4A-C), and 70% had lesions at the CSB at E18.5 (Fig. 4D-F). The cavities rapidly resorbed overtime, within 24 hours, suggesting that while Spp1/OPN contributes to maintaining structural integrity in the developing brain, additional factors or microglial properties appear to be implicated. Importantly, ATM factors, including Mac2 and GPNMB, were still expressed in *Spp1* mutants at both the CSA and CSB (Fig. 4B,F), indicating that Spp1 is not required for the induction of ATM-core factors but rather contributes to microglial function in brain integrity at cortical boundaries.

Microglia prevent the formation of cavitary lesions due to morphogenetic stress

The involvement of microglia and Spp1 in maintaining tissue cohesion at cortical boundaries raised the question of what properties might be specific to these boundaries. The CSB, located at the border between the cerebral cortex and the septum, is subjected to morphogenetic

constraints that increase as the cerebral cortex grows, and displays a normally occurring cavity called the cavum septum that resorbs over development [56,61]. The CSA, similarly to the CSB, is located at the border between the cerebral cortex and structures growing at different rates and in distinct directions, making it a region of morphogenetic tensions and tissue reorganization [62-64]. We therefore investigated whether these boundaries exhibited specific features and whether they could be affected by morphogenetic constraints, focusing on the CSA.

We first characterized the local niche of eATM at the CSA during normal physiological development at E14.5. Interestingly, the CSA was characterized by distinctive microdomains that were only sparsely populated by cells and that were bordered by microglia expressing the eATM markers Mac2 and Spp1 (Fig. 5A). Electron microscopy confirmed the presence of microcavities that were consistently adjacent to CSA microglia (Fig. 5A). These microcavities lacked a basal lamina, contained cell membrane fragments, and systematically abutted microglia that exhibited an amoeboid morphology, which is a hallmark of eATM in the CSA (Fig. 5A). Our observations suggested that such physiological microcavities might contribute to the local microglial recruitment and/or the induction of an ATM-like state. Furthermore, they raised the possibility that in the absence of microglia, microcavities might progress into larger lesions due to local morphogenetic constraints, with notable effects on fetal brain integrity.

To experimentally test the hypothesis that the CSA cavitary lesions form due to unrestrained local stress linked to morphogenesis, we examined the embryonic brains of mice in which genetic mutations generate increased or decreased developmental constraints. First, we used a genetic model of conditional *RhoA* inactivation (*Emx1*$^{cre/+}$*; RhoA*$^{fl/fl}$), in which a large periventricular nodular heterotopia forms from E15.5 [65] (Fig. 5B,C), increasing cortical thickness and organization without drastically altering microglial distribution at early stages (Fig. S4). At E18.5 and onwards, when the heterotopia is large and cortical morphogenesis is affected, we observed visible lesions at the CSA in 50% of mutant embryos, progressing into a large lesion observed in all cases at P8 (Fig. 5B,C). This process correlated with the marked

recruitment of microglia at the CSA and an increased number of cells expressing of ATM core markers Spp1, Mac2 and GPNMB at E18.5, even in embryos that did not show marked lesions at th timepoint (Fig. 5D,E and data not shown). Our findings hence reveal that drastically increasing morphogenetic tensions can drive microglial recruitment, increase the density of ATM-like microglia and ultimately lead to local CSA lesions.

Conversely, we studied the brains of *Brn4^{cre}; Wnt3A^{dta}* embryos, which lack a large brain structure, the thalamus[66], and therefore experience reduced morphogenetic stress in the developing forebrain. As expected, the CSA was preserved in E15.5 mutant embryos (Fig. 6A). We observed a conserved recruitment of microglia at the mutant CSA, although with a reduced number of cells co-expressing the ATM core factors Spp1, Mac2 and GPNMB (Fig. 6B,C and data not shown). These observations indicate that, conversely, alleviating morphogenetic constraints limits ATM-like microglial recruitment at the CSA. To further test whether alleviating morphogenetic constraints would limit the formation of lesions in the context of microglial absence, we treated *Brn4^{cre}; Wnt3A^{dta}* pregnant dams with PLX3397 during a short time-window between E12.5 and E15.5 (Fig. 6D,E). Importantly, while wild-type animals treated with PLX3397 exhibited clear CSA lesions, mutant embryos with reduced morphogenetic stress showed fewer and smaller lesions (Fig. 6D,E), highlighting that the extent of CSA lesions is driven by morphogenetic constraints.

Taken together, our results indicate that the CSA is a site of developmental vulnerability, where ATM-like microglia accumulate in response to morphogenetic constraints. Microglia prevent the progression of cavitary lesions due to morphogenetic stress, thereby preserving the structural integrity of this fetal cortical boundary.

ATM-like microglia are induced by lesions and contribute to rapid repair

Our results indicate that microglia prevent the formation of lesions at sites of morphogenetic tensions. Since microglia are known to help repair exogenous damage in the adult brain and

neonatal spinal cord [67], we further investigated whether lesions could induce microglial recruitment, ATM-like features, and whether microglia or Spp1 could contribute to the repair of large lesions at the CSA and CSB.

To test these hypotheses, we induced *in utero* lesions (IUL) in the neocortex of E14.5 *Cx3cr1*^{gfp} embryos by performing a stab-wound using a glass pipette (Fig. 7A-E). We examined the brains 2.5 h after the injury to assess the initial response (Fig. 7A). After 2.5 h, we already observed a marked accumulation of *Cx3cr1*^{gfp}–positive cells at the lesion site, with approximately 30% of these cells also expressing the ATM markers Spp1 or Mac2, and 10% expressing GPNMB (Fig. 7B, C). Thus, *in utero* stab-lesions led to very rapid recruitment of *Cx3cr1*^{gfp}–positive cells that expressed at least some ATM-core markers at the injury site (Fig. 7A-C). To assess whether these recruited cells may contribute to the rapid repair of lesions, we performed a similar experiment on PLX3397-treated embryos (Fig. 7D,E). We observed that microglial depletion delayed healing at the 2.5 h timepoint (Fig. 7D,E), a difference that was not observed after 24h (data not shown), suggesting that *Cx3cr1*^{gfp}–positive recruited cells might contribute to the early phases of efficient tissue repair.

We then examined whether microglial could contribute to the repair of large lesions at the CSA and CSB (Fig. 2, S2 and 3) and took advantage of the fact that after PLX3397-prenatal treatment, microglia repopulate the brain postnatally. We found that in pups prenatally exposed to PLX3397, CSA lesions rapidly resorbed within the first postnatal days, concomitantly to the progressive microglial repopulation (Fig. 7F): while all mice bore cavities at P0, 60% had already fully closed by P3 (Fig. 7F). Furthermore, lesion closure was consistently associated with a dense microglial accumulation at the scar, and these microglia co-expressed ATM markers Spp1, GPNMB and Mac2 (Fig. 7F, G). At P7, over 70% of the mice had their CSA lesions closed (Fig. 7F). Notably, at all stages, mice that still exhibited a cavity at the CSA showed microglial repopulation in other brain regions but lacked a local accumulation of microglia at the CSA (Fig. S5). All CSA cavities were systematically resorbed by P20 (Fig. 7F), and we observed a similar timeline of resorption at the CSB (data not shown). Although the

repair process was rapid, long-lasting morphological defects persisted at the CSA (Fig. S6), underscoring the importance of preserving structural integrity during morphogenesis.

Finally, as for the prevention of cavitary lesion formation, we found that this rapid repair process also relied on Spp1 (Fig. 7H, I). Indeed, by comparing at P7 wild-type and *Spp1*$^{-/-}$ pups exposed to PLX3397-prenatally, we observed a comparable microglial recruitment and Mac2 induction (Fig. 7I), but a significant inhibition of lesion closure in mice lacking Spp1 (Fig. 7H).

Taken together, these data show that microglia and Spp1 play crucial roles in preventing the progression of CSA microcavities into large lesions and promoting their prompt closure, which is essential for preserving brain integrity during development. Our study reveals novel functions of microglia and Spp1 in maintaining structural integrity in response to morphogenetic stress and lesions, underscoring the importance of these immune cells in early brain development.

DISCUSSION

Microglia have been associated with multiple functions, including axonal progression, cortical interneuron wiring, synaptic development and refinement, through a variety and of receptors and signaling pathways including Cx3cr1/Cx3cl1, Trem2/Dap12, Complement, and purinergic P2Y12 receptors[2,11-14,35,68-71]Our study reveals a novel and essential role of microglia in preserving brain tissue integrity during the development cerebral cortex develops, before the emergence of potentially redundant or complementary glial cells, such as astrocytes [37,72]. Indeed, because microglia colonize the brain from early embryonic stages and astrocytes or oligodendrocytes are produced later, microglia constitute a unique and a large contingent of embryonic glial cells [2,35].

In the absence of microglia, lesions form at specific cortical boundaries that constitute sites of fragility and normally host eATM, a microglial state resembling postnatal ATM, which has been linked with myelination [21,27,40,41,43]. Our study uses a combination of global, transient and selective models of microglial depletion, unambiguously establish a role for these immune cells in preventing the progression of microcavities into large cavitary lesions at cortical boundaries (Fig. 2, S2, 3, 5, S5 and 6). However, as we were unable to efficiently deplete microglia locally or manipulate their transient cellular states, it is possible that the accumulation of local eATM at these sites might not be the only factor responsible for the observed phenotypes. Nonetheless, we discovered that transient microglial hotspots at the CSA and CSB contained dense accumulations of eATM that were remarkably similar to their postnatal counterparts, confirming that the ATM state spans the prenatal and postnatal periods [22,30]. Interestingly, while the functions of postnatal ATM have largely been attributed to Igf1 [40-42], our study reveals that Spp1/OPN, an atypical extracellular matrix (ECM)-interacting factor previously linked to bone development, wound healing, inflammation [57-59], and microglial phagocytosis [59,60], contributes to tissue integrity at the cortical boundaries and the rapid repair of large lesions in the developing brain. While inactivating *Spp1* alone did not fully mimic the impact of microglial depletion, suggesting that other factors are likely involved, our findings

support a key contribution of the Spp1 core-ATM factor to microglial functions in both tissue integrity and repair. Importantly, we also reveal that Spp1 and other ATM factors are quickly induced in microglia that accumulate at sites of prenatal tissue lesions (Fig. 7), revealing the remarkable ability of these cells to switch states and exhibit plasticity in response to experimentally induced injury.

Core ATM-factors, including Spp1/OPN, are involved in immune cell responses, ECM organization, wound-healing and regulation of inflammation, and have been detected in a wide range of macrophages, during skin lesion, heart-repair after myocardial infarction or liver fibrosis [57-59,73-75]. This observation indicates that at least some aspects of the "ATM program" involved in brain integrity and repair are likely not unique to microglia but rather represent a basic feature shared across macrophages which is important for the general maintenance of tissue homeostasis, particularly in response to exogenous damage or lesions. In microglia, Spp1 and ATM factors are also expressed by damage-induced microglia during stroke [76] or neonatal spinal cord repair [67], as well as in DAM and TAM, which are respectively associated with neurodegeneration and tumors [18,20,23,27,77]. Thus, the "ATM program" may overlap with a basic repair macrophagic program that is triggered by tissue disruption in different contexts of health and disease. Whether Spp1 is consistently involved and how it acts, which other factors contribute to ATM functions in tissue cohesion and repair, and whether other cell types could exert similar functions in the adult brain constitute key questions to address in future studies.

The genuinely glial role of developing microglia described in this study has not been reported in other species, such as zebrafish, which provides various genetic models to examine brain development in the absence of microglia [78]. Notably, no evidence of dense ATM hotspots has been reported in zebrafish [78,79]. These observations raise the intriguing possibility that the embryonic ATM state, and associated repair properties, might have been co-opted during evolution to ensure the proper morphogenesis of a growing cerebral cortex, which is a hallmark of mammals. In agreement, we found that increasing morphogenetic constraints in a model of cortical periventricular nodular heterotopia [65] can lead to a selective breaking at the

CSA boundary strengthening the hypothesis that the CSA represents a site of morphogenetic fragility in mammals. In contrast, when morphogenetic constraints were alleviated in a genetic model of thalamus ablation, microglia and eATM were found to be less crucial in preventing lesions. However, in both models, we observed that the recruitment of ATM-like cells was influenced by morphogenetic constraints and the presence of lesions, underscoring the interaction between immune brain cells and their local niches, as seen in the aging white matter and postnatal cerebral cortex [29,32]. There is thus a delicate balance between tissue fragility, eATM localization and microglial functions, which warrants further investigation into the pathways involved in ATM induction and their role in mice and across species. Overall, our findings demonstrate that the proper development of the cerebral cortex depends on the mitigation of tissue damage by brain resident macrophages, allowing for the morphogenesis of complex structures, which is a hallmark of brain evolution.

In the context of pathological brain wiring, lesions are typically associated with damage induced by abnormally “activated” microglia in response to various triggers, such as hypoxia, inflammation, preterm birth, or congenital viral infections. For example, bilateral cysts in the temporal lobes, where the CSA is located, or midline cavities such as cavum septum pellucidum and midline cystic lesions, have been reported in several neurodevelopmental disorders [80,81]. Our study demonstrates the critical role of microglia and the ATM-like state in maintaining tissue integrity, suggesting that such lesions may also result from a lack of microglial function during crucial stages of morphogenesis. These findings have not only significant implications for our understanding of the fundamental mechanisms that govern brain morphogenesis and the state-specific functions of microglia but also provide new avenues for exploring microglial contributions to brain pathology.

Limitations of the study

While our study identified a novel role for microglia and their remarkable Spp1-dependent repair properties at cortical boundaries, it is important to acknowledge several limitations of our research. Firstly, morphogenetic stress could not be directly measured due to the difficulty of performing these experiments *in utero*, but rather indirectly assessed through genetic manipulations that distort brain morphogenesis. However, we believe that this caveat is compensated by leveraging two models that selectively increase and reduce morphogenetic constraints. Secondly, the lack of local or state-specific manipulations of CSA and CSB microglial accumulations is a limitation. Despite several attempts to selectively manipulate this state, we were unable to efficiently and selectively eliminate this cell population, which is consistent with a local interplay between the local niche and microglia. Nonetheless, our results provide insights into the contribution of microglia and their diversity to brain development, evolution, and pathology, highlighting their novel bona fide role in fetal cortical morphogenesis.

ACKNOWLEDGEMENTS

We thank M. Keita and S. Viguier for excellent technical assistance and E. Touzalin, A. Delecourt, and C. Le Moal, for assistance with mouse colonies. We are grateful to Denis Jabaudon and members of the Garel team for helpful discussions and critical review of the manuscript. We are grateful to Ana-Maria Lennon-Duménil, Silvia Cappello and Cord Brackebusch for the kind gifts of reagents and mouse models. We thank Lucy Robinson and Ilya Demchenko of Insight Editing London for scientific editing of the manuscript. We thank the IBENS Imaging Facility (France BioImaging, supported by ANR-10-INBS-04, ANR-10-LABX-54 MEMO LIFE and ANR-11-IDEX-000-02 PSL* Research University, “Investments for the future”). We thank the midwives of the Gynecology Department, Jeanne de Flandre Hospital of Lille (Centre d’Orthogenie), France, for their kind assistance and support. The authors acknowledge the support of the Inserm Cross-Cutting Scientific Program (HuDeCA to P.G.). This work was supported by grants to S.G. from INSERM, CNRS, the ERC Consolidator NImO 616080, ANR Microsenso, FSER dotation, Fondation du Collège de France (Fonds St Michel support) and FRM équipe (FRM, EQU202003010195). A.L. is a recipient of a fellowship from Ecole des Neurosciences de Paris Ile-de-France network and of an ATER position from the College de France; C.B. is supported by an AMX PhD fellowship; N.O. by the Fondation pour la Recherche Médicale (FRM, EQU202003010195); C.L. is a recipient of an FRM PhD fellowship (FRM, ECO202006011600).

AUTHOR CONTRIBUTIONS

Conceptualization: A.L., C.B., M.S.T, L.L and S.G.; Formal analysis: A.L., A.C., C.B., N.O., C.L., D.B., L.C, A.C., A.G., D.T., L.C., M.S.T, L.L. ; Investigation: A.L., A.C., C.B., N.O., C.L., G.O., P.S., L.C., L.C., M.S.T, L.L.; Resources: D.M., A.F.,C.A., F.W., J.B.M., C.P, J.P., P.G., F.G. ; Writing – Original Draft: A.L., C.L., M.S.T, L.L. and S.G.; All authors contributed to Manuscript editing; Visualization: A.L., A.C., C.A., N.O., C.L., M.S.T., L.L; Project

Administration: M.S.T, L.L. and S.G.; Supervision: M.S.T, L.L. and S.G.; Funding acquisition: S.G.

DECLARATION OF INTERESTS

The authors declare no conflicts of interest.

INCLUSION AND DIVERSITY STATEMENT

One or more of the authors of this paper self identifies as an underrepresented ethnic minority in science. We support inclusive, diverse, and equitable conduct of research.

STAR METHODS

- **EXPERIMENTAL MODELS**

Mouse Lines

Cx3cr1$^{+/gfp}$ [82] (RRID:IMSR_JAX:005582), *Pu.1*$^{+/-}$ [49], *Cd11c-eYFP* [83] (RRID:IMSR_JAX:007567), *Csf1r*$^{\Delta FIRE/+}$[50], *Spp1*$^{-/-}$ [57] (RRID:IMSR_JAX:004936), *CR3*$^{-/-}$ (*Cd11b*$^{-/-}$)[84] (RRID:IMSR_JAX:003991), *Dap12/TyroBP*$^{-/-}$ [85] (RRID:MGI:3818477), *RhoA*$^{fl/fl}$ [86], *Emx1*$^{cre/+}$*;RhoA*$^{fl/+}$ [65], *WntA3*^{dta} and *Brn4*^{cre} mice [66] were maintained on a C57BL/6J background, except for *Csf1r*$^{\Delta FIRE/+}$ mice that were kept on a mixed C57BL/6 CBA background. C57BL/6J wild-type mice or heterozygote littermates were used as controls for mutant mice, as they did not exhibit any phenotype, with the exception of repair analyses (Fig. 7), in which we compared *Spp1*$^{+/+}$ and Spp*1*$^{-/-}$, and in periventricular nodular heterotopia analyses (Fig. 5), in which we compared *Emx1*$^{cre/+}$*;RhoA*$^{fl/fl}$ with cre- littermates. The day of vaginal plug formation was considered E0.5. Animals were handled in accordance with the regulations of the European Union and the local ethics committee.

Human fetuses

Fetal tissues were made available in accordance with French bylaws (Good Practice Concerning the Conservation, Transformation, and Transportation of Human Tissue to Be Used Therapeutically, published on December 29, 1998). The studies on human fetal tissue were approved by the French agency for biomedical research (Agence de la Biomédecine, Saint-Denis la Plaine, France, protocol n°: PFS16-002). Three human fetuses without known pathologies were obtained at gestational weeks (GW) 9, GW11 and GW14 from voluntarily terminated pregnancies upon obtaining written informed consent form the parents (Gynaecology Department, Jeanne de Flandre Hospital, Lille, France). Fetuses were fixed by immersion in 4% paraformaldehyde (PFA) at 4°C for 3 (GW9 fetus) or 5 days (GW11 and GW14 fetuses). The tissues were cryoprotected in 30% sucrose/PBS at 4°C overnight,

embedded in Tissue-Tek OCT compound (Sakura Finetek, USA), frozen on dry ice and stored at -80°C until sectioning. Frozen samples were cut serially at 16 µm using a Leica CM 3050S cryostat (Leica Biosystems Nussloch GmbH, Germany). Sections were kept at -80°C.

- **METHOD DETAILS**

Transcriptomic analysis

Single-cell RNA-seq data reanalysis

10X scRNA-seq microglia data from [22] and [30] were downloaded from the GSE121654 series and loom file http://mousebrain.org/development ("dev_all.loom"), respectively. The raw count matrix and metadata for microglia-annotated cells in [30] were extracted from the loom file using R v4.1.2. The data include a total of 1711 cells (510 ATM, 415 cycling microglia, 786 non-cycling microglia cells). Genes were filtered as described by the authors (expressed in at least 10 cells for [30] and at least 20 cells for [22]). For the data set from [22], additional metadata such as published t-distributed stochastic neighbor embedding (tSNE) coordinates and reported clusters were provided by the authors to select the 76,149 cells, including 2,517 ATM cells.

The Seurat v4.1.1[87] scRNA-seq pipeline was used to produce uniform manifold approximation and projection (UMAP) and tSNE plots of the microglia data [22,30]. Default parameters were used, unless stated otherwise. For [30], data were first normalized and scaled using SCTransform [88]. PCA was performed and UMAP coordinates were computed using 5 principal components. Plots were created using Seurat v4.1.1, ggplot2 v3.3.6, scCustomize 0.7.0, and the viridis v0.6.2 palette.

Differential expression analysis

Differentially expressed genes (DEGs) of ATM-annotated cells from [30] were identified using the "FindAllMarkers" Seurat function (Wilcoxon signed-rank test, assay = "RNA", min.pct=0.1, only.pos=TRUE). DEGs were further filtered (Fold Change > 1.5, Bonferroni adjusted *p-value*

< $1e^{-10}$). To construct venn diagrams, the same threshold was applied to published DEGs of ATM [22] and PAM[21].

Gene set enrichment analysis

To determine gene set enrichment in the scRNA-seq dataset, the "AddModuleScore" Seurat function (ctrl.size = length of gene list, nbin=24) was used. Several gene signatures were tested for enrichment in the microglia scRNA-seq data from [30]: (i) top enriched ATM DEGs from [22], corresponding to the 9 reported markers (i.e., *Spp1*, *Gpnmb*, *Igf1*, *Lgals3*, *Fapb5*, *Lpl*, *Lgals1*, *Ctsl*, *Anxa5*), and (ii) top enriched PAM DEGs from[21] (i.e., *Spp1*, *Clec7a*, *Gpnmb*, *Igf1*, *Lpl*, *Pld3*, *Ctsl*, *Ctsb*, *Slc23a2*, *Gpx3*) (Table S1).

Microglial Depletion

Pregnant C57BL/6J females were given anti-CSF1R mAb (αCSF1R, clone AFS98) or the rat IgG2a isotype control (clone R35-95; BD Biosciences) by intraperitoneal injection at E6.5 and E7.5, as described previously[38]. Alternatively, pregnant mice were given the CSF1R inhibitor PLX3397 (Plexxikon) mixed into standard chow (Ssniff) from E6.5 or E12.5 until E15.5. The dose of PLX3397 was 290 mg/kg and respective controls received standard chow. The efficiency of depletion procedures was verified by immunohistochemistry at embryonic stages and in one newborn P0 per litter for postnatal litters.

Maternal Immune activation

Lipopolysaccharide in sterile PBS (0.12 µg/g mouse; InvivoGen and Sigma) was injected intraperitoneally into pregnant mice at E13.5. Sterile PBS was injected into control pregnant females by the same route and at the same timepoint, without detectable effects on embryonic phenotype.

Immunohistochemistry on sections

For immunohistochemistry, mouse embryonic brains were fixed in 4% PFA at 4°C for 2 h to overnight, depending on the developmental stage. For the analysis of postnatal brains, animals were perfused with 4% PFA, brains were dissected out, then post-fixed overnight at 4°C before cutting into sections in PBS. The preparation of human fetal brain tissue is described above. Immunohistochemistry was performed on free-floating 40-100 µm-thick vibratome-cut mouse brain sections or 25 µm-thick cryostat-cut human tissue sections. Slices were first incubated for 1 h at room temperature (RT) in 0.2% Triton X-100, 0.2% Gelatin in PBS (blocking solution), and then incubated at 4°C overnight in the same blocking solution with the following primary antibodies: rat anti-CD68 (1/500; Bio-Rad Cat# MCA1957, RRID:AB_322219), chicken anti-GFP (1/1000; Aves Labs Cat# GFP-1020, RRID:AB_10000240), rabbit anti-IBA1 (1/500; FUJIFILM Wako Shibayagi Cat# 019-19741, RRID:AB_839504), rat anti-Lgals3 (MAC2) (1/1000; CEDARLANE Cat# CL8942AP, RRID:AB_10060357), rat anti-L1 (1/100; Millipore Cat# MAB5272, RRID:AB_2133200), biotinylated rat anti-LYVE1 (1/200; Thermo Fisher Scientific Cat# 13-0443-82, RRID:AB_1724157), rat anti-Myelin Basic Protein (MBP) (1/300; Millipore Cat# MAB386, RRID:AB_94975), rat anti-mDectin-1 (CLEC7A) (1/30; InvivoGen Cat# mabg-mdect, RRID:AB_2753143), mouse anti-neurofilament marker SMI-312 (1/300; BioLegend Cat# 837904, RRID:AB_2566782), goat anti-mouse Osteoactivin (GPNMB) (1/200; R and D Systems Cat# AF2330, RRID:AB_2112934), rabbit anti-P2Y12 (1/500; AnaSpec; EGT Group Cat# 55043A, RRID:AB_2298886) and goat anti-SPP1 (1/400; R and D Systems Cat# AF808, RRID:AB_2194992). Sections were rinsed in PBS-0.1% TritonX-100 and incubated at 4°C from 2 h to overnight with the following secondary antibodies (1/400 in PBS, Jackson ImmunoResearch Labs): Alexa 10 Fluor® 488-conjugated donkey anti-chicken (Cat# 703-545-155, RRID:AB_2340375), Alexa 10 Fluor® 488-conjugated donkey anti-goat (Cat# 705-545-147, RRID:AB_2336933), Alexa 10 Fluor® 488-conjugated donkey anti-rat (Cat# 712-545-150, RRID:AB_2340683), Alexa 10 Fluor® 488-conjugated donkey rabbit (Cat# 711-545-152, RRID:AB_2313584), Cy3-conjugated donkey anti-goat (Cat# 705-165-147, RRID:AB_2307351), Cy3-conjugated donkey anti-rabbit (Cat# 711-165-152,

RRID:AB_2307443), Cy3-conjugated donkey anti-rat (Cat# 712-165-150, RRID:AB_2340666), Alexa 10 Fluor® 647-conjugated donkey anti-goat (Cat# 705-605-147, RRID:AB_2340437), Cy5-conjugated donkey anti-goat (Cat# 705-175-147, RRID:AB_2340415), Cy5-conjugated donkey anti-goat (Jackson ImmunoResearch Labs Cat# 705-175-147, RRID:AB_2340415) and Cy5-conjugated donkey anti-rat (Cat# 712-175-150, RRID:AB_2340671). Hoechst (1/1000; Sigma) was used for fluorescent nuclear counterstaining.

Tissue Clearing

We used an adapted version of the previously published iDISCO+ clearing protocol [54,55]. All incubation steps were performed at RT in a fume hood, on a tube rotator (SB3, Stuart) at 0.045 *g*, using a 15 mL centrifuge tube (Falcon) covered with aluminum foil to block light. E16.5 brain samples were first dehydrated by sequential 90 min incubation in a graded series (20%, 40%, 60%, 80%, and 100%) of methanol (MeOH, Sigma-Aldrich) diluted in H_2O. This was followed by de-lipidation in dichloromethane (DCM; Sigma-Aldrich) for 30 min. Finally, samples were cleared overnight in dibenzylether (DBE; Sigma-Aldrich) and then stored in brown glass vials filled with DBE in the dark at RT.

Tissue preparation for transmission electron microscopy (TEM)

E14.5 mouse embryos were perfused with 4% PFA, 2.5% glutaraldehyde (EM grade) in PBS. Fixed embryos, wrapped in aluminum foil, were kept on ice for 30 min to allow glutaraldehyde impregnation. Brains were then dissected out of embryos and incubated at 4°C overnight in a buffer of 4% PFA in PBS. 100 µm vibratome sections were collected, washed 3 times in PBS and fixed in 2% osmium tetroxide in PBS for 2 h. Samples were colored en bloc with 1.5% aqueous uranyl acetate at 4°C for 1.5 h. Then, the samples were then dehydrated by sequential 10 min incubation in graded concentrations of ethanol (25%, 50%, 70%, 90% and three times 100%) and rinsed by incubation in anhydrous acetone 3 times for 10 min. Samples were infiltrated with graded concentrations of Araldite 502 resin (50%, 90%, 1 hour per step)

and incubated for 2 h in freshly prepared pure resin. Samples were then mounted in a minimal amount of resin between two ACLAR 33C films, with polymerization performed at 60°C for 48 h. Before cutting, sample blocks were glued parallel to the flat surface of a cylinder bloc of resin used as a support. 70 nm ultrathin sections of the samples were obtained using an ultramicrotome (UC6, Leica). Ultrathin sections were collected on formvar-coated slot (2 x 1 mm) grids. Positive staining of grids was performed by 2 min incubation in UranyLess aqueous solution (Delta Microscopy) followed by lead citrate staining for 1 min.

MRI scans

After fixation, embryos were stored in a 1:250 mixture of 0.5 mmol gadoteric acid (Dotarem®, Guerbet) in PBS for at least 72 h. For imaging, the embryos were embedded in 2% low melting point agar gel (Sigma-Aldrich) and were placed in small Plexiglass containers. Acquisitions were performed on a 17.2 T (1H Larmor frequency = 730.2 MHz) Bruker Biospec preclinical scanner equipped with a 25 mm inner diameter quadrature birdcage volume coil (Rapid Biomedical). 3D images were acquired using a Fast-Low Angle Shot (FLASH) sequence with the following acquisition parameters: TE = 7 ms, TR = 150 ms, FA = 30°, resolution = 40 × 40 × 40 μm^3, signal averaging = 2.

Induction of *in utero* cortical lesions

Pregnant female mice at E14.5 were anesthetized with isoflurane (3.5% for induction, 2% during the surgery) and given 0.1 mg/kg of buprenorphine injected subcutaneously for analgesia. The uterine horns were exposed after laparotomy. Cortical *in utero* lesions were induced unilaterally using a 100 µm diameter glass capillary, by poking through the cortical plate up to the lateral ventricle, as usually done for *in utero* electroporation or viral infection [89]. Lesioned embryos were left to recover in the mother's womb for 2.5 h after surgery, after which their brains were collected and fixed in 4% PFA at 4°C overnight.

Ex vivo phagocytic assay

Slice preparation was performed as previously described[90] with the following modifications. Dissecting medium was prepared from minimum essential medium (MEM) (Gibco) with 20 mM TRIS powder pH7-9 (Sigma) and 45 mM D-glucose (Sigma). After telencephalic brains were cut into 250 µm vibratome coronal sections, slices of interest were stored in this medium on ice until use. For *ex vivo* phagocytosis, pH-rodo (Life technologies) was resuspended at 0.5 mg/mL in dissection medium containing 2.5 mM CaCl2, 2.5 mM MgSO4, 1 mM $NaHCO_3$ and with 300 µL HEPES (Gibco) per 50 mL. After careful removal of MEM, 15 µL of pH-rodo solution was added to the top of each slice and incubated for 1 h at 37°C in 5% CO_2. The reaction was stopped by adding cold pH-rodo suspension medium. After three washes, slices were fixed in 4% PFA in PBS for 45 min, followed by immunohistochemistry as described above.

Image acquisition and analysis

Slice imaging

Images of immunohistochemistry on sections were acquired with a fluorescence binocular microscope (Leica MZ16 F), a fluorescence microscope (Leica DMi8) or a confocal microscope (Leica TCS SP5 and TSP8). Image analyses were performed with FIJI (ImageJ; RRID: SCR_003070), Imaris (Bitplane; RRID:SCR_007370) and Adobe Photoshop CS6 software (Adobe Sytems; RRID:SCR_014199).

3D Imaging and Processing

3D imaging was performed with an ultramicroscope II (LaVision BioTec) using ImspectorPro software (LaVision BioTec). The light sheet was generated by a laser (wavelength 488 Coherent Sapphire Laser, LaVision BioTec) and two cylindrical lenses. Samples were placed in an imaging reservoir made of 100% quartz (LaVision BioTec) filled with ethyl cinnamate and illuminated from the side by the laser light. Images were acquired with a PCO Edge SCMOS CCD camera (2.560×2.160-pixel size, LaVision BioTec). The step size between each image was fixed at 3 µm. For all samples, background fluorescence recorded from exposure to the

488 nm wavelength was acquired in order to reconstruct brain morphology and lesions. Images, 3D volume, and movies were generated using Imaris x64 software (version 9.5, Bitplane). Stack images were first converted to an imaris file (.ims) using ImarisFileConverter. File size was next reduced to 8 bits. 3D reconstruction of the sample was performed using "volume rendering" (Imaris). The sample could be optically sliced at any angle using the "orthoslicer" or "obliqueslicer" tools to validate phenotypic alterations. Lesions due to microglial depletion were highlighted by creating a mask around the volume using the "surface" tool. To this end, low intensity pixels resulting from low background fluorescence (i.e. absence of cells in the lesions) in the 488nm exposure condition were selected in order to create the "surface". 3D pictures and movies were generated using the "snapshot" and "animation" tools. Movie legends were generated using FIJI ImageJ software.

Transmission electron microscopy (TEM) imaging

TEM was performed using a Philips Tecnai 12 Transmission Electron Microscope (Philips/FEI, Eindhoven, The Netherlands) at the electronic imaging department of the Imachem imaging platform (France BioImaging) at the Institut de Biologie de l'Ecole Normale Supérieure, Paris. The Gatan DigitalMicrograph software was used to acquire TEM images at various magnifications with a 4K CCD Orius 1000 camera (Gatan).

- **QUANTIFICATIONS AND STATISTICAL ANALYSIS**

Co-labelling of IBA1^{+} or CX3CR1-GFP^{+} macrophages with P2Y12 microglial marker and eATM markers was quantified specifically in cells accumulated along the CSA, CSB, and around *in utero*-induced lesions in the cortex using the Cell Counter tool in FIJI ImageJ software. Microglial distribution in the CSA region in E18.5 control and *Emx1*$^{cre/+}$*;RhoA*$^{fl/fl}$ mutant mice was quantified using the Cell Counter tool in FIJI ImageJ. Quantification was performed in 3

distinct areas defined as follows: (1) the CSA, centered on the boundary and with a width of 100 µm, (2) the Surrounding area to the CSA with a width of 200 µm and (3) the Remote area, which encircles the Surrounding area (2) with a width of 250 µm (Fig. S4A). For assessing post-depletion lesion severity in *Emx1*$^{cre/+}$*;RhoA*$^{fl/fl}$ mice, *Brn4*^{cre}*; Wnt3A*^{dta} mice (Fig. 5C, 6E and S4), or PLX3397-exposed embryos and pups (Fig. 7) we established a scoring system based on the lesion area measured via FIJI ImageJ software, as controls may display some microcavities (Fig. 5A). For each brain, the area of the largest lesion observed on the slice was selected, and scores were assigned based on the absence of lesion (score 0), mild lesion (score 1) or severe lesions (score 2). Table S2 displays the detailed scoring of lesions. The mean scores for lesion severity across different experimental conditions were then compared statistically. All data are presented as mean ± standard error of the mean (SEM). Non-parametric two-sided Mann-Whitney U-tests were used to compare two distributions in the co-labeling and lesion severity experiments. Fisher's exact test was used to compare contingent presence or absence of CSA/CSB lesions in controls, *Spp1*$^{-/-}$, and PLX3397-treated mice. All graphs and statistical analyses were generated using GraphPad Prism 8.0 software (GraphPad Software; RRID:SCR_002798). *p < 0.05, **p < 0.01, ***p < 0.001.

- **RESOURCE AVAILABILITY**

Lead contact

Further requests and information concerning this study should be addressed to the lead contact, Sonia Garel (garel@biologie.ens.fr).

Materials availability

This study did not generate new reagents.

DATA AND CODE AVAILABILITY

Further information concerning the analysis should be addressed to the lead contact, Sonia Garel (garel@biologie.ens.fr).

FIGURES

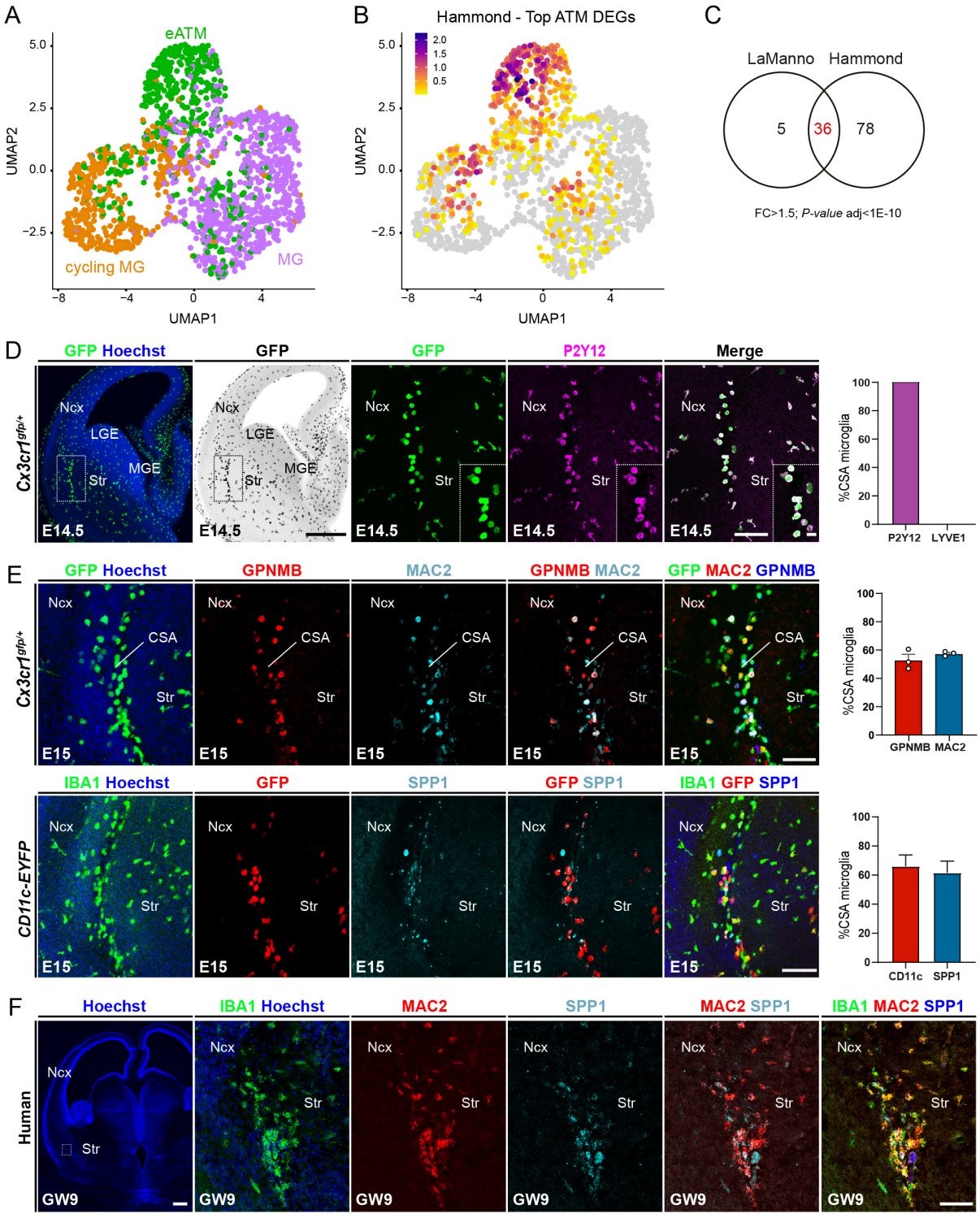

Figure 1. Embryonic ATM are located at the CSA in mouse and human embryos

(A) Single-cell transcriptomic UMAP plot of embryonic microglial cells (n = 1711) extracted from the La Manno dataset [30], showing cycling microglia (MG) (orange), non-cycling MG

(purple) and embryonic ATM (eATM) (green). **(B)** Projection of the postnatal ATM signature (top enriched DEGs) from the Hammond dataset [22] onto the UMAP from (A). **(C)** Venn diagram showing the overlap between the embryonic ATM (eATM) and postnatal ATM signature DEGs respectively identified from La Manno [30] and Hammond [22] datasets (fold change > 1.5, Bonferroni adjusted p-value < 1e-10). **(D-F)** Immunolabeling of brain sections from embryonic mice at E14.5 **(D)** or E15 **(E),** or human fetuses at gestational week (GW)9 (**F**), showing *Cxc3cr1*^{gfp}-positive or IBA1-positive microglia expressing ATM markers at the cortico-striato-amygdalar (CSA) boundary. CSA close-ups are delineated by dotted lines. Immunolabeling was performed on brain sections from at least 3 mice from 2 different litters and on one GW9 human sample. Values are presented as mean ± SEM. Scale bars equal 500 µm (D-left panels), 100 µm (D-right panels), 20 µm (D insets), 200 µm (E) and 1 mm (F).

ATM, axon-tract-associated microglia; CSA, cortico-striato-amygdalar boundary; DEGs, differentially expressed genes; eATM, embryonic ATM; LGE, lateral ganglionic eminence; MGE, medial ganglionic eminence; MG, microglia; Ncx, neocortex; Str, striatum.

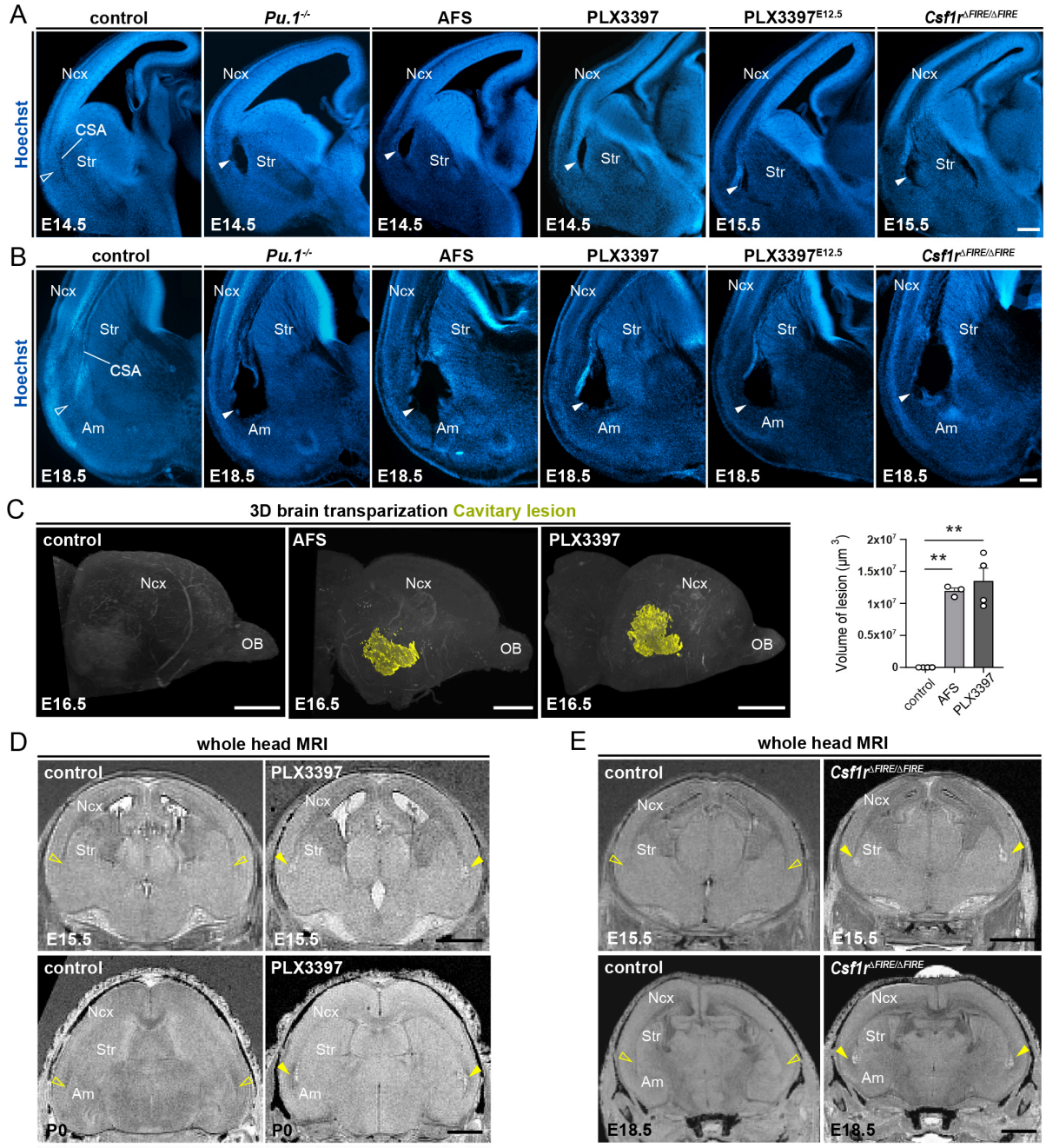

Figure 2. Microglia are required for tissue integrity at the embryonic CSA

(A,B) Hoechst staining of hemibrain coronal sections from E14.5 or E15.5 embryos **(A)**, showing CSA integrity in wild types (open arrowhead) and cavitary lesions in the absence of microglia (solid arrowheads) ($n_{controls}$=27, n_{Pu1KO}=6, n_{AFS}=4, $n_{PLX3397}$=8, $n_{PLX3397\text{-}E12}$=11, $n_{CSF1RFire}$=7); and from E18.5 embryos **(B)**, showing the localization of cavitary lesions at the border between the neocortex (Ncx), striatum (Str) and amygdala (Am) ($n_{controls}$=35, n_{Pu1KO}=5, n_{AFS}=7, $n_{PLX3397}$=13, $n_{PLX3397\text{-}E12}$=11, $n_{CSF1RFire}$=6). **(C)** Cavity reconstruction (yellow) after whole

hemibrain clearing using the iDISCO method, highlighting the absence of cavities in controls and stereotypically located cavities in two models of microglial depletion ($n_{controls}$=4, n_{AFS}=3, $n_{PLX3397}$=4), and enabling the 3D quantification of the lesion volumes in both depletion models using the Imaris Software. **(D)** Whole-head MRI scans of E15.5 and newborn mice, showing low-intensity signals at the CSA of PLX3397-treated embryos (n=3) (yellow solid arrowheads) in contrast to controls (n=3) (yellow open arrowheads), confirming the formation of a cavitary lesion in PLX3397-treated embryos.

(D) Whole-head MRI scans of E15.5, P0 or E18.5 or mice, showing low-intensity signals at the CSA of PLX3397-treated and *Csf1r*$^{\Delta FIRE/\Delta FIRE}$ embryos (yellow solid arrowheads) in contrast to controls (yellow open arrowheads), confirming the formation of a cavitary lesion in PLX3397-treated and *Csf1r*$^{\Delta FIRE/\Delta FIRE}$ mice ($n_{controls\text{-}E15}$=4, $n_{PLX3397\text{-}E15}$=3, $n_{CSF1RFire\text{-}E15}$=2, $n_{controls\text{-}P0}$=3, $n_{PLX3397\text{-}P0}$=3, $n_{controls\text{-}E18}$=3, $n_{CSF1RFire\text{-}E18}$=3). CSA close-ups are delineated by dotted lines. Graphs show means ± SEM. Mann-Whitney U Tests were performed for statistical comparison, **p<0.01. Scale bars equal 200 µm (A, B), 800 µm (C) and 1mm (D).

Am, amygdala; CSA, cortico-striato-amygdalar boundary; Ncx, neocortex; OB, olfactory bulb; Str, striatum.

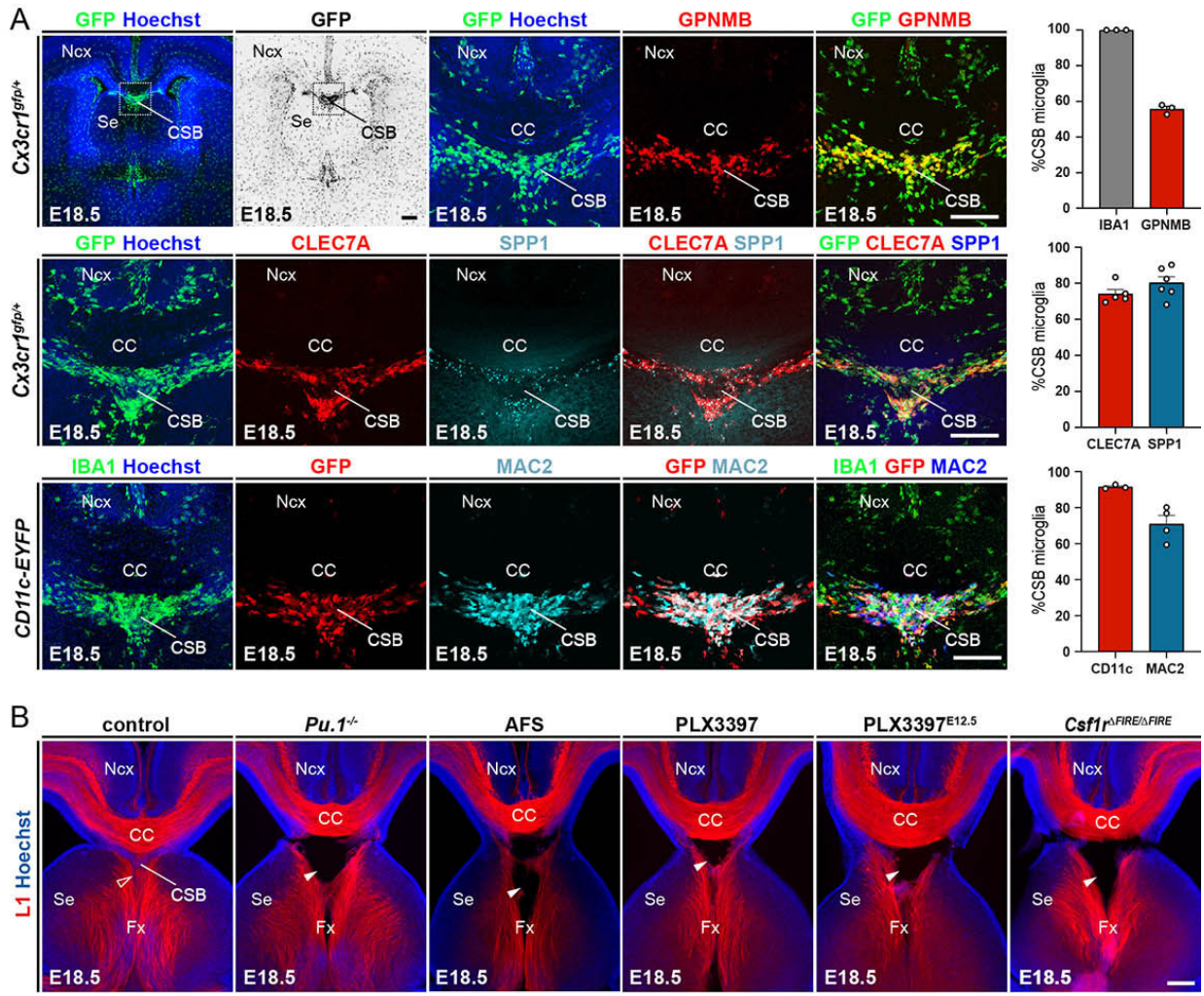

Figure 3. Embryonic microglia maintain tissue integrity at the midline CSB hotspot

(A) Immunolabeling of coronal brain sections from E18.5 *Cxc3cr1*^{gfp} or *CD11c-EYFP* embryos showing co-expression of microglia and eATM markers at the cortico-septal boundary (CSB), below the corpus callosum (CC). CSB close-ups are delineated by dotted lines. GFP-positive microglia in *Cxc3cr1*^{gfp} brains fully colocalized with the IBA1 marker, which was used to label all microglia in *CD11c-EYFP* brains. Immunolabeling was performed on brain sections of at least 3 mice from 2 different litters. **(B)** L1-immunolabeling enables the visualization of CC and Fornix (Fx) axons (open arrowhead) and highlights a lesion at the CSB (solid arrowheads) in various pharmacological and genetic models with disrupted microglial colonization and density ($n_{controls}$=21, n_{Pu1KO}=4, n_{AFS}=5, $n_{PLX3397}$=9, $n_{PLX3397\text{-}E12}$=11, $n_{CSF1RFire}$=5). Values are presented as mean ± SEM. Scale bars equal 100 µm (A) and 200 µm (B).

CC, corpus callosum; CSB, cortico-septal boundary; Fx, Fornix; Ncx, neocortex; Se, Septum.

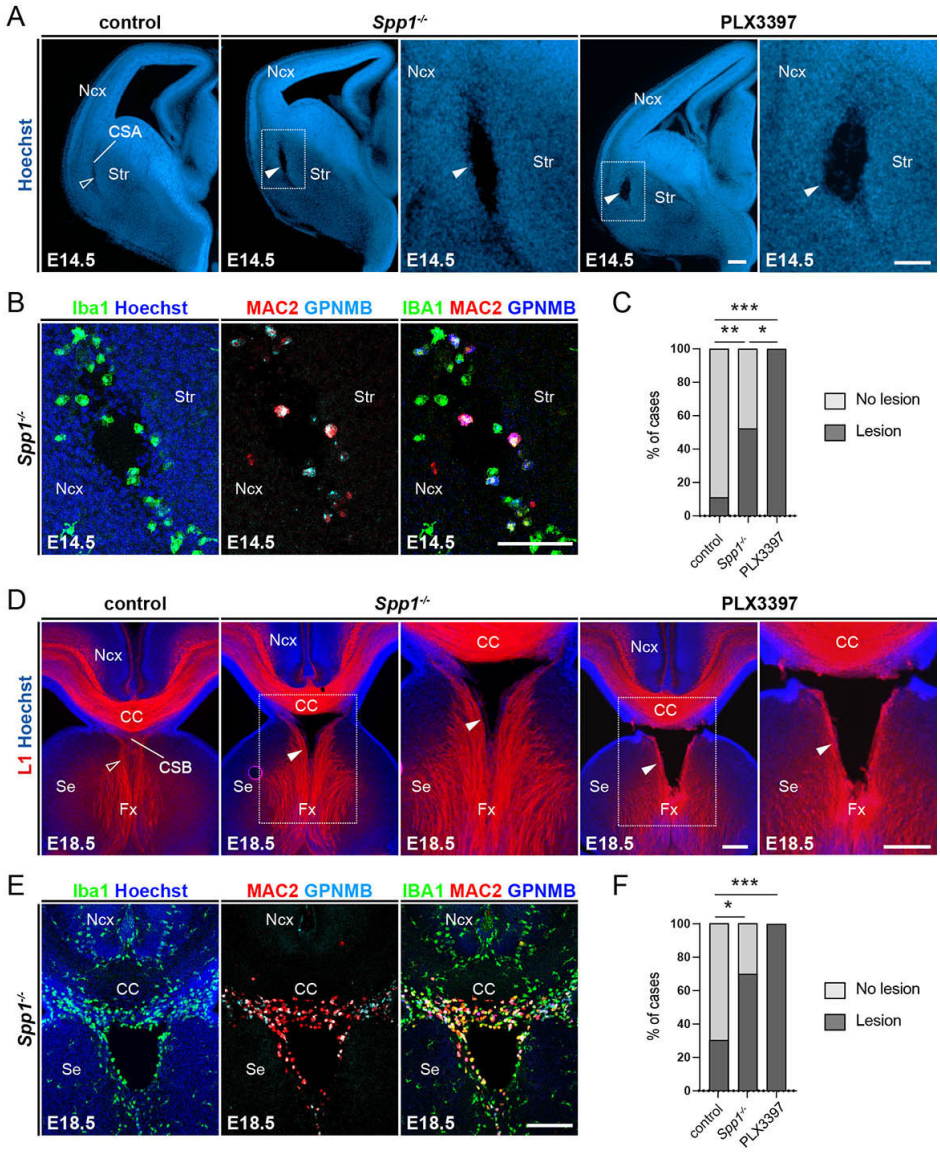

Figure 4. ATM-core factor Spp1 contributes to tissue integrity at the CSA and CSB

(A) Coronal hemisections of E14.5 brains stained with Hoechst reveal CSA disruption in 50% of *Spp1*$^{-/-}$ mutants (solid arrowheads), compared to controls (open arrowheads) and in 100% of PLX3397-treated embryos (solid arrowheads) ($n_{controls}$=18, n_{Spp1KO}=21, $n_{PLX3397}$=13). **(B)** E14.5 coronal hemisections showing expression of Mac2 and GPNMB at the CSA in controls (open arrowheads) and *Spp1*$^{-/-}$ embryos ($n_{controls}$=3, n_{Spp1KO}=3). **(C)** Quantification of the embryos showing CSA lesions across models. **(D)** L1 immunolabeling enables the visualization of axons (open arrowheads) and midline lesions (solid arrowheads) in *Spp1/OPN*$^{-}$

$^{/-}$ mutants in approximately 70% of cases compared to 100% in PLX3397-exposed embryos ($n_{controls}$=23, n_{Spp1KO}=20, $n_{PLX3397}$=8). **(E)** E18.5 coronal hemisections showing expression of Mac2 and GPNMB at the CSB in controls (open arrowheads) and *Spp1*$^{-/-}$ embryos ($n_{controls}$=3, n_{Spp1KO}=3). **(F)** Quantification of the embryos showing CSB lesions across models. Graphs show the percentages. Fisher's exact test was performed to compare distributions of cases with lesions in controls, *Spp1*$^{-/-}$, and PLX3397-exposed embryos, * $p<0.05$; ** $p<0.001$; *** $p<0.0001$. Scale bars equal 200 µm (A,D; low magnification) and 100 µm (B,E and A,D; high magnification).

CC, corpus callosum; CSA, cortico-striato-amygdalar boundary; CSB, cortico-septal boundary; Fx, fornix; Ncx, neocortex; Se, Septum; Str, striatum.

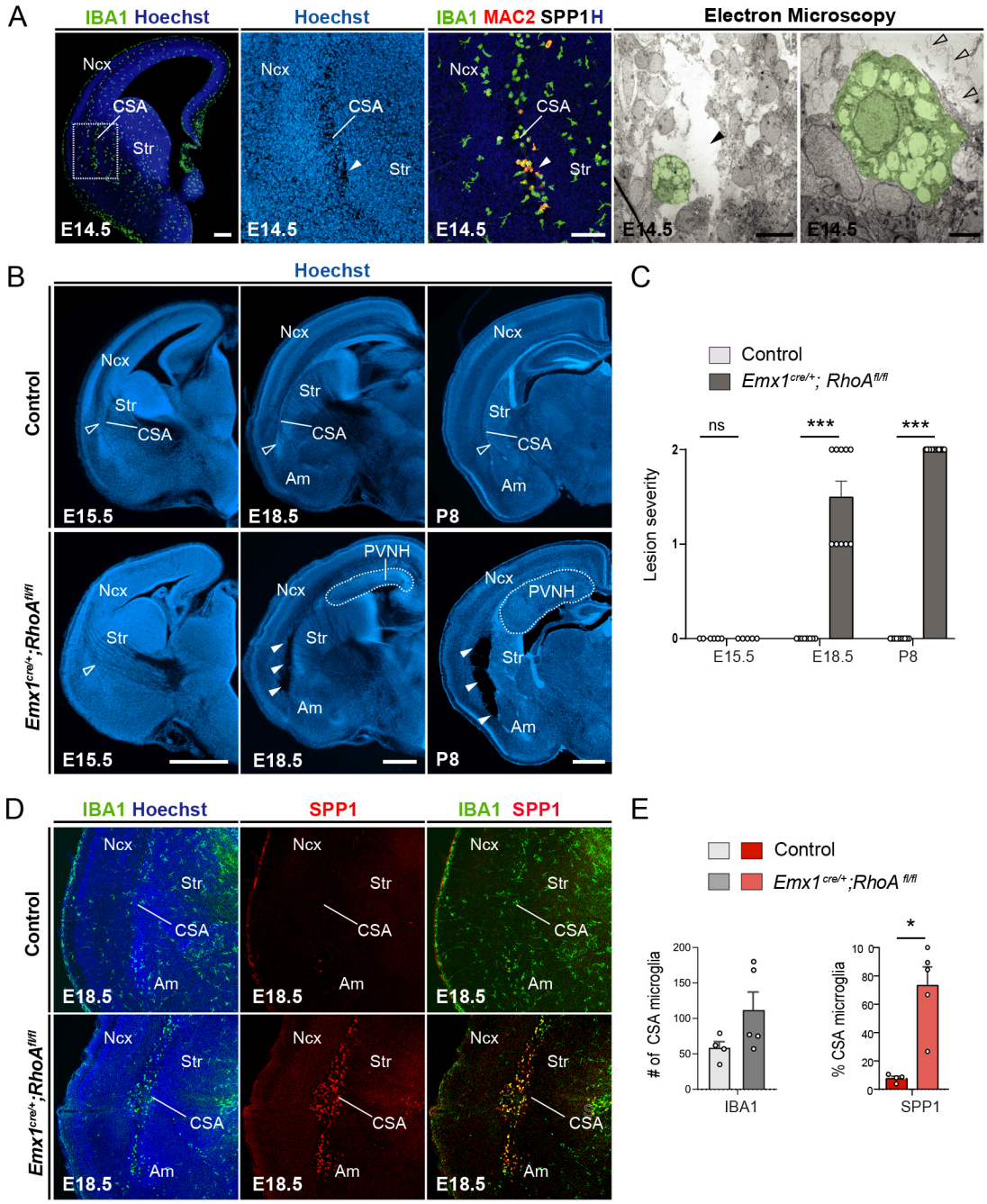

Figure 5. The CSA is a site of morphogenetic fragility and embryonic ATM recruitment

(A) Immunolabeling for IBA1, Spp1 and Mac2 indicate that at E14.5, ATM line microcavities (solid arrowheads) are visible by Hoechst counterstaining. Transmitted Electron Microscopy (EM) also reveals the presence of microcavities (solid arrowheads), lined with microglia (pseudo-colored in green) that show a characteristic amoeboid morphology, and containing membrane fragments (open arrowheads) (n=6 for immunolabeling and n=3 for EM, from at

least two distinct litters). **(B,C)** Coronal hemisections from control and *Emx1$^{cre/+}$;RhoA$^{fl/fl}$* mice, the latter displaying a periventricular nodular heterotopia (PVNH) visible from E18.5 onwards (dotted lines). Hoechst counterstaining shows the absence of a lesion at the CSA of controls and mutants at E15.5 (open arrowheads), a striking CSA lesion in 50% of the mutants (solid arrowheads), and in 100% of the mutants at P8 (solid arrowheads) ($n_{controlsE15}$=6, $n_{heterotopiaE15}$=5, $n_{controlsE18}$=8, $n_{heterotopiaE18}$=10, $n_{controlsP7}$=10, $n_{heterotopiaP7}$=15). Quantification in **(C)** uses values that represent scoring of lesion severity, scored from 0 to 2, as detailed in Table S2. **(D,E)** Iba1 and Spp1 co-immunolabeling shows a marked recruitment of Spp1-expressing microglia at the CSA of *Emx1$^{cre/+}$;RhoA$^{fl/fl}$* mice, with approximately 75% of Spp1-positive CSA microglia in mutants, but 8% of CSA cells detected in controls at this stage (n=4 at least from 2 different litters). Graphs show means ± SEM. Mann-Whitney U Tests were performed for statistical comparison, * $p<0.05$; *** $p<0.0001$.

Am, Amygdala; CSA, cortico-striato-amygdalar boundary; PVNH, periventricular nodular heterotopia; Ncx, neocortex; Str, striatum.

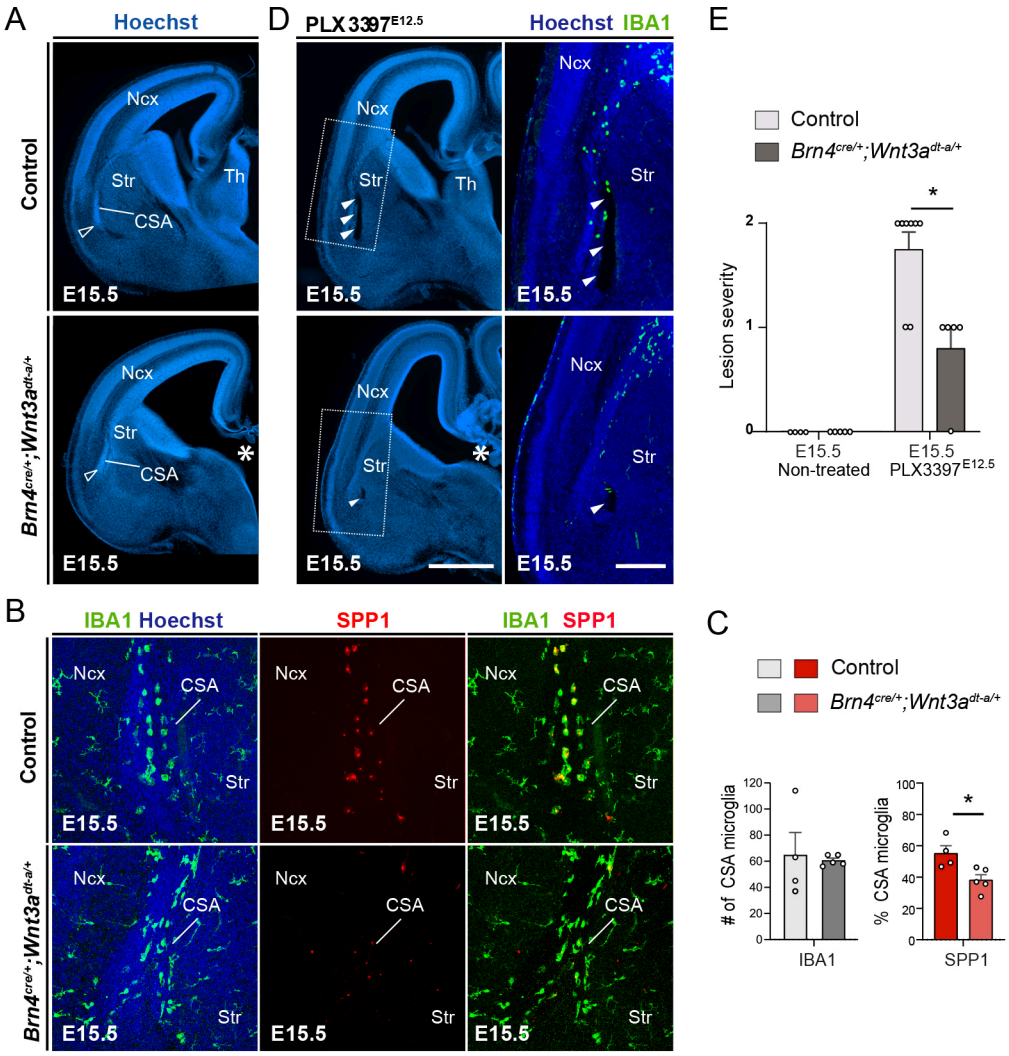

Figure 6. Alleviating morphogenetic constraints reduces ATM recruitment and lesion induction at the CSA

(A) Coronal hemisections of brains from E15.5 control and *Bnr4*$^{cre/+}$*; Wnt3a*^{dta} mice, showing the absence of the thalamus in *Bnr4*$^{cre/+}$*; Wnt3a*^{dta} mice (white asterisk) and a global modification of the brain shape but conserved CSA in mutant versus control embryos - ($n_{controls}$=4, $n_{thalamusdeleted}$=5). **(B,C)** IBA1 and Spp1 co-immunostaining at E15.5 showing a significantly diminished percentage of CSA microglia expressing Spp1 in E15.5 *Bnr4*$^{cre/+}$*; Wnt3a*$^{dta/+}$ mutant mice compared to controls, despite a conserved number of accumulating cells (n=4 at least from 2 different litters). **(D-E)** Coronal hemisections of brains from E15.5 control and *Bnr4*$^{cre/+}$*; Wnt3a*^{dta} mice exposed to PLX3397 between E12.5 and E15.5. While

PLX3397-exposed controls consistently displayed a lesion (open arrowheads), PLX3397-treated mutants exhibited a smaller lesion or no lesion (solid arrowheads) despite effective local depletion as assessed by IBA1 staining ($n_{controls}$=4, $n_{thalamusdeleted}$=5, $n_{PLX3397}$=8, $n_{thalamusdeleted\text{-}PLX3397}$=5). Quantification in **(E)** uses values that represent the scoring of lesion severity, scored from 0 to 2, as detailed in Table S2. Graphs show mean ± SEM. Mann-Whitney U Tests were used for statistical comparison, * $p<0.05$. Scale bars equal 200 µm (A,D; low magnification) and 100 µm (C and D; high magnification).

Am, Amygdala; CSA, cortico-striato-amygdalar boundary; Ncx, neocortex; Str, striatum; Th, thalamus.

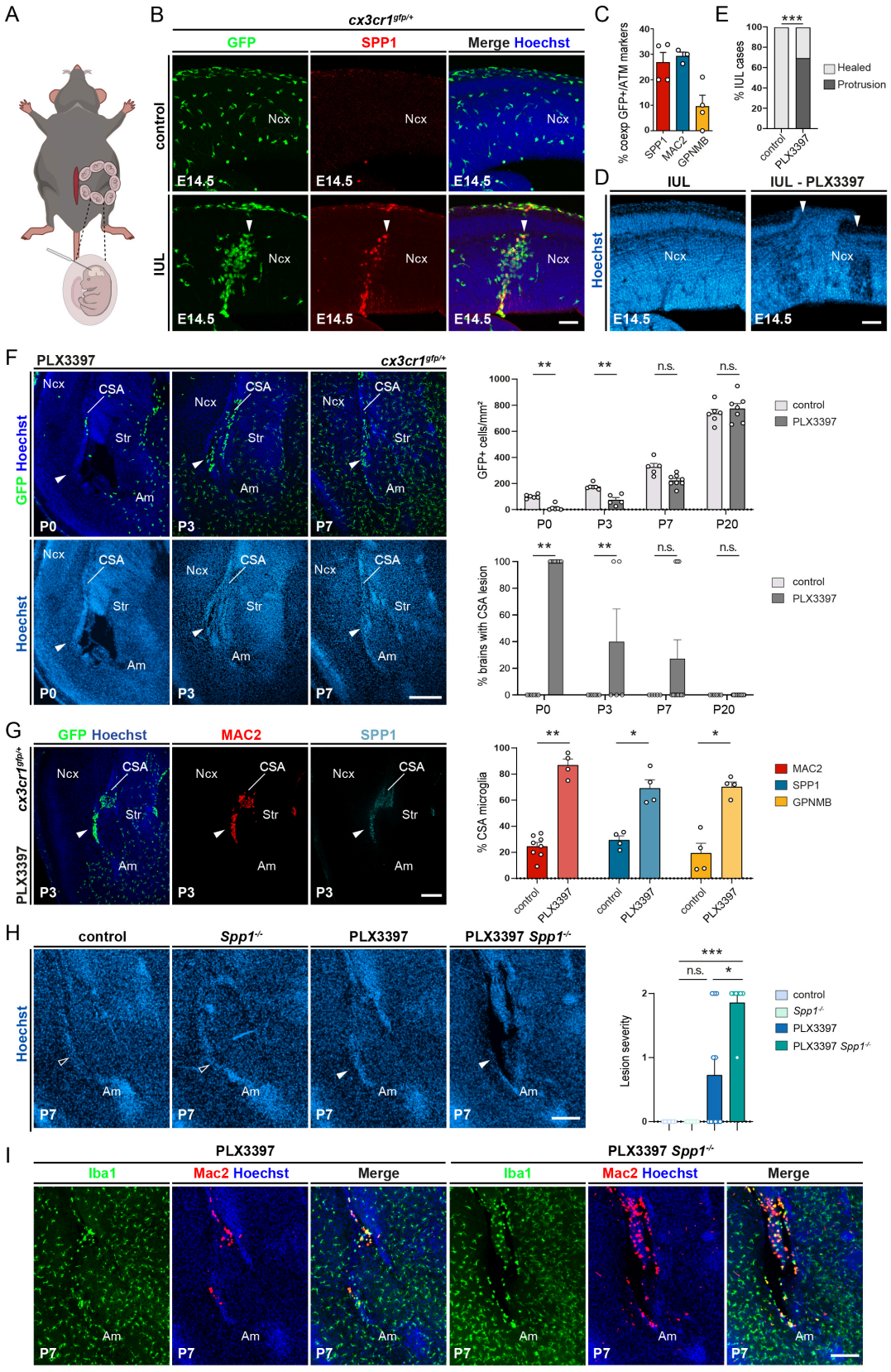

Figure 7. ATM factors are induced by mechanical damage and involved in lesion repair

(A) Schematic representation of *in utero* lesion (IUL) procedure induced by mechanical poking of the neocortex using a glass capillary. **(B)** Coronal sections through the E14.5 neocortex of control and IUL embryos collected 2.5 h after lesion induction, showing amoeboid *Cx3cr1*^{gfp}-positive cells accumulating at the lesion site and the co-expression of Spp1 and Mac2 (solid arrowheads) in IUL embryos, but dispersed *Cx3cr1*^{gfp}-positive cells and no expression of ATM markers in controls ($n_{controls}$=3, n_{IUL}=3). **(C)** Quantification of the percentage of *Cx3cr1*^{gfp}-positive cells co-expressing ATM markers ($n_{controls}$=3, n_{IUL}=3). **(D)** Coronal sections after IUL in control and PLX3397-exposed E14.5 embryos showing an altered morphology (bulge, solid arrowheads) in the absence of microglia. **(E)** Quantification of the morphological bulges observed in control and PLX3397-treated embryos (n_{IUL}=17; $n_{IUL-\ PLX3397}$=13). **(F)** Coronal sections showing the CSA region (solid arrowheads) in pups prenatally exposed to PLX3397 at postnatal days (P) 0, P3, P7 and P20. Cavitary lesions progressively resorbed, concurrently with the repopulation of *Cx3cr1*^{gfp}-positive cells, which accumulated at the site of lesion closure (solid arrowhead) ($n_{controls\text{-}P0}$=6; $n_{PLX3397\text{-}P0}$=6; $n_{controls\text{-}P3}$=6; $n_{PLX3397\text{-}P3}$=5; $n_{controls\text{-}P7}$=5; $n_{PLX3397\text{-}P7}$=8; $n_{controls\text{-}P20}$=7; $n_{PLX3397\text{-}P20}$=7). **(G)** *Cx3cr1*^{gfp}-positive cells accumulating at the site of lesion closure co-expressed ATM markers Spp1, Mac2 and GPNMB, as shown and quantified at P3 ($n_{controls}$=4; $n_{PLX3397}$=4). **(H)** In contrast to controls, *Spp1*$^{-/-}$ mutants and PLX3397-exposed controls, PLX3397-exposed *Spp1*$^{-/-}$ mutants reproducibly displayed lesions visible by Hoechst staining ($n_{controls}$=7; n_{Spp1KO}=8; $n_{control\text{-}PLX3397}$=11; $n_{Spp1KO\text{-}PLX3397}$=7). Values represent the scoring of lesion severity, scored from 0 to 2, as detailed in Table S2. **(I)** While few CSA IBA1-positive cells co-expressed Mac2 in resorbed PLX3397-treated controls at P7, they accumulated around the lesions in PLX3397-treated *Spp1* mutants, indicating that *Spp1* inactivation did not prevent the expression of selected ATM markers ($n_{control\text{-}PLX3397}$=3; $n_{Spp1KO\text{-}PLX3397}$=7). Graphs show the percentages (E,F) or means ± SEM (C,F-H). Fisher's exact test (E,F) and Mann-Whitney U Test (C,F-H) were performed for statistical comparison, * $p<0.05$; ** $p<0.001$; *** $p<0.0001$. Scale bars equal 100 µm (B, D), 200 µm (F-G), and 150 µm (H-I).

Am, Amygdala; CSA, cortico-striato-amygdalar boundary; IUL, *in utero* lesion; Ncx, neocortex.

REFERENCES

1. Colonna, M., and Butovsky, O. (2017). Microglia Function in the Central Nervous System During Health and Neurodegeneration. Annu Rev Immunol *35*, 441-468. 10.1146/annurev-immunol-051116-052358.
2. Li, Q., and Barres, B.A. (2018). Microglia and macrophages in brain homeostasis and disease. Nat Rev Immunol *18*, 225-242. 10.1038/nri.2017.125.
3. Hammond, T.R., Robinton, D., and Stevens, B. (2018). Microglia and the Brain: Complementary Partners in Development and Disease. Annu Rev Cell Dev Biol *34*, 523-544. 10.1146/annurev-cellbio-100616-060509.
4. Thion, M.S., Ginhoux, F., and Garel, S. (2018). Microglia and early brain development: An intimate journey. Science *362*, 185-189. 10.1126/science.aat0474.
5. Sierra, A., Paolicelli, R.C., and Kettenmann, H. (2019). Cien Anos de Microglia: Milestones in a Century of Microglial Research. Trends Neurosci *42*, 778-792. 10.1016/j.tins.2019.09.004.
6. Prinz, M., Jung, S., and Priller, J. (2019). Microglia Biology: One Century of Evolving Concepts. Cell *179*, 292-311. 10.1016/j.cell.2019.08.053.
7. Prinz, M., Masuda, T., Wheeler, M.A., and Quintana, F.J. (2021). Microglia and Central Nervous System-Associated Macrophages-From Origin to Disease Modulation. Annu Rev Immunol *39*, 251-277. 10.1146/annurev-immunol-093019-110159.
8. Cserep, C., Posfai, B., and Denes, A. (2021). Shaping Neuronal Fate: Functional Heterogeneity of Direct Microglia-Neuron Interactions. Neuron *109*, 222-240. 10.1016/j.neuron.2020.11.007.
9. Badimon, A., Strasburger, H.J., Ayata, P., Chen, X., Nair, A., Ikegami, A., Hwang, P., Chan, A.T., Graves, S.M., Uweru, J.O., et al. (2020). Negative feedback control of neuronal activity by microglia. Nature *586*, 417-423. 10.1038/s41586-020-2777-8.
10. McNamara, N.B., Munro, D.A.D., Bestard-Cuche, N., Uyeda, A., Bogie, J.F.J., Hoffmann, A., Holloway, R.K., Molina-Gonzalez, I., Askew, K.E., Mitchell, S., et al. (2023). Microglia regulate central nervous system myelin growth and integrity. Nature *613*, 120-129. 10.1038/s41586-022-05534-y.
11. Thion, M.S., Mosser, C.A., Ferezou, I., Grisel, P., Baptista, S., Low, D., Ginhoux, F., Garel, S., and Audinat, E. (2019). Biphasic Impact of Prenatal Inflammation and Macrophage Depletion on the Wiring of Neocortical Inhibitory Circuits. Cell Rep *28*, 1119-1126 e1114. 10.1016/j.celrep.2019.06.086.
12. Scott-Hewitt, N., Perrucci, F., Morini, R., Erreni, M., Mahoney, M., Witkowska, A., Carey, A., Faggiani, E., Schuetz, L.T., Mason, S., et al. (2020). Local externalization of phosphatidylserine mediates developmental synaptic pruning by microglia. EMBO J *39*, e105380. 10.15252/embj.2020105380.
13. Favuzzi, E., Huang, S., Saldi, G.A., Binan, L., Ibrahim, L.A., Fernandez-Otero, M., Cao, Y., Zeine, A., Sefah, A., Zheng, K., et al. (2021). GABA-receptive microglia selectively sculpt developing inhibitory circuits. Cell *184*, 5686. 10.1016/j.cell.2021.10.009.
14. Cserep, C., Schwarcz, A.D., Posfai, B., Laszlo, Z.I., Kellermayer, A., Kornyei, Z., Kisfali, M., Nyerges, M., Lele, Z., Katona, I., and Adam, D. (2022). Microglial control of neuronal development via somatic purinergic junctions. Cell Rep *40*, 111369. 10.1016/j.celrep.2022.111369.
15. Gallo, N.B., Berisha, A., and Van Aelst, L. (2022). Microglia regulate chandelier cell axo-axonic synaptogenesis. Proc Natl Acad Sci U S A *119*, e2114476119. 10.1073/pnas.2114476119.
16. Bisht, K., Sharma, K.P., Lecours, C., Sanchez, M.G., El Hajj, H., Milior, G., Olmos-Alonso, A., Gomez-Nicola, D., Luheshi, G., Vallieres, L., et al. (2016). Dark microglia: A new phenotype predominantly associated with pathological states. Glia *64*, 826-839. 10.1002/glia.22966.

17. Krasemann, S., Madore, C., Cialic, R., Baufeld, C., Calcagno, N., El Fatimy, R., Beckers, L., O'Loughlin, E., Xu, Y., Fanek, Z., et al. (2017). The TREM2-APOE Pathway Drives the Transcriptional Phenotype of Dysfunctional Microglia in Neurodegenerative Diseases. Immunity *47*, 566-581 e569. 10.1016/j.immuni.2017.08.008.
18. Keren-Shaul, H., Spinrad, A., Weiner, A., Matcovitch-Natan, O., Dvir-Szternfeld, R., Ulland, T.K., David, E., Baruch, K., Lara-Astaiso, D., Toth, B., et al. (2017). A Unique Microglia Type Associated with Restricting Development of Alzheimer's Disease. Cell *169*, 1276-1290 e1217. 10.1016/j.cell.2017.05.018.
19. Deczkowska, A., Keren-Shaul, H., Weiner, A., Colonna, M., Schwartz, M., and Amit, I. (2018). Disease-Associated Microglia: A Universal Immune Sensor of Neurodegeneration. Cell *173*, 1073-1081. 10.1016/j.cell.2018.05.003.
20. Stratoulias, V., Venero, J.L., Tremblay, M.E., and Joseph, B. (2019). Microglial subtypes: diversity within the microglial community. EMBO J *38*, e101997. 10.15252/embj.2019101997.
21. Li, Q., Cheng, Z., Zhou, L., Darmanis, S., Neff, N.F., Okamoto, J., Gulati, G., Bennett, M.L., Sun, L.O., Clarke, L.E., et al. (2019). Developmental Heterogeneity of Microglia and Brain Myeloid Cells Revealed by Deep Single-Cell RNA Sequencing. Neuron *101*, 207-223 e210. 10.1016/j.neuron.2018.12.006.
22. Hammond, T.R., Dufort, C., Dissing-Olesen, L., Giera, S., Young, A., Wysoker, A., Walker, A.J., Gergits, F., Segel, M., Nemesh, J., et al. (2019). Single-Cell RNA Sequencing of Microglia throughout the Mouse Lifespan and in the Injured Brain Reveals Complex Cell-State Changes. Immunity *50*, 253-271 e256. 10.1016/j.immuni.2018.11.004.
23. Masuda, T., Sankowski, R., Staszewski, O., Bottcher, C., Amann, L., Sagar, Scheiwe, C., Nessler, S., Kunz, P., van Loo, G., et al. (2019). Spatial and temporal heterogeneity of mouse and human microglia at single-cell resolution. Nature *566*, 388-392. 10.1038/s41586-019-0924-x.
24. Sala Frigerio, C., Wolfs, L., Fattorelli, N., Thrupp, N., Voytyuk, I., Schmidt, I., Mancuso, R., Chen, W.T., Woodbury, M.E., Srivastava, G., et al. (2019). The Major Risk Factors for Alzheimer's Disease: Age, Sex, and Genes Modulate the Microglia Response to Abeta Plaques. Cell Rep *27*, 1293-1306 e1296. 10.1016/j.celrep.2019.03.099.
25. Kracht, L., Borggrewe, M., Eskandar, S., Brouwer, N., Chuva de Sousa Lopes, S.M., Laman, J.D., Scherjon, S.A., Prins, J.R., Kooistra, S.M., and Eggen, B.J.L. (2020). Human fetal microglia acquire homeostatic immune-sensing properties early in development. Science *369*, 530-537. 10.1126/science.aba5906.
26. Bian, Z., Gong, Y., Huang, T., Lee, C.Z.W., Bian, L., Bai, Z., Shi, H., Zeng, Y., Liu, C., He, J., et al. (2020). Deciphering human macrophage development at single-cell resolution. Nature *582*, 571-576. 10.1038/s41586-020-2316-7.
27. Masuda, T., Sankowski, R., Staszewski, O., and Prinz, M. (2020). Microglia Heterogeneity in the Single-Cell Era. Cell Rep *30*, 1271-1281. 10.1016/j.celrep.2020.01.010.
28. Marschallinger, J., Iram, T., Zardeneta, M., Lee, S.E., Lehallier, B., Haney, M.S., Pluvinage, J.V., Mathur, V., Hahn, O., Morgens, D.W., et al. (2020). Lipid-droplet-accumulating microglia represent a dysfunctional and proinflammatory state in the aging brain. Nat Neurosci *23*, 194-208. 10.1038/s41593-019-0566-1.
29. Safaiyan, S., Besson-Girard, S., Kaya, T., Cantuti-Castelvetri, L., Liu, L., Ji, H., Schifferer, M., Gouna, G., Usifo, F., Kannaiyan, N., et al. (2021). White matter aging drives microglial diversity. Neuron *109*, 1100-1117 e1110. 10.1016/j.neuron.2021.01.027.
30. La Manno, G., Siletti, K., Furlan, A., Gyllborg, D., Vinsland, E., Mossi Albiach, A., Mattsson Langseth, C., Khven, I., Lederer, A.R., Dratva, L.M., et al. (2021). Molecular architecture of the developing mouse brain. Nature *596*, 92-96. 10.1038/s41586-021-03775-x.

31. Silvin, A., Uderhardt, S., Piot, C., Da Mesquita, S., Yang, K., Geirsdottir, L., Mulder, K., Eyal, D., Liu, Z., Bridlance, C., et al. (2022). Dual ontogeny of disease-associated microglia and disease inflammatory macrophages in aging and neurodegeneration. Immunity *55*, 1448-1465 e1446. 10.1016/j.immuni.2022.07.004.
32. Stogsdill, J.A., Kim, K., Binan, L., Farhi, S.L., Levin, J.Z., and Arlotta, P. (2022). Pyramidal neuron subtype diversity governs microglia states in the neocortex. Nature *608*, 750-756. 10.1038/s41586-022-05056-7.
33. Paolicelli, R.C., Sierra, A., Stevens, B., Tremblay, M.E., Aguzzi, A., Ajami, B., Amit, I., Audinat, E., Bechmann, I., Bennett, M., et al. (2022). Microglia states and nomenclature: A field at its crossroads. Neuron *110*, 3458-3483. 10.1016/j.neuron.2022.10.020.
34. Park, M.D., Silvin, A., Ginhoux, F., and Merad, M. (2022). Macrophages in health and disease. Cell *185*, 4259-4279. 10.1016/j.cell.2022.10.007.
35. Thion, M.S., and Garel, S. (2020). Microglial ontogeny, diversity and neurodevelopmental functions. Curr Opin Genet Dev *65*, 186-194. 10.1016/j.gde.2020.06.013.
36. Menassa, D.A., Muntslag, T.A.O., Martin-Estebane, M., Barry-Carroll, L., Chapman, M.A., Adorjan, I., Tyler, T., Turnbull, B., Rose-Zerilli, M.J.J., Nicoll, J.A.R., et al. (2022). The spatiotemporal dynamics of microglia across the human lifespan. Dev Cell *57*, 2127-2139 e2126. 10.1016/j.devcel.2022.07.015.
37. Cossart, R., and Garel, S. (2022). Step by step: cells with multiple functions in cortical circuit assembly. Nat Rev Neurosci *23*, 395-410. 10.1038/s41583-022-00585-6.
38. Squarzoni, P., Oller, G., Hoeffel, G., Pont-Lezica, L., Rostaing, P., Low, D., Bessis, A., Ginhoux, F., and Garel, S. (2014). Microglia modulate wiring of the embryonic forebrain. Cell Rep *8*, 1271-1279. 10.1016/j.celrep.2014.07.042.
39. Thion, M.S., and Garel, S. (2017). On place and time: microglia in embryonic and perinatal brain development. Curr Opin Neurobiol *47*, 121-130. 10.1016/j.conb.2017.10.004.
40. Wlodarczyk, A., Holtman, I.R., Krueger, M., Yogev, N., Bruttger, J., Khorooshi, R., Benmamar-Badel, A., de Boer-Bergsma, J.J., Martin, N.A., Karram, K., et al. (2017). A novel microglial subset plays a key role in myelinogenesis in developing brain. EMBO J *36*, 3292-3308. 10.15252/embj.201696056.
41. Hagemeyer, N., Hanft, K.M., Akriditou, M.A., Unger, N., Park, E.S., Stanley, E.R., Staszewski, O., Dimou, L., and Prinz, M. (2017). Microglia contribute to normal myelinogenesis and to oligodendrocyte progenitor maintenance during adulthood. Acta Neuropathol *134*, 441-458. 10.1007/s00401-017-1747-1.
42. Ueno, M., Fujita, Y., Tanaka, T., Nakamura, Y., Kikuta, J., Ishii, M., and Yamashita, T. (2013). Layer V cortical neurons require microglial support for survival during postnatal development. Nat Neurosci *16*, 543-551. 10.1038/nn.3358.
43. Nemes-Baran, A.D., White, D.R., and DeSilva, T.M. (2020). Fractalkine-Dependent Microglial Pruning of Viable Oligodendrocyte Progenitor Cells Regulates Myelination. Cell Rep *32*, 108047. 10.1016/j.celrep.2020.108047.
44. Erblich, B., Zhu, L., Etgen, A.M., Dobrenis, K., and Pollard, J.W. (2011). Absence of colony stimulation factor-1 receptor results in loss of microglia, disrupted brain development and olfactory deficits. PLoS One *6*, e26317. 10.1371/journal.pone.0026317.
45. Pridans, C., Raper, A., Davis, G.M., Alves, J., Sauter, K.A., Lefevre, L., Regan, T., Meek, S., Sutherland, L., Thomson, A.J., et al. (2018). Pleiotropic Impacts of Macrophage and Microglial Deficiency on Development in Rats with Targeted Mutation of the Csf1r Locus. J Immunol *201*, 2683-2699. 10.4049/jimmunol.1701783.
46. Hoeffel, G., Wang, Y., Greter, M., See, P., Teo, P., Malleret, B., Leboeuf, M., Low, D., Oller, G., Almeida, F., et al. (2012). Adult Langerhans cells derive predominantly from embryonic fetal liver monocytes with a minor contribution of yolk sac-derived macrophages. J Exp Med *209*, 1167-1181. 10.1084/jem.20120340.

47. Elmore, M.R., Najafi, A.R., Koike, M.A., Dagher, N.N., Spangenberg, E.E., Rice, R.A., Kitazawa, M., Matusow, B., Nguyen, H., West, B.L., and Green, K.N. (2014). Colony-stimulating factor 1 receptor signaling is necessary for microglia viability, unmasking a microglia progenitor cell in the adult brain. Neuron *82*, 380-397. 10.1016/j.neuron.2014.02.040.
48. Green, K.N., Crapser, J.D., and Hohsfield, L.A. (2020). To Kill a Microglia: A Case for CSF1R Inhibitors. Trends Immunol *41*, 771-784. 10.1016/j.it.2020.07.001.
49. Back, J., Dierich, A., Bronn, C., Kastner, P., and Chan, S. (2004). PU.1 determines the self-renewal capacity of erythroid progenitor cells. Blood *103*, 3615-3623. 10.1182/blood-2003-11-4089.
50. Rojo, R., Raper, A., Ozdemir, D.D., Lefevre, L., Grabert, K., Wollscheid-Lengeling, E., Bradford, B., Caruso, M., Gazova, I., Sanchez, A., et al. (2019). Deletion of a Csf1r enhancer selectively impacts CSF1R expression and development of tissue macrophage populations. Nat Commun *10*, 3215. 10.1038/s41467-019-11053-8.
51. Munro, D.A.D., Bradford, B.M., Mariani, S.A., Hampton, D.W., Vink, C.S., Chandran, S., Hume, D.A., Pridans, C., and Priller, J. (2020). CNS macrophages differentially rely on an intronic Csf1r enhancer for their development. Development *147*. 10.1242/dev.194449.
52. Kiani Shabestari, S., Morabito, S., Danhash, E.P., McQuade, A., Sanchez, J.R., Miyoshi, E., Chadarevian, J.P., Claes, C., Coburn, M.A., Hasselmann, J., et al. (2022). Absence of microglia promotes diverse pathologies and early lethality in Alzheimer's disease mice. Cell Rep *39*, 110961. 10.1016/j.celrep.2022.110961.
53. Esteban, H., Blondiaux, E., Audureau, E., Sileo, C., Moutard, M.L., Gelot, A., Jouannic, J.M., Ducou le Pointe, H., and Garel, C. (2015). Prenatal features of isolated subependymal pseudocysts associated with adverse pregnancy outcome. Ultrasound Obstet Gynecol *46*, 678-687. 10.1002/uog.14820.
54. Belle, M., Godefroy, D., Dominici, C., Heitz-Marchaland, C., Zelina, P., Hellal, F., Bradke, F., and Chedotal, A. (2014). A simple method for 3D analysis of immunolabeled axonal tracts in a transparent nervous system. Cell Rep *9*, 1191-1201. 10.1016/j.celrep.2014.10.037.
55. Renier, N., Wu, Z., Simon, D.J., Yang, J., Ariel, P., and Tessier-Lavigne, M. (2014). iDISCO: a simple, rapid method to immunolabel large tissue samples for volume imaging. Cell *159*, 896-910. 10.1016/j.cell.2014.10.010.
56. Hankin, M.H., Schneider, B.F., and Silver, J. (1988). Death of the subcallosal glial sling is correlated with formation of the cavum septi pellucidi. J Comp Neurol *272*, 191-202. 10.1002/cne.902720204.
57. Liaw, L., Birk, D.E., Ballas, C.B., Whitsitt, J.S., Davidson, J.M., and Hogan, B.L. (1998). Altered wound healing in mice lacking a functional osteopontin gene (spp1). J Clin Invest *101*, 1468-1478. 10.1172/JCI2131.
58. Rosmus, D.D., Lange, C., Ludwig, F., Ajami, B., and Wieghofer, P. (2022). The Role of Osteopontin in Microglia Biology: Current Concepts and Future Perspectives. Biomedicines *10*. 10.3390/biomedicines10040840.
59. Shen, X., Qiu, Y., Wight, A.E., Kim, H.J., and Cantor, H. (2022). Definition of a mouse microglial subset that regulates neuronal development and proinflammatory responses in the brain. Proc Natl Acad Sci U S A *119*. 10.1073/pnas.2116241119.
60. De Schepper, S., Ge, J.Z., Crowley, G., Ferreira, L.S.S., Garceau, D., Toomey, C.E., Sokolova, D., Rueda-Carrasco, J., Shin, S.H., Kim, J.S., et al. (2023). Perivascular cells induce microglial phagocytic states and synaptic engulfment via SPP1 in mouse models of Alzheimer's disease. Nat Neurosci. 10.1038/s41593-023-01257-z.
62. Saito, K., Okamoto, M., Watanabe, Y., Noguchi, N., Nagasaka, A., Nishina, Y., Shinoda, T., Sakakibara, A., and Miyata, T. (2019). Dorsal-to-Ventral Cortical Expansion Is Physically Primed by Ventral Streaming of Early Embryonic Preplate Neurons. Cell Rep *29*, 1555-1567 e1555. 10.1016/j.celrep.2019.09.075.
63. Van Essen, D.C. (2020). A 2020 view of tension-based cortical morphogenesis. Proc Natl Acad Sci U S A. 10.1073/pnas.2016830117.

64. Das, J.M., and Dossani, R.H. (2022). Cavum Septum Pellucidum. In StatPearls.
65. Cappello, S., Bohringer, C.R., Bergami, M., Conzelmann, K.K., Ghanem, A., Tomassy, G.S., Arlotta, P., Mainardi, M., Allegra, M., Caleo, M., et al. (2012). A radial glia-specific role of RhoA in double cortex formation. Neuron *73*, 911-924. 10.1016/j.neuron.2011.12.030.
66. Deck, M., Lokmane, L., Chauvet, S., Mailhes, C., Keita, M., Niquille, M., Yoshida, M., Yoshida, Y., Lebrand, C., Mann, F., et al. (2013). Pathfinding of corticothalamic axons relies on a rendezvous with thalamic projections. Neuron *77*, 472-484. 10.1016/j.neuron.2012.11.031.
67. Li, Y., He, X., Kawaguchi, R., Zhang, Y., Wang, Q., Monavarfeshani, A., Yang, Z., Chen, B., Shi, Z., Meng, H., et al. (2020). Microglia-organized scar-free spinal cord repair in neonatal mice. Nature *587*, 613-618. 10.1038/s41586-020-2795-6.
68. Paolicelli, R.C., Bolasco, G., Pagani, F., Maggi, L., Scianni, M., Panzanelli, P., Giustetto, M., Ferreira, T.A., Guiducci, E., Dumas, L., et al. (2011). Synaptic pruning by microglia is necessary for normal brain development. Science *333*, 1456-1458. 10.1126/science.1202529.
69. Schafer, D.P., Lehrman, E.K., Kautzman, A.G., Koyama, R., Mardinly, A.R., Yamasaki, R., Ransohoff, R.M., Greenberg, M.E., Barres, B.A., and Stevens, B. (2012). Microglia sculpt postnatal neural circuits in an activity and complement-dependent manner. Neuron *74*, 691-705. 10.1016/j.neuron.2012.03.026.
70. Miyamoto, A., Wake, H., Ishikawa, A.W., Eto, K., Shibata, K., Murakoshi, H., Koizumi, S., Moorhouse, A.J., Yoshimura, Y., and Nabekura, J. (2016). Microglia contact induces synapse formation in developing somatosensory cortex. Nat Commun *7*, 12540. 10.1038/ncomms12540.
71. Weinhard, L., di Bartolomei, G., Bolasco, G., Machado, P., Schieber, N.L., Neniskyte, U., Exiga, M., Vadisiute, A., Raggioli, A., Schertel, A., et al. (2018). Microglia remodel synapses by presynaptic trogocytosis and spine head filopodia induction. Nat Commun *9*, 1228. 10.1038/s41467-018-03566-5.
72. Allen, N.J., and Lyons, D.A. (2018). Glia as architects of central nervous system formation and function. Science *362*, 181-185. 10.1126/science.aat0473.
73. Frangogiannis, N.G. (2014). The inflammatory response in myocardial injury, repair, and remodelling. Nat Rev Cardiol *11*, 255-265. 10.1038/nrcardio.2014.28.
74. Pellicoro, A., Ramachandran, P., Iredale, J.P., and Fallowfield, J.A. (2014). Liver fibrosis and repair: immune regulation of wound healing in a solid organ. Nat Rev Immunol *14*, 181-194. 10.1038/nri3623.
75. Vannella, K.M., and Wynn, T.A. (2017). Mechanisms of Organ Injury and Repair by Macrophages. Annu Rev Physiol *79*, 593-617. 10.1146/annurev-physiol-022516-034356.
76. Shin, Y.J., Kim, H.L., Choi, J.S., Choi, J.Y., Cha, J.H., and Lee, M.Y. (2011). Osteopontin: correlation with phagocytosis by brain macrophages in a rat model of stroke. Glia *59*, 413-423. 10.1002/glia.21110.
77. Rentsendorj, A., Sheyn, J., Fuchs, D.T., Daley, D., Salumbides, B.C., Schubloom, H.E., Hart, N.J., Li, S., Hayden, E.Y., Teplow, D.B., et al. (2018). A novel role for osteopontin in macrophage-mediated amyloid-beta clearance in Alzheimer's models. Brain Behav Immun *67*, 163-180. 10.1016/j.bbi.2017.08.019.
78. Lyons, D.A., and Talbot, W.S. (2014). Glial cell development and function in zebrafish. Cold Spring Harb Perspect Biol *7*, a020586. 10.1101/cshperspect.a020586.
79. Sharma, K., Bisht, K., and Eyo, U.B. (2021). A Comparative Biology of Microglia Across Species. Front Cell Dev Biol *9*, 652748. 10.3389/fcell.2021.652748.
80. Teissier, N., Fallet-Bianco, C., Delezoide, A.L., Laquerriere, A., Marcorelles, P., Khung-Savatovsky, S., Nardelli, J., Cipriani, S., Csaba, Z., Picone, O., et al. (2014). Cytomegalovirus-induced brain malformations in fetuses. J Neuropathol Exp Neurol *73*, 143-158. 10.1097/NEN.0000000000000038.
81. Nunes, R.H., Pacheco, F.T., and da Rocha, A.J. (2014). Magnetic resonance imaging of anterior temporal lobe cysts in children: discriminating special imaging features in a

particular group of diseases. Neuroradiology *56*, 569-577. 10.1007/s00234-014-1356-9.
82. Jung, S., Aliberti, J., Graemmel, P., Sunshine, M.J., Kreutzberg, G.W., Sher, A., and Littman, D.R. (2000). Analysis of fractalkine receptor CX(3)CR1 function by targeted deletion and green fluorescent protein reporter gene insertion. Mol Cell Biol *20*, 4106-4114. 10.1128/MCB.20.11.4106-4114.2000.
83. Lindquist, R.L., Shakhar, G., Dudziak, D., Wardemann, H., Eisenreich, T., Dustin, M.L., and Nussenzweig, M.C. (2004). Visualizing dendritic cell networks in vivo. Nat Immunol *5*, 1243-1250. 10.1038/ni1139.
84. van Spriel, A.B., Leusen, J.H., van Egmond, M., Dijkman, H.B., Assmann, K.J., Mayadas, T.N., and van de Winkel, J.G. (2001). Mac-1 (CD11b/CD18) is essential for Fc receptor-mediated neutrophil cytotoxicity and immunologic synapse formation. Blood *97*, 2478-2486. 10.1182/blood.v97.8.2478.
85. Tomasello, E., Desmoulins, P.O., Chemin, K., Guia, S., Cremer, H., Ortaldo, J., Love, P., Kaiserlian, D., and Vivier, E. (2000). Combined natural killer cell and dendritic cell functional deficiency in KARAP/DAP12 loss-of-function mutant mice. Immunity *13*, 355-364. 10.1016/s1074-7613(00)00035-2.
86. Jackson, B., Peyrollier, K., Pedersen, E., Basse, A., Karlsson, R., Wang, Z., Lefever, T., Ochsenbein, A.M., Schmidt, G., Aktories, K., et al. (2011). RhoA is dispensable for skin development, but crucial for contraction and directed migration of keratinocytes. Mol Biol Cell *22*, 593-605. 10.1091/mbc.E09-10-0859.
87. Hao, Y., Hao, S., Andersen-Nissen, E., Mauck, W.M., 3rd, Zheng, S., Butler, A., Lee, M.J., Wilk, A.J., Darby, C., Zager, M., et al. (2021). Integrated analysis of multimodal single-cell data. Cell *184*, 3573-3587 e3529. 10.1016/j.cell.2021.04.048.
88. Hafemeister, C., and Satija, R. (2019). Normalization and variance stabilization of single-cell RNA-seq data using regularized negative binomial regression. Genome Biol *20*, 296. 10.1186/s13059-019-1874-1.
89. Genescu, I., Anibal-Martinez, M., Kouskoff, V., Chenouard, N., Mailhes-Hamon, C., Cartonnet, H., Lokmane, L., Rijli, F.M., Lopez-Bendito, G., Gambino, F., and Garel, S. (2022). Dynamic interplay between thalamic activity and Cajal-Retzius cells regulates the wiring of cortical layer 1. Cell Rep *39*, 110667. 10.1016/j.celrep.2022.110667.
90. de Frutos, C.A., Bouvier, G., Arai, Y., Thion, M.S., Lokmane, L., Keita, M., Garcia-Dominguez, M., Charnay, P., Hirata, T., Riethmacher, D., et al. (2016). Reallocation of Olfactory Cajal-Retzius Cells Shapes Neocortex Architecture. Neuron *92*, 435-448. 10.1016/j.neuron.2016.09.020.

Microglia maintain structural integrity during fetal brain morphogenesis

Lawrence et al.

Supplementary data include

Supplemental Figures 1 to 7

Tables S1 to S2

Legends of Movies S1 to S4

Other Supplementary data include

Table S1

Movies S1 to S4

Supplementary Figures

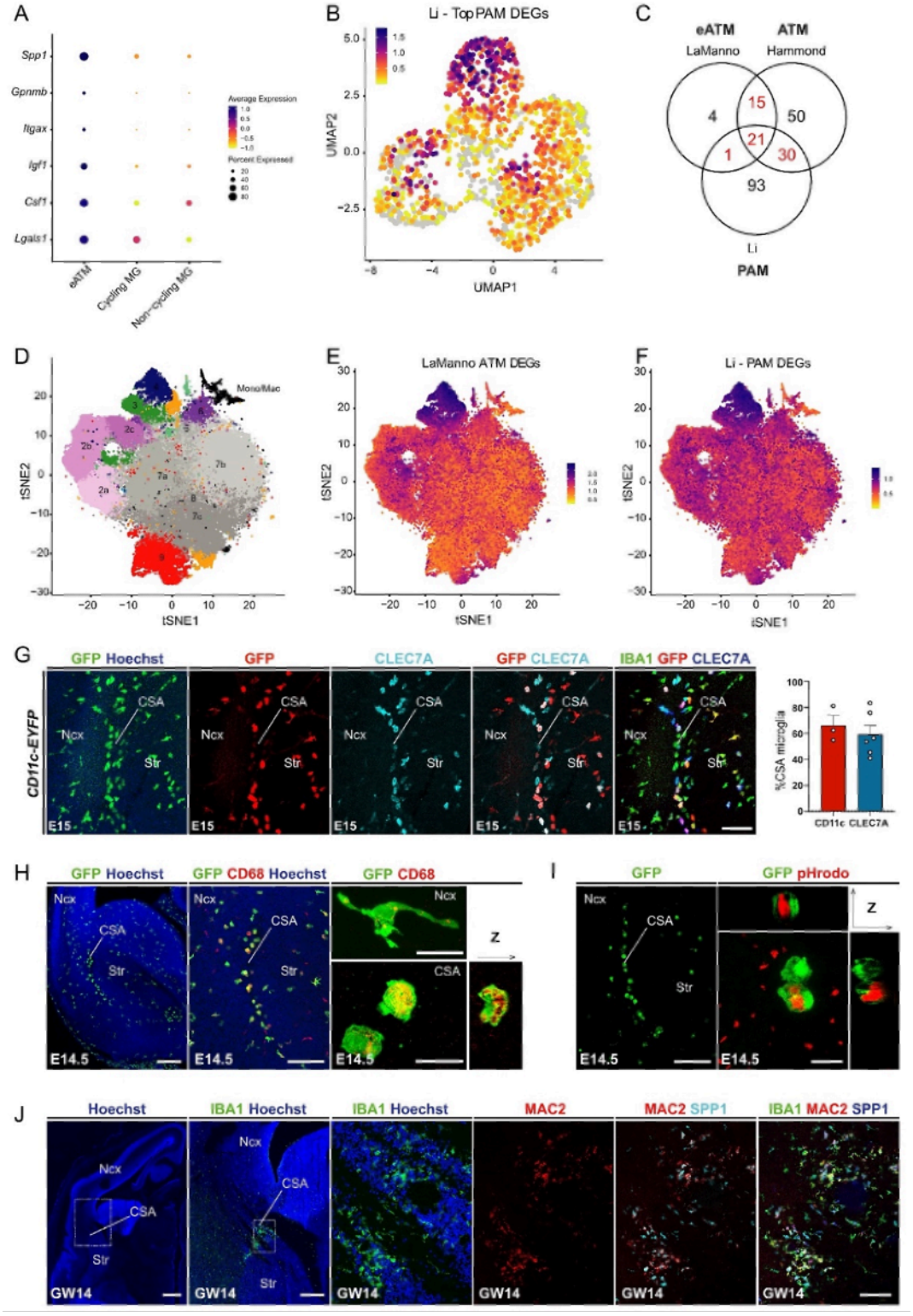

Figure S1, related to Figure 1. Embryonic ATM resemble postnatal ATM

(A) Dot plot showing the expression levels of core ATM genes in embryonic ATM (eATM) compared to non-cycling or cycling embryonic microglia (MG) in the La Manno scRNA-seq dataset (*1*). The color represents the scaled expression level across all cells within a cluster, while the dot size indicates the percentage of cells expressing each gene in that cluster. **(B)** Projection of the postnatal PAM signature from the Li dataset (*2*) onto the UMAP plot from Fig. 1A showing eATM. **(C)** Venn diagram highlighting the overlap between embryonic brain ATM DEGs identified in the La Manno dataset (*1*), postnatal ATM in the Hammond dataset (*3*), and postnatal PAM in the Li dataset (*2*). **(D)** Reproduced tSNE plot of the 76,149 cells characterized by scRNA-seq in the La Manno dataset (*3*). **(E,F)** Projections of the eATM signature defined in the La Manno dataset (*1*) **(E)** and the PAM signature defined in the Li dataset (*2*) **(F)**, showing the overlap with the Hammond ATM cluster 4. **(G)** Immunolabeling of an embryonic E15.0 *CD11c-EYFP* brain section showing IBA1-positive microglia expressing YFP (n=3) and ATM marker CLEC7A (n=6) at the CSA. **(H-I)** Immunolabeling for CD68 (**G**, n=3) and the pHrodo assay (**H**, n=4) conducted on *ex vivo* brain slices (at least n=3) showing intense staining in CSA microglia at E14.5. **(J)** Immunolabeling of human GW14 transverse sections showing co-expression of ATM markers with IBA1 at the CSA. Values are presented as mean ± SEM. Scale bars equal 1500 µm (left panel), 500 µm (second panel), and 100 µm (right panels).

ATM, axon-tract-associated microglia; CSA, cortico-striato-amygdalar boundary; DEGs, differentially expressed genes; eATM, embryonic ATM; MG, microglia; Ncx, neocortex; PAM, proliferative associated microglia; Str, striatum.

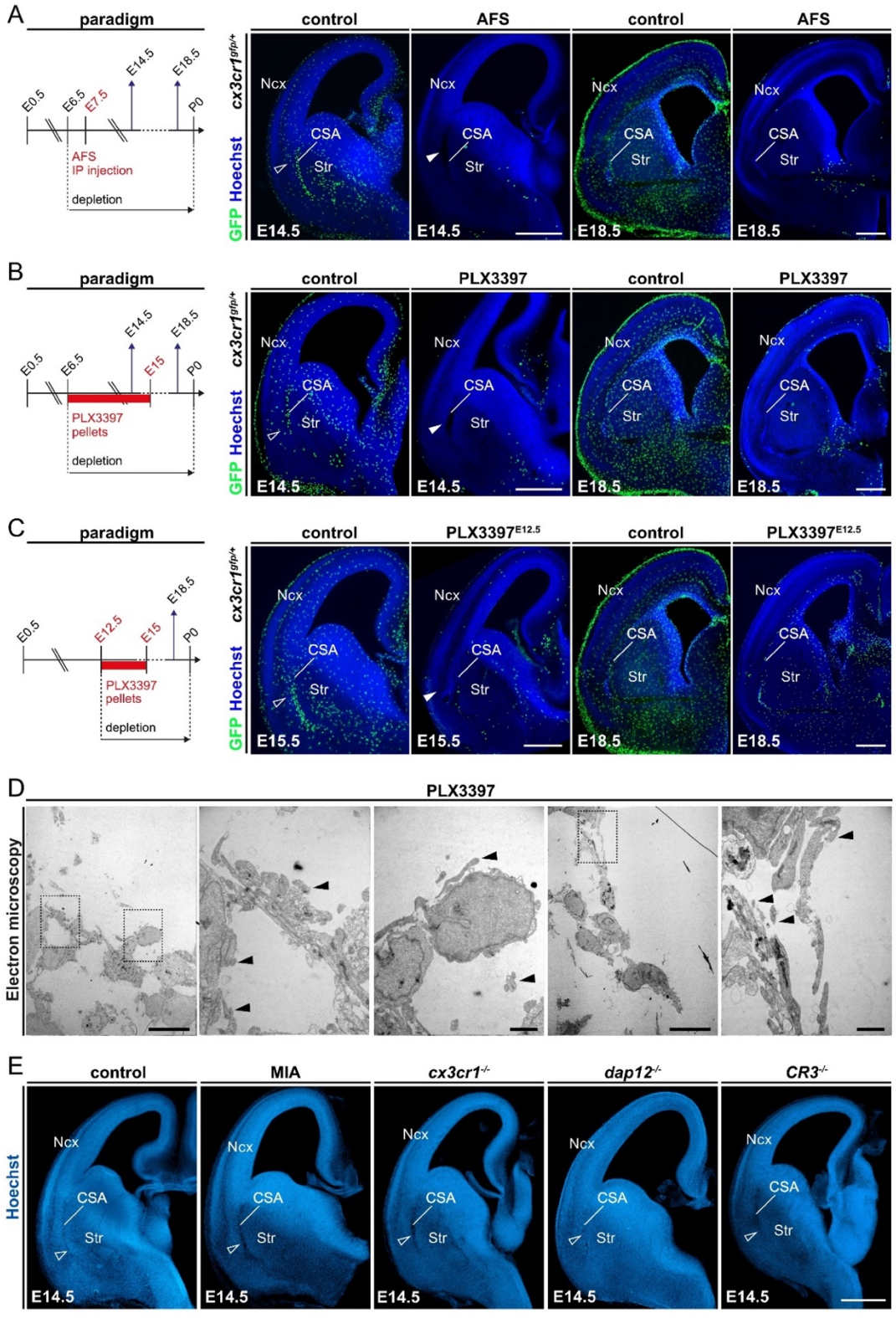

Figure S2, related to Figure 2. Models of macrophage depletion and functional alteration

(A-C) Confirmation of the depletion of microglia in brains of embryonic *Cx3cr1*^{gfp} mice at E14.5 and E18.5, where pregnant dams were subjected to **(A)** intraperitoneal injection of a CSF1R

blocking antibody (AFS) at E6.5 and E7.5 (E14.5, $n_{controls}$=21, n_{AFS}=6; E18.5, $n_{controls}$=15, n_{AFS}=17); **(B)** feeding with PLX3397, a pharmacological inhibitor of the CSF1R pathway, from E6.5 to E15.0 (E14.5, $n_{controls}$=5, $n_{PLX3397}$=5; E18.5, $n_{controls}$=12, $n_{PLX3397}$=11); and **(C)** feeding with PLX3397 from E12.5 to E15.0 (E15.5, $n_{controls}$=5, $n_{PLX3397\text{-}E12}$=9; E18.5, $n_{controls}$=12, $n_{PLX3397\text{-}E12}$=10). Open and solid arrowheads indicate the accumulation of GFP-positive cells at the CSA and local CSA tissue lesion in the absence of GFP-positive cells, respectively. **(D)** Transmission electron microscopy image of the CSA lesion in the brain of E14.5 embryos from PLX3397-treated dams, showing the presence of cell debris (solid arrowheads) but the absence of basal membrane (n=3). **(E)** Coronal sections through hemibrains of E14.5 embryos from wild-type mice, those exposed to mild maternal immune activation (MIA), and *Cxc3cr1*$^{-/-}$, *Dap12/TyroBP*$^{-/-}$ and *CR3*$^{-/-}$ mutant embryos showing the absence of CSA lesions (open arrowheads) (at least n=6 for each condition). Scale bars equal 500 μm (A, B, C, E), 10 μm (D; low magnification), and 2 μm (D; high magnification).

CSA, cortico-striato-amygdalar boundary; Ncx, neocortex; Str, striatum.

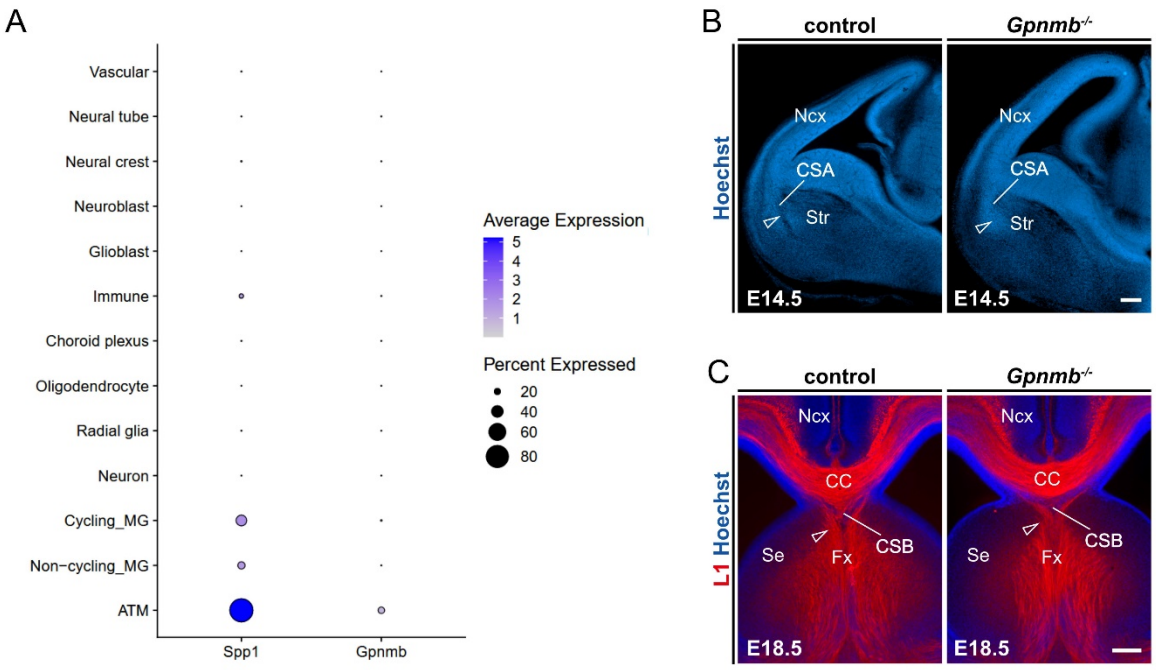

Figure S3, related to Figure 4. *Gpnmb* inactivation does not alter CSA or CSB integrity

(A) Dot plot reporting the average expression level of *Spp1* and *Gpnmb* in various cell types of La Manno et al. (*1*) scRNA-seq data across different embryonic time points (229,948 cells). Color represents the average expression level across all cells within a cluster, while the dot size indicates the percentage of cells expressed in that cluster. **(B)** E14.5 coronal hemisection stained with Hoechst, showing the integrity of the CSA in control mice and *Gpnmb*$^{-/-}$ mutants (open arrowheads) ($n_{controls}$=18, $n_{GpnmbKO}$= 13). (**C**) L1 immunolabeling showing the integrity at the CSB in control mice and *Gpnmb*$^{-/-}$ mutants (open arrowheads) ($n_{controls}$=23, $n_{GpnmbKO}$=8). Scale bars equal 200 µm.

CC, corpus callosum; CSA, cortico-striato-amygdalar boundary; CSB, cortico-septal boundary; Fx, fornix; Ncx, neocortex; Se, Septum; Str, striatum.

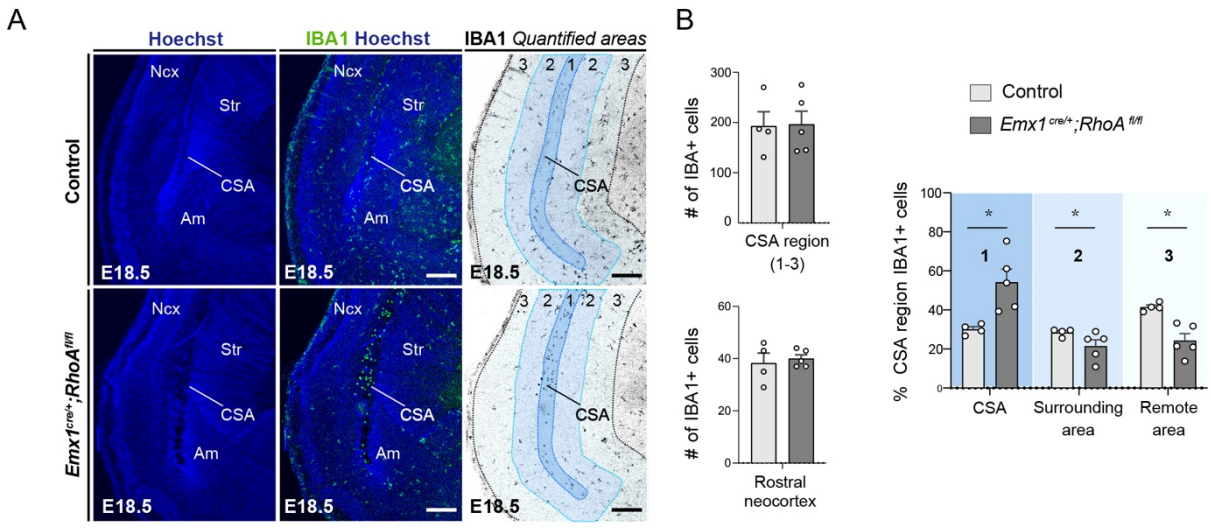

Figure S4, related to Figure 5. Microglial recruitment and expression of ATM-factor Spp1 is modulated by global changes in brain morphogenesis

(A) IBA1 immunolabeling in coronal sections showing the distribution of microglia in control and *Emx1*$^{cre/+}$*; RhoA*$^{fl/fl}$ mutant brains at E18.5. Mutant mice display the accumulation of microglia at the lesioned CSA and reduced numbers in surrounding areas, despite a lack of overall difference in microglial numbers in the caudal CSA region or the rostral neocortex (n=4 at least from 2 different litters for both controls and mutants). **(B)** Quantification of IBA1+ cells in the entire CSA region, rostral neocortex, and within CSA subregions (1 to 3). Graphs show means ± SEM. Mann-Whitney U Tests were performed for statistical comparison, * $p<0.05$. Scale bars equal 200 µm.

Am, Amygdala; CSA, cortico-striato-amygdalar boundary; Ncx, neocortex; Str, striatum.

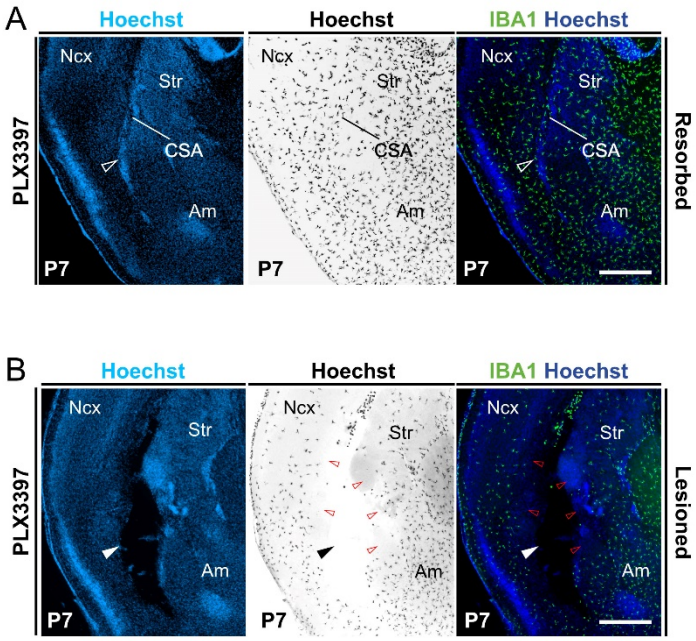

Fig S5, related to Figure 7. Lesion repair correlates with local microglial repopulation

(A) Representative examples showing that in most PLX3397-exposed pups, repopulation triggers lesion closure and leads to a "resorbed" phenotype at the CSA by P7 (open arrowheads). **(B)** By contrast, the cases in which the resorption did not occur and were still "lesioned" at P7 (solid arrowheads) correlate with a lack of local CSA repopulation (smaller arrows indicate a lack of repopulated microglia at the lesion edges) ($n_{Resorbed}$=8; $n_{Lesioned}$=3). Scale bars equal 500 µm.

Am, Amygdala; CSA, cortico-striato-amygdalar boundary; Ncx, neocortex; Str, striatum.

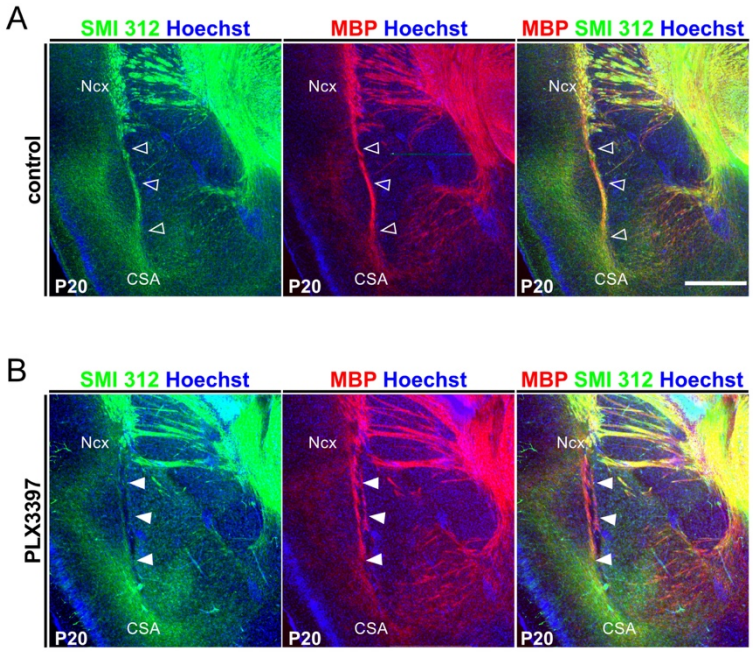

Fig S6, related to Figure 7. Long-term impact on CSA morphology after PLX3397-prenatal exposure and lesion closure

(A,B) P20 coronal hemisections of brains immunostained with the pan axonal neurofilament marker SMI-312, Myelin Basic Protein (MBP), and Hoechst reveal alterations in the axonal organization at the CSA in mice prenatally exposed to PLX3397 (solid arrowheads) (B) compared to controls (open arrowheads) (A). Axonal tracts of the amygdalar capsule are disorganized, highlighting a long-term morphological consequence of embryonic and early life CSA lesions ($n_{controls}$=9, $n_{PLX3397}$=7). Scale bars equal 500 µm.

CSA, cortico-striato-amygdalar boundary; Ncx, neocortex.

Supplementary Tables

Table S1. Comparison of ATM genes between datasets. Table S1 (excel sheet) provides a comparison of overlap in differentially expressed genes and their mean raw count expression between embryonic ATM from La Manno et al. (*1*), ATM from Hammond et al. (*3*), and PAM from Li et al. (*2*), related to the Venn diagrams Fig.1C and Fig.S1C.

Table S2. Tables delineating lesion severity. This table shows lesion area ranges used to score lesion severity in Figure 4, Figure S5, and Figure 5.

Lesion area	E15.5	E18.5	P7
Severity 0	0-2,000 μm^2	0-2,000 μm^2	0-2,000 μm^2
Severity 1	2,000-18,000 μm^2	2,000-18,000 μm^2	2,000-30,000 μm^2
Severity 2	>18,000 μm^2	>18,000 μm^2	>30,000 μm^2

Legends to Supplementary Movies

Movie S1. This movie shows a lateral rotation of an AFS-treated E16.5 hemibrain cleared by iDISCO, imaged on a light-sheet microscope and reconstructed using the Imaris software, showing a cavitary lesion at the CSA (yellow indicates the reconstructed cavity). Green signal encompasses non-depleted CX3CR1-GFP+ cells and tissue autofluorescence delineating hemibrain morphology. The cavitary lesion was reconstructed and pseudocolored in yellow in the Imaris software. Due to size limitations, a **low-resolution file** has been provided.

Movie S2. This movie shows a lateral rotation of a PLX3397-treated E16.5 hemibrain cleared by iDISCO, imaged on a light-sheet microscope and reconstructed using the Imaris software, showing a cavitary lesion at the CSA (yellow indicates the reconstructed cavity). Green signal encompasses tissue autofluorescence delineating hemibrain morphology. The cavitary lesion was reconstructed and pseudocolored in yellow in the Imaris software. Due to size limitations, a **low-resolution file** has been provided.

Movie S3. This movie shows a rostrocaudal progression through an E16.5 control hemibrain cleared by iDISCO, imaged on a light-sheet microscope and reconstructed using the Imaris software, showing normal morphology at the CSA and CSB (open arrowheads). The movie progresses through light sheet photographs acquired along the coronal rostrocaudal axis of the sample at a 3 μm Z step size.

Movie S4. This movie shows a rostrocaudal progression through a PLX3397-treated E16.5 hemibrain cleared by iDISCO, imaged on a light-sheet microscope and reconstructed using the Imaris software, showing a cavitary lesion at the CSA (solid arrowheads). The movie

progresses through light sheet photographs acquired along the coronal rostrocaudal axis of the sample at a 3 μm Z step size.

Review

Multifaceted Microglia during Brain Development: Models and Tools

Summary

Over the past decades, a growing interest in microglia has supported the development of numerous mouse lines and tools to label, target or deplete microglia. Focusing on murine development, we here provide a review summarizing the available tools at hand for scientists interested in microglia, highlighting their advantages and limitations. In particular, we detail which one are specific and which one also target the border associated macrophages, overlooked until recently but which diversity and importance is just starting to emerge.

frontiers | Frontiers in Neuroscience

TYPE Mini Review
PUBLISHED 23 March 2023
DOI 10.3389/fnins.2023.1125729

OPEN ACCESS

EDITED BY
Subashika Govindan,
DBT/Wellcome Trust India Alliance, India

REVIEWED BY
Deborah R. Winter,
Northwestern University, United States
Kathryn M. Lenz,
The Ohio State University, United States

*CORRESPONDENCE
Morgane Sonia Thion
✉ thion@biologie.ens.fr

SPECIALTY SECTION
This article was submitted to Translational Neuroscience, a section of the journal Frontiers in Neuroscience

RECEIVED 16 December 2022
ACCEPTED 24 February 2023
PUBLISHED 23 March 2023

CITATION
Bridlance C and Thion MS (2023) Multifaceted microglia during brain development: Models and tools.
Front. Neurosci. 17:1125729.
doi: 10.3389/fnins.2023.1125729

Multifaceted microglia during brain development: Models and tools

Cécile Bridlance[1,2,3] and Morgane Sonia Thion[1,2]*

[1]Institut de Biologie de l'École Normale Supérieure (IBENS), École Normale Supérieure, CNRS, INSERM, Université PSL, Paris, France, [2]Center for Interdisciplinary Research in Biology, Collège de France, CNRS, INSERM, Université PSL, Paris, France, [3]Collège Doctoral, Sorbonne Université, Paris, France

Microglia, the brain resident macrophages, are multifaceted glial cells that belong to the central nervous and immune systems. As part of the immune system, they mediate innate immune responses, regulate brain homeostasis and protect the brain in response to inflammation or injury. At the same time, they can perform a wide array of cellular functions that relate to the normal functioning of the brain. Importantly, microglia are key actors of brain development. Indeed, these early brain invaders originate outside of the central nervous system from yolk sac myeloid progenitors, and migrate into the neural folds during early embryogenesis. Before the generation of oligodendrocytes and astrocytes, microglia thus occupy a unique position, constituting the main glial population during early development and participating in a wide array of embryonic and postnatal processes. During this developmental time window, microglia display remarkable features, being highly heterogeneous in time, space, morphology and transcriptional states. Although tremendous progress has been made in our understanding of their ontogeny and roles, there are several limitations for the investigation of specific microglial functions as well as their heterogeneity during development. This review summarizes the current murine tools and models used in the field to study the development of these peculiar cells. In particular, we focus on the methodologies used to label and deplete microglia, monitor their behavior through live-imaging and also discuss the progress currently being made by the community to unravel microglial functions in brain development and disorders.

KEYWORDS

microglia, brain, development, models, tools

Introduction

Microglia, the central nervous system (CNS) resident macrophages remained poorly studied until an exponential growth in interest during the last two decades led to fascinating insights into the origin of microglia, their functions, as well as dysfunctions in pathological conditions (Mosser et al., 2017; Hammond et al., 2018; Hoeffel and Ginhoux, 2018; Li and Barres, 2018; Thion et al., 2018a; Prinz et al., 2019). Contrary to most brain cells, microglia were shown to originate from mesodermal yolk sac (YS) macrophage progenitors that travel to reach the CNS during early embryonic development, around Embryonic day (E)9 in mice and gestational week 4/5 in humans (Monier et al., 2007; Ginhoux et al., 2010; Verney et al., 2010; Menassa et al., 2022). As such, these brain invaders constitute the main glial population before the emergence of other glial cells such as oligodendrocytes and astrocytes. After closure of the blood brain barrier around E14 in mice, microglia are believed to be

enclosed in the brain under steady-state conditions. These pioneer microglia thus proliferate, seed the entire parenchyma and progressively mature in symbiosis with the neural tissue microenvironment (Matcovitch-Natan et al., 2016; Thion et al., 2018b; Kracht et al., 2020) before self-renewing throughout life. This situation is different in zebrafish where microglia are fully replaced by another source of microglia by adulthood (Xu et al., 2015; Ferrero et al., 2018). A key aspect of their development is the high heterogeneity in their colonization patterns, morphologies and molecular properties. In particular, microglial colonization of the brain parenchyma is a long-lasting process that spans embryogenesis until the end of the second postnatal week, following a very stereotypical and uneven spatiotemporal pattern (Swinnen et al., 2013; Squarzoni et al., 2014; Menassa et al., 2022). These cells transiently accumulate at specific hotspots such as the cortico-striatal-amygdalar boundary and are excluded from others regions such as the cortical plate. In addition, they display a variety of morphologies (ameboid, poorly ramified, and elongated) associated with different brain localizations. Finally, owing to high throughput approaches, microglia have been shown to exhibit different transcriptomic states, specifically during development, in both mice and humans (Hammond et al., 2019; Li et al., 2019; Sankowski et al., 2019; Kracht et al., 2020). This high developmental heterogeneity contrasts with a relatively uniform distribution in the whole parenchyma alongside homogeneously ramified morphologies and molecular signatures at adult stages. Finally, sex-specific microglial features have been highlighted in postnatal steady-state conditions but also in response to environmental challenges (Schwarz et al., 2012; Lenz et al., 2013; Rebuli et al., 2016; Hanamsagar et al., 2017; Guneykaya et al., 2018; Thion et al., 2018b; Villa et al., 2018; VanRyzin et al., 2019).

Several seminal studies have demonstrated that, beyond their immune functions, microglia also perform a wide array of cellular functions that relate to the normal functioning of the brain and importantly to its development. In particular, they interact with synapses to mediate remodeling, pruning and transmission but have also been involved in synaptogenesis (Andoh and Koyama, 2021). They further participate to neurogenesis and oligodendrogenesis, partly through their regulation of cell death and survival (Sierra et al., 2010; Cunningham et al., 2013; Hagemeyer et al., 2017; Wlodarczyk et al., 2017; Nemes-Baran et al., 2020; Sherafat et al., 2021; Cserep et al., 2022). They also contribute to the refinement of axonal tracts (Pont-Lezica et al., 2014; Squarzoni et al., 2014) and to the development of cortical inhibitory circuits (Squarzoni et al., 2014; Thion et al., 2019; Favuzzi et al., 2021; Yu et al., 2022). Besides, microglia express various pattern recognition, purinergic, chemokine and cytokine receptors, collectively described as the sensome (Hickman et al., 2013), enabling them to detect and integrate environmental changes. Importantly and consistently with their wide array of cellular functions, microglial dysfunction has been associated with the etiology of neurodevelopmental disorders, including autism spectrum disorders and schizophrenia in humans and mouse models (Lukens and Eyo, 2022). Therefore, during this crucial period of development, it is key to better grasp their functions, the regulatory mechanisms underpinning their heterogeneity and how their molecular states may regulate their roles. Furthermore, elucidating how external signals can impact on these fundamental processes is a major challenge. This will be crucial to illuminate specific and diverse microglial contributions to brain wiring as well as shed light on pathological mechanisms of neurodevelopmental disorders.

Beside microglia, other non-parenchymal macrophages called Border-Associated Macrophages (BAMs) are present at the interfaces of the brain: the meninges, choroid plexus and perivascular space (Lee et al., 2021; **Figure 1**). Although microglia and BAMs originate from yolk-sac derived progenitors and seed the brain during embryogenesis, some of them are further replaced by monocyte-derived cells, arising from hematopoietic stem cells (Goldmann et al., 2016; Mrdjen et al., 2018; Van Hove et al., 2019; Utz et al., 2020; Masuda et al., 2022). Moreover, while generally referred to as BAMs, they display age- and tissue-specific signatures (Kierdorf et al., 2019; Mildenberger et al., 2022). Most of the well-recognized microglial markers, reporter mouse lines and models that currently exist to label and deplete microglia can also target a large part of macrophages such as the BAMs in the CNS but also populations of peripheral macrophages (Green et al., 2020). Consequently, despite intense research efforts, these limitations prevent the identification and characterization of specific microglia functions, especially during development. Herein, we discuss about the current murine tools and models available to label or deplete microglia and subsequently assess their developmental functions in physiological and disease conditions.

From broad microglial targeting to specific states labeling

Catch me if you can: Microglia and other brain macrophages

Historically, microglia were mainly identified either through Iba1 immunostaining or using the *Cx3cr1*$^{GFP/+}$ (Jung et al., 2000) that labels many macrophages, including microglia and BAMs. Similarly, the well-established *Cx3cr1*^{creERT2} mouse lines have been very useful to inactivate genes in these cells (Parkhurst et al., 2013; Yona et al., 2013). Nevertheless, they are not specific to microglia and may trigger microglial reactivity in neonates upon tamoxifen administration (Sahasrabuddhe and Ghosh, 2022). Recent studies, including single cell RNA sequencing analyses, highlighted more specific homeostatic microglia markers including *p2ry12*, *Sall1*, *Tmem119*, *Hexb*, *Siglech* (Gautier et al., 2012; Buttgereit et al., 2016; Satoh et al., 2016; Cserep et al., 2020; Masuda et al., 2020) allowing the use of specific antibodies to label either microglia (P2ry12, Tmem119, and SiglecH) or BAMs (CD206, Lyve1, and Siglec1) (Mrdjen et al., 2018; **Figure 1**). Fluorescent *In Situ* Hybridization (FISH) has also been used to circumvent the absence of specific antibodies, particularly by taking advantage of the RNAscope technique (Matcovitch-Natan et al., 2016; Hammond et al., 2019). To specifically visualize, manipulate and assess microglia functions, reporter and *creERT2*-expressing lines were generated with minor recombination in BAMs: *Tmem119*^{eGFP} and *Tmem119*^{creERT2} (Kaiser and Feng, 2019), *Tmem119*^{tdTomato} (Ruan et al., 2020), *Hexb*^{tdTomato} and *Hexb*^{creERT2} (Masuda et al., 2020), *p2ry12*^{creERT2} (McKinsey et al., 2020), *Sall1*^{GFP}, and *Sall1*^{creERT2} (Buttgereit et al., 2016), the latter recombining in neurons and other glia (Chappell-Maor et al., 2020; **Table 1**). Nonetheless, since most of these genes start to be expressed as microglia mature (Bennett et al., 2016), it is important to stress that there are so far no

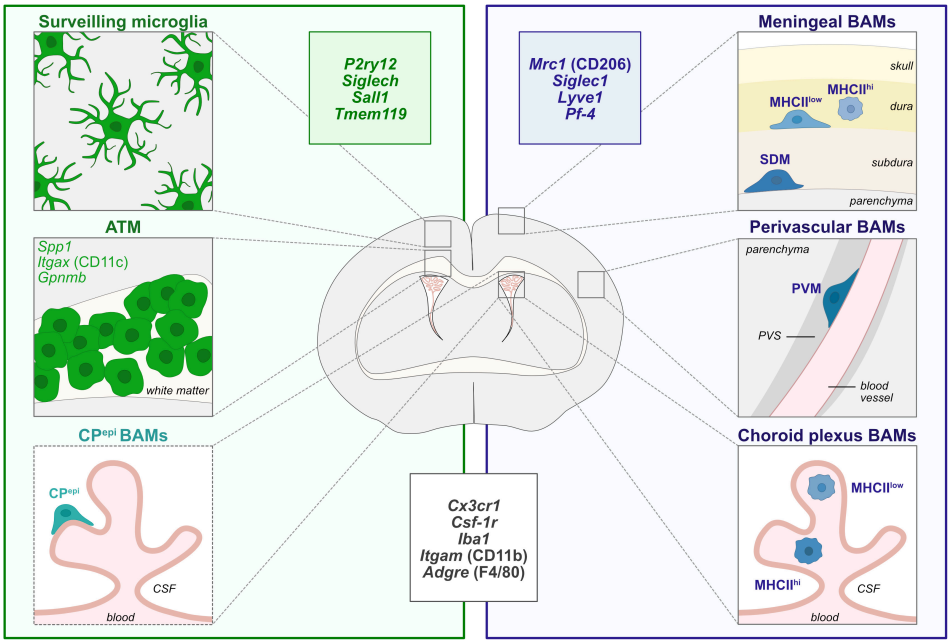

FIGURE 1
Diversity of CNS macrophages in steady-state conditions. During steady-state, microglia are localized within the brain parenchyma and are highly heterogeneous in morphologies, localization and molecular signatures throughout brain development. In particular, axon tract-associated microglia (ATM)/proliferative-region-associated microglia (PAM)/Cd11c-positive microglia have been described during early postnatal development in the corpus callosum and other white matter regions. Border-associated macrophages (BAMs) reside at distinct interfaces of the CNS such as the meninges, choroid plexus and perivascular space (Goldmann et al., 2016; Mrdjen et al., 2018; Van Hove et al., 2019; Utz et al., 2020; Masuda et al., 2022). Non-parenchymal microglia-like Kolmer's epiplexus BAMs (CP^{epi}) reside in the apical surface of the choroid plexus facing the cerebrospinal fluid (CSF) and share some transcriptional features with microglia and ATM signature (Van Hove et al., 2019). In particular, meningeal $MHCII^{low}$ and $MHCII^{high}$ macrophages are localized in the dura matter while subdural macrophages (SDM) are restrained to the subdural area. Finally, while perivascular macrophages (PVM) are found in the perivascular space, between the vascular basement membrane and the glia limitans of the parenchyma, choroid plexus contains $MHCII^{low}$ and $MHCII^{high}$ BAMs. The insets depict the most commonly used markers for microglia (green), BAMs (blue), and common markers to both populations (black). ATM, axon tract-associated microglia; BAMs, border-associated macrophages; CP^{epi}, Kolmer's epiplexus; CSF, cerebrospinal fluid; MHCII, major histocompatibility complex class II; PVS, perivascular space; PVM, perivascular macrophage; SDM, subdural macrophage.

alternatives to the $Cx3cr1^{GFP/+}$ or $Cx3cr1^{creERT2}$ lines to efficiently target early embryonic microglia.

Targeting microglia more specifically is crucial, since studies often assign a variety of roles to microglia using depletion models that target both microglia and BAMs. Kim et al. (2021) took advantage of an elegant "split cre" binary genetic construct to generate the $Cx3cr1^{ccre}$:$Sall1^{ncre}$ and $Cx3cr1^{ccre}$:$Lyve1^{ncre}$, to selectively target microglia and BAMs, respectively. Furthermore, several mouse lines including the $Siglec1^{cre}$ (Utz et al., 2020), *Pf4-Cre* (McKinsey et al., 2020), $Lyve1^{creERT2}$, and $Mrc1^{CreERT2}$ lines (Masuda et al., 2022) have been shown to specifically label BAMs during development and thereby enable to follow their trajectory (**Table 1**). In addition, while no circulating cells are thought to enter in the brain parenchyma during steady-state after BBB closure, monocyte infiltration can occur in disease, aging and injury, and can be monitored using bone marrow chimeras (Mills et al., 2022). These new tools will be important to decipher the relative contributions of microglia, BAMs or infiltrating myeloid cells, but still require thorough characterization with regards to efficiency and rate of spontaneous recombination at different timepoints along development.

Finally, cell-specific viral gene delivery has been extensively used to target different CNS population but robust transduction in microglia remained quite inefficient until recently (Maes et al., 2019). In a ground-breaking study, Lin et al. (2022) successfully targeted 80% of microglia *in vivo* using adeno-associated viruses without inducing microglia reactivity or changes in gene expression, although it remains elusive to what extend BAMs were also affected. Such approach opens new avenues to study microglia but also have tremendous translational potential.

Looking with new eyes

Along with new markers, mouse lines and viral approaches to target microglia, technical advances in diverse fields shed new light on ways to study microglia, in particular going from fixed immobile imaging in brain slices to dynamic and global approaches. First, tissue clearing methods are constantly improving, with some of them perfectly preserving the signal from reporter lines and antibodies [reviewed in Eme-Scolan and Dando (2020)]. This allows visualization of microglia in whole intact brains. However, while these techniques are becoming well-established and easier to use routinely, the difficulty lies in the analysis of the generated data. Annotated 3D atlases of the developing brain will offer many exciting possibilities toward a more comprehensive study of microglia development.

Another revolution in the field of microglia came with two-photon live-imaging experiments, which revealed never resting microglia with their processes constantly surveilling their

TABLE 1 Tools to label, target and deplete microglia and BAMs.

Tagging models	Microglia	BAMs	Prenatal and early postnatal	Adulthood	Remarks	References
Cx3cr1$^{GFP/+}$	Yes	Yes	GFP expressed by E9.5	>99%	Targets peripheral immune cells and myeloid BM progenitors	Jung et al., 2000
Cx3cr1^{creERT2} (1,2)	Yes	Yes	40H-Tam. E9.0: 99% efficiency at E10.5 (2)	>99%	Spontaneous recombination reported	Parkhurst et al., 2013 (1); Yona et al., 2013 (2)
Tmem119^{eGFP}	Yes	Few	GFP expressed by P1	>99%	Transiently labels blood vessels at P1	Kaiser and Feng, 2019
Tmem119^{creERT2}	Yes	Few	Tam. P2, P3 and P4: 90% efficiency by P14	>99%	Targets few CD45+ cells in blood	
Tmem119^{tdTomat}	Yes	Few	N.A.	>95%		Ruan et al., 2020
Hexb^{tdTomato}	Yes	Few	TdTomato expressed by E12.5	>99%	Labels few meningeal and perivascular BAMs	Masuda et al., 2020
Hexb^{creERT2}	Yes	Few	Tam. P1 and P3: 90% efficiency at P42	~80%	Targets peripheral macrophages in kidney	
P2ry12^{creERT2}	Yes	Few	Tam. E13.5, E15.5 and E17.5: robust efficiency by E18.5 in microglia and subsets of BAMs (40% in choroid plexus, 10% in meninges, few PVM)	90–95%	Targets 20–25% of BAMs in choroid plexus and meninges	McKinsey et al., 2020
Sall1^{GFP}	Yes	No	GFP expressed in 20% microglia by E12.5, 69% by E14.5, 90% by P2	>95%	Targets <10% other CNS cells	Buttgereit et al., 2016; Utz et al., 2020
Sall1^{creERT2}	Yes	No	Tam. E14.5 and E16.5: 75% efficiency at E18.5	>95%	Targets <10% other CNS cells	
Cx3cr1^{ccre}:*Sall1*^{ncre}	Yes	No	N.A.	~90%		Kim et al., 2021
Cx3cr1^{ccre}:*Lyve1*^{ncre}	No	Yes	N.A.	20% of Lyve1+ cells		
Lyve1^{CreERT2}	No	Yes	40H-Tam. E16.5: 50% efficiency in meningeal and perivascular macrophages at P14	N.A.	Targets lymphatic endothelial cells	Masuda et al., 2022
Siglec1^{cre}	No	Yes	Efficiently floxes gene in BAMs at E18.5	N.A.	*Siglec1* expressed by 60% BAMs at E14.5, 100% at E18.5	Utz et al., 2020
Pf4-Cre	Few	Yes	N.A.	>99%		McKinsey et al., 2020
Mrc1^{CreERT2}	No	Yes	40H-Tam. E9.0: 10% efficiency in BAMs and 5% in microglia by E18.5	>95%		Masuda et al., 2022
Adenoviruses	Yes	N.A.	N.A.	80%		Lin et al., 2022

(Continued)

10.3389/fnins.2023.1125729

TABLE 1 (Continued)

Depletion models	Microglia	BAMs	Prenatal and early postnatal	Adulthood	Remarks	References
Killing by numbers						
Cx3cr1^{CreER}:*R26*^{iDTR}	Yes	Yes	N.A.	>99%	Fast repopulation	Parkhurst et al., 2013
IBA1-tTA::$^{DTAtetO/tetO}$	Yes	Yes	Withdrawal of doxycycline from maternal diet from P5: 50% depletion at P8	~90% in retina	Fast repopulation	Miyamoto et al., 2016; Takeda et al., 2018
Siglech$^{DTR/DTR}$	Yes	No	Injection at E10.5: 80% depletion at E12.5, 60% at E14.5	80–85%	Fast repopulation	Konishi et al., 2017; Li et al., 2021
CSF-1R inhibitors						
Anti CSF-1R antibodies	Yes	Yes	Injections at E6 and E7: >98% depletion at E14.5	No effect	Fast repopulation	MacDonald et al., 2010; Squarzoni et al., 2014
Anti CSF-1 antibodies	Yes	No	Injections at E6 and E7: >50% depletion at P0.5	60% in white matter region	Dose-dependent efficiency	Easley-Neal et al., 2019
Anti IL-34 antibodies	Yes	No	Injections at E6 and E7: no effect at P0.5. Injection at P0.5: 30% depletion at P4	50% in grey matter region	Dose-dependent efficiency	
PLX5622	Yes	Yes	Chow PLX from E3.5: 99% depletion at E15.5	>95% within 7 days	Fast repopulation	Huang et al., 2018; Rosin et al., 2018; Marsters et al., 2020
PLX3397	Yes	Yes	Chow PLX from E14 followed by s.c. injections in pups: 90% depletion at P5 in spinal cord	>99% within 7 days	Fast repopulation	Elmore et al., 2014; Li et al., 2020
Genetic models						
Pu.1$^{-/-}$	Yes	Yes	100%	100%	Homozygotes die shortly after birth	McKercher et al., 1996
Csf1$^{op/op}$	Yes	Yes	N.A.	0–30%	Abnormal brain development	Michaelson et al., 1996
Il34$^{LacZ/LacZ}$ (1,2)	Yes	N.A.	>80% decrease at P2 (1); normal colonization of the brain from E10.5 to newborn (2)	50% (1; 2)		Wang et al., 2012 (1); Greter et al., 2012 (2)
Csf1r$^{-/-}$	Yes	Yes	>99%	100%	Shortened lifespan and abnormal brain development	Erblich et al., 2011
Sall1^{CreER};*Csf1r*$^{fl/fl}$	Yes	No	N.A.	70–90%	Spatial variability in efficiency	Buttgereit et al., 2016
Hexb^{CreERT2};*Csf1r*$^{fl/fl}$	Yes	No	N.A.	60%		Masuda et al., 2020
Csf1r$^{\Delta FIRE/\Delta FIRE}$	Yes	Few	Absence of CPepi in the choroid plexus, other BAMs reduced	100%		Rojo et al., 2019; Munro et al., 2020
Nestin^{cre};*Csf1*$^{fl/fl}$	Yes	N.A.	60% decrease in E17.5 cerebellum	~50% in cerebellum		Kana et al., 2019
Nestin^{cre};*Il34*$^{fl/fl}$	Yes	N.A.	N.A.	~85% in striatum		Badimon et al., 2020

Table summarizing the main mouse lines and tools available to label, target and deplete microglia and BAMs, indicating their specificity and efficiency in development and adulthood. BAMs, border-associated macrophages; BM, bone marrow; CNS, central nervous system; CPepi, Kolmer's epiplexus; DTA, diphtheria toxin fragment A; DTR, diphtheria toxin receptor; iDTR, inducible diphtheria toxin receptor; i.p., intraperitoneal; N.A., non-applicable; PVM, perivascular macrophages; s.c., subcutaneous; Tam, tamoxifen; 40H-Tam, 4-hydroxytamoxifen.

10.3389/fnins.2023.1125729

environment as well as rapidly reacting in case of injury (Davalos et al., 2005; Nimmerjahn et al., 2005). In combination with other markers, it is thus possible to monitor microglial interaction with blood vessels (Csaszar et al., 2022), radial glia (Rosin et al., 2021), neuronal populations as well as track microglial processes and their specific contact with synapses (Wake et al., 2009) or nodes of Ranvier (Ronzano et al., 2021). While some experiments are performed on brain slices, inducing tissue damage and possibly altering microglial behavior, most studies use cranial windows or skull thinning that allows microglial observation in their homeostatic environment. For pups, adapted approaches are being developed taking advantage of the thinness of the embryonic skull to perform *ex utero* live-imaging of microglia and macrophages in the brain of intact embryos (Hattori et al., 2020, 2022; Munz et al., 2022), that will probably be critical to better characterize key aspects of microglia development such as their entry in the brain parenchyma (Stremmel et al., 2018).

As a self-renewing population arising from a restricted pool of pioneer cells, the questions of microglial expansion during development, their migration and turnover were raised–and still retain some mystery. The "Microfetti" mice developed by Tay et al. (2017) in which microglia express randomly one out of four fluorophores after tamoxifen induction, highlighted clonal expansion of adult microglia in pathology. In addition, Ratz et al. (2022) developed the new TREX technique, which combines single-cell and spatial transcriptomic coupled to early (E9.5) *in vivo* barcoding, in order to analyze the lineage relationships between mature cells and progenitors. Thereby, they highlighted drastic microglial expansion from a limited pool of progenitors. Though not extensively used yet, these tools for clonal analysis and lineage tracing will be valuable in the context of development to better understand microglial expansion, migration and final distribution in the brain.

Targeting the different flavors of microglia

Historically, microglia were classified as displaying either a neurotoxic pro-inflammatory M1 or neuroprotective anti-inflammatory M2 phenotype but this binary perspective has been largely revisited (Paolicelli et al., 2022). The development of high throughput technologies such as single cell and single nucleus RNA sequencing (sc/snRNA-seq), cytometry by time-of-flight (CyTOF), or multiplex error-robust fluorescent *in situ* hybridization (MERFISH) revealed a richer heterogeneity in microglial profiles. While microglia constitute a relatively homogeneous population in adulthood, they display a striking heterogeneity during prenatal/early postnatal development, aging and neurodegeneration (Deczkowska et al., 2018; Hammond et al., 2019; Li et al., 2019; Masuda et al., 2019; Sankowski et al., 2019; Kracht et al., 2020; Marschallinger et al., 2020; Safaiyan et al., 2021; Stogsdill et al., 2022). Nevertheless, we should not underestimate the experimental bias introduced by cell dissociation and sorting-strategies, sequencing technologies and subsequent analyzes selected to characterize microglial heterogeneity (Marsh et al., 2022; Paolicelli et al., 2022; Sankowski et al., 2022). To avoid extensive confusion in the field, it remains crucial to be cautious about the semantic implication of microglial heterogeneity and the subsequent functional diversity associated with it (Paolicelli et al., 2022).

Specific developmental microglial states are thus starting to be described such as the Axon Tract-associated Microglia (ATM), also known as Proliferative-region-Associated Microglia (PAM), Cd11c-positive microglia, and Youth-Associated Microglia (YAM). They are characterized by the expression of several genes such as *Spp1, Itgax, Gpnmb* and were initially identified in the postnatal white matter as regulators of the development of oligodendrocyte precursors and of subsequent myelinogenesis (Hagemeyer et al., 2017; Wlodarczyk et al., 2017; Hammond et al., 2019; Li et al., 2019; Silvin et al., 2022). Interestingly, there are remarkable similarities in transcriptomic signatures between ATM and Disease Associated Microglia (DAM), initially characterized in mouse models of Alzheimer's disease (Keren-Shaul et al., 2017; Krasemann et al., 2017), raising the question of their potential similarities, differences–and relationship. Apart from the use of specific antibodies or *in situ* hybridization probes, the field lacks genetic tools to specifically label and target microglia states. So far, only a $CD11c^{cre}$ line has been used to target ATM (Wlodarczyk et al., 2017), but was unsuccessful in depleting ATM in combination with Diphtheria Toxin strategies. In addition, a novel $Spp1^{tdTomato}$ mouse line has been generated and used to monitor SPP1 from perivascular macrophages (De Schepper et al., 2022), and could constitute an interesting tool for ATM-lineage studies. Based on their emerging molecular characterization, novel mouse lines or viral approaches will enable specific depletion or inactivation of microglial states to further assess their fates and functions. Moreover, in-depth characterization of transcriptomic, epigenomic, and metabolomic landscapes in microglia would enable to better understand their regulatory mechanisms, the transientness of these states and to which extent they can be induced by the microenvironment at different stages of life. Along these lines, the progress of spatial transcriptomics toward increased structural resolution should lead to a tremendous breakthrough to characterize microglial heterogeneity (Stogsdill et al., 2022), in particular at hotspots of accumulating microglia during development. Altogether, the field is moving onto a specific targeting of developmental microglial states which should shed new light on their regulatory mechanisms, their plasticity and functions in steady-state and disease conditions.

En route for specific depletion approaches

Microglial functions in brain development, homeostasis and diseases were historically assessed using *in vivo* depletion strategies summarized in **Table 1**. Though a lot of techniques have been developed, their diversity illustrates the difficulty to obtain a specific, efficient and long-lasting depletion of microglia while limiting its off-target effects.

Killing by numbers

The first strategies employed were aiming to directly trigger microglial apoptosis by administration of clodronate liposomes,

that are specifically phagocytosed by microglia and BAMs and induce cell death upon cytoplasmic release (Green et al., 2020). This approach is efficient in the early post-natal brain and in adults, but the inability of the clodronate liposomes to cross the blood brain barrier requires an intracerebral injection, inducing an injury and possible release of inflammatory cytokines (Han et al., 2019). Another approach uses the diphtheria-toxin (DT) based systems, either with direct expression of the DTA or with DT receptor, the latter needing administration of DT. The first studies were performed in *Cx3cr1*^{CreER}:*R26*^{iDTR} and *Iba1-tTA*:$^{DTAtetO/tetO}$ targeting both microglia and BAMs (Parkhurst et al., 2013; Miyamoto et al., 2016; Takeda et al., 2018). On the contrary, the use of the *Siglech*$^{dtr/+}$ mice led to specific and transient depletion of embryonic microglia, without affecting BAMs (Li et al., 2021). Thus, the constitutive or inducible DTR/DTA expression, combined with specific microglial lines provides a better temporal control as well as selective effect, though their efficiency remains variable.

CSF-1R inhibitors

The CSF-1 receptor (CSF-1R) is expressed by microglia, macrophages and their progenitors and its signaling is essential for their survival and proliferation. It thus became a preferential target in the quest for microglial depletion methods. Injections of an anti-CSF-1R antibody performed at E6.5 and E7.5 lead to a drastic depletion of myeloid progenitors, macrophages and microglia, while repopulation spans the first postnatal week (Squarzoni et al., 2014; Hoeffel and Ginhoux, 2015; Thion et al., 2019). On the other hand, embryonic targeting of CSF-1, one of the two CSF-1R ligands, through anti-CSF-1 antibody, leads to a drastic depletion of forebrain microglia (Easley-Neal et al., 2019), with possible off-target effects of the circulating antibodies. Pharmacological inhibitors of the CSF-1R injected or delivered non-invasively *via* food pellets have been broadly developed to deplete adult microglia, such as PLX3397 and PLX5622, the latter having a higher specificity and improved brain penetrance (Elmore et al., 2014; Green et al., 2020) while it efficiently depletes embryonic microglia, enabling a temporal control of the depletion during gestation (Rosin et al., 2018; Marsters et al., 2020). Nevertheless, as this treatment can affect lactation by depleting maternal macrophages essential for mammary gland development (O'Brien et al., 2012), it can impact pup survival following birth. For early postnatal depletion, direct subcutaneous injections of PLX3397 or PLX5622 during the first post-natal week allows for an efficient depletion of microglia (Li et al., 2020; Favuzzi et al., 2021; Gesuita et al., 2022). Although beyond the scope of this review, CSF-1R inhibitors are also used in other species including humans, bringing novel therapeutic approaches [reviewed in Han et al. (2022)]. Overall, targeting the CSF-1R pathway has proven to be efficient and convenient, but also affects peripheral macrophages and BAMs, preventing the identification of specific microglial functions.

Genetic models

Different genetic models, including constitutive knock-outs of fundamental transcription or survival factors, like *Pu.1*$^{-/-}$ (McKercher et al., 1996) and *Csf1r*$^{-/-}$ (Erblich et al., 2011), fail to develop microglia as well as most macrophages (Green et al., 2020). This results in many off-target effects and early death in *Pu.1*$^{-/-}$ and *Csf1r*$^{-/-}$. On the other hand, the *Csf1r*$^{fl/fl}$ allows for a more specific targeting of microglia, thanks to the microglia specific mouse lines now available and their possible temporal induction. This strategy has been used with *Sall1*^{CreER};*Csf1r*$^{fl/fl}$ (Buttgereit et al., 2016) and *Hexb*^{CreERT2};*Csf1r*$^{fl/fl}$ mice (Masuda et al., 2020), with a respective efficiency varying across brain regions from 70% to 90% and of 60%.

An additional important model is the *Csf1r*$^{\Delta FIRE/\Delta FIRE}$ mice, in which a *Csf1r* enhancer is deleted (Rojo et al., 2019; Munro et al., 2020). This leads to the absence of microglia from the brain parenchyma, and of resident macrophages of the skin, kidney, heart and peritoneum; while other macrophages and monocytes are unaffected. Importantly, these mice are healthy and fertile in a mixed B6CBAF1/C57BL/6J background, and do not display strong developmental defects described in the *Csf1r*$^{-/-}$. So far, they were used to investigate the role of resident microglia in Alzheimer disease mice (Kiani Shabestari et al., 2022) and they will provide a more specific and long-lasting model to explore microglial functions.

Finally, full inactivation of CSF-1R ligands, *Csf-1* (Chang et al., 1994; Kondo and Duncan, 2009) or *Il34* (Greter et al., 2012; Wang et al., 2012), expressed by the neural tissue, results in time- and region-dependent partial depletion of microglia albeit there are still some controversies amongst studies and major impact on peripheral macrophages (Green et al., 2020; **Table 1**). Nevertheless, under the pan neuronal driver *Nestin*^{cre} that restricts depletion to the nervous system, thus mainly affecting microglia, the *Nestin*^{cre};*Csf1*$^{fl/fl}$ and *Nestin*^{cre};*Il34*$^{fl/fl}$ are respectively deprived of microglia in the white matter and cerebellum or in the gray matter highlighting region-specific dependency (Kana et al., 2019; Badimon et al., 2020). On the other hand, macrophages are unaffected in the yolk sac, fetal liver and fetal limbs. Last, because the CSF-1R ligands are differentially expressed and required from microglia through development, these lines provide promising models to investigate local microglial functions.

Concluding remarks

Microglia now appear as key actors of brain development, interacting with most brain cells and regulating several crucial developmental processes. Nevertheless, these exciting advances were done in models affecting both microglia and BAMs. Thus, dissecting their respective contributions thanks to new specific tools will be key to the field. In addition, further understanding microglial diversity during development and the functions played by specific states should bring new light on their importance in neurodevelopmental pathologies and open new avenues for therapeutic intervention.

Author contributions

CB and MST wrote the review. Both authors contributed to the article and approved the submitted version.

Funding

The laboratories acknowledge support from the INSERM, CNRS, École Normale Supérieure, Collège de France and Fondation du Collège de France. CB was supported by an AMX doctoral fellowship and an ARC fellowship. MST is a CNRS investigator supported by the Foundation for Brain Research (FRC).

Acknowledgments

We are grateful to members of the Thion and Garel laboratories for stimulating discussions and comments on the manuscript.

Conflict of interest

The authors declare that the research was conducted in the absence of any commercial or financial relationships that could be construed as a potential conflict of interest.

Publisher's note

References

Andoh, M., and Koyama, R. (2021). Microglia regulate synaptic development and plasticity. *Dev. Neurobiol.* 81, 568–590. doi: 10.1002/dneu.22814

Badimon, A., Strasburger, H. J., Ayata, P., Chen, X., Nair, A., Ikegami, A., et al. (2020). Negative feedback control of neuronal activity by microglia. *Nature* 586, 417–423. doi: 10.1038/s41586-020-2777-8

Bennett, M. L., Bennett, F. C., Liddelow, S. A., Ajami, B., Zamanian, J. L., Fernhoff, N. B., et al. (2016). New tools for studying microglia in the mouse and human CNS. *Proc. Natl. Acad. Sci. U.S.A.* 113, E1738–E1746. doi: 10.1073/pnas.1525528113

Buttgereit, A., Lelios, I., Yu, X., Vrohlings, M., Krakoski, N. R., Gautier, E. L., et al. (2016). Sall1 is a transcriptional regulator defining microglia identity and function. *Nat. Immunol.* 17, 1397–1406. doi: 10.1038/ni.3585

Chang, Y., Albright, S., and Lee, F. (1994). Cytokines in the central nervous system: Expression of macrophage colony stimulating factor and its receptor during development. *J. Neuroimmunol.* 52, 9–17. doi: 10.1016/0165-5728(94)90156-2

Chappell-Maor, L., Kolesnikov, M., Kim, J. S., Shemer, A., Haimon, Z., Grozovski, J., et al. (2020). Comparative analysis of CreER transgenic mice for the study of brain macrophages: A case study. *Eur. J. Immunol.* 50, 353–362. doi: 10.1002/eji.201948342

Csaszar, E., Lenart, N., Cserep, C., Kornyei, Z., Fekete, R., Posfai, B., et al. (2022). Microglia modulate blood flow, neurovascular coupling, and hypoperfusion via purinergic actions. *J. Exp. Med.* 219:e20211071. doi: 10.1084/jem.20211071

Cserep, C., Posfai, B., Lenart, N., Fekete, R., Laszlo, Z. I., Lele, Z., et al. (2020). Microglia monitor and protect neuronal function through specialized somatic purinergic junctions. *Science* 367, 528–537. doi: 10.1126/science.aax6752

Cserep, C., Schwarcz, A. D., Posfai, B., Laszlo, Z. I., Kellermayer, A., Kornyei, Z., et al. (2022). Microglial control of neuronal development via somatic purinergic junctions. *Cell Rep.* 40:111369. doi: 10.1016/j.celrep.2022.111369

Cunningham, C. L., Martinez-Cerdeno, V., and Noctor, S. C. (2013). Microglia regulate the number of neural precursor cells in the developing cerebral cortex. *J. Neurosci.* 33, 4216–4233. doi: 10.1523/JNEUROSCI.3441-12.2013

Davalos, D., Grutzendler, J., Yang, G., Kim, J. V., Zuo, Y., Jung, S., et al. (2005). ATP mediates rapid microglial response to local brain injury in vivo. *Nat. Neurosci.* 8, 752–758. doi: 10.1038/nn1472

De Schepper, S., Ge, J. G., Crowley, G., Ferreira, L. S. S., Garceau, D., Toomey, C. E., et al. (2022). Perivascular SPP1 mediates microglial engulfment of synapses in Alzheimer's disease models. *bioRxiv* [Preprint]. doi: 10.1101/2022.04.04.486547

Deczkowska, A., Keren-Shaul, H., Weiner, A., Colonna, M., Schwartz, M., and Amit, I. (2018). Disease-associated microglia: A universal immune sensor of neurodegeneration. *Cell* 173, 1073–1081. doi: 10.1016/j.cell.2018.05.003

Easley-Neal, C., Foreman, O., Sharma, N., Zarrin, A. A., and Weimer, R. M. (2019). CSF1R ligands IL-34 and CSF1 are differentially required for microglia development and maintenance in white and gray matter brain regions. *Front. Immunol.* 10:2199. doi: 10.3389/fimmu.2019.02199

Elmore, M. R., Najafi, A. R., Koike, M. A., Dagher, N. N., Spangenberg, E. E., Rice, R. A., et al. (2014). Colony-stimulating factor 1 receptor signaling is necessary for microglia viability, unmasking a microglia progenitor cell in the adult brain. *Neuron* 82, 380–397. doi: 10.1016/j.neuron.2014.02.040

Eme-Scolan, E., and Dando, S. J. (2020). Tools and approaches for studying microglia in vivo. *Front. Immunol.* 11:583647. doi: 10.3389/fimmu.2020.583647

Erblich, B., Zhu, L., Etgen, A. M., Dobrenis, K., and Pollard, J. W. (2011). Absence of colony stimulation factor-1 receptor results in loss of microglia, disrupted brain development and olfactory deficits. *PLoS One* 6:e26317. doi: 10.1371/journal.pone.0026317

Favuzzi, E., Huang, S., Saldi, G. A., Binan, L., Ibrahim, L. A., Fernandez-Otero, M., et al. (2021). GABA-receptive microglia selectively sculpt developing inhibitory circuits. *Cell* 184, 4048–4063.e32. doi: 10.1016/j.cell.2021.06.018

Ferrero, G., Mahony, C. B., Dupuis, E., Yvernogeau, L., Di Ruggiero, E., Miserocchi, M., et al. (2018). Embryonic microglia derive from primitive macrophages and are replaced by cmyb-dependent definitive microglia in zebrafish. *Cell Rep.* 24, 130–141. doi: 10.1016/j.celrep.2018.05.066

Gautier, E. L., Shay, T., Miller, J., Greter, M., Jakubzick, C., Ivanov, S., et al. (2012). Gene-expression profiles and transcriptional regulatory pathways that underlie the identity and diversity of mouse tissue macrophages. *Nat. Immunol.* 13, 1118–1128. doi: 10.1038/ni.2419

Gesuita, L., Cavaccini, A., Argunsah, A. O., Favuzzi, E., Ibrahim, L. A., Stachniak, T. J., et al. (2022). Microglia contribute to the postnatal development of cortical somatostatin-positive inhibitory cells and to whisker-evoked cortical activity. *Cell Rep.* 40:111209. doi: 10.1016/j.celrep.2022.111209

Ginhoux, F., Greter, M., Leboeuf, M., Nandi, S., See, P., Gokhan, S., et al. (2010). Fate mapping analysis reveals that adult microglia derive from primitive macrophages. *Science* 330, 841–845. doi: 10.1126/science.1194637

Goldmann, T., Wieghofer, P., Jordao, M. J., Prutek, F., Hagemeyer, N., Frenzel, K., et al. (2016). Origin, fate and dynamics of macrophages at central nervous system interfaces. *Nat. Immunol.* 17, 797–805. doi: 10.1038/ni.3423

Green, K. N., Crapser, J. D., and Hohsfield, L. A. (2020). To kill a microglia: A case for CSF1R Inhibitors. *Trends Immunol.* 41, 771–784. doi: 10.1016/j.it.2020.07.001

Greter, M., Lelios, I., Pelczar, P., Hoeffel, G., Price, J., Leboeuf, M., et al. (2012). Stroma-derived interleukin-34 controls the development and maintenance of langerhans cells and the maintenance of microglia. *Immunity* 37, 1050–1060. doi: 10.1016/j.immuni.2012.11.001

Guneykaya, D., Ivanov, A., Hernandez, D. P., Haage, V., Wojtas, B., Meyer, N., et al. (2018). Transcriptional and translational differences of microglia from male and female brains. *Cell Rep.* 24, 2773–2783.e6. doi: 10.1016/j.celrep.2018.08.001

Hagemeyer, N., Hanft, K. M., Akriditou, M. A., Unger, N., Park, E. S., Stanley, E. R., et al. (2017). Microglia contribute to normal myelinogenesis and to oligodendrocyte progenitor maintenance during adulthood. *Acta Neuropathol.* 134, 441–458. doi: 10.1007/s00401-017-1747-1

Hammond, T. R., Dufort, C., Dissing-Olesen, L., Giera, S., Young, A., Wysoker, A., et al. (2019). Single-Cell RNA sequencing of microglia throughout the mouse lifespan and in the injured brain reveals complex cell-state changes. *Immunity* 50, 253–271.e6. doi: 10.1016/j.immuni.2018.11.004

Hammond, T. R., Robinton, D., and Stevens, B. (2018). Microglia and the brain: Complementary partners in development and disease. *Annu. Rev. Cell Dev. Biol.* 34, 523–544. doi: 10.1146/annurev-cellbio-100616-060509

Han, J., Chitu, V., Stanley, E. R., Wszolek, Z. K., Karrenbauer, V. D., and Harris, R. A. (2022). Inhibition of colony stimulating factor-1 receptor (CSF-1R) as a potential therapeutic strategy for neurodegenerative diseases: Opportunities and challenges. *Cell Mol. Life Sci.* 79, 219. doi: 10.1007/s00018-022-04225-1

Han, X., Li, Q., Lan, X., El-Mufti, L., Ren, H., and Wang, J. (2019). Microglial depletion with clodronate liposomes increases proinflammatory cytokine levels, induces astrocyte activation, and damages blood vessel integrity. *Mol. Neurobiol.* 56, 6184–6196. doi: 10.1007/s12035-019-1502-9

Hanamsagar, R., Alter, M. D., Block, C. S., Sullivan, H., Bolton, J. L., and Bilbo, S. D. (2017). Generation of a microglial developmental index in mice and in humans reveals a sex difference in maturation and immune reactivity. *Glia* 65, 1504–1520. doi: 10.1002/glia.23176

Hattori, Y., Kato, D., Murayama, F., Koike, S., Naito, Y., Kawaguchi, A., et al. (2022). Border-associated macrophages transventricularly infiltrate the early embryonic cerebral wall to differentiate into microglia. *bioRxiv* [Preprint]. doi: 10.1101/2022.07.27.501563

Hattori, Y., Naito, Y., Tsugawa, Y., Nonaka, S., Wake, H., Nagasawa, T., et al. (2020). Transient microglial absence assists postmigratory cortical neurons in proper differentiation. *Nat. Commun.* 11:1631. doi: 10.1038/s41467-020-15409-3

Hickman, S. E., Kingery, N. D., Ohsumi, T. K., Borowsky, M. L., Wang, L. C., Means, T. K., et al. (2013). The microglial sensome revealed by direct RNA sequencing. *Nat. Neurosci.* 16, 1896–1905. doi: 10.1038/nn.3554

Hoeffel, G., and Ginhoux, F. (2015). Ontogeny of tissue-resident macrophages. *Front Immunol.* 6:486. doi: 10.3389/fimmu.2015.00486

Hoeffel, G., and Ginhoux, F. (2018). Fetal monocytes and the origins of tissue-resident macrophages. *Cell Immunol.* 330, 5–15. doi: 10.1016/j.cellimm.2018.01.001

Huang, Y., Xu, Z., Xiong, S., Sun, F., Qin, G., Hu, G., et al. (2018). Repopulated microglia are solely derived from the proliferation of residual microglia after acute depletion. *Nat Neurosci.* 21, 530–540. doi: 10.1038/s41593-018-0090-8

Jung, S., Aliberti, J., Graemmel, P., Sunshine, M. J., Kreutzberg, G. W., Sher, A., et al. (2000). Analysis of fractalkine receptor CX(3)CR1 function by targeted deletion and green fluorescent protein reporter gene insertion. *Mol. Cell Biol.* 20, 4106–4114. doi: 10.1128/MCB.20.11.4106-4114.2000

Kaiser, T., and Feng, G. (2019). Tmem119-EGFP and tmem119-CreERT2 transgenic mice for labeling and manipulating microglia. *eNeuro* 6, ENEURO.0448–18.2019. doi: 10.1523/ENEURO.0448-18.2019

Kana, V., Desland, F. A., Casanova-Acebes, M., Ayata, P., Badimon, A., Nabel, E., et al. (2019). CSF-1 controls cerebellar microglia and is required for motor function and social interaction. *J. Exp. Med.* 216, 2265–2281. doi: 10.1084/jem.20182037

Keren-Shaul, H., Spinrad, A., Weiner, A., Matcovitch-Natan, O., Dvir-Szternfeld, R., Ulland, T. K., et al. (2017). A unique microglia type associated with restricting development of Alzheimer's disease. *Cell* 169, 1276–1290.e17. doi: 10.1016/j.cell.2017.05.018

Kiani Shabestari, S., Morabito, S., Danhash, E. P., McQuade, A., Sanchez, J. R., Miyoshi, E., et al. (2022). Absence of microglia promotes diverse pathologies and early lethality in Alzheimer's disease mice. *Cell Rep.* 39:110961. doi: 10.1016/j.celrep.2022.110961

Kierdorf, K., Masuda, T., Jordao, M. J. C., and Prinz, M. (2019). Macrophages at CNS interfaces: Ontogeny and function in health and disease. *Nat. Rev. Neurosci.* 20, 547–562. doi: 10.1038/s41583-019-0201-x

Kim, J. S., Kolesnikov, M., Peled-Hajaj, S., Scheyltjens, I., Xia, Y., Trzebanski, S., et al. (2021). A binary Cre transgenic approach dissects microglia and CNS border-associated macrophages. *Immunity* 54, 176–190.e7. doi: 10.1016/j.immuni.2020.11.007

Kondo, Y., and Duncan, I. D. (2009). Selective reduction in microglia density and function in the white matter of colony-stimulating factor-1-deficient mice. *J. Neurosci. Res.* 87, 2686–2695. doi: 10.1002/jnr.22096

Konishi, H., Kobayashi, M., Kunisawa, T., Imai, K., Sayo, A., Malissen, B., et al. (2017). Siglec-H is a microglia-specific marker that discriminates microglia from CNS-associated macrophages and CNS-infiltrating monocytes. *Glia* 65, 1927–1943. doi: 10.1002/glia.23204

Kracht, L., Borggrewe, M., Eskandar, S., Brouwer, N., Chuva de Sousa Lopes, S. M., Laman, J. D., et al. (2020). Human fetal microglia acquire homeostatic immune-sensing properties early in development. *Science* 369, 530–537. doi: 10.1126/science.aba5906

Krasemann, S., Madore, C., Cialic, R., Baufeld, C., Calcagno, N., El Fatimy, R., et al. (2017). The TREM2-APOE pathway drives the transcriptional phenotype of dysfunctional microglia in neurodegenerative diseases. *Immunity* 47, 566–581.e9. doi: 10.1016/j.immuni.2017.08.008

Lee, E., Eo, J. C., Lee, C., and Yu, J. W. (2021). Distinct features of brain-resident macrophages: Microglia and non-parenchymal brain macrophages. *Mol. Cells* 44, 281–291. doi: 10.14348/molcells.2021.0060

Lenz, K. M., Nugent, B. M., Haliyur, R., and McCarthy, M. M. (2013). Microglia are essential to masculinization of brain and behavior. *J. Neurosci.* 33, 2761–2772. doi: 10.1523/JNEUROSCI.1268-12.2013

Li, C., Konishi, H., Nishiwaki, K., Sato, K., Miyata, T., and Kiyama, H. (2021). A mouse model of microglia-specific ablation in the embryonic central nervous system. *Neurosci. Res.* 173, 54–61. doi: 10.1016/j.neures.2021.06.002

Li, Q., and Barres, B. A. (2018). Microglia and macrophages in brain homeostasis and disease. *Nat. Rev. Immunol.* 18, 225–242. doi: 10.1038/nri.2017.125

Li, Q., Cheng, Z., Zhou, L., Darmanis, S., Neff, N. F., Okamoto, J., et al. (2019). Developmental heterogeneity of microglia and brain myeloid cells revealed by deep single-cell RNA sequencing. *Neuron* 101, 207–223.e10. doi: 10.1016/j.neuron.2018.12.006

Li, Y., He, X., Kawaguchi, R., Zhang, Y., Wang, Q., Monavarfeshani, A., et al. (2020). Microglia-organized scar-free spinal cord repair in neonatal mice. *Nature* 587, 613–618. doi: 10.1038/s41586-020-2795-6

Lin, R., Zhou, Y., Yan, T., Wang, R., Li, H., Wu, Z., et al. (2022). Directed evolution of adeno-associated virus for efficient gene delivery to microglia. *Nat. Methods* 19, 976–985. doi: 10.1038/s41592-022-01547-7

Lukens, J. R., and Eyo, U. B. (2022). Microglia and neurodevelopmental disorders. *Annu. Rev. Neurosci.* 45, 425–445. doi: 10.1146/annurev-neuro-110920-023056

MacDonald, K. P., Palmer, J. S., Cronau, S., Seppanen, E., Olver, S., Raffelt, N. C., et al. (2010). An antibody against the colony-stimulating factor 1 receptor depletes the resident subset of monocytes and tissue- and tumor-associated macrophages but does not inhibit inflammation. *Blood* 116, 3955–3963. doi: 10.1182/blood-2010-02-266296

Maes, M. E., Colombo, G., Schulz, R., and Siegert, S. (2019). Targeting microglia with lentivirus and AAV: Recent advances and remaining challenges. *Neurosci. Lett.* 707:134310. doi: 10.1016/j.neulet.2019.134310

Marschallinger, J., Iram, T., Zardeneta, M., Lee, S. E., Lehallier, B., Haney, M. S., et al. (2020). Lipid-droplet-accumulating microglia represent a dysfunctional and proinflammatory state in the aging brain. *Nat. Neurosci.* 23, 194–208. doi: 10.1038/s41593-019-0566-1

Marsh, S. E., Walker, A. J., Kamath, T., Dissing-Olesen, L., Hammond, T. R., de Soysa, T. Y., et al. (2022). Dissection of artifactual and confounding glial signatures by single-cell sequencing of mouse and human brain. *Nat. Neurosci.* 25, 306–316. doi: 10.1038/s41593-022-01022-8

Marsters, C. M., Nesan, D., Far, R., Klenin, N., Pittman, Q. J., and Kurrasch, D. M. (2020). Embryonic microglia influence developing hypothalamic glial populations. *J. Neuroinflammation* 17:146. doi: 10.1186/s12974-020-01811-7

Masuda, T., Amann, L., Monaco, G., Sankowski, R., Staszewski, O., Krueger, M., et al. (2022). Specification of CNS macrophage subsets occurs postnatally in defined niches. *Nature* 604, 740–748. doi: 10.1038/s41586-022-04596-2

Masuda, T., Amann, L., Sankowski, R., Staszewski, O., Lenz, M., d'Errico, P., et al. (2020). Novel Hexb-based tools for studying microglia in the CNS. *Nat. Immunol.* 21, 802–815. doi: 10.1038/s41590-020-0707-4

Masuda, T., Sankowski, R., Staszewski, O., Bottcher, C., Amann, L., Sagar, et al. (2019). Spatial and temporal heterogeneity of mouse and human microglia at single-cell resolution. *Nature* 566, 388–392. doi: 10.1038/s41586-019-0924-x

Matcovitch-Natan, O., Winter, D. R., Giladi, A., Vargas Aguilar, S., Spinrad, A., Sarrazin, S., et al. (2016). Microglia development follows a stepwise program to regulate brain homeostasis. *Science* 353:aad8670. doi: 10.1126/science.aad8670

McKercher, S. R., Torbett, B. E., Anderson, K. L., Henkel, G. W., Vestal, D. J., Baribault, H., et al. (1996). Targeted disruption of the PU.1 gene results in multiple hematopoietic abnormalities. *EMBO J.* 15, 5647–5658.

McKinsey, G. L., Lizama, C. O., Keown-Lang, A. E., Niu, A., Santander, N., Larpthaveesarp, A., et al. (2020). A new genetic strategy for targeting microglia in development and disease. *Elife* 9:e54590. doi: 10.7554/eLife.54590

Menassa, D. A., Muntslag, T. A. O., Martin-Estebane, M., Barry-Carroll, L., Chapman, M. A., Adorjan, I., et al. (2022). The spatiotemporal dynamics of microglia across the human lifespan. *Dev. Cell* 57, 2127–2139.e6. doi: 10.1016/j.devcel.2022.07.015

Michaelson, M. D., Bieri, P. L., Mehler, M. F., Xu, H., Arezzo, J. C., Pollard, J. W., et al. (1996). CSF-1 deficiency in mice results in abnormal brain development. *Development* 122, 2661–2672. doi: 10.1242/dev.122.9.2661

Mildenberger, W., Stifter, S. A., and Greter, M. (2022). Diversity and function of brain-associated macrophages. *Curr. Opin. Immunol.* 76:102181. doi: 10.1016/j.coi.2022.102181

Mills, J., Ladner, L., Soliman, E., Leonard, J., Morton, P. D., and Theus, M. H. (2022). Cross-talk and subset control of microglia and associated myeloid cells in neurological disorders. *Cells* 11:3364. doi: 10.3390/cells11213364

Miyamoto, A., Wake, H., Ishikawa, A. W., Eto, K., Shibata, K., Murakoshi, H., et al. (2016). Microglia contact induces synapse formation in developing somatosensory cortex. *Nat. Commun.* 7:12540. doi: 10.1038/ncomms12540

Monier, A., Adle-Biassette, H., Delezoide, A. L., Evrard, P., Gressens, P., and Verney, C. (2007). Entry and distribution of microglial cells in human embryonic and fetal cerebral cortex. *J. Neuropathol. Exp. Neurol.* 66, 372–382. doi: 10.1097/nen.0b013e3180517b46

Mosser, C. A., Baptista, S., Arnoux, I., and Audinat, E. (2017). Microglia in CNS development: Shaping the brain for the future. *Prog. Neurobiol.* 14, 1–20. doi: 10.1016/j.pneurobio.2017.01.002

Mrdjen, D., Pavlovic, A., Hartmann, F. J., Schreiner, B., Utz, S. G., Leung, B. P., et al. (2018). High-dimensional single-cell mapping of central nervous system immune

cells reveals distinct myeloid subsets in health, aging, and disease. *Immunity* 48:599. doi: 10.1016/j.immuni.2018.02.014

Munro, D. A. D., Bradford, B. M., Mariani, S. A., Hampton, D. W., Vink, C. S., Chandran, S., et al. (2020). CNS macrophages differentially rely on an intronic Csf1r enhancer for their development. *Development* 147:dev194449. doi: 10.1242/dev.194449

Munz, M., Bharioke, A., Kosche, G., Moreno-Juan, V., Brignall, A., Graff-Meyer, A., et al. (2022). Embryonic cortical layer 5 pyramidal neurons form an active, transient circuit motif perturbed by autism-associated mutations. *bioRxiv* [Preprint]. doi: 10.1101/2022.08.31.506080

Nemes-Baran, A. D., White, D. R., and DeSilva, T. M. (2020). Fractalkine-dependent microglial pruning of viable oligodendrocyte progenitor cells regulates myelination. *Cell Rep.* 32:108047. doi: 10.1016/j.celrep.2020.108047

Nimmerjahn, A., Kirchhoff, F., and Helmchen, F. (2005). Resting microglial cells are highly dynamic surveillants of brain parenchyma in vivo. *Science* 308, 1314–1318. doi: 10.1126/science.1110647

O'Brien, J., Martinson, H., Durand-Rougely, C., and Schedin, P. (2012). Macrophages are crucial for epithelial cell death and adipocyte repopulation during mammary gland involution. *Development* 139, 269–275. doi: 10.1242/dev.071696

Paolicelli, R. C., Sierra, A., Stevens, B., Tremblay, M. E., Aguzzi, A., Ajami, B., et al. (2022). Microglia states and nomenclature: A field at its crossroads. *Neuron* 110, 3458–3483. doi: 10.1016/j.neuron.2022.10.020

Parkhurst, C. N., Yang, G., Ninan, I., Savas, J. N., Yates, J. R. III, Lafaille, J. J., et al. (2013). Microglia promote learning-dependent synapse formation through brain-derived neurotrophic factor. *Cell* 155, 1596–1609. doi: 10.1016/j.cell.2013.11.030

Pont-Lezica, L., Beumer, W., Colasse, S., Drexhage, H., Versnel, M., and Bessis, A. (2014). Microglia shape corpus callosum axon tract fasciculation: Functional impact of prenatal inflammation. *Eur. J. Neurosci.* 39, 1551–1557. doi: 10.1111/ejn.12508

Prinz, M., Jung, S., and Priller, J. (2019). Microglia biology: One century of evolving concepts. *Cell* 179, 292–311. doi: 10.1016/j.cell.2019.08.053

Ratz, M., von Berlin, L., Larsson, L., Martin, M., Westholm, J. O., La Manno, G., et al. (2022). Clonal relations in the mouse brain revealed by single-cell and spatial transcriptomics. *Nat. Neurosci.* 25, 285–294. doi: 10.1038/s41593-022-01011-x

Rebuli, M. E., Gibson, P., Rhodes, C. L., Cushing, B. S., and Patisaul, H. B. (2016). Sex differences in microglial colonization and vulnerabilities to endocrine disruption in the social brain. *Gen. Comp. Endocrinol.* 238, 39–46. doi: 10.1016/j.ygcen.2016.04.018

Rojo, R., Raper, A., Ozdemir, D. D., Lefevre, L., Grabert, K., Wollscheid-Lengeling, E., et al. (2019). Deletion of a Csf1r enhancer selectively impacts CSF1R expression and development of tissue macrophage populations. *Nat. Commun.* 10:3215. doi: 10.1038/s41467-019-11053-8

Ronzano, R., Roux, T., Thetiot, M., Aigrot, M. S., Richard, L., Lejeune, F. X., et al. (2021). Microglia-neuron interaction at nodes of Ranvier depends on neuronal activity through potassium release and contributes to remyelination. *Nat. Commun.* 12:5219. doi: 10.1038/s41467-021-25486-7

Rosin, J. M., Marsters, C. M., Malik, F., Far, R., Adnani, L., Schuurmans, C., et al. (2021). Embryonic microglia interact with hypothalamic radial glia during development and upregulate the TAM receptors MERTK and AXL following an insult. *Cell Rep.* 34:108587. doi: 10.1016/j.celrep.2020.108587

Rosin, J. M., Vora, S. R., and Kurrasch, D. M. (2018). Depletion of embryonic microglia using the CSF1R inhibitor PLX5622 has adverse sex-specific effects on mice, including accelerated weight gain, hyperactivity and anxiolytic-like behaviour. *Brain Behav. Immun.* 73, 682–697. doi: 10.1016/j.bbi.2018.07.023

Ruan, C., Sun, L., Kroshilina, A., Beckers, L., De Jager, P., Bradshaw, E. M., et al. (2020). A novel Tmem119-tdTomato reporter mouse model for studying microglia in the central nervous system. *Brain Behav. Immun.* 83, 180–191. doi: 10.1016/j.bbi.2019.10.009

Safaiyan, S., Besson-Girard, S., Kaya, T., Cantuti-Castelvetri, L., Liu, L., Ji, H., et al. (2021). White matter aging drives microglial diversity. *Neuron* 109, 1100–1117.e10. doi: 10.1016/j.neuron.2021.01.027

Sahasrabuddhe, V., and Ghosh, H. S. (2022). Cx3Cr1-Cre induction leads to microglial activation and IFN-1 signaling caused by DNA damage in early postnatal brain. *Cell Rep.* 38:110252. doi: 10.1016/j.celrep.2021.110252

Sankowski, R., Bottcher, C., Masuda, T., Geirsdottir, L., Sagar, Sindram, E., et al. (2019). Mapping microglia states in the human brain through the integration of high-dimensional techniques. *Nat. Neurosci.* 22, 2098–2110. doi: 10.1038/s41593-019-0532-y

Sankowski, R., Monaco, G., and Prinz, M. (2022). Evaluating microglial phenotypes using single-cell technologies. *Trends Neurosci.* 45, 133–144. doi: 10.1016/j.tins.2021.11.001

Satoh, J., Kino, Y., Asahina, N., Takitani, M., Miyoshi, J., Ishida, T., et al. (2016). TMEM119 marks a subset of microglia in the human brain. *Neuropathology* 36, 39–49. doi: 10.1111/neup.12235

Schwarz, J. M., Sholar, P. W., and Bilbo, S. D. (2012). Sex differences in microglial colonization of the developing rat brain. *J. Neurochem.* 120, 948–963. doi: 10.1111/j.1471-4159.2011.07630.x

Sherafat, A., Pfeiffer, F., Reiss, A. M., Wood, W. M., and Nishiyama, A. (2021). Microglial neuropilin-1 promotes oligodendrocyte expansion during development and remyelination by trans-activating platelet-derived growth factor receptor. *Nat. Commun.* 12:2265. doi: 10.1038/s41467-021-22532-2

Sierra, A., Encinas, J. M., Deudero, J. J., Chancey, J. H., Enikolopov, G., Overstreet-Wadiche, L. S., et al. (2010). Microglia shape adult hippocampal neurogenesis through apoptosis-coupled phagocytosis. *Cell Stem Cell* 7, 483–495. doi: 10.1016/j.stem.2010.08.014

Silvin, A., Uderhardt, S., Piot, C., Da Mesquita, S., Yang, K., Geirsdottir, L., et al. (2022). Dual ontogeny of disease-associated microglia and disease inflammatory macrophages in aging and neurodegeneration. *Immunity* 55, 1448–1465.e6. doi: 10.1016/j.immuni.2022.07.004

Squarzoni, P., Oller, G., Hoeffel, G., Pont-Lezica, L., Rostaing, P., Low, D., et al. (2014). Microglia modulate wiring of the embryonic forebrain. *Cell Rep.* 8, 1271–1279. doi: 10.1016/j.celrep.2014.07.042

Stogsdill, J. A., Kim, K., Binan, L., Farhi, S. L., Levin, J. Z., and Arlotta, P. (2022). Pyramidal neuron subtype diversity governs microglia states in the neocortex. *Nature* 608, 750–756. doi: 10.1038/s41586-022-05056-7

Stremmel, C., Schuchert, R., Wagner, F., Thaler, R., Weinberger, T., Pick, R., et al. (2018). Yolk sac macrophage progenitors traffic to the embryo during defined stages of development. *Nat. Commun.* 9:75. doi: 10.1038/s41467-017-02492-2

Swinnen, N., Smolders, S., Avila, A., Notelaers, K., Paesen, R., Ameloot, M., et al. (2013). Complex invasion pattern of the cerebral cortex bymicroglial cells during development of the mouse embryo. *Glia* 61, 150–163. doi: 10.1002/glia.22421

Takeda, A., Shinozaki, Y., Kashiwagi, K., Ohno, N., Eto, K., Wake, H., et al. (2018). Microglia mediate non-cell-autonomous cell death of retinal ganglion cells. *Glia* 66, 2366–2384. doi: 10.1002/glia.23475

Tay, T. L., Mai, D., Dautzenberg, J., Fernandez-Klett, F., Lin, G., Sagar, et al. (2017). A new fate mapping system reveals context-dependent random or clonal expansion of microglia. *Nat. Neurosci.* 20, 793–803. doi: 10.1038/nn.4547

Thion, M. S., Ginhoux, F., and Garel, S. (2018a). Microglia and early brain development: An intimate journey. *Science* 362, 185–189. doi: 10.1126/science.aat0474

Thion, M. S., Low, D., Silvin, A., Chen, J., Grisel, P., Schulte-Schrepping, J., et al. (2018b). Microbiome influences prenatal and adult microglia in a sex-specific manner. *Cell* 172, 500–516.e16. doi: 10.1016/j.cell.2017.11.042

Thion, M. S., Mosser, C. A., Ferezou, I., Grisel, P., Baptista, S., Low, D., et al. (2019). Biphasic impact of prenatal inflammation and macrophage depletion on the wiring of neocortical inhibitory circuits. *Cell Rep.* 28, 1119–1126.e14. doi: 10.1016/j.celrep.2019.06.086

Utz, S. G., See, P., Mildenberger, W., Thion, M. S., Silvin, A., Lutz, M., et al. (2020). Early fate defines microglia and non-parenchymal brain macrophage development. *Cell* 181, 557–573.e18. doi: 10.1016/j.cell.2020.03.021

Van Hove, H., Martens, L., Scheyltjens, I., De Vlaminck, K., Pombo Antunes, A. R., De Prijck, S., et al. (2019). A single-cell atlas of mouse brain macrophages reveals unique transcriptional identities shaped by ontogeny and tissue environment. *Nat. Neurosci.* 22, 1021–1035. doi: 10.1038/s41593-019-0393-4

VanRyzin, J. W., Marquardt, A. E., Argue, K. J., Vecchiarelli, H. A., Ashton, S. E., Arambula, S. E., et al. (2019). Microglial phagocytosis of newborn cells is induced by endocannabinoids and sculpts sex differences in juvenile rat social play. *Neuron* 102, 435–449.e6. doi: 10.1016/j.neuron.2019.02.006

Verney, C., Monier, A., Fallet-Bianco, C., and Gressens, P. (2010). Early microglial colonization of the human forebrain and possible involvement in periventricular white-matter injury of preterm infants. *J. Anat.* 217, 436–448. doi: 10.1111/j.1469-7580.2010.01245.x

Villa, A., Gelosa, P., Castiglioni, L., Cimino, M., Rizzi, N., Pepe, G., et al. (2018). Sex-specific features of microglia from adult mice. *Cell Rep.* 23, 3501–3511. doi: 10.1016/j.celrep.2018.05.048

Wake, H., Moorhouse, A. J., Jinno, S., Kohsaka, S., and Nabekura, J. (2009). Resting microglia directly monitor the functional state of synapses in vivo and determine the fate of ischemic terminals. *J. Neurosci.* 29, 3974–3980. doi: 10.1523/JNEUROSCI.4363-08.2009

Wang, Y., Szretter, K. J., Vermi, W., Gilfillan, S., Rossini, C., Cella, M., et al. (2012). IL-34 is a tissue-restricted ligand of CSF1R required for the development of Langerhans cells and microglia. *Nat. Immunol.* 13, 753–760. doi: 10.1038/ni.2360

Wlodarczyk, A., Holtman, I. R., Krueger, M., Yogev, N., Bruttger, J., Khorooshi, R., et al. (2017). A novel microglial subset plays a key role in myelinogenesis in developing brain. *EMBO J.* 36, 3292–3308. doi: 10.15252/embj.201696056

Xu, J., Zhu, L., He, S., Wu, Y., Jin, W., Yu, T., et al. (2015). Temporal-spatial resolution fate mapping reveals distinct origins for embryonic and adult microglia in zebrafish. *Dev. Cell* 34, 632–641. doi: 10.1016/j.devcel.2015.08.018

Yona, S., Kim, K. W., Wolf, Y., Mildner, A., Varol, D., Breker, M., et al. (2013). Fate mapping reveals origins and dynamics of monocytes and tissue macrophages under homeostasis. *Immunity* 38, 79–91. doi: 10.1016/j.immuni.2012.12.001

Yu, D., Li, T., Delpech, J. C., Zhu, B., Kishore, P., Koshi, T., et al. (2022). Microglial GPR56 is the molecular target of maternal immune activation-induced parvalbumin-positive interneuron deficits. *Sci. Adv.* 8:eabm2545. doi: 10.1126/sciadv.abm2545

Microglia in the somatosensory cortex at P7.

DISCUSSION & PERSPECTIVES

1. Microglial entry, distribution and proliferation in the developing brain

Microglia, generated in the embryonic yolk-sac, migrate through the embryo and settle in the brain as early as E9 in mice or GW5 in humans (Alliot, Godin and Pessac, 1999; Ginhoux *et al.*, 2010; Verney *et al.*, 2010; Menassa and Gomez-Nicola, 2018; Menassa *et al.*, 2022). Their early entry is important to provide immune defense to the developing brain, not yet protected by the BBB. It also positions microglia as the main glial population of the brain until the generation of astrocytes and oligodendrocytes, coherent with their diverse roles in shaping neural circuits. Nevertheless, their exact developmental trajectory and routes of entry are less clear. Regarding their entry, microglia have been suggested to cross the pial surface and ventricular walls, because of their close proximity to these structures early on (Verney *et al.*, 2010), and could alternatively extravasate from blood vessels (Navascués *et al.*, 2000; Rigato *et al.*, 2011). Novel groundbreaking *in utero* imaging techniques recently developed (Hattori, Kato, *et al.*, 2022) highlighted the entry in the cortex of cells coming from the ventricle, and should keep on bringing new light on this process. Next, most microglia are believed to travel directly from the yolk-sac to the brain (Ginhoux *et al.*, 2010), but some, including *Hoxb8*-expressing microglia, have been suggested to transit through the fetal liver and enter in the brain by E12.5 (De *et al.*, 2018; Van Deren *et al.*, 2022). In addition, while two populations, CD206+ and CD206-, can be distinguished early on in the embryonic yolk-sac (Utz *et al.*, 2020) and were originally thought to give rise respectively to BAMs and microglia, it has recently been suggested by fate-mapping in $Mrc1^{creER};R26^{tdT/tdT}$ mice that at least some microglia could descend from CD206+ progenitors (Masuda *et al.*, 2022). This is consistent with another study showing CD206+ BAMs-like cells coming from the floor plate, that migrate along the ventricular wall and finally enter and settle in the neocortex, where they acquire microglial features (losing CD206 expression and turning on P2RY12 expression)(Hattori, Kato, *et al.*, 2022). While BAMs and microglia appear distinguishable as early as the embryonic yolk-sac, could some cells committed to a BAM fate switch later on to become microglia? New fate-mapping tools should help understand microglial trajectories and routes of entry. Whether these different routes/developmental trajectories confer specific features to microglia, in link with their developmental heterogeneity, and how they could respectively contribute to the mature microglial population is to date not well understood.

1.1. Microglial proliferation: embryonic phase

During my PhD, I focused on microglial colonization following their entry in the brain: their expansion and stereotyped distribution, from E12.5 onwards. Though the timing of closure of the BBB in the forebrain is not extensively described, it is believed that by E14, after BBB closure, very few circulating cells should be able to enter the parenchyma (Mildner *et al.*, 2007; Ginhoux *et al.*, 2010; Hoeffel and Ginhoux, 2015). This suggests that proliferation is a major process in order for the pioneer microglial cells already in the brain to give rise to the entire population. Their great proliferative capacity has been described in several studies: observed both in the rodent and human brain (Alliot, Godin and Pessac, 1999; Dalmau *et al.*, 2003; Swinnen *et al.*, 2013; Nikodemova *et al.*, 2015; Menassa *et al.*, 2022; Barry-Carroll *et al.*, 2023) or in transcriptomic studies (Matcovitch-Natan *et al.*, 2016; Hammond *et al.*, 2019; Li *et al.*, 2019; La Manno *et al.*, 2021), it is highlighted by the large numbers of clonally-related microglia (Ratz *et al.*, 2022; Barry-Carroll *et al.*, 2023). Essential during development, this proliferative capacity can emerge again in mature microglia throughout the lifespan in case of injury or disease: they are able of clonal expansion (Füger *et al.*, 2017; Tay *et al.*, 2017) as well as exceptional repopulation from very few remaining microglia (Elmore *et al.*, 2014; Zhan *et al.*, 2019; Hohsfield *et al.*, 2021). Nevertheless, a limited number of studies investigated this process in detail during development.

Here, we found that microglial proliferation follows two waves, one very global early on and conserved amongst regions; and a second postnatal burst showing more regional variability. The first wave, with a very high proportion of proliferative microglia at E12.5 (around 60%) that decreases drastically by E16.5, is coherent with what has previously been described in the neocortex (Swinnen *et al.*, 2013), and spans all regions studied (cortex, striatum and POA). Looking at the whole forebrain, Barry-Carroll and colleagues showed that microglial average proliferation was much lower throughout embryonic development (below 5% of Ki-67 positive microglia – except for a peak around 10% at E11.5)(Barry-Carroll *et al.*, 2023). These differences in numbers can come from the quantification methods as well as regional heterogeneity, as they made no distinction between regions. Nevertheless, microglia here again seem more proliferative at E11.5 as compared to E16.5, similarly to our observations. More strikingly, this pattern of dynamic waves of proliferation that we pointed out is also found in the human developing neocortex (Menassa *et al.*, 2022).

In the neocortex (Article 1) and other regions analyzed (data not shown), our analysis of proliferation seems to be predictive, to some extent, of the numbers of microglia observed in the following days. This suggests that the entry of microglia after E12.5 most probably brings little contribution to the microglial population and underlies again the importance of local proliferation, coherently with what can be observed in the human neocortex (Menassa *et al.*, 2021).

What drives the early microglial intense proliferation, and what makes it pause? Many hypotheses exist, non-exhaustively: microglia that reached the brain recently could have some internal progenitor-like program of intense proliferation, that would be replaced as they mature; cues from the circulation could be necessary for their early proliferation, and be later prevented from reaching the parenchyma due to BBB closure; or changing cues from the neural environment could regulate these shifts. Regarding their intrinsic imprinting, great advances have recently been made in the field thanks to single-cell analysis (single-cell RNAseq, ATACseq,…), but the scarcity of microglial cells analyzed at each embryonic steps has made it difficult so far to assess their precise properties and trajectories along time. Amongst the possible cues that could support microglial early colonization, we investigated how the CSF-1R pathway, known to regulate microglial survival and proliferation (Stanley and Chitu, 2014), was involved in microglial colonization and what were the relative contributions of its ligands. This is further discussed in 3.

1.2. Early microglial turnover?

In parallel, even though we focused our analysis on microglial proliferation because of its critical aspect in microglial colonization of the developing brain, our data suggest that cleaved-Caspase 3 positive microglia can be found, in small amounts, in the neocortex of control animals at E14.5 (Article 1), as described in the embryonic human cortex (Menassa *et al.*, 2022). Their scarcity suggests that it is not a major mechanism regulating their precise numbers, but could also be in part explained by the very transient and fast activity of cleaved-Caspase 3, or could translate the contribution of other types of microglial cell death, like necroptosis, observed in remyelination (Lloyd *et al.*, 2019), or autophagy (Plaza-Zabala, Sierra-Torre and Sierra, 2017). Though microglial colonization of the zebrafish brain is different in many ways from the mammal brains, microglial turnover during its development has been

suggested to be high, with a lifespan estimated to be below 3 days (Gordon, Schafer and Smith, 2023). Thus, the contribution of microglial death – and which type of cell death – to their early colonization of the mammal brain remains to be characterized and could be of importance alongside with proliferation.

1.3. Microglial proliferation: postnatal stages

At the beginning of postnatal life, microglia tend to proliferate again, peaking around P9 (Article 1). This second wave of proliferation has different intensities and timings across regions, and is almost absent in the POA. It leads to the postnatal increase in density, peaking around P14, that we described across the cortex, striatum and hippocampus and which was previously evidenced globally through FACs sorting of microglia, as well as across mesolimbic nuclei (Nikodemova *et al.*, 2015; Biase *et al.*, 2018; Hope *et al.*, 2020; Barry-Carroll *et al.*, 2023). Microglia later establish their final density after a refinement thought to be mediated, in part, by microglial cell death after the second postnatal week (Nikodemova *et al.*, 2015; Hope *et al.*, 2020; Menassa *et al.*, 2022; Barry-Carroll *et al.*, 2023). Microglial density is later regulated and maintained through coupled proliferation and apoptosis (Askew *et al.*, 2017). Displaying regional heterogeneities, it appears to be driven by local cues, and is re-established after depletion/repopulation phases (Elmore *et al.*, 2014; Biase *et al.*, 2018). During early postnatal development, these local cues could require microglia to proliferate to meet their target density, which would be coherent with the "overshoot" seen at the end of the second postnatal week and later refined. Alternatively, local cues could directly induce their proliferation, leading to increased densities, while other mechanisms could later take over and refine microglial numbers. High amounts of microglia during postnatal development could in particular be important in order to achieve their developmental functions. Whether microglial proliferation is driven by crucial developmental processes remains unclear: microglial densities are increased in key neurodevelopmental structures like the subplate in humans (Penna *et al.*, 2021; Menassa *et al.*, 2022), but no correlations were observed between the proliferation patterns of microglia and developmental events such as surrounding cell death or proliferation, nor phagocytosing events in mice, within mesolimbic nuclei and other regions (Hope *et al.*, 2020; Barry-Carroll *et al.*, 2023). In addition, we found that even though changes in microglial densities were drastic during the first postnatal weeks, matching the period when cortical circuits become mature and functional, their densities seemed to be unaffected by modulations

of neuronal activity. This is surprising considering their ability to sense finely neuronal activity (York, Bernier and MacVicar, 2018; Umpierre and Wu, 2021), and their response to specific patterns of activity, like their altered numbers observed when neuronal circuits are stimulated to promote Gamma oscillations (Iaccarino *et al.*, 2016). While we focused on the first postnatal week, it is possible that modulations of neuronal activity could impact microglial numbers later on during development.

1.4. Microglial migration

Microglia enter in the brain where they settle and further proliferate (Alliot, Godin and Pessac, 1999; Dalmau *et al.*, 2003). Known to migrate long distances before colonizing the brain parenchyma, from the yolk-sac through the embryo, little is known about their later redistribution via migration between brain regions. Using clonal analysis, performed with barcoded lentiviruses at E9 and analyzed at P14, microglia from the same clone could be observed scattered across the brain, which could suggest some migration of microglia (Ratz *et al.*, 2022). Nevertheless, the early tagging led to mixed clones containing both microglia and perivascular macrophages, also of yolk-sac origin, and might instead suggest that progenitors could have been labeled before their entry in the parenchyma, thus explaining the widely scattered population obtained. Conversely, microglial multicolor labeling performed at P0 and analyzed at P14 or P30 also underlined clonal expansion of microglia, with clones of diverse sizes and which cells were mostly grouped together, suggesting little microglial migration at postnatal stages (Barry-Carroll *et al.*, 2023).

We tried to perform clonal analysis using the *CAG-Cytbow* mice (Loulier *et al.*, 2014), kindly provided by the team of Jean Livet (Institut de la Vision): under the cre recombinase expression, it gives rise to a unique cytoplasmic labelling made of multiple copies of three different fluorophores. Our aim was to tag in a temporally-controlled manner microglia, using distinct inducible cre lines. Targeting different periods of microglial proliferation, we would thus have been able to track their relative dispersion and shed new light on their migratory patterns. We thus crossed the *CAG-Cytbow* line with the *Cx₃cr1*$^{creER/+}$ and *p2ry12*$^{creER/+}$ mice (McKinsey *et al.*, 2020), but achieved little or no recombination in microglia whatever the dose or doses of tamoxifen administered, in contrast to other reporter lines. We thus believe that the

CAG-Cytbow construct, which was optimized to work in neural cell types, is tough not recombine in microglial cells.

In parallel, we performed two-photon live imaging on acute brain slices in *Cx3cr1*$^{gfp/+}$ mice. This technique presents limitations: the sectioning induces injury, axons can be cut leading to neuronal damage and altered neuronal activity, and slices eventually die after a few hours, since they are bathed in a solution used by electrophysiologists to "just" maintain the tissue alive. Nevertheless, we found that imaging microglia at the center of 300µm-thick slices, avoiding microglial recruitment at the surface of the damage tissue, led to surprisingly interesting results: there was no sign of microglial aberrant activation, even after 6 hours; microglial morphology was comparable to what can be seen in fixed tissue and microglia could be tracked proliferating or migrating. We found that microglia were highly mobile in the neocortex at E14.5, but not in the striatum nor at other stages. Why E14.5 cortical microglia are much more mobile, and more generally what could drive their mobility remains to be further investigated. In particular, preliminary results showed that most microglia were moving in randomly distributed directions, suggesting the absence of long migratory routes as can be observed for migrating interneurons. Microglia in the neocortex have instead been shown to migrate along blood vessels (Smolders *et al.*, 2017), something coherent with the trajectories we observe, and which could help microglia move away from each other to scatter within the brain parenchyma. On the other hand, few microglia were detected crossing the cortical plate, from the subplate to the marginal zone. This is thought to be in part regulated by attraction cues present in the marginal zone/meninges, as proposed for Cxcl12 (Hattori *et al.*, 2020). Such mechanism could be needed to fuel the marginal zone, isolated between the cortical plate and the meninges. As microglial numbers in the marginal zone remain low, it suggests that at this stage, no or very few microglia would enter from the pia surface. It thus highlights local redistribution through migration in a zone where microglia are heterogeneously distributed. At postnatal stages, microglia have been shown in the cortex to migrate along blood capillaries (Mondo *et al.*, 2020), which could again participate, along with proliferation, in local redistribution across cortical layers; but are not likely to result in long-range migration due to the small distances traveled. Thus, in spite of some limitations of the experimental approaches, our findings overall support the hypothesis that local redistribution of microglia can be mediated by microglial migration, but that microglial general pattern of colonization is mainly the consequence of local proliferation.

1.5. Microglial colonization across sexes, species and environmental challenges

Our study provides a characterization of microglial proliferation and densities in different regions of the brain through development. Such a longitudinal study, from E12.5 to P60 with many timepoints across development, comes to complete fragmented data previously available, which were done focusing on one specific region or on the whole brain with no information about location; spanning only embryonic or postnatal development but rarely both; with the use of different techniques (Dalmau *et al.*, 2003; Swinnen *et al.*, 2013; Nikodemova *et al.*, 2015; Hope *et al.*, 2020; Barry-Carroll *et al.*, 2023). It thus brings a more comprehensive understanding of microglial proliferation and distribution along development.

In our study, we found no sex differences in terms of microglial densities or proliferation, consistently to what has been observed in humans (Menassa *et al.*, 2022), but in contrast to what has been described in rats (Schwarz, Sholar and Bilbo, 2012; Lenz *et al.*, 2013). This could be due to region or specie-specific specialization of sexual dimorphism that is not observed in the structures we examined in mice.

For experimental purposes, our study was done in heterozygous *Cx3cr1*$^{gfp/+}$ mice, an important microglial signaling pathway (Paolicelli, Bisht and Tremblay, 2014). Importantly, we checked at multiple timepoints and across regions that we did not find overt differences in microglial numbers and distribution compared to control animals. Instead, we observed some interindividual variability in our quantifications. Moreover, knowing that microglia can be sensitive to extrinsic signals, including ones derived from the maternal environment, chemical compounds, early-life stress or the gut microbiota (Gómez-González and Escobar, 2010; Delpech *et al.*, 2016; Hanamsagar and Bilbo, 2017; Thion *et al.*, 2018; Zhang *et al.*, 2019; Huang *et al.*, 2023), precise numbers and densities could display some variability amongst conditions, genetic background or animal facilities.

Nevertheless, it is overall reassuring that, even though slightly different in zebrafish (Xu *et al.*, 2016; Wu *et al.*, 2018), many features of microglial pattern of colonization in mice are conserved across mammalian species and studies, such as their dynamic phases of proliferation, accumulation in hotspots and exclusion from the cortical plate, also described in humans (Lawrence *et al.*, under revision; Alliot, Godin and Pessac, 1999; Dalmau *et al.*, 2003; Hristova *et al.*, 2010; Verney *et al.*, 2010; Swinnen *et al.*, 2013; Nikodemova *et al.*, 2015; Menassa *et al.*, 2022). This reinforces the interest and validity of our animal model and suggests that better

understanding microglial colonization in mice could also drive our comprehension of this process in humans.

In this work, we thus provided a thorough characterization of microglial distribution and proliferation spanning forebrain development from early embryonic stages to juvenile and adult stages, and in several regions of interest. The wide spatiotemporal setting of our study allowed us to point out two waves of microglial proliferative expansion, one very intense and global in the embryonic brain, and a second one heterogeneous across regions around the end of the first postnatal week. We evidenced little contribution of long-range migration but believe it is a combination of local proliferation and short-range migration that drives microglial distribution and redistribution along time. In parallel to these canonical regions, we found atypic hotspots of microglial accumulation, which are further described below.

2. Microglial developmental hotspots

2.1. Transient ATM accumulations

Along with slight regional differences, microglial colonization of the brain is a highly heterogeneous process. At E12.5, microglia are not numerous in the brain parenchyma and can be found dispersed in all regions. Strikingly, they will then distribute heterogeneously. In particular, they accumulate in several hotspots of white matter where they adopt an ameboid morphology, such as the cortico-striato-amygdalar boundary (CSA) as early as E14.5 (Lawrence *et al.*, under revision; Squarzoni *et al.*, 2014), or the corpus callosum and cortico-septal boundary (CSB) in the early postnatal brain (Lawrence *et al.*, under revision; Hristova *et al.*, 2010; Hagemeyer *et al.*, 2017; Wlodarczyk *et al.*, 2017; Hammond *et al.*, 2019; Li *et al.*, 2019; Nemes-Baran, White and DeSilva, 2020). By P14, when microglial densities peak in most regions (Nikodemova *et al.*, 2015; Hope *et al.*, 2020), no accumulation of ameboid microglia can be found: microglia all display a highly ramified morphology and have already established their homogeneous tiling of the parenchyma with individual territories (Hope *et al.*, 2020; Barry-Carroll *et al.*, 2023).

Along with their ameboid morphology and uncommon accumulation, microglia in the early postnatal white matter have been shown to display an atypical profile characterized by the expression of *Igf-1*, *Spp1*, *Lgals3*, *Gpnmb*, *Clec7a* and *Itgax*, and called alternatively axon-tract associated microglia (ATM)(Hammond *et al.*, 2019), proliferative region associated microglia (PAM)(Li *et al.*, 2019), CD11c+ microglia (Wlodarczyk *et al.*, 2017) or youth-associated microglia (YAM)(Silvin *et al.*, 2022) across diverse studies. We will hereafter refer to them as ATM. While this subtype was evidenced during postnatal development, we validated through immunohistochemistry or genetic tools the expression of the core ATM factors Spp1, Gpnmb, Clec7a, CD11c and Gal3/Mac2 (encoded by *Lgals3*) in accumulating microglia at the CSA and CSB (Lawrence *et al.*, under revision). We thus confirmed the specific location of these atypical embryonic ATM-like cells, hereafter referred to as embryonic ATM-like. We additionally were able to identify them in white matter regions of the embryonic human brain, which presence had been suggested by scRNA-seq (Kracht *et al.*, 2020). They thus share some core characteristics with postnatal ATM. Further transcriptomic analysis will nevertheless be needed to better understand how similar they are to postnatal ATM. Isolation of these embryonic ATM-like cells through microdissection or sorting, followed by scRNA-seq, appears challenging.

Instead, spatial transcriptomic should help us in the near future in understanding their relationships, similarities and possible discrepancies. Additionally, their mosaic expression of the different markers suggests that slightly different states or functional modules could be encapsulated under the "ATM" label. Whether these states could have slightly different and specialized functions, or whether they are a consequence of dynamic changes in expression profiles need further investigation. This being discussed, embryonic ATM-like will thereafter be referred to as ATM, a general designation encompassing both embryonic and postnatal ATM.

2.2. Formation of microglial hotspots and induction of the ATM profile

The presence of microglial transient accumulations and transcriptional heterogeneity in zones of white matter, found across different species, is highly intriguing. What could possibly recruit microglia there, induce their ameboid morphology, phagocytic properties and ATM features still remain to be fully investigated. In this work, we nevertheless bring new clues regarding this process, and showed that ATM induction can be linked to tissue damage/tension in several cases (Lawrence *et al.*, under revision). Indeed, we first found through *in utero* mechanical pokes in the neocortex, that microglia are quickly recruited to the vicinity of acute lesions. This is similar to what has been observed in the neonatal spinal cord (Li *et al.*, 2020). In both cases, microglia upregulate core ATM factors such as Spp1 or Gpnmb. In addition, the CSB is a known zone of high morphogenetic stress inducing a transient cavity, the cavum septum, during normal brain development (Kaur and Ling, 2017). We found that at the CSA, where morphogenetic tensions are particularly important (van Essen, 2020), transient microlesions can be observed in physiological conditions at E14.5. In this region, we showed that both microglial accumulation and ATM profile induction are correlated to morphogenetic stress: in a model where it is reduced, we found less microglia accumulating at the CSA, and less expression of ATM markers, and vice versa (Lawrence *et al.*, under revision). Thus, coherent with what can be observed in wounds, tissue fragility could induce ATM accumulation in both regions. Signaling through piezo receptors could directly sense mechanical tensions and occasion changes in their accumulation and phagocytic capacities, as suggested in the case of AD (Hu *et al.*, 2023). Alternatively, it could be local cell death or cell damage, resulting from the tensions, that could play this role. Instead, to our knowledge, nothing is known about morphogenetic tension or developmental fragility at the EDWM. Last, and possibly

concomitant to the previous hypothesis, microglial phagocytic activity, important in all these accumulations (Lawrence *et al.*, under revision; Hagemeyer *et al.*, 2017; Nemes-Baran, White and DeSilva, 2020), could induce microglial reprogramming towards the ATM profile in these hotspots, as well as microglial recruitment - possibly in a microglia-microglia communication.

2.3. Intrinsic microglial expression of *Csf-1*

Interestingly, a common feature to embryonic or postnatal ATM and DAM is their selective expression of autocrine *Csf-1*. More particularly, we confirmed using RNAscope that *Csf-1* expression in ameboid ATM-like microglia of the hotspots is very strong – contrasting with lower levels of the surrounding environment and coherent with our scRNA-seq reanalysis. We further showed that microglial *Csf-1* mediates the sustained proliferation at the CSA and in the EDWM (Article 1). Thereby, microglial *Csf-1* participate in the formation of the hotspots through *in situ* proliferation. Interestingly, as *Csf-1* can regulate macrophage chemotaxis (Stanley and Chitu, 2014), microglial *Csf-1* could also participate in microglia-microglia recruitment at the hotspots. In any case, we showed using two-photon live-imaging on acute brain slices that this proliferation is not supporting any fueling of the neighboring regions when the hotspots are active, as no microglia can be seen actively migrating away (Article 1). Instead, this mode of intrinsic microglial *Csf-1* signaling appears as an important feature of ATM accumulations and contrasts with the dogma of CSF-1R ligands being solely provided by the neural environment. We expect that by inactivating microglial *Csf-1* earlier, numbers of ATM should be reduced – something we could not evidence in our present paradigm. Whether it is a way to become independent from the environment, which could be shared by DAM, or not, microglial *Csf-1* appears particularly important, as it mediates microglial numbers in a specific zone where they assume developmental functions.

2.4. Developmental functions of microglia at the hotspots

Indeed, these hotspots of microglial accumulations are far from being anecdotic and instead are zones were microglia play developmental roles (Hagemeyer *et al.*, 2017; Wlodarczyk *et al.*, 2017; Nemes-Baran, White and DeSilva, 2020; McNamara *et al.*, 2023). Postnatal ATM of the corpus callosum have been shown to regulate oligodendrogenesis and

subsequent proper myelination, something recently questioned using *Csf1r*$^{\Delta FIRE/\Delta FIRE}$ mice (McNamara *et al.*, 2023), through the release of the ATM factor IGF-1, and via phagocytosis of viable OPCs in a fractalkine-dependent manner (Hagemeyer *et al.*, 2017; Wlodarczyk *et al.*, 2017; Nemes-Baran, White and DeSilva, 2020). In addition, we showed that at the CSA and CSB, microglia participate in the maintenance of tissue integrity (Lawrence *et al.*, under revision). In absence of microglia, both display lesions that are postnatally resorbed, concomitant with microglial repopulation. Lesions were absent when inactivating canonical signaling pathways in microglia such as *Cx3cr1*, *Dap12/TyroBP* or *CR3*. At the CSA, we showed instead that microglial prevention of lesion as well as repair is mediated, in part, by the ATM factor Spp1. Secretion of Spp1 and other ECM-modifying proteins also included in the core ATM factors, have been shown to be part of the repair and ECM remodeling programs common to all macrophages: microglial functions in these zones of morphogenetic tensions could be a core attribute of their macrophage identity (Liaw *et al.*, 1998; Frangogiannis, 2014; Pellicoro *et al.*, 2014; Vannella and Wynn, 2017; Rosmus *et al.*, 2022). In particular, Spp1 could promote microglial phagocytic activity, as previously shown (De Schepper *et al.*, 2022; Shen *et al.*, 2022). Importantly, while several evidence point at a specific role of ATM at the CSA and CSB, our inability to specifically target and deplete this subset prevents us to rule out a possible involvement of other factors. For example, could other microglia or BAMs contribute to the phenotype? While the *Csf1r*$^{\triangle FIRE\triangle/FIRE}$ mice (Rojo *et al.*, 2019; Munro *et al.*, 2020) offers a more specific model of microglial depletion (Kiani Shabestari *et al.*, 2022; McNamara *et al.*, 2023), this novel model still needs to be extensively characterized.

Whether microglia also assume some function of tissue integrity maintenance at the EDWM still remains to be investigated, something we will do using our *Il-34* postnatal conditional knockouts or in the *Csf1r*$^{\triangle FIRE\triangle/FIRE}$ mice in which microglial depletion lasts through postnatal stages. Finally, microglia could be involved in other functions not yet identified. Indeed, some mystery remains on what happens in the hotspots: we observe many proliferating cells, both at the CSA and EDWM, which are not microglia. If some of them probably are OPCs in the EDWM, there might be other cells in the CSA and EDWM that microglia could interact with. In particular, microglia have been shown to regulate PV-interneuron wiring (Thion *et al.*, 2019; Favuzzi *et al.*, 2021; Gallo, Berisha and Van Aelst, 2022) as well as positioning (Squarzoni *et al.*, 2014; Thion *et al.*, 2019), though mechanisms at stake remain unclear. In particular, the CSA could constitute a route for migrating interneurons; on the other hand specific interneurons have been shown to perform their final division in the

EDWM, before migrating to the cingular and prefrontal cortex (Riccio *et al.*, 2012). Thus, whether the CSA and EDWM could be zones of microglia-interneuron interplay, and underlying functional consequences, remain to be investigated.

2.5. Disappearance of the hotspots and ATM fate

Of course, the transient character of developmental ATM accumulations raises the question of the end of these hotspots and of the future of ATM. What happens to ATM before they become mostly undetectable? If the ATM state is believed to be locally induced by the microenvironment, little information is available about whether this is reversible and transient. If the ATM state is transient and microglia go back to a homeostatic state, a massive migration from the hotspots should be visible before their disappearance. By performing two photon live imaging on acute brain slices we found no evidence of such migration, but this need to be further investigated, more specifically when numbers of accumulating microglia decrease. More powerful and hopefully soon available, tools to target and label ATM should allow us to track precisely their evolution: to what extent can ATM later dilute amongst other microglia in the brain parenchyma; do they remain at a predominant location; are they imprinted in any way? In particular, the intriguing similarities between ATM and DAM interrogates about their possible relationship: could ATM turn down their specific profile, become undetectable, but be more prone to become DAM in disease context? Or are all microglia likely to become DAM in a given microenvironment?

Microglia at the hotspots could also die and thus disappear. This mechanism has been suggested in the developing zebrafish (Gordon, Schafer and Smith, 2023), where vacuolated microglia, reminiscent of the morphology we observe for microglia at the hotspots, eventually die. Microglia in remyelination, where they are ameboid and phagocytic, also display a high turnover (Lloyd *et al.*, 2019). It is possible that excessive phagocytosis could lead to microglial cell death, and could in the end participate in the disappearance of the hotspots. Phagocytosis-associated cell death could support the need for an increased proliferation to maintain the accumulation, independent of the neural environment but rather self-sustained, as we evidenced with microglial expression of *Csf-1*.

3. Role of the CSF-1R signaling pathway in microglial colonization and new depletion model

3.1. Embryonic cortical microglia transiently and locally depend on neural CSF-1

The CSF-1R pathway is known to be essential for macrophage survival and proliferation (Stanley and Chitu, 2014), including microglia and their progenitors. As neural progenitors have also been suggested to transiently express the CSF-1R during development (Nandi *et al.*, 2012), we first took advantage of an available scRNA-seq dataset (Di Bella *et al.*, 2021) to check the expression of *Csf-1r* in neural cells. We found no expression of *Csf-1r* in neural progenitors, except for very low levels in intermediate precursor cells. Consistent with low levels or absence of *Csf-1r* expression in non-microglial cells, using RNAscope experiments, we did not detect *Csf-1r* mRNA outside microglia in the brain, spanning E14.5, E16.5, E18.5, P0, P3 and P7 stages (Article 1 and data not shown). Though controversial (Chitu *et al.*, 2017), expression of *Csf-1r* by neural progenitors, even at low levels, could be important for their maturation, as previously suggested (Nandi *et al.*, 2012), and whether they could be affected in conditional knock-outs of CSF-1R ligands needs to be closely characterized.

Instead, remarkably little is known about the sources of each CSF-1R ligands and how they are respectively involved in early microglial colonization. From the same scRNA-seq dataset (Di Bella *et al.*, 2021), we investigated neural sources of *Csf-1* and *Il-34* during cortical development. We found that *Csf-1*, but not *Il-34*, is expressed at low levels by progenitors and immature neurons throughout embryonic development. We thus performed conditional inactivation of *Csf-1* in all cortical progenitors and excitatory neurons or in post-mitotic cortical neurons using respectively the $Emx1^{cre}$ or $Nex1^{cre}$ combined to the $Csf1^{fl/fl}$ mouse line. We found a drastic depletion of microglia from the E14.5 neocortex of $Emx1^{cre};Csf1^{fl/fl}$ animals. This highlights the importance of embryonic CSF-1, confirming previous observations (Easley-Neal *et al.*, 2019). More precisely, it shows that even though a circulating isoform of CSF-1 displays humoral regulation and is present in the embryonic circulation (Roth and Stanley, 1996; Stanley and Chitu, 2014), it is rather the local CSF-1 produced by the neural environment that controls microglial survival. Additionally, very few microglia can be seen in the E12.5 neocortex of $Emx1^{cre};Csf1^{fl/fl}$ animals. On the one hand, their very reduced number suggests that absence of CSF-1 from the neural tissue could prevent microglial recruitment to the parenchyma, pointing

at a chemotactic role of neural CSF-1 which could bring new light on mechanisms of microglial entry in the brain. The presence of few microglia instead suggests that local neural CSF-1 is not essential for their entry in the brain or its colonization, while some other compensatory mechanisms can not be excluded. Regarding potential compensatory mechanisms, we looked for *Il-34* mRNA abundance in our *Csf-1* knock-out cortex through RNAscope experiments but found no striking difference – something that will need more quantitative evaluation. Microglial presence could also be linked to changing needs of microglia along their sequential phases of maturation: early microglia could be less dependent on local CSF-1 than E14.5 microglia. Finally, these few microglia in the neocortex could be allowed by the timing of Cre recombinase expression in the $Emx1^{cre};Csf1^{fl/fl}$ animals, possibly leaving a developmental window where *Csf-1* is expressed in the early developing neocortex. On the other hand, the drastic depletion of cortical microglia in E14.5 $Emx1^{cre};Csf1^{fl/fl}$ animals underlines the necessity of CSF-1 signaling for embryonic microglial survival. In particular, our study highlights through scRNA-seq analysis (Article 1) and RNAscope experiments (data not shown) that neural progenitors are the major source of CSF-1. Nevertheless, a more modest decrease in microglial numbers of the subplate and intermediate zone in E14.5 $Nex1^{cre};Csf1^{fl/fl}$ animals suggests that CSF-1 from neurons also contributes to microglial number regulation. Preliminary results suggest that *Il-34*, for which we find no expression in neural cells during cortical embryonic development, has no detectable impact on E15.5 cortical microglia.

Strikingly, we showed here that the effect of neural *Csf-1* is dose-dependent: microglial numbers in the cortex of heterozygous $Emx1^{cre};Csf1^{fl/+}$ animals at E14.5 are approximately reduced by half. Our data suggest that *Csf-1* reduced abundance influence both microglial proliferation and survival to reach intermediate microglial numbers. This mirrors the effect of *Csf-1* overexpression, which increases microglial numbers and proliferation in 3 weeks-old mice (De *et al.*, 2014). Overall, even though neural *Csf-1* levels appear low, they finely tune microglial numbers at E14.5, underlying the importance of a fine balance between the neural environment and invading microglia.

While microglial early depletion is followed by a progressive repopulation, we could observe that repopulating microglia have an ameboid morphology, important loss of P2RY12 reactivity lasting at least until E18.5, and sometimes accompanied by a CD206+ immunostaining (data not shown), altogether pointing at an immature profile of microglia (Article 1). Though reminiscent of repopulating microglia after CSF-1R inhibition, it would be of great interest to further investigate their expression profile along repopulation and how they

could be altered at short and long term – something we will do thank to scRNA-seq experiments. In particular, CSF-1 signaling could be needed in order for microglia to achieve their step-wise maturation (Matcovitch-Natan *et al.*, 2016; Bennett *et al.*, 2018; Thion *et al.*, 2018), something that remains to be studied.

3.2. CSF-1 signaling in other brain regions and from non-neural sources

Our specific targeting of the neocortex in *Emx1^{cre};Csf1$^{fl/fl}$* animals resulted in an efficient and local depletion of microglia at E14.5. We thus aimed for other brain regions, hoping for specific depletions of microglia: we targeted most neural cells of the whole parenchyma with *Nestin^{cre};Csf1$^{fl/fl}$* animals; and we generated *Dlx5/6::cre;Csf1$^{fl/fl}$* and *Nkx2.1^{cre};Csf1$^{fl/fl}$* animals to target the ventral part of the brain. We found a wide depletion of microglia at E14.5 in *Nestin^{cre};Csf1$^{fl/fl}$* animals, suggesting that the local role of CSF-1 is needed throughout the brain (data not shown). Instead, we found no major changes in microglial numbers in *Dlx5/6::cre;Csf1$^{fl/fl}$* and *Nkx2.1^{cre};Csf1$^{fl/fl}$* E14.5 animals. This puzzling result could indicate a contribution of other CSF-1 sources in the ventral part of the brain. Screening through different available scRNA-seq datasets (Di Bella *et al.*, 2021; La Manno *et al.*, 2021), we found that during development, CSF-1 can also be expressed in endothelial cells, vascular and leptomeningeal cells and later in perivascular macrophages (data not shown), which might altogether provide alternative support to microglia. Why these sources might be more prominent in the ventral part of the brain and absent from the cortex remains to be addressed. Importantly, *Csf-1* expressing cells are found in abundance in the meninges and additionally express *Il-34*: they are thus probably needed for BAMs maintenance. Alternatively, it is possible that recombination of the *Csf1$^{fl/fl}$* does not occur in our models using subpallial Cre drivers, something we are investigating through RNAscope experiments but made difficult by the low levels of *Csf-1* mRNA detected at these stages (coherent with our analysis of the scRNA-seq dataset of Di Bella and colleagues).

3.3. CSF-1R independent microglia?

Intriguingly, some microglia still remain at E14.5 in *Nestin^{cre};Csf1$^{fl/fl}$* animals, mostly in the ventral part of the brain, and in increasing densities from rostral to caudal. In particular,

some microglia are found at the CSA and in the MGE, two spots where we find embryonic ATM-like at this stage. In addition, in the MGE we observe some microglia that are less sensitive to PLX3397 treatment administered from E6.5 (unpublished data). In the adult brain, some resistant microglia have also been described and shown to express higher levels of *Lgals3* (Zhan *et al.*, 2020), one of the ATM signature genes. In parallel, ATM express lower levels of *Csf-1r* (Hammond *et al.*, 2019; Li *et al.*, 2019). Whether the ATM profile is linked to a decreased dependence on CSF-1R signaling has indeed been suggested in the developing retina (Anderson *et al.*, 2022). Do they rely on different signals to survive? Do they temporally become independent from any environmental cues? For example, could their autocrine signaling of *Csf-1* allow them to survive independently from other survival cues? These issues remain to be investigated but our data suggest that along with alternative sources of *Csf-1* in the ventral part of the brain, it is likely that all microglia may not rely in the same way on local, neural *Csf-1*.

3.4. IL-34 signaling

Taking advantage of the *Il-34*$^{fl/fl}$ mouse line, we will also investigate its role in regulating microglial numbers and proliferation during early embryonic and postnatal development: its absence seems not to affect E14.5 cortical microglia (Article 1) but could be of importance in other regions of the brain; in parallel it is known to be important for grey matter microglia in the adult (Easley-Neal *et al.*, 2019; Kana *et al.*, 2019). More precisely, IL-34 signaling appears to have a local and dose-dependent effect in the adult: this is beautifully illustrated by Badimon and colleagues who compared the microglial densities in the striatum of specific *Il-34* knock-outs in all neural cells, leading to an important microglial depletion, or restricted to either D1 or D2 striatal neurons and leading to an intermediate effect on microglial densities (Badimon *et al.*, 2020). Nevertheless, microglial developmental switch from CSF-1 to IL-34 signaling needs better spatio-temporal resolution (Greter *et al.*, 2012; Wang *et al.*, 2012; Kana *et al.*, 2019). Whether it is an intrinsic shift of maturing microglia or whether it is driven by ligands availability still remains unknown, but expression patterns of both ligands suggest that the latter is contributing. Last, we are studying the early role of IL-34 in regulating microglial numbers and proliferation. Indeed, *Il-34* expression starts to be increased in early postnatal development heterogeneously across regions (Wei *et al.*, 2010; Easley-Neal *et al.*, 2019), and could be an important driver of the second postnatal wave of proliferation that we highlighted.

3.5. Repopulating microglia

Very interestingly, microglial depletion from the E14.5 neocortex of *Emx1^{cre};Csf1$^{fl/fl}$* animals is then followed by a progressive repopulation, starting as early as E16.5 and completed by P7. By P3, microglia are preferentially located in cortical layer V, where *Il-34* starts to be expressed by neurons, as shown by our analysis of the scRNA-seq dataset generated by Di Bella and colleagues (Di Bella *et al.*, 2021) and previous RNAscope experiments (Nandi *et al.*, 2012; Kana *et al.*, 2019). This suggests a possible early postnatal role for *Il-34* in microglial repopulation, which we plan to investigate thanks to the double knockout *Emx1^{cre};Csf1$^{fl/fl}$;Il34$^{fl/fl}$* mice. This leaves open the question of the origin of these cells: their distribution and morphology do not indicate that they would be migrating from populated areas like the striatum. Could invading BAMs-like cells suffice in seeding repopulating microglia? Could the absence of microglia promote the recruitment of microglia-like cells from an alternative source? In particular, microglia participate in vasculature formation and are involved in BBB maintenance (Checchin *et al.*, 2006; Fantin *et al.*, 2010; Ronaldson and Davis, 2020). Their early role in the closure of the BBB is not known: could this process be delayed in absence of microglia, allowing for the entry of circulating cells? Indeed, if microglial repopulation after CSF-1R inhibition has been shown to result from the proliferation of remaining resident microglia in the adult, with no contribution from the circulation (Zhan *et al.*, 2019; Hohsfield *et al.*, 2021), this could be different in the developing brain. We are currently investigating this question in the context of early administration of PLX3397 (from E6 to E15.5), which should help enlighten this process.

3.6. New model for local and specific depletion of microglia

While microglia appear as important actors of brain development, with many functions described at postnatal stages, our understanding of their roles in the embryonic brain is still limited – even though it is a unique moment where they constitute the main glial cells of the brain, before the generation of astrocytes and oligodendrocytes. In the embryo, microglia modulate the positioning of a subset of interneurons, regulate axonal outgrowth of dopaminergic fibers (Squarzoni *et al.*, 2014), maintain tissue integrity (Lawrence *et al.*, under revision), participate in axon fasciculation of the corpus callosum (Pont-Lezica *et al.*, 2014), act on neurogenesis (Cunningham, Martínez-Cerdeño and Noctor, 2013; Arnò *et al.*, 2014;

Shigemoto-Mogami *et al.*, 2014) and modulate vasculature development (Fantin *et al.*, 2010) - though the exact mechanisms at stake are not fully understood. One limitation to study embryonic microglia is our lack of specific tools to assess their local functions (Bridlance and Thion, 2023). Indeed, few microglia-specific lines can be used at embryonic stages, and depletion tools often display important side-effects and target microglia along with BAMs. This raises the question of a possible involvement of BAMs in functions previously attributed to microglia. The *Csf1r*$^{\triangle FIRE\triangle/FIRE}$ model (Rojo *et al.*, 2019; Munro *et al.*, 2020) brings a promising tool to specifically target microglia and disentangle microglia versus BAMs functions. Nevertheless, characterization of this model in the embryo probably needs further work, and an absence of different BAMs subsets has already been highlighted (Munro *et al.*, 2020). We additionally showed in this study that these mice present cavitary lesions at the CSA at E14.5 and E18.5. Such disruption of tissue integrity during development could impact brain function and wiring, something suggested by the disorganized structure of the amygdalar capsule axon tracts we highlighted (Lawrence *et al.*, under revision). This thus underlines the need for more local and specific tools to investigate microglial functions.

Here, we provide a new model that does not greatly impact BAMs number, while efficiently depleting cortical microglia. How BAMs are possibly affected in their maturation is under study through scRNA-seq experiments. While the mechanisms regulating their density seem independent of neural CSF-1, whether they can be altered by signaling from the parenchyma is an interesting perspective in our understanding of BAMs. In addition, microglial depletion is local and transient, allowing to investigate more finely microglial functions. For example, is microglial impact on interneuron positioning a consequence of local microglia-interneuron interactions in the neocortex, or of a possible action of microglia on neurogenesis in the ventricular zones of the medial and lateral ganglionic eminences, where interneurons are generated? In our *Emx1*^{cre}*;Csf1*$^{fl/fl}$ animals, neocortex development does not seem to be overtly impacted: the size of the cortex and respective cortical layers are not affected, as well as corpus callosum fasciculation, numbers of OPCs or myelin coverage by P14. We are investigating in this model the effect of transient microglial absence on vascular formation and neuronal progenitors numbers and maturation. More importantly, we are performing scRNA-seq experiments which should allow a finer resolution and possibly highlight more subtle alterations in all different cell populations of the neocortex. In parallel, our model validates this strategy of conditional knock-outs of neural *Csf-1*, opening new opportunities for microglial local models of depletion using different Cre lines.

General conclusions

Altogether, my PhD work sheds new light on microglial distribution and proliferation in the developing brain. It highlights microglial embryonic diversity, with transient hotspots of accumulating microglia, resembling postnatal ATM, that are important for the maintenance of tissue integrity in spots of increased morphogenetic tensions. Finally, it illustrates how microglia rely on local neural CSF-1 during embryonic development as well as on microglial CSF-1 in ATM hotspots.

Microglia are fascinating multifaceted cells, sensitive to environmental signals and inflammation, which roles during brain development are varied. Nevertheless, our understanding of their functions is still limited, especially when it comes to embryonic stages or to underlying specific mechanisms involved. More importantly, microglia are associated to the etiology of numerous neurodevelopmental disorders in mice as well as in humans but their exact contribution remains to be further investigated. They increasingly appear as subtle helpers of brain wiring, which alterations lead to neurodevelopmental disorders only in synergy with genetic and environmental risks, in a “second hit” model. This new understanding prompts the field for finer and more specific tools to investigate microglial functions. In this context, we here bring a new model for microglial specific, local and transient depletion, which novelty and precision will hopefully be valuable to future investigations on the early roles of microglia.

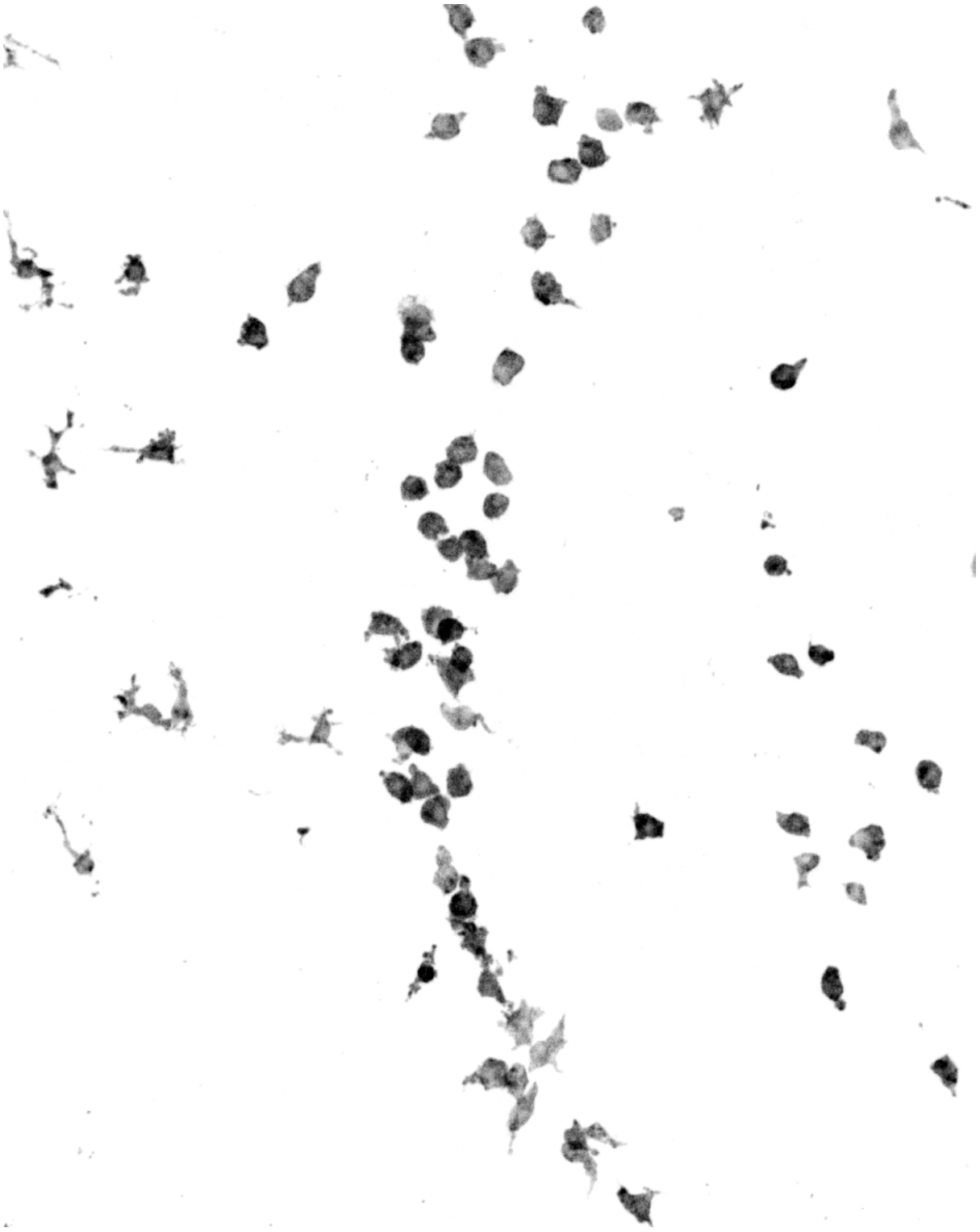

Microglia accumulating at the CSA at E14.5.

ANNEXES

Article 3

Dual ontogeny of disease-associated microglia and disease inflammatory macrophages in aging and neurodegeneration

Summary

In this work, Silvin *et al*. took advantage of different single-cell RNA sequencing datasets which spanned myeloid cells from embryonic, adult and old mice, as well as mice with Alzheimer's Disease. Complemented with two in-house generated datasets, their integration allowed for unprecedented characterization of the different myeloid populations present throughout life. In particular, they could interrogate ATM resemblance with DAMs, as well as DAMs heterogeneity. They found that the previously defined DAMs signature actually encompassed two distinct macrophage subsets: one corresponding to proper DAMs, made of microglia expressing a profile in many ways similar to ATM – or youth-associated microglia (YAM); and a second subset instead corresponding to infiltrating macrophages of the monocyte lineage, displaying a strong inflammatory program and termed disease inflammatory macrophages (DIMs).While DAMs are TREM2-dependent as previously described, and can be found in the brain mainly in neurodegenerative diseases, DIMs are TREM2-independent and also infiltrate the brain during aging. Excitingly, by examining human scRNA-seq datasets, they were able to identify YAM, DAMs as well as DIMs in human brains. This work thus clarifies myeloid cell heterogeneity along brain development, homeostasis, aging and disease.

Author's contribution

As part of a collaboration between my host laboratory and Florent Ginhoux's laboratory (Institut Gustave Roussy), I participated in this study by characterizing through immunohistochemistry the abundance and location of monocyte-derived Ms4a3-TdT positive infiltrating cells, in control or AD brains.

Article

Immunity

Dual ontogeny of disease-associated microglia and disease inflammatory macrophages in aging and neurodegeneration

Graphical abstract

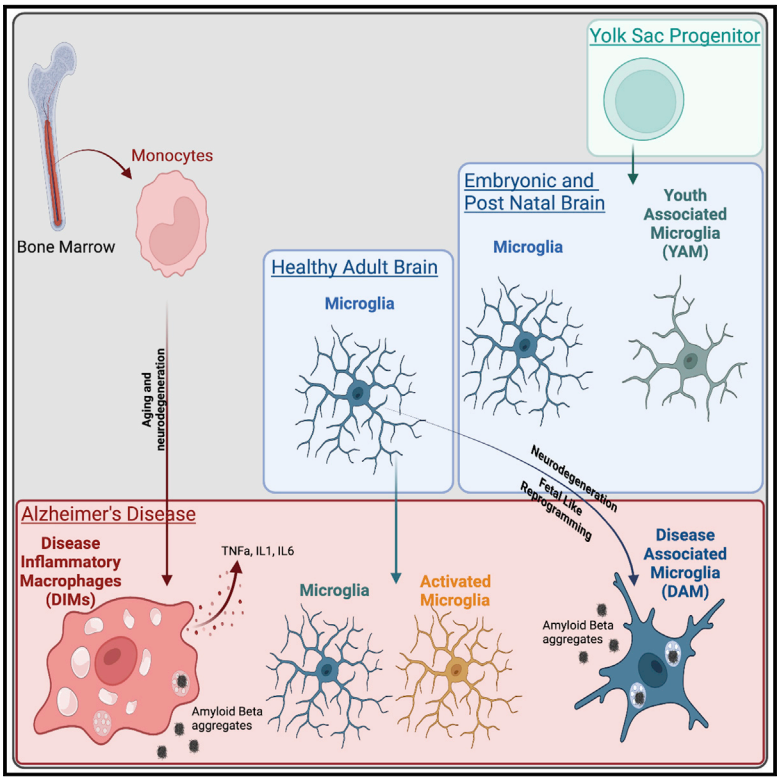

Highlights

- M-Verse as a global cross-comparison of developing and adult murine brain macrophages
- DAM correspond to a fetal-like reprogramming similar to Youth-Associated Microglia
- DIMs appear during aging and increase in neurodegenerative diseases
- DAM are embryonic derived, whereas DIMs are TREM2-independent monocyte derived

Authors

Aymeric Silvin, Stefan Uderhardt, Cecile Piot, ..., Ido Amit, Jonathan Kipnis, Florent Ginhoux

Correspondence

florent_ginhoux@immunol.a-star.edu.sg

In brief

Through 6 scRNA-seq brain dataset integration, the authors generated a myeloid map called M-Verse to delineate macrophage population heterogeneity. M-Verse revealed two distinct macrophage populations expressing published disease-associated microglia (DAM) signature: embryonically derived TREM2-dependent DAM and monocyte-derived TREM2-independent disease inflammatory macrophages (DIMs).

Silvin et al., 2022, Immunity *55*, 1448–1465
August 9, 2022
https://doi.org/10.1016/j.immuni.2022.07.004

CellPress

CellPress

Immunity

Article

Dual ontogeny of disease-associated microglia and disease inflammatory macrophages in aging and neurodegeneration

Aymeric Silvin,[1,2] Stefan Uderhardt,[3,4,5] Cecile Piot,[1] Sandro Da Mesquita,[6,7] Katharine Yang,[1] Laufey Geirsdottir,[8] Kevin Mulder,[2] David Eyal,[8] Zhaoyuan Liu,[9] Cecile Bridlance,[10] Morgane Sonia Thion,[10] Xiao Meng Zhang,[1] Wan Ting Kong,[1] Marc Deloger,[11] Vasco Fontes,[3,4,5] Assaf Weiner,[8] Rachel Ee,[1] Regine Dress,[1] Jing Wen Hang,[12] Akhila Balachander,[1] Svetoslav Chakarov,[1,9] Benoit Malleret,[1,12] Garett Dunsmore,[2] Olivier Cexus,[2,13] Jinmiao Chen,[1] Sonia Garel,[10] Charles Antoine Dutertre,[1,2] Ido Amit,[8] Jonathan Kipnis,[6,14] and Florent Ginhoux[1,2,9,15,16,*]

[1]Singapore Immunology Network, Agency for Science, Technology and Research, Singapore 138648, Singapore
[2]INSERM U1015, Gustave Roussy Cancer Campus, Villejuif 94800, France
[3]Department of Medicine 3 – Rheumatology and Immunology, Friedrich-Alexander-University Erlangen-Nürnberg (FAU) and Universitätsklinikum Erlangen, 91054 Erlangen, Germany
[4]Deutsches Zentrum für Immuntherapie, FAU, 91054 Erlangen, Germany
[5]Exploratory Research Unit, Optical Imaging Centre Erlangen, FAU, 91058 Erlangen, Germany
[6]Department of Neuroscience, Center for Brain Immunology and Glia, University of Virginia, Charlottesville, VA 22908, USA
[7]Department of Neuroscience, Mayo Clinic, Jacksonville, FL 32224, USA
[8]Department of Immunology, Weizmann Institute of Science, Rehovot 76100, Israel
[9]Shanghai Institute of Immunology, Department of Immunology and Microbiology, Shanghai Jiao Tong University School of Medicine, Shanghai 200025, China
[10]Institut de Biologie de l'Ecole Normale Supérieure (IBENS), Ecole Normale Supérieure, CNRS, INSERM, PSL Research University, 75005 Paris, France
[11]INSERM US23, CNRS UMS 3655, Gustave Roussy Cancer Campus, Villejuif 94800, France
[12]Department of Microbiology and Immunology, Immunology Translational Research Programme, Yong Loo Lin School of Medicine, Immunology Programme, Life Sciences Institute, National University of Singapore, Singapore 117543, Singapore
[13]School Biosciences and Medicine, Faculty of Health and Medical Sciences, University of Surrey, Guildford GU2 7XH, UK
[14]Center for Brain Immunology and Glia, Department of Pathology and Immunology, School of Medicine, Washington University in St Louis, St Louis, MO 63110, USA
[15]Translational Immunology Institute, SingHealth Duke-NUS Academic Medical Centre, Singapore 169856, Singapore
[16]Lead contact
*Correspondence: florent_ginhoux@immunol.a-star.edu.sg
https://doi.org/10.1016/j.immuni.2022.07.004

SUMMARY

Brain macrophage populations include parenchymal microglia, border-associated macrophages, and recruited monocyte-derived cells; together, they control brain development and homeostasis but are also implicated in aging pathogenesis and neurodegeneration. The phenotypes, localization, and functions of each population in different contexts have yet to be resolved. We generated a murine brain myeloid scRNA-seq integration to systematically delineate brain macrophage populations. We show that the previously identified disease-associated microglia (DAM) population detected in murine Alzheimer's disease models actually comprises two ontogenetically and functionally distinct cell lineages: embryonically derived triggering receptor expressed on myeloid cells 2 (TREM2)-dependent DAM expressing a neuroprotective signature and monocyte-derived TREM2-expressing disease inflammatory macrophages (DIMs) accumulating in the brain during aging. These two distinct populations appear to also be conserved in the human brain. Herein, we generate an ontogeny-resolved model of brain myeloid cell heterogeneity in development, homeostasis, and disease and identify cellular targets for the treatment of neurodegeneration.

INTRODUCTION

Macrophages are a diverse population of immune cells occupying multiple tissue niches and exhibiting microenvironment-specific phenotypes and functions (Blériot et al., 2020; Guilliams and Scott, 2017). Together, these populations support tissue development, maintain homeostasis, and respond to invading pathogens; however, dysregulation of their functions can promote pathological processes including inflammatory diseases, cancer, fibrosis, and impaired tissue repair, making

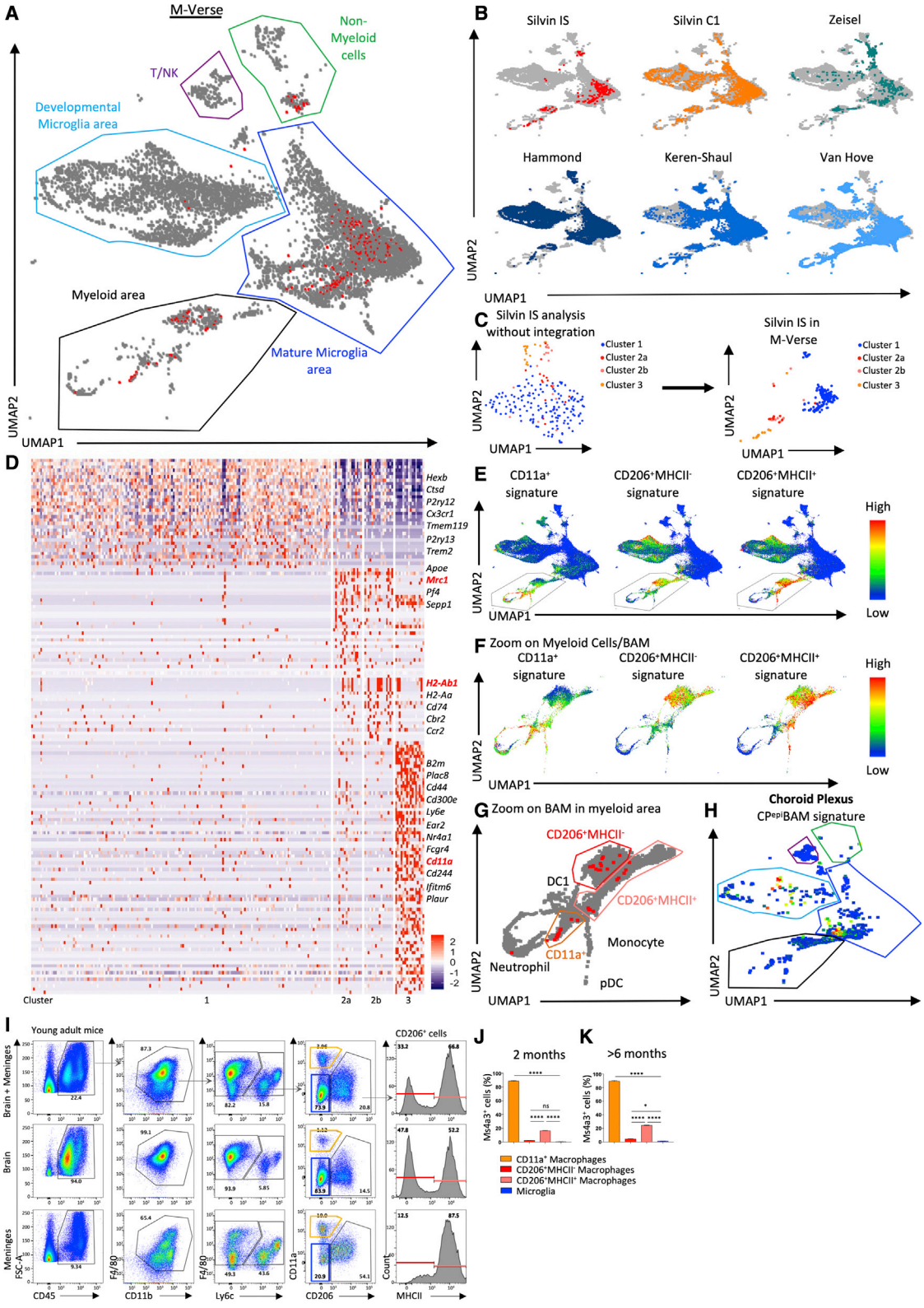

Figure 1. M-Verse, a global consensus of murine brain macrophage heterogeneity

(A) Six scRNA-seq dataset integration (186,026 cells): M-Verse. Red dots correspond to Silvin indexed-sort (IS) cells.

(B) M-Verse split by individual datasets. In gray, cells from other datasets; in color, cells of respective dataset.

(C) Silvin IS scRNA-seq dataset UMAP plot (left panel). M-Verse representation of Silvin IS dataset (right panel).

(legend continued on next page)

them important subjects of research and potential therapeutic targets (Jaitin et al., 2019; Low and Ginhoux, 2018; Wynn and Vannella, 2016).

Macrophages of the central nervous system (CNS) develop and work alongside nerve cells from the earliest stages of embryonic development, as in the case of microglia (Ginhoux et al., 2010), through adulthood and into old age (Tay et al., 2017). Alongside microglia, steady-state brain also contains border-associated macrophages (BAMs) that are located in meninges, choroid plexus, and perivascular spaces of the CNS (Mrdjen et al., 2018). Following inflammation, these populations are joined by macrophages derived from infiltrating monocytes, whose functions are implicated in pathophysiology and tissue damage (Ajami et al., 2018; Mrdjen et al., 2018). By contrast, the recently discovered disease-associated microglia (DAM), which are found at sites of neurodegeneration, have been suggested to play a protective role (Deczkowska et al., 2018; Keren-Shaul et al., 2017). Among these cell populations, there is much controversy surrounding the origin, maintenance, and homogeneity of BAMs, and even more so for DAM: are they distinct from, or related to microglia; how are DAM related to BAMs; and are they in fact even newly differentiated monocyte-derived cells? Hence, to advance the field, we must accurately map, understand the ontogeny of, and functionally characterize each of the various CNS macrophage populations.

Technical developments in next-generation sequencing such as single-cell RNA sequencing (scRNA-seq) have made it possible to interrogate brain heterogeneous immune populations at the single-cell level (Matcovitch-Natan et al., 2016; Mathys et al., 2017; Zeisel et al., 2015), revealing their individual transcriptomes and thereby their heterogeneity. In addition, by subjecting immune cells to multi-parameter flow cytometry or cytometry by time-of-flight (CyTOF) mass spectrometry, expression of up to 40 different proteins of interest on and in a single cell can be measured, providing detailed phenotypic profiles and a degree of implied functional information (Ajami et al., 2018; Mrdjen et al., 2018). Although these studies have undoubtedly advanced our knowledge, most of scRNA-seq methods used have favored breadth over depth and so have not examined potentially important smaller differences in transcriptomic signatures between cell populations. Moreover, no study has yet convincingly linked the populations described by scRNA-seq with those identified by protein expression using flow cytometry, CyTOF or immunostaining, nor validated their ontogeny with fate-mapping approaches. Hence, a consensus global analysis is urgently needed to validate identities, inter-relationships, and possible functions of macrophage populations described in these studies.

Here, we analyzed both mouse and human brain macrophage subsets during development, homeostasis, and disease. We first isolated myeloid cells from the brains of adult mice and generated an indexed-sorted (IS) scRNA-seq dataset that identified microglia, two subsets of CD206$^+$ BAMs differentially expressing major histocompatibility class II molecule (MHCII) transcripts, and a subset of CD11a$^+$ monocyte-derived vascular-associated cells. We then performed a global analysis of four major published scRNA-seq datasets to generate a global myeloid cell map (termed the "M-Verse") of the murine brain, which enabled us to establish common macrophage populations present in each dataset. Using this map in combination with fate-mapping models to dissect the recently identified DAM population, we revealed the presence of two ontogenetically distinct cell lineages with expression profiles consistent with neuroprotective versus inflammatory functions. Our data clarify brain myeloid cell heterogeneity in development, homeostasis, and disease and identify new cell populations to target or protect during aging and neuroinflammation in mice and in humans.

RESULTS

The M-Verse: generating a universal integration to identify murine brain macrophage subsets across multiple datasets

Given varied approaches and conclusions drawn by different scRNA-seq studies of macrophage subsets in murine brain, we first aimed to integrate six datasets collected in other studies (Hammond et al., 2019; Keren-Shaul et al., 2017; Van Hove et al., 2019; Zeisel et al., 2015) and two generated in-house (Silvin IS, Silvin C1) (Table S1), using Seurat (Stuart et al., 2019). To ensure that the resulting integration—which we named "M-Verse" (Figure 1A)—was truly comprehensive, we selected published datasets to cover a broad set of conditions within the CNS: one focused on comparing microglia and neurons, interneurons, oligodendrocytes, and astrocytes from juvenile and adult mice (Zeisel); whereas another tracked the embryonic-to-aged microglia transition, with time points at E14.5, P4, P5, P30, P100, and P540 (Hammond); and one characterized microglia in neurodegeneration, incorporating the first description of DAM (Keren-Shaul). Van Hove dataset added a spatial aspect to the analysis as it included cells from different brain regions: choroid plexus, dura mater meninges, sub-dura mater-enriched meninges (SDMs), and the brain parenchyma (whole brain). Our own datasets consisted of flow cytometry-sorted microglia from brains of embryonic (E12.5, E16.5, and E18.5), early post-natal (P7, P14) and adult (P60) mice (Silvin C1), alongside index-sorted CD45$^+$ macrophages from adult mice (P60) (Silvin IS). We

(D) Cluster DEG heatmap, identifying putative signatures of microglia (1), CD206$^+$ (*Mrc1*) MHCII$^+$ *(H2-Ab1)* (2b), CD206$^+$ MHCII$^-$ (2a), and CD11a$^+$ macrophages (3).
(E) Projection of gene signatures of BAM clusters established in (D) on M-Verse.
(F) Projection of gene signatures of BAM clusters established in (D) on the M-Verse myeloid cell/BAM area.
(G) BAM regions among M-Verse based on (F) and localization of Silvin IS cells (in red).
(H) CPepiBAM signature (Van Hove) projected on Van Hove cells within the M-Verse.
(I) Gating strategy for microglia, CD206$^+$MHCII$^+$ macrophages, CD206$^+$MHCII$^-$ macrophages, and CD11a$^+$ macrophages identified by flow cytometry of C57BL/6 young adult mouse brains (with meninges), meninges, and brain alone (n = 3).
(J) Macrophage ontogeny in 2-month-old fate mapping mouse (n > 3).
(K) Macrophage ontogeny in >6-month-old fate mapping mouse (n > 3).
One-way ANOVA; *p value < 0.05, ****p value < 0.0001.

hypothesized that bringing these diverse datasets together would allow us to generate a powerful tool with which to resolve murine brain macrophage heterogeneity.

The M-Verse (available online at https://macroverse.gustaveroussy.fr/2021_M-VERSE) allowed us to extract expression data of 14,794 common genes detected across all datasets. By comparing these datasets, we were able to generate an unbiased global map of myeloid cells in developing and adult mouse brain. We then identified five regions within the map (Figures 1A and S1A): one corresponding to non-myeloid cells including a cluster corresponding to neurons and one to interneurons, oligodendrocytes, and astrocytes; one to T and NK cells; one that was enriched in cells expressing a developmental microglia signature; one that was enriched in cells exhibiting a mature microglia signature; and a fifth containing non-microglia myeloid cells.

When we projected the data from each study separately back onto the M-Verse map (Figure 1B), we found that Van Hove dataset was enriched in myeloid cells, likely due to scRNA-seq of meningeal and choroid plexus areas (Figures S1B and S1C). Silvin C1 and Hammond datasets were the only two datasets containing embryonic and early post-natal microglia, and both generated a clear developmental microglia signature cluster (Figures S1D and S1E). Zeisel dataset contained a high proportion of non-myeloid cells (differentiating neurons [*Tubba2*, *Sox11*], interneurons [*Slc32a1*, *Pnoc*], oligodendrocytes [*Hapln2*, *Olig1*], and astrocytes [*Slc1a2*, *Slc1a3*], clearly visualized close to the neuron area of the M-Verse [*Stmn1*, *Tubb2b*] [Figure 1B]); despite this, microglia contained in Zeisel dataset had expression profiles that overlapped perfectly with microglia from the other datasets, indicating that the integration was successful. Of note, Zeisel dataset also contained some microglia that clustered in the developmental signature area, likely due to their use of adolescent or juvenile mice (from P21 to 1 month). Similarly, we observed a small number of cells in the developmental microglia signature area from 60–100 days old mice in Hammond, Silvin C1, and Silvin IS datasets (Figures 1A, 1B, S1D, and S1E), but we also observed an increase of cells in this area from old mice with neurodegenerative disease compared with old WT mice (Keren-Shaul and Van Hove) (Figure 1B), suggesting that in these neurodegenerative disease models, some microglia may acquire a developmental-like program.

Refining the M-Verse using targeted index-sorting data from murine brain macrophages

scRNA-seq approaches provide invaluable data, but supplementing their broader analysis with in-depth profiling of a smaller number of cells can facilitate more precise identification of cell sub-populations. Therefore, we next analyzed the Silvin IS dataset, which combines information on protein expression with deep gene expression measurement, using Seurat V2 (cells shown in red in Figure 1A). This dataset includes information from 213 adult murine brain CD45$^+$Ly6C$^-$F4/80$^+$CD11b$^+$ macrophages (Figures S1F and S1G) (regardless of their CD45 amount) and was generated using the Smart-Seq2 method, which allows measurement of the expression of similar number of genes compared with 10X Genomics, but with more reads per cell (Vieth et al., 2019). This was combined with IS to isolate individual cells with known characteristics (e.g., defined size, granularity, and selected marker expression) (Figures S1H–S1J). To assist with an unambiguous identification of BAMs within the traditionally gated microglia population, we used cells from 2-month-old *Lyz2GFP* mice (Figure S1F), in which GFP marks the lysozyme-expressing BAMs and not microglia (Van Hove et al., 2019). The 213 sequenced cells, using Seurat V2 and Phenograph clustering method allowed us to determine three clusters based only on their scRNA-seq expression profile: a large cluster 1 and two minor clusters 2 and 3 (Figure S1K).

To further characterize these 3 clusters, we measured the expression of a panel of "indexed" surface molecules obtained by flow cytometry. We found that the minor clusters 2 and 3 expressed higher amount of CD45 and *Lyz2*GFP (Figure S1L), whereas the major cluster, cluster 1, exhibited an intermediate amount of CD45, F4/80, CD11b, and Ly6C expression and a low amount of *Lyz2*GFP: a phenotype reminiscent of microglia (Figure S1M; Table S1). To better understand the composition of clusters 2 and 3 (Figure S1K), we reanalyzed the *Lyz2*GFP$^+$ cells (BAMs) independently of the other cells using the previous parameters. Based on gene expression profile, cluster 2 was resolved into two sub-clusters that we annotated 2a and 2b (Figures 1C and S1N, panel left). Then, based on flow cytometry data, we could see that cluster 2a was more like microglia (cluster 1), whereas cluster 2b was clearly separated from cluster 1, notably expressing high amount of MHCII protein (Figure S1M). To further investigate the clusters' identity, we used differentially expressed gene (DEG) analysis, which showed that cluster 1 corresponded to microglia (high expression of *Tmem119*). Although cluster 2 was generally characterized by high expression of BAM marker *Mrc1* (*Cd206*), cluster 2b exhibited higher expression of *H2-Ab1*, *H2-Aa*, and *Cd74* compared with cluster 2a at the RNA and protein amount (Figures 1D and S1M). Finally, cluster 3 represented a unique population of cells characterized by expression of *Cd11a*, *Cd44*, *Cd300e*, *Plac8*, *Nr4a1*, *Ear2*, and *Fcgr4* (Figures 1D and S1M). The amount of *Cd11a* RNA and CD11a protein correlated among cells from cluster 3 (Figures 1D and S1M).

We then used these new in-depth data from IS scRNA-seq (Silvin IS) to generate robust signatures for each cell populations within the M-Verse. This allowed us to confirm that CD11a$^+$ (cluster 3) and CD206$^+$ macrophages (clusters 2a and 2b) in the M-Verse clustered distinctly from microglia (cluster 1) (Figure 1C). We then projected these signatures onto the M-Verse to extend and validate their heterogeneity across other datasets. The projection of the CD11a$^+$, CD206$^+$MHCII$^-$, and CD206$^+$MHCII$^+$ macrophage signatures allowed us to highlight specific regions within the myeloid cell area that contained the highest numbers of cells expressing similar patterns of genes (Figure 1E). By focusing on these areas (Figure 1F), we identified a region corresponding to BAMs that was common to all datasets (Figure 1G). This approach enabled us to bring greater resolution to the cell identities proposed in other published studies: when we used Van Hove choroid plexus BAM (CPepiBAM) signature to interrogate their dataset region containing choroid plexus cells, we found that cells expressing this signature were in fact localized predominantly within the mature and developmental microglia area defined by the M-Verse (Figure 1H). Therefore, the cells proposed as BAMs in the original study are likely to be microglia: this is further supported by the published finding that choroid plexus

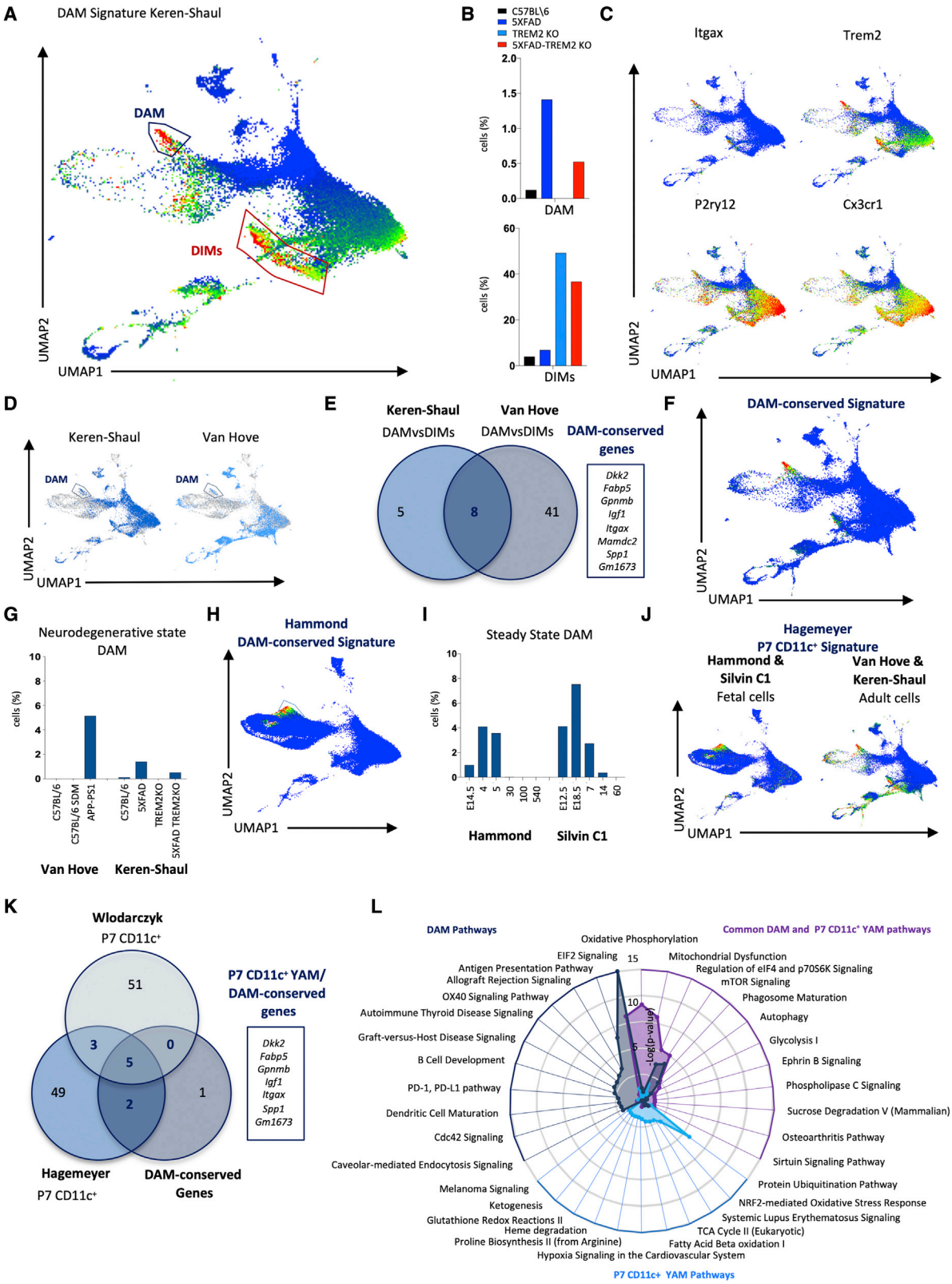

Figure 2. DAM signature includes two distinct cell populations

(A) Heatmap of DAM signature determined by Keren-Shaul et al., projected onto Keren-Shaul dataset with M-Verse coordinates, revealing two regions enriched with the Keren-Shaul DAM signature, named DAM and DIMs.

(legend continued on next page)

"BAMs" express the transcription factor *Sall1*, which was previously found to be expressed among brain macrophages only by microglia within the murine CNS (Buttgereit et al., 2016).

In conclusion, integrating six brain macrophage scRNA-seq datasets generated using different techniques allowed us to perform a global cross-comparison of developing and adult murine brains. By further applying IS single-cell analysis, we increased the resolution of the M-Verse and identified a consensus set of mRNA marker transcripts that enable reliable and accurate identification of murine microglia and brain macrophage populations across multiple life stages.

M-Verse-directed analysis resolves the origin of BAMs

Based on the M-Verse, and the expression of signature DEG-encoded proteins, we designed a stringent flow cytometry gating strategy to identify the brain macrophage populations defined above. These marker genes and proteins included *Mrc1* (coding for CD206), *Itgal* (coding for CD11a), and *H2-Ab1* (coding for MHCII) (Figure 1D). We first assessed cell suspensions from whole young adult mouse brains (brain, pia, arachnoid, and dura), brains with meninges removed (brain and pia), and meninges alone (arachnoid and dura). As expected (Van Hove et al., 2019), CD11a$^+$ and CD206$^+$MHCII$^+$ macrophages were enriched in meningeal fraction compared with brain only fraction, which instead was enriched in CD206$^+$MHCII$^-$ cells (Figure 1I). Thus, this gating strategy, based on signature DEGs identified by our integrated analysis, allowed us to accurately identify microglia as well as two subsets of CD206$^+$ BAMs differentially expressing MHCII, and a subset of macrophages expressing the integrin CD11a.

Having established these baselines, we moved into fate-mapping models using the recently described Ms4a3 fate mapping model that tracks contribution of blood monocytes to cell populations (Liu et al., 2019): less than 1% of microglia was labeled, while more than 87% of CD11a$^+$ macrophages were, suggesting that the latter are mostly monocyte derived. CD206$^+$MHCII$^+$ macrophages exhibited a higher amount of monocyte contribution (20%) compared with CD206$^+$MHCII$^-$ (<5%) (Figure 1J). However, we observed a slightly higher percentage of CD206$^+$MHCII$^+$ monocyte-derived cells (26%) and microglia-like monocyte-derived cells (2%–3%) in >6-month-old mice (Figure 1K). Altogether, these results show that meningeal CD206$^+$MHCII$^+$ macrophages have a higher monocytic contribution and thus are replaced to a greater extent than previously thought, compared with perivascular macrophages. This is in contrast to an initial report (Goldmann et al., 2016) but is in accordance with more recent work (Van Hove et al., 2019).

Phenotypic heterogeneity within DAM population

DAM are a population of CNS macrophages that are thought to play a protective role in mouse models of Alzheimer's disease (AD) and are also present in brain of human patients with AD (Keren-Shaul et al., 2017). Another study has suggested that DAM also accumulate in brains of aged mice, but it is debated whether their role is protective or not (Mrdjen et al., 2018). DAM were originally identified using scRNA-seq analysis as expressing high amount of *Cd11c*, *Csf1*, and *Cd9* and low amount of *Tmem119*, *P2ry12*, and *Cx3cr1* and depending on the expression of the triggering receptor expressed on myeloid cells 2 (TREM2) (Keren-Shaul et al., 2017). At this time, ontogeny of DAM remains elusive, with recent studies drawing contradictory conclusions that they could be potentially related to BAMs (Van Hove et al., 2019) or monocytes (Jay et al., 2015).

We therefore asked what the M-Verse could tell us about the nature of DAM within the context of extended brain macrophage populations across development, adulthood, aging, and neurodegeneration. We projected Keren-Shaul DAM gene expression signature (Table S2) onto Keren-Shaul dataset with M-Verse coordinates and found that cells highly expressing DAM gene signature were located in not one, but two, distinct areas: some within the developmental microglia area (DAM) and others within the mature microglia area (Figure 2A), which we will define as disease inflammatory macrophages (DIMs) due to their high expression of inflammatory genes. When we used Keren-Shaul DAM signature to screen the other datasets, we similarly observed two cell clusters in these distinct regions (Figure S2A). To assess whether the two DAM signature-expressing subsets were both equally TREM2-dependent, we compared their relative abundance in brains of aged C57BL/6 WT, 5XFAD (AD model), TREM2$^{-/-}$, and 5XFAD-TREM2$^{-/-}$ mice from Keren-Shaul dataset. We found that AD-TREM2$^{-/-}$ mice had approximately half the frequency of DAM cells in their cortex compared with AD mice, whereas DIMs markedly increased in frequency in all TREM2$^{-/-}$ mice (Figure 2B). At the RNA level, both populations highly expressed *Trem2* (Figure 2C) but differed in their expression of other markers: DAM exhibited relatively lower expression of *P2ry12* and *Cx3cr1* compared with DIMs, with higher expression of *Itgax* (*Cd11c*) (Figure 2C). Thus, the M-Verse, coupled with molecular comparisons of the cells within the two regions, has allowed us to identify two cell populations

(B) DAM and DIM percentage among total cells from Keren-Shaul mouse AD models.
(C) Relative RNA expression heatmap of specific DAM markers described by Keren-Shaul et al., projected on Keren-Shaul dataset with M-Verse coordinates.
(D) DAM cells in Keren-Shaul and Van Hove datasets with M-Verse coordinates. In blue, cells from the respective dataset and in gray, cells included in the M-Verse.
(E) Venn diagram representing the common and unique DEGs overexpressed in DAM compared with DIMs in Keren-Shaul and Van Hove datasets, establishing a DAM-conserved signature.
(F) DAM-conserved signature heatmap on Keren-Shaul and Van-Hove datasets with M-Verse coordinates.
(G) Percentage of cells in the DAM region in Van Hove and Keren-Shaul datasets for each mouse AD model.
(H) DAM-conserved signature heatmap on Hammond dataset with M-Verse coordinates.
(I) Percentage of cells in the DAM region in Hammond and Silvin C1 datasets.
(J) P7 CD11c$^+$ signature heatmap on Hammond and Silvin C1 datasets (left), Van Hove, and Keren-Shaul datasets (right), with M-Verse coordinates.
(K) Venn diagram representing common and unique DEGs between DAM-conserved signature and the P7 CD11c$^+$ signature and establishment of YAM/DAM-conserved signature.
(L) Pathways associated with DAM and/or YAM.

sharing DAM-signature gene expression but also uniquely expressing genes consistent with profound functional differences. These data strongly suggest that DAM, but not DIMs, represent *bona fide* DAM described by Keren-Shaul.

Bona fide adult DAM exhibit overlapping gene expression signatures with YAM

We then asked whether we could detect DAM cells within the other datasets used to generate the M-Verse and found that they were also present in the Van Hove dataset containing cells from APP-PS1 AD mouse model (Figure 2D). In both datasets, cells expressing DAM signature were contained within the developmental microglia area, suggesting that adult *bona fide* DAM shared patterns of gene expression otherwise typical of embryonic microglia. We therefore performed a DEG analysis comparing DAM and DIMs in both datasets, seeking to define a set of genes expressed at a higher amount in DAM and representing a truly specific signature (Figures 2E, S2B, and S2C). We found eight genes that were specifically expressed by DAM in both datasets: *Dkk2*, *Fabp5*, *Gpnmb*, *Igf1*, *Itgax*, *Mamdc2*, *Spp1*, and *Gm1673*. When we projected the mean expression amount of signature genes onto both datasets (Keren-Shaul and Van Hove overlaid) within the M-Verse to visualize the specificity of their expression (Figure 2F) and assess their frequencies in the different mice used in these studies (Figure 2G). Cells from Silvin C1 and Hammond datasets (WT mice) were present in the DAM gate (Figure 2H), but in this case, corresponding to cells from embryonic (E12.5, E14.5, and E18.5) and early post-natal (P4, P5, and P7) time points (Figure 2I). DAM-conserved expression signature for each separate dataset is presented in Figure S2D.

Together, our analysis shows that adult DAM share a common gene expression signature with developmental (fetal and early post-natal) microglia from non-AD mice, including expression of integrin *Itgax* (CD11c) already shown to be expressed on a subset of microglia named P7 CD11c$^+$ (Hagemeyer et al., 2017; Hammond et al., 2019; Li et al., 2019; Wlodarczyk et al., 2017). To understand how these two separately described cell types might be related, we projected P7 CD11c$^+$ transcriptomic signature, onto the M-Verse and observed a remarkable overlap with DAM signature from Keren-Shaul (Figures 2J and 2A). Five of the seven genes contained in our DAM-conserved signature (*Dkk2*, *Gpnmb*, *Igf1*, *Itgax*, and *Spp1*) were also expressed by P7 CD11c$^+$ cells from Hagemeyer and Wlodarczyk datasets (Figure 2K), and at embryonic time points, within Hammond and Silvin C1 datasets (Figures 2H and 2J). Thus, DAM-conserved signature seen in neurodegenerative disease closely resembles that of a group of cells present within the brains of healthy wild-type mouse embryos and neonates. Based on these observations, we propose here to call the CD11c$^+$ P7 microglia youth-associated microglia (YAM).

We next wanted to better understand similarities and differences between these two microglial subsets that share a similar gene expression signature but appear in radically different contexts. We performed a comparative pathway analysis of DEGs between YAM from Silvin C1 and Hammond datasets, and DAM from Keren-Shaul and Van Hove datasets. YAM and DAM both expressed high number of genes associated with phagocytosis, autophagy, and mitochondrial metabolism, whereas YAM exclusively expressed genes implicated in fatty acid, proline, and glutathione metabolisms, and DAM alone express genes linked with an anti-inflammatory response (Figure 2L). Thus, adult DAM appears to undergo a fetal-like reprogramming, transcriptionally converging to embryonic and neonatal YAM. However, although YAM and DAM share common patterns of gene expression, the former appears naturally during embryogenesis and the early post-natal period and represents a microglial population associated to brain development, whereas DAM, in contrast, appears uniquely in the context of neurodegeneration and may be involved in aiming to restore brain homeostasis.

DIMs appear during aging and expand in neurodegenerative diseases

We then explored the nature of the DIM population, which we first detected alongside DAM during neurodegeneration in mice (Figure 2A). When we examined other scRNA-seq datasets, we also detected DIMs in healthy aged mice in Hammond, Keren-Shaul, and Van Hove datasets (Figure 3A). To understand the kinetics of their appearance during murine lifespan, we quantified their relative abundance at the different time points from Hammond and Silvin C1 datasets: DIMs appeared after birth and increased drastically in mice older than a year (Figure 3B). In neurodegenerative states studied by Van Hove and Keren-Shaul datasets, DIMs were more abundant compared with age-matched WT mice (Figures 3C, S2E, and S2F). Strikingly, and in contrast to DAM, DIMs drastically increased in frequency in AD-TREM2$^{-/-}$ mice in Keren-Shaul dataset, showing their TREM2 independence (Figures 2B, 3C, and S2E). By comparing gene expression data from Hammond, Keren-Shaul, and Van Hove datasets, we then established a DIM-conserved signature that included genes linked to the pro-inflammatory response and immune activation including *Il1a*, *Il1b*, *Tnf*, *Nfkbia*, *Cd49f*, *Cd54*, and *Cd83* (Figures 3D, 3E, and S2G). This signature was enriched in DIM area compared with the rest of the M-Verse. Thus, given such high expression amount of inflammation-related genes and their increase in frequency in the context of neurodegenerative conditions, we named this population expressing TREM2 (Figure 2C), but TREM2-independent (Figures 2B, 3C, and S2E) disease inflammatory macrophages (DIMs). By performing pathway analysis of the genes exclusively expressed by DIMs compared with DAM, we observed that DIMs expressed higher amount of genes involved in many inflammation-related pathways, among them *Tnf*, *Il6*, and *Il1*, as well as Toll-like receptor signaling and production of nitric oxyde (NO) and reactive oxygen species (ROS) (Figure 3F), consistent with a potential pro-inflammatory status. However, we also observed some immunosuppressive pathways, including IL-10 signaling, glucocorticoid receptor signaling, and peroxisome proliferator-activated receptor (PPAR) signaling (Figure 3F) due to expression of genes such as *Ccr5*, *Il10ra*, *Tnf*, *Hsp90aa1*, *Cited2*, *Icam1*, *Ccl2*, *Stat1*, *Fcgr1a*, and *Adbr2*, likely reflecting a feedback loop integrating an inflammatory environment (Shemer et al., 2020). However, no notable expression of gene coding for immunosuppressive cytokines and chemokines was observed.

Brain inflammation induces the accumulation of monocyte-derived CD83$^+$ DIMs

Alongside the inflammatory environment that characterizes neurodegeneration in mice, we also wanted to understand whether

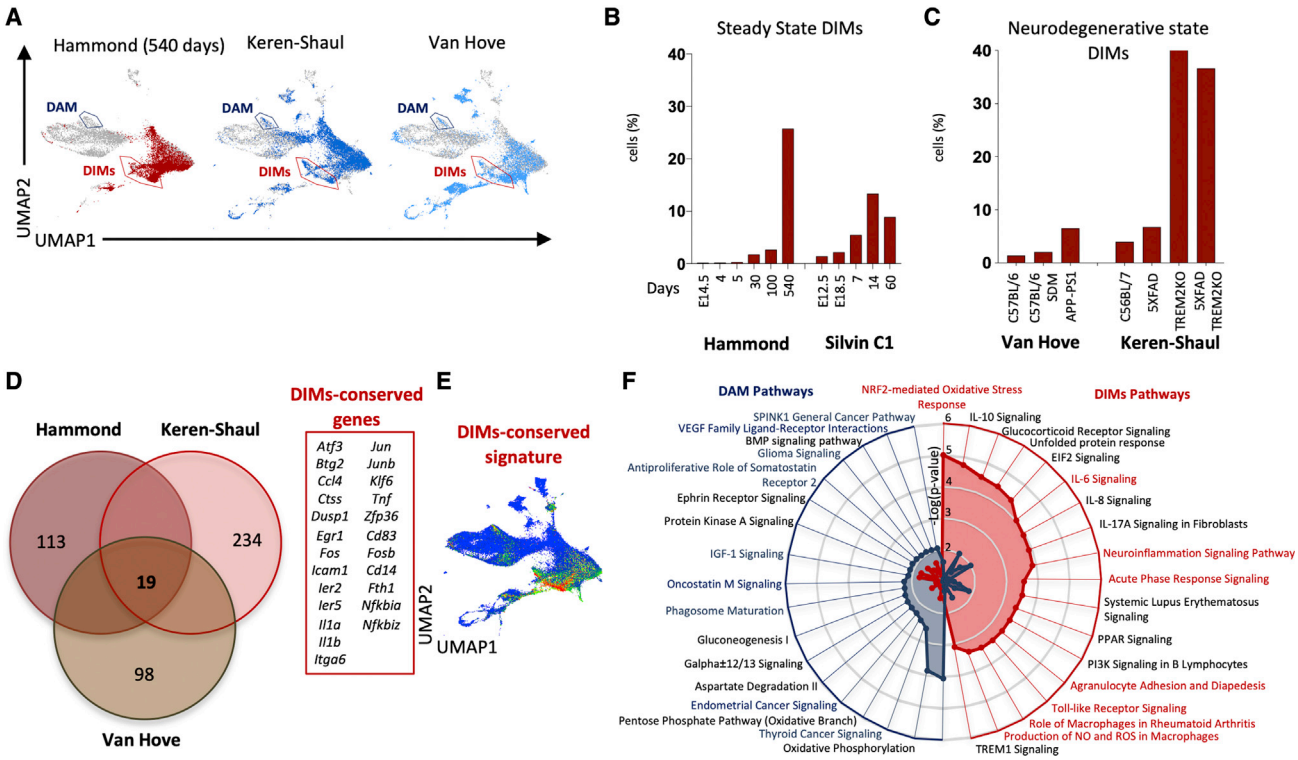

Figure 3. DIMs increase in frequency during aging and in AD murine models

(A) Visualization of DAM and DIM regions on Hammond, Keren-Shaul, and Van Hove datasets with M-Verse coordinates. Color: cells from old mice in each dataset; gray: cells from other datasets.

(B) DIM percentage in Hammond and Silvin C1 datasets.

(C) DIM percentage in Van Hove and Keren-Shaul datasets.

(D) Venn diagram showing common and unique DEGs expressed at a higher level in DIMs compared with DAM in Hammond, Keren-Shaul, and Van Hove datasets and establishment of a DIM-conserved gene signature.

(E) DIM-conserved signature heatmap among all the M-Verse.

(F) Pathways associated with DAM or DIM signatures.

DAM/DIMs-like cells appeared when the CNS is inflamed in other contexts. In humans, cranial ionizing radiation exposure induces progressive cognitive dysfunction and neuroinflammation that is associated with release of pro-inflammatory cytokines such as TNF-α, IL-1α, and IL-6 in mice (Greene-Schloesser et al., 2012; Lee et al., 2012; Parihar et al., 2015). A related process of microglial depletion followed by irradiation and congenic BM transfer leads to monocytes infiltrating the brain and giving rise to cells similar to microglia (Cronk et al., 2018; Lund et al., 2018). Aiming to bridge these observations, we investigated the presence of monocyte-derived macrophages and microglia-like cells in the brain after ionizing radiation to understand whether they might be related to DIMs or DAM. We generated BM chimeras by irradiating 1-month-old C57BL/6 WT mice and reconstituting their BM with cells from *Ms4a3*^{Cre}*Rosa*^{Tomato} mice, before analyzing their brains 5 or 10 months later (Figure S3A). After engraftment, the amount of Ms4a3-TdT^{+} monocytes was over 96% (Figure S3B), but at steady state, fewer than 25% of brain macrophages (identified based on expression of CD45, CD11b, F4/80, and low amount of Ly6C) expressed Ms4a3CreRosaTomato even at 10 months post-reconstitution (Figure S3C). In contrast, after irradiation, there was a significantly increase in monocyte-derived macrophages, reaching over 20% at later time point (Figure S3C). These Ms4a3-TdT^{+} macrophages expressed higher amount of F4/80 and CD83 and lower amount of CD206 compared with their non-monocyte-derived counterparts in the brain (Figure S3D). We then confirmed the presence of Ms4a3-TdT^{+} macrophages in the brain by microscopy. This revealed that Ms4a3-TdT^{+} cells also expressed IBA1^{+} and were found in diverse brain regions (Figure S3E).

The high amount of CD83 expression on Ms4a3-TdT^{+} macrophages in post-irradiation brain were particularly interesting to us because *Cd83* was one of the genes specifically overexpressed in DIMs, based on the M-Verse. Therefore, we sorted and compared CD83^{+}Ms4a3-TdT^{+} macrophages, microglia CD83^{+}Ms4a3-TdT^{-}, and microglia CD83^{-}Ms4a3-TdT^{-} by transmission electron microscopy (TEM) and H&E staining. Compared with microglia, CD83^{+} Ms4a3T-TdT^{+} macrophages were larger and contained more intracellular vesicles (Figure S3F), which likely correspond to lipid droplets visible by TEM (Figure S3G). We also performed bulk RNA-sequencing on these populations to compare their profiles of gene expression and understand how they might be related to DAM and DIMs (Figure 4A). The three cell populations were sorted based on their expression of CD45, F4/80, CD11b, Ly6C, CD83,

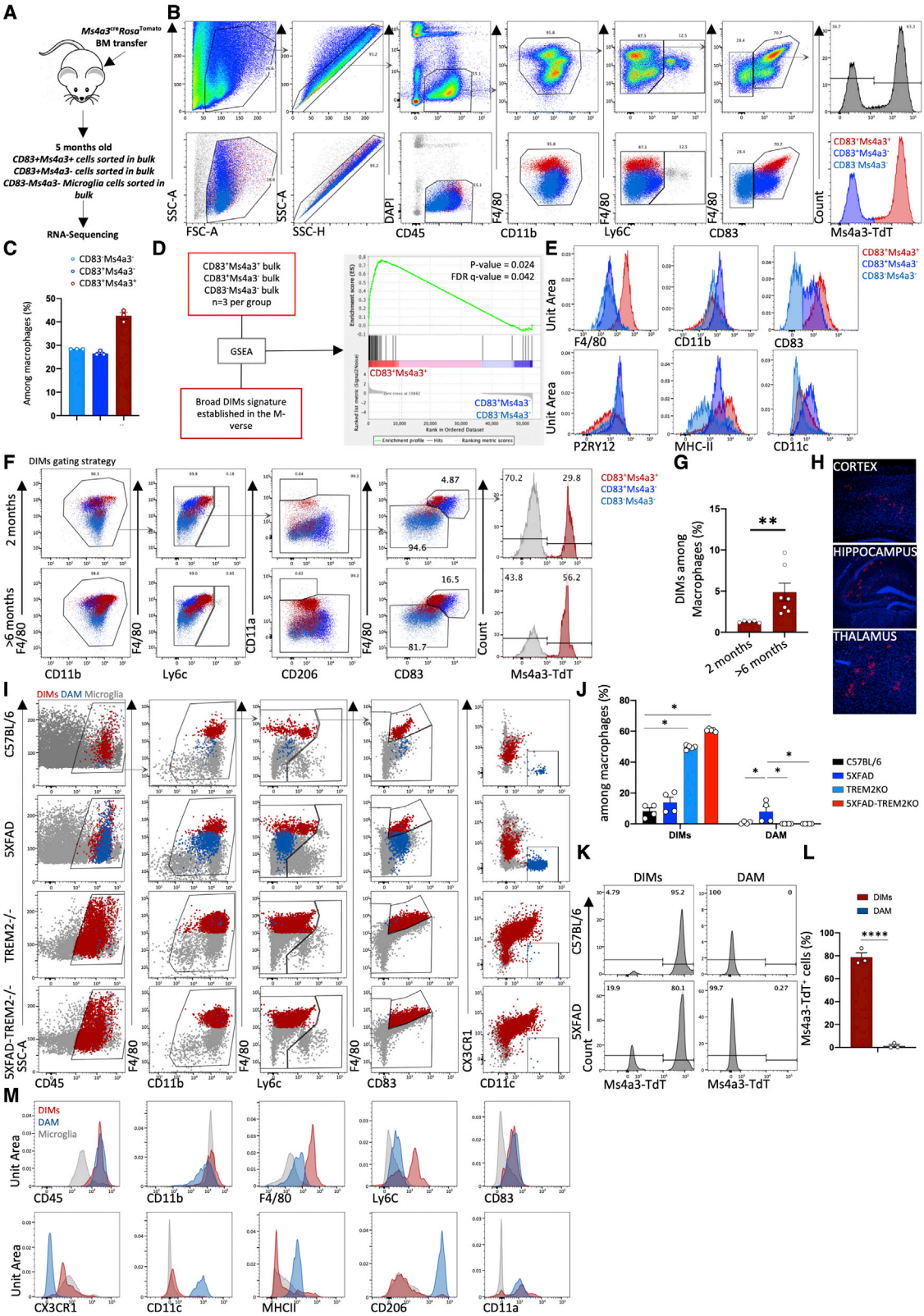

Figure 4. DIMs are monocyte derived, whereas DAM are embryonic derived

(A) Schematic overview of irradiated mice and cell populations sorted from 5-month-old mice brain.

(B) Gating strategy to sort corresponding populations (top panel). Visualization of the three cell populations along the gating strategy (bottom panel).

(legend continued on next page)

and Ms4a3-TdT (gating strategy shown in Figure 4B top panel): approximately 30% of all brain macrophages corresponded to CD83$^-$Ms4a3-TdT$^-$ microglia, 30% to CD83$^+$Ms4a3-TdT$^-$ microglia, and 40% to CD83$^+$Ms4a3-TdT$^+$ macrophages (Figure 4C). We first asked whether any of these three populations corresponded to DIMs at RNA level using a gene set enrichment analysis (GSEA) based on the broader DIM gene signature established by the M-Verse (Table S1). GSEA showed a clear DIM signature enrichment exclusively in the CD83$^+$Ms4a3-TdT$^+$ macrophage population (Figures 4D and S3H). Extending this to protein amount analysis, CD83$^+$Ms4a3-TdT$^+$ macrophages expressed similar amount of CD11c and CD11b compared with CD83$^-$Ms4a3-TdT$^-$ microglia but slightly lower amount of P2RY12 and higher amount of MHCII on their surface (Figure 4E). 68 genes significantly differed in expression amount between CD83$^+$Ms4a3-TdT$^+$ macrophages and CD83$^+$Ms4a3-TdT$^-$ microglia (data not shown), including *Axl*, *Irf7*, and *Clec12a* and genes involved in neuroinflammatory signaling pathways, which were uniquely upregulated in CD83$^+$Ms4a3-TdT$^+$ DIMs (Figure S3I). These results show that post-irradiation brain monocyte-derived macrophages are characterized by a higher expression of CD83 and F4/80 at their surface and express genes corresponding to the DIM population defined in the M-Verse.

Finally, we used the *Ms4a3*^{Cre}*Rosa*^{Tomato} model to monitor the quantity of DIMs in brains from two and >6-month-old mice and confirm their accumulation during aging. Using a similar gating strategy (Figure 4F), we uncovered a significant increase of DIM proportions among macrophages (Figures 4F and 4G) in young adult (2 months old) compared with adult mice (>6 months old). In comparison, frequencies of CD83$^-$Ms4a3-TdT$^-$ and CD83$^+$Ms4a3-TdT$^-$ microglia were not altered during this time (Figures S3J and S3K). These DIMs were localized in the hippocampus, thalamus, and cortex (Figure 4H). In conclusion, DIMs are monocyte-derived macrophages that accumulate in the brain with aging.

Monocyte-derived DIMs and YS-derived DAM accumulate in the brains of 5XFAD mice

We then assessed the presence of DIMs and DAM in the brain of 12-month-old C57BL/6-*Ms4a3*^{Cre}*Rosa*^{Tomato}, 5XFAD-*Ms4a3*^{Cre}*Rosa*^{Tomato}, C57BL/6-TREM2$^{-/-}$, and 5XFAD-TREM2$^{-/-}$ mice using flow cytometry to formally assess their ontogeny. Applying our previous gating strategy (Figure 4B) and adding antibodies targeting CX3CR1, CD11c, CD206, and CD11a, we observed an increase in percentage of DIMs (high expression of CD83 and F4/80, deep red dots) and DAM (high expression of CD11c and low expression of CX3CR1, deep blue dots) among total brain macrophages in AD versus WT mice (Figures 4I and 4J). DAM frequency was drastically decreased in TREM2$^{-/-}$ and AD-TREM2$^{-/-}$ mice, as described in the Keren-Shaul dataset, whereas we found that DIM frequency was significantly increased in these two models (Figures 4I and 4J). Most DIMs expressed high amount of Tomato reporter, confirming their monocytic origin, whereas DAM did not, confirming their embryonic origin (Figures 4K and 4L). Phenotypically, DIMs in AD model were characterized by the expression of higher amount of CD45, F4/80, CD83, and Ly6C compared with microglia, whereas DAM were characterized by higher expression of CD45, CD83, CD206, CD11c, and a lower amount of CX3CR1 compared with microglia (Figure 4M). These observations reveal that DAM and DIMs are two ontogenetically distinct cell lineages that can be distinguished by F4/80, CD83, CX3CR1, CD11c, and CD206 expression amount and exhibit differential reliance upon TREM2, but both accumulate during neurodegeneration.

DIMs co-localize with amyloid beta aggregates in AD mouse brains

We next used 5XFAD-*Ms4a3*^{Cre}*Rosa*^{Tomato} model to ask about the distribution of DIMs within AD brain. By examining whole-brain slices by immunofluorescence microscopy, we observed that DIMs were not uniformly distributed but rather localized as clusters within the hippocampus, meninges, basolateral amygdala, and cortex (Figures 5A and 5B). We also confirmed *in vivo* their phenotype: Ms4a3-TdT$^+$ DIMs expressed similar amount of Iba1 compared with Ms4a3-TdT$^-$ microglia (Figures 5C and 5D) and significantly higher amount of F4/80 (Figures 5C and 5E). We then examined DIMs clustering in more detail using spatial density estimation, revealing a marked overlap between DIMs clusters and some of the brain areas with high amyloid beta (Aβ) aggregate density (Figures 5F and 5G). At the individual cell level, three-dimensional image reconstructions showed DIMs in very close contact with Aβ aggregates of various sizes, sometimes almost as big as DIMs themselves (Figures 5H and 5I). However, it seemed that there were population-level limits to the extent of DIM co-localization with Aβ aggregates: local DIM density increased until a certain regional aggregate density was reached (plaque density from 0.0010 to 0.0013), above which, the number

(C) Histogram percentages of sub-populations among all brain macrophages (n = 3).
(D) GSEA enrichment analysis of DIM signature established in the M-Verse among the three brain macrophage populations sorted from irradiated mice.
(E) Flow cytometry measurement of F4/80, CD11b, CD83, P2RY12, MHCII, and CD11c expression by indicated populations.
(F) Gating strategy to delineate brain DIMs among brain cells from *Ms4a3*^{cre}*Rosa*^{Tomato} 2- and >6-month-old mice. Representative dot plot.
(G) Histogram showing DIM percentage among all brain macrophages (n > 5).
(H) Zoom on the three areas enriched in Ms4a3-TdT$^+$ cells in >6-month-old mouse brain, representative of 3 mice.
(I) Representative gating strategy for the identification of DIMs (red) and DAM (blue) in C57BL/6, 5XFAD, TREM2$^{-/-}$, and 5XFAD-TREM2$^{-/-}$ 12-month-old mice. One-way ANOVA *p value < 0.05.
(J) Histogram showing DIM and DAM percentage among all macrophages in C57BL/6, 5XFAD, TREM2$^{-/-}$, and 5XFAD-TREM2$^{-/-}$ mice (12 months old; one-way ANOVA *p value < 0.05).
(K) Histogram showing Ms4a3-TdT expression among DIMs and DAM from 12-month-old C57BL/6 and 5XFAD mice (representative n = 4).
(L) Histogram showing Ms4a3-TdT$^+$ percentage among DIMs and DAM in 12-month-old 5XFAD mice (n = 3).
(M) Histogram showing CD45, CD11b, F4/80, Ly6C, CD83, CX3CR1, CD11c, MHCII, CD206, and CD11a expression among DAM, DIMs, and microglia (12-month-old 5XFAD mice).
Mann-Whitney test **p value < 0.01, ****p value < 0.0001.

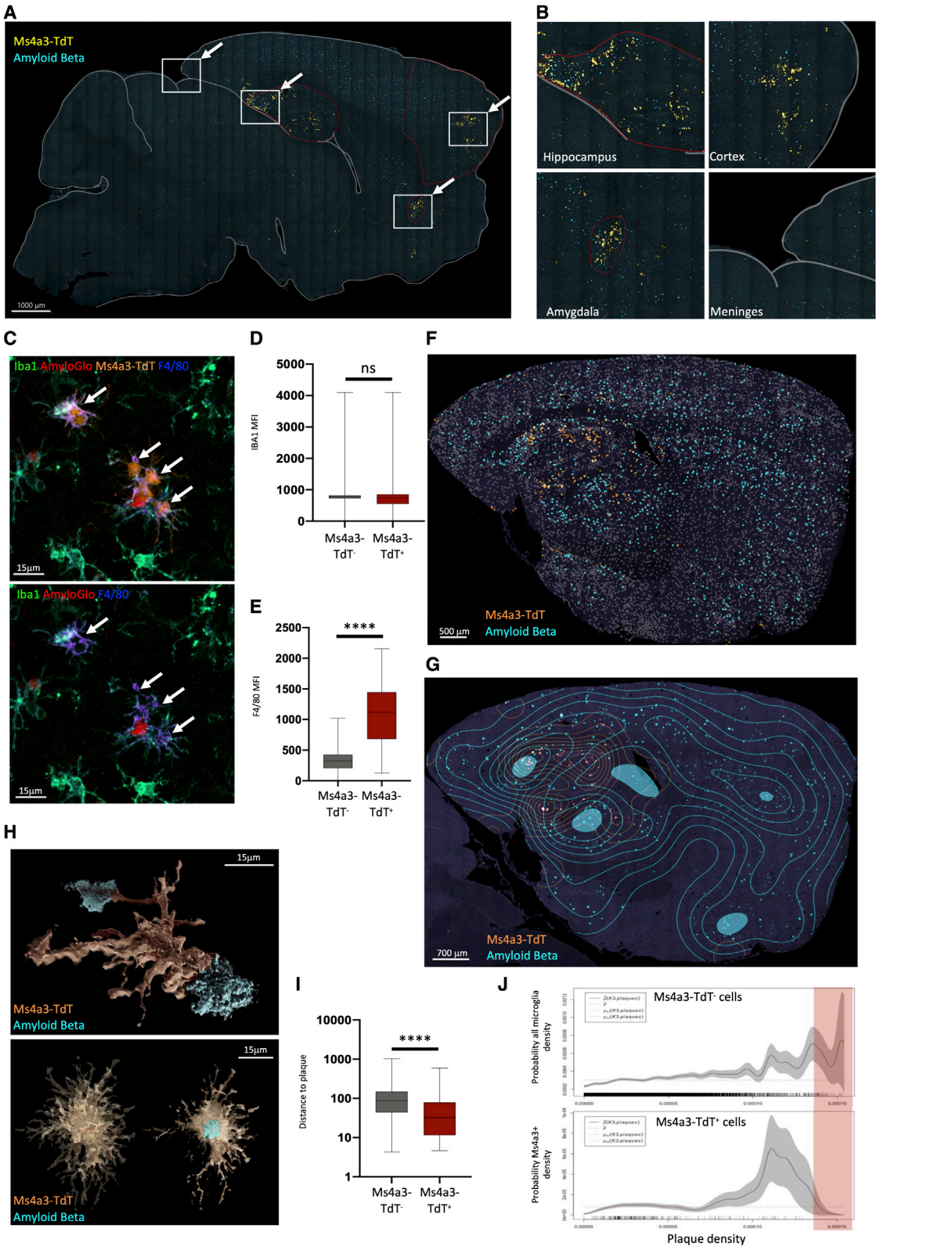

Figure 5. DIM clustering in 12-month-old 5XFAD mice specific brain regions

(A) Full brain slice imaging of Ms4a3-TdT$^+$ and Aβ aggregates. White square, area enriched in Ms4a3-TdT$^+$ cells.

(B) Areas enriched in Ms4a3-TdT$^+$ cells from (A).

(legend continued on next page)

of DIMs decreased dramatically, whereas Ms4a3-TdT^{-} microglia kept clustering (Figure 5J). These results suggest that DIMs accumulate in specific brain areas (hippocampus and basolateral amygdala) which do not correspond to DAM area showed to be in the cortex (Keren-Shaul et al., 2017). Thus, DIMs can be found near Aβ plaques, but only up to a certain aggregate density, above which, in turn, microglia are more likely to come into contact with Aβ plaques (Figure S4A).

DIM, DAM, and YAM equivalents are present in human fetal and AD brains

To understand how our observations relate to human brain, we first reanalyzed human adult scRNA-seq brain dataset from Thrupp et al., using Seurat V3 (Thrupp et al., 2020). We identified 18 clusters of cells (Figure S4B), including BAMs (*MRC1*, *F13A1*), CD14^{+} and CD16^{+} monocytes (*FCGR1A*, *FCGR3A*, *HMGB1*), microglia (*CX3CR1*, *P2RY12*), and contaminating astrocytes (*SNAP25*) and oligodendrocytes (*PLP1*) (Figure S4B). When we examined the microglia cluster in more detail, nine sub-clusters emerged (Figures 6A and S4B), with similar DEGs found in mouse DIMs or DAM signatures: clusters 11Up, 11Down, and 9 differentially expressed some DAM signature genes, whereas clusters 12, 14, and 15 differentially expressed some DIM signature genes (Figure 6B). However, only cluster 11Up cells exhibited significantly lower expression of *CX3CR1* and *P2RY12*, in combination with higher expression of *GPNMB*, *SPP1*, *APOE*, *TREM2*, *CD63*, and *ITGAX*, which corresponded to murine DAM profile (Figure 6B). Alongside, only cluster 12 displayed higher amount of expression of *CD83*, *EGR1*, *IER2*, *FOS*, *JUN*, and *AXL* together compared with other clusters, corresponding to murine DIM profile (Figure 6B). Overall, cluster 11Up highly expressed eight of the 20 genes characterized in murine broad DAM signature (*B2M*, *CD63*, *MAMDC2*, *CCL3*, GPNMB, *SPP1*, *TYROBP*, and *TREM2*), whereas cluster 12 expressed 15 of the 40 genes characterized in broad DIM murine signature (*CCL4*, *CD14*, *CD83*, *CSF2RA*, *EIF1*, *FOS*, *IER2*, *JUN*, *JUNB*, *IL1B*, *TNF*, *PLAUR*, *SAT1*, and *BTG2*) (Figure 6C). We then used the total DEGs of cluster 11Up and 12 to determine pathways in which these cells were enriched and again found substantial overlap: eight of the top 15 pathways in cluster 11up were also enriched in mouse DAM (pathways highlighted in blue Figure 6D), and seven of the top 19 pathways in cluster 12 were shared with human DIMs (pathways highlighted in red Figure 6D). Thus, we may consider cluster 11up the likely human equivalent of murine DAM, and cluster 12 the likely counterpart of murine DIMs.

To identify human YAM, DAM-like cell population present in the normally developing brain, we integrated Thrupp dataset with the human embryonic scRNA-seq dataset (brain from 13- to 18-week fetuses) from Kracht et al., (Kracht et al., 2020), based on 8,000 genes in common to both datasets. We also performed clustering on Kracht dataset using similar parameters to those used for Thrupp dataset (Figure S4B). By applying the human DIMs (cluster 12) and DAM (cluster 11Up) parameters generated above, we were not only able to identify these clusters not only within the integrated Thrupp dataset (Figure 6E), but also assess their parallels within the integrated Kracht dataset (Figure 6F). This revealed a clear cluster of DAM-like cells in fetal brains from Kracht dataset, thereby representing the human equivalent of murine YAM. By looking at the transcriptional data of cells within this cluster, we were able to define a human YAM signature (Figure 6F). We also uncovered similar patterns in the relative abundance of DIMs, DAM, and YAM in embryonic and aged humans: in adult Thrupp dataset, there was a higher proportion of DIMs and a lower proportion of DAM (Figure 6G), whereas in the fetal Kracht dataset, we observed a high proportion of YAM and a very low proportion of DIMs (Figure 6H). Human YAM also expressed high amount of genes involved in similar metabolic pathways as in murine YAM, including pathways linked to proteolysis, mitochondria organization, glutathione redox, and oxydation phosphorylation (OXPHOS) (Figure S4C). These cells further displayed even higher lipid alteration and degradation pathway enrichment than their murine counterparts (Figure S4C). Among cellular processes and signaling pathways that were commonly enriched in mouse and human YAM, we found neurodegenerative diseases and brain development pathways (Figure S4D), further suggesting that the DAM program and functions are indeed a program shared with YAM during embryonic development stages. In conclusion, DIMs, DAM, and YAM scRNA-seq profiles identified in mice can be extended to humans and the program of these three different populations during brain development, aging, and neurodegeneration appears to be conserved between the two species.

CD83^{+}TNF-α^{+} DIMs accumulate in AD-patient leptomeninges

We next asked whether DIMs exhibited the same pattern of distribution and Aβ plaque co-localization as seen in AD mouse model in human (Table S3). We performed P2RY12, CD83, Aβ, and TNF-α immunohistochemistry on brain slices from patients with AD and non-AD controls and found P2RY12^{+}CD83^{+} cells in the leptomeninges (Figures 6I and 6J), but not in the parenchyma (Figure S4E), of AD patients. When we looked at the localization of Aβ and DIMs, we found Aβ aggregates around blood vessels in leptomeninges (Figure 6J) and inside the cortex of the brain parenchyma (Figure S4E); similarly, there were significantly higher densities of P2RY12^{+}CD83^{+}TNF-α^{+} cells in AD-patients leptomeninges compared with non-AD

(C) Iba1 and F4/80 expression by Ms4a3-TdT^{+} cells and amyloGlo.
(D) Iba1 expression intensity among microglia and Ms4a3-TdT^{+} cells (n = 3).
(E) Intensity of F4/80 expression among microglia and Ms4a3-TdT^{+} cells (n = 3).
(F) Analysis of the distribution of Aβ aggregates and Ms4a3-TdT^{+} cells.
(G) Density analysis of the distribution of Aβ aggregates and Ms4a3-TdT^{+} cells.
(H) 3D reconstruction of Ms4a3-TdT^{+} cells interacting with Aβ aggregates without (top panel) or with (bottom panel) transparency.
(I) Histogram of the distance-to-plaque (μm) from microglia or Ms4a3-TdT^{+} cells (n = 3).
(J) Microglia or Ms4a3-TdT^{+} cell density analysis depending on plaque density.
Mann-Whitney test ****p value < 0.0001.

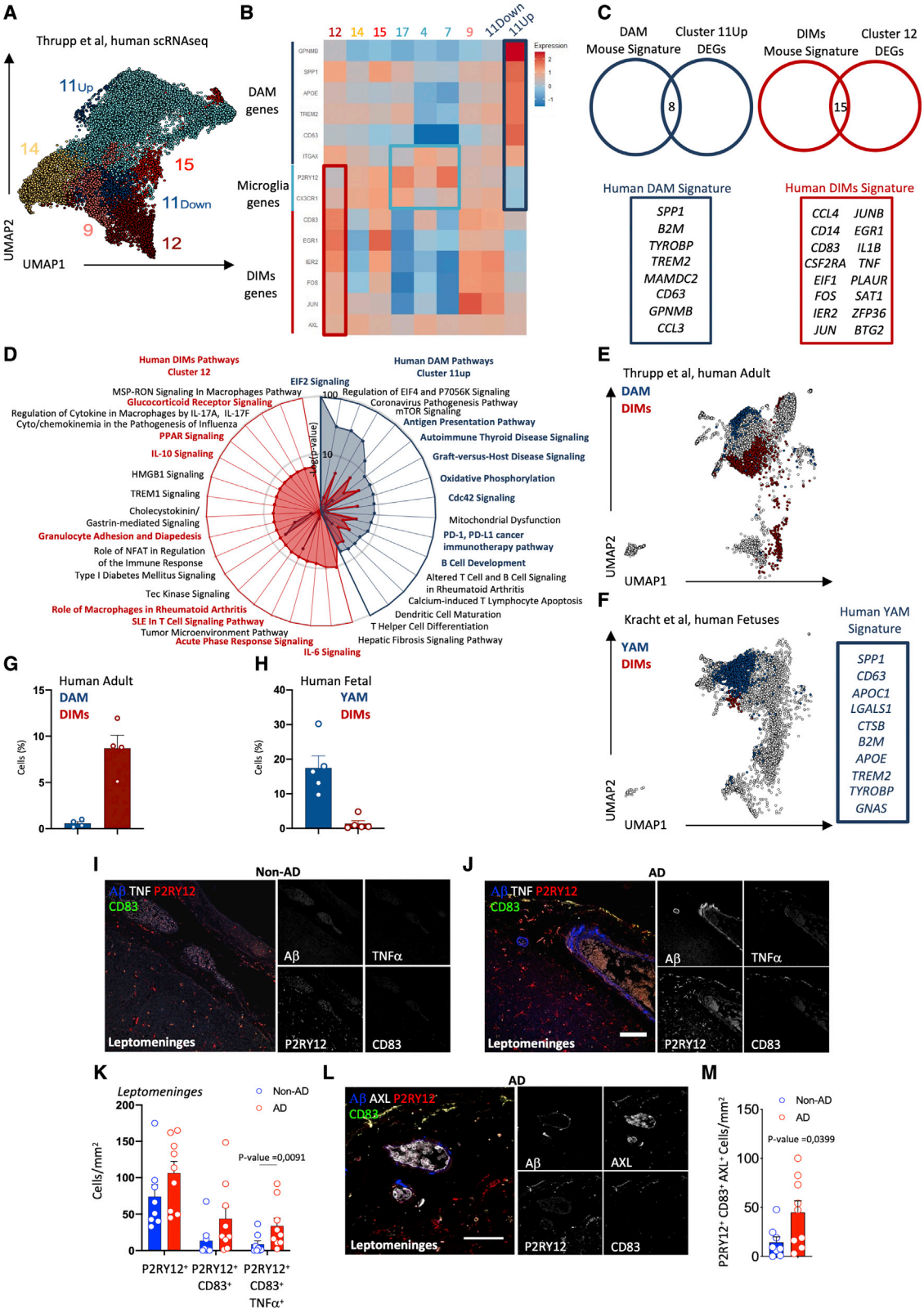

Figure 6. Increased number of P2RY12^{+}CD83^{+}TNF^{+} cells in AD patient cortical leptomeninges

(A) Thrupp dataset UMAP. Annotated clusters expressing genes in common with DIMs or DAM.

(B) Microglia, DAM, or DIM genes heatmap (mean expression per cluster).

(legend continued on next page)

patients (Figures 6J and 6K). The P2RY12 signal was higher in samples of leptomeninges from patients with AD compared with non-AD controls (Figure 6K). Moreover, there was a significantly higher density of P2RY12^{+}CD83^{+} cells expressing the DIMs-signature-associated molecule AXL in leptomeninges from AD compared with non-AD brains (Figures 6L and 6M). Thus, cells expressing DIM markers including CD83 and TNF-α accumulate around AD-patients leptomeninges, where they may be involved in the neuroinflammation typically seen in these regions during AD.

DISCUSSION

Here, using the integration of multiple brain immune scRNA-seq datasets across stages of development and disease, first in mice and then in humans, we comprehensively map the landscape of macrophages and microglia in the brain, highlighting the population's complexity and heterogeneity especially in the context of aging and neuroinflammation.

M-Verse generation through the integration of six diverse datasets allowed us to create an immune cell map spanning the distance from embryonic development to aging and neurodegeneration, unraveling the complexity of microglia and macrophage subsets. Moving on to investigate DAM heterogeneity, we uncovered that the gene signature initially used to define this population could be further deconvoluted, revealing two ontogenetically and functionally distinct cell lineages. Embryonic-derived DAM appear only in the context of neurodegeneration and not significantly during normal aging, whereas monocyte-derived DIMs accumulate with age, during inflammation and AD neurodegeneration. These observations parallel those in a mouse model of Niemann Pick disease (Gabandé-Rodríguez et al., 2019) that suggested the coexistence of microglial subsets playing antagonistic roles: in that study, mutated microglial cells clearly exhibited neurodegenerative functions due to the mutation inducing lysosomal lipid overloading. However, when all microglia and macrophages were depleted, disease progression worsened, suggesting that another subset of cells played a neuroprotective function. A recent article highlighting the localization of DAM in the cortex of AD mice suggested that these cells shared an embryonic origin with microglia because impairing microglia proliferation affected DAM proportions (Hu et al., 2021). The canonical DAM initially described by Keren-Shaul et al., also localized within the embryonic microglia cluster in this study, suggesting that DAM in the context of neurodegeneration may undergo a developmental-like transcriptional reprogramming, coming to resemble patterns of gene expression typically observed in CD11c^{+} microglia (initially described as CD11c^{+} microglia: re-termed here as YAM) during embryogenesis and in early post-natal stages. In addition, Li et al., characterized cells enriched in the white mater and highly proliferating expressing *Spp1*, *Gpnmb*, *Apoe*, *Tyrobp*, and *Igf1* genes that are highly enriched in YAM and called them proliferative-region associated microglia (PAM) (Li et al., 2019) or axon track microglia (ATM) (Hagemeyer et al., 2017). These P7 CD11c^{+} microglia have been found to promote myelination (Hagemeyer et al., 2017; Wlodarczyk et al., 2017), and hence, it is tempting to speculate that the transcriptionally similar DAM might exert a protective role in neurodegeneration via a putative capacity to induce remyelination for tissue repair, as suggested by Sala Frigerio et al. (2019). Further studies will be required to directly assess the roles of both YAM in embryogenesis and DAM in neurodegenerative disease.

Contrasting with DAM, we found that monocyte-derived DIMs accumulated in the brain with age. This observation suggests their increased recruitment into the brain in later life, which is in line with the proposal that the integrity of the blood brain barrier is reduced in advanced age or in neurodegeneration (Rustenhoven and Kipnis, 2019); this could be one of the first events leading to the recruitment of inflammatory cells into the CNS and their differentiation into DIMs. DIMs expressed many inflammatory genes, such as *Tnf*, as well as genes limiting tissue repair. Interestingly, these pathways may be directly linked, as TNF-α was recently described to promote expression of the transcription factor sterol regulatory element-binding protein 2, which under inflammatory conditions is thought to inhibit wound repair in murine models (Kusnadi et al., 2019). Moreover, peripheral TNF-α has been shown to increase monocyte infiltration in brain parenchyma, as well as to increase neuronal damage and synaptic loss (Paouri et al., 2017). Several of the cytokines expressed by DIMs are detected in AD patients' serum, cerebrospinal fluid, and brain samples (Jia et al., 2005; Mrak and Griffin, 2001). Finally, in the case of AD mouse models, it has been reported that anti-TNF-α may reduce the Aβ plaques density and disease progression (Shi et al., 2011; Tweedie et al., 2007). In humans, administration of Enbrel, an anti-TNF-α antibody, to patients suffering from rheumatoid arthritis reduces the risk of AD by 64% (Chou et al., 2016); however, a randomized, placebo-controlled, double-blinded phase two trial on patients with established AD showed only a trend toward improvement and no significant results (Butchart et al., 2015). These data could suggest that anti-TNF-α administered early in neurodegeneration might slow down monocyte infiltration and differentiation into DIMs in the brain, whereas, later in the disease, it is unable to reverse the phenomenon or protect the

(C) Venn diagram showing common DEGs between murine DAM signature and cluster 11Up (left panel) and between murine DIMs and cluster 12 (right panel). Identification of human DAM and DIM signatures, below.
(D) Pathways upregulated in human DAM and DIMs. In blue, common pathways with mouse DAM. In red common, pathways with mouse DIMs.
(E) Integration UMAP of adult Thrupp dataset, featuring Thrupp dataset DAM and DIMs.
(F) Integration UMAP of fetal Kracht dataset, featuring Kracht dataset YAM and DIMs.
(G) DAM and DIM percentage histogram among macrophages in Thrupp dataset.
(H) YAM and DIM percentage histogram among macrophages in Kracht dataset.
(I) Representative leptomeninges images, amyloid beta deposits (Aβ), TNF-α, CD83, and P2RY12, from non-AD patients (n = 8).
(J) Representative leptomeninges images, Aβ, TNF-α, CD83, and P2RY12, from AD patients (n = 9).
(K) P2RY12^{+}, P2RY12^{+}CD83^{+}, or P2RY12^{+}CD83^{+}TNF-α^{+} cells number per mm^{2} of leptomeninges. Two-way ANOVA with Sidak's multiple comparison test.
(L) Representative images leptomeninges, Aβ, AXL, CD83, and P2RY12 from patients diagnosed with AD (n = 9).
(M) Graphs P2RY12^{+}CD83^{+}AXL^{+} cells number in non-AD and AD groups. Two-tailed unpaired Student's t test, scale bars, 100 μm.

brain from the egregious consequences of the disease. In a recent study, Da Mesquita et al., showed that ablation of lymphatic vessels in 5XFAD mice worsened the deposition of Aβ and an associated increase in inflammatory microglial cells that could be related to DIMs (Mesquita et al., 2021).

We also observed that DIMs contained numerous lipid-droplet-like structures, which suggests that DIMs could be related to the lipid-droplet accumulating microglia (LDAM) previously described as dysfunctional and pro-inflammatory (Marschallinger et al., 2020). In addition, we found that DIMs were enriched in crucial brain regions such as the hippocampus, where "dark microglia" associated with pathologies have been described (Bisht et al., 2016). We hypothesize that DIMs, LDAM, and "dark microglia" might represent the same cell population, being inflammatory monocyte-derived macrophages and not a *bona fide* microglial population, which infiltrates the brain in aging and neuropathology.

M-Verse allowed us to cross-compare several studies and to identify and resolve important questions regarding the nature and ontogeny of the various macrophage populations conserved across datasets. Perhaps, the clearest example is the case of TREM2: mutations in the gene encoding this protein are one of the major risk factors for AD (Guerreiro et al., 2013), and TREM2 mutation is known to directly impact microglial function by impairing interaction with Aβ plaques, cell surface transport, and phagocytosis (Kleinberger et al., 2014; Song et al., 2018; Wang et al., 2016). DAM express TREM2 and depend on it for their differentiation (Keren-Shaul et al., 2017), but Jay et al., found that TREM2 is also expressed by monocyte-derived cells in the brain, although they do not require it for their development (Jay et al., 2015). Until now, reconciling these data into a coherent picture of TREM2's involvement in CNS macrophage and microglia development and functions was not possible. Here, we show that TREM2 plays a crucial role for YS-derived microglia and DAM by allowing these cells to acquire a developmental-like transcriptional program, which may support a role in tissue repair (Sala Frigerio et al., 2019), whereas TREM2 in monocyte-derived DIMs plays a different, yet undefined, role. As shown in M-Verse, although DAM was absent in AD-TREM2$^{-/-}$, the amount of DIMs increased drastically in AD-TREM2$^{-/-}$. It is tempting to speculate that such an increase in DIMs could be responsible for worsening some AD symptoms. A parallel could be made in the context of experimental autoimmune encephalomyelitis (EAE), the most commonly used experimental model for the human inflammatory demyelinating disease, multiple sclerosis (MS), in which blockade of TREM2 exacerbated its symptoms partly due to an increased monocyte-derived macrophage infiltration (Piccio et al., 2007). Thus, TREM2 as a potential therapeutic target in AD would need to be handled very carefully, since any changes could impact both neuroprotective DAM and potentially neurodegenerative DIM populations in, at present, unpredictable ways.

Limitations of the study

The transformed matrix is made in such a way that only genes common to all of the included datasets were taken forward. Consequently, some genes were lost in the process, but those included are conserved across studies and thus have a greater chance to be detected in any other study not included here. The M-Verse could continuously be improved by mapping more recent and upcoming datasets through reintegration. (https://macroverse.gustaveroussy.fr/2021_M-VERSE). In addition, we were limited in the evaluation of DIM function and contribution to the pathophysiology of AD by the absence of mouse models that could have allowed us to target or delete specifically this cell population during the course of the disease. Nevertheless, in addition to their unique pro-inflammatory RNA gene expression profile, we were able to define them using immunostaining or flow cytometry through protein expression, confirming their high expression of TNF-α and their unique accumulation in old and AD brain. Finally, full validation of the presence of such populations in the human brain and in AD patients was limited due to the scarce access to human brain samples.

STAR★METHODS

Detailed methods are provided in the online version of this paper and include the following:

- KEY RESOURCES TABLE
- RESOURCE AVAILABILITY
  - Lead contact
  - Materials availability
  - Data and code availability
- EXPERIMENTAL MODEL AND SUBJECT DETAILS
  - Animals
  - Human samples
- METHOD DETAILS
  - Preparation of cell suspensions
  - Macrophage labelling for flow cytometry
  - Flow cytometry, indexed-sort cytometry, and library generation
  - RNA-sequencing C1
  - Pre-processing, quality assessment, and scRNA-seq analysis
  - scRNA-seq dataset integration and clustering
  - Differentially expressed genes (DEGs) conserved
  - Differentially expressed genes (DEGs) integrated
  - Cibersort
  - Bone marrow transplant
  - Bulk RNA sequencing
  - Scanning electron microscopy
  - Transmission electron microscopy
  - Mouse immunofluorescence microscopy
  - Mouse immunohistochemistry
  - Microscopy
- QUANTIFICATION AND STATISTICAL ANALYSIS
  - Human immunohistochemistry
  - Human immunofluorescence microscopy

SUPPLEMENTAL INFORMATION

Supplemental information can be found online at https://doi.org/10.1016/j.immuni.2022.07.004.

ACKNOWLEDGMENTS

We thank all the laboratory's members for helpful discussions. Flow cytometry, cell sorting, and RNA library preparation were carried out on SIgN platforms

established by A*STAR Singapore. SIgN platforms are supported by a BMRC IAF311006 grant and BMRC transition funds #H16/99/b0/011 from A*STAR. S.U. is supported by DFG (448121430, 448121523, and 405969122) and by ERC starting grant (101039438). F.G. is supported by EMBO YIP, SIgN core funding (A*STAR) and Singapore NRF Senior Investigatorship (NRFI2017-02). B.M. was funded by NUHS Start-up grant (NUHSRO/2018/006/SU/01) and core funds from SIgN/A*STAR. We also thank the Electron Microscopy Unit, National University of Singapore and the Research Support Centre A*STAR Microscopy Platform for Electron Microscopy and Analysis. We thank Insight Editing London for their help.

AUTHOR CONTRIBUTIONS

Conceptualization, A.S. and F.G.; methodology, A.S., C.P., S.U., and F.G.; investigation, A.S., S.U., C.P., S.D.M., K.Y., K.M., M.S.T., O.C., and F.G.; formal analysis, A.S., C.P., X.M.Z., K.M., G.D., M.D., B.M., J.C., and F.G.; data curation, A.S., S.U., S.D.M., K.Y., L.G., D.E., Z.L., C.B., M.S.T., W.T.K., A.W., R.E., R.D., J.W.H., A.B., and S.C.; writing, A.S. and F.G.; visualization, A.S., J.C., S.G., C.A.D., I.A., J.K., and F.G.; resource, S.U., M.D., B.M., O.C., J.C., S.G., A.M.B., I.A., J.K., and F.G.; funding acquisition, F.G.; supervision, F.G.

DECLARATION OF INTERESTS

A.S. and F.G. are inventors on a patent filed, owned, and managed by A*ccelerate technologies Pte Ltd, A*STAR, Singapore, on technology related to the work presented in this manuscript.

Received: February 18, 2022
Revised: April 18, 2022
Accepted: July 7, 2022
Published: August 9, 2022

REFERENCES

Ajami, B., Samusik, N., Wieghofer, P., Ho, P.P., Crotti, A., Bjornson, Z., Prinz, M., Fantl, W.J., Nolan, G.P., and Steinman, L. (2018). Single-cell mass cytometry reveals distinct populations of brain myeloid cells in mouse neuroinflammation and neurodegeneration models. Nat. Neurosci. *21*, 541–551. https://doi.org/10.1038/s41593-018-0100-x.

Becht, E., McInnes, L., Healy, J., Dutertre, C.-A., Kwok, I.W.H., Ng, L.G., Ginhoux, F., and Newell, E.W. (2018). Dimensionality reduction for visualizing single-cell data using UMAP. Nat. Biotechnol. https://doi.org/10.1038/nbt.4314.

Bisht, K., Sharma, K.P., Lecours, C., Sánchez, M.G., El Hajj, H., Milior, G., Olmos-Alonso, A., Gómez-Nicola, D., Luheshi, G., Vallières, L., et al. (2016). Dark microglia: A new phenotype predominantly associated with pathological states. Glia *64*, 826–839. https://doi.org/10.1002/glia.22966.

Blériot, C., Chakarov, S., and Ginhoux, F. (2020). Determinants of resident tissue macrophage identity and function. Immunity *52*, 957–970. https://doi.org/10.1016/j.immuni.2020.05.014.

Butchart, J., Brook, L., Hopkins, V., Teeling, J., Püntener, U., Culliford, D., Sharples, R., Sharif, S., McFarlane, B., Raybould, R., et al. (2015). Etanercept in Alzheimer disease: A randomized, placebo-controlled, double-blind, phase 2 trial. Neurology *84*, 2161–2168. https://doi.org/10.1212/WNL.0000000000001617.

Buttgereit, A., Lelios, I., Yu, X., Vrohlings, M., Krakoski, N.R., Gautier, E.L., Nishinakamura, R., Becher, B., and Greter, M. (2016). Sall1 is a transcriptional regulator defining microglia identity and function. Nat. Immunol. *17*, 1397–1406. https://doi.org/10.1038/ni.3585.

Chou, R.C., Kane, M., Ghimire, S., Gautam, S., and Gui, J. (2016). Treatment for rheumatoid arthritis and risk of Alzheimer's disease: A nested case-control analysis. CNS Drugs *30*, 1111–1120. https://doi.org/10.1007/s40263-016-0374-z.

Cronk, J.C., Filiano, A.J., Louveau, A., Marin, I., Marsh, R., Ji, E., Goldman, D.H., Smirnov, I., Geraci, N., Acton, S., et al. (2018). Peripherally derived macrophages can engraft the brain independent of irradiation and maintain an identity distinct from microglia. J. Exp. Med. *215*, 1627–1647. https://doi.org/10.1084/jem.20180247.

Da Mesquita, S., Papadopoulos, Z., Dykstra, T., Brase, L., Farias, F.G., Wall, M., Jiang, H., Kodira, C.D., de Lima, K.A., Herz, J., et al. (2021). Meningeal lymphatics affect microglia responses and anti-Aβ immunotherapy. Nature *593*, 255–260. https://doi.org/10.1038/s41586-021-03489-0.

Deczkowska, A., Keren-Shaul, H., Weiner, A., Colonna, M., Schwartz, M., and Amit, I. (2018). Disease-associated microglia: a universal immune sensor of neurodegeneration. Cell *173*, 1073–1081. https://doi.org/10.1016/j.cell.2018.05.003.

Dobin, A., Davis, C.A., Schlesinger, F., Drenkow, J., Zaleski, C., Jha, S., Batut, P., Chaisson, M., and Gingeras, T.R. (2013). STAR: ultrafast universal RNA-seq aligner. Bioinformatics *29*, 15–21. https://doi.org/10.1093/bioinformatics/bts635.

Du, P., Kibbe, W.A., and Lin, S.M. (2008). lumi: a pipeline for processing Illumina microarray. Bioinformatics *24*, 1547–1548. https://doi.org/10.1093/bioinformatics/btn224.

Gabandé-Rodríguez, E., Pérez-Cañamás, A., Soto-Huelin, B., Mitroi, D.N., Sánchez-Redondo, S., Martínez-Sáez, E., Venero, C., Peinado, H., and Ledesma, M.D. (2019). Lipid-induced lysosomal damage after demyelination corrupts microglia protective function in lysosomal storage disorders. EMBO J. *38*, e99553. https://doi.org/10.15252/embj.201899553.

Ginhoux, F., Greter, M., Leboeuf, M., Nandi, S., See, P., Gokhan, S., Mehler, M.F., Conway, S.J., Ng, L.G., Stanley, E.R., et al. (2010). Fate mapping analysis reveals that adult microglia derive from primitive macrophages. Science *330*, 841–845. https://doi.org/10.1126/science.1194637.

Goldmann, T., Wieghofer, P., Jordão, M.J.C., Prutek, F., Hagemeyer, N., Frenzel, K., Amann, L., Staszewski, O., Kierdorf, K., Krueger, M., et al. (2016). Origin, fate and dynamics of macrophages at central nervous system interfaces. Nat. Immunol. *17*, 797–805. https://doi.org/10.1038/ni.3423.

Greene-Schloesser, D., Robbins, M.E., Peiffer, A.M., Shaw, E.G., Wheeler, K.T., and Chan, M.D. (2012). Radiation-induced brain injury: a review. Front. Oncol. *2*, 73. https://doi.org/10.3389/fonc.2012.00073.

Guerreiro, R., Wojtas, A., Bras, J., Carrasquillo, M., Rogaeva, E., Majounie, E., Cruchaga, C., Sassi, C., Kauwe, J.S.K., Younkin, S., et al. (2013). TREM2 variants in Alzheimer's disease. N. Engl. J. Med. *368*, 117–127. https://doi.org/10.1056/NEJMoa1211851.

Guilliams, M., and Scott, C.L. (2017). Does niche competition determine the origin of tissue-resident macrophages? Nat. Rev. Immunol. *17*, 451–460. https://doi.org/10.1038/nri.2017.42.

Hagemeyer, N., Hanft, K.-M., Akriditou, M.-A., Unger, N., Park, E.S., Stanley, E.R., Staszewski, O., Dimou, L., and Prinz, M. (2017). Microglia contribute to normal myelinogenesis and to oligodendrocyte progenitor maintenance during adulthood. Acta Neuropathol. *134*, 441–458. https://doi.org/10.1007/s00401-017-1747-1.

Hahne, F., and Ivanek, R. (2016). Visualizing genomic data using Gviz and bioconductor. Methods Mol. Biol. *1418*, 335–351. https://doi.org/10.1007/978-1-4939-3578-9_16.

Hammond, T.R., Dufort, C., Dissing-Olesen, L., Giera, S., Young, A., Wysoker, A., Walker, A.J., Gergits, F., Segel, M., Nemesh, J., et al. (2019). Single-cell RNA sequencing of microglia throughout the mouse lifespan and in the injured brain reveals complex cell-state changes. Immunity *50*, 253–271.e6. https://doi.org/10.1016/j.immuni.2018.11.004.

Hu, Y., Fryatt, G.L., Ghorbani, M., Obst, J., Menassa, D.A., Martin-Estebane, M., Muntslag, T.A.O., Olmos-Alonso, A., Guerrero-Carrasco, M., Thomas, D., et al. (2021). Replicative senescence dictates the emergence of disease-associated microglia and contributes to Aβ pathology. Cell Rep. *35*, 109228. https://doi.org/10.1016/j.celrep.2021.109228.

Jaitin, D.A., Adlung, L., Thaiss, C.A., Weiner, A., Li, B., Descamps, H., Lundgren, P., Bleriot, C., Liu, Z., Deczkowska, A., et al. (2019). Lipid-associated macrophages control metabolic homeostasis in a Trem2-dependent manner. Cell *178*, 686–698.e14. https://doi.org/10.1016/j.cell.2019.05.054.

Jay, T.R., Miller, C.M., Cheng, P.J., Graham, L.C., Bemiller, S., Broihier, M.L., Xu, G., Margevicius, D., Karlo, J.C., Sousa, G.L., et al. (2015). TREM2 deficiency eliminates TREM2+ inflammatory macrophages and ameliorates pathology in Alzheimer's disease mouse models. J. Exp. Med. *212*, 287–295. https://doi.org/10.1084/jem.20142322.

Jia, J.P., Meng, R., Sun, Y.X., Sun, W.J., Ji, X.M., and Jia, L.F. (2005). Cerebrospinal fluid tau, Abeta1-42 and inflammatory cytokines in patients with Alzheimer's disease and vascular dementia. Neurosci. Lett. *383*, 12–16. https://doi.org/10.1016/j.neulet.2005.03.051.

Keren-Shaul, H., Spinrad, A., Weiner, A., Matcovitch-Natan, O., Dvir-Szternfeld, R., Ulland, T.K., David, E., Baruch, K., Lara-Astaiso, D., Toth, B., et al. (2017). A unique microglia type associated with restricting development of Alzheimer's disease. Cell *169*, 1276–1290.e17. https://doi.org/10.1016/j.cell.2017.05.018.

Kleinberger, G., Yamanishi, Y., Suárez-Calvet, M., Czirr, E., Lohmann, E., Cuyvers, E., Struyfs, H., Pettkus, N., Wenninger-Weinzierl, A., Mazaheri, F., et al. (2014). TREM2 mutations implicated in neurodegeneration impair cell surface transport and phagocytosis. Sci. Transl. Med. *6*, 243ra86. https://doi.org/10.1126/scitranslmed.3009093.

Kracht, L., Borggrewe, M., Eskandar, S., Brouwer, N., Chuva de Sousa Lopes, S.M., Laman, J.D., Scherjon, S.A., Prins, J.R., Kooistra, S.M., and Eggen, B.J.L. (2020). Human fetal microglia acquire homeostatic immune-sensing properties early in development. Science *369*, 530–537. https://doi.org/10.1126/science.aba5906.

Krämer, A., Green, J., Pollard, J., and Tugendreich, S. (2014). Causal analysis approaches in ingenuity pathway analysis. Bioinformatics *30*, 523–530. https://doi.org/10.1093/bioinformatics/btt703.

Kusnadi, A., Park, S.H., Yuan, R., Pannellini, T., Giannopoulou, E., Oliver, D., Lu, T., Park-Min, K.-H., and Ivashkiv, L.B. (2019). The cytokine TNF promotes transcription factor SREBP activity and binding to inflammatory genes to activate macrophages and limit tissue repair. Immunity *51*, 241–257.e9. https://doi.org/10.1016/j.immuni.2019.06.005.

Langmead, B., Trapnell, C., Pop, M., and Salzberg, S.L. (2009). Ultrafast and memory-efficient alignment of short DNA sequences to the human genome. Genome Biol. *10*, R25. https://doi.org/10.1186/gb-2009-10-3-r25.

Lawrence, M., Huber, W., Pagès, H., Aboyoun, P., Carlson, M., Gentleman, R., Morgan, M.T., and Carey, V.J. (2013). Software for computing and annotating genomic ranges. PLoS Comput. Biol. *9*, e1003118. https://doi.org/10.1371/journal.pcbi.1003118.

Lee, M.-O., Song, S.-H., Jung, S., Hur, S., Asahara, T., Kim, H., Kwon, S.-M., and Cha, H.J.-. (2012). Effect of ionizing radiation induced damage of endothelial progenitor cells in vascular regeneration. Arterioscler. Thromb. Vasc. Biol. *32*, 343–352. https://doi.org/10.1161/ATVBAHA.111.237651.

Levine, J.H., Simonds, E.F., Bendall, S.C., Davis, K.L., Amir, E.D., Tadmor, M.D., Litvin, O., Fienberg, H.G., Jager, A., Zunder, E.R., et al. (2015). Data-Driven Phenotypic Dissection of AML Reveals Progenitor-like Cells that Correlate with Prognosis. Cell *162*, 184–197. https://doi.org/10.1016/j.cell.2015.05.047.

Li, Q., Cheng, Z., Zhou, L., Darmanis, S., Neff, N.F., Okamoto, J., Gulati, G., Bennett, M.L., Sun, L.O., Clarke, L.E., et al. (2019). Developmental heterogeneity of microglia and brain myeloid cells revealed by deep single-cell RNA sequencing. Neuron *101*, 207–223.e10. https://doi.org/10.1016/j.neuron.2018.12.006.

Liao, Y., Smyth, G.K., and Shi, W. (2014). featureCounts: an efficient general purpose program for assigning sequence reads to genomic features. Bioinformatics *30*, 923–930. https://doi.org/10.1093/bioinformatics/btt656.

Liu, Z., Gu, Y., Chakarov, S., Bleriot, C., Kwok, I., Chen, X., Shin, A., Huang, W., Dress, R.J., Dutertre, C.-A., et al. (2019). Fate mapping via Ms4a3-expression history traces monocyte-derived cells. Cell *178*, 1509–1525.e19. https://doi.org/10.1016/j.cell.2019.08.009.

Love, M.I., Huber, W., and Anders, S. (2014). Moderated estimation of fold change and dispersion for RNA-seq data with DESeq2. Genome Biol. *15*, 550. https://doi.org/10.1186/s13059-014-0550-8.

Low, D., and Ginhoux, F. (2018). Recent advances in the understanding of microglial development and homeostasis. Cell. Immunol. *330*, 68–78. https://doi.org/10.1016/j.cellimm.2018.01.004.

Lund, H., Pieber, M., Parsa, R., Han, J., Grommisch, D., Ewing, E., Kular, L., Needhamsen, M., Espinosa, A., Nilsson, E., et al. (2018). Competitive repopulation of an empty microglial niche yields functionally distinct subsets of microglia-like cells. Nat. Commun. *9*, 4845. https://doi.org/10.1038/s41467-018-07295-7.

Marschallinger, J., Iram, T., Zardeneta, M., Lee, S.E., Lehallier, B., Haney, M.S., Pluvinage, J.V., Mathur, V., Hahn, O., Morgens, D.W., et al. (2020). Lipid-droplet-accumulating microglia represent a dysfunctional and proinflammatory state in the aging brain. Nat. Neurosci. *23*, 194–208. https://doi.org/10.1038/s41593-019-0566-1.

Matcovitch-Natan, O., Winter, D.R., Giladi, A., Vargas Aguilar, S., Spinrad, A., Sarrazin, S., Ben-Yehuda, H., David, E., Zelada González, F., Perrin, P., et al. (2016). Microglia development follows a stepwise program to regulate brain homeostasis. Science *353*, aad8670. https://doi.org/10.1126/science.aad8670.

Mathys, H., Adaikkan, C., Gao, F., Young, J.Z., Manet, E., Hemberg, M., De Jager, P.L., Ransohoff, R.M., Regev, A., and Tsai, L.-H. (2017). Temporal tracking of microglia activation in neurodegeneration at single-cell resolution. Cell Rep. *21*, 366–380. https://doi.org/10.1016/j.celrep.2017.09.039.

Mrak, R.E., and Griffin, W.S. (2001). Interleukin-1, neuroinflammation, and Alzheimer's disease. Neurobiol. Aging *22*, 903–908. https://doi.org/10.1016/s0197-4580(01)00287-1.

Mrdjen, D., Pavlovic, A., Hartmann, F.J., Schreiner, B., Utz, S.G., Leung, B.P., Lelios, I., Heppner, F.L., Kipnis, J., Merkler, D., et al. (2018). High-dimensional single-cell mapping of central nervous system immune cells reveals distinct myeloid subsets in health, aging, and disease. Immunity *48*, 380–395.e6. https://doi.org/10.1016/j.immuni.2018.01.011.

Newman, A.M., Liu, C.L., Green, M.R., Gentles, A.J., Feng, W., Xu, Y., Hoang, C.D., Diehn, M., and Alizadeh, A.A. (2015). Robust enumeration of cell subsets from tissue expression profiles. Nat. Methods *12*, 453–457. https://doi.org/10.1038/nmeth.3337.

Paouri, E., Tzara, O., Kartalou, G.-I., Zenelak, S., and Georgopoulos, S. (2017). Peripheral tumor necrosis factor-alpha (TNF-α) modulates amyloid pathology by regulating blood-derived immune cells and glial response in the brain of AD/TNF transgenic mice. J. Neurosci. *37*, 5155–5171. https://doi.org/10.1523/JNEUROSCI.2484-16.2017.

Parihar, V.K., Pasha, J., Tran, K.K., Craver, B.M., Acharya, M.M., and Limoli, C.L. (2015). Persistent changes in neuronal structure and synaptic plasticity caused by proton irradiation. Brain Struct. Funct. *220*, 1161–1171. https://doi.org/10.1007/s00429-014-0709-9.

Piccio, L., Buonsanti, C., Mariani, M., Cella, M., Gilfillan, S., Cross, A.H., Colonna, M., and Panina-Bordignon, P. (2007). Blockade of TREM-2 exacerbates experimental autoimmune encephalomyelitis. Eur. J. Immunol. *37*, 1290–1301. https://doi.org/10.1002/eji.200636837.

Picelli, S., Faridani, O.R., Björklund, Å.K., Winberg, G., Sagasser, S., and Sandberg, R. (2014). Full-length RNA-seq from single cells using Smart-seq2. Nat. Protoc. *9*, 171–181. https://doi.org/10.1038/nprot.2014.006.

Robinson, M.D., McCarthy, D.J., and Smyth, G.K. (2010). edgeR: a Bioconductor package for differential expression analysis of digital gene expression data. Bioinformatics *26*, 139–140. https://doi.org/10.1093/bioinformatics/btp616.

Rustenhoven, J., and Kipnis, J. (2019). Bypassing the blood-brain barrier. Science *366*, 1448–1449. https://doi.org/10.1126/science.aay0479.

Sala Frigerio, C., Wolfs, L., Fattorelli, N., Thrupp, N., Voytyuk, I., Schmidt, I., Mancuso, R., Chen, W.-T., Woodbury, M.E., Srivastava, G., et al. (2019). The major risk factors for Alzheimer's disease: age, sex, and genes modulate the microglia response to Aβ plaques. Cell Rep. *27*, 1293–1306.e6. https://doi.org/10.1016/j.celrep.2019.03.099.

Shemer, A., Scheyltjens, I., Frumer, G.R., Kim, J.-S., Grozovski, J., Ayanaw, S., Dassa, B., Van Hove, H., Chappell-Maor, L., Boura-Halfon, S., et al. (2020). Interleukin-10 Prevents Pathological Microglia hyperactivation following

peripheral Endotoxin Challenge. Immunity *53*, 1033–1049.e7. https://doi.org/10.1016/j.immuni.2020.09.018.

Shi, J.-Q., Shen, W., Chen, J., Wang, B.-R., Zhong, L.-L., Zhu, Y.-W., Zhu, H.-Q., Zhang, Q.-Q., Zhang, Y.-D., and Xu, J. (2011). Anti-TNF-α reduces amyloid plaques and tau phosphorylation and induces CD11c-positive dendritic-like cell in the APP/PS1 transgenic mouse brains. Brain Res. *1368*, 239–247. https://doi.org/10.1016/j.brainres.2010.10.053.

Song, W.M., Joshita, S., Zhou, Y., Ulland, T.K., Gilfillan, S., and Colonna, M. (2018). Humanized TREM2 mice reveal microglia-intrinsic and -extrinsic effects of R47H polymorphism. J. Exp. Med. *215*, 745–760. https://doi.org/10.1084/jem.20171529.

Squarzoni, P., Oller, G., Hoeffel, G., Pont-Lezica, L., Rostaing, P., Low, D., Bessis, A., Ginhoux, F., and Garel, S. (2014). Microglia Modulate Wiring of the Embryonic Forebrain. Cell Rep. *8*, 1271–1279. https://doi.org/10.1016/j.celrep.2014.07.042.

Stuart, T., Butler, A., Hoffman, P., Hafemeister, C., Papalexi, E., Mauck, W.M., Hao, Y., Stoeckius, M., Smibert, P., and Satija, R. (2019). Comprehensive integration of single-cell data. Cell *177*, 1888–1902.e21. https://doi.org/10.1016/j.cell.2019.05.031.

Tay, T.L., Mai, D., Dautzenberg, J., Fernández-Klett, F., Lin, G., Sagar, N., Datta, M., Drougard, A., Stempfl, T., Ardura-Fabregat, A., et al. (2017). A new fate mapping system reveals context-dependent random or clonal expansion of microglia. Nat. Neurosci. *20*, 793–803. https://doi.org/10.1038/nn.4547.

Theocharidis, A., van Dongen, S., Enright, A.J., and Freeman, T.C. (2009). Network visualization and analysis of gene expression data using BioLayout Express(3D). Nat. Protoc. *4*, 1535–1550. https://doi.org/10.1038/nprot.2009.177.

Thrupp, N., Sala Frigerio, C., Wolfs, L., Skene, N.G., Fattorelli, N., Poovathingal, S., Fourne, Y., Matthews, P.M., Theys, T., Mancuso, R., et al. (2020). Single-nucleus RNA-seq is not suitable for detection of microglial activation genes in humans. Cell Rep. *32*, 108189. https://doi.org/10.1016/j.celrep.2020.108189.

Tweedie, D., Sambamurti, K., and Greig, N.H. (2007). TNF-alpha inhibition as a treatment strategy for neurodegenerative disorders: new drug candidates and targets. Curr. Alzheimer Res. *4*, 378–385. https://doi.org/10.2174/156720507781788873.

Van Hove, H., Martens, L., Scheyltjens, I., De Vlaminck, K., Pombo Antunes, A.R., De Prijck, S., Vandamme, N., De Schepper, S., Van Isterdael, G., Scott, C.L., et al. (2019). A single-cell atlas of mouse brain macrophages reveals unique transcriptional identities shaped by ontogeny and tissue environment. Nat. Neurosci. *22*, 1021–1035. https://doi.org/10.1038/s41593-019-0393-4.

Vieth, B., Parekh, S., Ziegenhain, C., Enard, W., and Hellmann, I. (2019). A systematic evaluation of single cell RNA-seq analysis pipelines. Nat. Commun. *10*, 4667. https://doi.org/10.1038/s41467-019-12266-7.

Wang, Y., Ulland, T.K., Ulrich, J.D., Song, W., Tzaferis, J.A., Hole, J.T., Yuan, P., Mahan, T.E., Shi, Y., Gilfillan, S., et al. (2016). TREM2-mediated early microglial response limits diffusion and toxicity of amyloid plaques. J. Exp. Med. *213*, 667–675. https://doi.org/10.1084/jem.20151948.

Wlodarczyk, A., Holtman, I.R., Krueger, M., Yogev, N., Bruttger, J., Khorooshi, R., Benmamar-Badel, A., de Boer-Bergsma, J.J., Martin, N.A., Karram, K., et al. (2017). A novel microglial subset plays a key role in myelinogenesis in developing brain. EMBO J. *36*, 3292–3308. https://doi.org/10.15252/embj.201696056.

Wynn, T.A., and Vannella, K.M. (2016). Macrophages in tissue repair, regeneration, and fibrosis. Immunity *44*, 450–462. https://doi.org/10.1016/j.immuni.2016.02.015.

Yu, G., Wang, L.-G., Han, Y., and He, Q.-Y. (2012). clusterProfiler: an R package for comparing biological themes among gene clusters. Omics *16*, 284–287. https://doi.org/10.1089/omi.2011.0118.

Zeisel, A., Muñoz-Manchado, A.B., Codeluppi, S., Lönnerberg, P., La Manno, G., Juréus, A., Marques, S., Munguba, H., He, L., Betsholtz, C., et al. (2015). Brain structure. Cell types in the mouse cortex and hippocampus revealed by single-cell RNA-seq. Science *347*, 1138–1142. https://doi.org/10.1126/science.aaa1934.

STAR★METHODS

KEY RESOURCES TABLE

REAGENT or RESOURCE	SOURCE	IDENTIFIER
Antibodies		
anti-CX3CR1 FITC (Mouse)	Biolegend	Cat# 149020
anti-CX3CR1 APC-Cy7 (Mouse)	Biolegend	Cat# 149040
anti-CD83 PE-Cy7 (Rat)	Biolegend	Cat# 121518
anti-Ly6c PerCP-Cy5.5 (Rat)	eBioscience	Cat# 45-5932-82
anti-Ly6c PE-Cy7 (Rat)	Biolegend	Cat# 128018
anti-Lyve1 Biotin (Rat)	eBioscience	Cat# 13-0443-82
anti-F4/80 PE-CF594 (Rat)	Biolegend	Cat# 123146
anti-CD45 BUV395 (Rat)	BD Bioscience	Cat# 564279
anti-CD45 APC-Cy7 (Rat)	Biolegend	Cat# 103116
anti-CD45 FITC (Rat)	Biolegend	Cat# 103108
anti-CD11b BUV737 (Rat)	BD Bioscience	Cat# 564443
anti-CD11b BV650 (Rat)	Biolegend	Cat# 101259
anti-CD44 BV605 (Rat)	Biolegend	Cat# 103047
anti-CD44 PerCP-Cy5.5 (Rat)	eBioscience	Cat# 45-5993-80
anti-CD11c BV650 (Hamster)	BD Bioscience	Cat# 564079
anti-CD206 BV786 (Rat)	Biolegend	Cat# 141729
anti-CD206 AF700 (Rat)	Biolegend	Cat# 141734
anti-P2RY12 APC (Rat)	Biolegend	Cat# 848006
anti-P2RY12 PE (Rat)	Biolegend	Cat# 848004
anti-CD49f APC-Cy7 (Rat)	Biolegend	Cat# 313632
anti-MHCII V500 (Rat)	BD Bioscience	Cat# 562366
anti-MHCII APC (Rat)	eBioscience	Cat# 17-5321-82
anti-MHCII AF700 (Rat)	eBioscience	Cat# 56-5321-82
anti-CD11a Pacific-Blue (Rat)	eBioscience	Cat# 48-0111-82
anti-CD64 PE (Mouse)	BD Bioscience	Cat# 558455
anti-CD64 BV711 (Mouse)	Biolegend	Cat# 139311
anti-CD14 V500 (Rat)	Biolegend	Cat# 123323
anti-FCERI PE-Cy7 (Hamster)	eBioscience	Cat# 25-5898-82
anti-CD90 in house coupled APC (Rat)	Bioxcell	Cat# BE0212
Streptavidin BUV737	BD Bioscience	Cat# 564293
anti-Iba1 (Rabbit)	Fujifilm	Cat# 019-19741
anti-MHCII (Rat)	eBioscience	Cat# 14-5321-85
anti-CD11a (Rat)	BD Bioscience	Cat# 553337
anti-CD206 (Rabbit)	Abcam	Cat# ab125028
anti-CD31 (Armenian Hamster)	Merck	Cat# MAB1398Z
anti-TNF (Goat)	Merck	Cat# T0813
anti-CD83 (Mouse)	R&D Systems	Cat# MAB1774
anti-P2RY12 (Rabbit)	Merck	Cat# HPA014518
anti-AXL (Goat)	R&D Systems	Cat# AF154
Chemicals, Peptides, and Recombinant Proteins		
Collagenase type IV	Sigma-Aldrich	Cat# C5138
DNAse I	Roche	Cat# 10104159001
Fetal Bovine Serum	GIBCO	Cat# 10270-106
Hoechst	Sigma-Aldrich	Cat# 33342

(*Continued on next page*)

Continued

REAGENT or RESOURCE	SOURCE	IDENTIFIER
Paraformaldehyde	Sigma-Aldrich	Cat# P6148
Percoll	GE-Healthcare	Cat# 17089101
RPMI	eBioscience\Invitrogen	Cat# 00433357
CD11b human/mouse Microbeads	Miltenyi	Cat# 130-049-601
Triton	Promega	Cat# H5142
EDTA	1st Base	Cat# BUF-3000-50
Rat serum	Sigma-Aldrich	Cat# R9759
Mouse Serum	Sigma-Aldrich	Cat# M5905
DAPI	ThermoFisher	Cat# 62248
BSA	Hyclone	Cat# SH30574.02
Sucrose	1st Base	Cat# 1090
PBS	1st Base	Cat# BUF-2040-10
Deposited Data		
Murine scRNA-Sequencing C1	Silvin et al.	GEO: GSE198531
Murine scRNA-Sequencing IS	Silvin et al.	GEO: GSE198531
Zeisel Murine scRNA-Sequencing	Zeisel et al., 2015	GEO: GSE60361
Hammond Murine scRNA-Sequencing	Hammond et al., 2019	GEO: GSE121654
Keren-Shaul Murine scRNA-Sequencing	Keren-Shaul et al., 2017	GEO: GSE98969
Van-Hove Murine scRNA-Sequencing	Van Hove et al., 2019	GEO: GSE128855
Experimental Models: Organisms/Strains		
C57BL/6j SPF	The Jackson Laboratory	N/A
C57BL/6j-LyzGFP	The Jackson Laboratory	N/A
C57BL/6j-Ms4a3creRosaTomato	Generated in the Laboratory of Dr. Florent Ginhoux	N/A
C57BL/6j-5XFAD	The Jackson Laboratory	N/A
C57BL/6j-5XFAD-Ms4a3creRosaTomato	Generated in the Laboratory of Dr. Ido Amit	N/A
C57BL/6j-TREM2KO	Generated in the Laboratory of Dr. Marco Colonna	N/A
C57BL/6j-5XFAD-TREM2KO	Generated in the Laboratory of Dr. Ido Amit	N/A
Software and Algorithms		
Bioconductor GenomicRanges v1.28.4	Lawrence et al., 2013	http://bioconductor.org/packages/release/bioc/html/GenomicRanges.html, RRID:SCR_000025
Bioconductor GenomicAlignments v1.12.2	Lawrence et al., 2013	http://bioconductor.org/packages/release/bioc/html/GenomicAlignments.html
Bioconductor DESeq2 v1.16.1	Love et al., 2014	http://bioconductor.org/packages/release/bioc/html/DESeq2.html, RRID:SCR_015687
Bioconductor Gviz v1.20.0	Hahne and Ivanek, 2016	http://bioconductor.org/packages/release/bioc/html/Gviz.html
Biolayout Express 3D 3.3	Theocharidis et al., 2009	http://www.biolayout.org/, RRID:SCR_7179
Bowtie v1.1.1	Langmead et al., 2009	http://bowtie-bio.sourceforge.net/index.shtml, RRID:SCR_005476
CIBERSORT analysis	Newman et al., 2015	https://cibersort.stanford.edu/
EdgeR package	Robinson et al., 2010	http://bioconductor.org/packages/release/bioc/html/edgeR.html
FeatureCount program	Liao et al., 2014	http://subread.sourceforge.net/
FlowJo v6.05	FlowJo	https://www.flowjo.com/
GraphPad Prism v6.05	GraphPad Software	https://www.graphpad.com/scientificsoftware/prism/

(*Continued on next page*)

Continued

REAGENT or RESOURCE	SOURCE	IDENTIFIER
Ingenuity Pathway Analysis	Krämer et al., 2014	https://www.qiagenbioinformatics.com/products/ingenuity-pathway-analysis/
R package clusterProfiler	Yu et al., 2012	http://www.rdocumentation.org/packages/clusterProfiler
R package lumi	Du et al., 2008	https://www.bioconductor.org/packages/release/bioc/html/lumi.html
STAR aligner	Dobin et al., 2013	https://github.com/alexdobin/STAR
Seurat v3	Stuart et al., 2019	https://satijalab.org/seurat/install.html
Imaris		https://imaris.oxinst.com/

RESOURCE AVAILABILITY

Lead contact

Further information and requests for resources and reagents should be directed to and will be fulfilled by the lead contact, Florent Ginhoux (Florent_ginhoux@immunol.a-star.edu.sg).

Materials availability

This study did not generate new unique reagents.

Data and code availability

The "M-Verse" can be explored and downloaded at https://macroverse.gustaveroussy.fr/2021_M-VERSE. Single-cell RNA-seq data from Silvin C1 and Silvin IS dataset have been deposited at GEO and are publicly available as of the date of publication. Accession numbers is GSE198531. Any additional information required to reanalyze the data reported in this paper is available from the lead contact upon request.

EXPERIMENTAL MODEL AND SUBJECT DETAILS

Animals

Mice used were housed in the A*STAR Biological Resource Centre (BRC) and included: C57/BL6 (The Jackson Laboratory), *Ms4a3*^{cre}*Rosa*^{Tomato} (Generated in the Laboratory of Dr. Florent Ginhoux) and Lyz2GFP (The Jackson Laboratory). Experiments using these mice were approved by the Institutional Animal Care and Use Committee of A*STAR, Singapore (Protocol 181402). Animals were bred, maintained, and used under Singaporean regulations, following the recommendations of the local ethics committee. Embryonic day (E) 0 was set as the day of vaginal plug formation on the dam, with postnatal day (P) 0 defined as the day of birth. 5XFAD, TREM2$^{-/-}$ and 5XFAD-TREM2$^{-/-}$ mice were generated as previously described (Keren-Shaul et al., 2017). 5XFAD and C57/BL6 were crossed with *Ms4a3*^{cre}*Rosa*^{Tomato} (Liu et al., 2019) to study the ontogeny of DIMs and DAM.

Human samples

Autopsy specimens of human brain and leptomeninges from non-AD (n = 8) or AD (n = 9) patients were obtained from the Department of Pathology at the University of Virginia. All samples were from consenting patients that gave no restriction to the use of their body for research and teaching (through an UVA's Institutional Review Board for Health Sciences Research). Diagnosis criteria and neuropathological score were performed following the National Institute on Aging/Alzheimer's Association guidelines 56, based on the ABC (Amyloid, Braak, CERAD) score, for seven of the AD cases; older CERAD guidelines were used to diagnose and score two of the AD cases (Table S3). All obtained samples were fixed in a 20% formalin solution and kept in paraffin blocks until further sectioning. Prior to immunohistochemical staining, slides containing 5-10 μm thick sections were heated to 70°C for 30 min, de-paraffinized and rehydrated by sequential washes (3 min each) in 100% xylene, xylene 1:1 ethanol (v/v), and 100, 95, 70 and 50% ethanol in water. Finally, tissue sections were rinsed with cold tap water.

METHOD DETAILS

Preparation of cell suspensions

Whole adult mouse brains were harvested, and the dura mater and arachnoid mater were removed from the skulls for individual analysis. Tissues were cut into small pieces and incubated in 3mL RPMI containing 10% fetal bovine serum, collagenase type IV (0.2 mg/mL, working activity of 770 U/mg) and DNAse (30 mg/mL) for one hour for brain tissue from adult and newborn mice, and 30 min for embryonic mouse tissues. Digested tissues were then passed through a blunt 19G needle to obtain a homogeneous cell suspension. In the case of C1 single-cell experiments, adult and postnatal brain cell suspensions were then resuspended in

40% isotonic Percoll and underlaid with 80% isotonic Percoll before centrifugation at 600g for 20 min at room temperature: embryonic brains for these experiments were directly processed without Percoll gradient centrifugation. For the other experiments, brain cell suspensions were instead filtered through a 70μM pore size cell strainer. The cells were washed with 14mL of FACS buffer (PBS+ 5% BSA + 2mM EDTA) and centrifuged for 4 min at 600g and 4°C before being resuspended in 1mL of FACS buffer containing 120μL of anti-mouse CD11b microbeads and incubated for 15 min at 4°C. Next, 5mL of FACS buffer were added and cells were centrifuged at 600g for 4 min at 4°C. Cells were finally resuspended in 2mL of FACS buffer and $CD11b^+$ cells were collected using the Automacs "pos-sel" function followed by centrifugation at 600g, for 4 min at 4°C.

Macrophage labelling for flow cytometry

Antibodies were diluted in blocking buffer (FACS buffer + 1% rat serum + 1% mouse serum). All antibodies were used at 1/200 dilution and applied at 100μL per brain cell suspension. Cells were incubated for 15 min with antibodies, mixing, at 4°C and then washed with 1 mL of FACS buffer, centrifuged at 600g, for 4 min at 4°C and resuspended in 200 μL of PBS+DAPI (1μg/mL).

Flow cytometry, indexed-sort cytometry, and library generation

Cell populations were identified by labelling using the antibodies listed in the key resources table, after gating for singlet live cells. Brain macrophages ($CD45^+CD11b^+F4/80^+Ly6c^-$) were indexed-sorted using the used for regular cytometry panel on a BD FACSARIAIII (BD Biosciences) into 96 well plates containing 3 μL Lysis buffer (see below) using a 70 μm nozzle. Single-cell cDNA libraries were prepared using the SMARTSeq v2 protocol (Picelli et al., 2014) with the following modifications: (i) 1 mg/mL BSA Lysis buffer (Ambion® Thermo Fisher Scientific, Waltham, MA, USA); and (ii) 200 pg cDNA with 1/5 reaction of Illumina Nextera XT kit (Illumina, San Diego, CA, USA). The length distribution of the cDNA libraries was monitored using a DNA High Sensitivity Reagent Kit on the Perkin Elmer Labchip (Perkin Elmer, Waltham, MA, USA). All samples were subjected to an indexed paired-end sequencing run of 2x151 cycles on an Illumina HiSeq 4000 system (Illumina, San Diego, CA, USA), with 300 samples/lane. To isolate cells for BM transfer, FACS was performed using a BD-Symphony. Data were analyzed using FlowJo software (Treestar).

RNA-sequencing C1

Single-cell suspensions of E16.5 mouse $CD45^{Int}F4/80^+CD11b^+Ly6c^-$ cells (300–500 cells/μL) were mixed at a 3:2 v/v ratio with C1 Cell Suspension Reagent (Fluidigm) and loaded onto a 5-10 μm-diameter C1 Single-Cell Auto Prep Integrated Fluidic Circuit (IFC; Fluidigm). LIVE/DEAD stain (2.5 μL ethidium homodimer-1 and 0.625 μL calcein AM (Life Technologies)) was diluted with 1.25 mL C1 Cell Wash Buffer (Fluidigm) and 20 μL of this solution were loaded onto the C1 IFC. After cells were captured and stained on the chip, they were imaged using phase-contrast and fluorescence microscopy before cell lysis, reverse transcription and cDNA amplification, which were performed on the IFC as specified by the manufacturer (Fluidigm Inc. protocol no. 100-5950 B1). The SMARTer Ultra Low RNA Kit (Clontech) was used for cDNA synthesis from single cells. The resulting cDNA was quantified with a Quant-iT PicoGreen dsDNA Assay Kit (PN P11496; Life Technologies), and quality was checked with High Sensitivity DNA Reagents (PN 5067-4626) according to the manufacturer's instructions (Agilent Technologies). Only cells with high-quality cDNA and concentration higher than 0.05ng/μl were processed for subsequent library preparation. The Illumina NGS library was constructed using the Nextera XT DNA Sample Prep kit (Illumina), according to the manufacturer's recommendations (protocol 100-7168 E1). Sequencing was then performed on an Illumina HiSeq2500 (Illumina) using high output mode by multiplexed single-read run with 51 cycles. The BCL files of raw sequence data were converted to FASTQ format via Illumina Casava 1.8.2. Reads were de-multiplexed according to their barcodes and quality was evaluated using FastQC. Reads were mapped to the reference genome (mm10) allowing one mismatch.

Pre-processing, quality assessment, and scRNA-seq analysis

Paired-end raw reads were aligned to the mouse reference genome (mm10) using RSEM version 1.3.0. Transcript Per Million read (TPM) values were calculated using RSEM and used for downstream analysis. Quality control, selection of highly variable genes, PCA, and differential gene analysis was performed using the Seurat R package (https://satijalab.org/seurat). Uniform Manifold Approximation and Projection (UMAP) were carried out using significant PCs (based on Seurat analysis). UMAP was run using 50 nearest neighbours (nn), a min_dist of 0.08 and Euclidean distance (Becht et al., 2018) Phenograph clustering (Levine et al., 2015) was performed using all markers or significant PCs (based on Seurat analysis) before dimension reduction. All scRNA-seq dot plots and meaning plots displaying the gene expression amount or mean signature genes were generated using SeqGec software (Flow Jo).

scRNA-seq dataset integration and clustering

Datasets were downloaded from the NIH GEO database (Van Hove dataset GSE128855; Hammond dataset GSE121654; Keren-Shaul dataset GSE98969, Zeisel dataset GSE60361) and integrated using the Seurat V3 anchoring method (Stuart et al., 2019). Briefly, the datasets were normalized independently, and the highly variable genes were identified for each dataset using the Seurat pipeline. A corrected data matrix with all six datasets was generated using the Seurat v3 anchoring procedure to allow for joint analysis: the matrix was then scaled and a Principal Component Analysis (PCA) was performed using the Seurat v3 pipeline. UMAP was performed on the 50 first Principal Components (PCs) (Becht et al., 2018). Data were then visualized using the SeqGec software (Flow Jo). Integrated clusters were established using the FindClusters function based on the shared nearest neighbor (SNN) modularity optimization clustering algorithm and using default parameters (resolution 0.8).

Differentially expressed genes (DEGs) conserved

Conserved DEG analyses were performed using Seurat v3 package (Stuart et al., 2019) for each datasets independently. DEGs obtained from the "RNA" matrix of the Seurat object were calculated on normalised values with a logFC threshold of 0.25 for each dataset. The likelihood-ratio test for single-cell gene expression (bimodal test) was used, and correction for multiple testing was carried out using the Bonferroni method. Then each DEGs list obtained for each dataset were compared using Venn Diagram to established conserved-DEG signature.

Differentially expressed genes (DEGs) integrated

Integrated DEG analyses were performed using the Seurat v3 package on all datasets together. DEGs obtained from the "RNA" matrix of the Seurat object were calculated on normalised values with a logFC threshold of 0.25 and constitute the integrated DEGs list. The likelihood-ratio test for single-cell gene expression (bimodal test) was used, and correction for multiple testing was carried out using the Bonferroni method.

Cibersort

To perform Cibersort, microglia, CD11a^{+} macrophages and CD206^{+} macrophages were isolated in bulk from brains of 2-month-old C57/BL6 mice, using a BD-FACS ARIA with the gating strategy shown in Figure 1I.

Bone marrow transplant

C57BL/6J (CD45.2) WT mice at eight weeks of age were lethally irradiated (950 rad) and then reconstituted via i.v. injection of 2.0×10^{6} total BM cells from Ms4a3creRosaTomato mice. Tissue from BM transplanted mice was analyzed when they reached five months of age.

Bulk RNA sequencing

Five hundred cells from each macrophage population (CD83^{-}Ms4a3-TdT^{-}, CD83^{+}Ms4a3-TdT^{-}, CD83^{+}Ms4a3-TdT^{+}) were isolated using a BD-FACS ARIA. Total RNA was extracted from the sorted cells using TRIzol reagent (Invitrogen), according to the manufacturer's protocol, then reverse transcribed with the SMART-seq2 protocol (Picelli et al., 2014). Samples were sequenced on an Illumina NextSeq 500 sequencer using pair-end 75 base pair reading. Sequencing data were aligned to the mouse reference genome (version mm10).

Scanning electron microscopy

For scanning electron microscopy (SEM), sorted cells were allowed to adhere onto poly-lysine- (Sigma) coated glass coverslips before fixation in 2.5% glutaraldehyde, washing, treatment with 1% osmium tetroxide (Ted Pella), and critical point drying (CPD 030, Bal-Tec). Glass coverslips were then sputter-coated with gold in a high-vacuum sputtering device (SCD005 sputter coater, Bal-Tec) and imaged with a field emission scanning electron microscope (JSM-6701F, JEOL) at an acceleration voltage of 8 kV.

Transmission electron microscopy

Flow-cytometry-sorted cells were embedded in 4% gelatin, fixed in 2.5% glutaraldehyde 0.1M HEPES (pH7.4) and post-fixed in 1% osmium tetroxide. After washing in distilled water, samples were dehydrated in ethanol (including en bloc staining with 1% uranyl acetate) and propylenoxide, embedded in epoxy resin EPON 812 (Serva) and polymerized at 60°C for 48 hours. Ultrathin sections were cut with a diamond knife (Diatome) on an EM UC7 ultramicrotome (LEICA Microsystems), collected onto Formvar-carbon-coated copper grids (EMS), post-contrasted with lead citrate and analyzed under a JEM1010 transmission electron microscope (JEOL) operating at 80 kV. Images were acquired with SIA model 12C CCD camera (16bit, 4K).

Mouse immunofluorescence microscopy

Mice were perfused with 4% paraformaldehyde, brains were dissected and post-fixed in 1% paraformaldehyde overnight at 4°C. After a second overnight incubation with 30% sucrose (Sigma-Aldrich), tissues were kept at -80°C until further processing. Using a rotary microtome cryostat (Leica, CM3050 S), 100 μm thickness sagittal brain sections were cut then blocked for 4 hours with PBS/0.1%-Tween containing 2% BSA and 5% normal rat serum. The same buffer was used to dilute the following primary antibodies/reagents for overnight incubation at room temperature: rabbit anti-mouse Iba1 (Wako), rat anti-mouse F4/80 (Biolegend; BM8), Amylo-Glo RTD Amyloid Plaque Stain Reagent (Biosensis), and DAPI (ThermoFisher). To allow effective imaging of thick volume sections, optical clearing was achieved using the Ce3D protocol (Biolegend). Volume imaging was then performed with sequential 1-photon/confocal and 2-photon excitation to better visualize tdTom fluorescence, using a Zeiss LSM 780 microscope with internal and external non-descanned GaAsP detectors and ZEN black software (Zeiss). Images were captured with a 20x water immersion objective (NA 1.0, Zeiss) as tiles at a resolution of 512x512 (16bit), in stacks with a slice distance of 3 μm over a z-range of the entire tissue volume. 1P- and 2P-stacks were computationally aligned using ZEN blue 3.2 (Zeiss), and multiplex volumetric reconstruction; visualization was performed in IMARIS 9.7 (Bitplane). Individual cell positions were defined based on the fluorescence intensity thresholds of their somata using the spot detection function in IMARIS. Border-corrected kernel density estimations of microglia (tdTom-Iba1+), DIMs (tdTom+Iba1+) and amyloid plaques (AmyloGlo+) were calculated in R studio (REF: 10.1007/s10707-015-0232-z) and displayed with and overlayed onto the original images using the *ggplot2* package. Positional data were

used to estimate the local densities of tdTom+ or tdTom- as a function of amyloid aggregate densities using the *rhohat* function of R studio's *spatstat* package (REF ISBN 9781482210200).

Mouse immunohistochemistry

Dissected brains were fixed by overnight incubation in 4% paraformaldehyde at 4°C. Immunohistochemistry was performed on 40uM thick free-floating vibratome sections, as previously described (Squarzoni et al., 2014). Non-specific antibody binding was prevented by incubating sections for 2 hours with PBS containing 10% fetal bovine serum and 0.01% Triton X-100, followed by several PBS washes, before overnight incubation with secondary antibodies (1/400 PBS). Cryo-sectioning was performed on a Leica CM3050 S Research Cryostat to give 17μM thick slices. Slides were placed in PBS+Triton 5% for 15 minutes before the addition of 100μl of blocking buffer (0.3% Triton-X-100 + BSA 0.2% in PBS + 5% DMSO + 0.1% sodium azide + 5% mouse serum) for 30 min on the slides. Next 100μL of primary antibodies diluted in blocking buffer were incubated on the slides at 4°C overnight. Following washing with PBS+5% Triton three times, 100μL of secondary antibodies diluted in blocking buffer were incubated on the slides at 4°C overnight. Slides were then washed with PBS+5% Triton three times and then once with PBS+DAPI before mounting in Prolong Diamond Anti-fade and covering with a glass-coverslip.

Microscopy

Images were acquired with a Leica TCS SP5 or an FV1000 Olympus confocal microscope, or using an Invitrogen EVOS FLAUTO2.

QUANTIFICATION AND STATISTICAL ANALYSIS

Significance for pathways analyses (Figures 1F, 3L, 4F, 5G, and S1H) was defined by the IPA software (QIAGEN). Unpaired T-tests were performed using Graphpad software.

Human immunohistochemistry

After de-paraffinization and rehydration, sections of human brain cortex and leptomeninges were submitted to heat-induced antigen retrieval using 10 mM citrate buffer for 10 min. Prior to immunofluorescence labelling, tissue sections were stained for β-sheet-enriched amyloid deposits using the Amylo-Glo® RTD™ reagent (Biosensis, Fine Bioscience Tools, South Australia), following the manufacturer's instructions. Tissue sections were then rinsed in PBS, pH 7.4, and washed with PBS 0.5% Triton-X-100 (PBS-T, Thermo Fisher Scientific) for 10 min, followed by incubation in PBS-T with 0.5% bovine serum albumin (BSA, Equitech Bio) for 30 min at room temperature (RT). This blocking step was followed by incubation with anti-TNF (Merck Sigma, T0813, lot MKCJ3649, used at 10 μg/mL), anti-CD83 (R&D Systems, MAB1774, clone HB15e, lot FUL0419071, used at 40 μg/mL) anti-P2RY12 (Merck Sigma, HPA014518, lot F119293, used at 5 μg/mL) and anti-AXL (R&D Systems, AF154, lot DMG0720031, used at 20 μg/mL) in PBS-T with 0.5% BSA, overnight at 4°C.

Human immunofluorescence microscopy

Tissue sections were then washed 3 times for 10 min each at RT in PBS-T, followed by incubation with the appropriate chicken anti-goat Alexa Fluor® 488, anti-mouse Alexa Fluor® 594 and anti-rabbit Alexa Fluor® 647 in PBS-T (at 1:500 from stock, all from Invitrogen, Thermo Fisher Scientific) for 1 hour at RT. The tissue sections were washed twice for 10 min with PBS-T and once with PBS at RT, left to dry at RT for ~5 min and mounted with Shandon™ Aqua-Mount (Thermo Fisher Scientific) and glass coverslips. Preparations were stored at 4°C for no more than one week until images were acquired using a confocal microscope (FV1200 Laser Scanning Confocal Microscope, Olympus). Acquired images of brain cortex containing leptomeninges were used for the quantification of $P2RY12^+$, $P2RY12^+CD83^+$ and $P2RY12^+CD83^+TNF^+$ cell density and of TNF amount on $P2RY12^+$ cells in the leptomeninges using the FIJI software. Briefly, five representative images of cortical leptomeninges were acquired per non-AD or AD sample; the number of each cell subtype was quantified using Fiji's Cell Counter plugin and divided by the total area (in mm2) of the region of interest (ROI, the area corresponding to the leptomeninges only). To measure the amount of TNF within $P2RY12^+TNF^+$ cells (in representative images where these cells were detected), the TNF and the P2RY12 channels were transformed into a binary signal (using the Threshold plugin in Fiji), the $P2RY12^+TNF^+$ cells were outlined with a mask, and the area corresponding to the TNF and P2RY12 signals was assessed using Fiji's Measure plugin. The area of TNF was considered "0" in representative images where leptomeningeal $P2RY12^+TNF^+$ cells were not detected. The % area of TNF labeling within $P2RY12^+$ cells in the leptomeninges was calculated by dividing the area of TNF by the area of P2RY12 in Microsoft Excel. Microsoft Excel was also used to calculate the final values (average of five representative images per sample) corresponding to cell density (cells per mm^2) and to the area % of TNF labeling within $P2RY12^+$ cells. Graphs showing comparisons between groups and statistical analysis were generated using Prism 8.3.0 (GraphPad Software, Inc.). Two-way ANOVA with Sidak's multiple comparisons test was used for multiple comparisons involving two independent variables and two-tailed unpaired Student's T test was used for comparing changes in a single variable between two groups.

Immunity, Volume *55*

Supplemental information

Dual ontogeny of disease-associated microglia and disease inflammatory macrophages in aging and neurodegeneration

Aymeric Silvin, Stefan Uderhardt, Cecile Piot, Sandro Da Mesquita, Katharine Yang, Laufey Geirsdottir, Kevin Mulder, David Eyal, Zhaoyuan Liu, Cecile Bridlance, Morgane Sonia Thion, Xiao Meng Zhang, Wan Ting Kong, Marc Deloger, Vasco Fontes, Assaf Weiner, Rachel Ee, Regine Dress, Jing Wen Hang, Akhila Balachander, Svetoslav Chakarov, Benoit Malleret, Garett Dunsmore, Olivier Cexus, Jinmiao Chen, Sonia Garel, Charles Antoine Dutertre, Ido Amit, Jonathan Kipnis, and Florent Ginhoux

Supplemental Information

Dual ontogeny of disease-associated microglia and disease inflammatory macrophages in ageing and neurodegeneration

Aymeric Silvin, Stefan Uderhardt, Cecile Piot, Sandro Da Mesquita, Katharine Yang, Laufey Geirsdottir, Kevin Mulder, David Eyal, Zhaoyuan Liu, Cecile Bridlance, Morgane Thion, Xiao Meng Zhang, Wan Ting Kong, Marc Deloger, Vasco Fontes, Assaf Weiner, Rachel Ee, Regine Dress, Jing Wen Hang, Akhila Balachander, Svetoslav Chakarov, Benoit Malleret, Garett Dunsmore, Olivier Cexus, Jinmiao Chen, Sonia Garel, Charles Antoine Dutertre, Ido Amit, Jonathan Kipnis, and Florent Ginhoux

List of supplemental information

Figure S1:

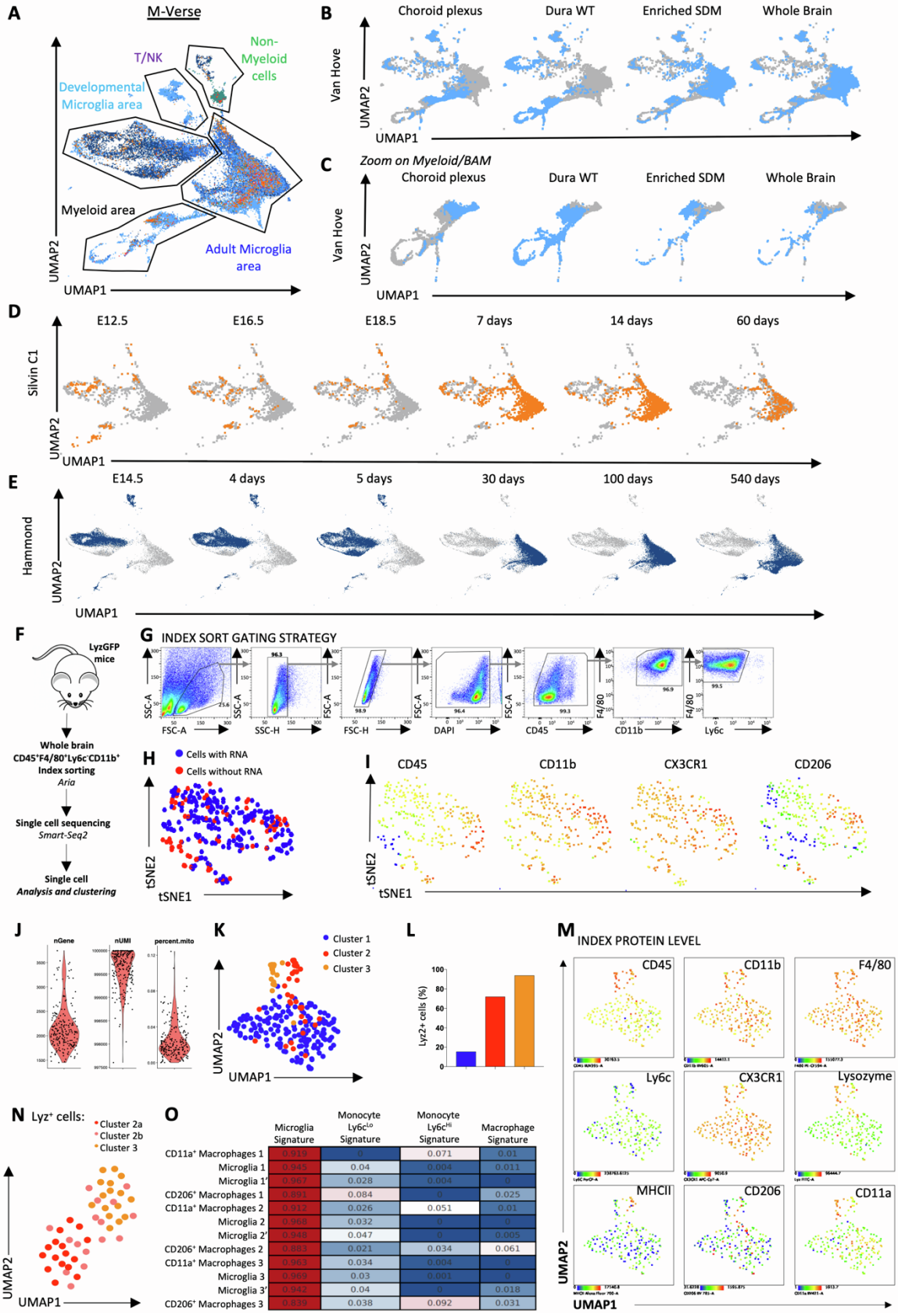
A
M-Verse
T/NK
Non-Myeloid cells
Developmental Microglia area
Myeloid area
Adult Microglia area
UMAP2
UMAP1
B
Choroid plexus
Dura WT
Enriched SDM
Whole Brain
Van Hove
UMAP2
UMAP1
C
Zoom on Myeloid/BAM
Choroid plexus
Dura WT
Enriched SDM
Whole Brain
Van Hove
UMAP2
UMAP1
D
E12.5
E16.5
E18.5
7 days
14 days
60 days
Silvin C1
UMAP2
UMAP1
E
E14.5
4 days
5 days
30 days
100 days
540 days
Hammond
UMAP2
UMAP1
F
LyzGFP mice
Whole brain
CD45+F4/80+Ly6c-CD11b+
Index sorting
Aria
Single cell sequencing
Smart-Seq2
Single cell
Analysis and clustering
G
INDEX SORT GATING STRATEGY
SSC-A
FSC-A
SSC-H
FSC-H
DAPI
CD45
CD11b
F4/80
Ly6c
H
Cells with RNA
Cells without RNA
tSNE2
tSNE1
I
CD45
CD11b
CX3CR1
CD206
tSNE2
tSNE1
J
nGene
nUMI
percent.mito
K
Cluster 1
Cluster 2
Cluster 3
UMAP2
UMAP1
L
Lyz2+ cells (%)
M
INDEX PROTEIN LEVEL
CD45
CD11b
F4/80
Ly6c
CX3CR1
Lysozyme
MHCII
CD206
CD11a
UMAP2
UMAP1
N
Lyz+ cells:
Cluster 2a
Cluster 2b
Cluster 3
UMAP2
UMAP1
O
Microglia Signature
Monocyte Ly6c^Lo Signature
Monocyte Ly6c^Hi Signature
Macrophage Signature
CD11a+ Macrophages 1 0.919 0 0.071 0.01
Microglia 1 0.945 0.04 0.004 0.011
Microglia 1' 0.967 0.028 0.004 0
CD206+ Macrophages 1 0.891 0.084 0 0.025
CD11a+ Macrophages 2 0.912 0.026 0.051 0.01
Microglia 2 0.968 0.032 0 0
Microglia 2' 0.948 0.047 0 0.005
CD206+ Macrophages 2 0.883 0.021 0.034 0.061
CD11a+ Macrophages 3 0.963 0.034 0.004 0
Microglia 3 0.969 0.03 0.001 0
Microglia 3' 0.942 0.04 0 0.018
CD206+ Macrophages 3 0.839 0.038 0.092 0.031

Supplementary Figure 1: M-Verse and brain macrophage heterogeneity, related to Figure 1
A. UMAP integration of the six scRNA-seq datasets with delimited areas: adult microglia, developmental microglia, myeloid cells, non-myeloid cells, NK and T cells. Color coding as in Figure 2B, indicating the different datasets integrated. **B.** Cells from the Van Hove dataset split by brain area origin in the M-Verse. **C.** Cells from the Van Hove dataset split by brain area origin in myeloid region of the M-Verse. **D.** Cells from the Silvin C1 dataset split by age of the mice. **E.** Cells from the Hammond dataset split by age of the mice. **F.** Experimental approach for the Index sort and SMART-seq2 of $CD45^+$ cells from brains of young adult Lyz2GFP C57BL/6 mice. **G.** Gating strategy used to isolate all brain macrophages ($CD45^+CD11b^+F4/80^+Ly6c^-$) for Indexed sort single-cell transcriptomic analysis. **H.** tSNE plot of the single cells that were indexed and assessed for RNA-sequencing. In blue are cells with sufficient RNA content to be sequenced. In red are cells without sufficient RNA content for RNA-seq. A total of 213 cells were sequenced. **I.** Protein expression level of CD45, CD11b, CX3CR1 and CD206 on the cells as in panel H. **J.** Violin representation of number of genes (nGene), number of unique molecular identifiers (nUMI) and percentage of mitochondrial genes (percent.mito) among cells with sufficient RNA for sequencing. **K.** tSNE plot of cells isolated from whole brain showing the three populations identified by unsupervised clustering after filtering based on nGene, nUMI and Percent Mito. **L.** Histogram of percentage of Lysozyme GFP^+ cells among Clusters 1, 2 and 3 determined by unsupervised clustering based on RNA expression. **M.** Protein expression level of the annotated markers as quantified by flow cytometry of each cell. **N.** UMAP plot and clustering based on transcriptome of Lyzozyme GFP^+ cells. **O.** Cibersort analysis performed on microglia, $CD11a^+$ macrophages and $CD206^+$ macrophages against the microglia signature, monocyte $Ly6c^{lo}$ signature, monocyte $Ly6c^{hi}$ signature and macrophage signature (red = closer to the signature, blue = further from the signature).

Figure S2:

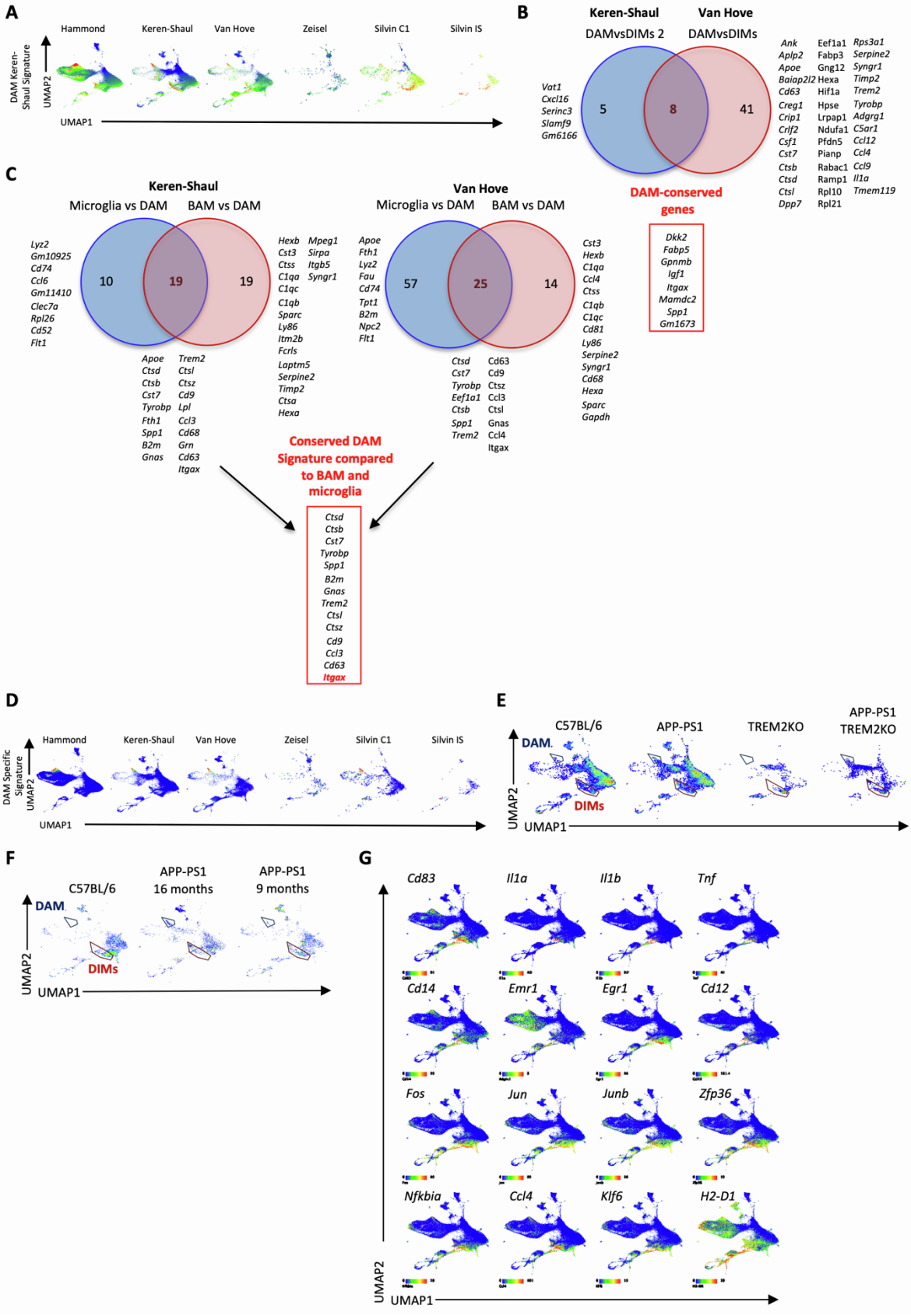
A
Hammond
Keren-Shaul
Van Hove
Zeisel
Silvin C1
Silvin IS
DAM Keren-Shaul Signature
UMAP2
UMAP1
B
Keren-Shaul
DAMvsDIMs 2
Van Hove
DAMvsDIMs
5
8
41
Vat1
Cxcl16
Serinc3
Slamf9
Gm6166
Ank
Aplp2
Apoe
Baiap2l2
Cd63
Creg1
Crip1
Crlf2
Csf1
Cst7
Ctsb
Ctsd
Ctsl
Dpp7
Eef1a1
Fabp3
Gng12
Hexa
Hif1a
Hpse
Lrpap1
Ndufa1
Pfdn5
Pianp
Rabac1
Ramp1
Rpl10
Rpl21
Rps3a1
Serpine2
Syngr1
Timp2
Trem2
Tyrobp
Adgrg1
C5ar1
Ccl12
Ccl4
Ccl9
Il1a
Tmem119
DAM-conserved genes
Dkk2
Fabp5
Gpnmb
Igf1
Itgax
Mamdc2
Spp1
Gm1673
C
Keren-Shaul
Microglia vs DAM
BAM vs DAM
10
19
19
Lyz2
Gm10925
Cd74
Ccl6
Gm11410
Clec7a
Rpl26
Cd52
Flt1
Apoe
Ctsd
Ctsb
Cst7
Tyrobp
Fth1
Spp1
B2m
Gnas
Trem2
Ctsl
Ctsz
Cd9
Lpl
Ccl3
Cd68
Grn
Cd63
Itgax
Hexb
Cst3
Ctss
C1qa
C1qc
C1qb
Sparc
Ly86
Itm2b
Fcrls
Laptm5
Serpine2
Timp2
Ctsa
Hexa
Mpeg1
Sirpa
Itgb5
Syngr1
Van Hove
Microglia vs DAM
BAM vs DAM
57
25
14
Apoe
Fth1
Lyz2
Fau
Cd74
Tpt1
B2m
Npc2
Flt1
Ctsd
Cst7
Tyrobp
Eef1a1
Ctsb
Spp1
Trem2
Cd63
Cd9
Ctsz
Ccl3
Ctsl
Gnas
Ccl4
Itgax
Cst3
Hexb
C1qa
Ccl4
Ctss
C1qb
C1qc
Cd81
Ly86
Serpine2
Syngr1
Cd68
Hexa
Sparc
Gapdh
Conserved DAM Signature compared to BAM and microglia
Ctsd
Ctsb
Cst7
Tyrobp
Spp1
B2m
Gnas
Trem2
Ctsl
Ctsz
Cd9
Ccl3
Cd63
Itgax
D
Hammond
Keren-Shaul
Van Hove
Zeisel
Silvin C1
Silvin IS
DAM Specific Signature
UMAP2
UMAP1
E
C57BL/6
APP-PS1
TREM2KO
APP-PS1 TREM2KO
DAM
DIMs
UMAP2
UMAP1
F
C57BL/6
APP-PS1 16 months
APP-PS1 9 months
DAM
DIMs
UMAP2
UMAP1
G
Cd83
Il1a
Il1b
Tnf
Cd14
Emr1
Egr1
Cd12
Fos
Jun
Junb
Zfp36
Nfkbia
Ccl4
Klf6
H2-D1
UMAP2
UMAP1

Supplementary Figure 2: DAM and DIMs conserved signature establishment, related to figure 2

A. DAM signature established by Keren-Shaul *et al.*, applied to each dataset of the M-Verse. **B.** Venn diagram representing the common and unique DEGs up in DAM between DAM versus DIMs in Keren-Shaul and Van Hove datasets. **C.** Venn diagram representing the common and unique DEGs up in DAM between DAM versus Microglia and DAM versus BAM in Keren-Shaul and Van Hove datasets. **D.** Heatmap representation of the relative RNA-expression levels of the newly established DAM-conserved signature among cells within each dataset of the M-Verse. **E.** DAM and DIMs visualization among Keren-Shaul dataset in the different mouse strains used. **F.** DAM and DIMs visualization among Van Hove dataset in the different mouse strains used. **G.** Heatmap representation of the relative RNA-expression levels of DIMs-conserved DEG projected onto the M-verse.

Figure S3:

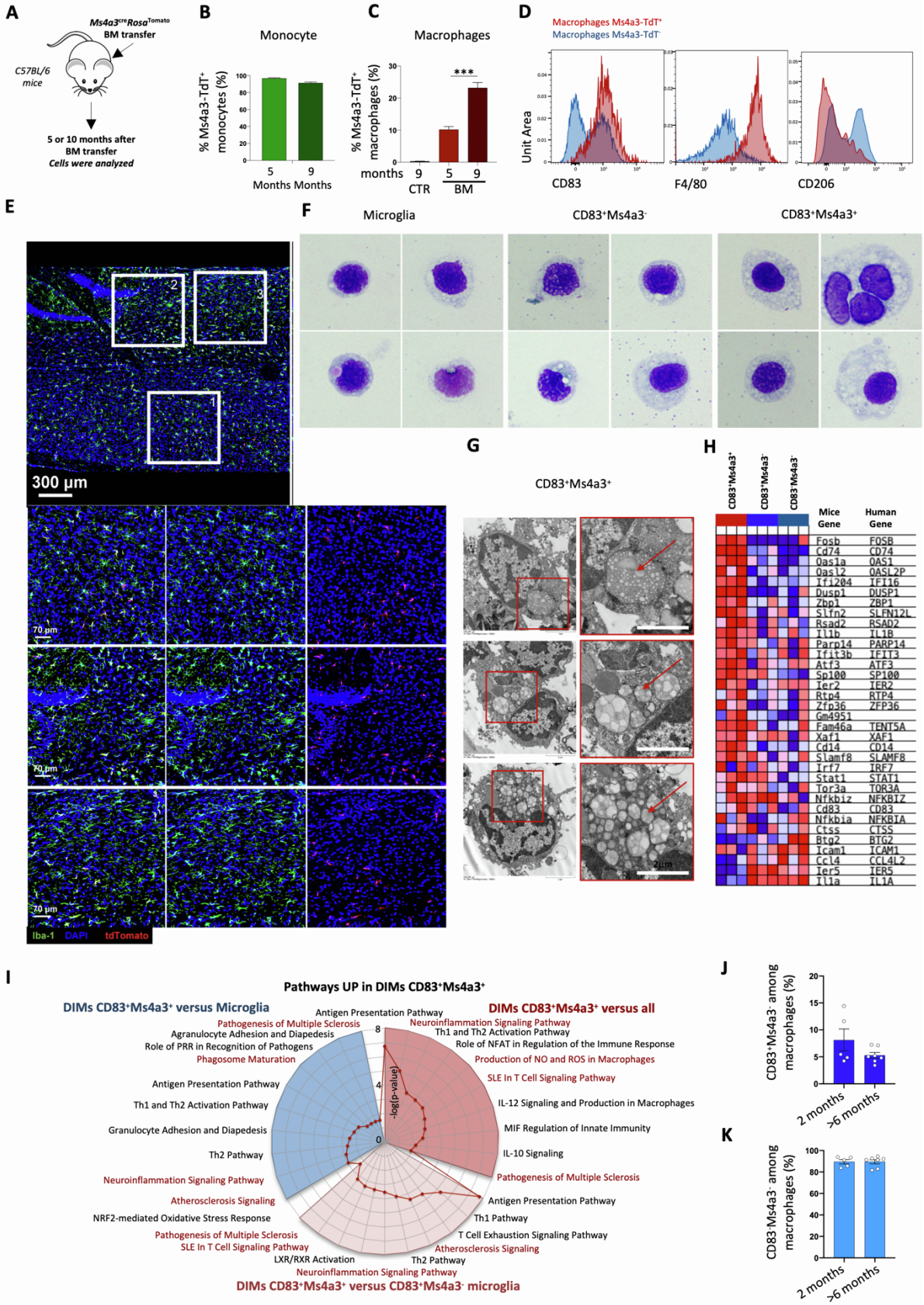
A
Ms4a3creRosaTomato
BM transfer
C57BL/6 mice
5 or 10 months after BM transfer
Cells were analyzed
B
Monocyte
% Ms4a3-TdT+ monocytes (%)
5 Months
9 Months
C
Macrophages
% Ms4a3-TdT+ macrophages (%)
***
months 9 5 9
CTR BM
D
Macrophages Ms4a3-TdT+
Macrophages Ms4a3-TdT-
Unit Area
CD83
F4/80
CD206
E
300 µm
70 µm
Iba-1 DAPI tdTomato
F
Microglia
CD83+Ms4a3-
CD83+Ms4a3+
G
CD83+Ms4a3+
2µm
H
CD83+Ms4a3+
CD83+Ms4a3-
CD83-Ms4a3-
Mice Gene
Human Gene
Fosb FOSB
Cd74 CD74
Oas1a OAS1
Oasl2 OASL2P
Ifi204 IFI16
Dusp1 DUSP1
Zbp1 ZBP1
Slfn2 SLFN12L
Rsad2 RSAD2
Il1b IL1B
Parp14 PARP14
Ifit3b IFIT3
Atf3 ATF3
Sp100 SP100
Ier2 IER2
Rtp4 RTP4
Zfp36 ZFP36
Gm4951
Fam46a TENT5A
Xaf1 XAF1
Cd14 CD14
Slamf8 SLAMF8
Irf7 IRF7
Stat1 STAT1
Tor3a TOR3A
Nfkbiz NFKBIZ
Cd83 CD83
Nfkbia NFKBIA
Ctss CTSS
Btg2 BTG2
Icam1 ICAM1
Ccl4 CCL4L2
Ier5 IER5
Il1a IL1A
I
Pathways UP in DIMs CD83+Ms4a3+
DIMs CD83+Ms4a3+ versus Microglia
DIMs CD83+Ms4a3+ versus all
DIMs CD83+Ms4a3+ versus CD83+Ms4a3- microglia
-log(p-value)
Antigen Presentation Pathway
Pathogenesis of Multiple Sclerosis
Agranulocyte Adhesion and Diapedesis
Role of PRR in Recognition of Pathogens
Phagosome Maturation
Antigen Presentation Pathway
Th1 and Th2 Activation Pathway
Granulocyte Adhesion and Diapedesis
Th2 Pathway
Neuroinflammation Signaling Pathway
Atherosclerosis Signaling
NRF2-mediated Oxidative Stress Response
Pathogenesis of Multiple Sclerosis
SLE In T Cell Signaling Pathway
LXR/RXR Activation
Neuroinflammation Signaling Pathway
Th1 and Th2 Activation Pathway
Role of NFAT in Regulation of the Immune Response
Production of NO and ROS in Macrophages
SLE In T Cell Signaling Pathway
IL-12 Signaling and Production in Macrophages
MIF Regulation of Innate Immunity
IL-10 Signaling
Pathogenesis of Multiple Sclerosis
Antigen Presentation Pathway
Th1 Pathway
T Cell Exhaustion Signaling Pathway
Atherosclerosis Signaling
Th2 Pathway
J
CD83+Ms4a3- among macrophages (%)
2 months
>6 months
K
CD83-Ms4a3- among macrophages (%)
2 months
>6 months

Supplementary Figure 3: Bone Marrow transfer to identify DIMs ontogeny, related to figure 4
A. Schematic overview of the *Ms4a3*^{Cre}*Rosa*^{Tomato} BM transfer into C57BL/6 mice with brain tissue analyzed 5 or 9 months later. **B.** Histogram showing the percentage of monocytes expressing Ms4a3-TdT in the brains of mice at 5- or 9-months post BM transfer (1-way ANOVA ***p-value<0.001). **C.** Histogram showing the percentage of macrophages expressing Ms4a3-TdT in the brains of mice at 5- or 9-months post BM transfer. **D.** Flow cytometry histogram of CD83, F4/80 and CD206 expression by Ms4a3-TdT^{+} and Ms4a3-TdT^{-} macrophages in the brains of mice at 9 months post BM transfer. **E.** Immunofluorescence microscopy images of iba-1 (green) Ms4a3-TdT^{+} (red) cells in the cortex (Zone 1), hippocampus-caudoputamen (Zone 2) and caudoputamen (Zone 3) of the brains of mice at 9 months post BM transfer. **F.** Hematoxylin and eosin staining of cytospin CD83^{+}Ms4a3-TdT^{+} DIMs, CD83^{+}Ms4a3-TdT^{-} microglia and microglia from mice at 9 months post BM transfer. **G.** Electron microscopy images of CD83^{+} DIMs. **H.** Heatmap showing relative expression level of DIMs signature genes among bulk CD83^{+}Ms4a3-TdT^{+}, CD83^{+} Ms4a3-TdT^{-} and CD83^{-} Ms4a3-TdT^{-} macrophages used for GSEA analysis. **I.** Specific pathways up-regulated in CD83^{+} Ms4a3-TdT^{+} DIMs as compared to all, CD83^{+} Ms4a3^{+} DIMs as compared to CD83^{+} Ms4a3-TdT^{-} microglia, and CD83^{+} Ms4a3-TdT^{+} DIMs as compared to microglia based on gene expression data. **J.** Histogram showing the percentage of CD83^{+}Ms4a3-TdT^{-} microglia among all brain macrophages in *Ms4a3*^{cre}*Rosa*^{Tomato} mice at two (n=5) and more than six months of age (n=7). **K.** Histogram showing the percentage of CD83^{-}Ms4a3-TdT^{-} microglia among all brain macrophages in *Ms4a3*^{cre}*Rosa*^{Tomato} mice at two (n=5) and more than six months of age (n=7).

Figure S4:

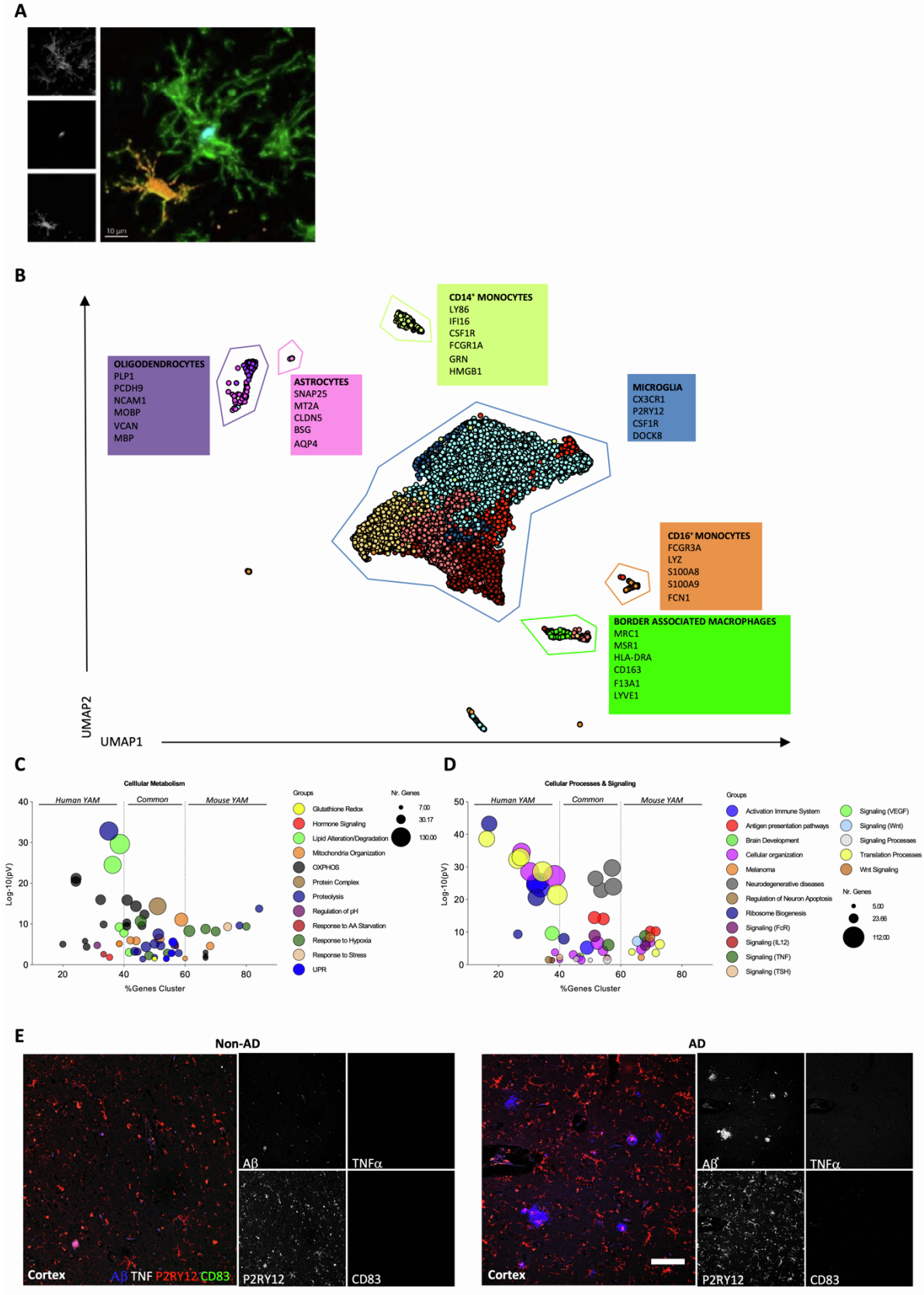
A
10 µm
B
CD14⁺ MONOCYTES
LY86
IFI16
CSF1R
FCGR1A
GRN
HMGB1
OLIGODENDROCYTES
PLP1
PCDH9
NCAM1
MOBP
VCAN
MBP
ASTROCYTES
SNAP25
MT2A
CLDN5
BSG
AQP4
MICROGLIA
CX3CR1
P2RY12
CSF1R
DOCK8
CD16⁺ MONOCYTES
FCGR3A
LYZ
S100A8
S100A9
FCN1
BORDER ASSOCIATED MACROPHAGES
MRC1
MSR1
HLA-DRA
CD163
F13A1
LYVE1
UMAP2
UMAP1
C
Cellular Metabolism
Human YAM
Common
Mouse YAM
Log-10(pV)
%Genes Cluster
Groups
Nr. Genes
7.00
30.17
130.00
Glutathione Redox
Hormone Signaling
Lipid Alteration/Degradation
Mitochondria Organization
OXPHOS
Protein Complex
Proteolysis
Regulation of pH
Response to AA Starvation
Response to Hypoxia
Response to Stress
UPR
D
Cellular Processes & Signaling
Human YAM
Common
Mouse YAM
Log-10(pV)
%Genes Cluster
Groups
Activation Immune System
Antigen presentation pathways
Brain Development
Cellular organization
Melanoma
Neurodegenerative diseases
Regulation of Neuron Apoptosis
Ribosome Biogenesis
Signaling (FcR)
Signaling (IL12)
Signaling (TNF)
Signaling (TSH)
Signaling (VEGF)
Signaling (Wnt)
Signaling Processes
Translation Processes
Wnt Signaling
Nr. Genes
5.00
23.66
112.00
E
Non-AD
AD
Aβ
TNFα
P2RY12
CD83
Cortex
Aβ TNF P2RY12 CD83

Supplementary Figure 4: DAM and DIMs in human brain, related to figure 6

A. Iba1 (green), amyloGlo (Cyan) and Ms4a3-TdT^{+} cells (orange) in brains from 12-month-old 5XFAD mice. **B.** UMAP of the scRNA-seq data from Thrupp *et al*., following analysis and clustering using Seurat V3. **C.** Cellular metabolism groups enriched in mouse and/or human YAM, based on mouse YAM DEGs and Human YAM DEGs. **D.** Cellular processes & signaling groups enriched in mouse and/or human YAM, based on mouse YAM DEGs and human YAM DEGs. **E.** Representative images of brain cortex labeled for amyloid deposits (blue), TNFa (grey), CD83 (green) and P2RY12 (red) from control patients without AD (non-AD) and patients diagnosed with AD (scale bar, 100 μm).

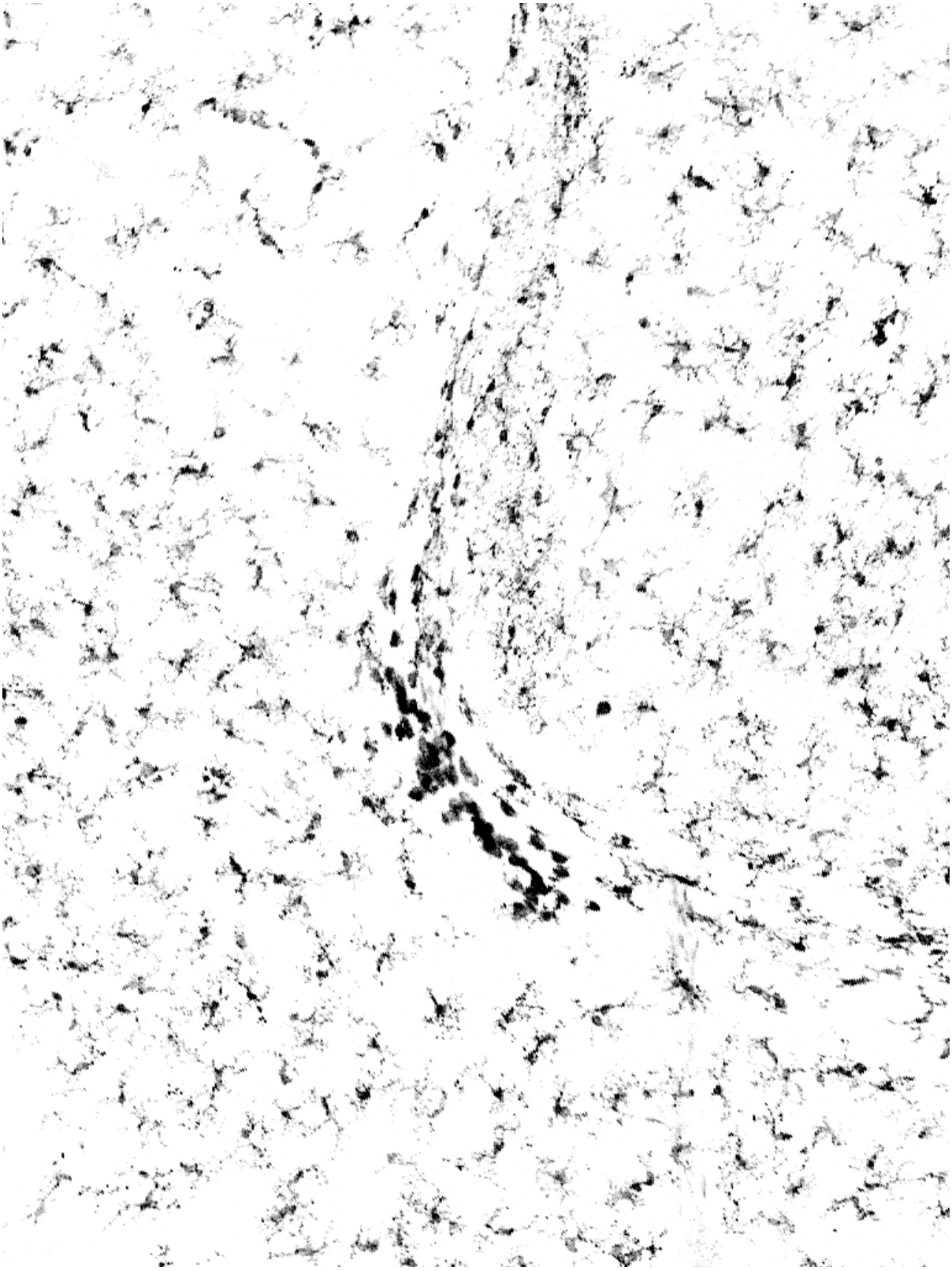

Microglia accumulating at the CSA atP5.

REFERENCES

Ajami, B. *et al.* (2007) 'Local self-renewal can sustain CNS microglia maintenance and function throughout adult life', *Nature Neuroscience*, 10(12), pp. 1538–1543. doi: 10.1038/nn2014.

Ajami, B. *et al.* (2018) 'Single-cell mass cytometry reveals distinct populations of brain myeloid cells in mouse neuroinflammation and neurodegeneration models', *Nature Neuroscience*, 21(4), pp. 541–551. doi: 10.1038/s41593-018-0100-x.

Akiyoshi, R. *et al.* (2018) 'Microglia enhance synapse activity to promote local network synchronization', *eneuro*. Society for Neuroscience, 5(5).

Albin, R. L., Young, A. B. and Penney, J. B. (1989) 'The functional anatomy of basal ganglia disorders', *Trends in Neurosciences*, 12(10), pp. 366–375. doi: 10.1016/0166-2236(89)90074-X.

Alliot, F., Godin, I. and Pessac, B. (1999) 'Microglia derive from progenitors, originating from the yolk sac, and which proliferate in the brain', *Developmental Brain Research*, 117(2), pp. 145–152. doi: 10.1016/S0165-3806(99)00113-3.

Alsema, A. M. *et al.* (2020) 'Profiling Microglia From Alzheimer's Disease Donors and Non-demented Elderly in Acute Human Postmortem Cortical Tissue', *Frontiers in Molecular Neuroscience*, 13(October), pp. 1–14. doi: 10.3389/fnmol.2020.00134.

Altman, J. and Das, G. D. (1965) 'Autoradiographic and histological evidence of postnatal hippocampal neurogenesis in rats', *Journal of Comparative Neurology*, 124(3), pp. 319–335. doi: https://doi.org/10.1002/cne.901240303.

Anderson, S. R. *et al.* (2019) 'Developmental Apoptosis Promotes a Disease-Related Gene Signature and Independence from CSF1R Signaling in Retinal Microglia', *Cell Reports*. ElsevierCompany., 27(7), pp. 2002-2013.e5. doi: 10.1016/j.celrep.2019.04.062.

Anderson, S. R. *et al.* (2022) 'Neuronal apoptosis drives remodeling states of microglia and shifts in survival pathway dependence', *eLife*, 11, pp. 1–28. doi: 10.7554/eLife.76564.

Arnò, B. *et al.* (2014) 'Neural progenitor cells orchestrate microglia migration and positioning into the developing cortex', *Nature Communications*, 5. doi: 10.1038/ncomms6611.

Arnoux, I. *et al.* (2013) 'Adaptive phenotype of microglial cells during the normal postnatal development of the somatosensory "Barrel" cortex', *GLIA*. John Wiley & Sons, Ltd, 61(10), pp. 1582–1594. doi: 10.1002/glia.22503.

Ashwell, K. (1991) 'The distribution of microglia and cell death in the fetal rat forebrain', *Developmental Brain Research*, 58(1), pp. 1–12. doi: https://doi.org/10.1016/0165-3806(91)90231-7.

Askew, K. *et al.* (2017) 'Coupled Proliferation and Apoptosis Maintain the Rapid Turnover of Microglia in the Adult Brain', *Cell Reports*, 18(2), pp. 391–405. doi: 10.1016/j.celrep.2016.12.041.

Audinat, É. and Arnoux, I. (2014) 'La microglie: Des cellules immunitaires qui sculptent et contrôlent les synapses neuronales', *Medecine/Sciences*, 30(2), pp. 153–159. doi: 10.1051/medsci/20143002012.

Ayata, P. *et al.* (2019) 'Epigenetic regulation of brain region-specific microglia clearance activity', *Nature Neuroscience*, 21(8), pp. 1049–1060. doi: 10.1038/s41593-018-0192-3.Epigenetic.

Badimon, A. *et al.* (2020) 'Negative feedback control of neuronal activity by microglia', *Nature*. Springer US, 586(7829), pp. 417–423. doi: 10.1038/s41586-020-2777-8.

Barber, H. M., Ali, M. F. and Kucenas, S. (2022) 'Glial Patchwork: Oligodendrocyte Progenitor Cells and Astrocytes Blanket the Central Nervous System', *Frontiers in Cellular Neuroscience*, 15(January), pp. 1–14. doi: 10.3389/fncel.2021.803057.

Barry-Carroll, L. *et al.* (2023) 'Microglia colonize the developing brain by clonal expansion of highly proliferative progenitors, following allometric scaling', *CellReports*. The Author(s), 42(5), p. 112425. doi: 10.1016/j.celrep.2023.112425.

Beattie, E. C. *et al.* (2002) 'Control of synaptic strength by glial TNFα', *Science*, 295(5563), pp. 2282–2285. doi: 10.1126/science.1067859.

Di Bella, D. J. *et al.* (2021) 'Molecular logic of cellular diversification in the mouse cerebral cortex', *Nature*. Springer US, 595(7868), pp. 554–559. doi: 10.1038/s41586-021-03670-5.

Benmamar-Badel, A., Owens, T. and Wlodarczyk, A. (2020) 'Protective Microglial Subset in Development, Aging, and Disease: Lessons From Transcriptomic Studies', *Frontiers in Immunology*, 11(April). doi: 10.3389/fimmu.2020.00430.

Bennett, F. C. *et al.* (2018) 'A Combination of Ontogeny and CNS Environment Establishes Microglial Identity', *Neuron*, 98(6), pp. 1170-1183.e8. doi: 10.1016/j.neuron.2018.05.014.

Bian, Z. *et al.* (2020) 'Deciphering human macrophage development at single-cell resolution', *Nature*, 582(7813), pp. 571–576. doi: 10.1038/s41586-020-2316-7.

Biase, L. M. De *et al.* (2018) 'Local cues establish and maintain region-specific phenotypes of basal ganglia microglia', *Neuron*, 95(2), pp. 341–356. doi: 10.1016/j.neuron.2017.06.020.Local.

Bolton, J. L. *et al.* (2017) 'Gestational Exposure to Air Pollution Alters Cortical Volume, Microglial Morphology, and Microglia-Neuron Interactions in a Sex-Specific Manner.', *Frontiers in synaptic neuroscience*. Switzerland, 9, p. 10. doi: 10.3389/fnsyn.2017.00010.

Bordeleau, M. *et al.* (2022) 'Maternal high-fat diet in mice induces cerebrovascular, microglial and long-term behavioural alterations in offspring', *Communications Biology*. Springer US, 5(1), pp. 1–13. doi: 10.1038/s42003-021-02947-9.

Böttcher, C. *et al.* (2019) 'Human microglia regional heterogeneity and phenotypes determined by multiplexed single-cell mass cytometry', *Nature Neuroscience*. Springer US, 22(1), pp. 78–90. doi: 10.1038/s41593-018-0290-2.

Bradl, M. and Lassmann, H. (2010) 'Oligodendrocytes: biology and pathology.', *Acta neuropathologica*. Germany, 119(1), pp. 37–53. doi: 10.1007/s00401-009-0601-5.

Bridlance, C. and Thion, M. S. (2023) 'Multifaceted microglia during brain development: Models and tools', *Frontiers in Neuroscience*, 17(March). doi: 10.3389/fnins.2023.1125729.

Brown, G. C. and Neher, J. J. (2014) 'Microglial phagocytosis of live neurons', *Nature Reviews Neuroscience*. Nature Publishing Group, 15(4), pp. 209–216. doi: 10.1038/nrn3710.

Bruttger, J. *et al.* (2015) 'Genetic Cell Ablation Reveals Clusters of Local Self-Renewing Microglia in the Mammalian Central Nervous System', *Immunity*, 43(1), pp. 92–106. doi: 10.1016/j.immuni.2015.06.012.

Butovsky, O. *et al.* (2014) 'Identification of a unique TGF-β-dependent molecular and functional signature in microglia', *Nature Neuroscience*, 17(1), pp. 131–143. doi: 10.1038/nn.3599.

Buttgereit, A. *et al.* (2016) 'Sall1 is a transcriptional regulator defining microglia identity and function', *Nature Immunology*, 17(12), pp. 1397–1406. doi: 10.1038/ni.3585.

Cahoy, J. D. *et al.* (2008) 'A transcriptome database for astrocytes, neurons, and oligodendrocytes: A new resource for understanding brain development and function', *Journal of Neuroscience*, 28(1), pp. 264–278. doi: 10.1523/JNEUROSCI.4178-07.2008.

Calcia, M. A. *et al.* (2016) 'Stress and neuroinflammation: a systematic review of the effects of stress on microglia and the implications for mental illness.', *Psychopharmacology*. Germany, 233(9), pp. 1637–1650. doi: 10.1007/s00213-016-4218-9.

Cameron, H. A. and Mckay, R. D. G. (2001) 'Adult neurogenesis produces a large pool of new granule cells in the dentate gyrus', *Journal of Comparative Neurology*, 435(4), pp. 406–417. doi: 10.1002/cne.1040.

Casali, B. T. *et al.* (2020) 'Microglia depletion rapidly and reversibly alters amyloid pathology by modification of plaque compaction and morphologies', *Neurobiology of Disease*. Elsevier, 142(March), p. 104956. doi: 10.1016/j.nbd.2020.104956.

Castillo-Ruiz, A. *et al.* (2018) 'The microbiota influences cell death and microglial colonization in the perinatal mouse brain', *Brain, Behavior, and Immunity*, 67, pp. 218–229. doi: https://doi.org/10.1016/j.bbi.2017.08.027.

Catale, C. *et al.* (2020) 'Microglial function in the effects of early-life stress on brain and behavioral development', *Journal of Clinical Medicine*, 9(2). doi: 10.3390/jcm9020468.

Checchin, D. *et al.* (2006) 'Potential Role of Microglia in Retinal Blood Vessel Formation AND', 47(8). doi: 10.1167/iovs.05-1522.

Chen, H.-R. *et al.* (2020) 'Fate mapping via CCR2-CreER mice reveals monocyte-to-microglia transition in development and neonatal stroke', *Science Advances*, 6(35), p. eabb2119. doi: 10.1126/sciadv.abb2119.

Chen, S. K. *et al.* (2010) 'Hematopoietic origin of pathological grooming in Hoxb8 mutant mice', *Cell*. Cell Press, 141(5), pp. 775–785. doi: 10.1016/j.cell.2010.03.055.

Chen, X. and Holtzman, D. M. (2022) 'Emerging roles of innate and adaptive immunity in Alzheimer's disease', *Immunity*. Elsevier Inc., 55(12), pp. 2236–2254. doi: 10.1016/j.immuni.2022.10.016.

Chen, Y. and Colonna, M. (2021) 'Microglia in Alzheimer's disease at single-cell level. Are there common patterns in humans and mice?', *Journal of Experimental Medicine*, 218(9), pp. 1–10. doi: 10.1084/jem.20202717.

Chihara, T. *et al.* (2010) 'IL-34 and M-CSF share the receptor Fms but are not identical in biological activity and signal activation', *Cell Death and Differentiation*. Nature Publishing Group, 17(12), pp. 1917–1927. doi: 10.1038/cdd.2010.60.

Chitu, V. *et al.* (2017) 'Emerging Roles for CSF-1 Receptor and its Ligands in the Nervous System CSF-1R and CSF-1R Ligands and their Expression Patterns in Brain', *Trends in Neurosciences*, 39(6), pp. 378–393. doi: 10.1016/j.tins.2016.03.005.Emerging.

Clavreul, S., Dumas, L. and Loulier, K. (2022) 'Astrocyte development in the cerebral cortex: Complexity of their origin, genesis, and maturation', *Frontiers in Neuroscience*, 16(September), pp. 1–11. doi: 10.3389/fnins.2022.916055.

Condello, C. *et al.* (2015) 'Microglia constitute a barrier that prevents neurotoxic protofibrillar Aβ42 hotspots around plaques', *Nature Communications*. Nature Publishing Group, 6(May 2014). doi: 10.1038/ncomms7176.

Cossart, R. and Garel, S. (2022) 'Step by step: cells with multiple functions in cortical circuit assembly', *Nature Reviews Neuroscience*. Springer US, 23(7), pp. 395–410. doi:

10.1038/s41583-022-00585-6.

Coull, J. A. M. *et al.* (2005) 'BDNF from microglia causes the shift in neuronal anion gradient underlying neuropathic pain', *Nature*, 438(7070), pp. 1017–1021. doi: 10.1038/nature04223.

Császár, E. *et al.* (2022) 'Microglia modulate blood flow, neurovascular coupling, and hypoperfusion via purinergic actions', *Journal of Experimental Medicine*, 219(3). doi: 10.1084/jem.20211071.

Cserép, C. *et al.* (2020) 'Microglia monitor and protect neuronal function through specialized somatic purinergic junctions', *Science*. American Association for the Advancement of Science, 367(6477), pp. 528–537. doi: 10.1126/science.aax6752.

Cserép, C. *et al.* (2022) 'Microglial control of neuronal development via somatic purinergic junctions', *Cell Reports*, 40(12). doi: 10.1016/j.celrep.2022.111369.

Cugurra, A. *et al.* (2021) 'Skull and vertebral bone marrow are myeloid cell reservoirs for the meninges and CNS parenchyma', *Science*. American Association for the Advancement of Science, 373(6553), p. eabf7844. doi: 10.1126/science.abf7844.

Cunningham, C. L., Martínez-Cerdeño, V. and Noctor, S. C. (2013) 'Microglia regulate the number of neural precursor cells in the developing cerebral cortex', *Journal of Neuroscience*, 33(10), pp. 4216–4233. doi: 10.1523/JNEUROSCI.3441-12.2013.

Dai, X. M. *et al.* (2004) 'Incomplete restoration of colony-stimulating factor 1 (CSF-1) function in CSF-1-deficient Csf1op/Csf1op mice by transgenic expression of cell surface CSF-1', *Blood*, 103(3), pp. 1114–1123. doi: 10.1182/blood-2003-08-2739.

Dalmau, I. *et al.* (2003) 'Dynamics of microglia in the developing rat brain', *Journal of Comparative Neurology*, 458(2), pp. 144–157. doi: 10.1002/cne.10572.

Davalos, D. *et al.* (2005) 'ATP mediates rapid microglial response to local brain injury in vivo', *Nature Neuroscience*, 8(6), pp. 752–758. doi: 10.1038/nn1472.

De, I. *et al.* (2014) 'CSF1 overexpression has pleiotropic effects on microglia in vivo', *Glia*, 62(12), pp. 1955–1967. doi: 10.1002/glia.22717.

De, S. *et al.* (2018) 'Two distinct ontogenies confer heterogeneity to mouse brain microglia', *Development*, 145(13), p. dev152306. doi: 10.1242/dev.152306.

Deczkowska, A. *et al.* (2018) 'Disease-Associated Microglia: A Universal Immune Sensor of Neurodegeneration', *Cell*. Elsevier Inc., 173(5), pp. 1073–1081. doi: 10.1016/j.cell.2018.05.003.

Del-Aguila, J. L. *et al.* (2019) 'A single-nuclei RNA sequencing study of Mendelian and sporadic AD in the human brain', *Alzheimer's Research and Therapy*. Alzheimer's Research & Therapy, 11(1), pp. 1–16. doi: 10.1186/s13195-019-0524-x.

Delpech, J.-C. *et al.* (2016) 'Early life stress perturbs the maturation of microglia in the developing hippocampus', *Brain, Behavior, and Immunity*, 57, pp. 79–93. doi: https://doi.org/10.1016/j.bbi.2016.06.006.

Van Deren, D. A. *et al.* (2022) 'Defining the Hoxb8 cell lineage during murine definitive hematopoiesis', *Development (Cambridge, England)*, 149(8). doi: 10.1242/dev.200200.

Ding, X. *et al.* (2021) 'Loss of microglial SIRPα promotes synaptic pruning in preclinical models of neurodegeneration', *Nature Communications*. Springer US, 12(1), pp. 1–17. doi: 10.1038/s41467-021-22301-1.

Djannatian, M. *et al.* (2021) 'Myelin biogenesis is associated with pathological ultrastructure

that is resolved by microglia during development 2 3 4', *bioRxiv*, p. 2021.02.02.429485. Available at: https://doi.org/10.1101/2021.02.02.429485.

Dubbelaar, M. L. *et al.* (2018) 'The Kaleidoscope of Microglial Phenotypes', *Frontiers in immunology*, 9(July), p. 1753. doi: 10.3389/fimmu.2018.01753.

Dudvarski Stankovic, N. *et al.* (2016) 'Microglia–blood vessel interactions: a double-edged sword in brain pathologies', *Acta Neuropathologica*, pp. 347–363. doi: 10.1007/s00401-015-1524-y.

Easley-Neal, C. *et al.* (2019) 'CSF1R Ligands IL-34 and CSF1 Are Differentially Required for Microglia Development and Maintenance in White and Gray Matter Brain Regions', *Frontiers in Immunology*, 10(September). doi: 10.3389/fimmu.2019.02199.

Edler, M., Mhatre-Winters, I. and Richardson, J. R. (2021) 'Microglia in Aging and Alzheimer's Disease: A Comparative Species Review', *Cells*, 10, pp. 1–30. doi: doi.org/10.3390/cells10051138.

Elmore, M. R. P. *et al.* (2014) 'Colony-stimulating factor 1 receptor signaling is necessary for microglia viability, unmasking a microglia progenitor cell in the adult brain', *Neuron*. Elsevier Inc., 82(2), pp. 380–397. doi: 10.1016/j.neuron.2014.02.040.

Elmore, M. R. P. *et al.* (2018) 'Replacement of microglia in the aged brain reverses cognitive, synaptic, and neuronal deficits in mice', *Aging Cell*, 17(6). doi: 10.1111/acel.12832.

Endele, M. *et al.* (2017) 'CSF-1–induced Src signaling can instruct monocytic lineage choice', *Blood*, 129(12), pp. 1691–1701. doi: https://doi.org/10.1182/blood-2016-05-714329.

Engelhardt, B., Vajkoczy, P. and Weller, R. O. (2017) 'The movers and shapers in immune privilege of the CNS', *Nature Immunology*, 18(2), pp. 123–131. doi: 10.1038/ni.3666.

Erblich, B. *et al.* (2011) 'Absence of colony stimulation factor-1 receptor results in loss of microglia, disrupted brain development and olfactory deficits', *PLoS ONE*, 6(10). doi: 10.1371/journal.pone.0026317.

Erny, D. *et al.* (2015) 'Host microbiota constantly control maturation and function of microglia in the CNS', *Nature Neuroscience*, 18(7), pp. 965–977. doi: 10.1038/nn.4030.

van Essen, D. C. (2020) 'A 2020 view of tension-based cortical morphogenesis', *Proceedings of the National Academy of Sciences of the United States of America*, 117(52), pp. 32868–32879. doi: 10.1073/PNAS.2016830117.

Fantin, A. *et al.* (2010) 'Tissue macrophages act as cellular chaperones for vascular anastomosis downstream of VEGF-mediated endothelial tip cell induction', *Blood*, 116(5), pp. 829–840. doi: 10.1182/blood-2009-12-257832.

Favuzzi, E. *et al.* (2021) 'GABA-receptive microglia selectively sculpt developing inhibitory circuits', *Cell*, 184(15), pp. 4048-4063.e32. doi: 10.1016/j.cell.2021.06.018.

Filipello, F. *et al.* (2018) 'The Microglial Innate Immune Receptor TREM2 Is Required for Synapse Elimination and Normal Brain Article The Microglial Innate Immune Receptor TREM2 Is Required for Synapse Elimination and Normal Brain Connectivity', *Immunity*. Elsevier Inc., 48(5), pp. 979-991.e8. doi: 10.1016/j.immuni.2018.04.016.

Frade, J. M. and Barde, Y. A. (1998) 'Microglia-derived nerve growth factor causes cell death in the developing retina', *Neuron*, 20(1), pp. 35–41. doi: 10.1016/S0896-6273(00)80432-8.

Francis, H. and Stevenson, R. (2013) 'The longer-term impacts of Western diet on human cognition and the brain', *Appetite*, 63, pp. 119–128. doi:

https://doi.org/10.1016/j.appet.2012.12.018.

Frangogiannis, N. G. (2014) 'The inflammatory response in myocardial injury, repair, and remodelling', *Nature Reviews Cardiology*, pp. 255–265. doi: 10.1038/nrcardio.2014.28.

Freeman, M. R. and Rowitch, D. H. (2013) 'Perspective Evolving Concepts of Gliogenesis : A Look Way Back and Ahead to the Next 25 Years', *Neuron*. Elsevier Inc., 80(3), pp. 613–623. doi: 10.1016/j.neuron.2013.10.034.

Freyer, C. and Renfree, M. B. (2009) 'The mammalian yolk sac placenta', *Journal of Experimental Zoology Part B: Molecular and Developmental Evolution*. Wiley Online Library, 312(6), pp. 545–554.

Frigerio, C. S. *et al.* (2019) 'The Major Risk Factors for Alzheimer ' s Disease : Age , Sex , and Genes Modulate the Microglia Response to A b Plaques Resource The Major Risk Factors for Alzheimer ' s Disease : Age , Sex , and Genes Modulate the Microglia Response to A b Plaques', pp. 1293–1306. doi: 10.1016/j.celrep.2019.03.099.

Füger, P. *et al.* (2017) 'Microglia turnover with aging and in an Alzheimer's model via long-term in vivo single-cell imaging', *Nature Neuroscience*. Nature Publishing Group, 20(10), pp. 1371–1376. doi: 10.1038/nn.4631.

Gallo, N. B., Berisha, A. and Van Aelst, L. (2022) 'Microglia regulate chandelier cell axo-axonic synaptogenesis', *Proceedings of the National Academy of Sciences of the United States of America*, 119(11), pp. 1–12. doi: 10.1073/pnas.2114476119.

Gandal, M. J. *et al.* (2018) 'Transcriptome-wide isoform-level dysregulation in ASD, schizophrenia, and bipolar disorder', *Science*. American Association for the Advancement of Science, 362(6420), p. eaat8127.

Geirsdottir, L. *et al.* (2019) 'Cross-Species Single-Cell Analysis Reveals Divergence of the Primate Microglia Program', *Cell*, 179(7), pp. 1609-1622.e16. doi: 10.1016/j.cell.2019.11.010.

Gesuita, L. *et al.* (2022) 'Microglia contribute to the postnatal development of cortical somatostatin-positive inhibitory cells and to whisker-evoked cortical activity', *Cell Reports*, 40(7). doi: 10.1016/j.celrep.2022.111209.

Gibson, E. M. *et al.* (2018) 'Methotrexate Chemotherapy Induces Persistent Tri-glial Dysregulation that Underlies Chemotherapy-Related Cognitive Impairment', *Cell*. Elsevier Inc., pp. 1–13. doi: 10.1016/j.cell.2018.10.049.

Ginhoux, F. *et al.* (2010) 'Fate mapping analysis reveals that adult microglia derive from primitive macrophages', *Science*, 330(6005), pp. 841–845. doi: 10.1126/science.1194637.

Ginhoux, F. and Prinz, M. (2015) 'Origin of microglia: Current concepts and past controversies', *Cold Spring Harbor Perspectives in Biology*, 7(8), pp. 1–16. doi: 10.1101/cshperspect.a020537.

Goldmann, T. *et al.* (2016) 'Origin, fate and dynamics of macrophages at central nervous system interfaces', *Nature Immunology*, 17(7), pp. 797–805. doi: 10.1038/ni.3423.

Gómez-González, B. and Escobar, A. (2010) 'Prenatal stress alters microglial development and distribution in postnatal rat brain', *Acta Neuropathologica*, 119(3), pp. 303–315. doi: 10.1007/s00401-009-0590-4.

Gomez Perdiguero, E. *et al.* (2015) 'Tissue-resident macrophages originate from yolk-sac-derived erythro-myeloid progenitors', *Nature*. Nature Publishing Group, 518(7540), pp. 547–551. doi: 10.1038/nature13989.

Gordon, H., Schafer, Z. T. and Smith, C. J. (2023) 'A paradox promoted by microglia cannibalism shortens the lifespan of developmental microglia', *bioRxiv*, p. 2023.03.15.532426. Available at: https://www.biorxiv.org/content/10.1101/2023.03.15.532426v1%0Ahttps://www.biorxiv.org/content/10.1101/2023.03.15.532426v1.abstract.

Gosselin, D. *et al.* (2017) 'An environment-dependent transcriptional network specifies human microglia identity.', *Science (New York, N.Y.)*. American Association for the Advancement of Science, 356(6344), p. eaal3222. doi: 10.1126/science.aal3222.

Götz, M. and Huttner, W. B. (2005) 'The cell biology of neurogenesis', *Nature Reviews Molecular Cell Biology*, 6(10), pp. 777–788. doi: 10.1038/nrm1739.

Green, K. N., Crapser, J. D. and Hohsfield, L. A. (2020) 'To Kill a Microglia: A Case for CSF1R Inhibitors', *Trends in Immunology*, 0(0), pp. 771–784. doi: 10.1016/j.it.2020.07.001.

Greter, M. *et al.* (2012) 'Stroma-Derived Interleukin-34 Controls the Development and Maintenance of Langerhans Cells and the Maintenance of Microglia', *Immunity*. NIH Public Access, 37(6), pp. 1050–1060. doi: 10.1016/j.immuni.2012.11.001.

Guneykaya, D. *et al.* (2018) 'Transcriptional and Translational Differences of Microglia from Male and Female Brains'. doi: 10.1016/j.celrep.2018.08.001.

Guo, J. and Anton, E. S. (2014) 'Decision making during interneuron migration in the developing cerebral cortex', *Trends in Cell Biology*. Elsevier Ltd, 24(6), pp. 342–351. doi: 10.1016/j.tcb.2013.12.001.

Guo, L. and Ikegawa, S. (2021) 'From HDLS to BANDDOS: fast-expanding phenotypic spectrum of disorders caused by mutations in CSF1R', *Journal of Human Genetics*. Springer US, 66(12), pp. 1139–1144. doi: 10.1038/s10038-021-00942-w.

Hagemeyer, N. *et al.* (2017) 'Microglia contribute to normal myelinogenesis and to oligodendrocyte progenitor maintenance during adulthood', *Acta Neuropathologica*, 134(3), pp. 441–458. doi: 10.1007/s00401-017-1747-1.

Hammond, T. R. *et al.* (2019) 'Single-Cell RNA Sequencing of Microglia throughout the Mouse Lifespan and in the Injured Brain Reveals Complex Cell-State Changes', *Immunity*. Cell Press, 50(1), pp. 253-271.e6. doi: 10.1016/j.immuni.2018.11.004.

Hanamsagar, R. *et al.* (2017) 'Generation of a microglial developmental index in mice and in humans reveals a sex difference in maturation and immune reactivity', *Glia*, 65(9), pp. 1504–1520. doi: 10.1002/glia.23176.

Hanamsagar, R. and Bilbo, S. D. (2017) 'Environment matters: microglia function and dysfunction in a changing world'. doi: 10.1016/j.conb.2017.10.007.

Hanamsagar, R. and Bilbo, S. D. (2018) 'Environment Matters: Microglia Function and Dysfunction in a Changing World Richa', *Physiology & behavior*, 176(1), pp. 139–148. doi: 10.1016/j.conb.2017.10.007.Environment.

Haq, R. A. *et al.* (2018) 'Microbiome – microglia connections via the gut – brain axis', *Journal of Experimental Medicine*, 216(1), pp. 41–59.

Hattori, Y. *et al.* (2020) 'Transient microglial absence assists postmigratory cortical neurons in proper differentiation', *Nature Communications*. Springer US, 11(1). doi: 10.1038/s41467-020-15409-3.

Hattori, Y., Kato, D., *et al.* (2022) 'Border-associated macrophages transventricularly infiltrate the early embryonic cerebral wall to differentiate into microglia', *bioRxiv*. Cold Spring Harbor

Laboratory. doi: 10.1101/2022.07.27.501563.

Hattori, Y., Itoh, H., *et al.* (2022) 'Embryonic Pericytes Promote Microglial Homeostasis and Their Effects on Neural Progenitors in the Developing Cerebral Cortex', *The Journal of neuroscience : the official journal of the Society for Neuroscience*, 42(3), pp. 362–376. doi: 10.1523/JNEUROSCI.1201-21.2021.

Hattori, Y. (2022) 'The microglia-blood vessel interactions in the developing brain', *Neuroscience Research*. Elsevier B.V., (September). doi: 10.1016/j.neures.2022.09.006.

Hayes, L. N. *et al.* (2022) 'Prenatal immune stress blunts microglia reactivity , impairing neurocircuitry', 610(May 2019).

Haynes, S. E. *et al.* (2006) 'The P2Y12 receptor regulates microglial activation by extracellular nucleotides', *Nature Neuroscience*, 9(12), pp. 1512–1519. doi: 10.1038/nn1805.

Hewett, S. J., Jackman, N. A. and Claycomb, R. J. (2012) 'Interleukin-1β in central nervous system injury and repair', *European journal of neurodegenerative disease*. NIH Public Access, 1(2), p. 195.

Hickman, S. E. *et al.* (2013) 'The microglial sensome revealed by direct RNA sequencing', *Nature Neuroscience*. Nature Publishing Group, 16(12), pp. 1896–1905. doi: 10.1038/nn.3554.

Hoeffel, G. and Ginhoux, F. (2015) 'Ontogeny of Tissue-Resident Macrophages', *Frontiers in Immunology*, 6. doi: 10.3389/fimmu.2015.00486.

Hohsfield, L. A. *et al.* (2021) 'Subventricular zone/white matter microglia reconstitute the empty adult microglial niche in a dynamic wave', *eLife*, 10. doi: 10.7554/eLife.66738.

Holtman, I. R. *et al.* (2015) 'Induction of a common microglia gene expression signature by aging and neurodegenerative conditions: a co-expression meta-analysis', *Acta neuropathologica communications*. ???, 3, p. 31. doi: 10.1186/s40478-015-0203-5.

Hope, K. T. *et al.* (2020) 'Maturation of the microglial population varies across mesolimbic nuclei', *European Journal of Neuroscience*, 52(7), pp. 3689–3709. doi: 10.1111/ejn.14740.

Hoshiko, M. *et al.* (2012) 'Deficiency of the Microglial Receptor CX3CR1 Impairs Postnatal Functional Development of Thalamocortical Synapses in the Barrel Cortex', *Journal of Neuroscience*. doi: 10.1523/JNEUROSCI.1167-12.2012.

Van Hove, H. *et al.* (2019) 'A single-cell atlas of mouse brain macrophages reveals unique transcriptional identities shaped by ontogeny and tissue environment', *Nature Neuroscience*, 22(6), pp. 1021–1035. doi: 10.1038/s41593-019-0393-4.

Hristova, M. *et al.* (2010) 'Activation and deactivation of periventricular white matter phagocytes during postnatal mouse development', *Glia*, 58(1), pp. 11–28. doi: 10.1002/glia.20896.

Hristovska, I. *et al.* (2022) 'Sleep decreases neuronal activity control of microglial dynamics in mice', *Nature Communications*. Springer US, 13(1), pp. 1–15. doi: 10.1038/s41467-022-34035-9.

Hu, J. *et al.* (2023) 'Microglial Piezo1 senses Aβ fibril stiffness to restrict Alzheimer's disease.', *Neuron*. United States, 111(1), pp. 15-29.e8. doi: 10.1016/j.neuron.2022.10.021.

Huang, Y. *et al.* (2011) 'Neuron-specific effects of interleukin-1β are mediated by a novel isoform of the IL-1 receptor accessory protein', *Journal of Neuroscience*. Soc Neuroscience, 31(49), pp. 18048–18059.

Huang, Y. *et al.* (2018) 'Repopulated microglia are solely derived from the proliferation of

residual microglia after acute depletion', *Nature Neuroscience*. Springer US, 21(4), pp. 530–540. doi: 10.1038/s41593-018-0090-8.

Huang, Y. *et al.* (2023) 'The gut microbiome modulates the transformation of microglial subtypes', *Molecular Psychiatry*. Springer US, (June 2022). doi: 10.1038/s41380-023-02017-y.

Hughes, A. N. and Appel, B. (2020) 'Microglia phagocytose myelin sheaths to modify developmental myelination', *Nature Neuroscience*. Springer US, 23(9), pp. 1055–1066. doi: 10.1038/s41593-020-0654-2.

Hughes, E. G. *et al.* (2018) 'Myelin remodeling through experience-dependent oligodendrogenesis in the adult somatosensory cortex', *Nature Neuroscience*, 21(5), pp. 696–706. doi: 10.1038/s41593-018-0121-5.

Iaccarino, H. F. *et al.* (2016) 'Gamma frequency entrainment attenuates amyloid load and modifies microglia', *Nature*. Nature Publishing Group, 540(7632), pp. 230–235. doi: 10.1038/nature20587.

Ikezu, S. *et al.* (2021) 'Inhibition of colony stimulating factor 1 receptor corrects maternal inflammation-induced microglial and synaptic dysfunction and behavioral abnormalities', *Molecular Psychiatry*. Springer US, 26(6), pp. 1808–1831. doi: 10.1038/s41380-020-0671-2.

Imamoto, K. and Leblond, C. P. (1978) 'Radioautographic investigation of gliogenesis in the corpus callosum of young rats II. Origin of microglial cells', *Journal of Comparative Neurology*, 180(1), pp. 139–163. doi: 10.1002/cne.901800109.

Jung, S. *et al.* (2000) ' Analysis of Fractalkine Receptor CX 3 CR1 Function by Targeted Deletion and Green Fluorescent Protein Reporter Gene Insertion ', *Molecular and Cellular Biology*, 20(11), pp. 4106–4114. doi: 10.1128/mcb.20.11.4106-4114.2000.

Kamphuis, W. *et al.* (2016) 'Transcriptional profiling of CD11c-positive microglia accumulating around amyloid plaques in a mouse model for Alzheimer's disease', *Biochimica et Biophysica Acta - Molecular Basis of Disease*. Elsevier B.V., 1862(10), pp. 1847–1860. doi: 10.1016/j.bbadis.2016.07.007.

Kana, V. *et al.* (2019) 'CSF-1 controls cerebellar microglia and is required for motor function and social interaction', *Journal of Experimental Medicine*, 216(10), pp. 2265–2281. doi: 10.1084/jem.20182037.

Kaur, C. and Ling, E. A. (2017) 'Transitory cystic cavities in the developing mammalian brain – normal or anomalous?', *Journal of Anatomy*, 230(2), pp. 197–202. doi: 10.1111/joa.12556.

Keren-Shaul, H. *et al.* (2017) 'A Unique Microglia Type Associated with Restricting Development of Alzheimer's Disease', *Cell*. Elsevier, 169(7), pp. 1276-1290.e17. doi: 10.1016/j.cell.2017.05.018.

Kiani Shabestari, S. *et al.* (2022) 'Absence of microglia promotes diverse pathologies and early lethality in Alzheimer's disease mice', *Cell Reports*. The Authors, 39(11), p. 110961. doi: 10.1016/j.celrep.2022.110961.

Kierdorf, K. *et al.* (2013) 'Microglia emerge from erythromyeloid precursors via Pu.1-and Irf8-dependent pathways', *Nature Neuroscience*, 16(3), pp. 273–280. doi: 10.1038/nn.3318.

Kierdorf, K. *et al.* (2019) 'Macrophages at CNS interfaces: ontogeny and function in health and disease', *Nature Reviews Neuroscience*. Springer US, 20(9), pp. 547–562. doi: 10.1038/s41583-019-0201-x.

Kieusseian, A. *et al.* (2012) 'Immature hematopoietic stem cells undergo maturation in the fetal

liver', *Development*, 139(19), pp. 3521–3530. doi: 10.1242/dev.079210.

Kober, D. L. and Brett, T. J. (2017) 'TREM2-Ligand Interactions in Health and Disease', *Journal of Molecular Biology*, pp. 1607–1629. doi: 10.1016/j.jmb.2017.04.004.

Kopec, A. M. *et al.* (2018) 'Microglial dopamine receptor elimination defines sex-specific nucleus accumbens development and social behavior in adolescent rats', *Nature Communications*, 9(1). doi: 10.1038/s41467-018-06118-z.

Koziol, L. F. *et al.* (2014) 'Consensus paper: the cerebellum's role in movement and cognition.', *Cerebellum (London, England)*. United States, 13(1), pp. 151–177. doi: 10.1007/s12311-013-0511-x.

Kracht, L. *et al.* (2020) 'Human fetal microglia acquire homeostatic immune-sensing properties early in development', *Science*, 369(6503), pp. 530–537. doi: 10.1126/science.aba5906.

Krasemann, S. *et al.* (2017) 'The TREM2-APOE Pathway Drives the Transcriptional Phenotype of Dysfunctional Microglia in Neurodegenerative Diseases', *Immunity*. Elsevier Inc., 47(3), pp. 566-581.e9. doi: 10.1016/j.immuni.2017.08.008.

Kreisel, T. *et al.* (2019) 'Unique role for dentate gyrus microglia in neuroblast survival and in VEGF-induced activation', *Glia*, 67(4), pp. 594–618. doi: 10.1002/glia.23505.

Kubota, Y. *et al.* (2009) 'M-CSF inhibition selectively targets pathological angiogenesis and lymphangiogenesis', *Journal of Experimental Medicine*, 206(5), pp. 1089–1102. doi: 10.1084/jem.20081605.

Kumaravelu, P. *et al.* (2002) 'Quantitative developmental anatomy of definitive haematopoietic stem cells/long-term repopulating units (HSC/RUs): role of the aorta-gonad-mesonephros (AGM) region and the yolk sac in colonisation of the mouse embryonic liver', *Development*, 129(21), pp. 4891–4899. doi: 10.1242/dev.129.21.4891.

Lavin, Y. *et al.* (2014) 'Tissue-Resident Macrophage Enhancer Landscapes Are Shaped by the Local Microenvironment', *Cell*, 159(6), pp. 1312–1326. doi: https://doi.org/10.1016/j.cell.2014.11.018.

Lawrence, A. *et al.* (no date) 'Microglia maintain structural integrity during fetal brain morphogenesis', *in preparation*.

Lawson, L. J., Perry, V. H. and Gordon, S. (1992) 'Turnover of resident microglia in the normal adult mouse brain', *Neuroscience*, 48(2), pp. 405–415. doi: https://doi.org/10.1016/0306-4522(92)90500-2.

Lehrman, E. K. *et al.* (2018) 'CD47 Protects Synapses from Excess Microglia-Mediated Pruning during Development', *Neuron*. Cell Press, 100(1), pp. 120-134.e6. Available at: https://www-sciencedirect-com.gate2.inist.fr/science/article/pii/S0896627318307906 (Accessed: 22 October 2018).

Lenz, K. M. *et al.* (2013) 'Microglia are essential to masculinization of brain and behavior', *Journal of Neuroscience*, 33(7), pp. 2761–2772. doi: 10.1523/JNEUROSCI.1268-12.2013.

Lenz, K. M. and McCarthy, M. (2017) 'A Starring Role for Microglia in Brain Sex Differences', *Physiology & behavior*, 176(3), pp. 139–148. doi: 10.1016/j.physbeh.2017.03.040.

Leyrolle, Q., Layé, S. and Nadjar, A. (2019) 'Direct and indirect effects of lipids on microglia function', *Neuroscience Letters*, 708, p. 134348. doi: https://doi.org/10.1016/j.neulet.2019.134348.

Li, J. *et al.* (2006) 'Conditional deletion of the colony stimulating factor-1 receptor (c-fms

proto-oncogene) in mice', *Genesis*. Wiley Online Library, 44(7), pp. 328–335.

Li, Q. *et al.* (2019) 'Developmental Heterogeneity of Microglia and Brain Myeloid Cells Revealed by Deep Single-Cell RNA Sequencing', *Neuron*. Elsevier Inc., 101(2), pp. 207-223.e10. doi: 10.1016/j.neuron.2018.12.006.

Li, Y. *et al.* (2020) 'Microglia-organized scar-free spinal cord repair in neonatal mice', *Nature*, 587(7835), pp. 613–618. doi: 10.1038/s41586-020-2795-6.

Li, Y. *et al.* (2022) 'Decoding the temporal and regional specification of microglia in the developing human brain', *Cell Stem Cell*. Elsevier Inc., pp. 1–15. doi: 10.1016/j.stem.2022.02.004.

Liaw, L. *et al.* (1998) 'Altered wound healing in mice lacking a functional osteopontin gene (spp1).', *Journal of Clinical Investigation*, 101(7), pp. 1468–1478. doi: 10.1172/jci2131.

Lim, S. H. *et al.* (2013) 'Neuronal synapse formation induced by microglia and interleukin 10', *PLoS ONE*, 8(11), pp. 1–13. doi: 10.1371/journal.pone.0081218.

Ling, E. A. (1979) 'Transformation of monocytes into amoeboid microglia in the corpus callosum of postnatal rats, as shown by labelling monocytes by carbon particles.', *Journal of anatomy*, 128(Pt 4), pp. 847–58. Available at: http://www.ncbi.nlm.nih.gov/pubmed/489472%0Ahttp://www.pubmedcentral.nih.gov/articlerender.fcgi?artid=PMC1232886.

Lloyd, A. F. *et al.* (2019) 'Central nervous system regeneration is driven by microglia necroptosis and repopulation', *Nature Neuroscience*. Springer US, 22(7), pp. 1046–1052. doi: 10.1038/s41593-019-0418-z.

Lokmane, L. and Garel, S. (2014) 'Map transfer from the thalamus to the neocortex: Inputs from the barrel field', *Seminars in Cell & Developmental Biology*, 35, pp. 147–155. doi: https://doi.org/10.1016/j.semcdb.2014.07.005.

Loulier, K. *et al.* (2014) 'Multiplex Cell and Lineage Tracking with Combinatorial Labels', *Neuron*, 81(3), pp. 505–520. doi: 10.1016/j.neuron.2013.12.016.

Lukens, J. R. and Eyo, U. B. (2022) 'Microglia and Neurodevelopmental Disorders', *Annual Review of Neuroscience*, 45, pp. 425–445. doi: 10.1146/annurev-neuro-110920-023056.

Luo, J. *et al.* (2013) 'Colony-stimulating factor 1 receptor (CSF1R) signaling in injured neurons facilitates protection and survival', *Journal of Experimental Medicine*, 210(1), pp. 157–172. doi: 10.1084/jem.20120412.

Madore, C. *et al.* (2020) 'Essential omega-3 fatty acids tune microglial phagocytosis of synaptic elements in the mouse developing brain', *Nature Communications*. Springer US, 11(1). doi: 10.1038/s41467-020-19861-z.

Mahmood, A. and Miron, V. E. (2022) 'Microglia as therapeutic targets for central nervous system remyelination', *Current Opinion in Pharmacology*. Elsevier Ltd, 63, p. 102188. doi: 10.1016/j.coph.2022.102188.

La Manno, G. *et al.* (2021) 'Molecular architecture of the developing mouse brain', *Nature*. Springer US, 596(7870), pp. 92–96. doi: 10.1038/s41586-021-03775-x.

Marín-Teva, J. L. *et al.* (2004) 'Microglia Promote the Death of Developing Purkinje Cells', *Neuron*, 41(4), pp. 535–547. doi: 10.1016/S0896-6273(04)00069-8.

Marín, O. (2013) 'Cellular and molecular mechanisms controlling the migration of neocortical interneurons', *European Journal of Neuroscience*, 38(1), pp. 2019–2029. doi:

10.1111/ejn.12225.

Marsters, C. M. *et al.* (2020) 'Embryonic microglia influence developing hypothalamic glial populations', *Journal of Neuroinflammation*. Journal of Neuroinflammation, 17(1), pp. 1–17. doi: 10.1186/s12974-020-01811-7.

Masuda, T. *et al.* (2019) 'Spatial and temporal heterogeneity of mouse and human microglia at single-cell resolution', *Nature*. Springer US, 566, pp. 388–392. doi: 10.1038/s41586-019-0924-x.

Masuda, T., Sankowski, R., *et al.* (2020) 'Microglia Heterogeneity in the Single-Cell Era', *Cell Reports*. ElsevierCompany., 30(5), pp. 1271–1281. doi: 10.1016/j.celrep.2020.01.010.

Masuda, T., Amann, L., *et al.* (2020) 'Novel Hexb-based tools for studying microglia in the CNS', *Nature Immunology*, 21(7), pp. 802–815. doi: 10.1038/s41590-020-0707-4.

Masuda, T. *et al.* (2022) 'Specification of CNS macrophage subsets occurs postnatally in defined niches', *Nature*, 604(7907), pp. 740–748. doi: 10.1038/s41586-022-04596-2.

Matcovitch-Natan, O. *et al.* (2016) 'Microglia development follows a stepwise program to regulate brain homeostasis', *Science*, 353(6301). doi: 10.1126/science.aad8670.

Mathys, H. *et al.* (2019) 'Single-cell transcriptomic analysis of Alzheimer's disease', *Nature*. Springer US, 570(7761), pp. 332–337. doi: 10.1038/s41586-019-1195-2.

McKinsey, G. L. *et al.* (2020) 'A new genetic strategy for targeting microglia in development and disease', *eLife*, 9, pp. 1–34. doi: 10.7554/eLife.54590.

McNamara, N. B. *et al.* (2023) 'Microglia regulate central nervous system myelin growth and integrity', *Nature*. Springer US, 613(7942), pp. 120–129. doi: 10.1038/s41586-022-05534-y.

Menassa, D. A. *et al.* (2021) 'Spatiotemporal Dynamics of Human Microglia are Linked with Brain Developmental Processes Across the Lifespan', *SSRN Electronic Journal*. doi: 10.2139/ssrn.3932600.

Menassa, D. A. *et al.* (2022) 'The spatiotemporal dynamics of microglia across the human lifespan', *Developmental Cell*, pp. 1–13. doi: 10.1016/j.devcel.2022.07.015.

Menassa, D. A. and Gomez-Nicola, D. (2018) 'Microglial dynamics during human brain development', *Frontiers in Immunology*, p. 1014. doi: 10.3389/fimmu.2018.01014.

Michaelson, M. D. *et al.* (1996) 'CSF-1 deficiency in mice results in abnormal brain development', *Development*, 122(9), pp. 2661–2672. doi: 10.1242/dev.122.9.2661.

Mildenberger, W., Stifter, S. A. and Greter, M. (2022) 'Diversity and function of brain-associated macrophages', *Current Opinion in Immunology*. Elsevier, 76, p. 102181. doi: 10.1016/j.coi.2022.102181.

Mildner, A. *et al.* (2007) 'Microglia in the adult brain arise from Ly-6ChiCCR2+ monocytes only under defined host conditions', *Nature Neuroscience*, 10(12), pp. 1544–1553. doi: 10.1038/nn2015.

Mink, J. W. (2003) 'The Basal Ganglia and Involuntary Movements', *Archives of Neurology*, 60(10), p. 1365. doi: 10.1001/archneur.60.10.1365.

Miyamoto, A. *et al.* (2016) 'Microglia contact induces synapse formation in developing somatosensory cortex', *Nature Communications*. Nature Publishing Group, 7(1), p. 12540. doi: 10.1038/ncomms12540.

Mizuno, T. *et al.* (2011) 'Interleukin-34 selectively enhances the neuroprotective effects of

microglia to attenuate oligomeric amyloid-β neurotoxicity', *American Journal of Pathology*. Elsevier Inc., 179(4), pp. 2016–2027. doi: 10.1016/j.ajpath.2011.06.011.

Molnár, Z., Luhmann, H. J. and Kanold, P. O. (2020) 'Transient cortical circuits match spontaneous and sensory-driven activity during development', *Science*. doi: 10.1126/science.abb2153.

Mondo, E. *et al.* (2020) 'A developmental analysis of juxtavascular microglia dynamics and interactions with the vasculature', *Journal of Neuroscience*, 40(34), pp. 6503–6521. doi: 10.1523/JNEUROSCI.3006-19.2020.

Monier, A. *et al.* (2006) 'Distribution and differentiation of microglia in the human encephalon during the first two trimesters of gestation', *Journal of Comparative Neurology*. John Wiley & Sons, Ltd, 499(4), pp. 565–582. doi: https://doi.org/10.1002/cne.21123.

Monier, A. *et al.* (2007) 'Entry and distribution of microglial cells in human embryonic and fetal cerebral cortex', *Journal of Neuropathology and Experimental Neurology*, 66(5), pp. 372–382. doi: 10.1097/nen.0b013e3180517b46.

Mrdjen, D. *et al.* (2018) 'High-dimensional single-cell mapping of central nervous system immune cells reveals distinct myeloid subsets in health, aging, and disease', *Immunity*. Elsevier, 48(2), pp. 380–395. doi: 10.1016/j.immuni.2018.01.011.

Mueller, F. S. *et al.* (2018) 'Mouse models of maternal immune activation: Mind your caging system!', *Brain, Behavior, and Immunity*, 73, pp. 643–660. doi: https://doi.org/10.1016/j.bbi.2018.07.014.

Muhr, J. and Ackerman, K. M. (2020) 'Embryology, gastrulation'.

Munro, D. A. D. *et al.* (2020) 'CNS macrophages differentially rely on an intronic Csf1r enhancer for their development', *Development (Cambridge, England)*, 147(23). doi: 10.1242/dev.194449.

Najafi, A. R. *et al.* (2018) 'A limited capacity for microglial repopulation in the adult brain', *GLIA*. John Wiley and Sons Inc., 66(11), pp. 2385–2396. doi: 10.1002/glia.23477.

Nandi, S. *et al.* (2006) 'Developmental and functional significance of the CSF-1 proteoglycan chondroitin sulfate chain', *Blood*, 107(2), pp. 786–795. doi: 10.1182/blood-2005-05-1822.

Nandi, S. *et al.* (2012) 'The CSF-1 receptor ligands IL-34 and CSF-1 exhibit distinct developmental brain expression patterns and regulate neural progenitor cell maintenance and maturation', *Developmental Biology*. Elsevier, 367(2), pp. 100–113. doi: 10.1016/j.ydbio.2012.03.026.

Nandi, S. *et al.* (2013) 'Receptor-type protein-tyrosine phosphatase ζ is a functional receptor for interleukin-34', *Journal of Biological Chemistry*. Â© 2013 ASBMB. Currently published by Elsevier Inc; originally published by American Society for Biochemistry and Molecular Biology., 288(30), pp. 21972–21986. doi: 10.1074/jbc.M112.442731.

Navascués, J. *et al.* (2000) 'Entry, dispersion and differentiation of microglia in the developing central nervous system', *Anais da Academia Brasileira de Ciencias*, 72(1), pp. 91–102. doi: 10.1590/S0001-37652000000100013.

Ndubaku, U. and de Bellard, M. E. (2008) 'Glial cells: Old cells with new twists', *Acta Histochemica*, pp. 182–195. doi: 10.1016/j.acthis.2007.10.003.

Nelson, L. H., Warden, S. and Lenz, K. M. (2017) 'Sex differences in microglial phagocytosis in the neonatal hippocampus', *Brain, Behavior, and Immunity*. Elsevier Inc., 64, pp. 11–22. doi: 10.1016/j.bbi.2017.03.010.

Nemes-Baran, A. D., White, D. R. and DeSilva, T. M. (2020) 'Fractalkine-Dependent Microglial Pruning of Viable Oligodendrocyte Progenitor Cells Regulates Myelination', *Cell Reports*. ElsevierCompany., 32(7), p. 108047. doi: 10.1016/j.celrep.2020.108047.

Nery, S., Fishell, G. and Corbin, J. G. (2002) 'The caudal ganglionic eminence is a source of distinct cortical and subcortical cell populations', *Nature Neuroscience*, 5(12), pp. 1279–1287. doi: 10.1038/nn971.

Nguyen, A. T. *et al.* (2020) 'APOE and TREM2 regulate amyloid-responsive microglia in Alzheimer's disease', *Acta Neuropathologica*, 140(4), pp. 477–493. doi: 10.1007/s00401-020-02200-3.

Nguyen, P. T. *et al.* (2020) 'Microglial Remodeling of the Extracellular Matrix Promotes Synapse Plasticity', *Cell*. Elsevier Inc., 182(0), pp. 1–16. doi: 10.1016/j.cell.2020.05.050.

Nikodemova, M. *et al.* (2015) 'Microglial numbers attain adult levels after undergoing a rapid decrease in cell number in the third postnatal week', *Journal of Neuroimmunology*. Elsevier, 278, pp. 280–288. doi: 10.1016/j.jneuroim.2014.11.018.

Nimmerjahn, A., Kirchhoff, F. and Helmchen, F. (2005) 'Resting microglial cells are highly dynamic surveillants of brain parenchyma in vivo', *Neuroforum*, 11(3), pp. 95–96. doi: 10.1515/nf-2005-0304.

Nott, A. *et al.* (2019) 'Brain cell type – specific enhancer – promoter interactome maps and disease-risk association', *Science*, 1139(November), pp. 1134–1139.

O'Brien, J. *et al.* (2012) 'Macrophages are crucial for epithelial cell death and adipocyte repopulation during mammary gland involution', *Development*, 139(2), pp. 269–275. doi: 10.1242/dev.071696.

Olah, M. *et al.* (2020) 'Single cell RNA sequencing of human microglia uncovers a subset associated with Alzheimer's disease', *Nature Communications*. Springer US, 11(1). doi: 10.1038/s41467-020-19737-2.

Olmos-Alonso, A. *et al.* (2016) 'Pharmacological targeting of CSF1R inhibits microglial proliferation and prevents the progression of Alzheimer's-like pathology', *Brain*, 139(3), pp. 891–907. doi: 10.1093/brain/awv379.

Olmos, G. and Lladó, J. (2014) 'Tumor necrosis factor alpha: a link between neuroinflammation and excitotoxicity', *Mediators of inflammation*. Hindawi, 2014.

Oosterhof, N. *et al.* (2018) 'Colony-Stimulating Factor 1 Receptor (CSF1R) Regulates Microglia Density and Distribution, but Not Microglia Differentiation In Vivo', *Cell Reports*. ElsevierCompany., 24(5), pp. 1203-1217.e6. doi: 10.1016/j.celrep.2018.06.113.

Oosterhof, N. *et al.* (2019) 'Homozygous Mutations in CSF1R Cause a Pediatric-Onset Leukoencephalopathy and Can Result in Congenital Absence of Microglia', *The American Journal of Human Genetics*. ElsevierCompany., pp. 1–12. doi: 10.1016/j.ajhg.2019.03.010.

Orłowski, D., Sołtys, Z. and Janeczko, K. (2003) 'Morphological development of microglia in the postnatal rat brain: A quantitative study', *International Journal of Developmental Neuroscience*, 21(8), pp. 445–450. doi: 10.1016/j.ijdevneu.2003.09.001.

Paolicelli, R. C. *et al.* (2011) 'Synaptic pruning by microglia is necessary for normal brain development', *Science*, 333(6048), pp. 1456–1458. doi: 10.1126/science.1202529.

Paolicelli, R. C. *et al.* (2022) 'Microglia states and nomenclature: A field at its crossroads', *Neuron*, 110(21), pp. 3458–3483. doi: 10.1016/j.neuron.2022.10.020.

Paolicelli, R. C., Bisht, K. and Tremblay, M. È. (2014) 'Fractalkine regulation of microglial physiology and consequences on the brain and behavior', *Frontiers in Cellular Neuroscience*. doi: 10.3389/fncel.2014.00129.

Parikshak, N. N. *et al.* (2016) 'Genome-wide changes in lncRNA, splicing, and regional gene expression patterns in autism', *Nature*. Nature Publishing Group, 540(7633), pp. 423–427. doi: 10.1038/nature20612.

Parkhurst, C. N. *et al.* (2013) 'Microglia Promote Learning-Dependent Synapse Formation through Brain-Derived Neurotrophic Factor', *Cell*, 155(7), pp. 1596–1609. doi: https://doi.org/10.1016/j.cell.2013.11.030.

Pasciuto, E. *et al.* (2020) 'Microglia Require CD4 T Cells to Complete the Fetal-to-Adult Transition', *Cell*. Elsevier, 182(3), pp. 625-640.e24. doi: 10.1016/j.cell.2020.06.026.

Pellicoro, A. *et al.* (2014) 'Liver fibrosis and repair: immune regulation of wound healing in a solid organ.', *Nature reviews. Immunology*. England, 14(3), pp. 181–194. doi: 10.1038/nri3623.

Penna, E. *et al.* (2021) 'Greater Number of Microglia in Telencephalic Proliferative Zones of Human and Nonhuman Primate Compared with Other Vertebrate Species.', *Cerebral cortex communications*. United States, 2(4), p. tgab053. doi: 10.1093/texcom/tgab053.

Perdiguero, E. G. and Geissmann, F. (2016) 'Development and maintainance of resident macrophages', *Nat Immunol*, 17(4), pp. 2–8. doi: 10.1038/ni.3341.Development.

Pereira, L. *et al.* (2015) 'IL-10 regulates adult neurogenesis by modulating ERK and STAT3 activity.', *Frontiers in cellular neuroscience*. Switzerland, 9, p. 57. doi: 10.3389/fncel.2015.00057.

Petersen, C. C. H. (2007) 'The functional organization of the barrel cortex.', *Neuron*. Cell Press, pp. 339–355. doi: 10.1016/j.neuron.2007.09.017.

Plaza-Zabala, A., Sierra-Torre, V. and Sierra, A. (2017) 'Autophagy and microglia: Novel partners in neurodegeneration and aging', *International Journal of Molecular Sciences*, p. 598. doi: 10.3390/ijms18030598.

Pont-Lezica, L. *et al.* (2014) 'Microglia shape corpus callosum axon tract fasciculation: Functional impact of prenatal inflammation', *European Journal of Neuroscience*, 39(10), pp. 1551–1557. doi: 10.1111/ejn.12508.

Pridans, C. *et al.* (2013) 'CSF1R mutations in hereditary diffuse leukoencephalopathy with spheroids are loss of function', *Scientific Reports*, 3, pp. 1–5. doi: 10.1038/srep03013.

Priller, J. and Prinz, M. (2019) 'Targeting microglia in brain disorders', *Science*, pp. 32–33. doi: 10.1126/science.aau9100.

Purves, D. (2001) *Neuroscience*. 2nd ed. Sunderland, Mass. : Sinauer Associates, c2001.

Rahimian, R. *et al.* (2021) 'The emerging tale of microglia in psychiatric disorders', *Neuroscience and Biobehavioral Reviews*. Elsevier Ltd, 131(September), pp. 1–29. doi: 10.1016/j.neubiorev.2021.09.023.

Ratz, M. *et al.* (2022) 'Clonal relations in the mouse brain revealed by single-cell and spatial transcriptomics', *Nature Neuroscience*. Springer US, 25(March). doi: 10.1038/s41593-022-01011-x.

Reemst, K. *et al.* (2016) 'The Indispensable Roles of Microglia and Astrocytes during Brain Development'. doi: 10.3389/fnhum.2016.00566.

Réu, P. *et al.* (2017) 'The Lifespan and Turnover of Microglia in the Human Brain', *Cell*

Reports, 20(4), pp. 779–784. doi: 10.1016/j.celrep.2017.07.004.

Riccio, O. *et al.* (2012) 'New pool of cortical interneuron precursors in the early postnatal dorsal white matter', *Cerebral Cortex*, 22(1), pp. 86–98. doi: 10.1093/cercor/bhr086.

Rice, R. A. *et al.* (2015) 'Elimination of microglia improves functional outcomes following extensive neuronal loss in the hippocampus', *Journal of Neuroscience*, 35(27), pp. 9977–9989. doi: 10.1523/JNEUROSCI.0336-15.2015.

Rigato, C. *et al.* (2011) 'Pattern of invasion of the embryonic mouse spinal cord by microglial cells at the time of the onset of functional neuronal networks', *GLIA*, 59(4), pp. 675–695. doi: 10.1002/glia.21140.

Rojo, R. *et al.* (2019) 'Deletion of a Csf1r enhancer selectively impacts CSF1R expression and development of tissue macrophage populations', *Nature Communications*. Nature Publishing Group, 10(1), p. 3215. doi: 10.1038/s41467-019-11053-8.

Ronaldson, P. T. and Davis, T. P. (2020) 'Regulation of blood – brain barrier integrity by microglia in health and disease : A therapeutic opportunity'. doi: 10.1177/0271678X20951995.

Ronzano, R. *et al.* (2021) 'Microglia-neuron interaction at nodes of Ranvier depends on neuronal activity through potassium release and contributes to remyelination', *Nature Communications*. Springer US, 12(1). doi: 10.1038/s41467-021-25486-7.

Rosin, J. M., Vora, S. R. and Kurrasch, D. M. (2018) 'Depletion of embryonic microglia using the CSF1R inhibitor PLX5622 has adverse sex-specific effects on mice, including accelerated weight gain, hyperactivity and anxiolytic-like behaviour', *Brain, Behavior, and Immunity*. Elsevier, 73(April), pp. 682–697. doi: 10.1016/j.bbi.2018.07.023.

Rosmus, D. D. *et al.* (2022) 'The Role of Osteopontin in Microglia Biology: Current Concepts and Future Perspectives', *Biomedicines*, 10(4). doi: 10.3390/biomedicines10040840.

Roth, P. and Stanley, E. R. (1996) 'Colony stimulating factor-1 expression is developmentally regulated in the mouse', *Journal of Leukocyte Biology*, 59(6), pp. 817–823. doi: 10.1002/jlb.59.6.817.

Rothhaas, R. and Chung, S. (2021) 'Role of the Preoptic Area in Sleep and Thermoregulation ', *Frontiers in Neuroscience* . Available at: https://www.frontiersin.org/articles/10.3389/fnins.2021.664781.

Ruggiero, M. J. *et al.* (2018) 'Sex Differences in Early Postnatal Microglial Colonization of the Developing Rat Hippocampus Following a Single-Day Alcohol Exposure', *Journal of Neuroimmune Pharmacology*. Springer US, 13(2), pp. 189–203. doi: 10.1007/s11481-017-9774-1.

Sankowski, R. *et al.* (2019) 'Mapping microglia states in the human brain through the integration of high-dimensional techniques', *Nature Neuroscience*, 22(12), pp. 2098–2110. doi: 10.1038/s41593-019-0532-y.

Sato-Hashimoto, M. *et al.* (2019) 'Microglial SIRPa regulates the emergence of CD11c+ microglia and demyelination damage in white matter', *eLife*, 8, pp. 1–29. doi: 10.7554/eLife.42025.

Scattolin, M. A. de A., Resegue, R. M. and Rosário, M. C. do (2022) 'The impact of the environment on neurodevelopmental disorders in early childhood', *Jornal de Pediatria*, 98, pp. S66–S72. doi: https://doi.org/10.1016/j.jped.2021.11.002.

Schafer, D. P. *et al.* (2012) 'Microglia Sculpt Postnatal Neural Circuits in an Activity and Complement-Dependent Manner', *Neuron*, 74(4), pp. 691–705. doi:

10.1016/j.neuron.2012.03.026.

Schafer, D. P. and Stevens, B. (2015) 'Microglia function in central nervous system development and plasticity', *Cold Spring Harbor Perspectives in Biology*, 7(10), pp. 1–18. doi: 10.1101/cshperspect.a020545.

De Schepper, S. *et al.* (2022) 'Perivascular SPP1 Mediates Microglial Engulfment of Synapses in Alzheimer's Disease Models', *bioRxiv*, p. 2022.04.04.486547. Available at: https://www.biorxiv.org/content/10.1101/2022.04.04.486547v1%0Ahttps://www.biorxiv.org/content/10.1101/2022.04.04.486547v1.abstract.

Schulz, C. *et al.* (2012) 'A Lineage of Myeloid Cells Independent of Myb and Hematopoietic Stem Cells', *Science*. American Association for the Advancement of Science, 336(6077), pp. 86–90. doi: 10.1126/science.1219179.

Schwarz, J. M., Sholar, P. W. and Bilbo, S. D. (2012) 'Sex differences in microglial colonization of the developing rat brain', *Journal of Neurochemistry*, 120(6), pp. 948–963. doi: 10.1111/j.1471-4159.2011.07630.x.

Sciences, I. of M. and N. A. of (1992) *Discovering the Brain*. Edited by S. Ackerman. Washington, DC: The National Academies Press. doi: 10.17226/1785.

Scott, E. P. *et al.* (2022) 'The zinc finger transcription factor Sall1 is required for the early developmental transition of microglia in mouse embryos', *Glia*, (February), pp. 1720–1733. doi: 10.1002/glia.24192.

Sedel, F. *et al.* (2004) 'Macrophage-Derived Tumor Necrosis Factor α, an Early Developmental Signal for Motoneuron Death', *The Journal of Neuroscience*, 24(9), pp. 2236 LP – 2246. doi: 10.1523/JNEUROSCI.4464-03.2004.

Segaliny, A. I. *et al.* (2015) 'Syndecan-1 regulates the biological activities of interleukin-34', *Biochimica et Biophysica Acta - Molecular Cell Research*. Elsevier B.V., 1853(5), pp. 1010–1021. doi: 10.1016/j.bbamcr.2015.01.023.

Shechter, R., London, A. and Schwartz, M. (2013) 'Orchestrated leukocyte recruitment to immune-privileged sites: absolute barriers versus educational gates', *Nature Reviews Immunology*, 13(3), pp. 206–218. doi: 10.1038/nri3391.

Shen, X. *et al.* (2022) 'Definition of a mouse microglial subset that regulates neuronal development and proinflammatory responses in the brain', *Proceedings of the National Academy of Sciences of the United States of America*, 119(8). doi: 10.1073/pnas.2116241119.

Sherafat, A. *et al.* (2021) 'Microglial neuropilin-1 promotes oligodendrocyte expansion during development and remyelination by trans-activating platelet-derived growth factor receptor', *Nature Communications*, 12(1). doi: 10.1038/s41467-021-22532-2.

Shigemoto-Mogami, Y. *et al.* (2014) 'Microglia enhance neurogenesis and oligodendrogenesis in the early postnatal subventricular zone', *Journal of Neuroscience*, 34(6), pp. 2231–2243. doi: 10.1523/JNEUROSCI.1619-13.2014.

Sierksma, A. *et al.* (2020) 'Novel Alzheimer risk genes determine the microglia response to amyloid-β but not to TAU pathology', *EMBO Molecular Medicine*, 12(3), pp. 1–18. doi: 10.15252/emmm.201910606.

Sierra, A. *et al.* (2010) 'Microglia shape adult hippocampal neurogenesis through apoptosis-coupled phagocytosis', *Cell Stem Cell*. Elsevier Inc., 7(4), pp. 483–495. doi: 10.1016/j.stem.2010.08.014.

Sierra, A. *et al.* (2016) 'The "Big-Bang" for modern glial biology: Translation and comments

on Pío del Río-Hortega 1919 series of papers on microglia', *Glia*, 64(11), pp. 1801–1840. doi: 10.1002/glia.23046.

Sierra, A., Paolicelli, R. C. and Kettenmann, H. (2019) 'Cien An ˜ os de Microglı ´ a : Milestones in a Century of Microglial Research Trends in Neurosciences', *Trends in Neurosciences*. Elsevier Inc., 42(11), pp. 778–792. doi: 10.1016/j.tins.2019.09.004.

Silvin, A. *et al.* (2022) 'Dual ontogeny of disease-associated microglia and disease inflammatory macrophages in aging and neurodegeneration', *Immunity*. Elsevier Inc., 55(8), pp. 1448-1465.e6. doi: 10.1016/j.immuni.2022.07.004.

Smith, J. A. *et al.* (2012) 'Role of pro-inflammatory cytokines released from microglia in neurodegenerative diseases', *Brain Research Bulletin*. Elsevier Inc., 87(1), pp. 10–20. doi: 10.1016/j.brainresbull.2011.10.004.

Smolders, S. M. T. *et al.* (2017) 'Age-specific function of α5β1 integrin in microglial migration during early colonization of the developing mouse cortex', *GLIA*, 65(7), pp. 1072–1088. doi: 10.1002/glia.23145.

Sofroniew, M. V and Vinters, H. V (2010) 'Astrocytes: biology and pathology', *Acta Neuropathologica*, 119(1), pp. 7–35. doi: 10.1007/s00401-009-0619-8.

Son, Y. *et al.* (2020) 'Inhibition of colony-stimulating factor 1 receptor by plx3397 prevents amyloid beta pathology and rescues dopaminergic signaling in aging 5xfad mice', *International Journal of Molecular Sciences*, 21(15), pp. 1–14. doi: 10.3390/ijms21155553.

Sosna, J. *et al.* (2018) 'Early long-term administration of the CSF1R inhibitor PLX3397 ablates microglia and reduces accumulation of intraneuronal amyloid, neuritic plaque deposition and pre-fibrillar oligomers in 5XFAD mouse model of Alzheimer's disease', *Molecular Neurodegeneration*. Molecular Neurodegeneration, 13(1), pp. 1–11. doi: 10.1186/s13024-018-0244-x.

Spector, R., Robert Snodgrass, S. and Johanson, C. E. (2015) 'A balanced view of the cerebrospinal fluid composition and functions: Focus on adult humans.', *Experimental neurology*. United States, 273, pp. 57–68. doi: 10.1016/j.expneurol.2015.07.027.

Spiteri, A. G. *et al.* (2022) 'PLX5622 Reduces Disease Severity in Lethal CNS Infection by Off-Target Inhibition of Peripheral Inflammatory Monocyte Production', *Frontiers in Immunology*, 13(March), pp. 1–16. doi: 10.3389/fimmu.2022.851556.

Squarzoni, P. *et al.* (2014) 'Microglia Modulate Wiring of the Embryonic Forebrain', *Cell Reports*. The Authors, 8(5), pp. 1271–1279. doi: 10.1016/j.celrep.2014.07.042.

Srinivasan, K. *et al.* (2020) 'Alzheimer's Patient Microglia Exhibit Enhanced Aging and Unique Transcriptional Activation', *Cell Reports*. ElsevierCompany., 31(13), p. 107843. doi: 10.1016/j.celrep.2020.107843.

Stanley, E. R. and Chitu, V. (2014) 'CSF-1 receptor signaling in myeloid cells', *Cold Spring Harbor Perspectives in Biology*, 6(6), pp. 1–22. doi: 10.1101/cshperspect.a021857.

Stephan, A. H., Barres, B. A. and Stevens, B. (2012) 'The complement system: An unexpected role in synaptic pruning during development and disease', *Annual Review of Neuroscience*, pp. 369–389. doi: 10.1146/annurev-neuro-061010-113810.

Stogsdill, J. A. *et al.* (2022) 'Pyramidal neuron subtype diversity governs microglia states in the neocortex', *Nature*, 608(7924), pp. 750–756. doi: 10.1038/s41586-022-05056-7.

Stremmel, C. *et al.* (2018) 'Yolk sac macrophage progenitors traffic to the embryo during defined stages of development', *Nature Communications*, 9(1). doi: 10.1038/s41467-017-

02492-2.

Swinnen, N. *et al.* (2013) 'Complex invasion pattern of the cerebral cortex bymicroglial cells during development of the mouse embryo', *GLIA*, 61(2), pp. 150–163. doi: 10.1002/glia.22421.

Szalay, G. *et al.* (2016) 'Microglia protect against brain injury and their selective elimination dysregulates neuronal network activity after stroke', *Nature Communications*, 7(May). doi: 10.1038/ncomms11499.

Takasato, M. *et al.* (2004) 'Identification of kidney mesenchymal genes by a combination of microarray analysis and Sall1-GFP knockin mice', *Mechanisms of development*. Elsevier, 121(6), pp. 547–557.

Takata, K. *et al.* (2017) 'Induced-Pluripotent-Stem-Cell-Derived Primitive Macrophages Provide a Platform for Modeling Tissue-Resident Macrophage Differentiation and Function', *Immunity*, 47(1), pp. 183-198.e6. doi: 10.1016/j.immuni.2017.06.017.

Tan, Y. L., Yuan, Y. and Tian, L. (2020) 'Microglial regional heterogeneity and its role in the brain', *Molecular Psychiatry*. Springer US, 25(2), pp. 351–367. doi: 10.1038/s41380-019-0609-8.

Tay, T. L. *et al.* (2017) 'A new fate mapping system reveals context-dependent random or clonal expansion of microglia', *Nature Neuroscience*, 20(6), pp. 793–803. doi: 10.1038/nn.4547.

Thion, M. S. *et al.* (2018) 'Microbiome Influences Prenatal and Adult Microglia in a Sex-Specific Manner', *Cell*. Elsevier Inc., 172(3), pp. 500-507.e16. doi: 10.1016/j.cell.2017.11.042.

Thion, M. S. *et al.* (2019) 'Biphasic Impact of Prenatal Inflammation and Macrophage Depletion on the Wiring of Neocortical Inhibitory Circuits', *Cell Reports*, 28(5), pp. 1119-1126.e4. doi: 10.1016/j.celrep.2019.06.086.

Thion, M. S., Ginhoux, F. and Garel, S. (2018) 'Microglia and early brain development: An intimate journey', *Science*. American Association for the Advancement of Science, 362(6411), pp. 185 LP – 189. doi: 10.1126/science.aat0474.

Van Tilborg, E. *et al.* (2018) 'Origin and dynamics of oligodendrocytes in the developing brain: Implications for perinatal white matter injury', *Glia*, 66(2), pp. 221–238. doi: 10.1002/glia.23256.

Tremblay, M. Ě. M.-E. `, Lowery, R. L. and Majewska, A. K. (2010) 'Microglial interactions with synapses are modulated by visual experience', *PLoS Biology*. Edited by M. Dalva. Public Library of Science, 8(11), p. e1000527. doi: 10.1371/journal.pbio.1000527.

Tsukahara, S. and Morishita, M. (2020) 'Sexually Dimorphic Formation of the Preoptic Area and the Bed Nucleus of the Stria Terminalis by Neuroestrogens', *Frontiers in Neuroscience*. Available at: https://www.frontiersin.org/articles/10.3389/fnins.2020.00797.

Ueno, M. *et al.* (2013) 'Layer v cortical neurons require microglial support for survival during postnatal development', *Nature Neuroscience*. Nature Publishing Group, 16(5), pp. 543–551. doi: 10.1038/nn.3358.

Umpierre, A. D. *et al.* (2020) 'Microglial calcium signaling is attuned to neuronal activity in awake mice', *Elife*. eLife Sciences Publications Limited, 9, p. e56502.

Umpierre, A. D. and Wu, L.-J. J. (2021) 'How microglia sense and regulate neuronal activity.', *Glia*. United States, 69(7), pp. 1637–1653. doi: 10.1002/glia.23961.

Utz, S. G. *et al.* (2020) 'Early Fate Defines Microglia and Non-parenchymal Brain Macrophage

Development', *Cell*. Elsevier, 181(3), pp. 557-573.e18. doi: 10.1016/j.cell.2020.03.021.

Uzunova, G., Pallanti, S. and Hollander, E. (2016) 'Excitatory/inhibitory imbalance in autism spectrum disorders: Implications for interventions and therapeutics.', *The world journal of biological psychiatry : the official journal of the World Federation of Societies of Biological Psychiatry*. England, 17(3), pp. 174–186. doi: 10.3109/15622975.2015.1085597.

Vannella, K. M. and Wynn, T. A. (2017) 'Mechanisms of Organ Injury and Repair by Macrophages.', *Annual review of physiology*. United States, 79, pp. 593–617. doi: 10.1146/annurev-physiol-022516-034356.

VanRyzin, J. W. *et al.* (2019) 'Microglial Phagocytosis of Newborn Cells Is Induced by Endocannabinoids and Sculpts Sex Differences in Juvenile Rat Social Play', *Neuron*, 102(2), pp. 435-449.e6. doi: 10.1016/j.neuron.2019.02.006.

Velmeshev, D. *et al.* (2019) 'Single-cell genomics identifies cell type–specific molecular changes in autism', *Science*, 364(6441), pp. 685–689. doi: 10.1126/science.aav8130.

Verney, C. *et al.* (2010) 'Early microglial colonization of the human forebrain and possible involvement in periventricular white-matter injury of preterm infants', *Journal of Anatomy*, 217(4), pp. 436–448. doi: 10.1111/j.1469-7580.2010.01245.x.

Villa, A. *et al.* (2018) 'Sex-Specific Features of Microglia from Adult Mice', *Cell Reports*. ElsevierCompany., 23(12), pp. 3501–3511. doi: 10.1016/j.celrep.2018.05.048.

Wake, H. *et al.* (2009) 'Resting microglia directly monitor the functional state of synapses in vivo and determine the fate of ischemic terminals', *Journal of Neuroscience*, 29(13), pp. 3974–3980. doi: 10.1523/JNEUROSCI.4363-08.2009.

Wakselman, S. *et al.* (2008) 'Developmental Neuronal Death in Hippocampus Requires the Microglial CD11b Integrin and DAP12 Immunoreceptor', *The Journal of Neuroscience*, 28(32), pp. 8138 LP – 8143. doi: 10.1523/JNEUROSCI.1006-08.2008.

Walls, J. R. *et al.* (2008) 'Three-Dimensional Analysis of Vascular Development in the Mouse Embryo', *PLOS ONE*. Public Library of Science, 3(8), p. e2853. Available at: https://doi.org/10.1371/journal.pone.0002853.

Wang, Y. *et al.* (2012) 'IL-34 is a tissue-restricted ligand of CSF1R required for the development of Langerhans cells and microglia', *Nature Immunology*, 13(8), pp. 753–760. doi: 10.1038/ni.2360.

Wang, Y. Q., Berezovska, O. and Fedoroff, S. (1999) 'Expression of colony stimulating factor-1 receptor (CSF-1R) by CNS neurons in mice', *Journal of Neuroscience Research*, 57(5), pp. 616–632. doi: 10.1002/(SICI)1097-4547(19990901)57:5<616::AID-JNR4>3.0.CO;2-E.

Wei, S. *et al.* (2010) 'Functional overlap but differential expression of CSF-1 and IL-34 in their CSF-1 receptor-mediated regulation of myeloid cells', *Journal of Leukocyte Biology*, 88(3), pp. 495–505. doi: 10.1189/jlb.1209822.

Weinhard, L. *et al.* (2018) 'Microglia remodel synapses by presynaptic trogocytosis and spine head filopodia induction', *Nature Communications*. Springer US, 9(1). doi: 10.1038/s41467-018-03566-5.

Wlodarczyk, A. *et al.* (2017) 'A novel microglial subset plays a key role in myelinogenesis in developing brain', *The EMBO Journal*, 36(22), pp. 3292–3308. doi: 10.15252/embj.201696056.

Wong, F. K. and Marín, O. (2019) 'Developmental cell death in the cerebral cortex', *Annual Review of Cell and Developmental Biology*, pp. 523–542. doi: 10.1146/annurev-cellbio-

100818-125204.

Wu, S. *et al.* (2018) 'Il34-Csf1r Pathway Regulates the Migration and Colonization of Microglial Precursors', *Developmental Cell*. Elsevier Inc., 46(5), pp. 552-563.e4. doi: 10.1016/j.devcel.2018.08.005.

Wylot, B. *et al.* (2019) 'Csf1 Deficiency Dysregulates Glial Responses to Demyelination and Disturbs CNS White Matter Remyelination', *Cells*, 9(1), p. 99. doi: 10.3390/cells9010099.

Xu, J. *et al.* (2016) 'Microglia Colonization of Developing Zebrafish Midbrain Is Promoted by Apoptotic Neuron and Lysophosphatidylcholine', *Developmental Cell*, 38(2), pp. 214–222. doi: 10.1016/j.devcel.2016.06.018.

Yamane, T. (2018) 'Mouse yolk sac hematopoiesis', *Frontiers in Cell and Developmental Biology*, 6(JUL), pp. 1–8. doi: 10.3389/fcell.2018.00080.

Yanguas-Casás, N. *et al.* (2018) 'Sex differences in the phagocytic and migratory activity of microglia and their impairment by palmitic acid', *Glia*, 66(3), pp. 522–537. doi: 10.1002/glia.23263.

York, E. M., Bernier, L. P. and MacVicar, B. A. (2018) 'Microglial modulation of neuronal activity in the healthy brain', *Developmental Neurobiology*, 78(6), pp. 593–603. doi: 10.1002/dneu.22571.

Zang, Y., Chaudhari, K. and Bashaw, G. J. (2021) 'New insights into the molecular mechanisms of axon guidance receptor regulation and signaling.', *Current topics in developmental biology*. United States, 142, pp. 147–196. doi: 10.1016/bs.ctdb.2020.11.008.

Zeisel, A. *et al.* (2015) 'Cell types in the mouse cortex and hippocampus revealed by single-cell RNA-seq', *Science*. American Association for the Advancement of Science, 347(6226), pp. 1138–1142. doi: 10.1126/science.aaa1934.

Zhan, L. *et al.* (2020) 'A MAC2-positive progenitor-like microglial population is resistant to CSF1R inhibition in adult mouse brain', *eLife*, 9, pp. 1–22. doi: 10.7554/elife.51796.

Zhan, L. I. *et al.* (2019) 'Proximal recolonization by self-renewing microglia re-establishes microglial homeostasis in the adult mouse brain', *PLoS Biology*, 17(2), pp. 1–35. doi: 10.1371/journal.pbio.3000134.

Zhan, Y. *et al.* (2014) 'Deficient neuron-microglia signaling results in impaired functional brain connectivity and social behavior', *Nature Neuroscience*. Nature Publishing Group, 17(3), pp. 400–406. doi: 10.1038/nn.3641.

Zhang, J. *et al.* (2019) 'Maternal immune activation altered microglial immunoreactivity in the brain of postnatal day 2 rat offspring', *Synapse*, 73(2), pp. 1–14. doi: 10.1002/syn.22072.

Zhang, Y. *et al.* (2014) 'An RNA-Sequencing Transcriptome and Splicing Database of Glia, Neurons, and Vascular Cells of the Cerebral Cortex', *The Journal of Neuroscience*, 34(36), pp. 11929 LP – 11947. doi: 10.1523/JNEUROSCI.1860-14.2014.

Zhao, Q. *et al.* (2014) 'Maternal sleep deprivation inhibits hippocampal neurogenesis associated with inflammatory response in young offspring rats.', *Neurobiology of disease*. United States, 68, pp. 57–65. doi: 10.1016/j.nbd.2014.04.008.

Zheng, J. *et al.* (2021) 'Single-cell RNA-seq analysis reveals compartment-specific heterogeneity and plasticity of microglia', *iScience*. Elsevier Inc., 24(3), p. 102186. doi: 10.1016/j.isci.2021.102186.

Mécanismes contrôlant la colonisation microgliale du cerveau antérieur

Résumé :

Les microglies, les macrophages résidants du cerveau, jouent un rôle essentiel dans le développement, le fonctionnement et l'homéostasie cérébrale. Issues de progéniteurs érythromyéloïdes du sac vitellin, elles colonisent le système nerveux central au début de l'embryogenèse, où elles prolifèrent ensuite, se répartissent et puis s'autorenouvellent tout au long de la vie. La voie de signalisation du récepteur CSF-1 (CSF-1R) est essentielle pour la survie et la prolifération des microglies, et ses deux ligands, les cytokines CSF-1 et IL-34, sont produites par l'environnement neural. Au cours du développement, outre une remarquable hétérogénéité cellulaire et transcriptionnelle des microglies, leur distribution dans le cerveau suit un schéma spatio-temporel stéréotypé. Par exemple, des microglies d'un sous-type particulier, appelées microglies associées à des faisceaux d'axones (ATM), forment des hotspots transitoires - une caractéristique conservée à travers espèces. Ces spécificités de colonisation et l'hétérogénéité microgliale ont été associées à des fonctions développementales des microglies. Néanmoins, leur régulation ainsi que la contribution des neurones et d'autres sources de CSF-1, restent encore largement inexplorées

Nous avons effectué une analyse détaillée de la prolifération et distribution des microglies dans le cerveau antérieur murin, et étudié comment cela pouvait être régulée par l'environnement neural, soit par l'activité neuronale ou l'expression de CSF-1. Nous avons mis en évidence deux vagues de prolifération microgliale : une première phase globale et intense pendant l'embryogenèse, et une seconde phase postnatale plus hétérogène. De plus, nous avons montré que les microglies des points d'accumulation sont particulièrement prolifératives. En utilisant l'imagerie à deux photons sur des tranches aiguës de cerveau, nous avons confirmé une prolifération et redistribution locale, mais n'avons trouvé aucune preuve de migration à longue distance. Dans l'ensemble, nos résultats indiquent que la prolifération est un moteur important de la colonisation microgliale et contribue à son schéma hétérogène.

En nous concentrant sur le cortex cérébral, nous avons d'abord testé le rôle de l'activité neuronale, connue pour être surveillée par les microglies, lorsqu'elle émerge, pendant la seconde vague de prolifération. Nous avons constaté que différentes perturbations de l'activité neuronale n'avaient pas d'effet fort sur le nombre et la distribution des microglies. Ensuite, nous avons examiné les rôles de CSF-1 grâce à des inactivation conditionnelles dans des populations neurales spécifiques. Nous avons montré que CSF-1 issu des progéniteurs et neurones était essentiel pour la colonisation microgliale embryonnaire : son inactivation dans le cortex entraine une déplétion drastique des microglies dans l'embryogenèse, sans affecter les macrophages des méninges. Plus précisément, CSF-1 a une action dose-dépendante, extrêmement locale et transitoire. En parallèle, nous avons montré que les ATM des hotspots exprimaient *Csf-1*. Grâce à des mutants conditionnels, nous avons révélé que la production autocrine de CSF-1 contribuait à la prolifération soutenue des ATM, mettant en évidence une contribution duale du CSF-1 neural et CSF-1 microglial dans la régulation de leur distribution au cours du développement.

De plus, j'ai participé à la description d'une nouvelle fonction microgliale, associée aux ATM, assurant le maintien de l'intégrité tissulaire au hotspots embryonnaire.

De façon plus large, notre étude met en lumière la façon dont les microglies prolifèrent et se distribuent dans le cerveau, ainsi que leur dépendance focale au CSF-1. De plus, notre mutant conditionnel dans le cortex fournit un modèle novateur pour étudier les rôles locaux et spécifiques des microglies pendant le développement prénatal et ouvre la voie à une analyse plus approfondie des contributions relatives des ligands de CSF-1R.

Mots clés : Microglie, Prolifération, CSF-1, Développement

Mechanisms controlling microglial colonization of the forebrain

Abstract :

Microglia are the central nervous system resident macrophages and the main immune sentinels of the brain. Beyond their immune functions, they play key roles in cerebral development and functioning. These immigrants derive from erythromyeloid progenitors generated in the yolk sac and colonize the brain during early embryogenesis. They further proliferate *in situ*, distribute within the brain parenchyma and self-renew throughout life. The CSF-1 receptor (CSF-1R) pathway regulates microglial survival and proliferation from embryogenesis up to adulthood, with its two ligands, the cytokines CSF-1 and IL-34, produced by the neural environment. During development, along with a remarkable cellular and transcriptional heterogeneity, microglial distribution follows a stereotypical spatiotemporal pattern. For instance, microglia of a specific subset, called axon-tract associated microglia (ATM), form transient and specific accumulations, or hotspots - a feature conserved across mammalian species. Such pattern of colonization and associated microglial heterogeneity have been linked to specific developmental functions. Yet, how early microglial distribution and heterogeneity are regulated, the potential contributions of neurons and of distinct cellular sources of CSF-1, remain largely to be investigated.

Here, we tackled these issues by performing a detailed analysis of microglial proliferation and distribution during mouse forebrain development, and examining how the neural environment may regulate this pattern, either through neuronal activity or CSF-1 expression. We first highlighted the existence of two waves of microglial proliferation: a first global and intense phase during mid-embryogenesis, and a second postnatal phase which intensity and timing vary across forebrain regions. In addition, we found that some transient developmental hotspots of microglia were particularly proliferative. Using two-photon live-imaging on acute brain slices, we confirmed local proliferation and redistribution, but found no evidence of long-range migration. Collectively, our findings indicate that proliferation is an important driver of microglial colonization and contributes to its heterogeneous pattern.

Focusing on the cerebral cortex, we first tested during this second wave of proliferation the role of neuronal activity, which emerges at these developmental stages and is known to be monitored by microglia. We found that different perturbations of neuronal activity had no broad effect on microglial numbers and distribution. Next, we examined the roles of CSF-1, using conditional mutants in specific neural populations. Through distinct cre drivers, we showed that CSF-1 from both cortical progenitors and neurons is required for microglial embryonic colonization. More specifically, CSF-1 acts in a dose-dependent manner and has a remarkably local effect, without severely affecting macrophages in the meninges. Consistently, *Csf-1* cortical inactivation leads to a drastic absence of microglia only during embryogenesis, supporting a later role of IL-34 as previously reported. In parallel, we examined ATM in the hotspots and observed that they express *Csf-1*. Using conditional mutants, we revealed that autocrine CSF-1 production by ATM contributes to their proliferation in hotspots. Our findings thus highlight a dual contribution of local neural CSF-1 and microglial CSF-1 in regulating their early developmental distribution.

In parallel, I participated in describing a novel function of microglia in the maintenance of tissue integrity at the embryonic ATM hotspot.

Altogether, our study sheds light on how microglia proliferate and distribute to colonize the brain as well as on their focal and cell-type dependency on CSF-1. In addition, our conditional cortical mutants provide a groundbreaking tool to study the local and specific roles of microglia during prenatal development and opens the path to further dissect the relative contributions of CSF-1R ligands.

Keywords : Microglia, Proliferation, CSF-1, Development